CONTENTS:

Chapt. 4: Stress

- Definitions, magnitudes and units
- Stress on a surface
- Stress at a point
- Stress components
- The stress tensor (matrix)
- Deviatoric stress and mean stress
- Mohr's circle and the Mohr diagram

Chapt. 5: Stress in the lithosphere

- Introduction
- Stress measurements
- Reference states of stress
- The thermal effect on horizontal stress
- Residual stress
- Tectonic stress
- Global stress patterns
- Differential stress, deviatoric stress and some implications

Chapt. 6: Rheology

- Rheology and continuum mechanics
- Idealized conditions
- Elastic materials
- Plasticity and flow: permanent deformation
- Combined models
- Experiments
- The role of temperature, water etc.
- Definition of plastic, ductile and brittle deformation
- Rheology of the lithosphere

Chapt. 7: Fracture and brittle deformation

- Brittle deformation mechanisms
- What is a fracture?
- Failure and fracture criteria
- Microdefects and failure
- Fracture termination and interaction
- Reactivation and frictional sliding
- Fluid pressure, effective stress and poroelasticity
- Deformation bands and fractures in porous rocks

Chapt. 8: Faults

- Basic terminology
- Fault anatomy
- Displacement distribution
- Identifying faults in an oil field setting

The birth and growth of faults
Growth of fault populations
Faults, communication and sealing properties

Chapt. 9: Kinematics and paleostress in the brittle regime

Kinematic criteria
Stress from faults
A kinematic approach to fault slip data
Contractional and extensional structures

Chapt. 10: Deformation at the microscale

Deformation mechanisms and microstructures
Brittle versus plastic deformation mechanisms
Brittle deformation mechanisms
Mechanical twinning
Crystal defects
From the atomic scale to microstructures

Chapt. 11: Folds and folding

Geometric description
Folding – mechanisms and processes
Fold interference patterns
Folds in shear zones

Chapt. 12: Foliation and cleavage

Basic concepts
Relative age terminology
Cleavage development
Cleavage, folds and strain
Foliation in quartzites, gneisses and mylonite zones

Chapt. 13: Lineations

Basic terminology
Lineations related to plastic deformation
Lineations in the brittle regime
Lineations and kinematics

Chapt. 14: Boudinage

Boudinage and pinch-and-swell structures
Geometry, viscosity and strain
Asymmetric boudinage and rotation
Foliation boudinage
Boudinage and the strain ellipse
Really large-scale boudinage

Chapt. 15: Shear zones and mylonites

CHAPTER 1

Structural geology and structural analysis

Structural geology involves the description of the structure of the lithosphere at various scales and seeks to understand how any given structure or set of structures formed. Our methods are field observations, laboratory experiments and numerical modeling. All of these methods have advantages and challenges. Field examples portray the final results of deformation processes, while the actual deformation history may be unknown. Histories that may span millions of years in nature must be performed in hours, days or weeks in the laboratory. In addition, numerical modeling is hampered by simplifications necessary for the models to be runable with today's codes and computers. However, by combining different approaches we are able to obtain realistic models of how structures form and what they mean. Field studies will always be the key to success. Any modeling, numerical or physical, must be based directly or indirectly on accurate and objective field observations and descriptions. Objectivity during field work is often a challenge.

1.1 Structural geology and tectonics

The word *structure* is derived from the Latin word *struere*, to build. The closely related word *tectonics* comes from the Greek word *tektos*, which has a similar, but often broader, meaning. Both terms relate to the building or structure of the Earth's crust, and to the continuous movements that change and shape the outer layers of our planet. *Plate tectonics* is the part of tectonics that involves the movement and interaction of lithospheric plates.

Tectonic structures may be the direct result of plate motions (plate tectonics), but are not limited to structures formed by plate movements.

Tectonic deformation is primarily caused by a regional horizontal stress that deviates from the state of stress that is to be expected based on such things as crustal depth, density of overburden and fluid pressure. However, there are important deformation structures that are of non-tectonic origin, and most or all of these are related to *gravity*. Such structures include those related to compaction of sediments, diapirism in magmatic settings and buoyancy-driven salt movements in some salt provinces. On a smaller scale there is syn-sedimentary folding, dewatering structures and structures related to landslides. Still, there is a gradual transition between tectonic and non-tectonic deformation. Typical non-tectonic deformation, such as gravity sliding and dewatering deformation, can be triggered by earthquakes, salt diapirism is usually linked to fracturing of the overburden by regional tectonic strain, and magmatism can be related to convergent or divergent plate motions. Furthermore, *gravity* controls the thickness of the crust in a collision zone and can be consider a (if not the) driving force in plate tectonics, creating ridge-push and slab pull, and in this sense actually generates tectonic stresses and deformation structures. Because of this intimate relationship these two popular terms are used somewhat variably within the geo-community, and it can be useful to be more specific by relating to the actual processes that control the deformation features in question.

Structural geology typically relates to the observation, description and interpretation of structures that can be mapped in the field. Structural data are analyzed in ways that lead to a tectonic model for an area. By *tectonic model* we mean a model that constrain the deformation history in space and time. Perhaps the data fits with a model of N-S rifting (extension) followed by N-S contraction where extensional faults were partly reactivated as reverse faults. Another large-scale example that does not involve deformation history could be the model where the Tibet plateau and all of its strike-slip faults are explained in terms of an escape tectonics

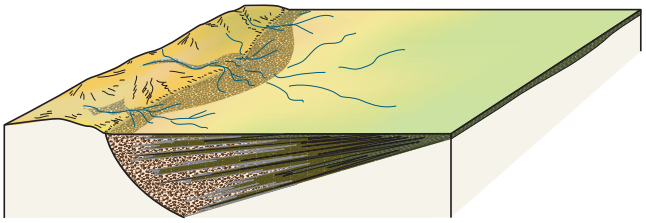

Figure 1.1 Illustration of the close relationship between sedimentary facies, layer thickness variations and faulting during the development of a growth fault along the margin of a sedimentary basin.

or lateral extrusion model (Fig. ??later chapter). More locally, a fault polulation can, based on fault measurements, be interpreted in terms of a transtension model. *Tectonics* concerns large-scale deformation structures and deformation histories, such as mountain building, rifting and basin developement, among others. At smaller scales, *microtectonics* describes microscale deformation and deformation structures visible under the microscope. *Neotectonics* is concerned with recent and ongoing crustal motions and the contemporaneous stress field. Neotectonic structures are the surface expression of faults in the form of fault scarps, and important data sets stem from seismic information from earthquakes (such as focal mechanisms, p. ??) and changes in elevation of regions detected by repeated satellite measurements.

How do we recognize deformation or strain in a rock? "Strained" means that something primary has been geometrically modified, be it cross stratification, pebble shape, a primary magmatic texture, static growth of metamorphic minerals or a preexisting deformation structure. Hence, recognizing strain and deformation structures actually requires solid knowledge of what undeformed rocks and their primary structures originally looked like.

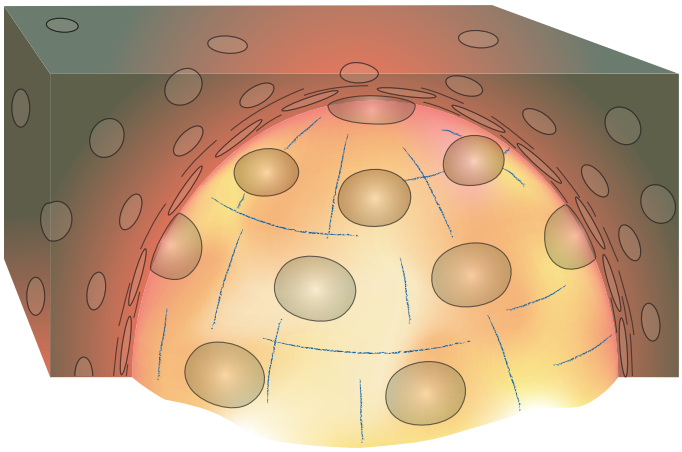

Figure 1.2 Structural geology can be linked with other processes. This figures illustrates the connection between forceful intrusion of magma (balloning) and foliation and strain in the country rock. Ellipses indicate amount of strain.

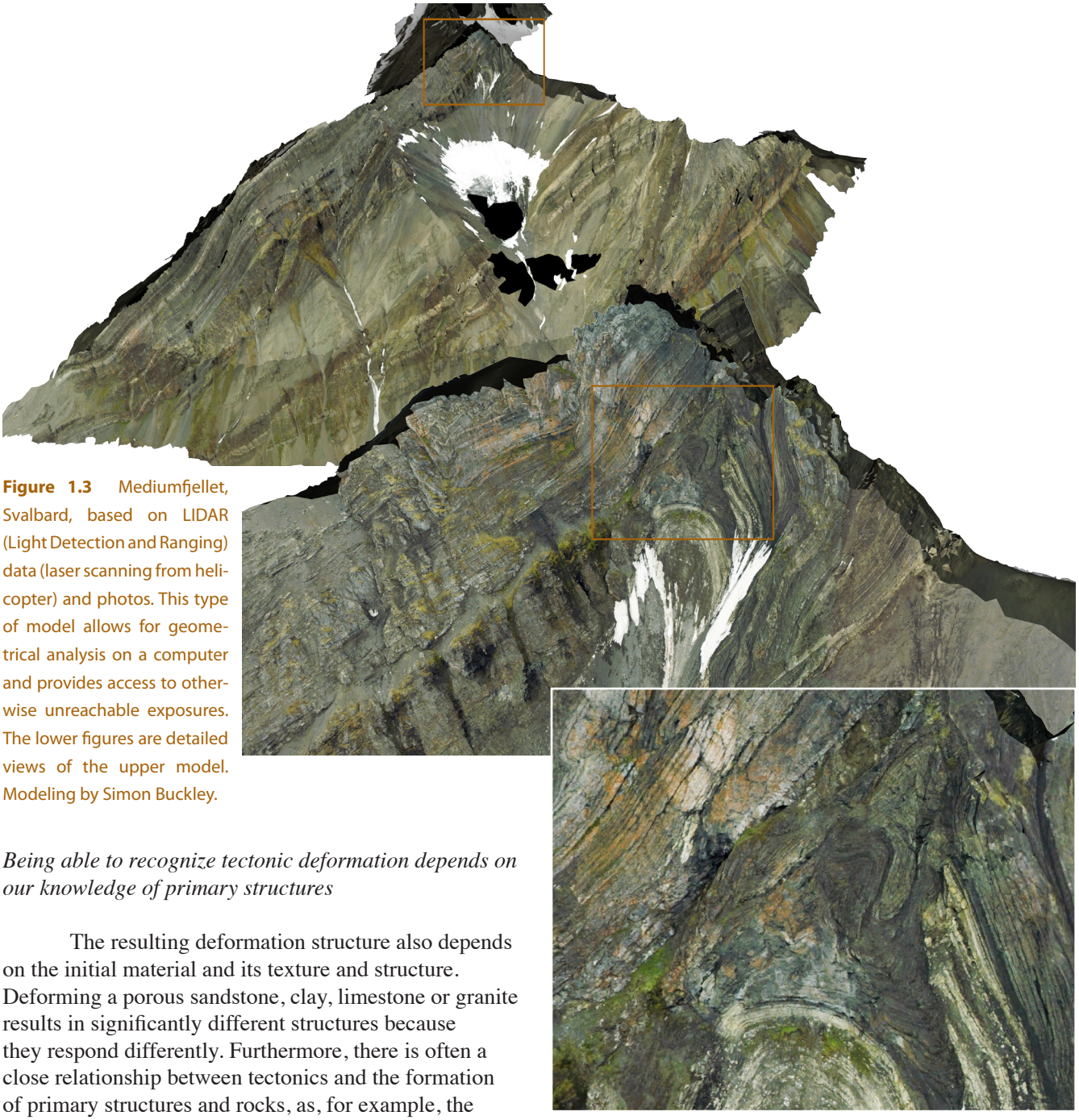

Figure 1.3 Mediumfjellet, Svalbard, based on LIDAR (Light Detection and Ranging) data (laser scanning from helicopter) and photos. This type of model allows for geometrical analysis on a computer and provides access to otherwise unreachable exposures. The lower figures are detailed views of the upper model. Modeling by Simon Buckley.

Being able to recognize tectonic deformation depends on our knowledge of primary structures

The resulting deformation structure also depends on the initial material and its texture and structure. Deforming a porous sandstone, clay, limestone or granite results in significantly different structures because they respond differently. Furthermore, there is often a close relationship between tectonics and the formation of primary structures and rocks, as, for example, the relationship between sedimentary facies and thickness in the hanging wall of a syndepositional fault with fault offset and movement history (Figure 1.1). Another is the deformation of magmatic rocks during forceful intrusion (ballooning) (Figure 1.2). Metamorphic growth of minerals before, during and after deformation may also provide important information about the pressure-temperature conditions during deformation, and may contain textures and structures reflecting kinematics and deformation history.

Structural geology covers deformation structures formed at or near the Earth's surface, in the cool, upper part of the crust, in the hotter lower crust and in the underlying mantle. It embraces structures at the scale of hundreds of kilometers down to micro- or atomic-scale structures, structures that form almost instantaneously, and structures that form over tens of millions of years. A large number of sub-disciplines and methodologies therefore exist within the field of structural geology. The oil exploration geologist may be considering sealing fault problems while the production geologist worries about the effect of deformation bands on fluid flow in his reservoir. The engineering geologist may consider fracture orientations and densities in relation to a tunnel project, while the university professor uses structural mapping, physical modeling or computer modeling to understand mountain building processes. The methods and approaches are many, but they serve to understand the structural or tectonic development of a region or to predict the structural pattern in an area. In most cases structural geology is founded on data and observations

that must be analyzed and interpreted. Structural analysis is therefore an important part of the field of structural geology.

1.2 Structural data sets

Planet Earth represents an incredibly complex physical system, and the structures that result from natural deformation reflect this fact through their multitude of expressions and histories. Field observations of deformed rocks and their structures represent the most direct and important source of information on how rocks deform, and objective observations and descriptions of naturally deformed rocks are the key to understand natural deformation. There is thus a need to simplify and identify the one or few most important factors that describe or lead to the recognition of deformation structures that can be seen or mapped in naturally deformed rocks. Experiments performed in the laboratory give us valuable knowledge of how various physical conditions, including stress field, boundary condition, temperature, or the physical properties of the deforming material, relate to deformation. Numerical models, where rock deformation is simulated on a computer, are also useful as they allow one to control the various parameters and properties that influence deformation.

Experiments and numerical models not only help us understand how external and internal physical conditions control or predict the deformation structures that form, but also give information on how deformation structures evolve, i.e. they provide insights into the deformation history. In contrast, naturally deformed rocks represent end-results of natural deformation histories, and the history may be difficult to read out of the rocks themselves. Numerical and experimental models allow one to control rock properties and boundary conditions and explore their effect on deformation and deformation history. Nevertheless, any deformed rock does contain some information about the history of deformation. The challenge is to know what to look for and to interpret this information. Numerical and experimental work aids in completing this task, together with objective and accurate field observations.

Figure 1.4 a) Landsat image over an area west of Bergen, Norway, and a more detailed aerial photo of a selected part of the satellite image. Satellite images are useful for regional analysis of fracture systems and foliations, while aerial photos are used for more detailed analyses.

1.2.1 Field data

It is hard to overemphasize the importance of traditional field observations of deformed rocks and their structures. Rocks contain more information than we will ever be able to extract from them, and the success of any physical or numerical model relies on the accuracy of observation of rock structures in the field. Direct contact with rocks and structures that have not been filtered or interpreted by man or computers is invaluable. Unfortunately, man's ability to make objective observations is limited. We tend to see what we expect to see and what we are trained to see. What we have learned and seen in the past strongly influences our visual impressions of deformed rocks. Any student of deformed rocks should therefore train himself or herself to be objective. Only then can we expect to discover the unexpected and make new interpretations that may contribute to our understanding of the

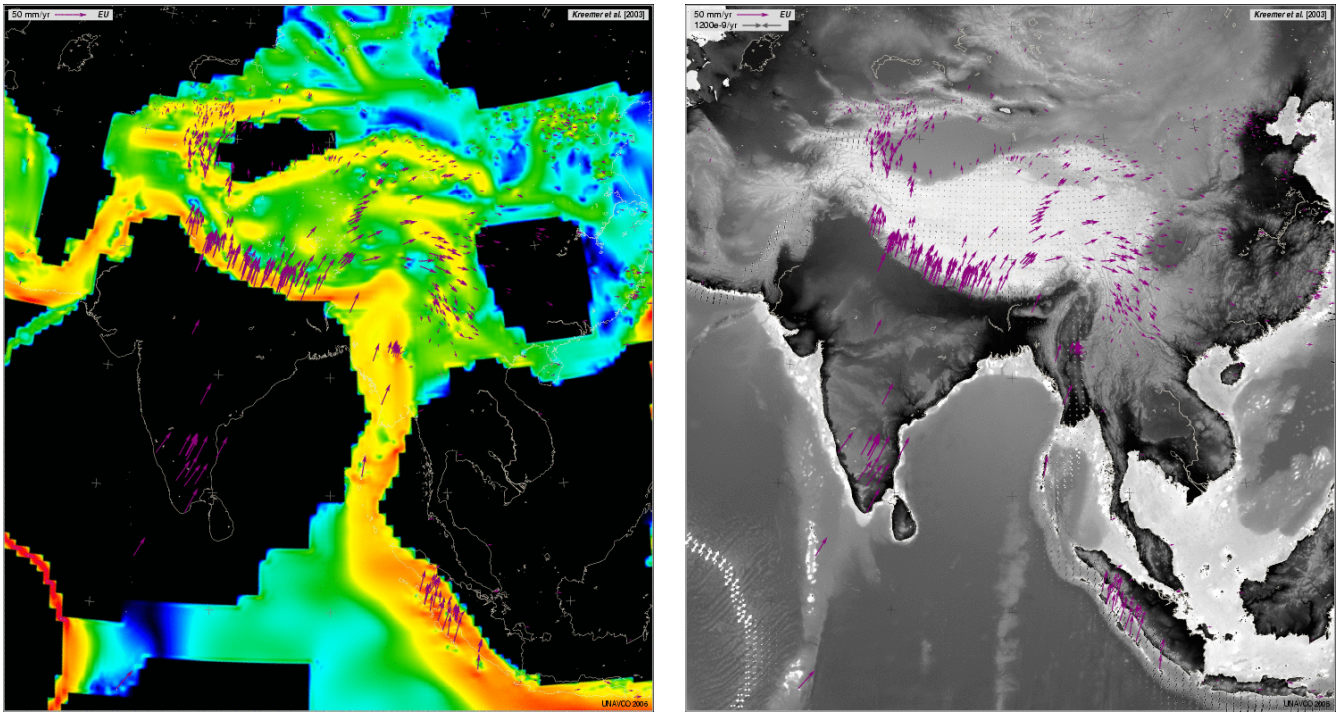

Figure 1.5 Use of GPS data from stationary GPS stations worldwide can be used to map relative plate motions, here shown as purple vectors. The vectors clearly shows how India is moving into Eurasia, causing deformation in the Himalaya-Tibetian Plateau region. Strain vectors are shown in the right figure. Calculated strain rates are generally less than 10^{-6} y^{-1} or 10^{-14} s^{-1}. The colored areas in the left figure are areas of significant strain rate, based on GPS data. Similar use of GPS data can be applied to much smaller areas where differential movements occur, for example across fault zones. From http://jules.unavco.org

structural development of a region and to the field of structural geology in general. Many structures have been overlooked until the day that someone pointed out their existence and meaning, upon which they all of a sudden appear "everywhere". Shear bands in strongly deformed ductile rocks (mylonites) is one such example. They were either overlooked or considered as cleavage until the late 1970's, when they were properly described and interpreted. After that, they have been described from almost every major shear zone or mylonite zone in the world.

Traditional fieldwork involves the use of simple tools such as a hammer, measuring device, topomaps, a hand lens and a compass, and the data collected are mainly structural orientations and samples for thin section studies. This type of data collection is still important, and is aided by modern GPS units and high-resolution aerial and satellite photos. More advanced and detailed work may now involve the use of a laser-scanning unit, where pulses of laser light strike the surface of the Earth and the time of return is recorded. This information can be used to build a detailed topographic or geometrical model of the outcrop, onto which one or more high-resolution field photographs can be draped (Figure 1.3). Geological observations such as the orientation of layering or fold axes can then be made on a computer. In many cases, the most important way of recording field data is by use of careful field sketches, aided by photographs, orientation measurements and other measurements that can be related to the sketch. Sketching also forces the field geologist to observe features and details that may otherwise be overlooked. At the same time, sketches can be made so as to emphasize relevant information and neglect irrelevant details. Field sketching is, largely, a matter of practice.

1.2.2 Remote sensing and geodesy

Satellite images (Figure 1.4) are now available at increasingly high resolutions and are a valuable tool for the mapping of map-scale structures. An increasing amount of such data is available freely on the world-wide-web, and may be combined with digital elevation data to create three-dimensional models. Orthorectified *aerial photos* may give more details (Figure 1.4, top), with resolutions down to tens of centimeters in some cases. Both ductile structures, such as folds and foliations, and brittle faults and fractures are mappable from satellite images and aerial photos.

In the field of neotectonics, *InSAR* (Interferometric Synthetic Aperture Radar) is a useful remote sensing technique that uses radar satellite images. Beams of radar waves are constantly sent towards the Earth, and an image is generated based on the returned information. The intensity of the reflected information reflects the composition of the ground, but

Offshore Seismic Aquisition

Seismic aquisition. A seismic vessel travels about 5 knots while towing arrays of air guns and streamers containing hydrophones a few meters below the surface of the water. The tail buoy helps the crew locate the end of the streamers. The air guns are activated periodically, such as every 25 m (about 10 seconds), and the resulting sound wave travels into the Earth, is reflected back by the underlying rock layers to hydrophones on the streamer and then relayed to the recording vessel for further processing.

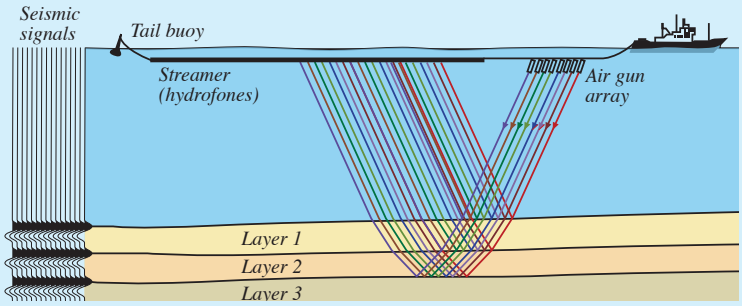

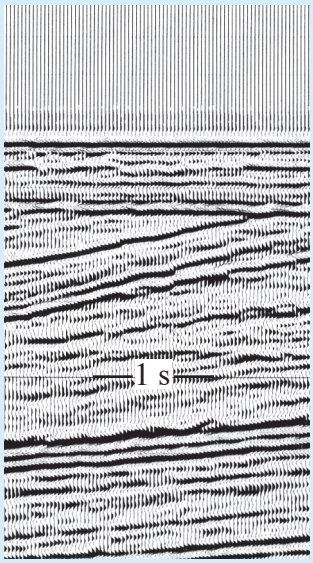

The few sound traces indicated on the figure indicate how the sound waves are both refracted and reflected from the interfaces between water and Layer 1, between Layer 1 and 2, and between Layer 2 and 3. Reflection occurs if there is an increase in the product between velocity and density from one layer to the next. Such interfaces are called reflectors. Reflectors from a seismic line image the upper stratigraphy of the North Sea basin (right). Note the upper, horizontal sea bed reflector, horizontal Quaternary reflectors and dipping Tertiary layers. Unconformities like this one tyically indicate a tectonic event. Note that most seismic sections have seconds (two-way time) as vertical scale.

the phase of the wave as it hits and becomes reflected is also recorded. Comparing the phases enables us to monitor millimeter-scale changes in elevation and geometry of the surface, which among other things may reflect active tectonic movements related to earthquakes. In addition, accurate digital elevation models and topographic maps can also be constructed from these types of data.

GPS positioning data in general are an important source of data that can be retrieved from GPS satellites to measure plate movements (Fig. 1.5). Such data can also be collected on the ground by means of stationary GPS-units with millimeter-scale accuracy.

1.2.3 Seismic reflection data

In the mapping of subsurface structures, seismic data are invaluable and since the 1960's have revolutionized our understanding of fault and fold geometry. Some seismic data are collected for purely academic purposes, but the vast majority of seismic data aquisition is motivated by exploration for petroleum and gas. Most seismic data are thus from rift basins and continental margins.

Marine seismic reflection data (Figure 1.6) are usually collected by boat, where a sound source (air gun) generates sound waves that penetrate the crustal layers under the sea bottom. Microphones can also be put on the sea floor. This method is more cumbersome, but enables both seismic S and P-waves to be recorded (S-waves do not travel through water). Seismic data can also be collected onshore, putting the sound source and microphones (geophones) on the ground. The onshore sound source would usually be an explosive device or a vibrating truck, but even a sledgehammer or special gun can be used for very shallow and local targets.

The sound waves are reflected from layer boundaries where there is an increase in acoustic impedance, i.e. where there is an abrupt change in density and/or the velocity by which sound waves travel in the rock. A long line of microphones, onshore called geophones and onshore referred to as hydrophones, record the reflected sound signals and the time they appear at the surface. These data are collected in digital form and processed by computers to generate a seismic image of the underground.

Seismic data can be processed in a number of ways, depending on the focus of the study. Standard reflection seismic lines are displayed with two-way travel time as the vertical axis. Depth conversion of either the seismic data or the seismic interpretation is therefore necessary to create a geologic profile from those data. Depth conversion is done using a velocity model that depends on the lithology (sound moves faster in sandstone than in shale, and yet faster in limestone) and burial depth (lithification leads to increased velocity). Sometimes the seismic data are

depth migrated. In this case a velocity model is needed. The convenient aspect of depth migrated sections is that the vertical scale is given in depth rather than time. Furthermore, it takes into account lateral changes in rock velocity that may cause visual or geometrical challenges to the interpreter when dealing with a time-migrated section. The accuracy of the depth migrated data does however rely on the velocity model.

Deep seismic lines can be collected where the energy emitted is sufficiently high to penetrate deep parts of the crust and even the upper mantle. Such lines are useful to explore the large-scale structure of the crust. While widely-spaced deep seismic lines and regional seismic lines are called 2-D, more and more commercial (petroleum company) data are collected as a 3-D cube where line spacing is close enough (ca 25 m) that the data can be processed in three dimensions, and where sections through the cube can be made in any direction. The lines parallel to the direction of collection are sometimes called inlines, those orthogonal to inlines are referred to as crosslines, while other vertical lines are random lines. Horizontal sections are called time slices, and can be useful during fault interpretation. Hence 3-D seismic data provide unique opportunities for three-dimensional mapping of faults and folds in the subsurface that is rarely possible even in areas of excellent exposure.

Seismic data is restricted by seismic resolution, which means that one can only distinguish layers that are a certain distance apart, and only faults with a certain minimum offset can be imaged and interpreted. The quality and resolution of 3-D data is generally better than that of 2-D lines, also because the reflected energy is restored more precisely through three-dimensional migration. The seismic resolution of high-quality 3-D data depends on depth, acoustic impedance of the layer interfaces, data collection method and so on, but would typically be at around 15-20 m for identification of fault throw.

More and more sophisticated methods of data analysis and visualization are becoming available for 3-D seismic data sets, helpful for identifying faults and other structures that are underground. Petroleum exploration and exploitation usually rely on seismic 3-D data sets interpreted on computers by geophysicists and structural geologists. The interpretation makes it possible to generate structural contour maps and geologic cross sections that can be analyzed structurally in various ways, e.g. by structural restoration.

1.2.4 Experimental data

Physical modeling of folding and faulting have been performed since the earliest days of structural geology, and since the middle part of the 20th century such modeling has been carried out in a more systematic way. Buckle folding, shear folding, reverse, normal and strike-slip faulting, fault populations, fault reactivation, porphyroclast rotation, diapirism and boudinage are only some of the processes and structures that have been modeled in the laboratory. The traditional way of modeling geologic structures is by filling a box with clay, sand, plaster, silicone putty, honey and other media and applying extension (Figure 1.7), contraction, simple shear deformation, extension followed by contraction or some other deformation history. A ring shear apparatus is used when large amounts of shear are required. In this set-up, the outer part of the disk-shaped volume is rotated relative to the inner part. Many models can be filmed and photographed during the deformation history or scanned using computer tomography. Another tool is the centrifuge, where material is deformed under the

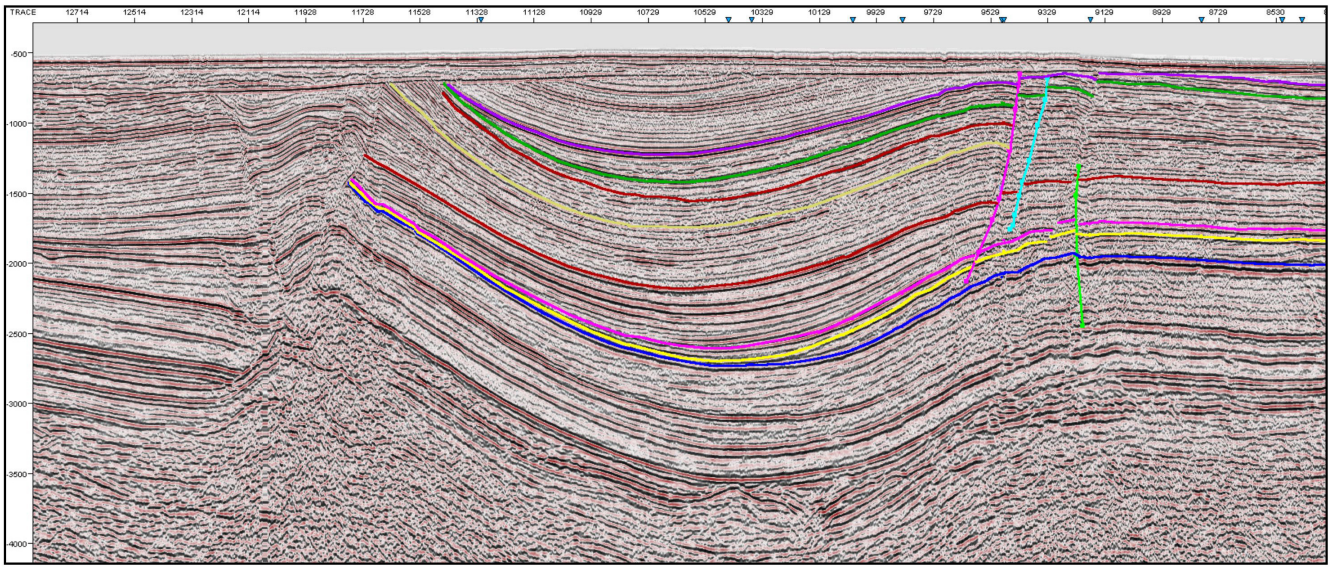

Figure 1.6 Seismic 2D line from the Barents Sea. Folded and faulted sedimentary strata above Permian salt (lower part of the section). Note that the vertical scale is in seconds while the horizontal scale indicates shotpoints (distance). Faults are identified as discontinuities in the seismic reflection pattern. Note the angular unconformity around 700 ms.

influence of the centrifugal force. Here the centrifugal force plays the same role in the models as the force of gravity does in geological processes.

Ideally we wish to use a scale model, where not only the size of the natural object or structure that it refers to is shrunk, but where also the physical properties (grain size, cohesion, ductility etc.) are scaled down. In practice, it is impossible to scale down every aspect or property of a deformed part of the Earth's crust. Sand has grains that, when scaled up to natural size, may be large as huge boulders, preventing the replication of small-scale structures. The grain size of clay may be more appropriate, but one may find that clay gets too cohesive. Moreover, plaster has properties that change during the course of the experiment and thus difficult to describe accurately in terms of rheology. Obviously, physical models have their limitations, but observation of progressive deformation under known boundary conditions still provide important information that can help understand natural structures.

Experimental deformation of rocks and soils in a deformation rig under the influence of an applied pressure (stress) is used to explore how materials react to various stress fields and strain rates. The samples may be a few tens of cm3 in size (Figure 1.8), and are exposed to uniaxial compression or tension (uniaxial means that a force is applied in only one direction) with a fluid-controlled confining pressure that relates to the crustal depth of interest. Triaxial tests are also performed, and the resulting deformation may be both plastic and brittle. For plastic deformation we run into the challenge of strain rate. Natural plastic strains accumulate over thousands or millions of years. We have to apply higher temperatures to our laboratory experiments to produce plastic structures at laboratory strain rates. We are thus back to the challenge of scaling, this time in terms of temperature, time and strain rate.

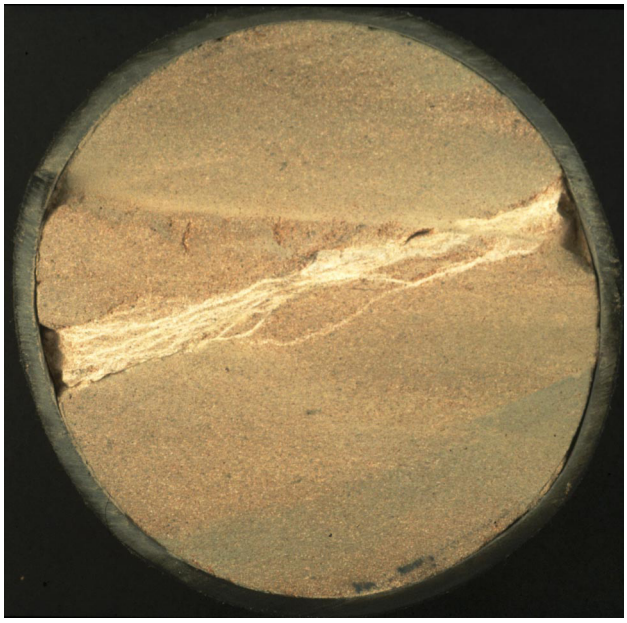

Figure 1.8 Section through a sandstone sample deformed in a tri-axial deformation rig. The light bands are called deformation bands (see Chapter 7), the sandstone is the Scottish Locharbrigg Sandstone and the diameter of the cylindrical sample is 10 cm. You can read about these experiments in Mair et al. (2000). Photo: Karen Mair.

1.2.5 Numerical modeling

Numerical modeling of geologic processes has become increasingly simple with the development of increasingly fast computers. Simple modeling can be performed using mathematical tools such as spreadsheets or Matlab™ . Other modeling requires more sophisticated and expensive software, often building on finite element and finite difference methods. The models may range from microscale, for instance dealing with mineral grain deformation, to the deformation of the entire lithosphere and anything in between. One can model stress fields during faulting and fault interaction, fracture formation in rocks, fold formation in various

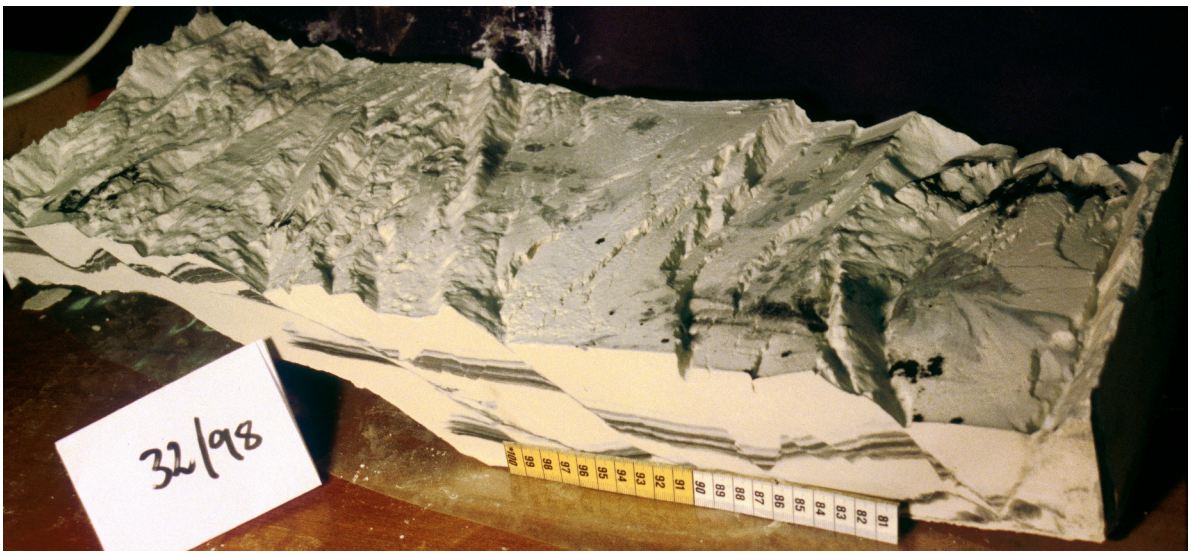

Figure 1.7 Plaster model of extensional faulting. The right-hand side has been pulled to the right before the plaster was completely solidified.

settings and conditions, microscale diffusion processes during plastic deformation among many others. However, nature is complex, and when the degree of complexity is increased, even the fastest supercomputer at some point reaches its physical limitations. Neither can every aspect of natural deformation be described by today's numerical theory. Hence, we have to consider our simplifications very carefully and use field and experimental data both during the planning of the modeling and during the evaluation of the results. Therefore there is a need for geologists who can combine field experience with a certain insight into numerical methodology including all of its advantages and limitations.

1.2.6 Other data sources

There is a long list of other data sources that can be of use in structural analysis. Gravimetric and magnetic data can be used to map large-scale faults and fault patterns in sedimentary basins. Magnetic anisotropy as measured from oriented hand samples can be related to finite strain. Thin section studies and electron microscope images reveal structural information on the microscale. Earthquake data and focal mechanism solutions give valuable information about intraplate stresses and neotectonism and may be linked with in situ stress measurements by means of strain gauges, borehole breakouts, hydraulic fracturing, overcoring etc. Radiometric data can be used to date tectonic events. Sedimentological data and results of basin analysis are closely related to fault activity in sedimentary basins (Figure 1.1). Dike intrusions are related to the stress field and pre-existing weaknesses, and geomorphologic features can reveal important structures in the underground. The list can be made longer, illustrating how the different geological disciplines rely on each other and should be used in concert to solve geological problems.

1.3 Organizing the data

Once collected, geologic data need to be analyzed. Structural field data represent a special source of data because they directly relate to the product of natural deformation in all its purity and complexity. Because of the vastness of information contained in a field area, or even a single outcrop, the field geologist is faced with the challenge of sorting out the information that is relevant to the problem in question. Collecting too much data slows down both collection and analyses of the data. At the same time an incomplete data set stops the geologist from reaching sound and statistically significant conclusions. Collecting the wrong type of data is of course not very useful, and the quality of the

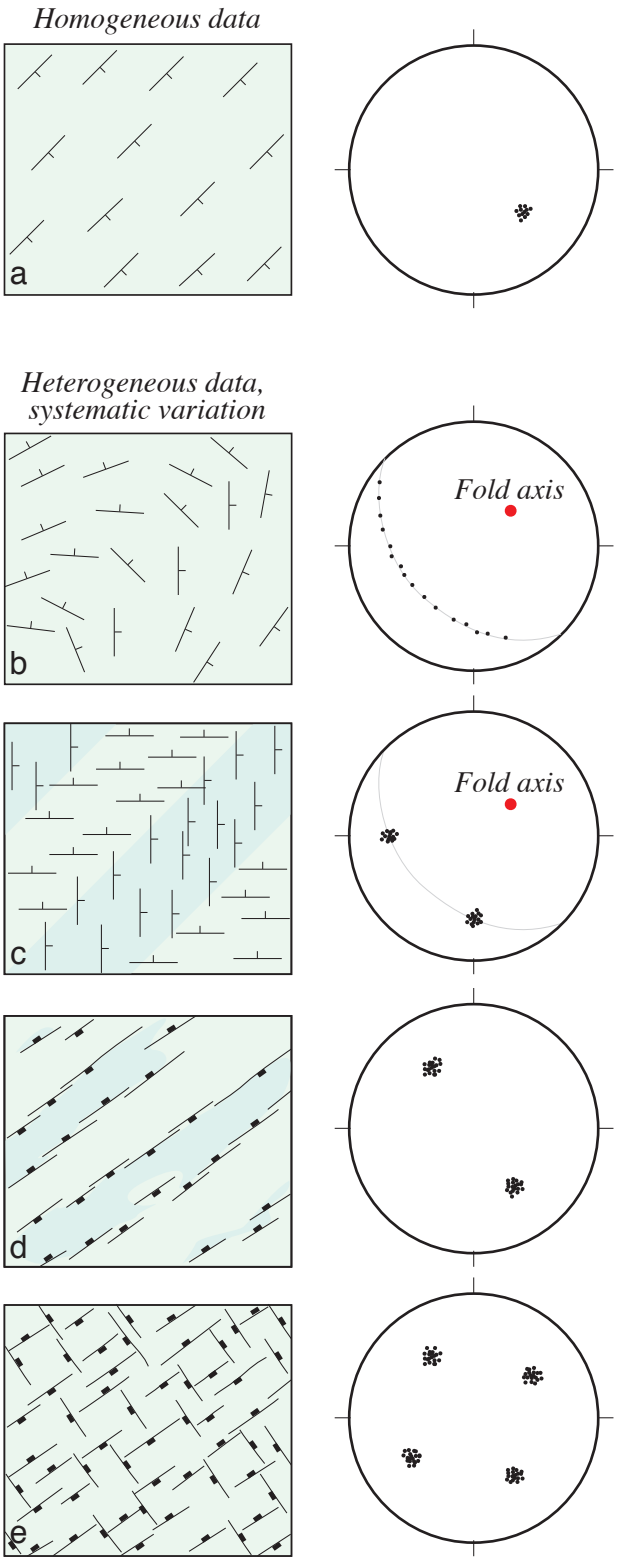

Figure 1.9 Synthetic structural data sets showing different degree of homogeneity. a) Synthetic homogeneous set of strike and dip measurements. b) Systematic variation in layer orientation measurements. c) Homogeneous subareas due to kink- or chevron folding. d-e) Systematic fracture systems. Note how the systematics are reflected in the strereonets.

data must be acceptable for further use. The quality of the analysis is limited by the quality of the data upon which it is based. It is therefore essential that the objective is clearly in mind before data collection starts. The same is the case for other data types, such as those gathered by seismic methods or remote sensing.

Once collected, data must be grouped and sorted in a reasonable way for further analysis. Field data may be subdivided based on orientation or relative age (e.g. cleavages, folds or fractures). The different parts of the data set are then referred to as subpopulations. In other cases field data are subdivided into subsets based on geographical subareas. A structural subarea is a geographic area within which the structural data set is approximately homogeneous or where it shows a systematic change (Figure 1.9 and 1.10). Completely non-systematic or chaotic structural data are very unusual; there is usually some fabric or systematic orientation of minerals or fractures resulting from rock deformation.

As an example, Figure 1.10 shows the overall pattern of lineations in a part of the Caledonian orogenic wedge in Scandinavia. Each lineation arrow represents the average orientation within the area that it covers on the map. The region can be subdivided into subareas in which the lineation pattern shows a relatively homogeneous orientation, as shown in Figure 1.10c. The actual variation within each subarea can be displayed by means of stereographic presentation of individual measurements (Figure 1.11). One could also distinguish between different types of lineation (stretching lineation, intersection lineation, mineral lineation etc.) (not shown).

A second example is taken from the petroleum province of the North Sea (Figure 1.12). It shows how fault populations look different at different scales and must therefore be treated at the scale suitable to serve the purpose of the study. The lower figures shows how the smallest mappable fault population within the Gullfaks Oilfield can be subdivided into subpopulations based on orientation. The maps show the geographical distribution of the fault populations. At this point each subgroup can be individually analyzed with respect to orientation (stereo plots), displacement, sealing properties, or other factors, depending on the purpose of the study.

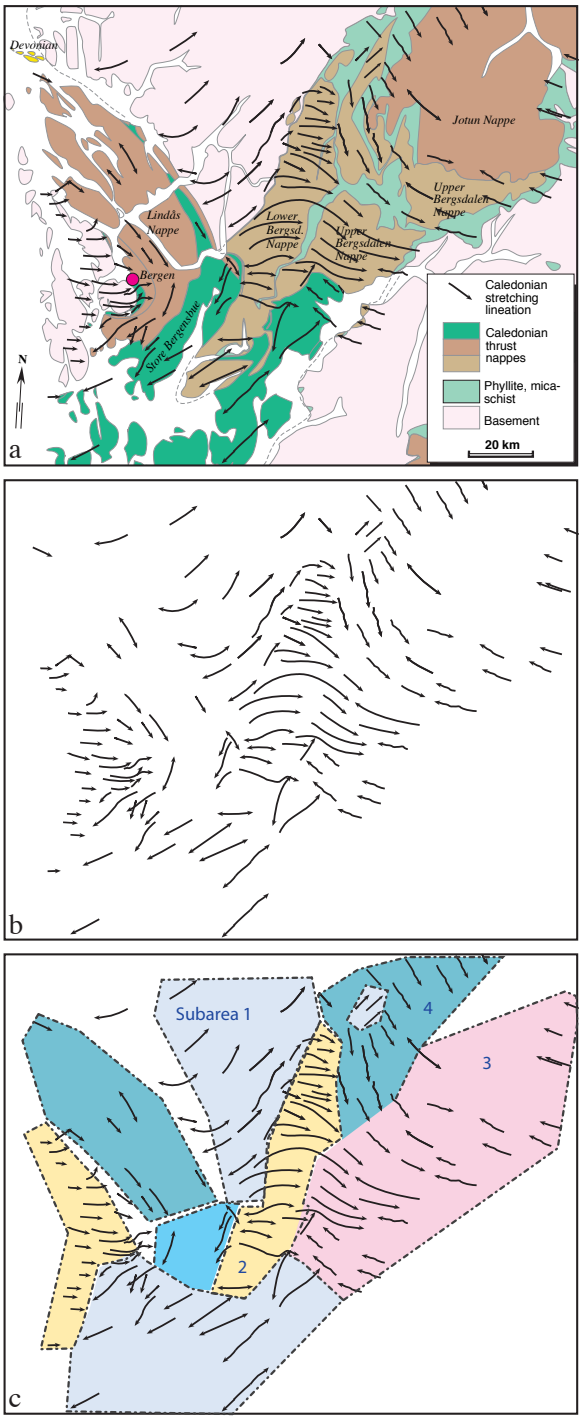

Figure 1.10 a-b) Caledonian lineation pattern in the Scandinavian Caledonides east of Bergen. To analyze this pattern, subareas of approximately uniform orientation are defined (c). From Fossen (1993a).

1.4 Structural analysis

Many structural processes span thousands to millions of years. Most structural data describe the final product of some deformation history, and the history itself can only be revealed through careful analysis of the data. When looking at a fold, it may not be obvious whether it formed by layer parallel shortening, shearing or passive bending. The same thing applies to a fault. What part of the fault formed first? Did it form by linkage of individual segments, or did it grow from a single point outward, and if so, was this point in the central part of the present fault surface? It may not always be easy to answer such questions, but the approach should always be to analyze the field information and compare with experimental and/or numerical models.

1.4.1 Geometric analysis

The analysis of the geometry of structures is referred to as geometric analysis. This includes the shape, geographic orientation, size and geometric relation between the main (first order) structure and related smaller-scale (second order) structures. The last point emphasizes the fact that most structures are composite and appear in association at different scales. Hence, various methods are needed to measure and describe structures and structural associations.

Shape is the spatial description of open or closed surfaces such as folded layer interfaces or fault surfaces. The shape of folded layers may give information about the fold forming process or the mechanical properties of the folded layer (p. ??), while fault curvature may have implications for hanging wall deformation (p. ??) or could give information about the slip direction (p. ??).

Orientation of linear and planar structures are perhaps the most common types of data, and shapes and linear features may be described by mathematical functions, for instance by use of vector functions. In most cases, however, natural surfaces are too irregular to be described accurately by simple vector functions, or it may be impossible to map continuous parts of a surface (e.g. a fault or folded layer) to the extent necessary for mathematical description. Nevertheless, it may be necessary to make geometric interpretations of partly exposed structures. Our data will always be incomplete at some level, and our minds tend to search for geometric models when analyzing geologic information. For example, when the Alps were mapped in great detail early in the 20th century, they were generally considered to be cylindrical (meaning that they were assumed to have straight fold axes). This model made it possible to project folds onto cross-sections, and impressive sections or geometric models were created. At a later stage it became clear that the folds were in fact noncylindrical, with curved hinge lines, requiring modification of earlier models.

In geometric analysis it is very useful to represent orientation data (e.g. Figures 1.9 and 1.11) by means of stereographic projection (see appendix). Stereographic projection is used to show or interpret both the orientation and geometry of a structure. The method is quick and efficient, and the most widely used tool for presenting and interpreting spatial data. In general, geometry may be presented in the form of maps, profiles, stereographic projections, rose diagrams or three-dimensional models based on observations made in the field, from geophysical data and other data sources.

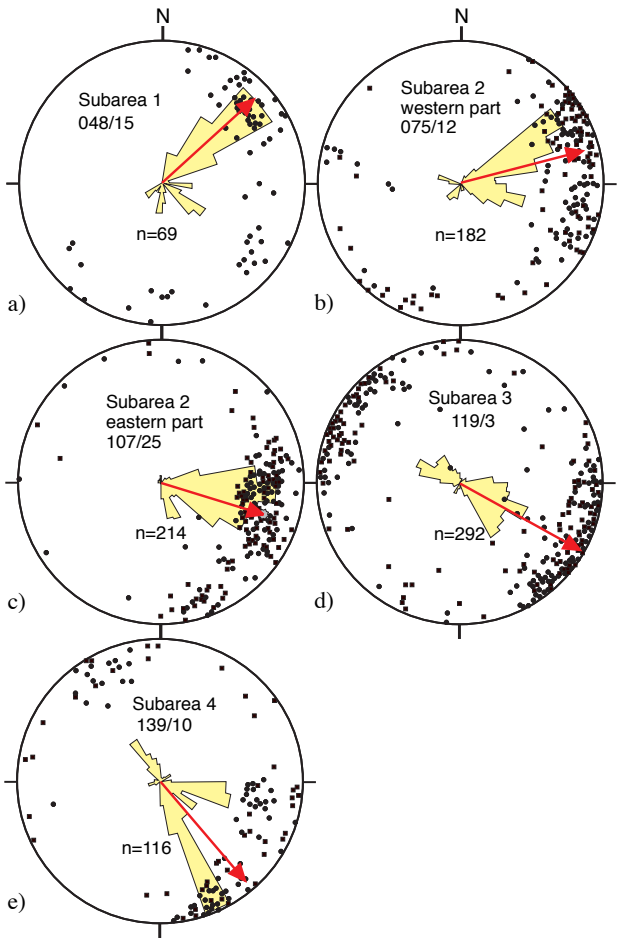

Figur 1.11 Lineation data from the subareas defined in the previous figure. The plots show the variations within each subarea, portrayed by means of poles, rose diagrams and an arrow indicating the average orientation. "n" indicates the number of data within each subarea. From Fossen (1993b).

1.4.2 Strain and kinematic analysis

Geometric description and analysis may form the basis for strain quantification or strain analysis. Such quantification is useful in many contexts, e.g. in the restoration of geologic sections through deformed regions. Strain analysis commonly involves finite strain analysis, which concerns changes in shape from the initial state to the very end result of the deformation. Structural geologists are also concerned with the deformation history, which can be explored by incremental strain analysis. In this case only a portion of the deformation history is considered, and a sequence of increments describe the deformation history.

By definition, strain is only applicable to continuous deformation, i.e. deformation where originally continuous structures such as bedding or dikes remain continuous also after the deformation. Another word for continuous deformation is ductile deformation. Ductile deformation occurs when rocks flow under the influence of stress. The opposite, discontinuous deformation or brittle deformation, occurs when rocks break or fracture. Modern geologists do however not restrict the use of strain to ductile deformation. In cases where fractures occur in a high number and on a scale that is significantly smaller than the discontinuity each

term brittle strain is used. It is a simplification, but it is useful in many cases. Strain analysis is thus also applied to brittle structures such as fault populations.

Geometric description also forms the foundation of kinematic analysis that concerns how rock masses have moved during deformation (the Greek word kinesis means movement). Striations on fault surfaces (Figure 1.13) and lineations in shear zones are among the structures that are useful in kinematic analysis.

To illustrate the connection between kinematic analysis and geometrical analysis, consider the folds depicted in Figure 1.14. The difference in geometry (shape) of the two folded layers can be used to distinguish between the kinematics involved during their formation, one by compression, the other by shear. In other words, a kinematic analysis can be performed based on geometric analysis. It also depends on physical boundary conditions such as rigid walls or a free surface from which rocks and sediments are free to extrude.

1.4.3 Dynamic analysis

Both strain (change in shape) and kinematics are a result of the accumulation and release of stress. The interplay between stress and kinematics is called dynamics. Dynamic analysis thus explores the connection between stress and the structures or strains that can be observed in the crust. Returning to the folds shown in Figure 1.14, it may be found that the forces or stress axes were differently oriented relative to the layering in the two cases. The upper, parallel fold may have been formed by the application of layer parallel compression, whereas the similar fold may be the result of significant shear stress acting parallel to the layer. Based on the geometric analysis and the kinematic

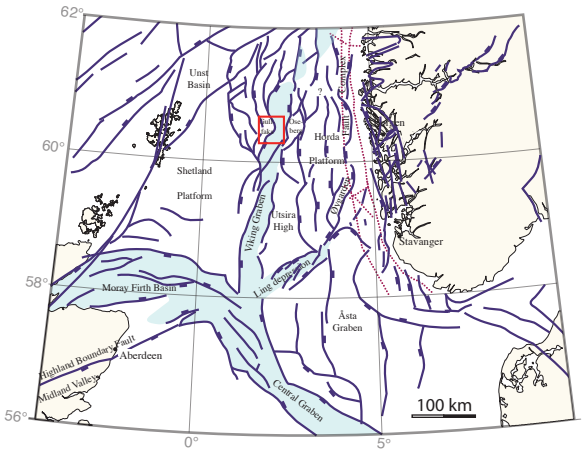

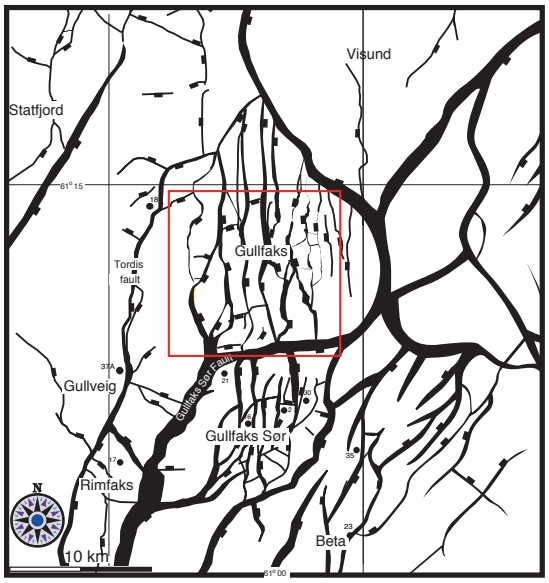

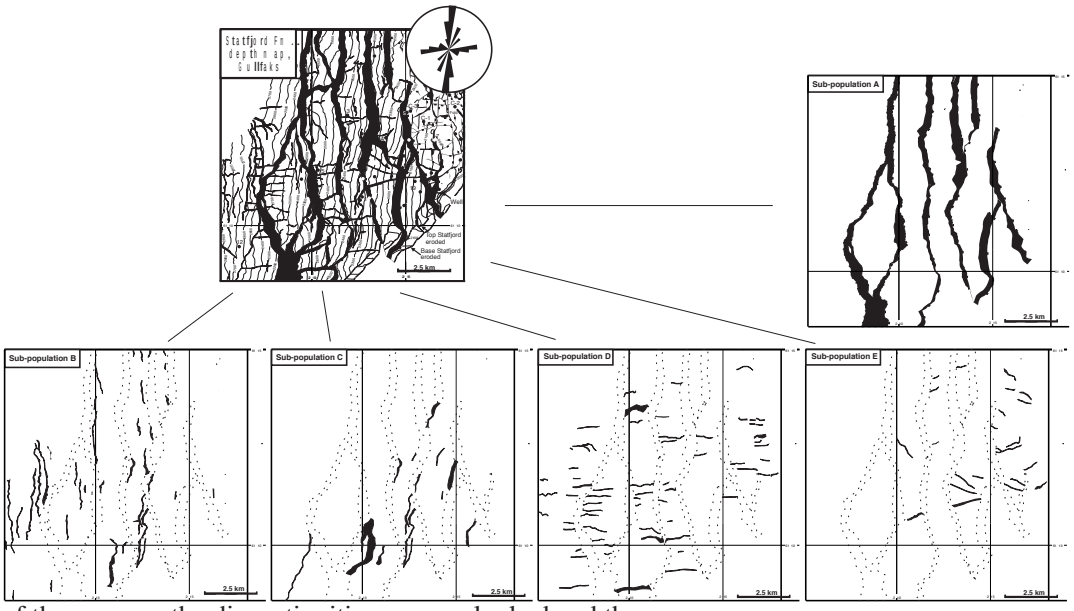

of them cause, the discontinuities are overlooked and the

Figure 1.12 This set of figures from the North Sea illustrates how fault patterns may change from one scale to another. Note the contrast between the N-S faults dominating the Gullfaks area and the different orientations of small (<100 m displacement) faults in lower panels. They should be separated as shown for further orientation or displacement analysis. See Fossen & Rørnes (1997) for more details.

model, we can therefore present a simple dynamic model for each of the folds.

Applying stress to syrup gives a different result than stressing a cold chocolate bar. The syrup will flow, while the chocolate bar will break. Both are dynamic analyses, but the part of dynamics related to the flow of rocks is referred to as rheological analysis. Similarly, the study of how rocks (or sugar) break or fracture is the field of mechanical analysis. In general, rocks flow when they get warm enough, which means when they get buried deep enough. □Deep enough□ means little more than surface temperatures for salt, around 300 °C for a quartz-rich rock, perhaps closer to 550 °C for a feldspathic rock and even more for olivine-rich rocks. Pressure also plays an important role, as does water content and strain rate. It is important to realize that different rocks behave differently under any given condition, but also that the same rock reacts differently to stress under different physical conditions. Rheological testing is done in the laboratory in order to understand how different rocks flow in the lithosphere.

1.4.4 Tectonic analysis

Tectonic analysis involves dynamic analysis of the geometry of structure (geometric analysis) and their kinematic development (kinematic analysis) at the scale of a basin or orogenic belt. This kind of analysis therefore involves elements of sedimentology, paleontology, and petrology among other subdisciplines of geology and related sciences in addition to structural geology. Structural geologists involved in tectonic analysis are sometimes referred to as tectonicists. On the opposite end of the scale range, some structural geologists analyze the structures and textures that can only be studied through the microscope. This is the study of how deformation occurs between and within individual mineral grains and is referred to as microstructural analysis or microtectonics by some. Both the optical microscope and Scanning Electron Microscope (SEM) (Figure 1.15)are useful tools in microstructural analysis.

Figure 1.13 Abrasive marks (slickenlines) on fault slip surfaces give local kinematic information. Seismically active fault in the Gulf of Corinth .

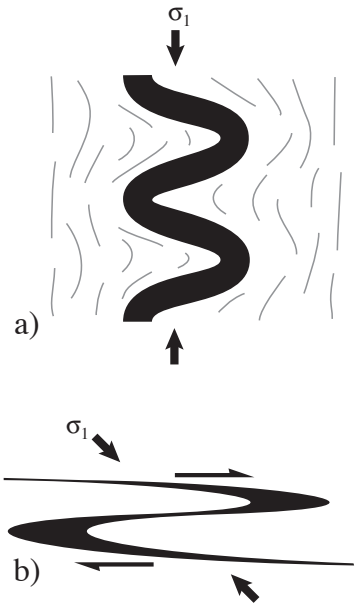

Figure 1.14 Parallel fold (a) and similar fold (b). These two types of folds can be distinguished by geometry, as discussed in the chapter on folding (class 1B and 2). They form in different ways, so that the geometric analysis (of thickness variations etc.) results in a kinematic model. Arrows indicate the approximate orientation of forces during folding.

1.5 Concluding comment

Structural geology has changed from being a descriptive discipline to one where analytical methods and physical and numerical modeling are increasingly important. Many new data types and methods have been added to structural geology over the last few decades, and more new methods will surely see their application in this field in the years to come. Nevertheless, it is hard to overemphasize the importance of field studies even

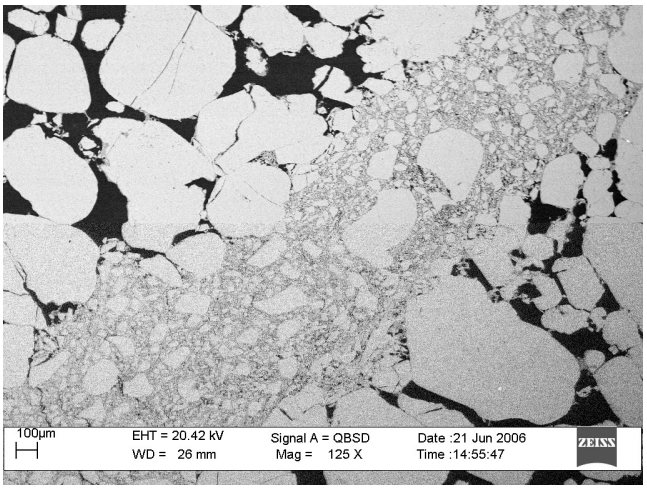

Figur 1.15 Scanning Electron Microphotograph of a mm-thin zone of grain deformation (deformation band) in the Nubian Sandstone in Sinai. Photo: Anita Torabi.

where the most sophisticated numerical algorithms are being used or where the best 3D-seismic dataset is available. The connection between field observations and modeling must be tight. It is the crust of the Earth and the processes acting in it that we seek to understand. It is the rocks themselves that contain the information that can reveal their structural or tectonic history. Models and analyses are useful tools to help us create models that we can relate to and to understand what is a likely and what is an unlikely or impossible interpretation. However, they must always comply with the information retrievable from the rocks.

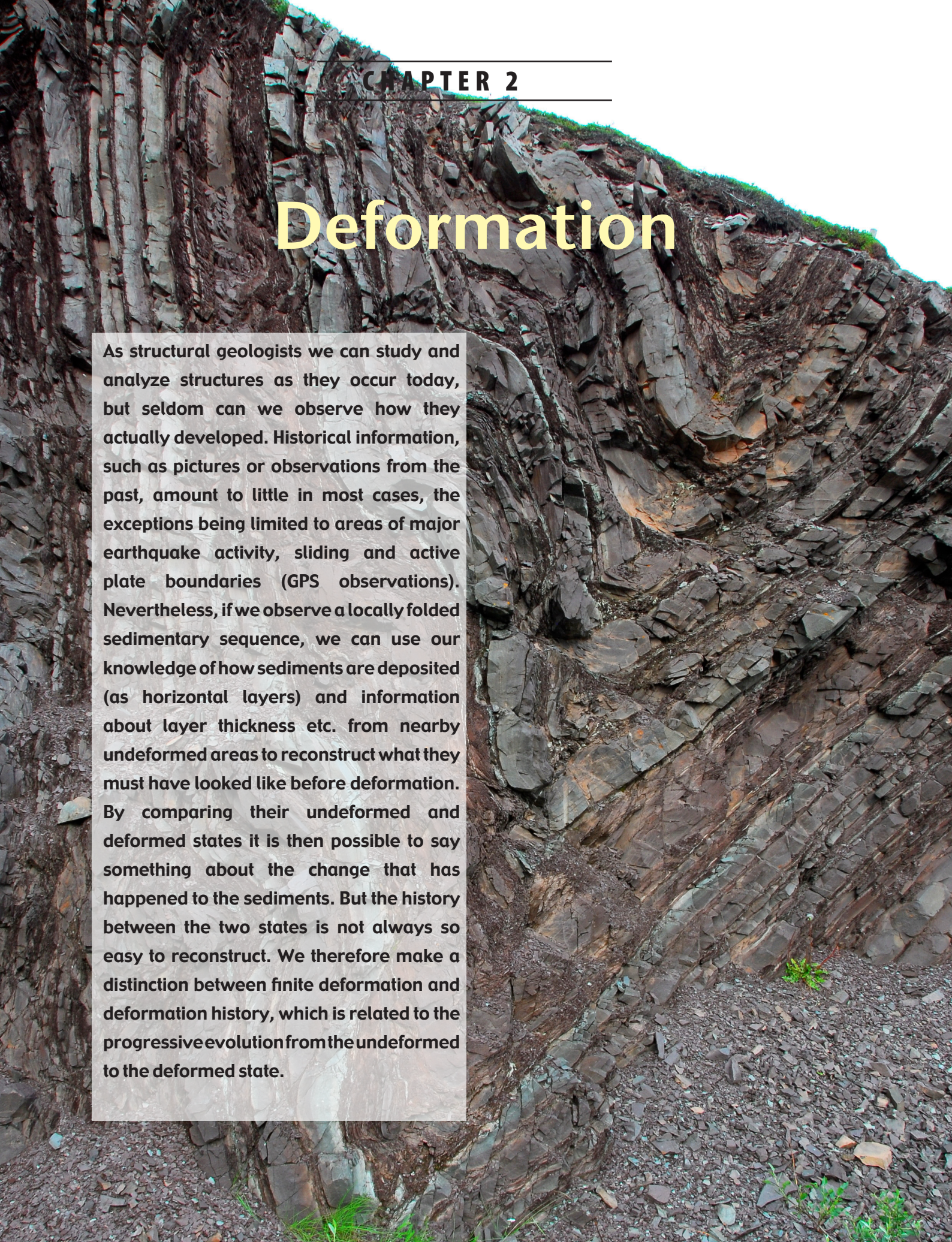

CHAPTER 2

Deformation

As structural geologists we can study and analyze structures as they occur today, but seldom can we observe how they actually developed. Historical information, such as pictures or observations from the past, amount to little in most cases, the exceptions being limited to areas of major earthquake activity, sliding and active plate boundaries (GPS observations). Nevertheless, if we observe a locally folded sedimentary sequence, we can use our knowledge of how sediments are deposited (as horizontal layers) and information about layer thickness etc. from nearby undeformed areas to reconstruct what they must have looked like before deformation. By comparing their undeformed and deformed states it is then possible to say something about the change that has happened to the sediments. But the history between the two states is not always so easy to reconstruct. We therefore make a distinction between finite deformation and deformation history, which is related to the progressive evolution from the undeformed to the deformed state.

1.1 What is deformation?

The term *deformation* is used in different ways by different people and under different circumstances. In a strict sense, deformation is defined as the difference between the position of particles in the object under consideration prior to and after the deformation has occurred. Less formally, and particularly in the field, it is commonly used about the change in shape (strain) that is expressed in a rock or geologic section. Since a change in shape involves relocation of rock particles (minerals, sand grains etc.), it is in keeping with the formal definition, but deformation may also include translation and rotation without any change in shape (see below). Still, it is only the change in shape that is directly visible in most deformed rocks, and why, for practical purposes, deformation is so closely associated with strain. Informally the term deformation is also used to describe the process or history that is involved (e.g. during a laboratory experiment). However, when specifically referring to the progressive changes that take place during deformation, terms such as *deformation history* or *progressive deformation* should be used.

Deformation is the difference between the position, shape and orientation of an object before and after the deformation has occurred.

It is useful to think of a rock in terms of a continuum of particles or a regular mesh attached to the rock during the deformation history. Since deformation relates the positions of particles before and after the deformation history, the positions of points before and after deformation can be connected with vectors. These vectors are called *displacement vectors*, and a field of such vectors is referred to as the *displacement field* (Figure 2.1). Displacement vectors do not tell us how the particles moved during the deformation history – they merely describe the difference between the undeformed and deformed state. The actual path that each particle follows during the deformation history is referred to as a particle path (Figure 2.1).

1.2 Components of deformation

The displacement field can be decomposed into various components, depending on the purpose of the decomposition. The classical way of decomposing it is by separating pure translation and rigid rotation from change in shape and volume (Figure 2.2).

1.2.1 Translation

Translation moves every particle in the rock in the same direction and the same distance, and its displacement field consists of parallel vectors of equal length. This component may be considerable, for instance where thrust nappes (detached slices of rocks) have been transported several tens or hundreds of kilometers. The Jotun Nappe (Figure 2.3) is an example from the Scandinavian Caledonides. In this case most of the deformation is rigid translation. We do not know the exact orientation of the nappe prior to the onset of deformation, so we cannot estimate the rigid rotation (see below), but field observations reveals that the change in shape, or strain, is largely restricted to the lower parts. The total deformation thus consists of a huge translation component, an unknown but possibly small rigid rotation component and a variable strain component.

On a smaller scale rock components (mineral grains, layers or fault blocks) may be translated along slip planes or planar faults without any internal change in shape. One model where there is only translation and rigid rotation is the classical domino fault model, which we will look at in the last chapter of this book.

1.2.2 Rotation

Rotation is here taken to mean rigid rotation of the entire deformed rock volume that is being studied. It should not be confused with the rotation of the (imaginary) axes of the strain ellipse during progressive deformation, which is called internal rotation. Rigid rotation involves a physical rotation of a rock volume (such as a shear zone) relative to an external coordinate system.

Large-scale rotations of a major thrust nappe or entire tectonic plates typically occur about the vertical axis. Fault blocks in extensional settings on the other hand may rotate around horizontal axes, and small-scale rotations may occur about any axis.

1.2.3 Strain

Any change in the shape of the deformed rock volume is referred to as *strain*. A rock volume can be transported (translated) and rotated rigidly in any way and sequence, but we will never be able to tell just from looking at the rock itself. All we can see in the field or in samples is strain and perhaps the way that strain has accumulated. Consider your lunch bag. You can bring it to school or work, which involves a lot of rotation and translation, but you cannot see the deformation directly unless it has been squeezed on the way. Then you can tell by compar-

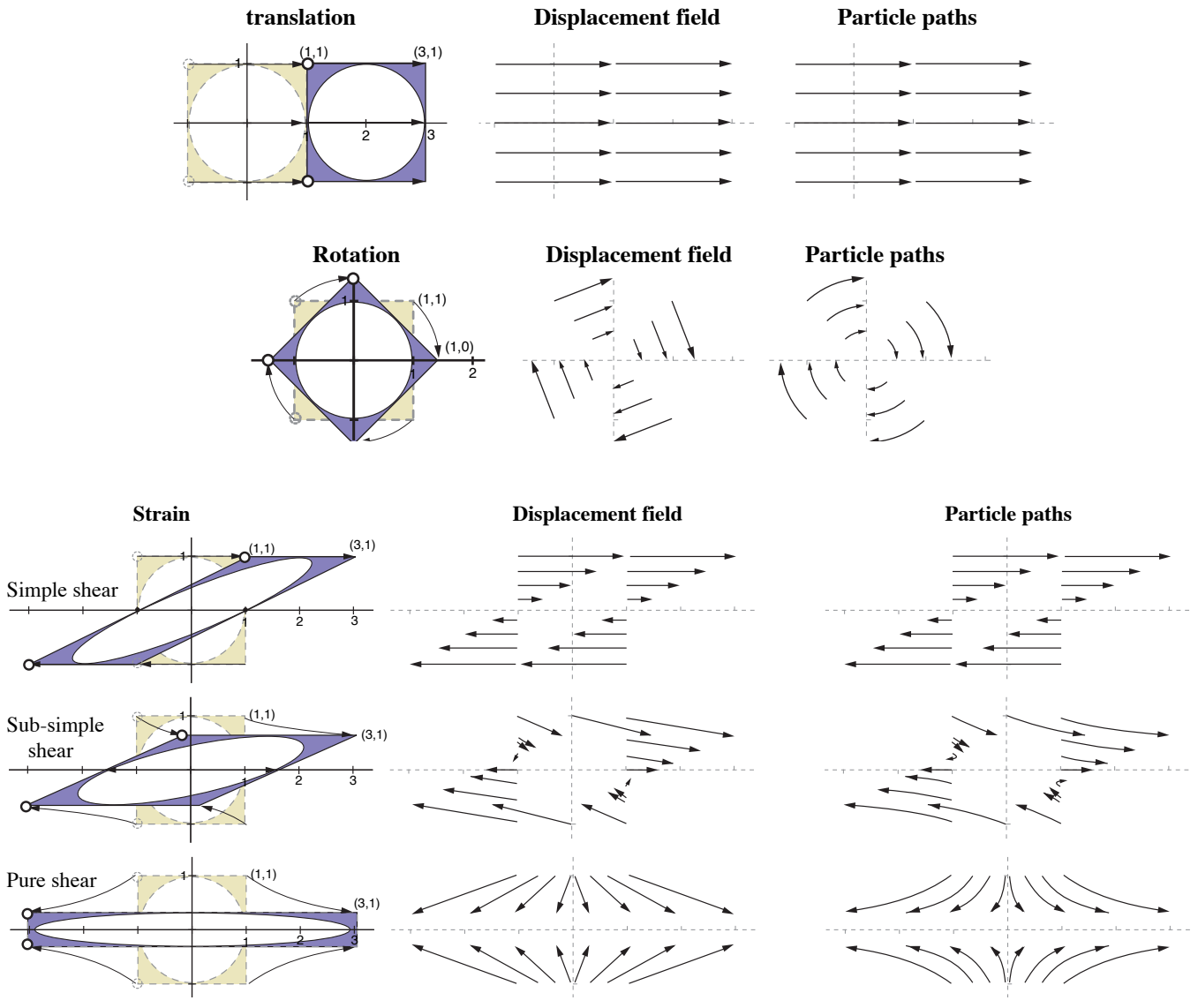

Figure 2.1 Displacement field and particle paths for rigid translation and rotation, and strain resulting from simple, shear, sub-simple shear and pure shear (explained later in this chapter). Particle paths trace the actual motion of individual particles in the deforming rock, while displacement vectors simply connect the initial and final positions. Hence, displacement vectors can be constructed from particle paths, but not the other way around.

ing it with what it looked like before you left home. If someone else prepared your lunch bag and put it in your bag, you would use your knowledge of how a lunch bag should be shaped.

The last point is very relevant, because with very few exceptions, we have not seen the deformed rock in its undeformed state. We then have to use our knowledge of what such rocks typically look like when unstrained. For example, if we find ooliths or reduction spots in the rock, we would expect them to have been spherical (circular in cross-section) in the undeformed state.

1.2.4 Volume change

Even if the shape of a rock volume has not changed, it may have shrunk or expanded. We therefore have to add volume change (area change in two dimensions) for a complete description of deformation. Volume change is commonly considered to be a special type of strain, called *volumetric strain*. However, it is useful to keep this type of deformation separate if possible. Clearly, it may be possible to determine a change in shape without being able to estimate the volume change and vice versa.

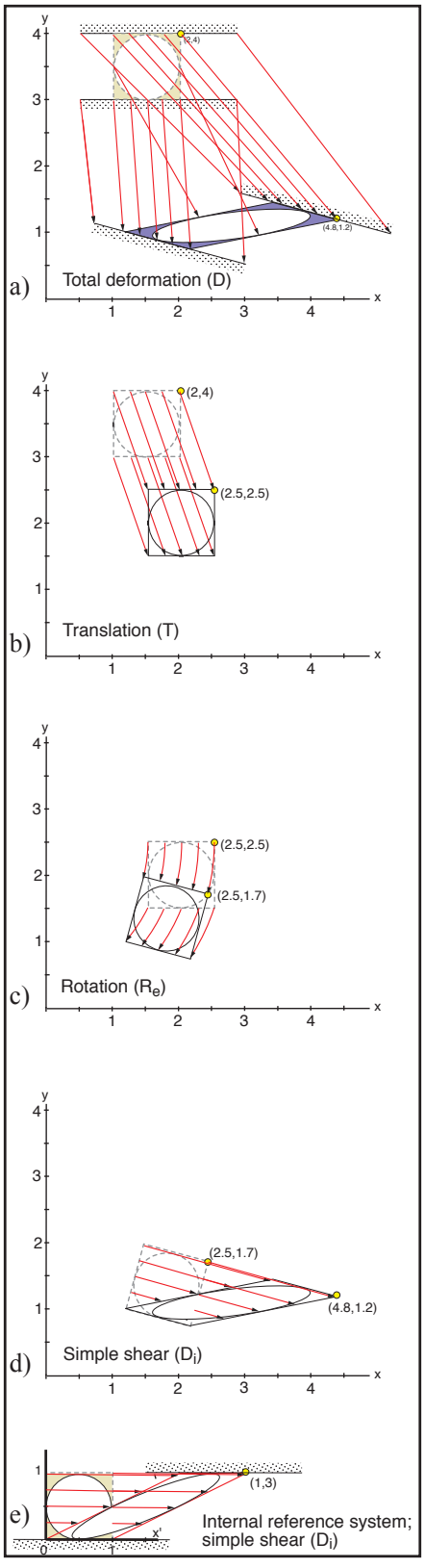

Figure 2.2 a) The total deformation of an object (square with an internal circle). Arrows are displacement vectors connecting initial and final particle positions. b-c) translation and rotation components of the deformation shown in a). d) the strain component. e) The coordinate system has been attached to the lower left corner of the square. This eliminates the translation and rotation (b-c) and makes it easier to reveal the strain component, which is here produced by a simple shear.

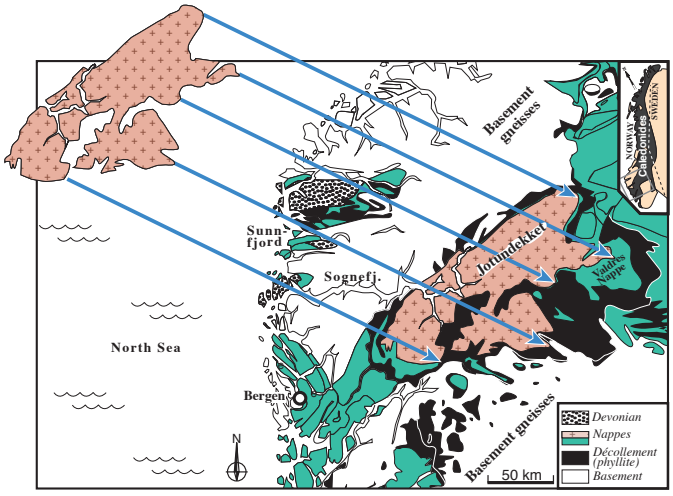

Figure 2.3 The Jotun Nappe in the Scandinavian Caledonides seems to have been transported more than 300 km to the southeast, based on restoration and the orientation of lineations see Chapter ?). The displacement vectors are indicated, but the amount of rigid rotation around the vertical axis is unknown. The amount of strain is generally concentrated to the base.

1.3 System of reference

For studies of deformation, a reference or coordinate system must be chosen. Standing on a dock watching a big ship entering or departing can give the impression that the dock, not the ship, is moving. Unconsciously, the reference system gets fixed to the ship, and the rest of the world moves by translation relative to the ship. While this is fascinating, it is not a very useful choice of reference. Rock deformation must also be considered in the frame of some reference coordinate system, and it must be chosen with care to keep the level of complexity down.

It is often useful to orient the coordinate system along important geologic structures. This could be the base of a thrust nappe, plate boundaries or local deformation zones (shear zones, see Chapter 15). In many cases we want to eliminate translation and rigid rotation. In the case of shear zones we normally place two axes parallel to the shear zone with the third being perpendicular to the zone. If we are interested in the deformation in the shear zone as a whole, the origin could be fixed to a particle at the margin of the zone. If we are interested in what is going on around any given particle in the zone, then we can "glue" the origin to a particle within the zone (still parallel/perpendicular to the shear zone boundaries). In both cases translation and rigid rotation of the shear zone are eliminated, because the coordinate system rotates and translates along with the shear zone. There is nothing wrong with a coordinate system that is oblique to the shear zone boundaries, but

visually and mathematically it is more complicated.

1.4 Deformation – detached from history

Deformation is the difference between the deformed and undeformed states. It tells nothing about what actually happened during the deformation history.

A given strain may have accumulated in an infinite number of ways

Imagine an unusually tired student who falls asleep in his boat while fishing. He knows where he was when he fell asleep, and he soon figures out where he is when he wakes up, but he does not know the exact path that currents and winds have taken him. He only knows the position of his boat before and after the nap, and he can check the strain or shape of his boat (hopefully zero). He can map the deformation, but not the deformation history.

Let us also consider "particle flow": Students walking from one lecture hall to another may follow infinitely many paths (the different paths may take longer or shorter time, but deformation does not involve time). All the lecturer knows, busy as he is between classes, is that the students have moved from one lecture hall to the other. Their history is unknown to him (although he may have some theories based on new cups of coffee etc.). In a similar way, rock particles may move along a variety of paths from the undeformed to the deformed state. One difference between rock particles and individual students is of course that students are free to move on an individual basis, while rock particles, such as mineral grains in a rock, are "glued" to one another in a solid continuum and cannot operate freely on an individual basis.

1.5 Homogeneous and heterogeneous deformation

Where the deformation applied to a rock volume is identical throughout that volume, the deformation is *homogeneous*. Rigid rotation and translation by definition are homogenous, so it is always strain and/or volume or area change that can be heterogeneous. Thus *homogeneous deformation* and *homogeneous strain* are identical expressions.

For homogeneous deformation, originally straight and parallel lines will be straight and parallel also after the deformation (Figure 2.4). Further,

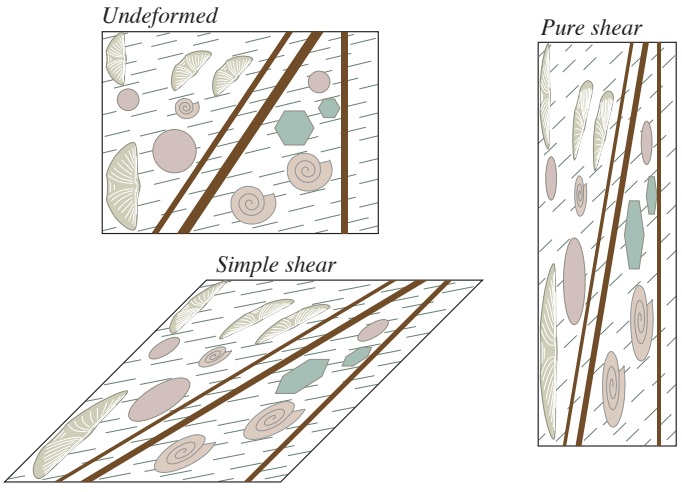

Figure 2.4 Homogeneous deformations of a rock with objects such as brachiopods, reduction spots, ammonites and dikes. Two different deformations are shown (pure and simple shear). Note that the brachiopods that are differently oriented before deformation obtain different shapes.

the strain and volume/area change will be constant throughout the volume of rock under consideration. If not, then the deformation is *heterogeneous* (inhomogeneous). This means that two objects with identical initial shape and orientation will end up having identical shape and orientation after the deformation. Note however that the initial shape and orientation in general will differ from the final shape and orientation. If two objects have identical shapes but different orientations before deformation, then they will generally have different shapes after deformation even if the deformation is homogeneous. An example is the deformed brachiopods in Figure 2.4. The difference reflects the strain imposed on the rock.

Homogeneous deformation: Straight lines remain straight, parallel lines remain parallel, and identically shaped and oriented objects will also be identically shaped and oriented after the deformation.

A circle will be converted into an ellipse during homogeneous deformation, where the ellipticity (ratio between the long and short axes of the ellipse) will depend on the type and intensity of the deformation. Mathematically, this is identical to saying that homogeneous deformation is a linear transformation. Homogeneous deformation can therefore be described by a set of first order equations (three in three dimensions) or, simpler, by a transformation matrix referred to as the deformation matrix.

Before looking at the deformation matrix, it must be emphasized that:

A deformation that is homogeneous on one scale may be considered heterogeneous on another (Figure 2.5).

A classical example is the increase in strain typically seen from the margin toward the center of a shear zone. The strain is heterogeneous on this scale, but can be subdivided into thinner elements or zones in which strain is approximately homogeneous. Another example is shown in Figure 2.6, where a rock volume is penetrated by faults. On a large scale, the deformation may be considered homogeneous because the discontinuities represented by the faults are relatively small. On a smaller scale, however, those discontinuities become more apparent, and the deformation must be considered heterogeneous.

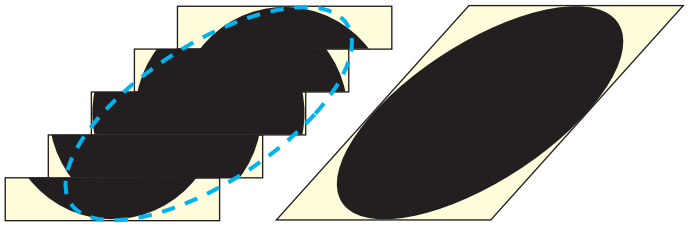

Figure 2.6 Discrete or discontinuous deformation can be approximated as continuous and even homogeneous in some cases. In this sense the concept of strain can also be applied to brittle deformation (*brittle strain*). The success of doing so depends on the scale of observation.

1.6 Mathematical description of deformation

Deformation is conveniently and accurately described and modeled by means of elementary linear algebra. Let us use a local coordinate system, such as one attached to a shear zone, to look at some fundamental deformation types. We will think in terms of particle positions (or vectors if you like) and see how particles change positions during deformation. If (x, y) is the original position of a particle, then the new position will be denoted (x´, y´). For homogeneous deformation in two dimensions (i.e. in a section) we have that

$$x' = D_{11}x + D_{12}y$$

$$y' = D_{21}x + D_{22}y \quad (2.1)$$

These equations can be written in terms of matrices and vectors as:

$$\begin{bmatrix} x' \\ y' \end{bmatrix} = \begin{bmatrix} D_{11} & D_{12} \\ D_{21} & D_{22} \end{bmatrix} \begin{bmatrix} x \\ y \end{bmatrix} \quad (2.2)$$

which can be written

$$\mathbf{x'} = \mathbf{Dx}. \quad (2.3)$$

The matrix **D** is called the deformation matrix and the equation describes a linear transformation, which means that it describes a homogeneous deformation.

There is a corresponding or inverse matrix $\mathbf{D}^{-1}$ (where $\mathbf{DD}^{-1}=\mathbf{I}$ and **I** is the identity matrix). $\mathbf{D}^{-1}$ represents the *reciprocal* or *inverse deformation*, and

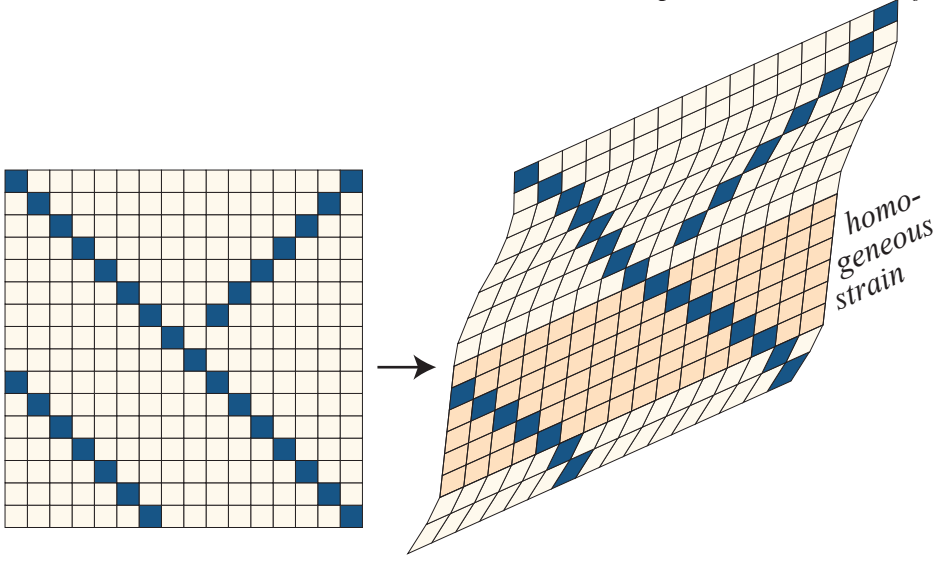

Figure 2.5 A regular grid in undeformed and deformed state. The overall strain is heterogeneous, so that some of the straight lines have become curved. However, in a restricted portion of the grid, the strain is homogeneous. In this case the strain is also homogeneous at the scale of a grid cell.

reverses the deformation imposed by **D**:

$$\mathbf{x}=\mathbf{D}^{-1}\mathbf{x}'. \qquad (2.4)$$

The reciprocal or inverse deformation takes the deformed rock back to its undeformed state

The deformation matrix **D** (also called position gradient tensor) is very useful if one wants to model deformation using a computer. Once the deformation matrix is defined any aspect of the deformation itself can be found. Once again, it tells nothing about the deformation history, nor does it tell how the deforming medium responds to the imposed deformation.

1.7 One-dimensional strain

In one dimension (a single direction), strain is about stretching and shortening (which is simply negative stretching) of lines or approximately linear (straight) objects. One might say that one-dimensional strain makes no sense, since strain is a change in shape and shape is in most people's mind at least two-dimensional. In this sense, a straight line that is extended does not change shape, just length. On the other hand, a change in shape, such as a circle changing into an ellipse can be described by the change in length of lines of different orientations. It is therefore convenient to include change of line lengths in the concept of strain. There are however special terms in use, such as elongation, extension, stretching, contraction, shortening, and, as any other strain quantity, they are dimensionless.

Elongation (e or ε) of a line is defined as $e=(l-l_0)/l_0$, where l_0 and l are the lengths of the line before and after deformation, respectively (Figure 2.7). The line may represent a horizontal line or bedding trace in a cross-section, the long axis of a belemnite or some other fossil on which a line can be defined, the vertical direction in a rock mechanics experiment

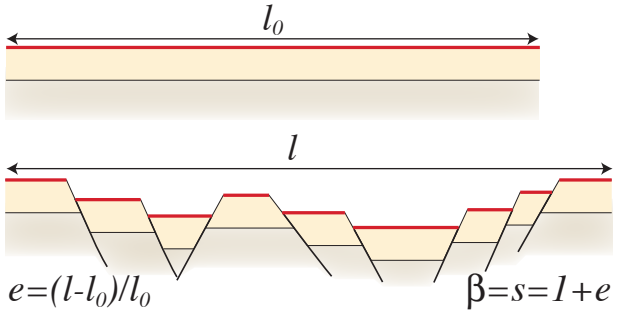

Figure 2.7 Extension of layers by faulting. The red layer has an original (l_0) and a new length, and the extension *e* is found by comparing the two. The beta-factor (β) is commonly used when considering extension across extensional basins.

THE SECTIONAL STRAIN ELLIPSE

X, Y and Z are the three principal strains or strain axes in three dimensional strain analysis. However, when considering a section, X and Y are commonly used regardless of the orientation of the section relative to the strain ellipsoid. It would be better to name them X' and Y' or something similar, and reserve the designations X, Y and Z for the true principal strains in three dimensions. An arbitrary section through a deformed rock contains a strain ellipse that is called the *sectional strain ellipse*. It is important to specify which section we are describing at any time.

and many other things. The logarithmic or natural elongation $\bar{e}=\ln(e)$ is also in use.

Extension of a line is identical to elongation (e) and is used in the analysis of extensional basins where the elongation of a horizontal line in the extension direction indicates the extension. Negative extension is called c*ontraction* (the related terms compression and tension area reserved for stress).

Stretching of a line is designated $s=1+e$, where s is called the stretch. Hence, $s=l/l_0$. *Stretching factors* are commonly referred to in structural analysis of rifts and extensional basins. These are sometimes called β-factors, but are identical to s.

Quadratic elongation[1], $\lambda=s^2$, is identical to the eigenvalues of the deformation matrix **D**.

Natural strain, $\bar{e}$, is simply ln (s) or ln(1+e).

1.8 Strain in two dimensions

Observations of strain in planes or sections are described by the following dimensionless quantities:

Angular shear, ψ, which describes the change in angle between two originally perpendicular lines in a deformed medium (Figures 2.8 and 2.9).

Shear strain, $\gamma=\tan\psi$, where ψ is the angular shear (Figure 2.8). The shear strain can be found where objects of known initial angular relations occur. Where a number of such objects occur within a homogeneously strained area, the strain ellipse can be found.

The *strain ellipse* is the ellipse that describes the amount of elongation in any direction in a plane of homogeneous deformation. It represents the de-

1 Quadratic stretch would be a better name, because it is the square value of the stretch, not the elongation. However, quadratic elongation is the name that is in common use.

MATRIX ALGEBRA

Matrices contain coefficients of systems of equations that represent linear transfomations. In two dimensions this means that the system of equations shown in equation 3.1 can be expressed by the matrix of equation 3.2. A linear transformation is the same as a homogeneous deformation. The matrix describes the shape and orientation of the strain ellipsoid, and the transformation is a change from a unit sphere (circle in two dimensions).

Matrices are simpler to handle than sets of equations, particularly when applied in computer programs. The most important matrix operations in structural geology are multiplication and finding eigenvectors and eigenvalues:

Multiplication by a vector:

$$\begin{bmatrix} D_{11} & D_{12} \\ D_{21} & D_{22} \end{bmatrix} \begin{bmatrix} x \\ y \end{bmatrix} = \begin{bmatrix} D_{11} \cdot x & D_{12} \cdot y \\ D_{21} \cdot x & D_{22} \cdot y \end{bmatrix}$$

Matrix multiplication:

$$\begin{bmatrix} D_{11} & D_{12} \\ D_{21} & D_{22} \end{bmatrix} \begin{bmatrix} d_{11} & d_{12} \\ d_{21} & d_{22} \end{bmatrix} = \begin{bmatrix} D_{11}d_{11} + D_{12}d_{21} & D_{11}d_{12} + D_{12}d_{22} \\ D_{21}d_{11} + D_{22}d_{21} & D_{21}d_{12} + D_{22}d_{22} \end{bmatrix}$$

Transposition means shifting coloumns and rows in a matrix:

$$\begin{bmatrix} D_{11} & D_{12} \\ D_{21} & D_{22} \end{bmatrix}^{T} = \begin{bmatrix} D_{11} & D_{21} \\ D_{12} & D_{22} \end{bmatrix}$$

The inverse of a matrix **D** is denoted $\mathbf{D}^{-1}$ and is the matrix that gives the identity matrix **I** when multiplied by **D**:

$$\begin{bmatrix} D_{11} & D_{12} \\ D_{21} & D_{22} \end{bmatrix}^{-1} \begin{bmatrix} D_{11} & D_{21} \\ D_{12} & D_{22} \end{bmatrix} = \begin{bmatrix} 1 & 0 \\ 0 & 1 \end{bmatrix} = I$$

Matrix multiplication is non-commutative:

$$D_1 D_2 \neq D_2 D_1$$

The determinant of a matrix **D** is:

$$\det D = \begin{vmatrix} D_{11} & D_{21} \\ D_{12} & D_{22} \end{vmatrix} = D_{11}D_{22} - D_{21}D_{12}$$

The determinant describes the volume change: det**D**=1 then there is no volume change involved.

Eigenvectors(x) and eigenvalues (l) are the vectors and values that fulfill;

$$Dx = \lambda x$$

Deformation matrices have two eigenvectors for two dimensions and three for three dimensions. The eigenvectors describe the orientation of the ellipsoid (ellipse), and the eigenvalues describe its shape. Eigenvalues and eigenvectors are easily found by means of a spreadsheet or computer program such as MatLab™.

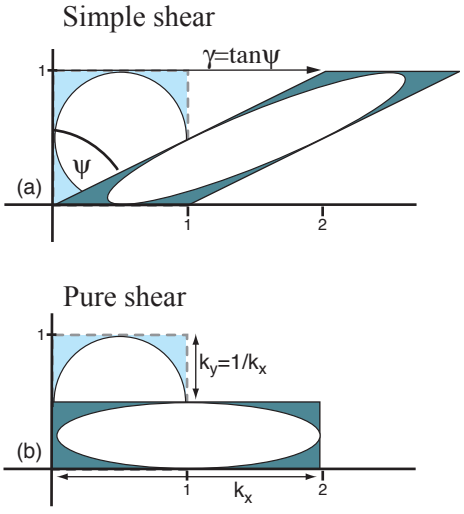

Figure 2.8 Simple and pure shear.

formed shape of an imaginary circle on the undeformed section. The strain ellipse is conveniently described by a long (X) and short (Y) axis. The two axes have lengths $1+e_1$ and $1+e_2$, and the ratio $R=X/Y$ or $(1+e_1)/(1+e_2)$ describes the ellipticity or eccentricity of the ellipse and thus the strain that it represents. For a circle (no strain) R=1.

Area change: For area change without any strain, R=X/Y=1. The circle "drawn" on the initial section remains a circle after a pure area change, albeit with a smaller or larger radius. In a simple diagram where X is plotted against Y, isochoric deformations will plot along the main diagonal (Figure 2.10). The same diagram illustrates strain fields characteristic for different combinations of area change and strain. We will later look at the different types of structures formed in these different fields.

Interestingly enough, it will always be possible to decompose a deformation into some combination of area change and strain. Figure 2.11 shows how compaction can be decomposed into a strain and an area change.

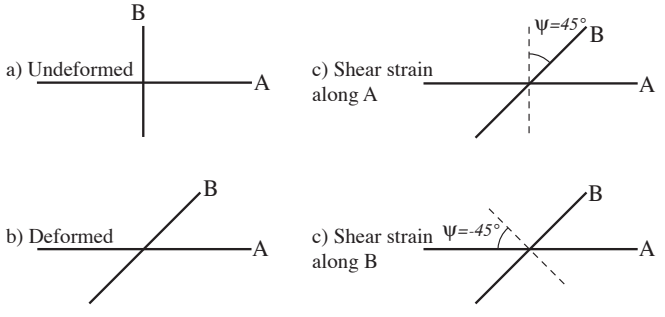

Figure 2.9 Angular shear strain is the change in angle between two initially perpendicular lines, and is positive for clockwise rotations and negative for anti-clockwise rotations. In this example the angular shear strain is 45° along line A and -45° along line B.

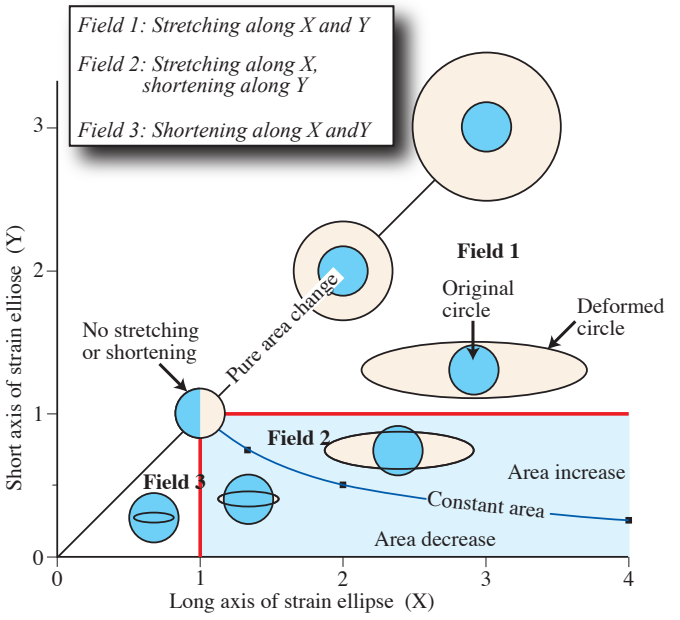

Figure 2.10 Classification of strain ellipses. Only the lower part of the diagram is in use because we have defined X≥Y. Note that Field 2 is divided in two by the constant area line. The plot is called an X-Y plot, but we could also have called it an X-Z plot if we plot the largest and smallest principal strains. Based on Ramsay & Huber (1983).

1.9 Three-dimensional strain

The degree of variation increases significantly when we allow for stretching and contraction in three dimensions. Classical reference situations are known as uniform extension, uniform flattening and plane strain (Figure 2.12). *Uniform extension*, also referred to as axisymmetric extension, is a state of strain where stretching in a direction X is compensated for by equal shortening in the plane orthogonal to X. *Uniform flattening* (axially symmetric flattening) is the opposite, with shortening in a direction Z compensated for by identical stretching in any direction perpendicular to Z. These two reference states

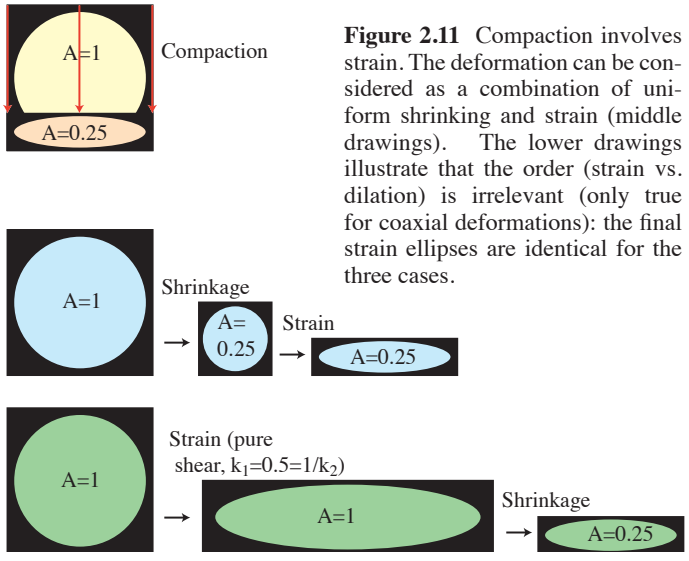

Figure 2.11 Compaction involves strain. The deformation can be considered as a combination of uniform shrinking and strain (middle drawings). The lower drawings illustrate that the order (strain vs. dilation) is irrelevant (only true for coaxial deformations): the final strain ellipses are identical for the three cases.

are end members in a continuous spectrum of deformation types. In the middle between uniform flattening and extension lies *plane strain*, where stretching in one direction is perfectly compensated by shortening in a single perpendicular direction. It is "plane" because all the stretching and shortening takes place within a single plane only.

1.10 The strain ellipsoid

The finite spatial change in shape that is connected with deformation is completely described by the *strain ellipsoid*. The strain ellipsoid is the deformed shape of an imaginary sphere with unit radius that is deformed along with the rock volume under consideration.

The strain ellipsoid has three mutually orthogonal planes of symmetry, the *principal planes of strain*, which intersect along three orthogonal axes that are referred to as the *principal strain axes*. Their lengths (values) are called the *principal stretches*. These axes are commonly designated X, Y and Z, but the designations $\sqrt{\lambda_1}$, $\sqrt{\lambda_2}$ and $\sqrt{\lambda_3}$, S_1, S_2 and S_3 as well as ε_1, ε_2 and ε_3 are also used. We will use X, Y and Z in this book, where X represents the longest axis, Z the shortest axis and Y the intermediate axis

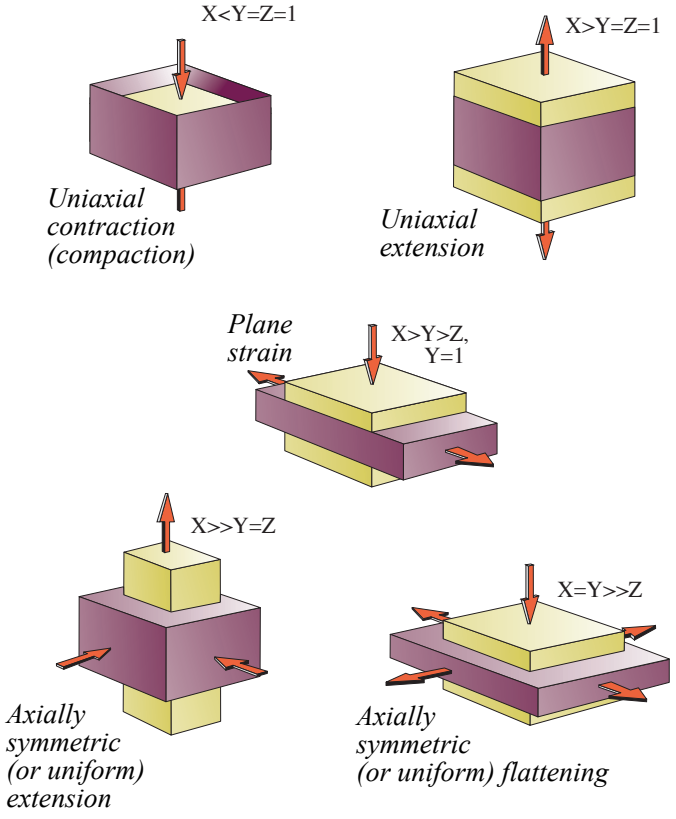

Figure 2.12 Some referance states of strain. The conditions are uniaxial (top), planar (middle) and three-dimensional (bottom).

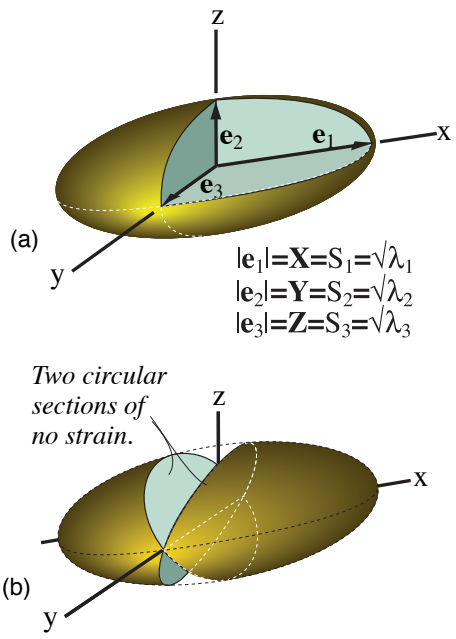

Figure 2.13 The strain ellipsoid is an imaginary sphere that has been deformed along with the rock that we are studying. It depends on homogeneous deformation and is described by three vectors, $\mathbf{e}_1$, $\mathbf{e}_2$ and $\mathbf{e}_3$, defining the principal axes of strain (X, Y and Z) and the orientation of the ellipsoid. The length of the vectors thus describes the shape of the ellipsoid, which is independent on choice of coordinate system. For plane strain there are two sections through the ellipsoid that display no strain.

that may have any value between the other two:

$$X>Y>Z$$

When the ellipsoid is fixed in space, the axes may be considered vectors of given lengths and orientations. Knowledge of these vectors thus means knowledge of both the shape and orientation of the ellipsoid. The vectors are named $\mathbf{e}_1$, $\mathbf{e}_2$ and $\mathbf{e}_3$, where $\mathbf{e}_1$ is the longest and $\mathbf{e}_3$ the shortest (Figure 2.13).

If we place a coordinate system with axes x, y and z along the principal strain axes X, Y and Z, we can write the equation for the strain ellipse as

$$\frac{x^2}{\lambda_1^2}+\frac{y^2}{\lambda_2^2}+\frac{z^2}{\lambda_3^2}=1 \qquad (2.4)$$

It can be shown that λ_1, λ_2 and λ_3 are the eigenvalues of the matrix product $\mathbf{DD}^T$, and that $\mathbf{e}_1$, $\mathbf{e}_2$ and $\mathbf{e}_3$ are the corresponding eigenvectors. So if $\mathbf{D}$ is known, one can easily calculate the orientation and shape of the strain ellipsoid or vice versa. A deformation matrix would look different depending on the choice of coordinate system. However, the eigenvectors and eigenvalues will always be identical for any given state of strain. Another way of saying the same

thing is that they are *strain invariants*[2]. Here is another characteristic related to the strain ellipsoid:

Lines that are parallel with the principal strain axes are orthogonal, and were also orthogonal in the undeformed state.

This means that they have experienced no finite shear strain. No other set of lines has this property. Thus, estimating shear strain from sets of originally orthogonal lines gives information about the orientation of X, Y and Z (see Chapter 4). This goes for two- as well as three-dimensional strain considerations. It should be noted that the rotation that is referred to here is related to the strain component of deformation, and is therefore different from the rigid rotation discussed in section 2.2.2.

1.11 More about the strain ellipsoid

Any strain ellipsoid contains two sur*faces of no finite longitudinal strain*. For constant volume deformations, known as *isochoric deformations*, these surfaces are found by connecting points along the lines of intersection between the ellipsoid and the unit sphere it was deformed from. For plane strain, where the intermediate principal strain axis has unit length, these surfaces are planar (Figure 2.13b). In general, when strain is three dimensional, the surfaces of no finite longitudinal strain are non-planar. Lines contained in these surfaces have the same length as in the undeformed state for constant volume deformations, or are stretched an equal amount if a volume change is involved. This means that:

A plane strain deformation produces two planes in which the rock appears unstrained.

It also means added that physical lines and particles move through these theoretical planes during progressive deformation.

The shape of the strain ellipsoid can be visualized graphically by plotting the axial ratios X/Y and Y/Z as coordinate axes, as shown in Figure 2.14a. This widely used diagram is called a *Flinn diagram* after the English geologist Derek Flinn who published it in 1962. The diagonal of the diagram describes strains where X/Y=Y/Z, i.e. planar strain. It separates *prolate* geometries or cigar shapes of the upper half of the field from *oblate* geometries or

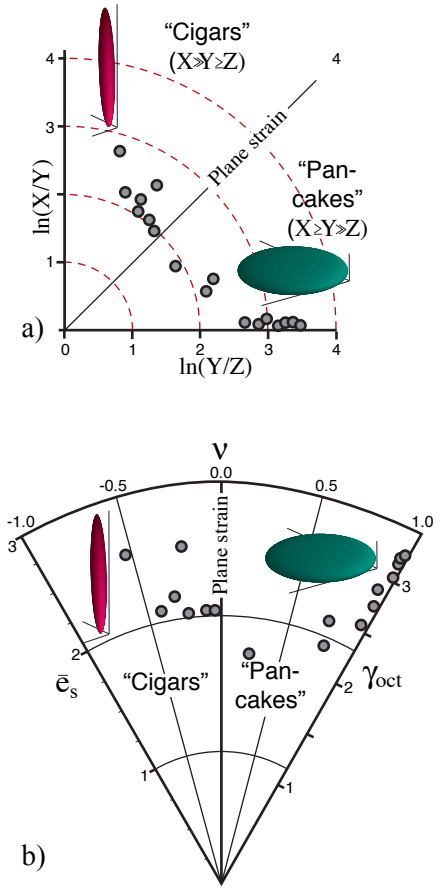

Figure 2.14 Strain data can be represented in a) the Flinn diagram (linear or logaritihmic axes) or b) the Hsü diagram. The same data are plotted in the two diagrams for comparison. Data from Holst & Fossen (1987).

pancake shapes of the lower half. The actual shape of the ellipsoid is characterized by the Flinn k-value: $k=(R_{XY}-1)/(R_{YZ}-1)$, where $R_{XY}=X/Y$ and $R_{YZ}=Y/Z$. A logarithmic scale is sometimes used to represent strain in such diagrams.

The horizontal and vertical axes in the Flinn diagram represent axially symmetric flattening and extension, respectively. Any point in the diagram represents a unique three-dimensional shape or *strain geometry*, i.e. a strain ellipsoid with a unique Flinn k-value. However, different types of deformations may in some cases produce ellipsoids with the same k-value, in which case other criteria are needed for separation. An example is pure shear and simple shear (see below), which both plot along the diagonal of the Flinn diagram. The orientation of the strain ellipse is different for simple and pure shear, but this is not reflected in the Flinn diagram. Thus, the diagram is useful but has its limitations.

In the Flinn diagram, the amount of strain gen-

2 Shear strain, volumetric strain and the kinematic vorticity number (W_k) are other examples of strain invariants

erally increases away from the origin[3]. Direct comparison of strain in the various parts of the diagram is however not trivial. How does one compare a given pancake-shaped and a cigar-shaped ellipsoid? Which one is more strained? We can use the radius (distance from the origin; stippled lines in Figure 2.14), although there is no good mathematical or physical reason why this would be an accurate measure of strain. An alternative parameter is given by the formula:

$$\bar{e}_s = \frac{\sqrt{3}}{2}\bar{\gamma}_{oct} \qquad (2.5)$$

The variable $\bar{e}_s$ is called the natural octahedral unit shear, and

$$\bar{\gamma}_{oct} = \frac{2}{3}\sqrt{(\bar{e}_1 - \bar{e}_2)^2 + (\bar{e}_2 - \bar{e}_3)^2 + (\bar{e}_3 - \bar{e}_1)^2} \qquad (2.6)$$

where the $\bar{e}$'s are the natural principal strains. This unit shear is directly related to the mechanical work that is performed during the deformation history. It does however not take into consideration the rotation of the strain ellipse that occurs for non-coaxial deformations (see section…) and is therefore best suited for coaxial deformations.

An alternative strain diagram can be defined by means of $\bar{\gamma}_{oct}$ (Figure 2.14b), where the natural octahedral unit shear is plotted against a parameter ν called Lodes parameter, which is defined by

$$\nu = \frac{2\bar{e}_2 - \bar{e}_1 - \bar{e}_3}{\bar{e}_1 - \bar{e}_3} \qquad (2.7)$$

This diagram is known as the Hsü diagram, and the radial lines indicate similar amounts of strain based on the natural octahedral unit shear.

1.12 Volume change

A pure volume change or *volumetric strain* of an object is given by $\Delta=(V-V_0)/V_0$, where V_0 and V are volumes of the object before and after the deformation, respectively. The volume factor Δ is thus negative for volume decrease and positive for volume increase. The deformation matrix that describes general volume change is:

$$\begin{bmatrix} D_{11} & 0 & 0 \\ 0 & D_{22} & 0 \\ 0 & 0 & D_{33} \end{bmatrix} = \begin{bmatrix} 1+\Delta_1 & 0 & 0 \\ 0 & 1+\Delta_2 & 0 \\ 0 & 0 & 1+\Delta_3 \end{bmatrix} \qquad (2.8)$$

The product $D_{11}D_{22}D_{33}$, which is identical to the determinant or det(**D**) of the matrix in equation 2.8, is always different from 1 for this and any other deformation that involves a change in volume (area change in two dimensions). The closer det(**D**) is to 1, the smaller the volume (area) change. Volume and area changes do not involve any internal rotation, meaning that lines parallel to the principal strain axes have the same orientations that they had in the undeformed state. Such deformation is called *coaxial*.

A distinction is sometimes drawn between isotropic and anisotropic volume change. *Isotropic volume change* (Figure 2.15) is real volume change where the object is equally shortened in all directions, i.e. the diagonal elements in equation 2.8 are equal. This means that the deformed object has decreased or increased in size, but retained its shape. So strictly speaking, there is no strain involved in isotropic volume change. In two dimensions, there is isotropic area change in which an initial circle remains a circle, albeit with a smaller or larger radius. *Anisotropic volume change* involves not only a volume (area) change but also a change in shape because its effect on the rock is different in different directions.

One may argue that anisotropic volume change is a redundant term, because any anisotropic strain can be decomposed into a combination of (isotropic) volume change and change in shape. The obvious example is compaction, as shown in Figure 2.11 and discussed in the next section. However, if we think about how compaction comes about in most cases, it makes sense to consider it as an anisotropic volume change rather than a combination of isotropic volume change and a strain. In practice, sediments compact by vertical shortening (Figure 2.11, top), not discretely by shrinking and then straining (Figure 2.11, middle). But the fact that deformation is not concerned with the deformation history makes any decomposition of the deformation into such components mathematically correct, even though they have nothing to do with the actual process of deformation in question. As geologists we are concerned with reality and retain the term anisotropic volume change where we find it useful. The most useful case

3 There are cases where primary ellipsoids, such as pebbles, are deformed into less elliptical shapes or even spherical shapes, which causes challenges to the strain analyst.

THE DETERMINANT OF THE DEFORMATION MATRIX D

The determinant of a matrix D is generally found by the following formula:

$$\det\begin{bmatrix} D_{11} & D_{12} & D_{13} \\ D_{21} & D_{22} & D_{23} \\ D_{31} & D_{32} & D_{33} \end{bmatrix} = D_{11}(D_{22}D_{33} - D_{23}D_{32}) - D_{12}(D_{21}D_{33} - D_{23}D_{31}) + D_{13}(D_{21}D_{32} - D_{22}D_{31})$$

If the matrix is diagonal, meaning that it has non-zero values along the diagonal only, then det(**D**) is the product of the diagonal entries of D. Fortunately, this is also the case for triangular matrices, i.e. matrices that have only zeros below (or above) the diagonal:

$$\det\begin{bmatrix} D_{11} & D_{12} & D_{13} \\ 0 & D_{22} & D_{23} \\ 0 & 0 & D_{33} \end{bmatrix} = D_{11}D_{22}D_{33}$$

The deformation matrices for volume change and pure shear are both examples of diagonal matrices, and those for simple and subsimple shear are triangular matrices. When det(**D**)=1, then the deformation represented by the matrix is isochoric, i.e. it involves no change in volume.

is probably the one where an object is shortened or extended in only one direction (no strain in the other directions). The result is called *uniaxial strain*.

1.13 Uniaxial strain (compaction)

Uniaxial strain is contraction or extension along one of the principal strain axes without any change in length along the other two. Such strain requires a reorganization, addition or removal of rock volume. If volume is lost, we have *uniaxial shortening* and volume reduction. This happens through grain reorganization during compaction of porous sediments and tuffs near the surface, leading to a denser packing of grains. Only water, oil or gas that filled the pore space leaves the rock volume, not the rock minerals themselves. In calcareous rocks and deeply buried siliciclastic sedimentary rocks, uniaxial strain can be accommodated by (pressure) solution, also referred to as chemical compaction. In this case, minerals are dissolved and transported out of the rock volume by fluids. Removal of minerals by diffusion can also occur under metamorphic conditions in the middle and lower crust. This can result in cleavage formation or can lead to compaction across shear zones. *Uniaxial extension* implies expansion in one direction. This may occur by the formation of tension fractures or veins or during metamorphic reactions.

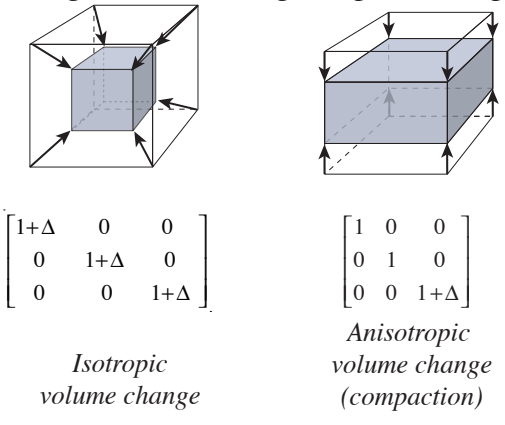

Figure 2.15 The difference between isotropic volume change, which involves no strain, and anisotropic volume change represented by uniaxial shortening (compaction).

Uniaxial strain may occur isolated, such as during compaction of sediments, or in concert with other deformation types such as simple shear. It has been found useful to consider many shear zones as zones of simple shear with an additional uniaxial shortening across the zone.

Uniaxial shortening or compaction is such an important and common deformation that it needs some further attention. The deformation matrix for uniaxial strain is:

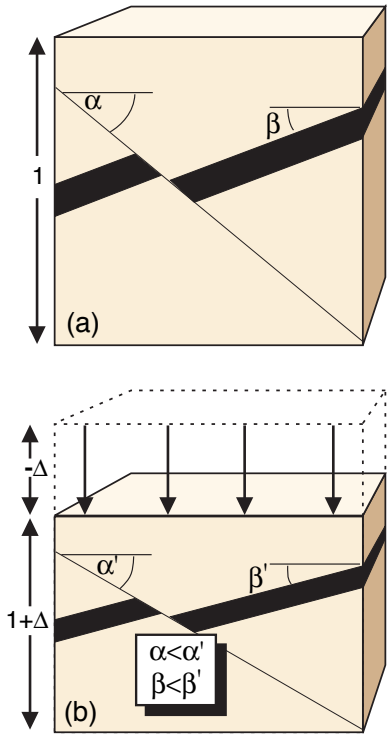

Figure 2.16 Compaction of faulted layer. Compaction lowers the dip of both layering and faults. The effect depends on the amount of post-faulting compaction and can be estimated using the deformation matrix for compaction (eq. 3.9).

$$\begin{bmatrix} 1 & 0 & 0 \\ 0 & 1 & 0 \\ 0 & 0 & 1+\Delta \end{bmatrix} \quad (2.9)$$

where Δ is the elongation in the vertical direction (negative for compaction) and 1+ Δ is the vertical stretch (Figure 2.16). The fact that only the third diagonal element is different from unity implies that elongation or shortening only occurs in one direction. The matrix gives the strain ellipsoid, which is oblate or pancake-shaped for compaction. It can also be used to calculate how planar features such as faults and bedding are affected by compaction (Figure 2.16).

If we can estimate the present and initial porosity of a compacted sediment or sedimentary rock, then we can use the equation

$$\Phi = \Phi_0 e^{-CZ} \quad (2.10)$$

to find 1+ Δ. Φ_0 is here the initial porosity, Z is the burial depth and C is a constant that typically is about 0.29 for sand, 0.38 for silt and 0.42 for shale. *e* is here the exponential function, not the extension factor. Equation 2.10 tells us that the porosity Φ changes with depth Z, and we are looking at a matrix of the form

$$\begin{bmatrix} 1 & 0 & 0 \\ 0 & 1 & 0 \\ 0 & 0 & 1+f(Z) \end{bmatrix} \quad (2.11)$$

It can be shown that $\Delta = (1-\Phi_0)/(1-\Phi_0 e^{-CZ})$, and the deformation matrix then becomes:

$$\begin{bmatrix} 1 & 0 & 0 \\ 0 & 1 & 0 \\ 0 & 0 & 1+(1-\Phi_0)/(1-\Phi_0 e^{-CZ}) \end{bmatrix} \quad (2.12)$$

Matrix (2.12) helps us predict the compaction at any point in a sedimentary basin, and it also predicts how structures such as folds and faults are modified by compaction. A relationship that can be found from matrix (2.12) relates the original dip (α) to the new dip (α´) after the compaction:

$$\alpha' = \tan^{-1}[(1+\Delta)\tan\alpha]. \quad (2.13)$$

In metamorphic rocks, uniaxial shortening or compaction can be estimated by comparing portions of the rock affected by compaction with those believed to be unaffected. If the concentration of an immobile mineral, such as mica or an opaque phase, is C in the compacted part of the rock, and is believed to have been C_0 before compaction, then the compaction factor is given by the relationship:

$$1+\Delta = \frac{C_0}{C}$$

C_0 is found outside of the deformation zone, which could be a millimeter-thick cleavage-related microlithon, as discussed in the chapter on cleavages and foliations. The deformation zone could also be a mesoscopic shear zone, where the wall rock is assumed to be unaffected by both shearing and compaction. As we will see in the chapter on shear zones, ideal shear zones can only accommodate compaction in addition to simple shear.

1.14 Pure shear

Pure shear (Figures 2.8b and 2.17) is a perfect *coaxial deformation*, which means that it involves

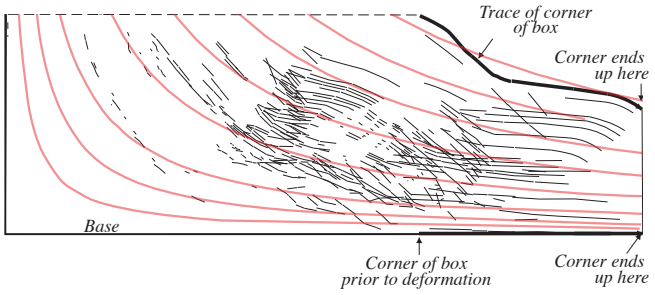

Figure 2.17 Particle path for a plaster experiment. The theoretical pure-shear pattern is shown for comparison. Based on Fossen & Gabrielsen (1996).

no internal rotation (see p.). The same is the case with uniaxial strain where the rock shrinks in one direction. Coaxial deformation also means that lines along the principal strain axes have the same orientation as they had in the undeformed state. Pure shear is traditionally considered a plane strain with no volume change, although some geologists also apply the term to three-dimensional coaxial deformations. Pure shear is identical to applying uniaxial shortening in one direction and an equal amount of uniaxial extension in the other. Since it affects only two dimensions, the deformation matrix can be written as the two-dimensional matrix

$$\begin{bmatrix} k_x & 0 \\ 0 & k_y \end{bmatrix} \quad (2.14)$$

where k_x and k_y are the stretch and shortening along the x and y coordinate axes, respectively. They are also the principal stretches for pure shear deformation, and their orientations coincide with the coordinate axes. Unless there is an additional area (volume) change, $k_y=1/k_x$.

1.15 Simple shear

Simple shear (Figure 2.8) is a special type of constant-volume two-dimensional deformation. There is no stretching or shortening, and no movement of particles in the third direction. Unlike pure shear, it is a *non-coaxial deformation*, meaning that lines parallel to the principal strain axes have rotated away from their initial positions. This internal rotation has caused several geologists to refer to simple shear and other non-coaxial deformations as rotational deformations. Another characteristic of non-coaxial deformations relates the orientation of the strain ellipsoid and the amount of strain:

In the case of non-coaxial deformations, the orientations of the principal strain axes are different for different amounts of strain, while for coaxial deformations they always are identical.

Simple shear involves the particular amount of internal rotation that causes one of the two circular sections of the strain ellipse (p.) to parallel the shear plane, regardless of the amount of strain involved.

The consideration of coaxiality and internal rotations is easier to discuss in terms of progressive deformation (below). But, for now, it is more important to study the deformation matrix for simple shear:

$$\begin{bmatrix} 1 & \gamma \\ 0 & 1 \end{bmatrix} \quad (2.15)$$

The factor γ is called the shear strain and $\gamma=\tan\psi$, where ψ is the angle of rotation of a line that was perpendicular to the shear plane in the undeformed state (Figure 2.8). Lines and planes that lie within (parallel to) the shear plane do not change orientation or length during simple shear. Lines and planes with any other orientation do. It is noteworthy that deformation matrices describing coaxial deformations are symmetric, while those describing non-coaxial deformations are asymmetric.

1.16 Subsimple shear

Between pure shear and simple shear there exists a spectrum of planar deformations referred to as subsimple shear (also referred to as general shear, although these deformations are just a subset of planar deformations and thus not very general). Subsimple shear can be considered as a mix of pure and simple shear, but the internal rotation involved is less than for simple shear. Mathematically we have to combine the deformation matrices for simple and pure shear, which is not as trivial as it may sound. The matrix can be written as:

$$\begin{bmatrix} k_x & \Gamma \\ 0 & k_y \end{bmatrix} \quad (2.16)$$

where $\Gamma=\gamma[(k_x-k_y)] / [\lambda_n(k_x-k_y)]$. If there is no area change in addition to the pure and simple shear components, then $k_y=1/k_x$ and $\Gamma=\gamma(k_x-1/k_x)/2\ln(k_x)$. An example of subsimple shear is shown in Figure 2.1.

1.17 Progressive deformation and flow parameters

Simple shear, pure shear, volume change and any other deformation type relate the undeformed to the deformed state only. The history that takes place between the two states is a different matter, and is the focus of the study of *flow* and *progressive deformation of rocks*.

It is useful to consider individual particles in the rock or sediment when discussing progressive deformation. If we keep track of a single particle during the deformation history, we can get a picture of a single *particle path*. If we map the motion of a number of such particles we get an impression of the *flow pattern*.

The flow pattern is the movement patterns described by individual particles, or the sum of particle paths in a deforming medium.

Particle paths can be recorded directly in experiment, either where individual particles or (colored) grains can be traced throughout the deformation history or where structures such as faults cross other structures or bedding. Filming an ongoing experiment enables the scientist to reconstruct the flow pattern during the experiment. In the field things are different and we can only see the final stage of the deformation, i.e. the last picture of the film roll.

Let us imagine that we can photograph some deformation from the start to the end. Then the difference between any two adjacent pictures represents a small interval of the total deformation. Based on the differences between the two pictures we may be able to find the size and orientation of the *incremental strain ellipsoid* for this interval and obtain an increment of the deformation history. The smaller such an interval gets, the closer we get to the *instantaneous* or *infinitesimal deformation parameters* (Figure 2.18). Parameters that act instantaneously during the deformation history are called flow parameters and rely on how particles flow during deformation. They also include the infinitesimal or instantaneous stretching axes, the flow apophyses, vorticity and the velocity field.

The Instantaneous Stretching[4] *Axes (ISA)* are the three perpendicular axes (two for plane deformations) that describe the directions of maximum and minimum stretching at any time during deformation.

4 They are all called instantaneous *stretching* axes although at least one tend to be the minimum stretching axis (ISA_3) is generally the direction of maximum *shortening*, or *negative stretching*.

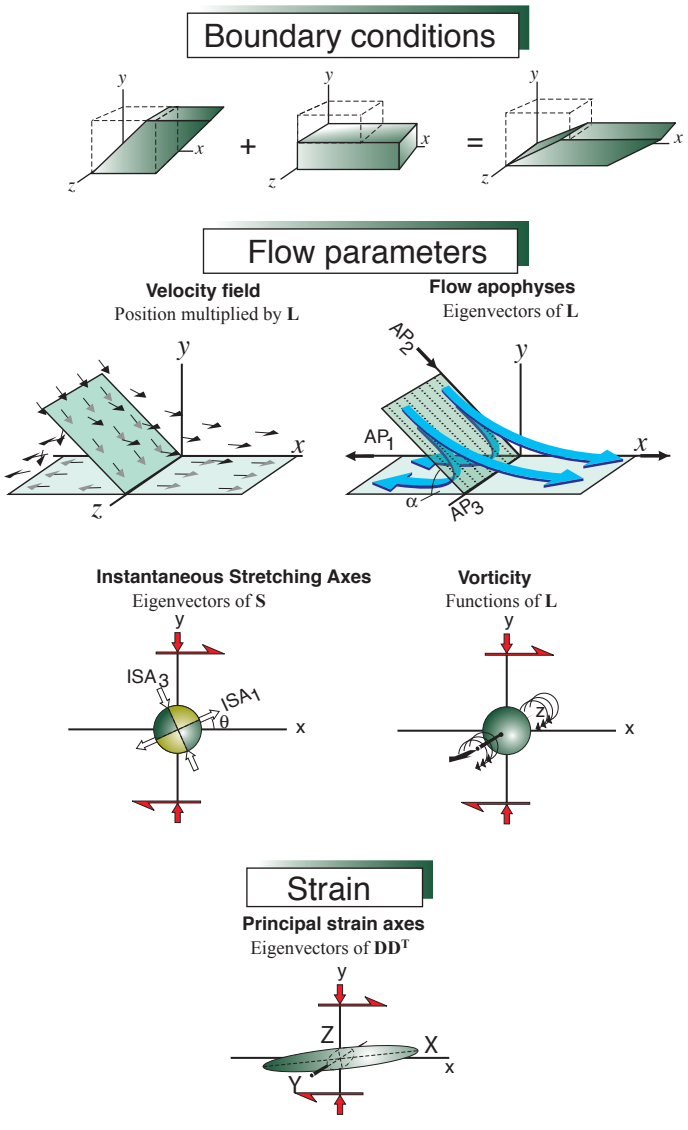

Figure 2.18 The most important deformation parameters.Boundary conditions control the flow parameters, which over time produce strain.

Lines along the longest axis (ISA_1) are extending faster than any other line orientation. Similarly, no line is stretching slower (or shortening faster) than those along the shortest instantaneous stretching axis (ISA_3).

Flow apophyses separate different domains of particle paths (AP in Figure 2.18). Particles located along the apophyses rest or move along the straight apophyses. Other particle paths are curved. No particle can cross a flow apophysis unless the conditions change during the deformation history.

Vorticity describes how fast a particle rotates in a soft medium during the deformation (Section 2.20). A related quantity is the *kinematic vorticity number* (W_k) which is 1 for simple shear and 0 for pure shear and somewhere between the two for sub-simple shear.

The *velocity field* describes the velocity of the particles at any instance during the deformation history. Let us have a closer look at these things.

1.18 Velocity field

The velocity (gradient) tensor is designed **L** and describes the velocity of the particles at any instant during the deformation. In three dimensions the velocity field is described by the equations:

$$v_1 = L_{11}x_1 + L_{12}x_2 + L_{13}x_3$$
$$v_2 = L_{21}x_1 + L_{22}x_2 + L_{23}x_3$$
$$v_3 = L_{31}x_1 + L_{32}x_2 + L_{33}x_3$$

which in matrix notation becomes

$$\begin{bmatrix} v_1 \\ v_2 \\ v_3 \end{bmatrix} = \begin{bmatrix} L_{11} & L_{12} & L_{13} \\ L_{21} & L_{22} & L_{23} \\ L_{31} & L_{32} & L_{33} \end{bmatrix} \begin{bmatrix} x_1 \\ x_2 \\ x_3 \end{bmatrix} \quad (2.17)$$

or

$$\mathbf{v}=\mathbf{L}x$$

Here, the vector **v** describes the velocity field and the vector **x** gives the particle positions.

If we consider flow with a 3-D coaxial component, such as flattening or constriction (Figure 2.19) in combination with a progressive simple shear whose shear plane is the x-y plane, then we have the following velocity matrix:

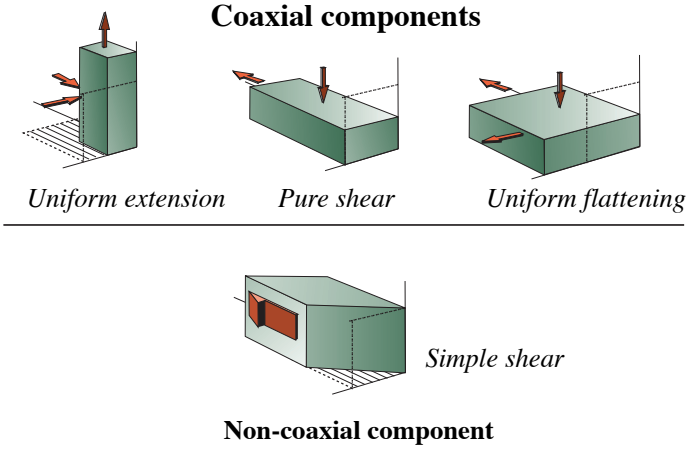

Figure 2.19 Coaxial deformation produces a spectrum of deformation between uniform extension and uniform flattening, of which pure shear is a special, plane-strain case. They can combine with simple shear to form more general deformations.

$$L = \begin{bmatrix} \dot{e}_x & \dot{\gamma} & 0 \\ 0 & \dot{e}_y & 0 \\ 0 & 0 & \dot{e}_z \end{bmatrix} \quad (2.18)$$

In this matrix, $\dot{e}_x$ and $\dot{e}_y$ are the elongation rates in the x and y directions, respectively, and $\dot{\gamma}$ is the shear strain rate (all with dimension s^{-1}). These deformation rates are related to the particle velocities during the deformation and thus related to the velocity field. The velocity field can thus be written:

$$v_1 = \dot{e}_x x + \dot{\gamma} y$$
$$v_2 = \dot{e}_y y \quad (2.19)$$
$$v_3 = \dot{e}_z z$$

The tensor **L** is composed of time-dependent deformation rate components, while the deformation matrix has spatial components that do not involve time or history. The matrix **L** for progressive subsimple shear now becomes:

$$L = \begin{bmatrix} \dot{e}_x & 0 \\ 0 & \dot{e}_y \end{bmatrix} + \begin{bmatrix} 0 & \dot{\gamma} \\ 0 & 0 \end{bmatrix} = \begin{bmatrix} 0 & \dot{\gamma} \\ 0 & 0 \end{bmatrix} + \begin{bmatrix} \dot{e}_x & 0 \\ 0 & \dot{e}_y \end{bmatrix} = \begin{bmatrix} \dot{e}_x & \dot{\gamma} \\ 0 & \dot{e}_y \end{bmatrix} \quad (2.20)$$

This equation illustrates a significant difference between deformation rate tensors and ordinary deformation matrices: while deformation matrices are non-commutative, strain rate tensors can be added in any order without changing the result. The disadvantage is that information about the strain ellipse is slightly more cumbersome to extract from deformation rate tensors, since we then need to integrate with respect to time over the interval in question.

L can be decomposed into a symmetric matrix $\dot{S}$ and a skew-symmetric matrix **W**:

$$L = \dot{S} + W \quad (2.21)$$

$\dot{S}$ is the stretching tensor and describes the portion of the deformation that over time produces strain. **W** is known as the vorticity or spin tensor and contains information about the internal rotation during the deformation. For progressive subsimple shear the decomposition becomes

$$L = \dot{S} + W = \begin{bmatrix} \dot{\varepsilon}_x & \frac{1}{2}\dot{\gamma} \\ \frac{1}{2}\dot{\gamma} & \dot{\varepsilon}_y \end{bmatrix} + \begin{bmatrix} 0 & \frac{1}{2}\dot{\gamma} \\ -\frac{1}{2}\dot{\gamma} & 0 \end{bmatrix} \quad (2.22)$$

The eigenvectors and eigenvalues to $\dot{S}$ give the orientations and lengths of the ISA (instantaneous stretching axes). The eigenvectors to **L** describe the flow apophyses, which are discussed in the next section. Whether one wants to work with strain rates or simple deformation parameters such as k and γ is a matter of personal preference in many cases. Both are in use, and both have their advantages and disadvantages.

1.19 Flow apophyses

Flow apophyses are theoretical lines (meaning that they cannot be seen or painted on the deforming medium – they are lines that are free to rotate independently of material lines) that separate different fields of the flow. Particles cannot cross an apophysis, but they can either move along the apophysis or not move at all in this direction. For the case of simple shearing (progressive simple shear), the particles will always move straight along the shear direction. This occurs because there is no shortening or extension perpendicular to the shear plane, and it tells us that one of the apophyses is parallel to the shear direction (Figure 2.20). As we shall see, there is only this one apophysis for simple shear. For pure shear there are two orthogonal apophyses along which particles move straight toward or away from the origin. Subsimple shear has two oblique apophyses; one parallel to the shear direction and one at an angle α to the first one. The angle α between the two apophyses varies from 90° (pure shear) to 0° (simple shear).

For simple shear, pure shear or subsimple shear, the two apophyses are given by:

$$\begin{bmatrix} 1 \\ 0 \end{bmatrix}, \begin{bmatrix} \dfrac{-\gamma}{\ln(k_x/k_y)} \\ 1 \end{bmatrix} \qquad (2.23)$$

which agrees with our statement that one of the apophyses is parallel and the other oblique to the shear direction (here chosen to be along the x-axis of our coordinate system). The angle α between the apophyses is directly related to how close to simple shear or pure shear the deformation is. α is zero for simple shear and 90° for pure shear, and W_k thus depends on α:

$$W_k = \cos(\alpha) \qquad (2.24)$$

To illustrate how flow apophyses can be useful in tectonics, consider the convergent motion of one tectonic plate relative to another. It actually turns out that the oblique apophysis is parallel to the convergence vector, which becomes apparent if we recall that straight particle motion can only occur in the direction of the apophyses. In other words, for oblique plate convergence (transpression, see Chap-

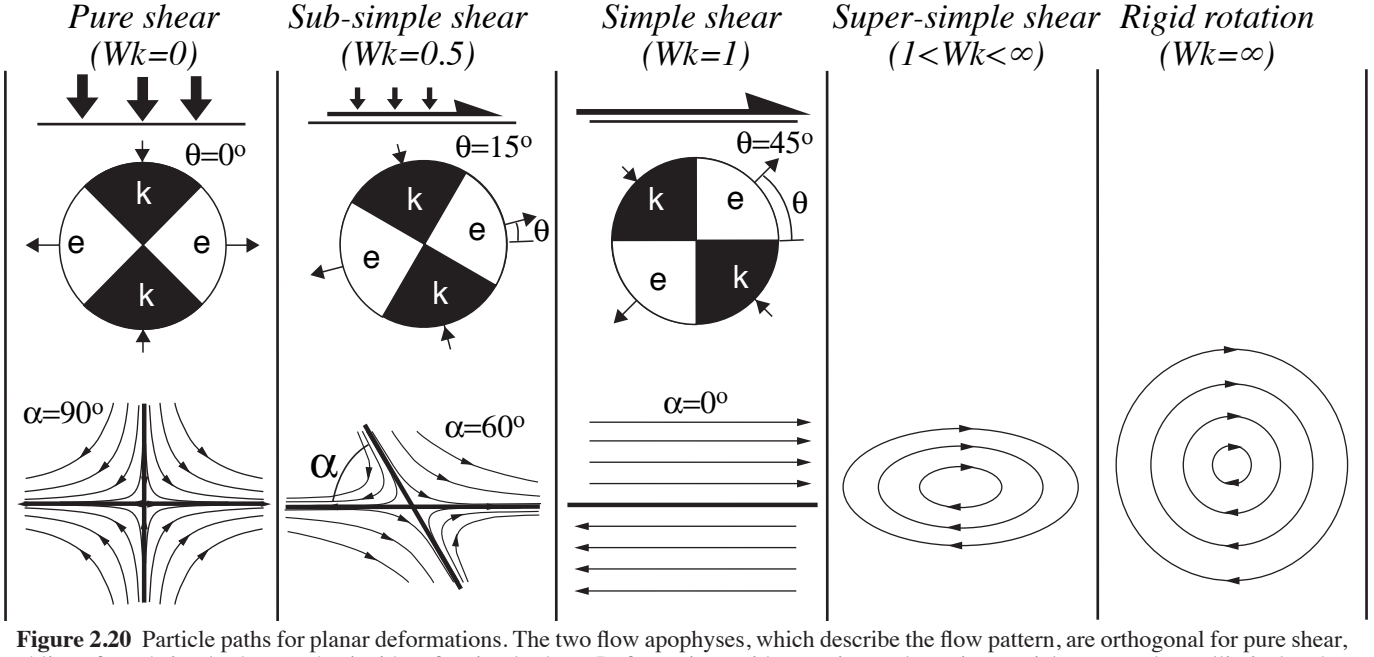

Figure 2.20 Particle paths for planar deformations. The two flow apophyses, which describe the flow pattern, are orthogonal for pure shear, oblique for subsimple shear and coincident for simple shear. Deformations with more internal rotation particles move along elliptical paths. The end-member is rigid rotation, where particles move along perfect circles. Rigid rotation involves perfect rotation without strain, while pure shear is simply strain with no rotation. Note that ISA are generally oblique to the flow apophyses for $W_k>0$.

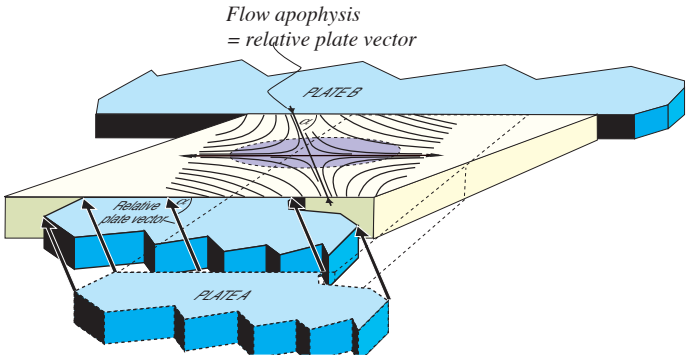

Figure 2.21 Two rigid plates (A and B) and an intermediate deforming zone (yellow). Standing on plate B, we will observe plate A moving obliquely towards us. If this shortening is compensated by lateral extension, then the oblique flow apophysis is parallel to the plate vector and the particle path is known. W_k can be calculated by means of Figure 2.21. Modified from Fossen & Tikoff (1998).

ter 18) α describes the angle of convergence and is 90° for head-on collision and 0° for perfect strike slip. Head-on collision is thus a pure shear on a large scale, while strike-slip or conservative boundaries deform by overall simple shear. Hence, if we know the plate vectors along a plate boundary, we can, at least in principle, estimate the orientations of the flow apophyses and W_k (Figure 2.21) and use this to model or evaluate deformation structures along the plate boundary.

1.20 Vorticity and W_k

We separate between *non-coaxial deformation histories*, where material lines (imagine lines drawn on a section through the deforming rock) that in one instance are parallel to ISA in the next instance have rotated away from them, and *coaxial deformation histories*, where the material lines along ISA remain along these axes for the entire deformation history. The degree of rotation or coaxiality is denoted by the kinematic vorticity number W_k. This number is 0 for perfectly coaxial deformation histories, 1 for progressive simple shear, and between 0 and 1 for subsimple shear. Values between 1 and ∞ are deformation histories where the strain ellipsoid continuously rotates rather than rotating toward a shear plane. $W_k>1$ deformations are therefore sometimes termed spinning deformations, and the result of such deformations is that the strain ellipsoid records a cyclic history of being successively strained and unstrained.

To get a better understanding of what W_k actually means, we need to explore the concept of vorticity. *Vorticity* is a measure of the internal rotation during the deformation. The term comes from the field of fluid dynamics, and the classical example is where a paddle wheel is moving with the flow (Fig. 2.22). If the paddle wheel does not turn, then there is no vorticity. If it does turn around, there is a (relative) vorticity, and the vector that describes the speed of rotation, the angular velocity vector ω, is closely associated with the vorticity vector **w**:

$$\mathbf{w} = 2\,\omega = \text{curl}\,\mathbf{v}, \quad (2.25)$$

where **v** is the velocity field.

Another illustration that may help is one where a spherical volume of the fluid freezes (Figure 2.23). If the sphere is infinitely small, then the vorticity vector w will represent the axis of rotation of the sphere, and its length would be proportional to the speed of the rotation. The vorticity vector can be interpreted as 1) the average rotation of all lines in the plane perpendicular to w, 2) the speed of rotation of a set of physical lines that are parallel to the ISA, 3) The average speed of rotation of two orthogonal physical lines in the plane perpendicular to w, or 4)

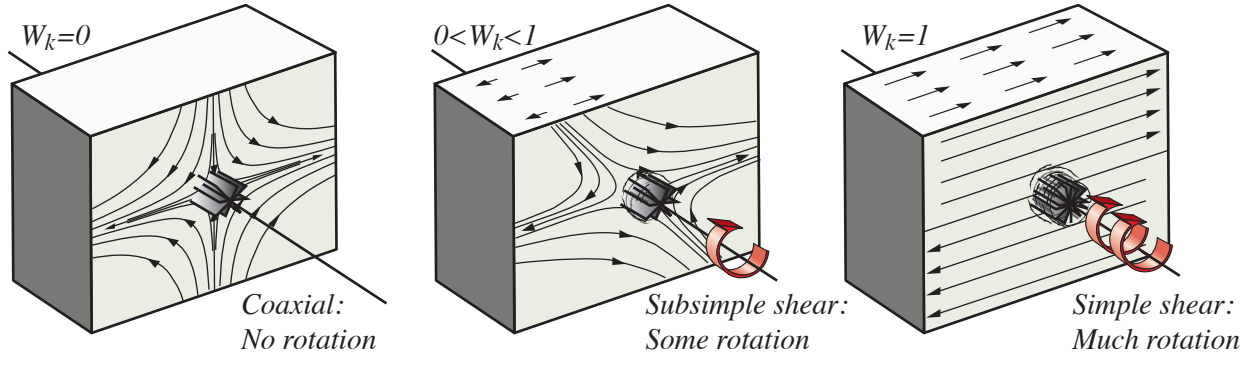

Figure 2.22 The paddle-weel interpretation of flow. The axis of the paddle weel is parallel to the vorticity vector and is not rotating for coaxial deformation (W_k=0) and shows an increasing tendency to rotate for increasing W_k.

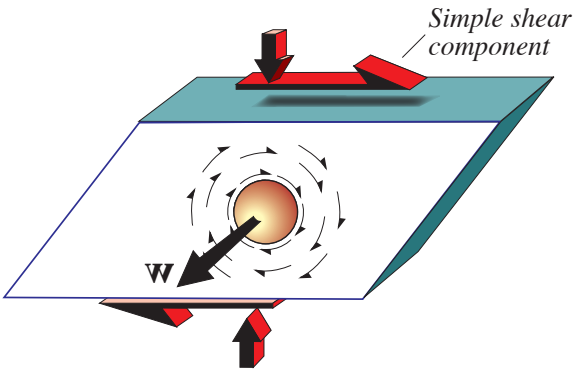

Figure 2.23 The vorticity vector (**w**) in progressive subsimple shear.

half the speed of rotation of a rigid spherical inclusion in a ductile matrix where there is no slip along the edge of the sphere and where the viscosity contrast is infinitely high.

As an example, let us put a rigid sphere in a deformation box filled with a softer material that contains strain markers. If we apply a coaxial deformation by squeezing the box in one direction and letting it extend in the other(s), the sphere will not rotate and the vorticity is 0. However, if we add a simple shear to the content of the box, the sphere will rotate, and we will observe that there is a relationship between the strain and the rotation, regardless of how fast we perform the experiment (strain rate): the more strain, the more rotation. This relation between strain and (internal) rotation is the kinematic vorticity number W_k. For a simultaneous combination of pure shear and simple shear, i.e. subsimple shear, there is less rotation of the sphere for a certain strain accumulation than for simple shear. Therefore W_k is less than 1 by an amount that depends on the relative amount of simple versus pure shear.

W_k is a measure of the relation between the vorticity (internal rotation) and how fast strain accumulates during the deformation.

Mathematically, the kinematic vorticity number is defined as:

$$W_k = \frac{w}{\sqrt{2(s_x^2 + s_y^2 + s_z^2)}}, \quad (2.26)$$

where S_n are the principal strain rates, i.e. the strain rates along the ISA. This equation can be rewritten in terms of pure and simple shear components if we assume steady flow (see next section) during the deformation:

$$W_k = \frac{\gamma}{\sqrt{2\left[(\ln k_x)^2 + (\ln k_y)^2 + (\gamma)^2\right]}} \quad (2.27)$$

which for constant area becomes

$$W_k = \cos[\arctan((2 \ln k)/\gamma)] \quad (2.28)$$

This expression is identical to the simpler equation $W_k = \cos(\alpha)$ (equation 2.24), where α and α' are the acute and obtuse angles between the two flow apophyses, respectively, and k and γ are the pure shear and simple shear components, as above. The relation between W_k and α is shown graphically in Figure 2.24, where also the corresponding relation between W_k and ISA_1 is shown.

1.21 Steady-state deformation

If the flow pattern and the flow parameters remain constant throughout the deformation history, then we have a steady-state flow or deformation. If, on the other hand, the ISA rotate, W_k changes value, or the particle paths change during the course of de-

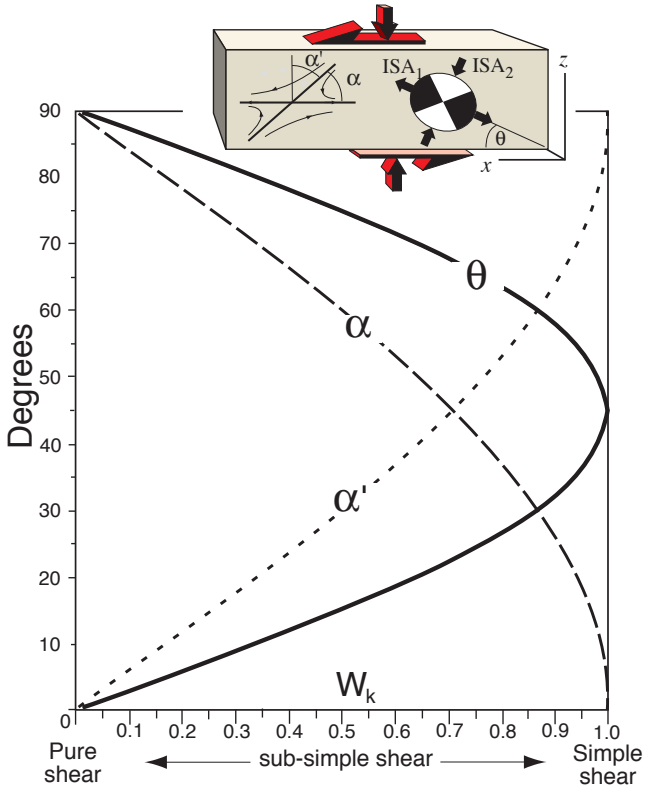

Figure 2.24 The relationship between W_k α, α' and θ.

formation, then we have a non-steady-state flow.

During steady-state deformation the ISA and flow apophyses retain their initial orientation throughout the deformation history, and W_k is constant.

An example of non-steady deformation is a subsimple shear that moves from being close to simple shearing towards a more pure shear dominated flow. For practical reasons, and because non-steady-state deformations are difficult to identify in may cases, steady-state flow is assumed. In nature, however, non-steady state deformation is probably quite common.

1.22 Incremental deformation

The theory around the deformation matrix can be used to model progressive deformation in a discrete way. We make a distinction between *finite deformation* or *finite strain* on one hand, which is the result of the entire deformation history, and *incremental deformation* or *incremental strain* on the other, which concerns only a portion of the same deformation history. When using an incremental approach, each deformation increment is represented by an *incremental deformation matrix*, and the product of all of the incremental deformation matrices equals the finite deformation matrix.

There is an important thing about matrix multiplication that we should be aware of: The order by which we multiply matrices (apply deformations) is not arbitrary. For example, a pure shear followed by a simple shear does not result in the same deformation as a simple shear followed by pure shear:

$$\begin{bmatrix} k_x & 0 \\ 0 & k_y \end{bmatrix}\begin{bmatrix} 1 & \gamma \\ 0 & 1 \end{bmatrix} \neq \begin{bmatrix} 1 & \gamma \\ 0 & 1 \end{bmatrix}\begin{bmatrix} k_x & 0 \\ 0 & k_y \end{bmatrix} \quad (2.29)$$

Interestingly, the matrix representing the first deformation or deformation increment is the last in the row of the matrices to be multiplied. For example, if a deformation is represented by three increments, D_1 representing the first part of the history and D_3 the last part, then the matrix representing the total deformation is the product $D_{tot} = D_3 D_2 D_1$.

Another point to be noted is that since we are here operating in terms of kinematics only (not time), it does not make any difference whether D_1-D_3 represent different deformation phases or increments of the same progressive history.

One can define as many increments as one needs to model progressive deformation. When the incremental matrices represent very small strain increments, the principal strain axes of the matrices approximate the ISA and other flow parameters can also be calculated for each increment and compared. Modeling progressive deformation numerically can provide useful information about the deformation history. It may be difficult however to extract information from naturally deformed rocks that reveal the actual deformation history. For this reason, steady-state deformations represent useful reference deformations, although natural deformations are not restricted by the limitations of steady state flow.

1.23 Strain compatibility and boundary conditions

If we deform a chunk of soft clay between our hands there will be free surfaces where the clay can extrude. This situation is quite different for a volume of rock undergoing natural deformation in the crust. Most deformation happens at depth where the rock volume is surrounded by other rock and under considerable pressure. The resulting strain will depend on the anisotropy of the rocks and their structures. Anisotropy, such as a weak layer or foliation, may control the deformation just as much as the stress field.

Let us illustrate this by a ductile shear zone with straight and parallel margins and undeformed walls, as shown in Figure 2.25a-b. In principle, simple shearing can continue “forever” in such a zone without any problem with the wall rock (challenges may arise at the points of termination, but we will neglect those for now).

Adding shortening across the shear zone as a result of anisotropic volume change is also easy to accommodate. However, adding a pure shear means that the shear zone will have to extrude laterally while the wall rock remains undeformed (Figure 2.25c-d). This causes a classical *strain compatibility problem* since the continuity across the shear zone boundaries is lost. The strain in the shear zone is no longer compatible with the undeformed walls.

For the state of strain in two adjacent layers to be compatible, the section through their respective strain ellipsoids parallel to their interface must be identical.

For our shear zone example, the rock on one

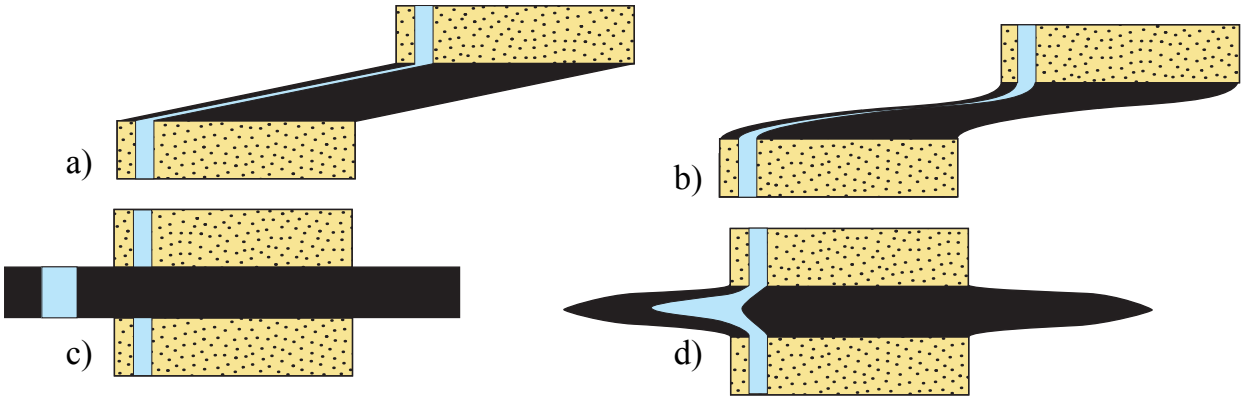

Figure 2.25 Homogeneous (a) and heterogeneous (b) simple shear create no compatibility problems between the deformed and undeformed rocks. Homogeneous pure shear (c) does, because material flows out sideways, creating discontinuities. The space problem is also apparent for heterogeneous pure shear (d), but the discontinuities can be eliminated.

side is undeformed, and the section must be circular, which it is for simple shear with or without shear zone-perpendicular compaction (Fig. 2.26). However, if a pure shear component is involved, compatibility between the deformed and undeformed volumes is not maintained.

A practical solution to this problem is to introduce a discontinuity (slip-surface or fault) between the zone and each of the walls. The shear zone material can then be squeezed sideways in the direction of the shear zone. The problem is that it has nowhere to go, since the neighboring part of a parallel-sided shear zone will try to do exactly the same thing. We can therefore conclude that a shear zone with parallel boundaries is not compatible with (cannot accommodate) pure shear. Besides, strain compatibility as a concept requires that the deformed volume is coherent and without discontinuities, overlaps or holes. Discontinuities and non-parallel shear zones are, as we know, common in many deformed rocks. The requirement of continuity in strain compatibility is thus negotiable.

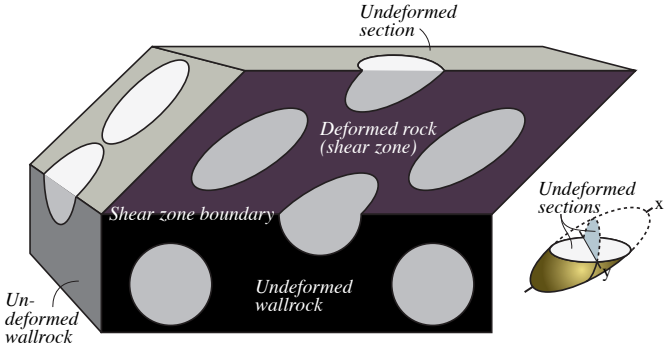

Figure 2.26 The compatibility between undeformed wall rock and a simple shear zone. Any section parallel to the shear zone wall will appear undeformed.

1.24 Deformation history from deformed rocks

It is sometimes possible to extract information about the deformation history from naturally deformed rocks. The key is to find structures that have developed during a limited part of the total deformation history only. In some cases the deformation has moved from one part of the deformed rock volume to another, leaving behind deformed rock that has recorded the conditions during earlier increments of the deformation. For example, strain may after some time localize to the central part of the shear zone. Thus the margins bear a record of the first increment of the deformation. But shear zones can also initiate as narrow zones and widen over time. In this case the outer portion of the shear zone records the last increments of deformation. The search for deformation history is not necessarily an easy task!

In other cases, there is evidence for mineral fiber growth at various stages or veins forming successively during deformation. The orientation of fibers and veins reflects the orientation of ISA and thus give information about the flow parameters.

If the metamorphic conditions change during the course of deformation, structures that carry information about incremental deformation may be separated by means of metamorphic mineralogy.

1.25 Coaxiality and progressive simple shear

Earlier in this chapter we defined certain reference deformation types such as simple shear, pure shear, subsimple shear and volume change. The same deformations define progressive deformation if every increment, large or small, represents the same defor-

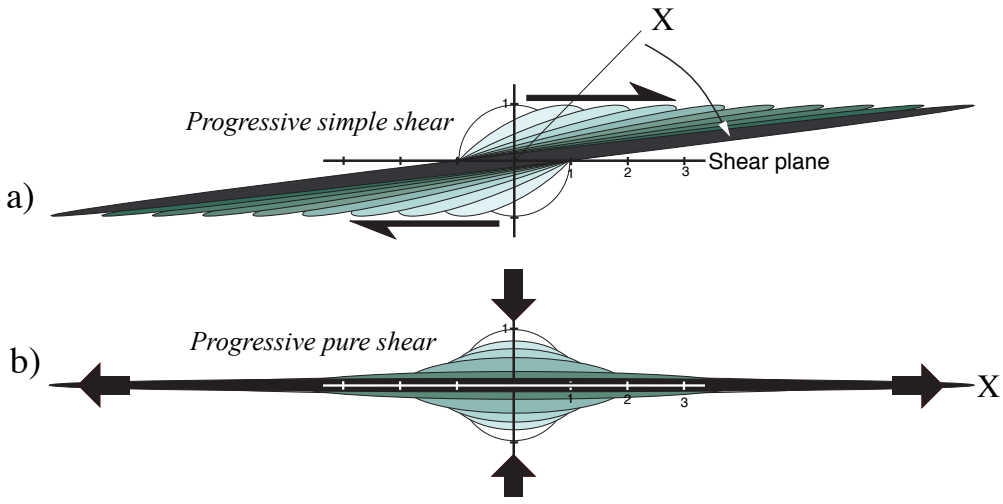

Figure 2.27 The evolution of strain during progressive simple (a) and pure (b) shear.

mation as the total one. Hence, a deformation that not only ends up at simple shear but where any interval of the deformation history can be represented by an incremental simple shear, then the deformation history is one of progressive simple shear or *simple shearing*. Similarly we have progressive pure shear or *pure shearing*, progressive subsimple shear or *subsimple shearing*, and progressive volume change or *dilating*.

Progressive deformations are separated into coaxial and non-coaxial ones. A *non-coaxial deformation history* implies that the orientation of the progressive strain ellipsoid is different at any to points in time during the deformation (Figure 2.27a). Another characteristic feature is that lines that are parallel to ISA or the principal strain axes rotate during deformation. These rotational features allow us to call them rotational deformation histories. During a *coaxial deformation history* the orientation of the strain ellipsoid is constant throughout the course of the deformation and lines parallel to ISA do not rotate. Coaxial deformation histories are therefore referred to as non-rotational.

Simple shearing involves no stretching, shortening or rotation of lines or planar structures parallel to the shear plane. Differently oriented lines will rotate towards the shearing direction as they change length, and planes will rotate towards the shear plane. The long axis of the strain ellipse also rotates towards the shear direction during the shearing history, although it will never reach parallelism with this direction.

In order to improve our understanding of simple shearing we will study a circle with six physical lines numbered from 1 to 6 (Figure 2.28). We will study what happens to three orthogonal pairs of lines, numbered 1 and 4, 2 and 5, and 3 and 6, at various stages during the shearing. At the moment the shearing starts, the rock (and circle) is stretched fastest in the direction of ISA_1 and slowest along ISA_3 (negative stretching, which actually means shortening along ISA_3). The ISA are constant during the entire history of deformation, since we are considering a steady-state deformation Two important pairs of fields occur in Figure 2.28a. In the two white fields lines are continuously being stretched, and we can call them the *fields of instantaneous stretching*. Similarly, lines in the two yellow fields continuously experience shortening and we call them the *fields of instantaneous shortening*. The borderline between these fields are the *lines of no stretching or shortening*. In three dimensions the fields become volumes and the borderlines become surfaces of no stretching or shortening. These fields remain constant during the deformation history while lines may rotate from one field to the next.

Lines 1 and 4 start out parallel to the boundary between active stretching and shortening. Line 1 lies in the shear plane and maintains its original orientation and length, i.e. remains undeformed. Line 4 quickly rotates into the stretching field towards ISA_1 (Figure 2.28b). In Figure 2.28c line 4 has rotated through ISA_1 and will also pass the long axis X of the strain ellipse if the deformation keeps going.

Lines 2 and 5 are located in the fields of shortening and stretching, respectively. In Figure 2.28b line 2 is shortened and line 5 extended, but the two lines are orthogonal at this point. They were orthogonal also before the deformation started, which means that the angular shear along these two directions is now zero. This also means that lines 2 and 5 are parallel to the strain axes at this point. They do

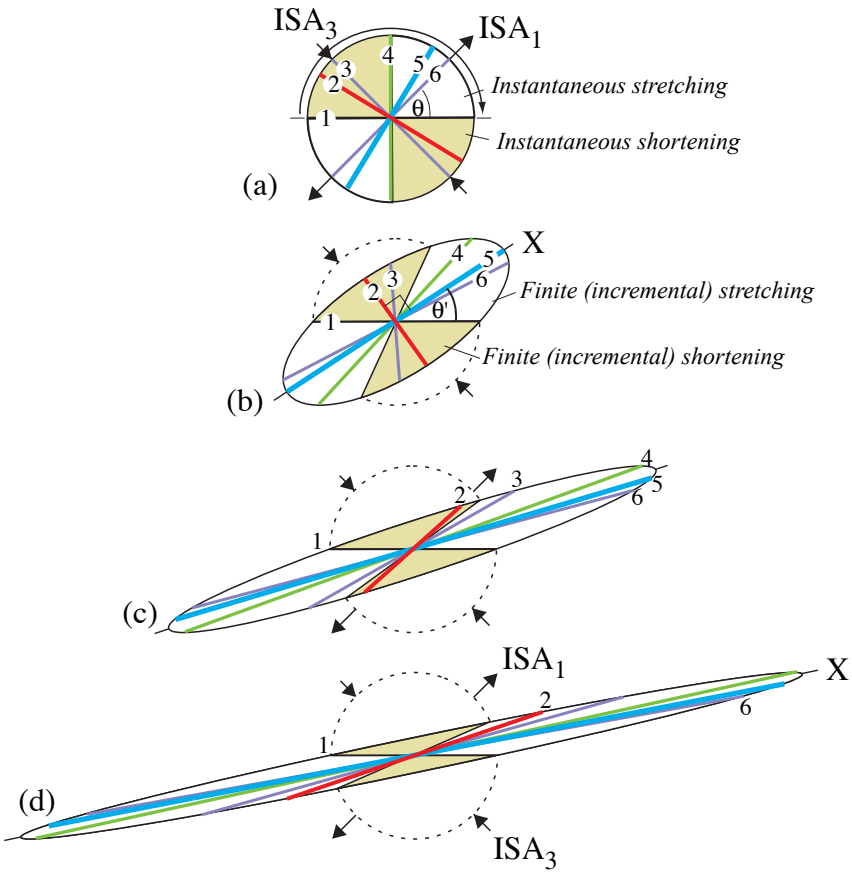

Figure 2.28 Simple shearing of a circle and three sets of orthogonal lines (1-6). The arrow along the circle in (a) indicates the rotation direction for lines during the deformation.

however rotate faster than the deformation ellipse, and in Figure 2.28c line 5 has passed X and line 2 has passed the shortest axis of the strain ellipse. In fact, line 2 is now parallel with ISA_1 and has passed the boundary between the fields of instantaneous shortening and stretching. This means that the line has gone from a history shortening into one of stretching[5]. On the way toward the last stage (Figure 2.28d) line 2 passes ISA_1 as well as the borderline between total stretching and shortening.

The last pair of lines (3 and 6) start out parallel with ISA_3 and ISA_1, respectively. Both lines immediately rotate away from the principal stretching directions because of the rotational or non-coaxial nature of simple shearing. Line 3 experiences shortening until stage (b). Soon thereafter it is stretched and its original length is restored as it passes through the borderline between the fields of instantaneous stretching and shortening (between stages b and c). It keeps being stretched as it rotates toward the shear direction. Line 6 experiences stretching during the entire deformation history, but less and less so as it rotates toward the shear direction and away from ISA. Clearly, line 6 rotates faster than X, with which it was parallel at the onset of deformation.

The deformation history can also be represented in terms of sectors, in which lines share a common history of contraction, extension or contraction followed by extension (Figure 2.29). If we start out with a randomly oriented set of lines we will soon see a field containing lines that first were shortened, then stretched (green fields in Figure 2.29). This field increases in size and will cover more and more of the field of instantaneous stretching. Note that the fields are asymmetrically distributed for simple shear and other non-coaxial deformations, but symmetric for coaxial deformations such as pure shearing (left column in Figure 2.29).

Even though the line rotations discussed here were in a plane perpendicular to the shear plane, simple shearing can cause lines and planes to rotate along many other paths. Figure 2.30 shows how lines (or particles if you wish) move along great circles when exposed to simple shearing. This is yet another characteristic feature of simple shearing that may help separating it from other deformations.

5 The total shortening is still > total stretching, which is why this line is still located in the contractional field of the cumulative strain ellipsoid.

Based on these observations we can list the following characteristics of simple shearing:

-Lines along the shear plane do not deform or rotate.
-Physical (material) lines rotate faster than the axes of the strain ellipse (generally true).
-The sense of line (and plane) rotation is the same for any line orientation.
-Lines that are parallel with the ISA rotate (generally true for non-coaxial progressive deformations).
-Lines can rotate from the field of instantaneous shortening to that of instantaneous stretching (to produce boudinaged folds) but never the other way (never folded boudins) for steady-state simple shearing
-In the Schmidt net, lines rotate along great circles toward the shearing direction

1.26 Progressive pure shear

Progressive pure shear or pure shearing is a two-dimensional coaxial deformation, i.e. the strain

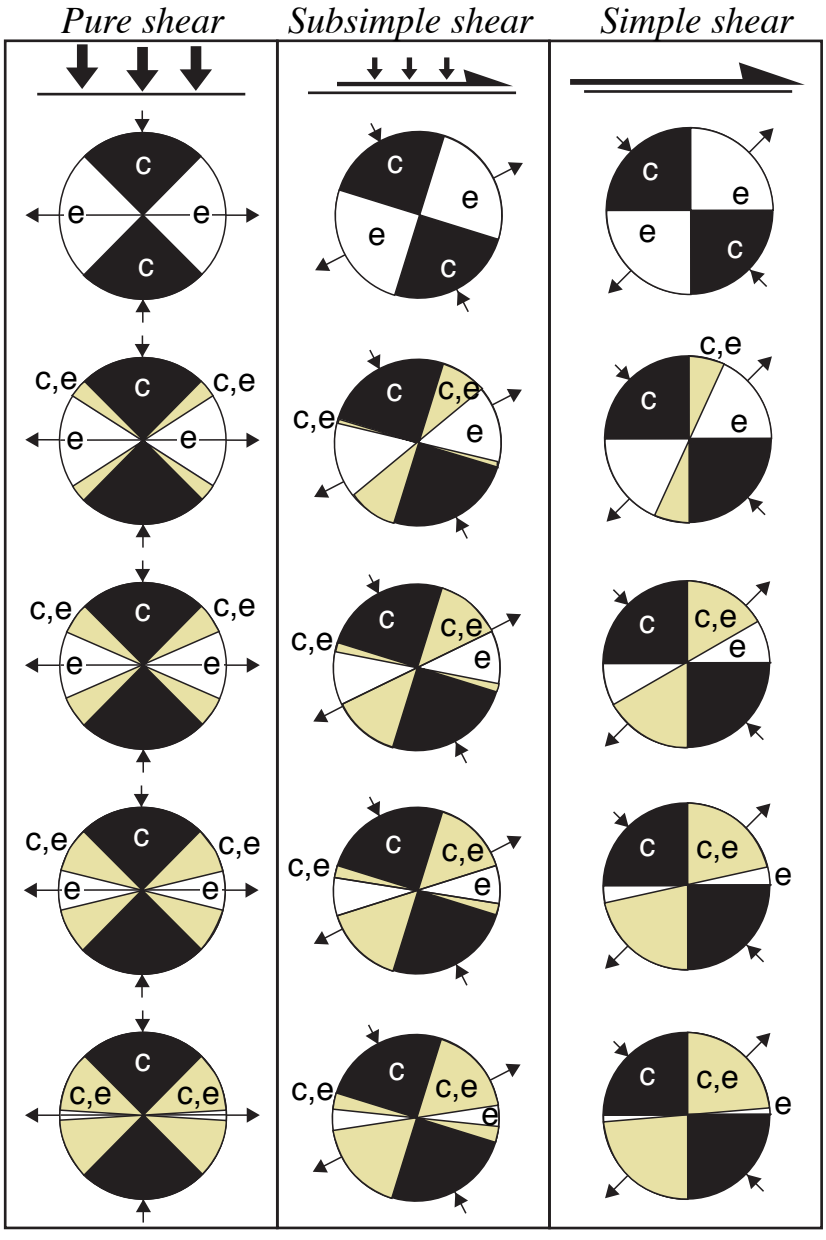

Figure 2.29 The development of sectors where lines experience a qualitatively common history. c= contractional field. e= extension field. c, e indicate that lines in this field were first shortened and then extended. Note the symmetric picture produced by pure shear and the asymmetry created by non-coaxial deformation histories. Field observations of deformed dikes and veins can be used to construct the sectors and thus the degree of coaxiality in some cases.

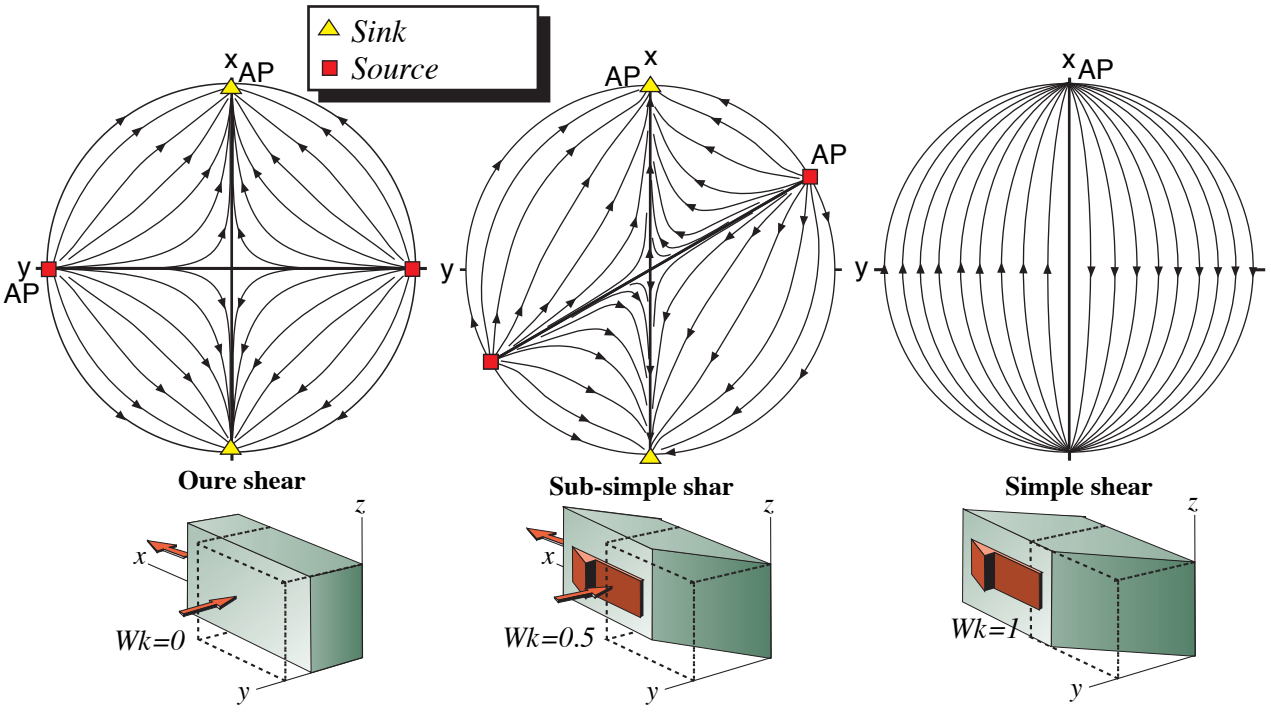

Figure 2.30 Stereographic representation of line rotation during pure shearing, subsimple shearing and simple shearing. AP=flow apophyses, where one is an attractor (sink) and the other is a repellor (source).

ellipsoid does not rotate and is fixed with respect to the ISA throughout the deformation (Figs. 2.27b and 2.29). Coaxial deformation histories result in coaxial (finite) deformations, which are characterized by symmetric deformation matrices. There is also a specter of three-dimensional coaxial deformations, as indicated in Figure 2.19.

For pure shearing the ISA and the fields of instantaneous stretching and shortening are symmetrically arranged with respect to the principal strain axes (axes of the strain ellipse). The following characteristics of pure shearing can be found by studying the different stages shown in Figure 2.31:

-The greatest principal strain axis (X) does not rotate and is always parallel with ISA_1.
-Lines that are parallel with the ISA do not rotate during the deformation.
-Any other line rotates toward X and ISA_1.
-The lines rotate both clockwise and anticlockwise in a symmetric pattern about the ISA.
-Lines that are parallel with ISA do not rotate (generally true for coaxial deformation histories)
-Lines can rotate from the shortening field and into the stretching field, but never the other way.

1.27 Progressive subsimple shear

Progressive subsimple shear or subsimple shearing can be described as a simultaneous combination of simple and pure shearing, and the component of simple shear reveals its non-coaxial nature.

The same sets of orthogonal lines that were discussed for simple and pure shearing can also be deformed under subsimple shearing. We have chosen a subsimple shearing where W_k=0.82 in Figure 2.32, which means that it has a substantial component of simple shearing. An important difference from simple shearing is that lines in the sector approximately between lines 1 and 2 rotate against the shearing direction. The size of this sector is identical to α or the angle between the flow apophyses α and depends on W_k and θ (see Figure 2.24). The smaller the pure shearing component, the larger the sector of back-rotation. For pure shearing (W_k=0) the two sectors of oppositely rotating lines are of equal size (Figure 2.31a), while for simple shearing one of them has vanished.

Line 1 is parallel to the shear plane and does not rotate, but in contrast to the case of simple shearing it is stretched in the shearing direction. Line 4 rotates clockwise and demonstrates the high degree

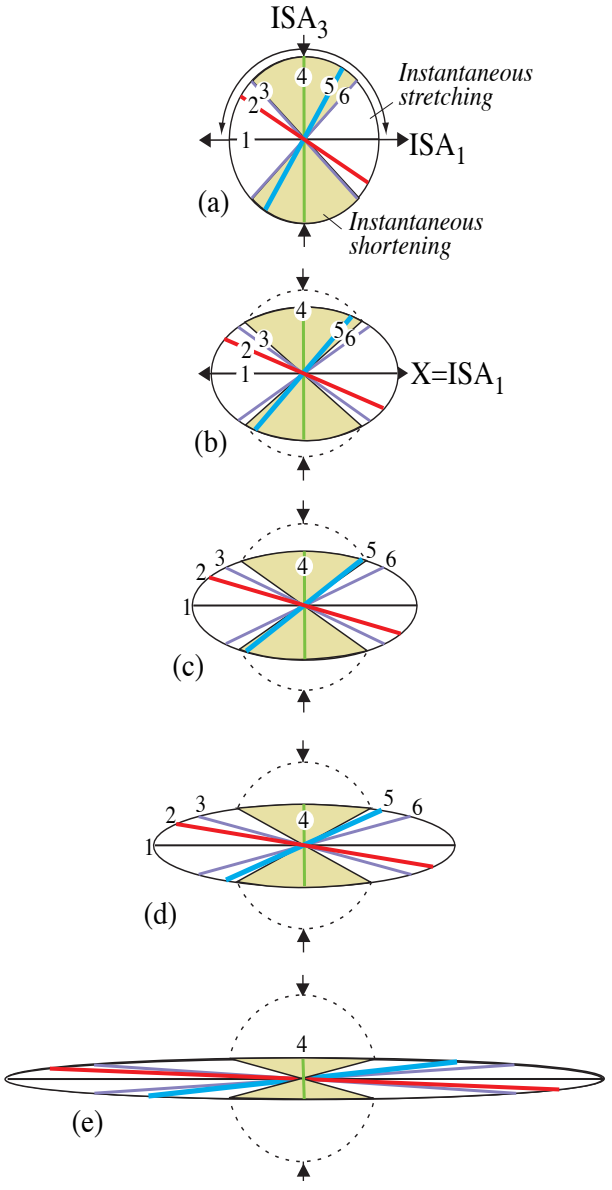

Figure 2.31 Pure shearing of a circle and three sets of orthogonal lines (1-6). The arrows along the circle in (a) indicate the rotation directions for lines during the deformation.

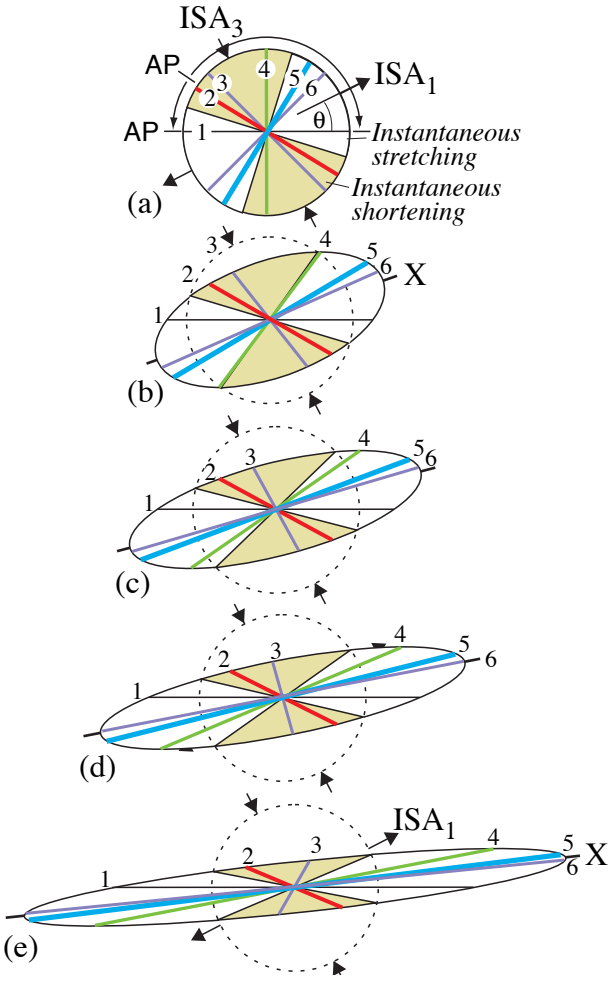

Figure 2.32 Subsimple shearing of a circle and three sets of orthogonal lines (1-6). The arrows along the circle in (a) indicate the rotation directions for lines during the deformation. AP=flow apophysis.

of non-coaxiality of this version of sub-simple shearing. Line 4 rotates from the instantaneous shortening field into that of stretching where it retains its original length at stage (b). From this point line 4 grows longer while it, together with all the other lines, rotates towards the horizontal apophysis, which is the shearing direction of the simple shearing component.

Line 2 rotates counterclockwise as it shortens, while lines 5 and 6 are stretched on their way towards the horizontal apophysis. At stage (e), line 6 has rotated through the theoretical X-axis, while line 5 has not quite reached that point.

Line 3 is in the field of instantaneous shortening. At stage (c) it parallels ISA_3 and rotates through this axis due to the non-coaxial nature of this deformation. From this point it follows the path already taken by line 4.

These are some of the characteristic features of subsimple shearing:

-Lines of any orientation rotate towards a flow apophysis (the shear direction).
-There are two sectors of opposite line rotation. The size and asymmetry of the fields is controlled by the flow apophyses and indicate W_k and one of the flow apophyses (shear direction).
-Lines of any orientation are being stretched or shortened during subsimple shearing.
-Lines parallel with ISA rotate. Only those parallel with the shear plane do not rotate.
-The long axis X of the strain ellipsoid rotates,

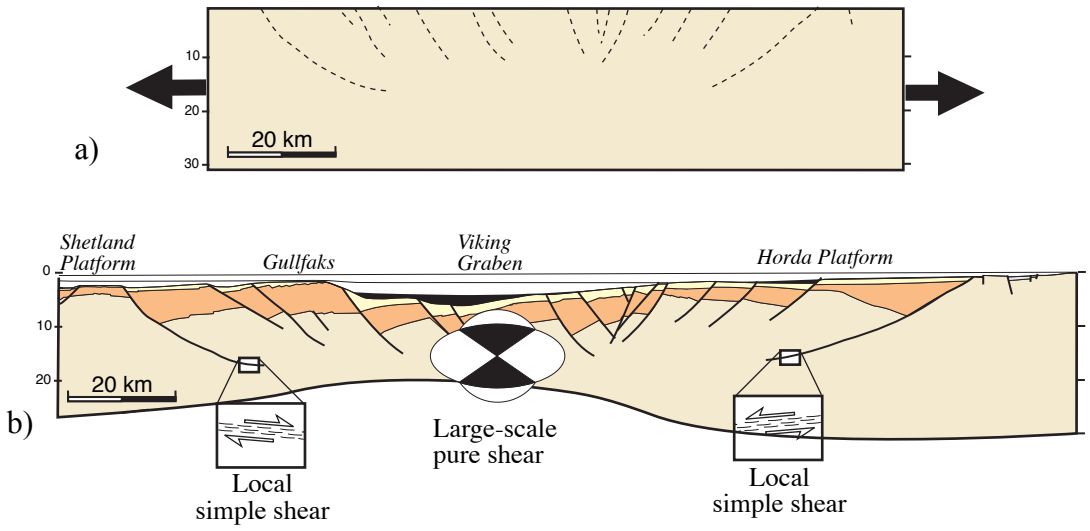

Figure 2.33 Profile across the northern North Sea rift (current and restored). Locally the deformation is simple shear, but is better treated as pure shear on a larger scale. Profile is based on Odinsen et al. (2000).

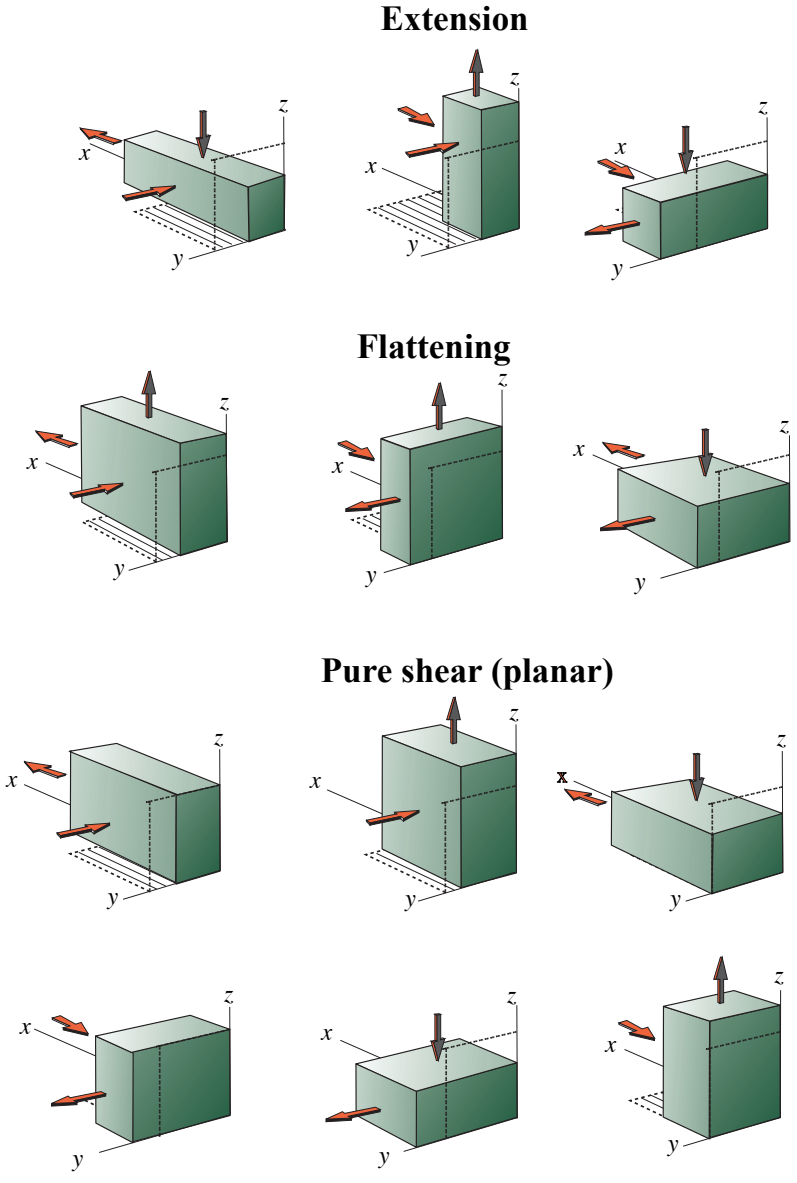

Figure 2.34 Types of coaxial strain.

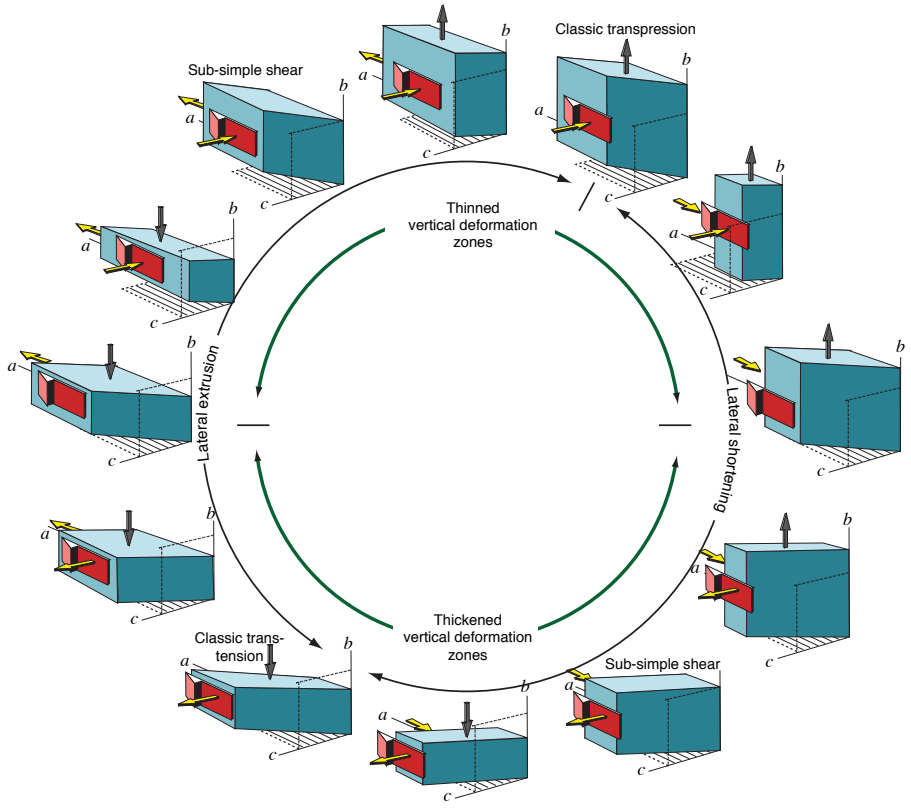

Figure 2.35 Spectrum of deformations based on combinations of a single simple shear and orthogonal coaxial deformations. Thinning shear zones occur in the upper half and thickening zones in the lower half of the circle. See Tikoff & Fossen (1999) for details.

but slower than for simple shearing.

-Lines rotate from the field of instantaneous shortening into that of instantaneous stretching, but never the other way.

1.28 Simple and pure shear and their scale dependence

Simple and pure shear(ing) are defined mathematically in this chapter. The practical use of these terms depends on the choice of coordinate system and scale. As an example, consider a simple shear zone in the crust that is 50 m thick and 5 km long. If we want to study this zone it would be natural to place a coordinate system with the x-axis in the shear direction and another axis perpendicular to the zone. One can then study or model the effect of simple shear in this zone. Now, if there should be some tens of such shear zones on a bigger scale dipping in opposite directions, then it would be better to orient the x-axis horizontally, which is parallel to the surface (or base) of the crust. In this case the deformation is closer to pure shear, although it contains simple shear zones and perhaps discrete faults on a smaller scale (Figure 2.33).

This example illustrates how deformation can be considered as simple shear on one scale and as pure shear on another. The opposite can also be the case, where there is a partitioning of the deformation on a smaller scale. Some shear zones contain small-scale domains of different deformation types that together constitute an overall simple shear. Hence, pure and simple shear are scale-dependent expressions.

1.29 General three-dimensional deformation

Strain measurements in deformed rocks typically indicate that strain is three-dimensional, i.e. they plot off the diagonal in the Flinn diagram (Figure 2.14). Three-dimensional deformation theory tends to be considerably more complex than that of plane deformation. Pure shear, which is a two-dimensional coaxial deformation, is replaced by a spectrum of coaxial deformations, where uniform extension and uniform flattening are the end members (Figure 2.19 and 2.34). Furthermore, there is room for several simple shear components in different directions, all of which can be combined with

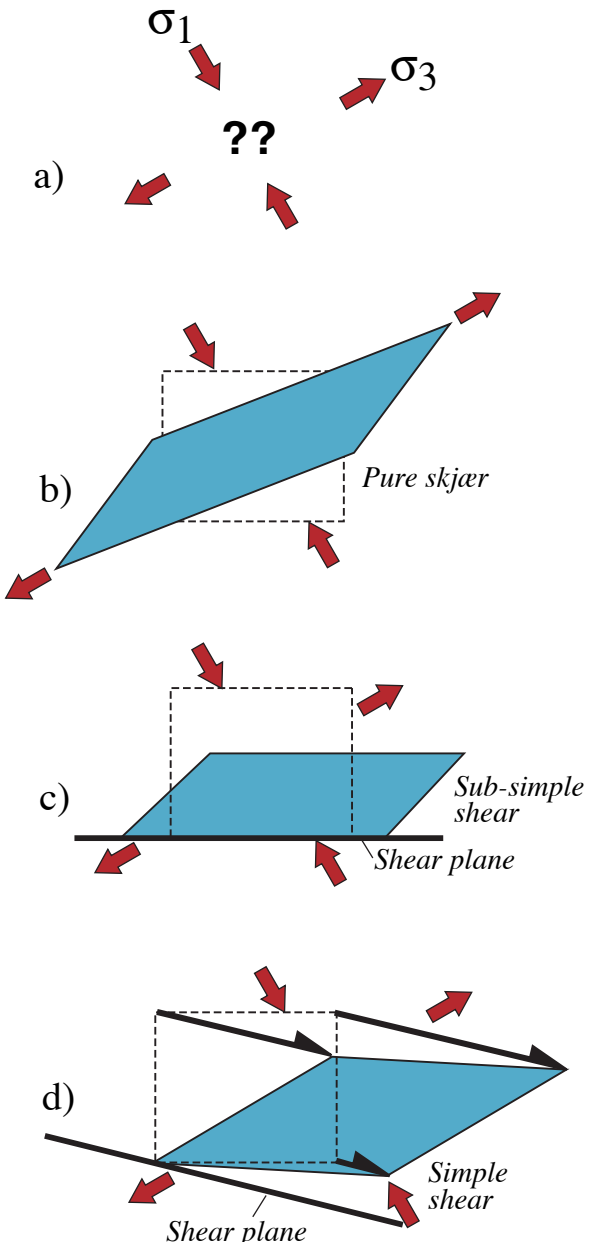

Figure 2.36 Knowledge about the orientations of the principal stresses (a) is not sufficient to predict the resulting deformation. In a perfectly isotropic medium the deformation will be a pure shear as shown in b). However, if we have a plane of weakness (shear plane), then we could have a subsimple (c) shear. In the special case where the angle between σ_1 and the weak plane is 45°, then a simple shear could result.

coaxial strain.

It is therefore useful to relate to a few simple three-dimensional deformation types, where two of the principal strain axes of the coaxial strain coincide with any shear plane involved by simple shear components. Figure 2.35 shows a spectrum of three-dimensional deformations that arises from a combination of coaxial deformations shown in Figure 2.34 with a simple shear. Transpression and transtension are some of the deformations found in this spectrum and will be discussed later in this book (Chapter 18). Also note that subsimple shear separates different types of three-dimensional deformations in Figure 2.35.

1.30 Stress versus strain

One would perhaps think that the deformation type (pure shear, simple shear, general flattening etc.) is given when the magnitudes and orientations of the three principal stresses are known. This is not so, and strain information combined with observable structures in deformed rocks usually gives more information about the deformation type than does stress information alone.

As an illustration, consider a homogeneous medium that is exposed to linear-viscous (Newtonian) deformation (Chapt. 5.1). In such an idealized medium there will be a simple relationship between stress and strain, and the ISA will parallel the principal stresses (this is the case for any isotropic medium that deforms according to a so-called power-law stress-strain rate).

Natural rocks are rarely (if ever) homogeneous, and linear-viscous deformation is an idealization of natural flow in rocks. Thus, even if we constrain our considerations to planar deformations, the orientation of the principal stresses does not predict the type of plane strain caused by the stresses in a heterogeneous rock. For a given state of stress, the deformation may be pure shear, simple shear or subsimple shear, depending on boundary conditions or heterogeneities of the deforming material. Figure 2.36 shows how the introduction of a rigid wall rock completely changes the way the rock deforms. In this case the boundary between the rigid rock and the weak, deforming rock is important. A related example is the deformation that can occur along plate boundaries. There will usually be a weak zone between the two plates along which most strain is accommodated, and the orientation of the plate boundaries will be important in addition to their relative motions. Further, the weak, deforming zone may contain faults, soft layers or other heterogeneities that cause the deformation to partition into domains dominated by coaxial and non-coaxial strains, respectively.

If it is difficult or impossible to predict strain from stress alone, can we more easily go from strain to stress? If we know only the shape and orientation

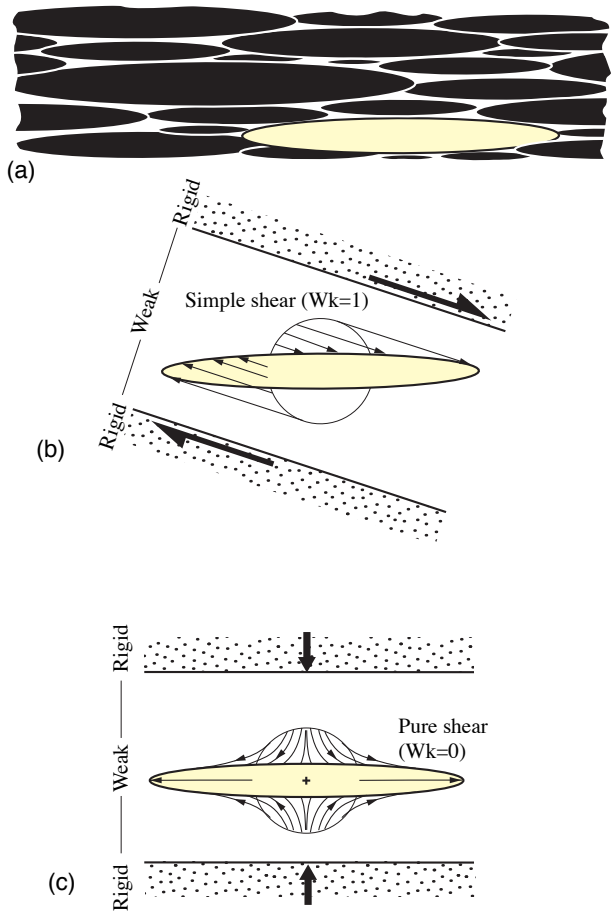

Figure 2.37 Deformed markers (a) such as strained pebbles or ooids give no information about the type of deformation. It could have been simple shear (b), pure shear (c) or any other type of deformation. Knowledge of the orientation of shear zone boundaries or lithological layering could however give us the necessary information. The yellow ellipses in the three illustrations are identical.

of the strain ellipse (ellipsoid in three dimensions), then Figure 2.37 reveals that we have no clue about the deformation type. However, if we can relate the strain to such things as shear zone boundaries, then we can find the orientation of the ISA (if we assume steady-state deformation). The question then is whether the ISA correspond to the principal stresses. Paleostress analysis relies on the assumption that they are equal, which is not necessarily quite true. We will return to this topic in Chapter 9.

----*---

In this chapter we have covered the basic theory of deformation and strain. The theory forms the foundation for most of the later chapters, where structures resulting from strain are treated. Concepts such as pure and simple shear, ISA and coaxiality will reappear throughout the text. But first of all we will look at how we can retrieve information about strain in deformed rocks.

Further reading:

General deformation theory:

Means, W.D., 1976. Stress and Strain. Springer-Verlag, New York, 339 p.

Means, W.D., 1990. Kinematics, stress, deformation and material behavior. Journal of Structural Geology, 12: 953-971.

Ramsay, J.G., 1980. Shear zone geometry: a review. Journal of Structural Geology, 2: 83-99.

Tikoff, B. & Fossen, H., 1999. Three-dimensional reference deformations and strain facies. Journal of Structural Geology, 21: 1497-1512.

The deformation matrix:

Flinn, D., 1979. The deformation matrix and the deformation ellipsoid. Journal of Structural Geology, 1: 299-307.

Fossen, H. & Tikoff, B., 1993. The deformation matrix for simultaneous simple shearing, pure shearing, and volume change, and its application to transpression/transtension tectonics. Journal of Structural Geology, 15: 413-422.

Ramberg, H., 1975. Particle paths, displacement and progressive strain applicable to rocks. Tectonophysics, 28: 1-37.

Sanderson, D.J., 1976. The superposition of compaction and plane strain. Tectonophysics, 30: 35-54.

Sanderson, D.J., 1982. Models of strain variations in nappes and thrust sheets: a review. Tectonophysics, 88: 201-233.

The strain ellipse:

Flinn, D., 1963. On the symmetry principle and the deformation ellipsoid. Geological Magazine, 102: 36-45.

Treagus, S.H. & Lisle, R.J., 1997. Do principal surfaces of stress and strain always exist. Journal of Structural Geology, 19: 997-1010.

Mohr's circle for strain:

Passchier, C.W., 1988. The use of Mohr circles to describe non-coaxial progressive deformation. Tectonophysics, 149: 323-338.

Volumetric strain:
Xiao, H. B., & Suppe, J., 1989. Role of compaction in listric shape of growth normal faults: American Association of Petroleum Geologists Bulletin, 73: 777-786.
Passchier, C. W., 1991. The classification of dilatant flow types: Journal of Structural Geology, 13: 101-104.

Vorticity and deformation history:
Elliott, D., 1972. Deformation paths in structural geology. Geological Society of America Bulletin, 83: 2621-2638.
Ghosh, S.K., 1987. Measure of non-coaxiality. Journal of Structural Geology, 9: 111-113.
Jiang, D., 1994. Vorticity determination, distribution, partitioning and the heterogeneity and non-steadiness of natural deformations. Journal of Structural Geology, 16: 121-130.
Passchier, C.W., 1990. Reconstruction of deformation and flow parameters from deformed vein sets. Tectonophysics, 180: 185-199.
Talbot, C.J., 1970. The minimum strain ellipsoide using deformed quartz veins. Tectonophysics, 9: 47-76.
Tikoff, B. & Fossen, H., 1995. The limitations of three-dimensional kinematic vorticity analysis. Journal of Structural Geology, 17: 1771-1784.
Truesdell, C., 1953. Two measures of vorticity. Journal of Rational Mechanics and Analysis, 2: 173-217.
Wallis, S.R., 1992. Vorticity analysis in a metachert from the Sanbagawa Belt, SW Japan. Journal of Structural Geology, 12: 271-280.

CHAPTER 3

Strain in rocks

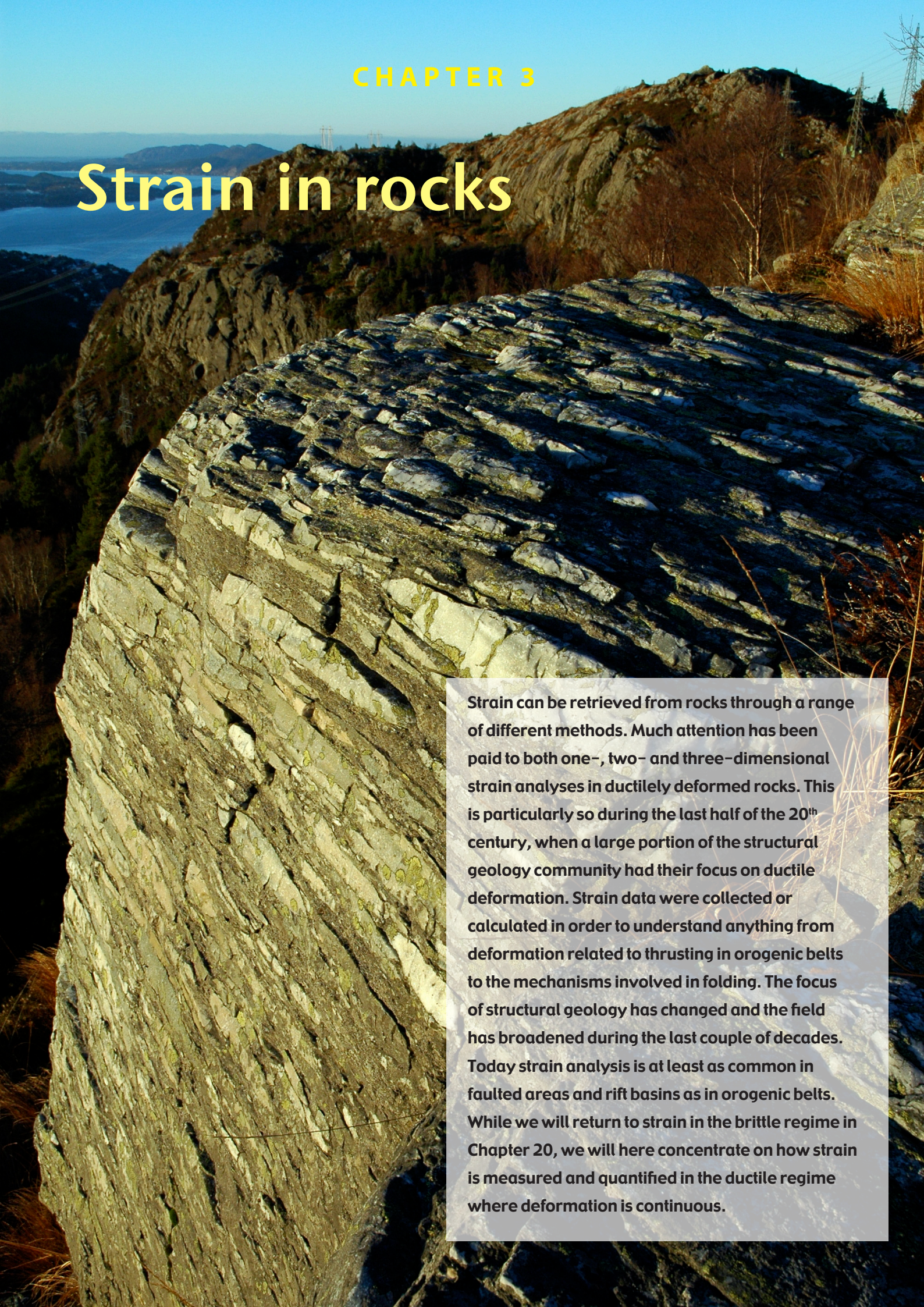

Strain can be retrieved from rocks through a range of different methods. Much attention has been paid to both one-, two- and three-dimensional strain analyses in ductilely deformed rocks. This is particularly so during the last half of the 20th century, when a large portion of the structural geology community had their focus on ductile deformation. Strain data were collected or calculated in order to understand anything from deformation related to thrusting in orogenic belts to the mechanisms involved in folding. The focus of structural geology has changed and the field has broadened during the last couple of decades. Today strain analysis is at least as common in faulted areas and rift basins as in orogenic belts. While we will return to strain in the brittle regime in Chapter 20, we will here concentrate on how strain is measured and quantified in the ductile regime where deformation is continuous.

1.1 Why perform strain analysis?

It can be important to retrieve information about strain from deformed rocks. First of all, strain analysis gives us an opportunity to explore the state of strain in a rock and to map out strain variations in a sample, an outcrop or a region. Knowledge about strain localization is important in the mapping and understanding of shear zones in orogenic belts. Strain measurements can also be used to estimate the amount of offset across a shear zone. As will be discussed in chapter 15, it is possible to extract important information from shear zones if strain is known.

In many cases it is useful to know if the strain is planar or three-dimensional. If planar, an important criterion for section balancing is fulfilled, be it across orogenic zones or extensional basins. The shape of the strain ellipsoid may also contain information about how the deformation occurred. Oblate (pancake-shaped) strain in an orogenic setting may for example indicate flattening strain related to deep gravity-driven collapse.

The orientation of the strain ellipsoid is also important, particularly in relation to rock structures. In a shear zone setting, it may tell us if the deformation was coaxial or not (Chapter 15). Strain in folded layers helps understand the fold-forming mechanism(s) (Chapter 11). Studies of deformed reduction spots in slates give good estimates on how much shortening has occurred across the foliation in such rocks (Chapter 12), and that has implications for things such as reconstruction of original sedimentary thickness. Strain will follow us through the chapters of this book.

Figure 3.1 Two elongated belemnites in Jurassic limestone in the Swiss Alps. The different ways that the two belemnites have been stretched gives us some two-dimensional information about the strain field: the upper belemnite has experienced significant sinistral shear strain while the lower one has not and is therefore close to the maximum stretching direction in this section.

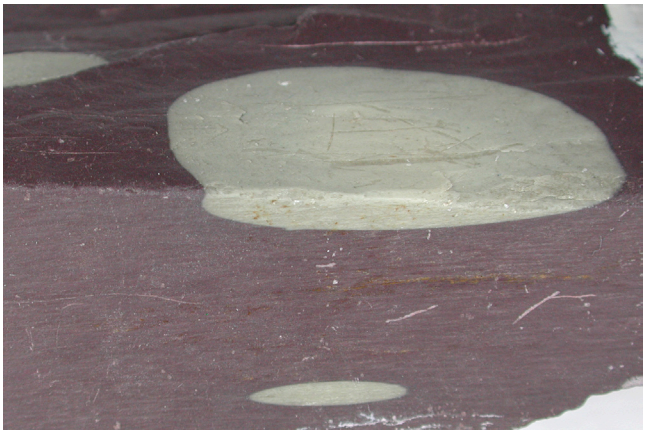

Figure 3.2 Reduction spots in Welsh slate. The light spots formed as spherical volumes of bleached (chemically reduced) rock. Their new shapes are elliptical in cross section and oblate (pancake-shaped) in three dimensions, reflecting the tectonic strain in these slates.

1.2 Strain in one dimension

One-dimensional strain analyses are concerned with changes in length only and therefore the simplest form of strain analysis we have. If we can reconstruct the original length of an object or linear structure we can also calculate the amount of stretching or shortening in that direction. Objects revealing the state of strain in a deformed rock are known as *strain markers*. Examples of strain markers indicating change in length are boudinaged dikes or layers, and minerals or linear fossils such as belemnites or graptolites that have been elongated (Figure 3.1). Or it could be a layer shortened by folding. It could even be a faulted reference horizon on a geologic or seismic profile, as will be discussed in Chapter 20. The horizon may be stretched by normal faults or shortened by reverse faults, and the overall strain is referred to as *brittle strain*. One-dimensional strain is revealed when the horizon, fossil, mineral or dike is restored to its pre-deformational state.

1.3 Strain in two dimensions

In *two-dimensional strain analyses* we look for sections that have objects with known initial shape (Figure 3.2) or contain linear markers with a variety of orientations (Figure 3.1). Sections through conglomerates, breccias, corals, reduction spots, oolites, vesicles, pillow lavas, columnar basalt, plutons and so on are examples of objects that have been used (Fig. 3.3). Two-dimensional strain can also be calculated from one-dimensional data that represent different directions in the same section. A typical example would be dikes with different orientations that show different amounts of extension.

1.3.1 Changes in angles

Strain can be found if we know the original angle between sets of lines. The original angular relations between structures such as dikes, foliations and bedding are sometimes found in both undeformed and deformed states, i.e. outside and inside a deformation zone. We can then see how the strain has affected the angular relationships and use this information to estimate strain. In other cases orthogonal lines of symmetry found in undeformed fossils such as trilobites, brachiopods, and worm burrows (angle with layering) can be used to determine the angular shear in some deformed sedimentary rocks. In general, all we need to know is the change in angle between sets of lines and that there is no strain partitioning due to contrasting mechanical properties of the objects with respect to the enclosing rock.

If the angle was 90° in the undeformed state, the change in angle is 90-ψ, where ψ is the local angular shear (Section 2.8). If, as you may recall from page ??, the two originally orthogonal lines remain orthogonal after the deformation, then they must represent the principal strains and thus the orientation of the strain ellipsoid. Observations of variously oriented line sets thus give information about the strain ellipse or ellipsoid. All we need is a useful method. Two of the most common methods used to find strain from initially orthogonal lines are known as the Wellman and Breddin methods, and are presented in the following sections.

Wellmann's method

This method dates back to 1962 and is a geometric construction for finding strain in two dimensions (in a section). It is typically demonstrated on fossils with orthogonal lines of symmetry in the undeformed state. In Figure 3.3a we use the hinge and symmetry lines of brachiopods. A line of reference must be drawn (with arbitrary orientation) and pairs of lines that were orthogonal in the unstrained state are identified. The reference line must have two defined endpoints, named A and B in Figure 3.4b. A pair of lines is then drawn parallel to both the hinge line and symmetry line for each fossil, so that they intersect at the endpoints of the reference line. The other two points of intersection (numbered in Figure 3.4b) are marked (numbered 1-6 in Figure 3.4b and c). If the rock is unstrained, the lines will define rectangles. If there is a strain involved, they will define parallelograms. To find the strain ellipse, simply fit an ellipse to the numbered corners of the parallelograms (Figure 3.4c). If no ellipse can be fitted to the corner points of the

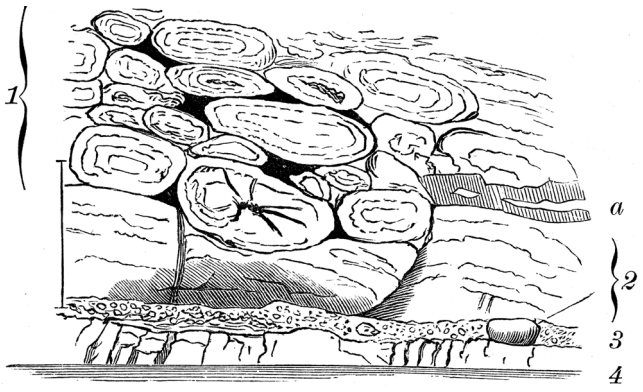

Figure 3.3 Section through a deformed Ordovician pahoe-hoe lava. The elliptical shapes were originally more circular, and Hans Reusch, who made the scetch in the 1880's, understood that they had been flattened during deformation.The R_f/ϕ-, center-to-center, and Fry methods would all be useful methods in this case.

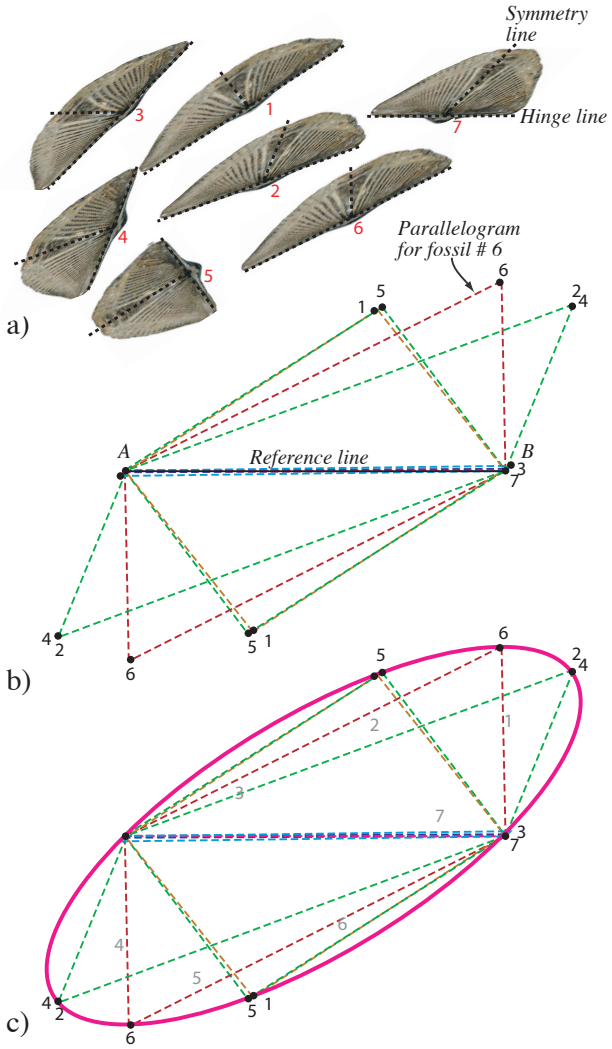

Figure 3.4 Wellman's method for construction of the strain ellipse by drawing parallelograms based on the orientation of originally orthogonal pairs of lines. The deformation was produced on a computer and is a homogeneous simple shear of γ=1. However, the strain ellipse itself tells nothing about the degree of coaxiality: the same result could have been attained by pure shear.

rectangles the strain is heterogeneous or, alternatively, the measurements or assumption of initial orthogonality is false. The challenge with this method is, of course, to find enough fossils or other features with initially orthogonal lines – typically 6-10 are needed.

Breddin's graph

We have already stated that the angular shear depends on the orientation of the principal strains: the closer the deformed orthogonal lines are to the principal strains, the lower the angular shear. This fact is utilized in a method first published in 1956 in German (with some errors). It is based on a graph where the angular shear changes with orientation and strain magnitude R. Input are the angular shears and the orientations of the sheared line pairs with respect to the principal strains. These data are plotted in the so-called Breddin's graph and the R-value (ellipticity of the strain ellipse) is found by inspection (Figure 3.5). This method works even for only one or two observations.

In many cases the orientation of the principal axes is unknown. In this case the data are plotted with respect to an arbitrarily drawn reference line. The data are then moved horizontally on the graph until they fit one of the curves, and the orientations of the strain axes are then found at the intersections with the horizontal axis (Figure 3.5). In this case a larger number of data are needed for good results.

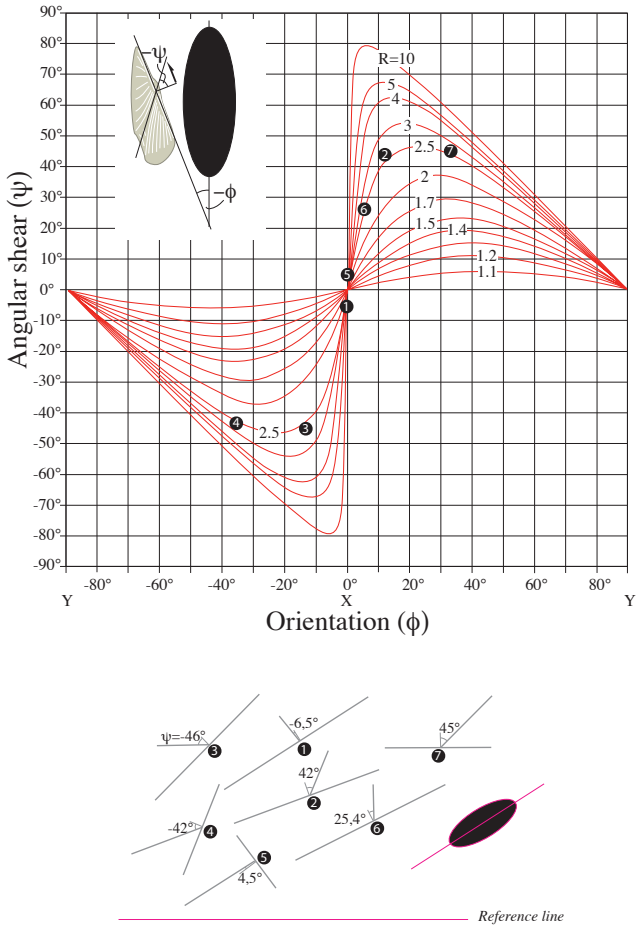

Figure 3.5 The data from the previous figure plotted in a Breddin graph. The data points are close to the curve for R=2.5.

1.3.2 Elliptical objects and the R_f/ϕ-method

Objects with circular (in sections) or spherical (in three dimensions) geometry are relatively uncommon but do occur. Reduction spots and ooliths perhaps form the most perfect spherical shapes in sedimentary rocks. When deformed homogeneously, they are transformed into ellipses and ellipsoids that reflect the local finite strain. Conglomerates are perhaps more common and contain clasts that reflect the finite strain. In contrast to oolites and reduction spots, few pebbles or cobbles in a conglomerate are spherical in the undeformed state. This will of course influence their shape in the deformed state and causes a challenge in strain analyses. However, the clasts tend to have their long axes in a spectrum of orientations in the undeformed state, in which case methods such as the R_f/ϕ-method may be able to take the initial shape factor into account.

The R_f/ϕ-method was first introduced by John Ramsay in his well known 1967 textbook and has later been improved. The method is illustrated in Figure 3.6. The markers are assumed to have approximately elliptical shapes in the deformed (and undeformed) state, and they must have somewhat different orientations for the method to work. The ellipticity (X/Y) in the undeformed (initial) state is called R_i. In our example (Figure 3.6) R_i=2.

After a strain R_s the markers exhibit new shapes. The new shapes are different and depend on the initial orientation of the elliptical markers. The new (final) ellipticity for each deformation marker is called R_f and the spectrum of R_f-values is plotted against their orientations, or more specifically against the angle ϕ' between the long axis of the ellipse and a reference line (horizontal in Figure 3.6). In our example we have applied two increments of pure shear to a series of ellipses with different orientations. All the ellipses have the same initial shape R_i=2, and they plot along a vertical line in the upper right diagram in Figure 3.6. Ellipse 1 is oriented with its long axis along the minimum principal strain axis, and it is converted into an ellipse that shows less strain (lower R_f -value) than the true strain ellipse (R_s). Ellipse 7, on the other hand, is oriented with its long axis parallel to the long axis of the strain ellipse, and the two ellipticities are added. This leads to an ellipticity that is higher than R_s. Once R_s=1.5, the true strain R_s is located somewhere between the shape represented by ellipses 1 and 7, as seen in Figure 3.6 (lower right diagram).

For R_s=1.5 we still have ellipses with the full spectrum of orientations (-90° to 90°; see middle

diagram in Figure 3.6), while for R_s=3 there is a much more limited spectrum of orientations (lower graph in Figure 3.6). The scatter in orientation is called the fluctuation F. An important change happens when ellipse 1, which has its long axis along the Z-axis of the strain ellipsoid, passes the shape of a circle (R_s=R_i,) and starts to develop an ellipse whose long axis is parallel to X. This happens when R_s=2, and for larger strains the data points define a circular shape. Inside this shape is the strain R_s that we are interested in. But where exactly is R_s? A simple average of the maximum and minimum R_f -value would depend on the original distribution of orientations. Even if the initial distribution is random, the average R-value would be too high, as high values tend to be overrepresented (Figure 3.6, lower graph).

To find R_s we have to treat the cases where R_s>R_i and R_s<R_i separately. In the latter case, which is represented by the middle graph in Figure 3.6, we have the following expressions for the maximum and minimum value for R_f:

$$R_{fmax} = R_s R_i$$
$$R_{fmin} = R_i / R_s$$

Solving for R_i and R_s gives

$$R_s = (R_{fmax} / R_{fmin})^{1/2}$$

$$R_i = (R_{fmax} R_{fmin})^{1/2}$$

which represent expressions for both the strain related to the deformation and the initial ellipticity.

For higher-strain cases, where R_s<R_i, we obtain:

$$R_{fmax} = R_s R_i$$
$$R_{fmin} = R_s / R_i$$

Solving for R_s gives

$$R_s = (R_{fmax} R_{fmin})^{1/2}$$

$$R_i = (R_{fmax} / R_{fmin})^{1/2}$$

In both cases the orientation of the long (X) axis of the strain ellipse is given by the location of the maximum R_f-values. Strain could also be found by fitting the data to pre-calculated curves for various values for R_i and R_s. In practice, such operations are most efficiently done by means of computer programs.

The example shown in Figure 3.6 and discussed above is idealized in the sense that all the undeformed elliptical markers have identical ellipticity. What if this was not the case, i.e. some markers were more elliptical than others? Then the data would not have defined a nice curve but a cloud of points in the R_f/ϕ-diagram. Maximum and minimum R_f-values could still be found and strain could be calculated using the equations above. The only change in the equation is that R_i now represents the maximum ellipticity present in the

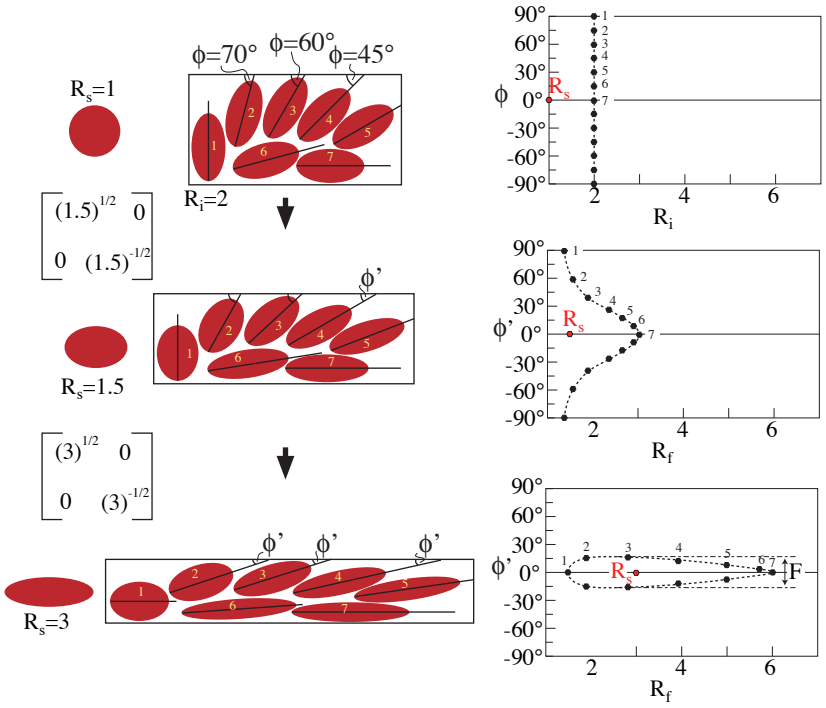

Figure 3.6 The R_f/ϕ method illustrated. The ellipses has the same ellipticity (R_i) before the deformation starts. The R_f-ϕ diagram to the right indicates that R_i=2. A pure shear is then added with R_S=1.5 followed by a pure shear strain of R_S=3. The deformation matrices for these two deformations are shown. Note the change in the distribution of points in the diagrams to the right. R_S in the diagrams is the actual strain that is added. Modified from Ramsay & Huber (1983).

undeformed state.

Another complication that may arise is that the initial markers may have had a restricted range of orientations. Ideally, the R_f/ϕ-method requires the elliptical objects to be more or less randomly oriented prior to deformation. Conglomerates, to which this method commonly is applied, tend to have clasts with a preferred orientation. This may result in a R_f-ϕ plot in which only a part of the curve or cloud is represented. In this case the maximum and minimum R_f-values may not be representative, and the formulas above may not give the correct answer and must be replaced by an computer-based iterative retrodeformation method where X is input. However, many conglomerates have a few clasts with initially anomalous orientations that allow the use of R_f-ϕ analysis.

1.3.3 Center-to-center method

This method is based on the assumption that circular objects have a more or less statistically uniform distribution in our section(s). This means that the distances between neighboring particle centers was fairly constant before deformation. The particles could represent sand grains in well-sorted sandstone, pebbles, ooids, mud crack centers, pillow-lava or pahoe-hoe lava centers, pluton centers or other objects that are of similar size and where the centers are easily definable. If you are unsure about how closely your section complies with this criterion, try anyway. If the method yields a reasonably well-defined ellipse, then the method works.

The method itself is simple: Measure the distance and direction from the centre of an ellipse to those of its neighbors. Repeat this for all ellipses and graph the distance d' between the centers and the angles α' between the center tie lines and a reference line (Figure 3.7). A straight line occurs if the section is unstrained, while a deformed section yields a curve with maximum (d'_{max}) and minimum values (d'_{min}). The ellipticity of the strain ellipse is then given by the ratio: $R_s=(d'_{max})/(d'_{min})$.

1.3.4 The Fry method

A quicker and visually more attractive method for finding two-dimensional strain was developed by Norman Fry at the end of the 1970's. This method is based on the center-to-center method and is most easily dealt with using one of several available computer programs. It can be done manually by placing a tracing overlay with a coordinate origin and pair of reference axes on top of a sketch or picture of the section. The origin is placed on a particle center and the centers of all

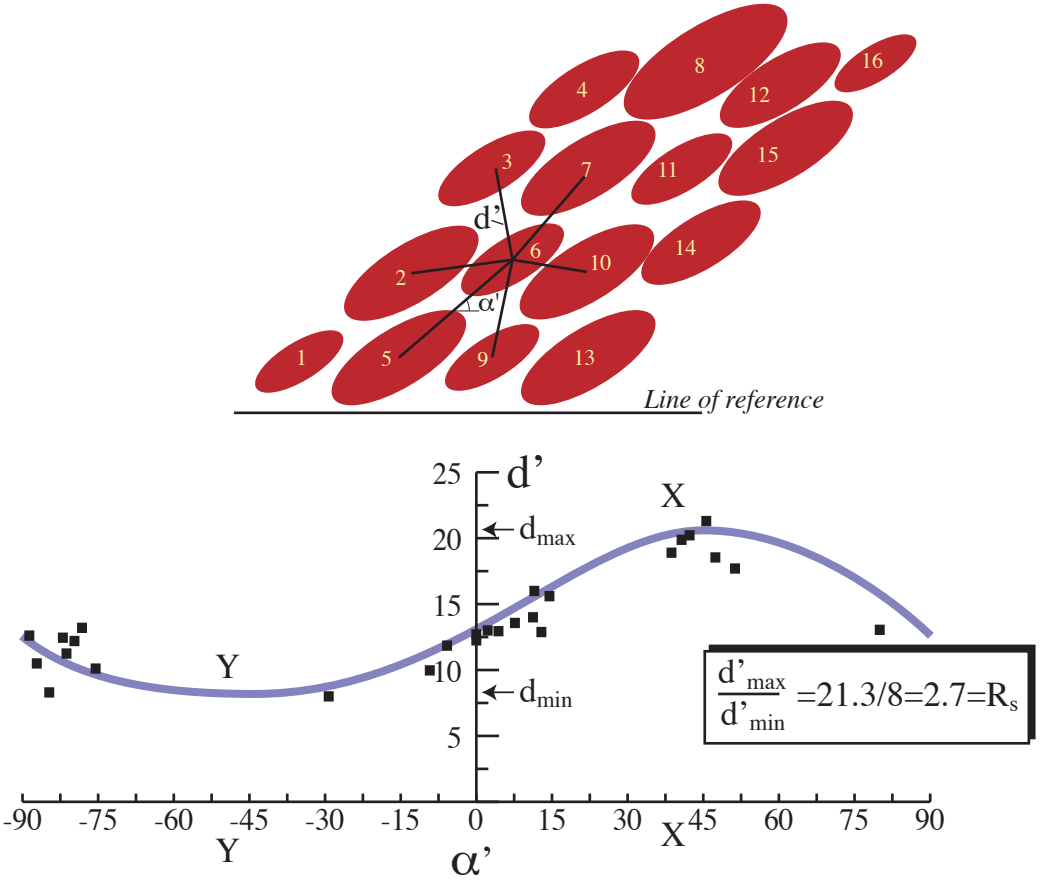

Figure 3.7 The center-to-center method. Straight lines are drawn between neighboring object centers. The length of each line (d') and the angle (α') that they make with a reference line are plotted in the diagram. The data define a curve which has a maximum at X and a minimum at the Y-value of the strain ellipse, and where R_S=X/Y

Strain around a fold

Deformed conglomerates are an important source of strain data in deformed rocks because conglomerates are relatively common and contain large numbers of objects (clasts). An example is shown where strain was evaluated at several stations around a folded conglomerate layer, deformed under greenschist facies conditions. It was found that the long limbs were totally dominated by flattening strain (oblate strain geometry) while there was a change towards constrictional strain in the hinge and short limb area. This information would have been difficult to achieve without the mesoscopic strain markers, because the rock is recrystallized so that the original sand grain boundaries are obliterated.

The conglomerate in a constrictional state of strain

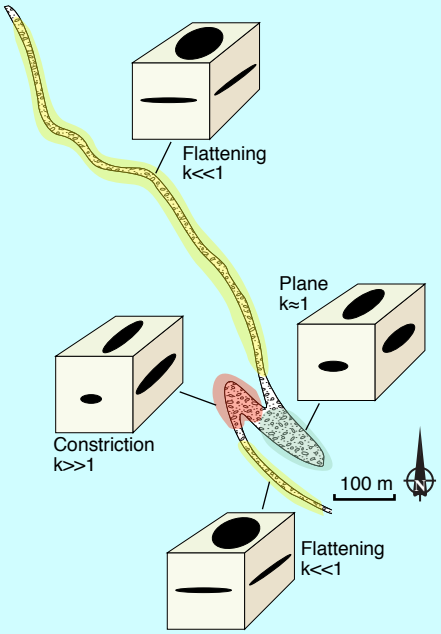

Map of the conglomerate layer. Note the thickened short fold limb.

The strain data then had to be explained, and were found to fit a model where an already flattened conglomerate layer is rotated into the field of constriction during shearing. A dextral shear rotates the foliation and the oblate clasts into the shortening field (k<1), which makes the Y-axis shrink. This takes the strain ellipsoid across the plane strain diagonal of the Flinn diagram and eventually into the constrictional field (k>1). At this point we are on the inverted limb or at the lower fold hinge. The process continues, and the strain ellipse again becomes flattened. This model explains strain data by means of a particular deformation history, defining a certain strain path which in this case is flattening to constriction and back to flattening strain.

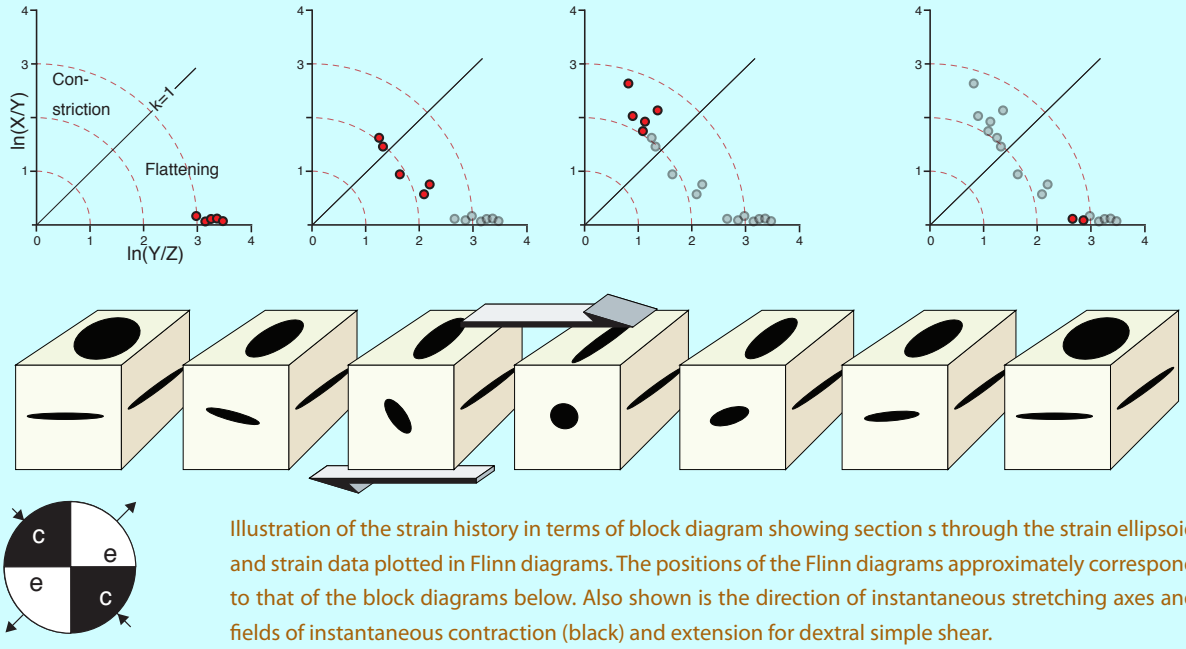

Illustration of the strain history in terms of block diagram showing section s through the strain ellipsoid and strain data plotted in Flinn diagrams. The positions of the Flinn diagrams approximately correspond to that of the block diagrams below. Also shown is the direction of instantaneous stretching axes and fields of instantaneous contraction (black) and extension for dextral simple shear.

other particles (not just the neighbors) are marked on the tracing paper. The tracing paper is then moved, without rotating the paper with respect to the section, so that the origin covers a second particle center, and the centers of all other particles are again marked on the tracing paper. This procedure is repeated until the area of interest has been covered. For objects with a more or less uniform distribution the result will be a visual representation of the strain ellipse. The ellipse is the void area in the middle, defined by the point cloud around (Figure 3.8c).

The Fry method, as well as the other methods presented in this section, output two-dimensional strain. Three-dimensional strain is found by combining strain estimates from two or more sections through

the deformed rock volume. If sections can be found that each contain two of the principal strain axes, then two sections are sufficient. In other cases three or more sections are needed, and the three-dimensional strain must be calculated by use of available computer software (see www.geo.uib.no/struct/).

1.4 Strain in three dimensions

A complete strain analysis is *three-dimensional*. Three-dimensional strain data are presented in the Flinn diagram or similar diagrams that describe the shape of the strain ellipsoid, also known as the *strain geometry*. In addition, the orientation of the principal strains can be presented by means of stereographic nets. Direct field observations of three-dimensional strain are rare. In almost all cases it is based on two-dimensional strain observations from two or more sections at the same locality (Fig. 3.9).

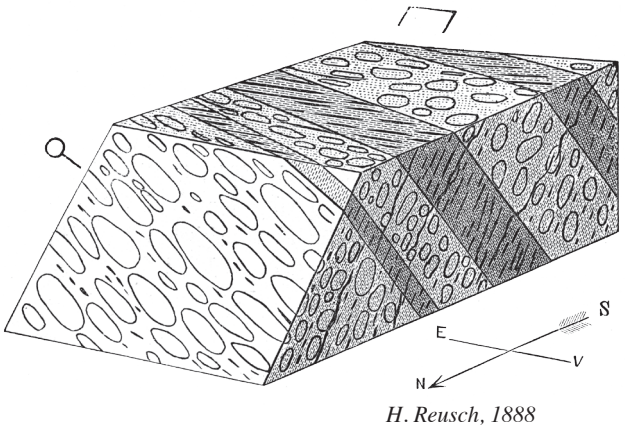

Figure 3.9. Three-dimensional strain expressed as ellipses on different sections through a conglomerate. The foliation (X-Y plane) and the lineation (X-axis) are annotated. This illustration was published in 1888, but what is now routine strain estimates were not developed until the 1960's.

In order to quantify ductile strain the following conditions need to be met:

The deformation must be homogeneous within the area or volume under consideration, the mechanical properties of the objects must have been similar to those of their host rock during the deformation, and we must have a reasonably good knowledge about the original shape of strain markers.

The first point is obvious. If the strain is heterogeneous we have to look at another scale, either a larger one where the heterogeneities vanish, or subareas where strain can be considered to be approximately homomgeneous.

The second point is an important one. For ductile rocks it means that the object and its surroundings must have had the same competence or viscosity (see chapter 5). Otherwise the strain recorded by the object would be different from that of its surroundings. This effect is one of several types of *strain partitioning*, where the overall strain is distributed unevenly in terms of intensity and/or geometry in a rock volume. As an example, we mark a perfect circle on a piece of clay before flattening it between two walls. The circle transforms passively into an ellipse that reveals the two-dimensional strain if the deformation is homogeneous. If we embed a colored sphere of the same clay, then it would again deform along with the rest of the clay, revealing the three-dimensional strain involved. However, if we put a stiff marble in the clay the result becomes quite different. The marble remains unstrained while the clay around gets more intensely and heterogeneously strained than in the previous case. In fact, it causes a more heterogeneous strain pattern to appear. Strain markers with the same mechanical properties as the surroundings are called *passive strain markers* because they deform passively along with its surroundings. Those that have

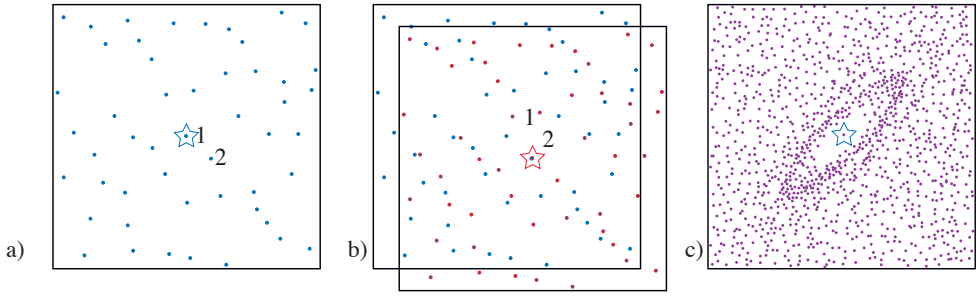

Figure 3.8 The Fry-method performed manually. a) The centerpoints for the deformed objects are transfered to a transparent overlay. A central point (1 at the figure) is defined. b) The transparent paper is then moved to another of the points (point 2) and the centerpoints are again transfered onto the paper (the overlay must not be rotated). The procedure is repeated for all of the points, and the result (c) is an image of the strain ellipsoid (shape and orientation). Based on Ramsay & Huber (1983).

Deformed quartzite conglomerates

Quartz or quartzite conglomerates with a quartzite matrix are commonly used for strain analyses. The more similar the mineralogy and grain size of the matrix and the pebbles, the less deformation partitioning and the better the strain estimates. A classical study of deformed quartzite conglomerates is Jake Hossack's study of the Norwegian Bygdin conglomerate, published in 1968. Hossack was fortunate – he found natural sections along the principal planes of the strain ellipsoid at each locality. Putting the sectional data together gave the three-dimensional state of strain (strain ellipsoid) for each locality. Hossack found that strain geometry and intensity varies within his field area. He related the strain pattern to static flattening under the weight of the overlying Caledonian Jotun Nappe. Although details of his interpretation may be challenged, his work demonstrates how conglomerates can reveal a complicated strain pattern that otherwise would have been impossible to map.

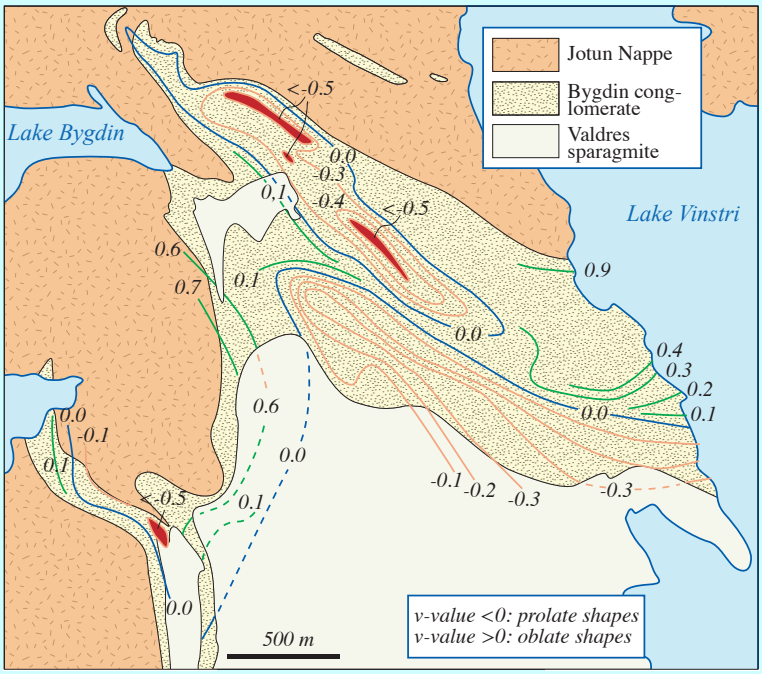

Hossack's strain map from the Bygdin area.
Left: The Bygdin conglomerate

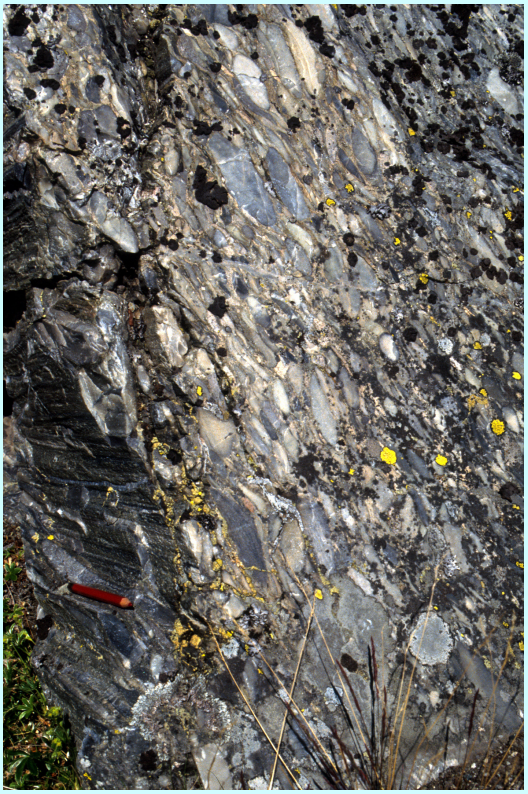

The Bygdin conglomerate at Bygdin.

Hossack noted the following sources of error:
- Inaccuracy connected with data collection (sections not being perfectly parallel to the principal planes of strain and measuring errors).
- Variations in pebble composition.
- The pre-deformational shape and orientation of the pebbles.
- Viscosity contrasts between clasts and matrix.
- Volume changes related to the deformation (pressure solution).
- The possibility of multiple deformation events.

anomalous mechanical properties respond differently than the surrounding medium to the overall deformation, and such markers are called *active strain markers*.

A natural example of active strain markers is shown in Figure 3.10. These data are collected from a deformed polymictic conglomerate where three-dimensional strain has been estimated from different clast types in the same rock and at the same locality. Clearly, the different clast types have recorded different amounts of strain. Competent (stiff) granitic clasts are less strained than less competent greenstone clasts. This is seen using the fact that strain intensity generally increases with increasing distance from the origin in Flinn space. But there is another interesting thing to note from this figure: It seems that competent clasts plot lower in the Flinn diagram (Fig. 3.10a) than incompetent ("soft") clasts (Fig. 3.10b), meaning that competent clasts take on a more prolate shape. Hence, not only strain intensity but also strain geometry may vary according to the mechanical properties of strain markers.

The way that the different markers behave depends on factors such as their mineralogy, preexisting fabric, grain size, water content and temperature-pressure conditions at the time of deformation. In the case of Figure 3.10, the temperature-pressure regime is that of lower to middle greenschist facies. At higher temperatures, quartz-rich rocks are more likely to behave as "soft" objects, and the relative positions of clast types in Flinn space are expected to change.

The last point above also requires attention: the initial shape of a deformed object clearly influences its post-deformational shape. If we consider two-

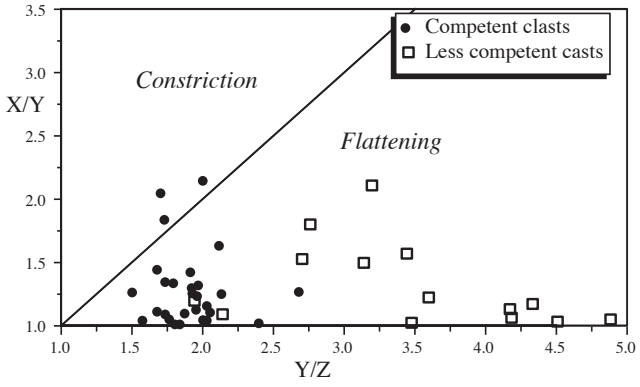

Figure 3.10 Strain obtained from deformed conglomerates, plotted in the Flinn diagram. Different pebble types show diferent shapes and finite strains. Polymict conglomerate of the Utslettefjell Formation, Stord, SW Norway. Data collected by D. Kirshner, R. Malt and the author.

dimensional objects such as sections through ooiltic rocks, sandstones or conglomerates, the R_i/ϕ method discussed above can handle this type of uncertainty. It is better to measure up two or more sections through a deformed rock using this method than digging out an object and measuring its three-dimensional shape. The one object could have an unexpected initial shape (conglomerate clasts are seldom perfectly spherical or elliptical), but by combining numerous measurements in several sections we get a statistical variation that can solve or reduce this problem.

Three-dimensional strain is usually achieved by combining two-dimensional data from several differently oriented sections.

There are now computer programs that can be used to extract three-dimensional strain from sectional data. If the sections each contain two of the principal strain axes everything becomes easy, and only two are strictly needed (although three would still be good). Otherwise, strain data from at least three sections are required.

_____***_____

Strain markers and the information that they contain are intriguing to structural geologists. Studying rocks in which strain can be estimated is very useful because one can then compare the structures, fabrics and microfabrics of these rocks with those of rocks without strain markers. The way that rocks accumulate strain depends on the stress field, boundary conditions, physical properties of the rock as well as external factors such as temperature, pressure, and state of stress. In the next chapter we will explore some of these relationships.

Further reading:

Bhattacharyya, P. & Hudleston, P., 2001. Strain in ductile shear zones in the Caledonides of northern Sweden: a three-dimensional puzzle. Journal of Structural Geology, 23: 1549-1565.

De Paor, D.G., 1990. Determination of the strain ellipsoid from sectional data. Journal of Structural Geology, 12: 131-137.

Erslev, E.A., 1988. Normalized center-to-center strain analysis of packed aggregates. Journal of Structural Geology, 10: 201-209.

Goldstein, A., Knight, J. & Kimball, K., 1999. Deformed graptolites, finite strain and volume loss during cleavage formation in rocks of the taconic slate belt, New York and Vermont, U.S.A. Journal of Structural Geology, 20: 1769-1782.

Holst, T.B. & Fossen, H., 1987. Strain distribution in a fold in the West Norwegian Caledonides. Journal of Structural Geology, 9: 915-924.

Hossack, J., 1968. Pebble deformation and thrusting in the Bygdin area (Southern Norway). Tectonophysics, 5: 315-339.

Ramsay, J.G. & Huber, M.I., 1983. The techniques of modern structural geology: Strain analysis, 1. Academic Press, London, 307 p.

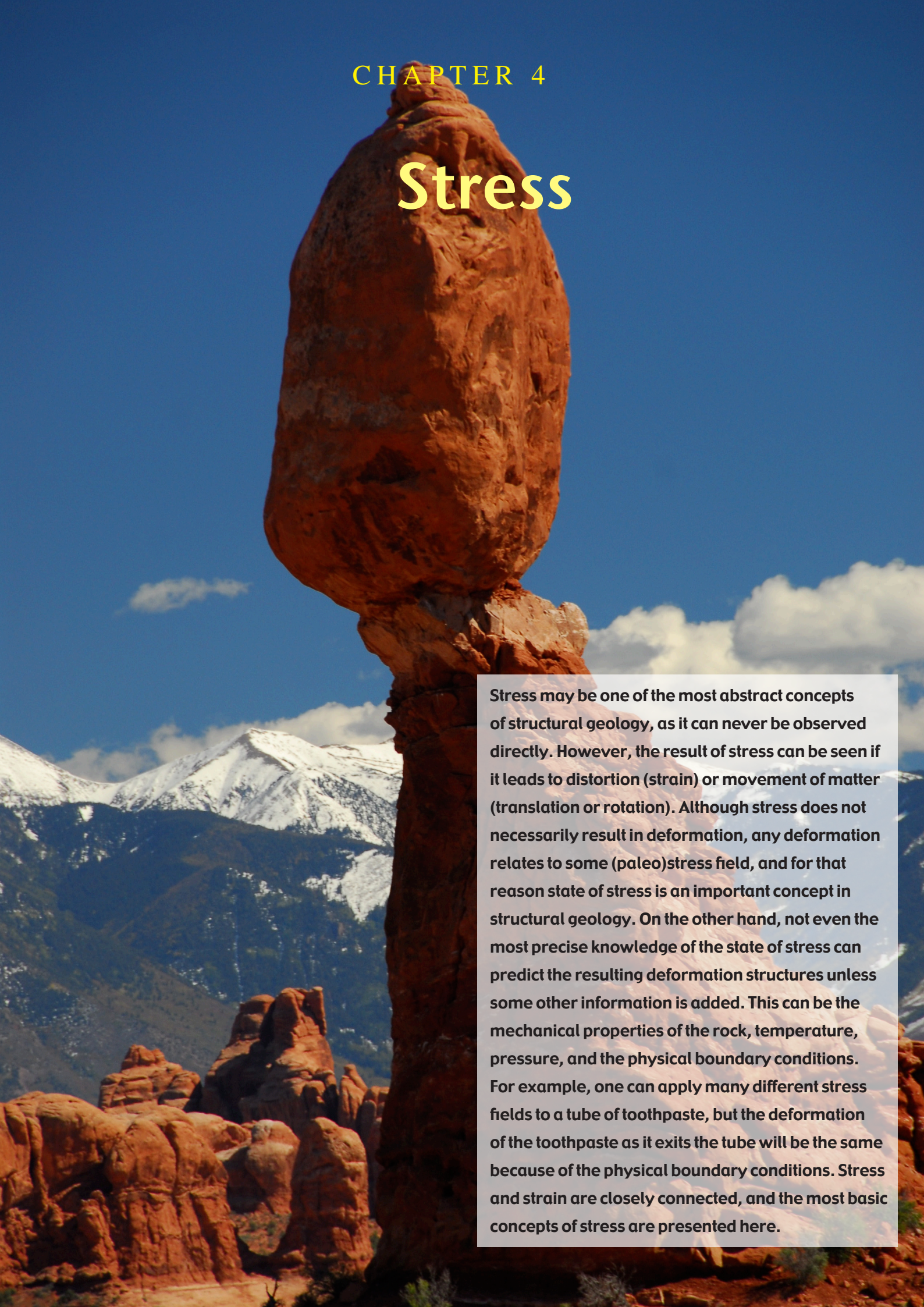

CHAPTER 4

Stress

Stress may be one of the most abstract concepts of structural geology, as it can never be observed directly. However, the result of stress can be seen if it leads to distortion (strain) or movement of matter (translation or rotation). Although stress does not necessarily result in deformation, any deformation relates to some (paleo)stress field, and for that reason state of stress is an important concept in structural geology. On the other hand, not even the most precise knowledge of the state of stress can predict the resulting deformation structures unless some other information is added. This can be the mechanical properties of the rock, temperature, pressure, and the physical boundary conditions. For example, one can apply many different stress fields to a tube of toothpaste, but the deformation of the toothpaste as it exits the tube will be the same because of the physical boundary conditions. Stress and strain are closely connected, and the most basic concepts of stress are presented here.

1.1 Definitions, magnitudes and units

There is a close relationship between how we use the terms pressure, force and stress in everyday conversation. As structural geologists we need to use these terms more carefully. *Pressure* (p) is always used about the condition in media with no shear resistance, which means fluids and gases. *Stress* (σ) is restricted to rocks and other media with a minimum of shear resistance. To check if a medium has a shear resistance, put some of it between your hands and move them in parallel but opposite directions. The resistance you feel reflects the shear resistance. Water will have no shear resistance (repeat the above exercise in a swimming pool, with just water between your hands), while clay and loose sand will resist shearing. In a porous sandstone layer in the crust we can talk about both pressure and stress: it has a certain pore *pressure* and it is in a certain state of *stress*. They are both related to the external forces that affect the rock volume.

There are two different types of forces. One type affects the entire volume of a rock, the outside as well as the inside, and is known as *body forces*. Body forces define three-dimensional fields. The most important type of body force in structural geology is gravity. Another example is magnetic forces.

The other type of force acts on surfaces only and is referred to as *surface forces*. Surface forces originate when one body pushes or pulls another body and acts across the contact area between the two bodies. Surface forces are of great importance during deformation of rocks. In a similar way we can talk about stress on a surface and state of stress at a point. Stress on a plane is a vector quantity, while stress at a point is a second-order tensor. We will start by looking at the first case.

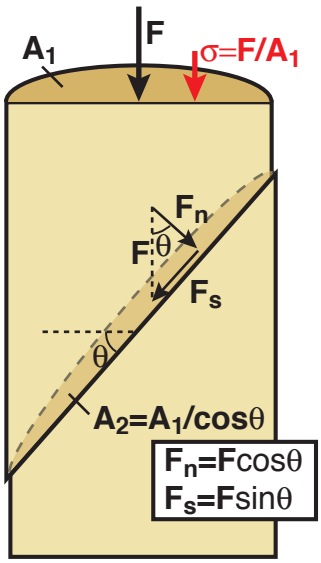

Figure 4.1 A force vector **F** acting vertically downward on a rock cylinder (sectioned in the figure) can be decomposed into a normal ($\mathbf{F}_n$) and a shear ($\mathbf{F}_s$) component by simple vector addition. The stress vector σ cannot be decomposed in this way, because it depends on the area across which the force acts. Trigonometric expressions for the components σ_n and σ_s are derived.

$\sigma_n = F_n/A_2 = F\cos\theta/A_2 = F\cos^2\theta/A_1 = \sigma\cos^2\theta$

$\sigma_s = F_s/A_2 = F\sin\theta/(A1/\cos\theta)$
$= F\sin\theta\cos\theta/A_1 = \sigma\sin\theta\cos\theta = \sigma 1/2\sin 2\theta$

What are tensors?

Tensors are simply arrays of numbers, or functions, that transform according to certain rules under a change of coordinates. In physics, tensors characterize the properties of a physical system. A tensor may be defined at a single point or collection of isolated points, or it may be defined over a continuum of points and thus forming a field (scalar field, vector field etc.). In the latter case, the elements of the tensor are functions of position and the tensor forms what is called a *tensor field*. This simply means that the tensor is defined at every point within a region of space (or space-time), rather than just at a point or collection of isolated points.

A tensor of order zero is identical to a scalar, which is a quantity that has magnitude only. It has no direction and is independent of the coordinate system. Examples are time, mass, density, volume and speed. Examples of a scalar field would be the density or gravitational potential energy of rock in a given volume of the crust.

A first-order tensor is identical to a vector, which is a quantity that has both magnitude and direction. It is completely described by its components along three (two for two-dimensional considerations) specified coordinate directions. In four-dimensional space-time, a vector has four components. Regardless, vectors can be written as a column or row of numbers and are therefore considered one-dimensional. Velocity, displacement, gravity and force in general are well-known vectors that may form vector fields relevant to structural geology. A surface traction (stress across a surface) is also a first order tensor or vector.

Second-order tensors are often referred to as matrices, which are two dimensional arrays of number (3x3 or 2x2 in most geological applications, meaning that they have 9 or 4 components). Just like vectors and scalars, second-order tensors are independent of any chosen frame of reference, meaning that the "quantity" represented by the tensor (such as the state of stress or strain at any point in a volume) remains the same regardless of the choice of coordinate system. The actual numbers in the matrix representing the tensor will however be different in different frames of reference. Stress and strain state are second order tensors since they are quantities associated with two directions (the shape of the stress or strain ellipsoid and its orientation).

Stress is used in two different meanings: stress on a surface, which is a vector (first-order tensor), and state of stress at a point, which is a second-order tensor.

Engineers and rock mechanics-oriented geologists refer to stress on a surface as *traction* and reserve the term stress to mean the state of stress at a point in a body. Also, as geologists we need to be aware of these two uses and avoid confusion between those two meanings of stress.

1.2 Stress on a surface

The *stress on a surface* such as a fracture or a grain-grain contact is a vector (σ) that can be defined

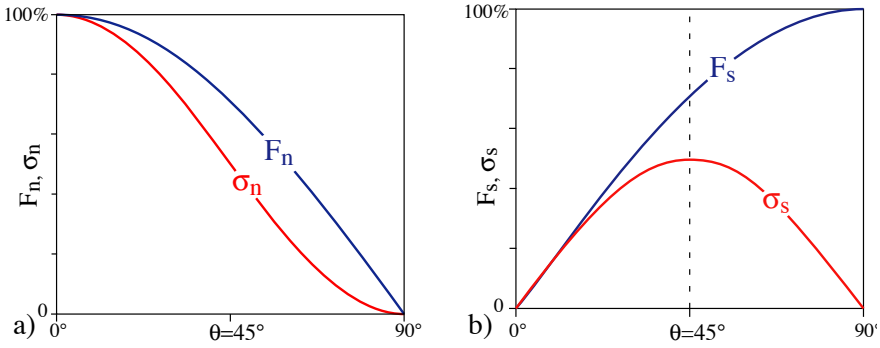

Figure 4.2 a) The normal components of the force (F_n) and stress (σ_n) vectors acting across a surface, plotted as a function of the orientation of the vectors relative to the surface (θ, see Figure 2.1). Note the difference between the two. b) the same for the shear components. Note that the shear stress is at its maximum at 45° to the surface while maximum shear force is obtained parallel to the surface.

as the ratio between a force (F) and the area (A) across which the force acts. The stress that acts on a point on the surface can be formulated as:

$$\bar{\sigma} = \lim_{\Delta A \to 0} (\Delta F / \Delta A) \qquad (5.1)$$

This formulation indicates that the stress value may change from place to place on a surface. The SI-unit for force (F) is Newton (N) = mkg/s^2. 1 N (Newton) is the force at the surface of the Earth that is created by the weight of 102 g. Some geologists use the unit dyne, where 1 dyne (g·cm/s^2) = 10^{-5} N. Differential stress or pressure given in *megapascal (MPa)*, where

1Pa = 1N/m^2 = 1kg/(ms^2)
1 MPa = 10 bar = 10.197 kp/cm^2 = 145 lb/in^2
100 MPa = 1 kbar

Compressive stresses are normally considered positive in geologic literature, while tension is regarded as negative. In material science the definition is reversed, so that tension becomes positive. This is related to the fact that the tensional strength of a material is lower than its compressional strength. Their tensional strength thus becomes more important, particularly during evaluation of constructions such as bridges and buildings. The crust, on the other hand, is dominated by compression, although tension creates important structures in the upper crust.

1.2.1 Normal stress and shear stress

A stress vector acting perpendicular to a surface is called the *normal stress*, while a stress vector that acts parallel to a surface is referred to as the *shear stress*. In general, stress vectors act obliquely on planes. The stress vector can then be resolved into normal and shear stress components. It is emphasized that the concept of normal and shear stress has a meaning only when related to a specific surface.

While the decomposition of forces is quite simple, the decomposition of stress vectors is slightly more complicated. The complications relate to the fact that stress depends on the area across which it acts while forces do not. Therefore, simple vector addition does not work for stress vectors. As shown in Figure 4.1 we have the relationships

$$\sigma_n = \sigma\cos^2\theta, \quad \sigma_s = (\sigma\sin 2\theta)/2 \qquad (5.2)$$

where θ is the angle between the stress vector and the surface in question, or the dip of the surface if the stress vector is vertical. For comparison, decomposition of the force vector into normal and shear force vectors (Figure 4.1) gives:

$$F_n = F\cos\theta, \quad F_s = F\sin\theta \qquad (5.3)$$

These four functions are illustrated graphically in Figure 4.2.

1.3 Stress at a point

We leave the concept of stress on a single plane to consider the state of stress at a given point in a rock, for example a point within a mineral grain. We may imagine that there are planes in an infinite number of orientations through this point. Perpendicularly across each of the planes there are two oppositely directed and equally long traction or stress vectors. Different pairs of stress vectors may be of different lengths, and when a representative family of such vectors are drawn about the point an ellipse emerges in two dimensions (Figure 4.3), and an

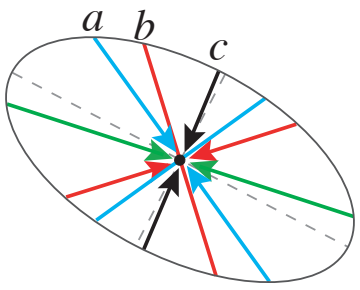

Figure 4.3 2D ilustration of stress in a point. Three planes (a, b and c) are oriented perpendicular to the page and their normal stresses are represented in the form of vectors. The stress vectors define an ellipse, and the ellipticity depends on the state of stress.

SIGN CONVENTIONS

Compressive normal forces are always positive in geology, while tensile ones are negative (in engineering geology the sign convention is opposite). Geologists like this convention because stresses tend to be compressive in the crust. Note however that shear stresses are subjected to at least two conventions. For the Mohr circle construction, we have the following convention: Shear stresses consistent with clockwise rotation are negative. For tensor notation the sign convention is different for the shear stresses (absolute values are identical): If the shear components on the negative (hidden) sides of the cube shown in the figures act in the positive directions of the coordinate axes, then the sign is positive and vice versa. This may be confusing, so always check if the signs of an output of a calculation make sense.

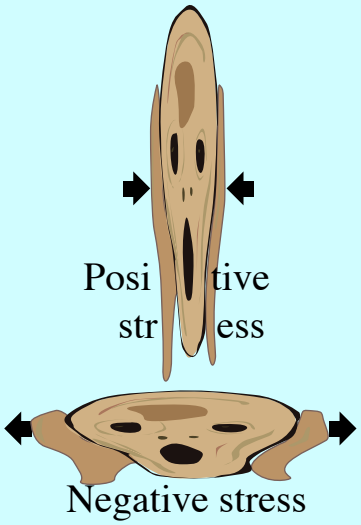

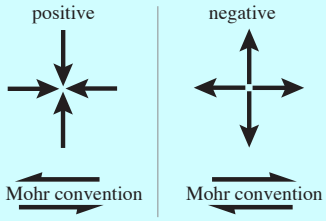

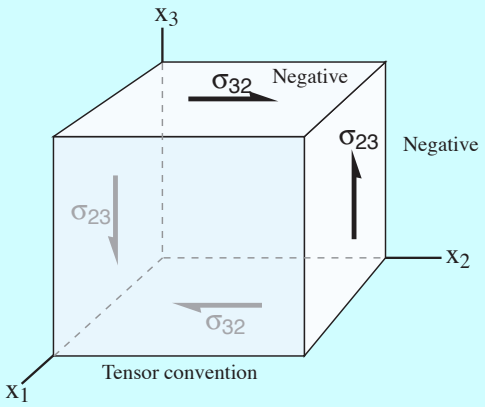

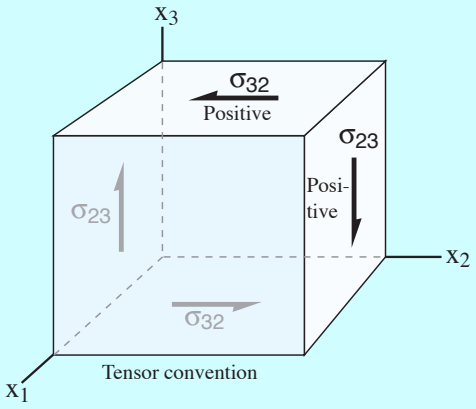

ellipsoid is defined in three dimensions (Figure 4.4). The requirement is that there is not a combination of positive and negative tractions. The ellipse is called the *stress ellipse*, and the ellipsoid is the *stress ellipsoid* .

The stress ellipsoid has three axes, denoted σ_1, σ_2 and σ_3. The longest (σ_1) is the direction of maximum stress while the shortest is normal to the (imaginary) plane across which there is less traction than across any other plane through the point. The axes are called the *principal stresses* and the planes to which they represent the poles are the *principal planes of stress*. These are the only planes where the shear stress is zero.

1.4 Stress components

The state of stress at a point is also defined by the stress components that act on each of the three orthogonal surfaces in a infinitesimal cube (yes, a cube has six surfaces, but they reduce to three as the cube gets infinitesimal). Each of the surfaces has a normal stress vector (σ_n) and a shear stress vector along each of its two edges (Figure 4.5). In total, this gives three normal stress vectors and six shear stress vectors. If the forces that act in opposite direction are of equal magnitude, then they cancel each other out and the cube does not move. The cube is then in a state of equilibrium. This implies that

$$\sigma_{xy}=-\sigma_{yx},\ \sigma_{yz}=-\sigma_{zy} \text{ and } \sigma_{xz}=-\sigma_{zx}, \qquad (5.4)$$

and we are left with six independent stress components.

If we now rotate our cube until all of the shear stresses are zero the only nonzero components are the three normal stress vectors. These vectors are now oriented along the principal stress directions and are the *principal stresses* or *principal axes of the stress ellipsoid*. The three surfaces that define the cube are the *principal planes of stress* that divide the stress ellipsoid into three.

1.5 The stress tensor (matrix)

It is useful to put the nine components of stress into a matrix (second-order tensor) known as the stress tensor or stress matrix:

$$\begin{bmatrix} \sigma_{11} & \sigma_{12} & \sigma_{13} \\ \sigma_{21} & \sigma_{22} & \sigma_{23} \\ \sigma_{31} & \sigma_{32} & \sigma_{33} \end{bmatrix} \qquad (5.5)$$

The normal stresses σ_{11}, σ_{22} and σ_{33} occupy the diagonal while the off-diagonal terms represent the shear stresses. We have that $|\sigma_{11}|=|\sigma_{xx}|$, $|\sigma_{12}|=|\sigma_{xy}|$, $|\sigma_{13}|=|\sigma_{xz}|$ etc., but they may have different signs because of different conventions

used for tensor components. In the stable situation where forces are balanced we have

$\sigma_{12}=\sigma_{21}$, $\sigma_{31}=\sigma_{13}$ and $\sigma_{23}=\sigma_{32}$,

and the stress tensor can be written as

$$\begin{bmatrix} \sigma_{11} & \sigma_{12} & \sigma_{13} \\ \sigma_{12} & \sigma_{22} & \sigma_{23} \\ \sigma_{13} & \sigma_{23} & \sigma_{33} \end{bmatrix} \qquad (5.6)$$

This is now a symmetric matrix (changing columns to rows does not change the matrix), but the values will change with choice of coordinate system or how we orient our little cube from Figure 4.5. If we are lucky we have the principal stresses along the edges of the box, in which case the matrix becomes:

$$\begin{bmatrix} \sigma_{11} & 0 & 0 \\ 0 & \sigma_{22} & 0 \\ 0 & 0 & \sigma_{33} \end{bmatrix} = \begin{bmatrix} \sigma_{1} & 0 & 0 \\ 0 & \sigma_{2} & 0 \\ 0 & 0 & \sigma_{3} \end{bmatrix} \qquad (5.7)$$

Being the only non-zero entries, the principal stresses can now readily be extracted from the matrix. The three principal stress vectors are the three columns $(\sigma_{11},0,0)$, $(0, \sigma_{22},0)$ and $(0,0, \sigma_{33})$. In other words:

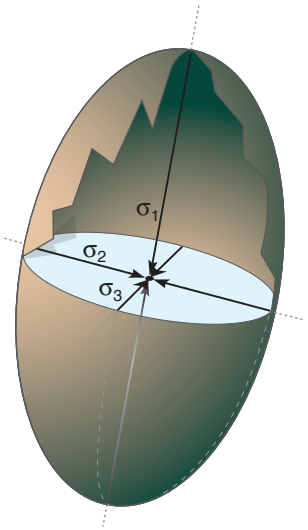

Figure 4.4 The stress ellipsoid.

The stress tensor is composed of the three principal stress vectors.

In other cases we have to find the eigenvectors and eigenvalues of the matrix, which are the principal stress vectors and principal stresses, respectively. This is easily done by means of readily available computer programs. It is important to know that even if the elements of the stress tensor vary for different coices of coordinate system, the eigenvalues and eigenvectors of the tensor remain the same.

Strain tensors represent the same state of stress and stress ellipsoid regardless of choice coordinate system.

1.6 Deviatoric stress and mean stress

Any stress tensor can be split into two symmetric matrices, where the first part represents the mean stress and the second is called the deviatoric stress. This is not just another boring mathematical exercise, but a very useful decomposition that allows us to distinguish two very important components of stress that we also can denote the isotropic and anisotropic components. The decomposition is:

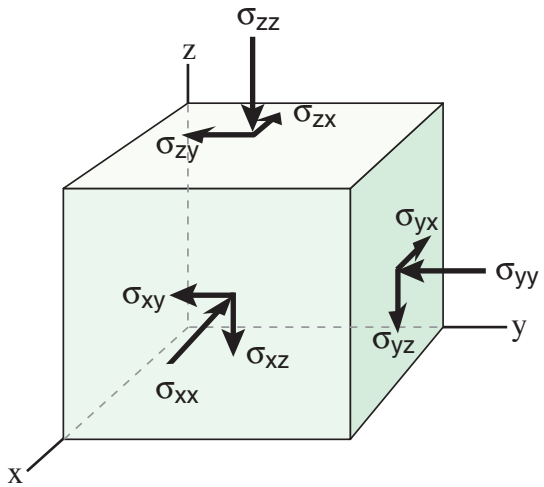

Figure 4.5 The stress components acting on the faces of a small cube. Positive stress components are shown – corresponding stress components exist on the negative and hidden faces of the cube. σ_{xx}, σ_{yy} and σ_{zz} are normal stresses, the others are shear stresses and parallel to the edges of the cube.

$$\begin{bmatrix} \sigma_{11} & \sigma_{12} & \sigma_{13} \\ \sigma_{12} & \sigma_{22} & \sigma_{23} \\ \sigma_{13} & \sigma_{23} & \sigma_{33} \end{bmatrix} =$$

total stress tensor

$$\begin{bmatrix} \sigma_m & 0 & 0 \\ 0 & \sigma_m & 0 \\ 0 & 0 & \sigma_m \end{bmatrix} + \begin{bmatrix} \sigma_{11}-\sigma_m & \sigma_{12} & \sigma_{13} \\ \sigma_{12} & \sigma_{22}-\sigma_m & \sigma_{23} \\ \sigma_{13} & \sigma_{23} & \sigma_{33}-\sigma_m \end{bmatrix}$$

(5.8)

isotropic component + anisotropic component
(mean stress tensor) (deviatoric stress tensor)

The σ_m in this decomposition is called the *mean stress* and is simply the arithmetic mean of the three principal stresses. Thus, $\sigma_m=(\sigma_1+\sigma_2+\sigma_3)/3$ gives an average measure of stress.

If there is no deviatoric stress so that the anisotropic component is zero (the deviatoric stress tensor is the identity matrix), then the stress or traction is identical on any plane through the point, regardless of the orientation of the plane. Furthermore, the stress ellipsoid is a perfect sphere, $\sigma_1=\sigma_2=\sigma_3$, there is no shear stress "anywhere" and there is no off-diagonal stress in the total stress tensor. Such a condition is commonly referred to as *hydrostatic stress* or *hydrostatic pressure*, and represents an isotropic state of stress. In the lithosphere, the mean stress is closely related to *lithostatic pressure*, which is controlled by burial depth and the density of the overlying rock column. We will return to this discussion in Chapter 6.

Deviatoric stress is the difference between the mean stress and the total stress: $\sigma_{dev}=\sigma_{tot}-\sigma_m$, or $\sigma_{tot}=\sigma_m+\sigma_{dev}$. The deviatoric stress tensor represents the *anisotropic* component of the total stress and the deviatoric stress is generally considerably smaller than the isotropic mean stress, but of greater significance when it comes to the formation of geologic structures in most settings. While isotropic stress results in dilation (inflation or deflation), only the anisotropic component results in strain. The relationship between its principal stresses influences on what type of structures are formed.

We will return to stress states in the crust in Chapters 6 and 7, but before we leave stress for strain we look at a practical graphical way of presenting and dealing with stress based on a diagram referred to as the Mohr diagram.

1.7 Mohr's circle and the Mohr diagram

In the 19th century, the German engineer Otto Mohr found a particularly useful way of dealing with stress. He constructed a diagram, now known as the Mohr diagram (Figure 4.6) where the horizontal and vertical axes represent the normal (σ_N) and shear (σ_S) stresses that act on a plane through a point. The value of the maximum and minimum principal stresses (σ_1 and σ_3, also denoted σ_1 and σ_2 for two dimensional cases) are plotted on the horizontal axis and the distance between σ_1 and σ_3 defines the diameter of a circle centered $((\sigma_1+\sigma_3)/2, 0)$. This circle is called *Mohr's circle*, and describes the normal and shear stress acting on planes of all possible orientations through the point. More specifically, for any given point on the circle a normal stress and a shear stress value can be read off the axes of the diagram. These are the normal and shear stresses acting on the plane represented by that point. How do we know the orientation of the plane that the point represents? In two dimensions and with σ_1 and σ_3 plotted on the horizontal axis the planes represented on the circle contain σ_2. If θ is the angle between the normal to the plane and σ_1, as shown in Figure 4.1, then the angle between the radius to the point on the circle and the horizontal axis is 2θ.

The difference between the maximum and minimum principal stresses (σ_1-σ_3) is the diameter of the circle. This difference is called *differential stress* and is important in fracture mechanics. In general, great differential stress promotes rock fracturing.

θ and other angles are measured in the same sense on the Mohr diagram as in physical space, but the angles are doubled in Mohr space. Two points representing perpendicular planes are thus separated by 180° in the Mohr diagram. This is why the two principal stresses both plot on the horizontal axis. Another reason is that

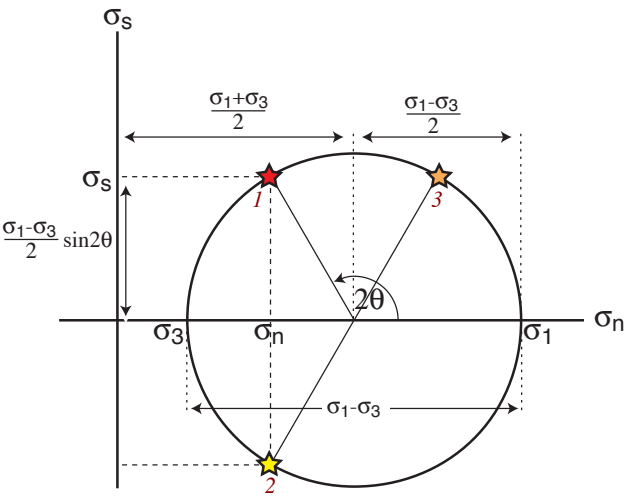

Figure 4.6 The Mohr circle. θ is the angle between the largest stress and a given plane. Note the use of double angles.

principal planes have no shear stress, which is fulfilled only along the horizontal axis. This illustrates how the Mohr space is different from physical space, and it is important to understand the connection between the two. Let us explore some more. The doubling of angles in Mohr space means that any plane, such as that indicated by point 1 in Figure 4.6, has a complementary plane (point 3 in the same figure) with identical shear stress and different normal stress. Point 1 in Figure 4.6 also has another complimentary plane (point 2) of identical normal stress and a shear stress that differ by sign only. Maximum shear stress occurs for planes where $2\theta=\pm 90°$, or where the angle to σ_1 is 45° (Figure 4.2b). The Mohr diagram used in geological applications is generally constructed so that compression is positive and tension is negative, while the opposite convention is common in the engineering literature. In most cases all principal stresses are positive in the lithosphere, but not always. For tensile stress, Mohr's circle is moved to the left of origin into the tensile field. If all principal stresses are tensile (a most unusual case in geology), then the entire circle is located to the left of the origin.

The Mohr diagram can also be used in three dimensions, where all three principal stresses are plotted along the horizontal axis. In his way we can represent three Mohr's circles in a single Mohr diagram. A number of important states of strain can be represented in the three-dimensional Mohr diagram, as shown in Figure 4.7.

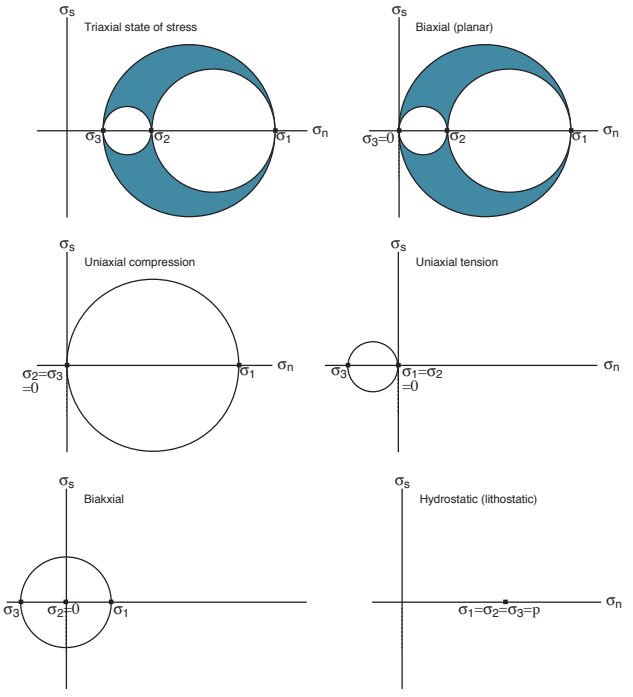

Figure 4.7 Characteristic states of stress are illustrated in the Mohr diagram for 3D stress. The three-dimensional state of stress is illustrated by means of three circles connecting the three principal stresses. The largest circle contains σ_1 og σ_3. The three circles reduce to two or one for special states of stress.

Later in this text we will look at stresses in the crust, both in the form of general stress conditions (Chapter 6) and more locally on fracture surfaces (Chapter 7 and 8). Before doing so, we will look at the visible effect of stress, generally known as deformation.

Further reading:

Means, W.D., 1976. Stress and Strain. Springer-Verlag, New York, 339 p.

Price, N.J. & Cosgrove, J.W., 1990. Analysis of geological structures. Cambridge University Press, Cambridge, 502 p.

Twiss, R.J. & Moore, E.M., 1992. Structural geology. H.W. Freeman and Company, 532 p.

CHAPTER 5

Stress in the lithosphere

A large number of stress measurements have been performed and compiled over the last few decades. The data indicate that the stress conditions in the crust are complex, partly because of geologic heterogeneities (faults, fracture zones and compositional contrasts), and partly because many areas have been exposed to multiple phases of deformation, each associated with different stress fields. The latter is of importance because the crust has the ability to "freeze in" a state of stress and preserve remnants of it over geologic time. Knowledge of the local and regional stress field has a number of practical applications, including evaluation of tunneling operations, drilling and stimulation of petroleum and water wells. Besides, knowledge of the present and past states of stress provides important information about tectonic processes, then and now.

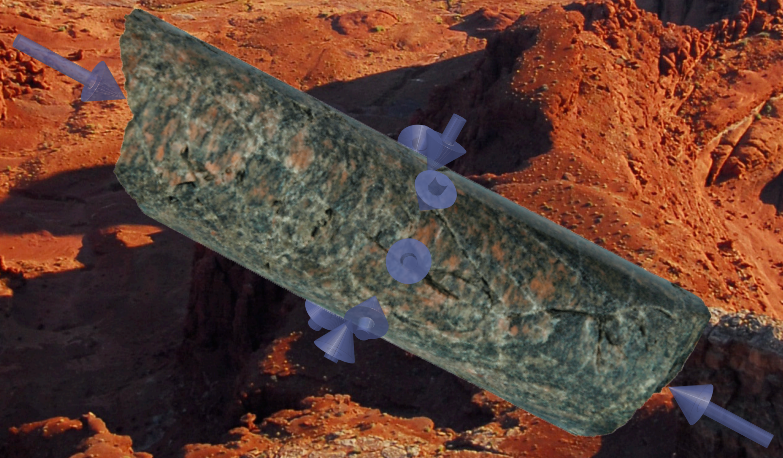

5.1 Introduction

Knowledge of stress is important for many reasons. Near the surface, drilling in highly stressed rock during underground construction, tunneling, quarrying and mining operations may cause pieces of rock to literally shoot off the walls, the floor or the roof, obviously a serious safety issue. Stress concentrations in underground openings may result in roof closure, sidewall movement and ground subsidence. Unlined pressure tunnels and shafts used in hydroelectric and water supply systems can leak (by hydrofracture) if the internal water pressure exceeds the minimum *in situ* principal stress in the surrounding rock mass. In this case high rock stresses are advantageous.

At greater depths, in oil fields for example, in-situ stress field during drilling helps steer the drill head in the desired direction, prevent sand production and maintain borehole stability. Stresses must also be monitored during production because pore pressure reduction during production may reduce horizontal stresses by a factor large enough to cause formations to collapse and the seafloor to subside. Hydrofracturing of reservoirs in order to increase permeability around producing wells also requires information about the stress field.

At any level in the crust stresses are related to the formation and orientation of geologic structures, i.e. the accumulation of strain. Any deformation can be related to some stress field that deviates from the "normal" stress situation. We have already looked at stress relative to strain during our discussion of rheology. In the deeper portions of the crust stress cannot be measured or estimated, except for the information obtained from focal mechanisms. There are however ways to estimate paleostress once the rocks have been exhumed and exposed at the surface.

5.2 Stress measurements

A challenging aspect of stress is that only its effects can be observed after released in the form of elastic or permanent strain. We have already seen how different media (rock types) react differently to stress (Chapter 5), and if the medium is anisotropic, such relations tend to get more complex. For small strains, however, typically involved in measurements of current stress fields, reasonable estimates of stress are possible.

A series of different methods are applied, depending on where stress data are to be collected. Some are particularly useful at the surface

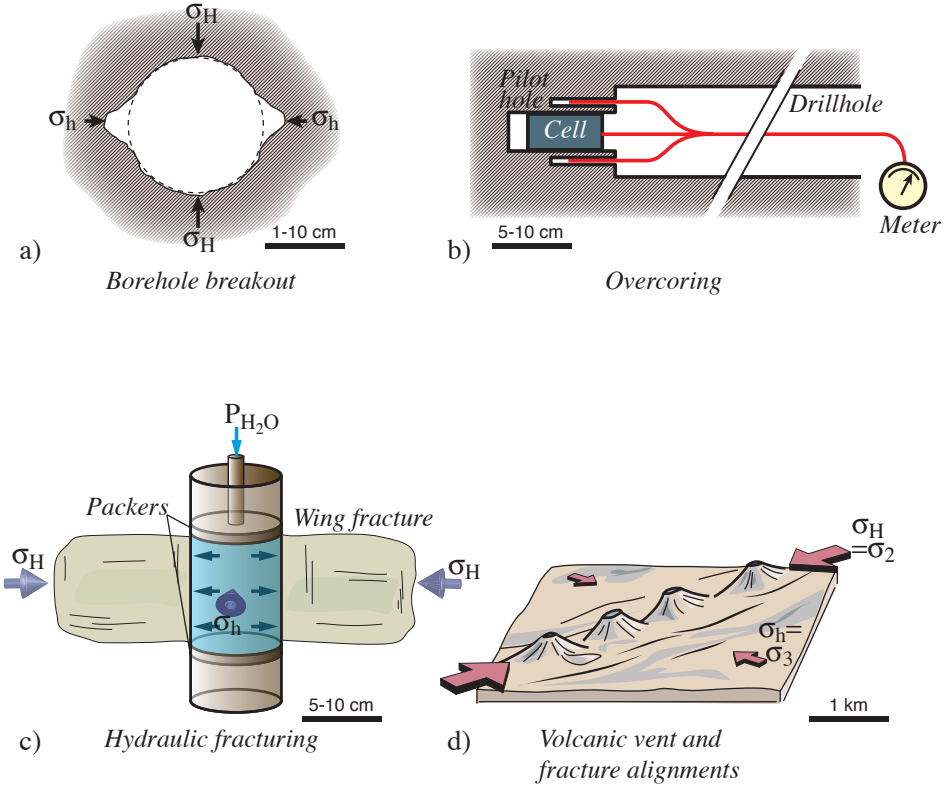

Figure 5.1 Examples of stress determination. a) Borehole breakouts as illustrated by a horizontal section through a vertical wellbore. Maximum and minimum horizontal stresses σ_H and σ_h are generally equal to or close to two of the principal stresses. b) The overcoring method. A pilot hole is drilled at the end of the main hole into which stress meters or a strain cell is placed. A wider core is cut outside the cell, and strain is calculated by comparing measurements before and after the drilling. Strain is related to stress by means of elastic theory, and the state of stress is found. c) Hydraulic fracturing. d) Recent surface structures related to the current stress field.

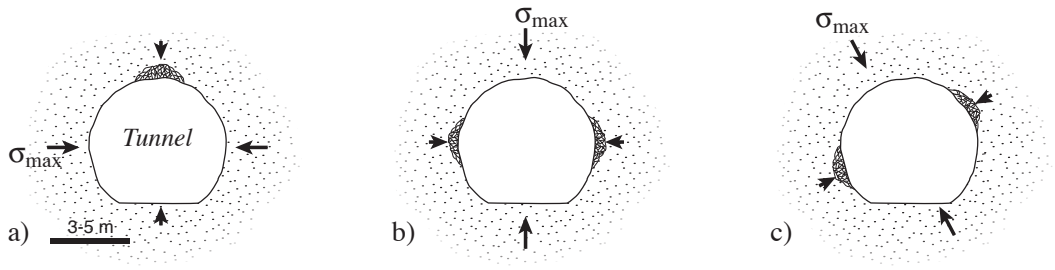

Figure 5.2 Spalling of rock fragments in certain parts of a tunnel gives information about the orientation of the principal stresses and the differential stress.

(overcoring and surface structures), some in deeper wells (borehole breakouts and hydraulic fracturing), and one is related to the first motion generated by stress release during the rupture of faults (focal mechanisms).

Borehole breakouts are zones of failure of the wall of a well that give the borehole an irregular and typically elongated shape (Figure 5.1a). It is assumed that the spalling of fragments from the wellbore occurs preferentially parallel to the minimum horizontal stress (S_h) and orthogonal to the maximum horizontal stress (S_H). The ellipticity of the hole thus indicates the orientation of the horizontal stress axes at a particular depth in the wellbore. Information about the shape of the hole is obtained by dipmeter tools or well imaging tools. These are tools with arms that are pressed against the borehole wall as the tool is moved along the wellbore. The arms record the diameter of the hole as well as the orientation of the tool. Thus, in addition to the ~~tool's~~ measurements of the orientation of planar structures intersecting the wellbore (the main purpose of a dipmeter tool), a record of the shape of the borehole is produced, yielding information about the horizontal stresses.

Borehole breakout data are primarily collected in wells drilled for petroleum exploration and production. The shape of holes drilled for road and tunnel blasting operations have also been used for stress analyses, although this method is not regarded as very reliable. Even in tubular tunnels preferred spalling of fragments sometimes indicates the orientation of the stress field (Figure 5.2). The principle is the same for all cases: the borehole takes on an "elliptical" shape where the elongated direction is assumed to parallel S_h.

Overcoring (Figure 5.1b) is a strain relaxation method where, in principle, a sample (core or block) is extracted from a rock unit, measured, and then released so that it can freely expand. The change in shape that occurs reflects the compressive stresses that have been released, but also depends on the rock's elasticity. In particular, maximum expansion occurs in the direction of σ_h.

Overcoring is done to map the state of stress at the surface and around[1]. Surface or near-surface overcoring is done by drilling a hole into the rock and adding a small pilot hole at the end of the main hole. Stressmeters or a strain cell are placed in the pilot hole before a wider core is cut. The stress release resulting from the overcoring causes elastic deformation that is recorded by the stressmeters or strain cell. The fact that the unit microstrain ($\mu e=10^{-6}e$) is used indicates that the strains involved are not great. At least six stressmeters are required in the hole to completely record the three-dimensional stress field. Young's modulus (E) and Poisson's ratio (ν) are measured in the laboratory, and elastic theory is applied to calculate the orientations and magnitudes of the principal stresses.

At the surface, the effect of local topography must be accounted for. Mountains and valleys create stress effects near the surface that influence regional stress patterns Figure 5.3). In tunnels and rock chambers the effect of free space in the rock on the stress field must be taken into consideration, or holes must be drilled far enough away from the tunnel that this effect is negligible. Even the perturbation of the stress field by the drill hole itself must be corrected for, although such a correction is

1 Less commonly, it is done by bringing a sample from a deep bore hole in confined condition to the surface, and measuring the three-dimensional expansion as the sample is unconfined.

easily done using modern equipment. Weak faults and fracture zones, weathering and contacts between rocks of contrasting physical properties are examples of geological structures that are likely to distort the stress field locally (Figure 5.4).

Hydraulic fracturing (hydrofracturing, "hydrofracking," Figure 5.1c) means increasing the fluid pressure until the rock fractures. The technique is frequently applied to petroleum reservoirs to increase the near-well permeability. In this case the interval of the wellbore that is to be fractured is sealed off and pressure is pumped up until tension fractures form. The pressure that is just enough to keep the fracture(s) open equals σ_h in the formation. Knowing the tensile strength of the rock, it is possible to calculate σ_H. Furthermore, the vertical stress is assumed to be a principal stress and equal to ρgz. Petroleum engineers use knowledge of the stress field to plan hydrofracturing of reservoir units to take advantage of predicted direction of fracture propagation.

Earthquake focal mechanisms (p. box Chapter 9) give information about the Earth's immediate response to stress release along new or preexisting fractures. They provide information about the stress regime (Section 6.6) as well as the relative magnitude of the principal stresses. The main problem with this method is that the P- and T-axes do not necessarily parallel principal stress axes.

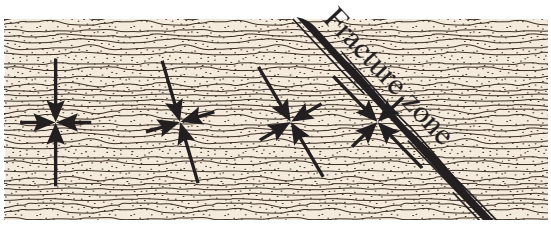

Figure 5.4 Deflection of the stress field near a fault or fracture zone. The structure is weaker than the surrounding rock and can support lower shear stresses than its surroundings. The situation is similar to that where an open surface exists, e.g. the free surface of the Earth (see Fig. 6.3).

Combining focal mechanisms of faults of different orientation helps reduce this problem.

Geological structures formed by active tectonic processes ~~may~~ also give reliable indications of certain aspects of the present day stress field. The orientation and pattern of recent fault scarps, fold traces, tension fractures (Figure 5.5) and volcanic vent alignments (Figures 6.1d) all indicate the orientation of the principal stresses.

Stress can be measured *in situ* from rocks in the upper crust, i.e. without taking samples away to a laboratory for stress determinations. The deepest reliable stress measurement reported so far was made at a depth of about 9 km in the German Continental Deep Drilling Project (hydrofracturing).

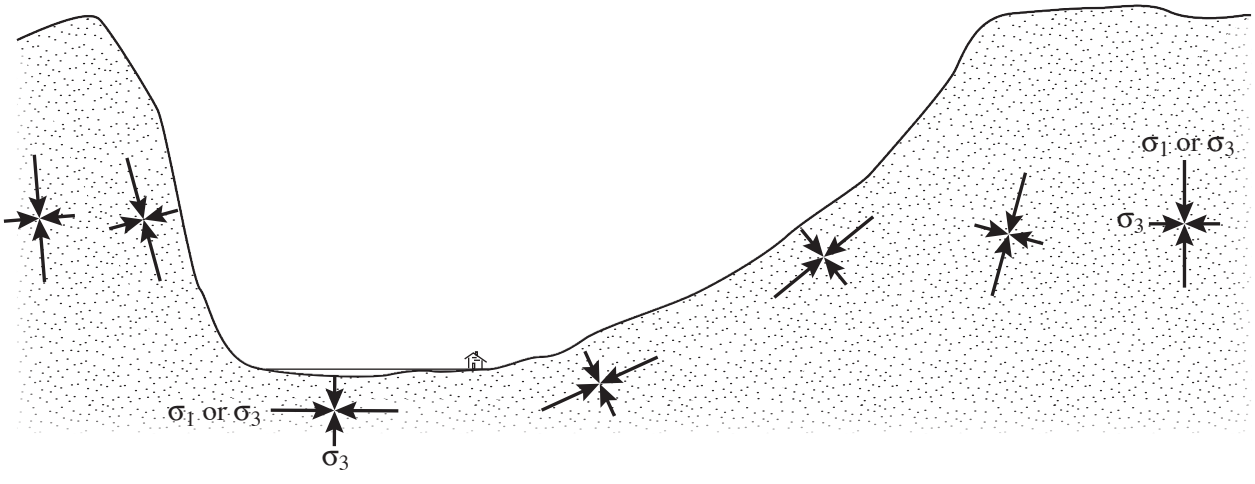

Figure 5.3 State of stress around a valley or fjord. One of the principal stresses will always be perpendicular to the free surface of the Earth, because the shear stress is zero along any free surface. Thus, a non-planar surface causes the orientation of the stresses to rotate as shown on the figure. Note that these deviations occur near the surface only, but must be considered when stress is measured at or near the surface or other free surfaces (tunnel walls etc.).

Figure 5.5 Active vertical fractures on the surface of Holocene lava flows in SE Iceland indicate the orientation of σ_h. Because the fractures occur at the surface, $\sigma_h = \sigma_3$, and σ_1 must be vertical. A historic basalt flow in the background is less influenced by the fractures.

Information about the stress conditions deeper ~~down~~ in the crust can only be inferred from focal mechanisms, theoretical considerations and through the use of paleostress methods, which will be treated in Chapter 9.

5.3 Reference states of stress

Various theoretical models of how the state of stress changes through the crust exist, and three of them are presented below. Such models are referred to as reference models or *reference states of stress*, and each of them defines idealized states of stress in the crust. Each assumes a planet with only one lithospheric shell without the complications of plate tectonics. Tectonic forces are not included in the reference states of stress. Thus, to find tectonic stress one needs to look at deviations from the reference models.

5.3.1 Lithostatic/hydrostatic reference state

The *lithostatic reference state* is the simplest general stress model for the interior of the Earth. It is based on an idealized situation where the rock has no shear strength (σ_s=0). A rock volume with this condition cannot support differential stress over geologic time (σ_1-σ_3=0), which means that its state of stress is described as a point on the horizontal axis of the Mohr diagram (Figure 2.8, hydrostatic/lithostatic). This means that stress is independent of direction:

$$\sigma_1 = \sigma_2 = \sigma_3 = \rho g z \quad (6.1)$$

This is an isotropic state of stress ~~is thus isotropic~~ and the vertical stress equals the horizontal stresses. The stress is completely controlled by the height and density of the overlying rock column. For continental rocks, which have a density of ~2.7 g/cm^3, this means a vertical stress gradient of 26.5 MPa/km (Figure 5.6a). Porous rocks have lower density (2.1-2.5 g/cm^3) depending on porosity and mineralogy, and the gradient becomes somewhat lower in sedimentary basins.

No real, solid rock experiences a perfectly lithostatic reference state. Only magma and other

PRESSURE AND METAMORPHISM

Metamorphic petrologists tend to talk about pressure rather than stress (commonly in terms of kilobars, where 1 kbar = 100 MPa), while structural geologists reserve the term pressure for fluids. Any rock in the lithosphere has a shear strength even over geologic time: rocks can sustain anisotropic stress as long as the melting point is not reached. The metamorphic petrologist uses the term pressure to discuss phase transitions and stability of metamorphic minerals, such as the Al_2SiO_5 system or the transformation of graphite into diamond. This use closely matches our lithostatic reference state. They can do this because they operate at relatively large depths, where anisotropic (tectonic) stresses do not make a big difference when for example andalusite changes into kyanite or graphite becomes diamond. Anisotropic stresses do however determine the tectonic regime and the structures formed.

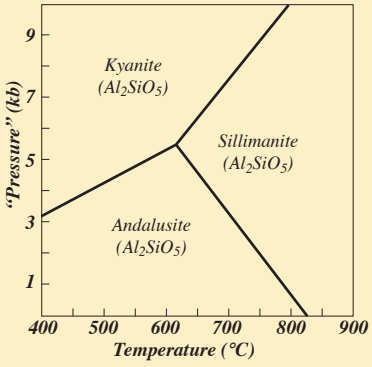

Field of stability for the Al_2SiO_5-system.

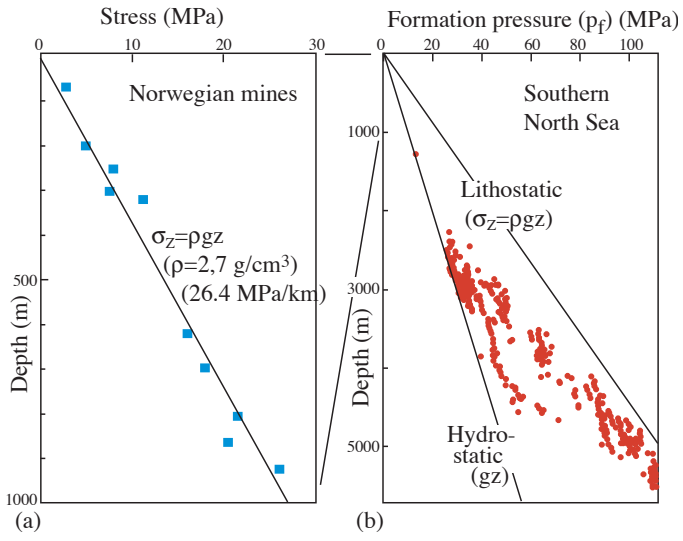

Figure 5.6 a) Vertical stress measurements compared to the theoretical curve for lithostatic stress (ρgz) in Norwegian mines down to 1 km depth (crystalline rocks). b) Pressure data from the southern North Sea (porous rocks) lie between the gradients for hydrostatic and lithostatic pressure. Individual linear trends are seen, indicating overpressured formations and multiple pressure regimes. Note that these pressure data are formation pressures, meaning fluid pressures. Data from Myrvang (2002) and Darby et al. (1996).

fluids do, in which case the term *hydrostatic pressure* is more appropriate. This is relevant in sedimentary basins where the formation fluid is generally water. The density contrast between water and rock forces us to operate with two different stress situations: The hydrostatic pressure is $P_{H2O}=\rho gz=gz$, since the density of water is 1 g/cm^3, while the lithostatic stress is larger by a factor of around 2.7 g/cm^3 (rock density). If the rock also contains oil and/or gas, the densities of hydrocarbons must also be considered.

In a rock column where the rock is porous, the lithostatic pressure is distributed over the grain contact area. This pressure/area ratio gives what is called the *effective stress* $\bar{\sigma}$. In addition we have the pore pressure of the water p_f (and perhaps hydrocarbons) in the pore volume. Hence, we have to operate with two different stress systems in porous media, and the sum of the two is the vertical stress at any given depth:

$$\sigma_v=\bar{\sigma}+p_f \quad (6.2)$$

If the fluid pressure (p_f), often referred to as the formation pressure, equals the hydrostatic pressure ρgz, then the pressure is normal (hydrostatic). In this case pores are interconnected all the way to the surface, and the pore fluid forms a continuous column. This is not always the situation, and deviations from hydrostatic pressure can occur. The pore fluid p_f is routinely measured in oil fields and exploration wells, and many reservoir formations are found to be overpressured.

Overpressure typically forms when formation fluid in porous formations is tapped between non-permeable layers. Typically sandstones sandwiched between shale layers become overpressured during burial because the pore fluid is trapped at the same time as the sandstone carries an increasingly heavy load. The deeper the burial, the larger the deviation between the actual pore pressure and the hydrostatic pressure. This explains deviations from hydrostatic pressure as seen in Figure 5.6b. This figure shows evidence of several pressure regimes in southern North Sea reservoirs, each with their own trends between the hydrostatic and lithostatic gradients.

Deviation from hydrostatic pore pressure is important. A high deviation may indicate that the sandstone is poorly compacted, which could mean sand production (sand flowing into the well together with oil during production) and unstable well conditions. This may occur because during overpressure p_f in Equation 6.2 increases, and the effective stress across the grain contact points decreases. Where the pore pressure approaches lithostatic pressure, very loose sand(stone) may be expected even at several kilometers depth.

Anomalously high pore pressure can have consequences for deformation. Overpressured layers are weak and may act as detachments during deformation. Thrust faults in foreland settings or accretionary prisms preferentially form in overpressured formations, and extensional detachments are known to develop along such zones. On a smaller scale, grain reorganization rather than cataclasis is promoted by overpressure during deformation of sandstones and other porous rocks.

Artificial overpressure in a formation can be created by increasing the mud weight (hydrostatic pressure) in a chosen interval of a wellbore. The rock responds by fracturing at some pressure level, and the operation is known as hydraulic fracturing (Figure 5.1c).

5.3.2 *Uniaxial-strain reference state*

The lithostatic state of stress is easy and convenient, but not necessarily realistic. A somewhat related model is called the *uniaxial-strain reference state*. This reference state is based on the boundary condition that no elongation (positive or negative) occurs in the horizontal directions (Figure 5.7). Strain only occurs in the vertical direction (i.e. strain is uniaxial), and the stress has to comply with this condition[2]. It is interesting to note that stress in this case is prescribed by strain (boundary conditions), whereas we often are inclined to think of strain being the product of stress. Is this really realistic?

The answer is, as you may suspect, yes. This is related to the fact that there is a free surface at top of any rock column, i.e. the face of the Earth, while any rock volume is surrounded by rock in the horizontal direction. Let us consider compaction, which conforms to the prescribed strain field. A rock or rock column can shorten (compact) in the vertical direction, but not in the horizontal plane.

Uniaxial strain is characteristic of compaction of sediments where tectonic stresses are absent or negligible. During burial the horizontal stresses are equal ($\sigma_H=\sigma_h$) and will increase as a function of increasing burial depth or σ_V, but, as shown in section 5.3, the vertical stress will increase faster than the horizontal stress if the crust is modeled as a linearly elastic medium.

The vertical stress is identical to that predicted by the lithostatic reference state, i.e. $\sigma_v=\rho gz=\sigma_1$, and the horizontal stress $\sigma_H=\sigma_h=\sigma_2=\sigma_3$ is given by the expression:

$$\frac{\nu}{1-\nu}\sigma_v = \frac{\nu}{1-\nu}\rho gz \quad (6.3)$$

where ν is Poisson's ratio (see section 5.3 for derivation). In contrast to the lithostatic model, the horizontal stress depends on the physical properties of the rock.

Let us explore equation 6.3 in more detail. Rocks typically have ν values in the range 0.25-0.33. For ν=0.25 the equation gives $\sigma_H=(1/3)\ \sigma_v$

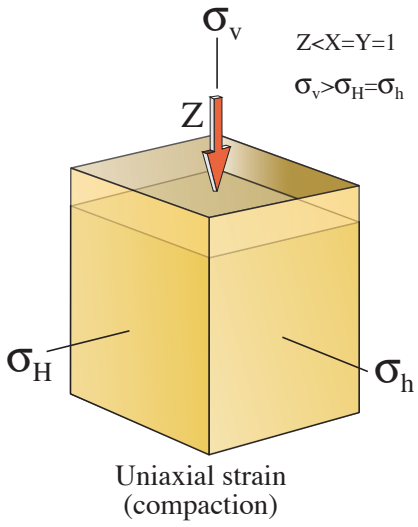

Figure 5.7 Uniaxial-strain reference state of lithospheric stress. Note the difference between the principal stresses (σ_v, σ_H and σ_h) and principal strains (X, Y and Z). Merk forskjellen på spenningsakser (here equal to σ_v, σ_H og σ_h). The strain is uniaxial One component different from zero), while stress is not. In this model the vertical stress comes from overburden while the horizontal one is influenced by the uniaxial strain boundary condition. The model fits well the effecet of compaction in sedimentary basins.

and for ν=0.33, $\sigma_H=(1/2)\ \sigma_v$. In other words, the horizontal stress is predicted to be between half and one third of the vertical stress, i.e. considerably less than what is predicted by the lithostatic reference state. The two models are identical ($\sigma_H=\sigma_h=\sigma_v$) only if the lithosphere is completely incompressible, i.e. if ν=0.5. As stated in Chapter 5, rocks do not even get close to incompressible, but for a sediment that progressively gets more and more cemented and lithified, its elastic property changes (ν increases) and the uniaxial-strain model gets closer to the lithostatic one.

The uniaxial-strain reference state predicts that the vertical stress is considerably larger than the horizontal stress, which again predicts tensional stress regimes ($\sigma_V>\sigma_H>\sigma_h$). However, compressional stress regimes ($\sigma_H>\sigma_h>\sigma_V$) are very common even in the upper crust, so the uniaxial-strain reference state does not sufficiently explain the state of strain in many cases. Besides, it predicts somewhat unrealistically large changes in σ_H during thermal changes and uplift events in the lithosphere. A third model has thus been proposed, called the constant-horizontal-stress reference state.

2 Make sure you do not confuse uniaxial strain with uniaxial stress, which was defined on p. ??. The uniaxial strain model discussed here results in a triaxial stress.

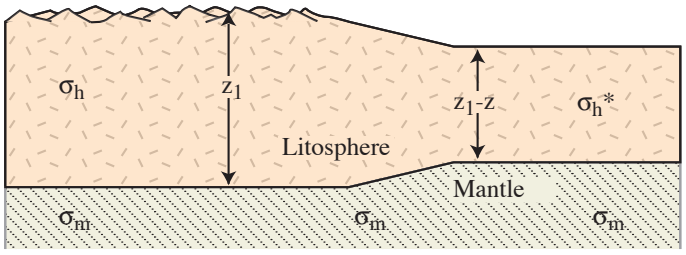

Figure 5.8 Schematic illustration of the relationship between erosion, isostasy and stress for a constant-horizontal-stress reference state, as indicated in equation 6.4. Erosion of the right hand side caused upward movement of the base of the lithosphere until isostatic equilibrium has been reached. The mantle is considered as a fluid where $\sigma_H=\sigma_h=\sigma_v=\sigma_m$. Based on Engelder (1983).

5.3.3 Constant-horizontal-stress reference state

The *constant-horizontal-stress reference state* is based on the assumption that the average stress in the lithosphere is everywhere the same to the depth of isostatic compensation under the thickest lithosphere (z_1 in Figure 5.8). In other words, the average horizontal stress in the lithosphere is more or less constant to the depth of compensation z_1 under the thickest lithosphere. Below z_1, the Earth is assumed to behave like a fluid ($\sigma_H=\sigma_h=\sigma_V=\sigma_m$ in Figure 5.8) where the lithostatic stress σ_m is generated by the overburden. This is a *plane strain model* with strain in the vertical and one horizontal direction only. In general, this model is probably the most realistic one for a lithosphere unaffected by tectonic forces.

The constant horizontal stress requirement is maintained by isostatic equilibrium. After erosion, but before isostatic reequilibration, the average horizontal stress (σ_h*) in the thinner portion of the lithosphere must be higher than that in the thicker portion (σ_h) if the horizontal forces are balanced. The depth of isostatic compensation is z_1, and it is assumed that the mantle below has no shear strength over geologic time. Hence, the state of stress is lithostatic below z_l. The average horizontal stress σ_h* can then be expressed by the equation:

$$\sigma_h^* = \sigma_h\,[z_1/(z_1-z)] - \rho_1 g z(\rho_1/\rho_m)[(z_1-z/2)/(z_1-z)] \quad (6.4)$$

where $\sigma h(z1/z1-z)$ describes the horizontal stress increase resulting from lithospheric thinning (horizontal forces must balance, and stress increases as the force act across a smaller area), and $\rho_l g z(\rho_l/\rho_m)[(z_l-z/2)/(z_l-z)]$ expresses the stress reduction caused by isostasy. Lithospheric thickening can be considered by making $z_l > z$.

Calculations indicate that the constant-horizontal-stress model predicts lower stress changes during uplift related to lithospheric thinning than the uniaxial-strain model.

5.4 The thermal effect on horizontal stress

Temperature changes occur as rocks are buried, uplifted or exposed to local heat sources (intrusions and lavas) and must be added to the three reference states of stress discussed above. The effect of temperature changes on horizontal stress can be significant, and can be calculated using the following equation for uniaxial strain behavior:

$$\Delta\sigma_h^T = \frac{E\alpha_T(\Delta T)}{1-\nu} \quad (6.5)$$

where E is Young's modulus, α_T is the linear thermal expansion coefficient, ΔT is the temperature change and ν is Poisson's ratio. As an example, a temperature change of 100 °C on a rock with ν=0.25 and $\alpha_T=7\times10^{-6}$ °C^{-1} results in a reduction of the horizontal stress of 93 MPa. Cooling during uplift thus has the potential of causing extension fractures in rocks and may in part explain why many uplifted rocks tend to be extensively jointed. Joints are particularly common in competent layers in sedimentary sequences (Figure 5.9). Let us explore this feature in terms of non-tectonic horizontal stress variations before turning to tectonic stress.

5.4.1 Stress variations during burial and uplift

Rocks that are buried and later uplifted go through a stress history that can be explored by means of thermal effects, the Poisson effect (p. ??) and the effect of overburden. The relationship between these effects are combined in the expression:

$$\sigma_H = \sigma_h = (\nu/(1-\nu))\sigma_Z + [\alpha E\Delta T/(1-\nu)] \quad (6.6)$$

where $(\nu/(1-\nu))\sigma_Z$ is the Poisson effect and $[\alpha Y\Delta T/$

Figure 5.9 Densely jointed Permian sandstones and siltstones of the Colorado Plateau, exposed by the Colorado River. Such joints would not occur in a reservoir sandstone unless it was uplifted and cooled substantially.

(1-ν)] is the thermal effect.

Equation 6.6 can be used to estimate σ_H for any given depth. The result depends on the mechanical properties of the rock (E and ν), which means that for instance adjacent sandstone and shale layers will develop different stress histories during burial and uplift. To simplify the calculations, we here use one set of mechanical properties during burial and another during uplift, assuming that lithification occurs at the deepest point of the burial curve only. In other words, sand and clay layers go down; sandstone and shale layers come back up. The result is illustrated in Figure 5.10 and shows that while the clay/shale is always in the compressional regime, the sandstone is likely to enter the tensional regime during uplift.

Tension fractures or joints are more likely to develop in rock layers with the highest Young's modulus and the lowest Poisson's ratio, which in simple terms means stiff and competent layers (i.e. sandstones and limestones) build up significant differential stress,. This may be important to geologists exploring petroleum reservoirs in uplifted areas where vertical tension fractures that may cause leakage of oil traps are more likely. It also means that a smaller overpressure is needed to produce fractures in sandstone than in claystone (Figure 5.11), which is why hydrofractures form in sandstone layers rather than in adjacent claystones.

5.5 Residual stress

Stress can be locked in and preserved after the external forces or stress field has been changed or removed. In principle, any kind of stress can be

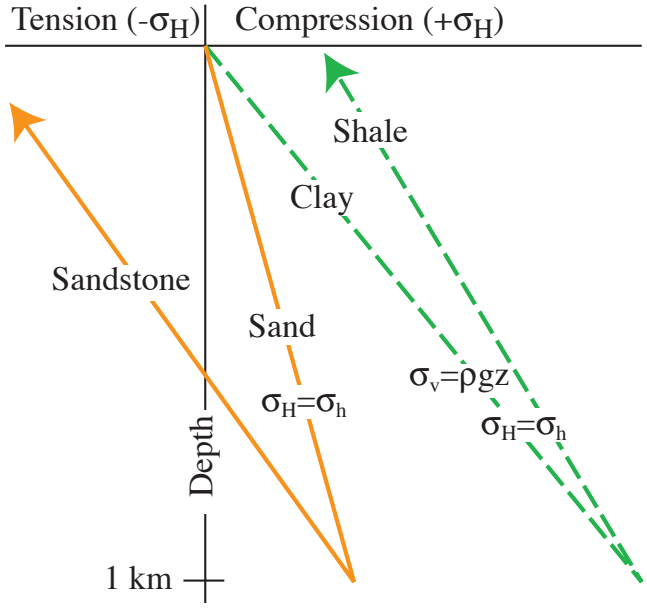

Figur 5.10 Stress variations during burial and uplift for sand(stone) and clay (shale). Lithification is assumed to occur instantaneously at maxumum burial depth. Based on Engelder (1985).

locked into a rock if for some reason elastic strain remains after the stress field is removed. The causes for the external stress may be overburden, tectonic stress or thermal effects.

Let us look at how residual stress can form in sandstone during compaction, cementation and uplift. During burial and physical loading, stress builds up across grain contact areas. Cementation occurs prior to removal of the external stress field or the overburden. Uplift and erosion exposes the sandstone at the surface with stress decrease. The elastic deformation of the grains caused by the now removed overburden will start to relax. However, relaxation is partly prevented by the cement, which itself was stressed. Hence some of the stress is transferred to the cement while the rest remains in the sand grains as locked-in stress. Stress that was imposed on the sand during burial thus remains locked in as residual stress.

Residual stress may thus stem from diagenesis, but may also be caused by metamorphic transformations that involve volumetric changes, by intrusions where magma cooling sets up stresses that are locked into the crust, by changes in temperature and/or pressure, or by past tectonic episodes. There is therefore no absolute distinction between residual stresses, thermal stress and tectonic stress, which will be treated next.

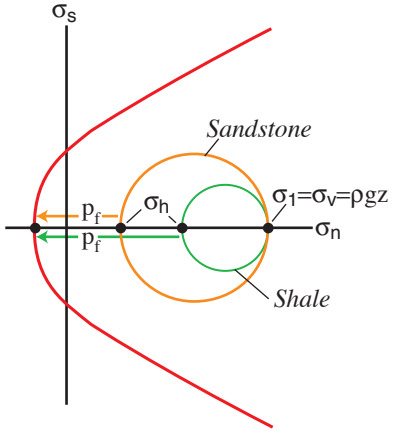

Figure 5.11 Stresses in alternating shale-sandstone layers. Sandstone is stronger and can sustain a higher differential stress than shale. The critical pore pressure needed to generate tension fractures in the sandstone is less than for shale, since the vertical stress is the same for the layers. The red curve defines the fracture criterion that describes the conditions at which the rocks fracture. Fracturing happens when the circle for sandstone or shale touches the red curve. This can happen due to increased pore fluid pressure (see next chapter) or due to uplift. In either case, the sandstone first touches the red line, and it happens at the tensile side of the normal stress axis, meaning that tension fractures form. Fracture criteria are treated in the next chapter (section 7.3).

5.6 Tectonic stress

The reference states of stress discussed above relate to natural factors such as rock density, boundary conditions (uniaxial vs. plane strain), thermal effects and the physical properties of rock. Natural deviations from a reference state are generally caused by *tectonic stresses*. On a large scale, tectonic stress generally means stress related to plate movements and plate tectonics. Locally, however, tectonic stresses may be related to such things as bending of layers, e.g. ahead of a propagating fault or fault intersection or interlocking. Local tectonic stress may be quite variable with respect to orientation, while regional tectonic stress patterns are often found to be constant over large areas.

Tectonic stresses can be defined as those parts of the local stress state in the lithosphere that deviate from the reference state of stress as a consequence of plate-scale and local tectonic processes.

Hence, tectonic stress is the deviation from any chosen reference state of stress. There are also other components of stress, including thermal and residual stresses, that one may want to distinguish from present tectonic stresses. Although individual components may be difficult to separate, the total state of stress in any given point in the lithosphere can be separated into a reference state of stress, residual stress, thermal stress, tectonic stress and terrestrial stress (related to seasonal and daily temperature changes, moon pull etc.):

Current tectonic stress = Total stress – (reference state of stress + non-tectonic residual stress + thermal stress + terrestrial stress)

It is seldom easy to separate the tectonic component of stress from the other contributions. Tectonic stresses are expressed in stress data from the upper crust, as discussed below. They appear on a regional scale, albeit with local significant deviations. In most cases, tectonic stress is a change in a horizontal component of a reference state of stress, and is usually related to plate tectonic processes. We will start by looking at Anderson's classical classification

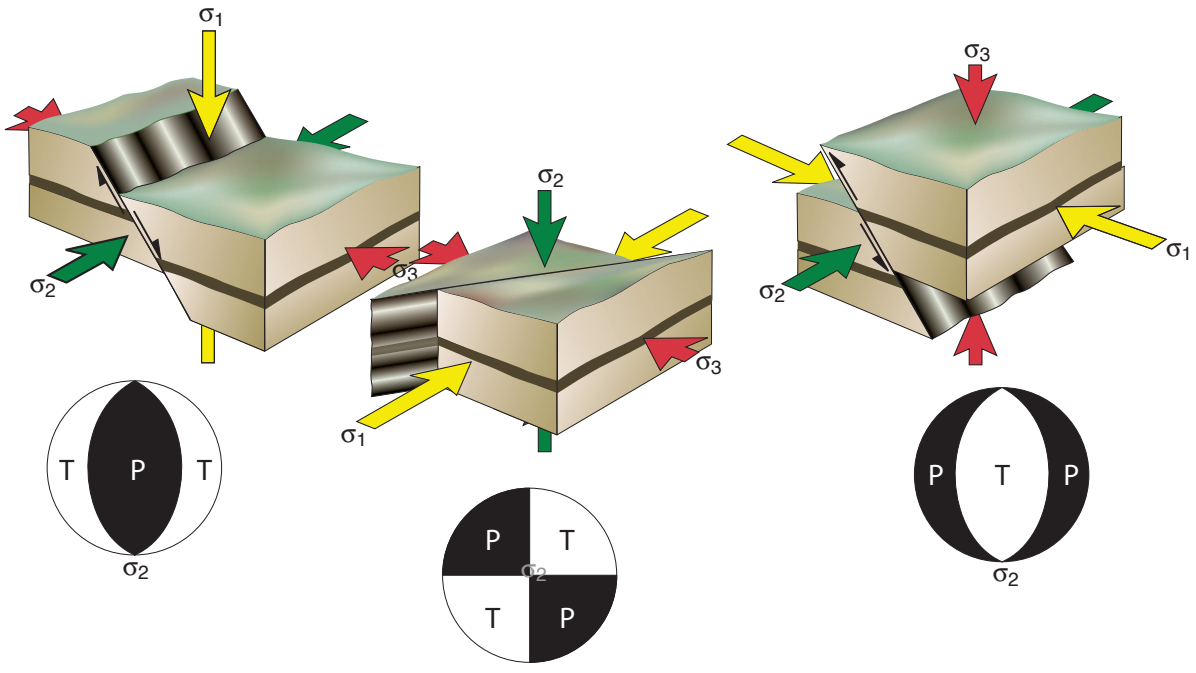

Figure 5.12 Relasjonships between the orientation of the principal stresses and tectonic regimes according to Anderson (1951). Stereonets show fields of compression (P) and tension (T).

of tectonic stress before looking at actual data.

5.6.1 Anderson's classification of tectonic stress

The traditional classification of tectonic stress regimes into normal, thrust and strike-slip regimes was coined in Anderson's famous 1951-publication. Anderson made the assumption that, since there is no shear stress at the Earth's surface (shear stress cannot occur in gases or fluids), one of the principal stresses has to be vertical, implying that the other two are horizontal. Depending on which of the three principal stresses is the vertical one, Anderson defined three regimes (Figure 5.12):

$\sigma_v = \sigma_1$; normal-fault regime,
$\sigma_v = \sigma_2$; strike-slip fault regime,
$\sigma_v = \sigma_3$; thrust-fault regime.

Anderson's classification is valid only in coaxial deformational regimes, where lines parallel to ISA and principal strain axes do not rotate. Furthermore, the deforming rock must be isotropic. The vertical stress can be related to the weight and density of the overlying rock column:

$$\sigma_v = \rho g z \quad (6.7)$$

One of the reference states of stress must be chosen to calculate the horizontal stresses. Let us use the *thrust-fault regime* as an example. A horizontal tectonic stress acts in this regime, which we can call σ^*_t. This stress is an addition to that specified by the reference state of stress (Equation 6.7). For a lithostatic state of stress, σ_H thus becomes

$$\sigma_H = \rho g z + \sigma^*_t \quad (6.8)$$

If instead we consider the uniaxial-strain reference state of stress, then we implicitly assume that the stress condition also depends on the physical properties of the rock. In this case (excluding any thermal effect) we use the designation σ_t for tectonic stress, and by adding this tectonic stress to the uniaxial-strain reference state (Equation 6.3) we have ~~that~~:

$$\sigma_H = [\nu/(1-\nu)]\rho g z + \sigma_t \quad (6.9)$$

It follows by comparing the two expressions that, since $[\nu/(1-\nu)]<0$, $\sigma_t > \sigma^*_t$. This means that the magnitude of the tectonic stress depends on our

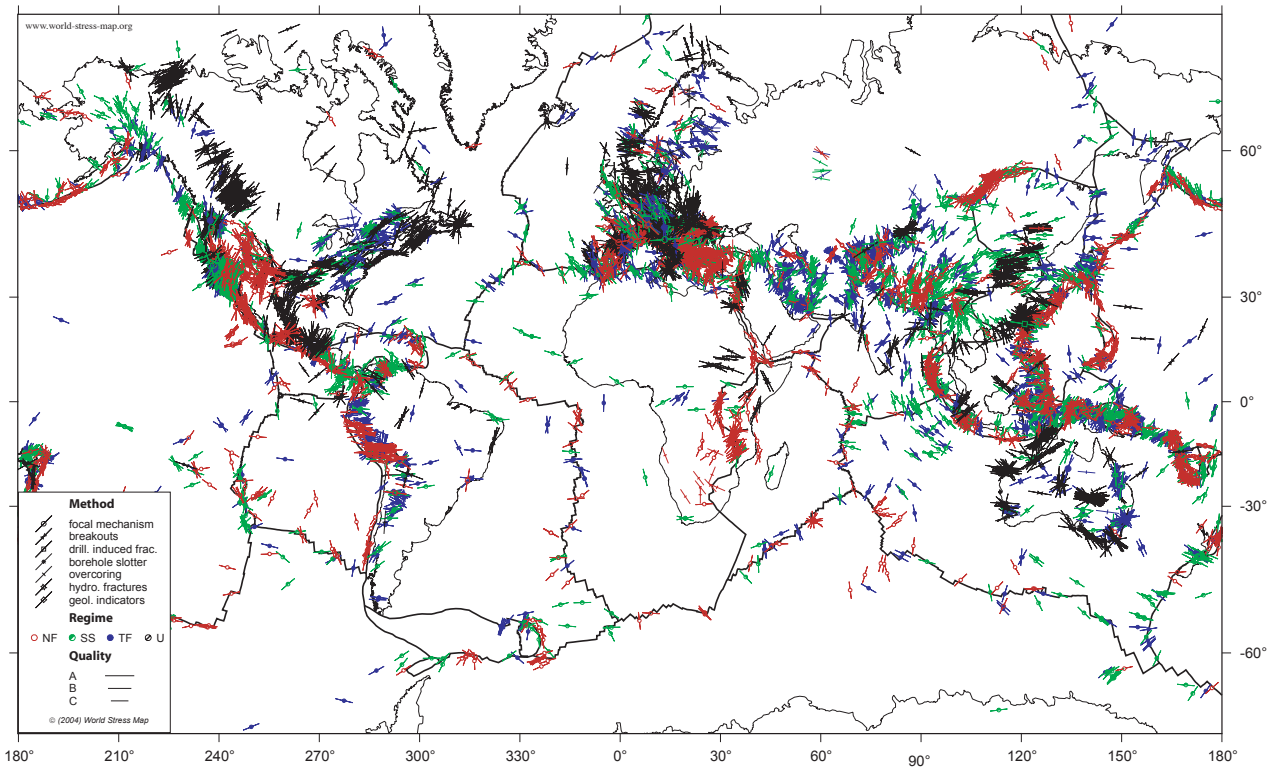

Figure 5.13 The World Stress Map, based on stress measurements from around the World. Lines indicate the orientation of σ_H. Colors indicate tectonic regime (NF=Normal Faulting, SS= Strike-Slip faulting, TF=Thrust Faulting, U=Unknown). From www-wsm.physik.uni-karlsruhe.de.

choice of reference state of stress. Note that when ν approaches 0.5, equation 6.8 approaches equation 6.9, i.e. σ_t approaches σ^*_t. These considerations also hold for the normal-fault regime, except that σ^*_t is tensional and thus becomes negative (σ_t is only negative or tensional in areas of very active normal faulting).

The examples ~~shown here~~ illustrate that the definition of tectonic stress is dependent on the choice of reference state of stress. Hence, the absolute value of tectonic stress is not always easy to estimate.

5.7 Global stress patterns

Stress is estimated around the world in mines, during construction and tunneling work, during onshore and offshore drilling operations, and in relation to earthquake monitoring. All together, these data are evaluated, compiled in *The World Stress Map Project* and are available on the world wide web (www-wsm.physik.uni-karlsruhe.de).

In the World Stress Map Project different types of stress indicators are used to determine the tectonic stress orientation. They are grouped into 1) earthquake focal mechanisms, 2) well bore breakouts and drilling-induced fractures, 3) in-situ stress measurements (overcoring, hydraulic fracturing) and 4) neotectonic geologic structural data (from fault-slip analysis and volcanic vent alignments). The data are ranked according to reliability, and it is assumed that one principal stress is vertical and the other two horizontal. Focal mechanisms completely dominate the deeper (4-20 km) portion of the dataset, while breakouts, hydrofractures and overcoring dominate the shallow data.

Figure 5.13 shows a concentration of stress data from areas near plate boundaries. The main reason for this is the high frequency of earthquakes and neotectonic structures in these areas, which again indicate that tectonic stresses are higher in these areas than elsewhere. The correlation between the orientation of the stress orientations and plate motion is also obvious many places, although the stress data clearly are influenced by stresses from many different sources. Hence, tectonic processes at plate margins are thought to have a significant influence on the regional stress pattern, and the main sources are thought to be slab pull, ridge push, collisional

resistance, trench suction and basal drag. Other, so-called second-order sources of stress are continental margins influenced by sediment loading, areas of glacial rebound, areas of thin crust and upwelling hot mantle material, ocean-continent transitions, orogenic belts and large, weak faults such as the San Andreas Fault. The many sources of stress may be difficult to identify from the present world stress database, but a combination of new stress data and modeling results may improve our understanding of stress in the lithosphere in the future.

A characteristic feature of the stress data (Figure 5.13) is that the horizontal stress field is fairly consistent within broad regions. Eastern North America and Western Europe are two such regions. Another feature is the distribution of the three different fault regimes (normal, strike-slip and thrust regimes). *Tensional stresses* are variably found along divergent plate boundaries, but are more pronounced in areas of rifting and extension. The East African Rift zone, the Aegean area and the Basin and Range Province of the western USA are obvious examples, but also elevated areas in convergent settings, such as the Tibetan Plateau, the high Andes, and the western US Cordillera, tend to be under tension. One of the most popular models for the (ex)tension in these areas is related to gravitational collapse of topographically high areas, which we will return to in Chapter 17. *Strike-slip stress data* are found many places, but a clear concentration is seen in areas of known strike-slip faulting, notably along the San Andreas Fault in California and the Dead Sea transform fault in the Middle East. *Compressional horizontal stresses*, where σ_2 or σ_3 is vertical, are particularly common along convergent plate boundaries and major active orogenic zones (e.g. the Himalayan orogenic belt and the Andes). In addition, many continental regions are dominated by compressive stress regimes.

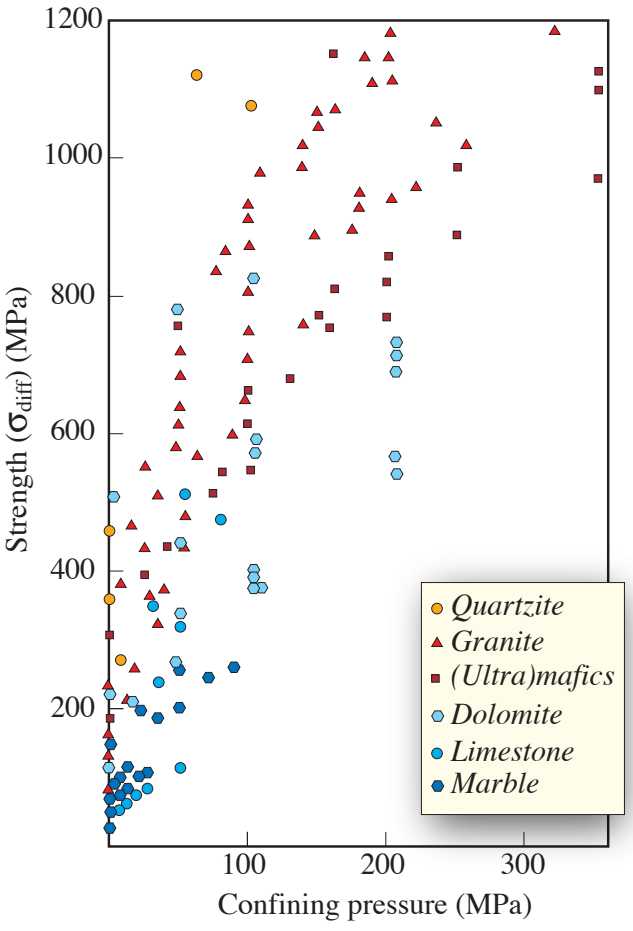

Figure 5.14 The strength of various rock types, plotted against confining pressure (burial depth). The data indicate that the strength of the brittle crust increases with depth, and that the absolute strength depends on lithology (mineralogy). Data compiled from a range of sources.

5.8 Differential stress, deviatoric stress and some implications

The amount of stress increases downwards from the surface into the lithosphere. How much stress can a rock withstand before deformation occurs? If we consider the reference states, stress increases all the way to the center of the earth. Rock forming minerals undergo phase changes and metamorphic reactions in response to this increase, and it takes a deviation from the reference state for rocks to deform by fracturing or shearing. Anderson gave us an idea of how the relative orientation of the tectonic stresses influences the style of faulting (close to the surface). We also want to know how faulting occurs in the lithosphere. Here it is not the absolute level of stress, but rather the difference between the maximum and minimum principal stresses that causes the rock to fracture or flow. This difference is called the *differential stress*:

$$\sigma_{diff} = \sigma_1 - \sigma_3. \quad (6.10)$$

For *lithostatic stress* (Figure 2.8) the principal stresses are all equal, and we have that

$$\sigma_{diff} = 0 \quad (6.11)$$

The lithostatic model itself provides no differential stress to the lithosphere, regardless of depth of burial.

For a *uniaxial-strain reference state* of stress the situation is:

$$\sigma_H = \sigma_h < \sigma_V \qquad (6.12)$$

and the differential stress becomes:

$$\sigma_{diff} = \sigma_1 - \sigma_3 = \sigma_V - \sigma_h = \sigma_V [(1-2\nu)/(1-\nu)] \quad (6.13)$$

For a rock with ν=0.3, $\sigma_{diff} = 0.57\sigma_V$ and σ_{diff} increases with depth at a rate of ~13 MPa/km for continental crust. While the uniaxial-strain reference state of stress may be reasonably realistic in sedimentary basins, it may not be very realistic deep in the lithosphere. Again we see that our choice of reference model has great implications.

Regardless of the choice of reference state of stress, tectonic stress adds to the total differential stress in a rock. The amount of differential stress that can exist in the lithosphere is, however, limited by the strength of the rock itself. When a rock deforms by brittle fracturing, its strength changes and σ_{diff} is reduced. Hence, while the vertical stress in the lithosphere is governed by the weight of the overburden, the horizontal stresses are limited by the strength of the rock at any given depth.

Differential stress at any given point in the Earth is limited by the strength of the rock itself. Any attempt to increase the differential stress above the ultimate rock strength will lead to deformation.

This does not mean that differential stress is independent of overburden. In fact, there is a positive relationship in the upper part of the crust between the amount of overburden and the differential stress that any given rock can support (Figure 5.14). Thus, the strength increases from the surface and down towards the depth at which the rock starts to flow plastically. For granitic rocks this generally means mid-crustal depths (10-15 km). This transition is controlled by temperature rather than σ_V, and is related to the brittle-plastic transition in the crust (Section 5.9).

The strength of rocks in the crust is in practice controlled by anisotropic features, particularly weak

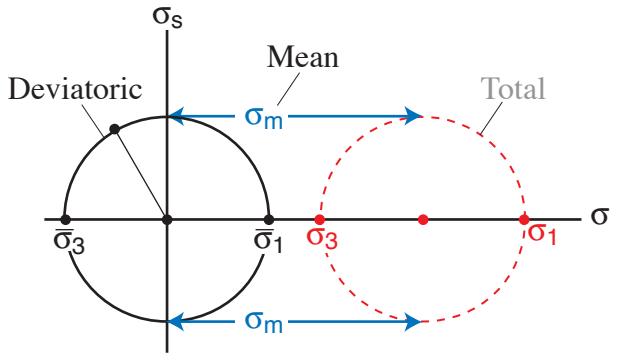

Figure 5.15 The total state of stress can be considered as consisting of an isotropic component, the mean normal stress, and an anisotropic component, the deviatoric stress. The center of the Mohr circle is moved to the origin when the mean stress is subtracted.

fractures and shear zones. We will look more closely at brittle deformation of rocks in the next chapter. Before that we will discuss another useful quantity, called deviatoric stress.

Deviatoric stress (σ_{dev}) is already defined in Chapter 2 as the difference between the total stress tensor and the mean stress tensor:

$$\sigma_{diff} = \sigma_{tot} - \sigma_m \quad (6.14)$$

where

$$\sigma_m = (\sigma_1 + \sigma_2 + \sigma_3)/3 \quad (6.15)$$

In three dimensions deviatoric stress is thus defined as:

$$\begin{bmatrix} \sigma_{11dev} & \sigma_{12dev} & \sigma_{13dev} \\ \sigma_{21dev} & \sigma_{22dev} & \sigma_{23dev} \\ \sigma_{31dev} & \sigma_{32dev} & \sigma_{33dev} \end{bmatrix} = \begin{bmatrix} \sigma_{11} & \sigma_{12} & \sigma_{13} \\ \sigma_{21} & \sigma_{22} & \sigma_{23} \\ \sigma_{31} & \sigma_{32} & \sigma_{33} \end{bmatrix} - \begin{bmatrix} \sigma_m & 0 & 0 \\ 0 & \sigma_m & 0 \\ 0 & 0 & \sigma_m \end{bmatrix}$$

$$= \begin{bmatrix} \sigma_{11} - \sigma_m & \sigma_{12} & \sigma_{13} \\ \sigma_{21} & \sigma_{22} - \sigma_m & \sigma_{23} \\ \sigma_{31} & \sigma_{32} & \sigma_{33} - \sigma_m \end{bmatrix} \qquad (6.16)$$

Or, if the principal stresses are oriented along the coordinate axes of our reference system:

$$\begin{bmatrix} \sigma_{1dev} & 0 & 0 \\ 0 & \sigma_{2dev} & 0 \\ 0 & 0 & \sigma_{3dev} \end{bmatrix} = \begin{bmatrix} \sigma_1 & 0 & 0 \\ 0 & \sigma_2 & 0 \\ 0 & 0 & \sigma_3 \end{bmatrix} - \begin{bmatrix} \sigma_m & 0 & 0 \\ 0 & \sigma_m & 0 \\ 0 & 0 & \sigma_m \end{bmatrix}$$

$$= \begin{bmatrix} \sigma_1 - \sigma_m & 0 & 0 \\ 0 & \sigma_2 - \sigma_m & 0 \\ 0 & 0 & \sigma_3 - \sigma_m \end{bmatrix} \quad (6.17)$$

This implies that the mean stress by definition is the *isotropic* component of the total stress, while the deviatoric stress is the *anisotropic* component at the same point. This becomes clearer if we rearrange the above equation (also see equation 2.?):

$$\begin{bmatrix} \sigma_1 & 0 & 0 \\ 0 & \sigma_2 & 0 \\ 0 & 0 & \sigma_3 \end{bmatrix} = \begin{bmatrix} \sigma_m & 0 & 0 \\ 0 & \sigma_m & 0 \\ 0 & 0 & \sigma_m \end{bmatrix} + \begin{bmatrix} \sigma_{1dev} & 0 & 0 \\ 0 & \sigma_{2dev} & 0 \\ 0 & 0 & \sigma_{3dev} \end{bmatrix}$$

Total stress = Isotropic + Anisotropic part
(6.18)

Deviatoric stress in two dimensions is visualized in Mohr space in Figure 5.15. The distance from the center of Mohr's circle to the origin is the mean stress. The two deviatoric stresses are positive (σ_1-σ_m) and negative (σ_3-σ_m), respectively. Their directions indicate the tectonic regime (normal, thrust or strike-slip). Note that even though one of the anisotropic stresses is negative (σ_3-σ_m), the isotropic component is generally large enough in the lithosphere that all principal stresses of the total state of stress become positive (compressive).

From these considerations of the state of stress in the crust we will move on to look at the brittle response of upper crustal rocks to stress. Fracturing and stress are closely connected, and we are now in a situation where we are able to consider the connection between fractures and stress.

Further reading:

Amadei, B & Stephansson, O., 1997: Rock stress and its measurement. Chapman & Hall, London, 490 pp.

Engelder, J.T., 1993. Stress regimes in the lithosphere. Princeton, 457 ss.

Means, W.D., 1976. Stress and Strain. Springer-Verlag, New York, 339 ss.

Olesen, O. et al., 1992. Neotectonics in the Precambrian of Finnmark, northern Norway. Norsk Geologisk Tidsskrift, 72: 301-306.

Turcotte, D.L. & Schubert, G., 2002. Geodynamics. Cambridge University Press: 472 pp.

CHAPTER 6

Rheology

Stress and strain are related, which is why different states of stress tend to produce different states of strain. However, the relationship is highly dependent on the rheology or mechanical properties of rock. The same rock may react differently depending on strain rate, temperature, pressure and other physical conditions. It may crush at low temperatures and flow like syrup at higher temperatures. Strain rate typically has a similar effect (Newtonian materials), unless perfectly plastic behavior is achieved. Perhaps stress causes only elastic strain that disappears once the stress field is relaxed. Elastic, Newtonian and perfectly plastic materials are ideal reference materials, useful when trying to understand natural deformation structures and textures. A very useful arena for exploring stress–strain relations and the way rocks deform is the rock deformation laboratory, where factors such as the stress conditions, deformation rate, pressure and temperature can be controlled. Experimenting with different media has greatly increased our knowledge about rock deformation and rheology.

5.1 Rheology and continuum mechanics

Rheology is the study of the mechanical properties of solid materials as well as fluids and gases. The name derives from the Greek word "rheo", which means "to flow". But what has flow and fluids got to do with solid rocks? In answering this question, it is interesting to consider the Greek philosopher Heraclitus' aphorism "Panta Rhei", meaning "everything flows". He argued that everything is in constant change, which is easier to accept if geologic time is involved.

It is not only water that flows, but also oil, syrup, asphalt, ice, glass and rock. The flow of oil and syrup can be studied over time spans of minutes, while it takes days, months or years to study the flow of ice and salt glaciers, which again flow considerably faster than glass. Old (100-200 years) window glasses tend to be thicker in their lower part than in their upper part simply because of the slow flow of glass under the influence of gravity.

If you watch a glassmaker at work you know how much quicker glass flows when heated. This is the case with most solids, including rock. Flow of rock mostly occurs in the middle and lower crust where temperatures are higher than in the cool upper crust. The upper crust tends to fracture, a feature outside of the field of rheology but still within the realm of *rock mechanics*. In addition to external factors, such as stress, temperature, pressure and fluids, the properties of the material itself are of course important. Hence, an old marble bench supported on the ends may be seen to have sagged in the middle, reflecting the fact that calcite is different from most other minerals in that it flows at relatively high rates even under surface conditions.

If we consider rock as a continuous medium, neglecting heterogeneities such as (micro)fractures, mineral grain boundaries, and pore space, and consider physical properties to be constant or evenly changing through the rock volume, simple mathematics and physics can then be used to describe and analyze rock deformation in what is known as *continuum mechanics*. Equations that mathematically describe the relationship between stress and strain or strain rate are the focus in this chapter. Such relations are called *constitutive laws* or *constitutive equations*. The term *constitutive* emphasizes the importance of the constitution of the material.

5.2 Idealized conditions

In a simple and idealized continuum mechanics context, materials can be said to react to stress in three fundamentally different ways; by perfectly elastic, plastic and viscous deformation. In addition there is brittle deformation and cataclastic flow, but these are beyond the field of continuum mechanics. As the physical conditions change during the deformation history, a given material can deform according to each of these types of flow.

Deformations are generally analyzed by plotting a stress-strain or stress-strain-rate curve where strain or strain rate is plotted along the horizontal axis and stress along the vertical axis (Figure 6.1). Time dependent deformations are also described by means of stress-time and strain-time graphs where time is plotted along the horizontal axis. Several curves can be plotted, either for the same material under different external conditions or for different materials under the same external conditions. Each curve can also be subdivided into stages distinguished by their characteristic stress-strain (rate) relationships. We will start by looking at the elastic response to stress, then move to permanent non-brittle deformation or flow.

It is always useful to start out by looking at simple cases, so let us consider a perfectly isotropic medium (rock). By *isotropic* we mean a medium that has the same mechanical properties in all directions, so that it reacts identically to stress regardless of its orientation. Much of the strains we will consider in this chapter are small, less than a few percent for elastic deformation (i.e. for elastic deformation). This contrasts to strains that we often face when studying rocks in the field. The advantage is that a simple relationship occurs between stress and strain for small strains in such an ideal medium. In particular, the instantaneous stretching axes (ISA) will be identical to the principal stresses, assumed throughout this chapter unless specified otherwise. We will deal with natural conditions and structures in later chapters.

5.3 Elastic materials

An *elastic material* resists a change in shape, but strains as more stress is applied (Figure 6.2). Ideally,

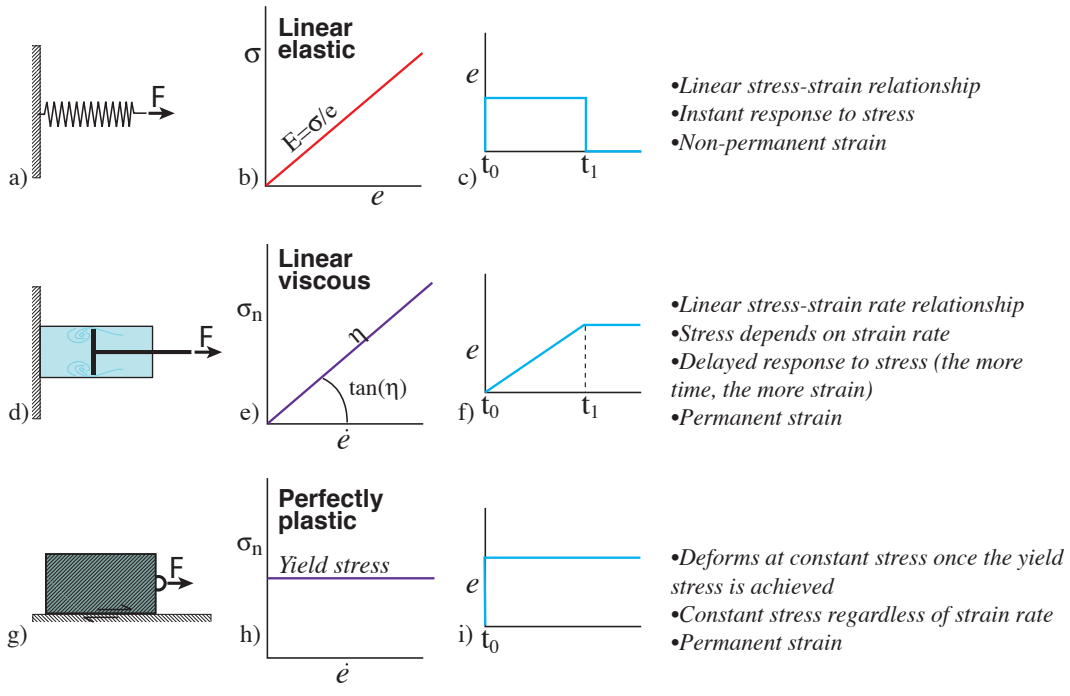

Figure 6.1 Elastic, viscous and plastic deformation illustrated by mechanical analogs, stress-strain (rate) curves and strain history curves (right).

it returns to its original shape once the applied stress (force) is removed.

Elastic strain is recoverable because it involves stretching rather than breaking atomic bonds.

Most rubber bands fit this definition very well: more stretching requires more force, and the band recovers its original shape once the force is removed. Rubber is, however, not a linear elastic material.

Linear elasticity and Hooke's law

A *linear elastic material* has a linear relationship between stress (or force) and strain. This means that if it flattens twice as much under two tons weight as under one, it will flatten four times as much under four tons weight. An analogy is often made to a simple spring (Figure 6.1a): If the weight on the spring is doubled then the change in length has also doubled and so on. In other words, the elongation of the spring is proportional to the force applied, and the spring will return to its original length once the force is removed. A similar example is shown in Figure 6.2, where a rod of some elastic material is pulled. Such a linear relationship between stress and strain is expressed by *Hooke's law*:

$$\sigma = Ee \qquad (6.1)$$

where σ=stress, e=extension (i.e., one-dimensional strain), and E=*Young's modulus* (sometimes denoted Y), also called the *elastic modulus* or, less formally, the stiffness of a material. Hooke's law is a constitutive equation for elastic materials.

Young's modulus can also be viewed as the

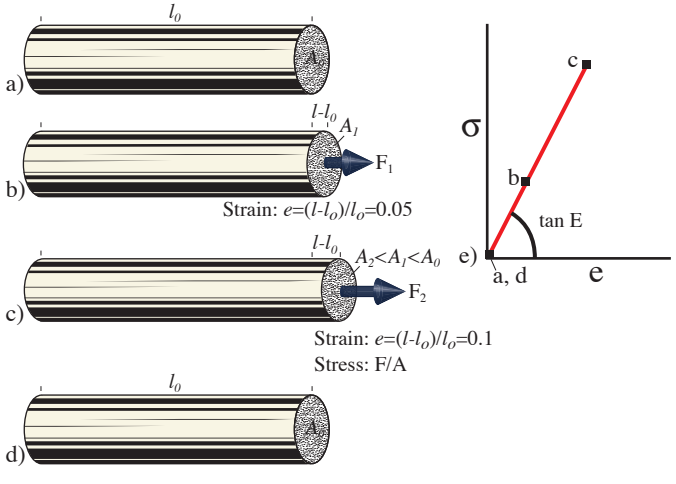

Figure 6.2 Elastic deformation illustrated (a-d) by uniaxial extension of a rod. The stronger the force F that acts on the end area A, the longer the rod (length *l*). If the material is linear elastic, then the relationship between the extension *e* and σ (=F/A) is linear and forms a line in e-σ-space (e). The gradient of the line is E (Youngs modulus). When the force is relaxed, the material returns to its original length (the origin).

Medium	E (GPa)	ν (Poisson's ratio)
Iron	196	0.29
Rubber	0.01-0.1	almost 0.5
Quartz	72	0.16
NaCl	40	~0.38
Diamond	1,050-1,200	0.2
Limestone	80	0.15-0.3
Sandstone	10-20	0.21-0.38
Shale	5-70	0.03-0.4
Gabbro	50-100	0.2-0.4
Granite	~50	0.1-0.25
Amphibolite	50-110	0.1-0.33
Marble	50-70	0.06-0.25

Figure 6.3 Representative values of Young's modulus (E) and Poisson's ratio for some rocks, minerals and familiar media.

stress/strain ratio:

$$E = \sigma/e \qquad (6.2)$$

and is closely related to the *shear modulus* μ (also denoted G and called the rigidity modulus, not to be confused with the friction coefficient introduced in Chapter 2). For uniaxial strain the relationship is simple:

$$E = 2\mu \qquad (6.3)$$

Shear modulus is related to the shear stress (γ), and Hooke's law can be written:

$$\sigma_s = \mu\gamma \qquad (6.4)$$

or:

$$\sigma = 2\mu e \qquad (6.5)$$

The constant E expresses the ratio between the normal stress and the related extension or shortening in the same direction and describes how hard it is to deform a certain elastic material or rock. Similarly, μ quantifies how hard it is to deform a rock elastically under simple shear (for very small finite strains). A rock with a low E-value is mechanically weak, as its resistance to deformation is small. Since strain is dimensionless, Young's modulus has the same dimension as stress, and is typically given in GPa (10^9 Pa). Young's modulus for diamond is more than 1000 GPa (very hard to strain), and for iron it is 196 GPa (under axial tension). It takes less force to squeeze aluminum witn E=69 GPa, and rubber is really easy to deform elastically with typical values of E in the range 0.01-0.1. Figure 6.3 gives some examples of experimentally determined strengths and their characteristic values of E.

Non-linear elasticity

Several minerals are linearly elastic, including quartz and dolomite (Figure 6.4). Even some granites and dolomites obey Hookean elasticity for small strains, but most elastic materials do not, meaning that the line in σ-*e*-space is not straight. This means that there is no constant stress-strain relationship, no single Young's modulus. The curves defined during straining (loading) and unstraining (unloading) may still be identical, in which case the material is *perfect elastic* (Figure 6.5b). In this case, the word *perfect* relates to the fact that the material perfectly recovers to its original shape. In many cases of experimental rock deformation, the stress-strain curves during elastic loading and unloading will differ, and the material is called *elastic with hysteresis* (Figure 6.5c).

If the deformed volume does not return to its original shape, then the deformation is inelastic. The remaining strain is referred to a *permanent strain*. However, when strain is small (a few percent or less), the deviations from elasticity generally are small enough that elastic theory can successfully be used to model fracture initiation and growth in natural rocks as well as in metals, concrete and many other media.

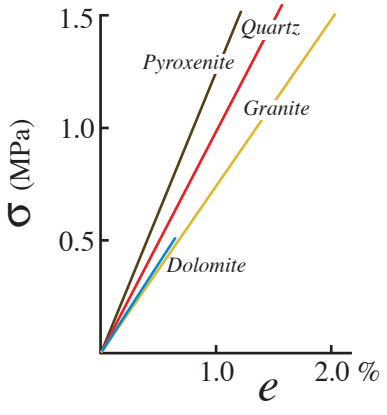

Figure 6.4 Some minerals and rocks show linear elasticity, which means that they follow the same linear path in stress-strain space during stress build-up as during unloading. Data from Griggs et al. (1960) and Hobbs et al. (1972).

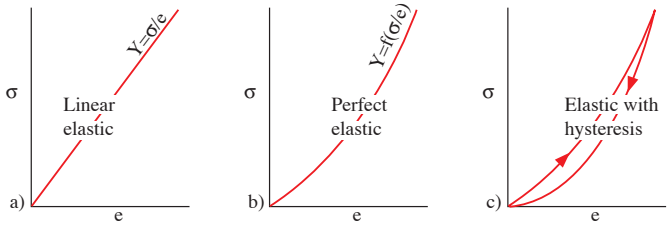

Figure 6.5 The three types of elasticity. a) Linear elasticity where the loading (straining) and unloading (unstraining) paths are both linear and identical and where the gradient is described by Young's modulus. b) Perfect elastic deformation follows the same non-linear path during loading and unloading. c) Elasticity with hysteresis is where the path is nonlinear and different during loading and unloading.

In particular, *linear elastic fracture mechanics* is used as a simple way to explore and model the state of stress around fractures. It describes stress orientations and stress concentrations based on the geometry of the object (fracture) and the overall (remote) state of stress.

Elastic deformation

Before looking at permanent deformation, let us return to our example of the elastically extended rod in Figure 6.2. Here, the axial stretching is accompanied with thinning of the rod. Therefore the area in Figure 6.2 shrinks as the rod extends. The same effect can be seen when pulling a rubber band: the more it is stretched, the thinner it gets. Because we are considering an isotropic material the shortening will be the same in any direction perpendicular to the elongation direction (long axis of the rod). If we put our rod in a coordinate system with the long axis along z and assume that volume is preserved, then the elongation along z is balanced by the elongations in the directions represented by the x- and y-axes (remember that negative elongations imply shortening):

$$e_z = -(e_x + e_y) \qquad (6.6)$$

Since $e_x = e_y$ we can write the equation:

$$e_z = -2e_x \qquad (5.7)$$

or

$$0.5\, e_z = -e_x \qquad (6.8)$$

where e_z is the elongation parallel to the long axis of the rod and e_x is the perpendicular elongation. In our example e_x becomes negative, because the rod gets thinner during stretching. We could of course shorten the rod in Figure 6.2, which represents a common geologic situation. In this case the shortening causes the sample to expand in the perpendicular direction.

Equation 6.8 tells us that shortening in one direction is perfectly balanced by elongation in the plane perpendicular to the shortening direction. This holds true only for perfectly incompressible materials, i.e. materials that do not change volume during deformation. Rubber is a familiar material that is almost incompressible. In low strain rock deformation there is always some volume change involved, and the 0.5 in equation 6.8 must be replaced with a constant ν that relates the axial and perpendicular extensions. This constant is known as *Poisson's ratio*. ν gives the ratio between the extensions normal and parallel to the stress vector σ_z in Figure 6.6:

$$\nu = -e_z/e_x \qquad (6.9)$$

The minus is commonly omitted when referring to Poisson's ratio for rocks. The closer the Poisson's ratio gets to 0.5, the less compressible the material.

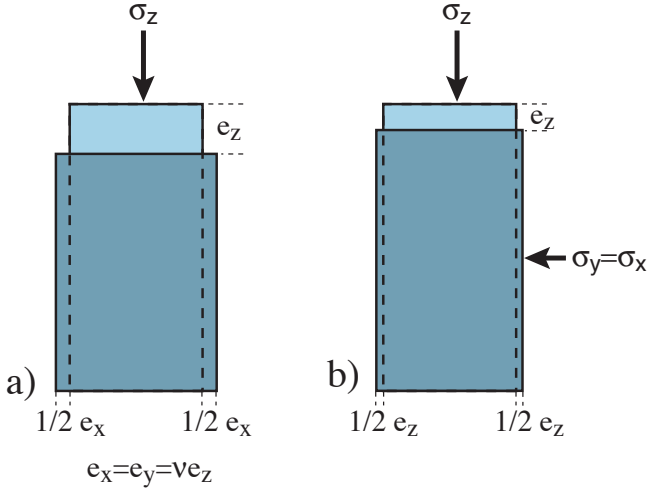

Figure 6.6 a) A vertical stress (σ_z) applied to a rectangular medium (unconstrained uniaxial compression). The stippled rectangle indicates the shape of the material prior to the uniaxial deformation. The horizontal elongation e_x is directly related to the vertical shortening through Poisson's ratio. b) Adding a confining pressure gives horizontal stresses that counteract the effect of the vertical stress (the Poisson effect).

Even steel changes volume, and most steels have ν-values around 0.3, meaning that a contraction in one direction is not fully compensated for by perpendicular elongation. Most rocks have ν values between 0.2 and 0.33. For comparison, cork is close to 0, meaning that it hardly expands or shortens perpendicular to an applied stress. Some materials, such as polymer foams, have a negative Poisson's ratio; if these materials are stretched in one direction, they become thicker in perpendicular directions, i.e. a quite unusual scenario for a rock. Some ν-values for rocks and familiar media are given in Figure 6.3.

If we confine our sample, the horizontal stresses will no longer be zero. Under these conditions horizontal stresses arise that reduce the axial shortening e_z. We now have the following expression for the component of vertical strain resulting from the vertical stress:

$$e_{z'} = \sigma_z / E \qquad (6.10)$$

The horizontal stresses will give rise to vertical strains that counteract the effect of Equation 6.10:

$$e_{z''} = \nu\sigma_x / E \qquad (6.11)$$

and

$$e_{z'''} = \nu\sigma_y / E \qquad (6.12)$$

Thus, the total axial strain is:

$$e_z = e_{z'} - e_{z''} - e_{z'''} \qquad (6.13)$$

By substituting Equations 5.2, 5.11 and 5.12 in Equation 6.13 we obtain the following expression for the axial strain:

$$e_z = (\sigma_z / E) - (\nu\sigma_x / E) - (\nu\sigma_y / E) = \frac{1}{E}\left[\sigma_z - \nu(\sigma_x + \sigma_y)\right] \qquad (6.14)$$

POISSON'S RATIO AND SOUND WAVES

Poisson's ratio, named after the French matematician Simeon Poisson (1781-1840), is a measure of a medium's compressibility perpendicular to an applied stress and can be expressed in terms of velocities of P-waves (V_P) and S-waves (V_S). P-waves or compressional waves are waves of elastic deformation or energy in which particles oscillate in the direction of wave propagation. Conventional seismic is based on P-waves. S-waves or shear waves are elastic body waves where particles oscillate perpendicular to the propagation direction. These are different ways of elastic deformation and their relation to Poisson's ratio is:

$$\nu = (V_p^2 - 2V_s^2) / 2(V_p^2 - V_s^2)$$

Hence, if V_P and V_S can be measured, Poisson's ratio can be calculated. The ratio is useful in estimating rock and fluid properties in a petroleum reservoir. For example, if $V_S = 0$, then $\nu = 0.5$, indicating either a fluid (shear waves do not pass through fluids) or an incompressible material (which as already stated is not found in the crust). V_S approaching zero is characteristic of a gas reservoir. Poisson's ratio for carbonate rocks is ~0.3, for sandstones ~0.2, and above 0.3 for shale. The Poisson's ratio of coal is ~0.4.

Similar expressions can be found for the horizontal stresses:

$$e_y = \frac{1}{E}\left[\sigma_y - \nu(\sigma_z + \sigma_x)\right] \qquad (6.15)$$

and

$$e_x = \frac{1}{E}\left[\sigma_x - \nu(\sigma_z + \sigma_y)\right] \qquad (6.16)$$

The generation of stresses perpendicular to the loading direction is known as the *Poisson effect*. This effect is very relevant to rocks in the crust, because any buried rock volume is confined by other rocks and therefore cannot expand in the horizontal (x-y) plane. As a consequence there will be no horizontal strain (e_x=e_y=0), which reduces the vertical shortening e_z.

In fact, e_z will depend on both ν and σ_z. Furthermore, horizontal stresses will result from the vertical stress because this stress cannot be released by lateral strain. To find the vertical stress e_z we use the boundary condition that e_x=0 in equation 6.16 and obtain:

$$\frac{1}{E}\left[\sigma_x - \nu(\sigma_z + \sigma_y)\right] = 0 \qquad (6.17)$$

Multiplying by E on each side gives:

$$\sigma_x - \nu(\sigma_z + \sigma_y) = 0 \qquad (6.18)$$

Rearranging and using $\sigma_x = \sigma_y$ gives

$$\sigma_x = \sigma_y = \frac{\nu}{1-\nu}\sigma_z \qquad (6.19)$$

We will return to this equation for elastic media in the next chapter because it represents one of several models for the state of stress in the crust.

If pressure changes cause elastic deformation rather than directed force, then the *bulk modulus* K relates the pressure change Δp to volume change (volumetric strain):

$$K = \frac{\Delta p}{\Delta V / V_0} \qquad (6.20)$$

The bulk modulus is the inverse of the compressibility of a medium, which is a measure of the relative volume change (volumetric strain) of a fluid or solid as a response to a pressure or mean stress change. The higher the value of bulk modulus, the more pressure is needed for the material to compress. Equation (5.20) is a specific form of Hooke's law and K is related to Young's modulus (E) and to the shear modulus (μ) by:

$$K = \frac{E}{3(1-2\nu)} = \frac{2(1+\nu)}{3(1-2\nu)}\mu \qquad (6.21)$$

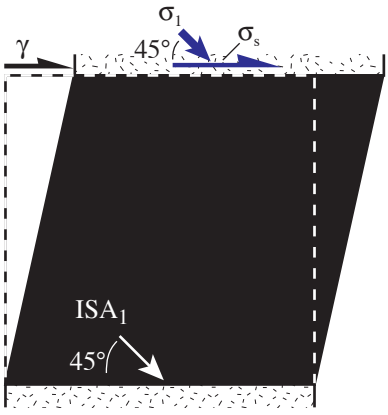

Figur 6.7 Shearing of a medium (fluid) implies that the maximum principal stress is acting at 45° to the surface. For small strains this is equal to the orientation of ISA1. Increasing the stress results in faster shearing if the material is viscous. The relation between the two is determined by the viscosity of the material.

5.4 Plasticity and flow: Permanent deformation

While elastic theory may work well for very small strains in the upper crust, heated rocks tend to flow and accumulate permanent deformation. In this context it is useful to consider how fluids respond to stress. Rocks can never quite become fluids unless they melt, but at high temperatures and over geologic time they may get fairly close in terms of rheology.

Viscous materials (fluids)

The ease with which fluids flow is described in terms of their viscosity η. Viscosity and laminar flowing fluids were first explored quantitatively by Sir Isaac Newton. He found that the shear stress and shear strain rate are closely related:

$$\sigma_s = \eta\dot{\gamma} \qquad (6.22)$$

where η is the viscosity constant, and $\dot{\gamma}$ is the shear strain rate or shear strain per time unit (Figure 6.7). A material that deforms according to this equation is a *Newtonian fluid* or a *linear* or *perfectly viscous material*. The constitutive equation for viscous materials can also be expressed in terms of normal stress and elongation rate:

HOW QUICKLY DO ROCKS DEFORM?

Strain rate is a measure of how fast a rock changes length or shape. Since strain is dimensionless it gets the somewhat peculiar dimension s^{-1} (per second). There are generally two different types of strain rate that we must consider. The simplest is the *rate of elongation* and is denoted $\dot{\varepsilon}$ or $\dot{e}$. This is elongation per time unit (second):

$$e = \frac{e}{t} = \left(\frac{l - l_0}{t l_0} \right)$$

We can also call this the extension rate or contraction rate. In an experiment this may be closely related to the speed at which we squeeze a sample. For an axial compression test that lasts for one hour, where the sample is shortened at 10%, the elongation rate becomes:

$$e = \frac{-0.1}{3600 s} = -2.778 \cdot 10^{-5} s^{-1}$$

In some geological settings the *shear strain rate* may be more appropriate. Here the change in shear strain over time is considered, and it is denoted γ. Its dimension (s^{-1}) is the same as for elongation rate, and they are clearly related, since shear deformation also results in elongation. The two are, however, not linearly related, and it is important to clearly distinguish between the two.

Natural geologic strain rates are on the order of 10^{-14}-10^{-15} s^{-1} and are much slower than the ones we observe in the rock deformation laboratory (10^{-7} s^{-1} or faster). Clearly, this is a challenge when applying experimental results to naturally deformed rocks. In many cases temperature is increased in the laboratory to "speed up" plastic deformation mechanisms and thus increase strain rates. Experimental strain rates must then be scaled down together with temperature. Alternatively, the processes must be studied at smaller length scales.

$$\sigma_n = \eta \dot{e} \qquad (6.23)$$

Viscous deformation involves dependence of stress on strain rate: higher stress means more rapid strain accumulation or flow.

These equations state that there is a simple, linear relationship between stress and strain rate (not strain): the higher the stress, the faster the flow. So while stress was proportional to strain for elastic deformation, it is proportional to strain rate for viscous media. Viscosity can therefore be said to be time dependent; strain is not instant but accumulates over time.

A perfectly viscous material flows like a fluid when influenced by an external force. This means that there is no elastic deformation involved. Hence, when the force is removed, a viscous material does not recover to its original shape. Viscous deformation is therefore *irreversible* and creates *permanent strain*.

A physical analogy to a perfectly viscous material is an oil-filled cylinder with a perforated piston (Figure 6.1d). When the piston is pulled, it moves through the oil at a constant speed that is proportional to the stress (Figure 6.1e). When the force is removed, the piston stops and remains where it is. If the oil is replaced by a more viscous fluid, such as syrup or warm asphalt, then the force must be increased for strain rate to be maintained. Otherwise, the piston will move at a lower speed. If the oil is heated, viscosity goes down and the force must be decreased to keep the strain rate constant. Thus, temperature is an important factor when viscosity is considered. In layered rocks the relative viscosity is also of great interest, as the most viscous (stiff) layers tend to boudinage/fracture or buckle under layer-parallel extension or shortening. Relative viscosity is related to *competency*, where a competent layer is

stiffer or more viscous than its surroundings.

Competency is resistance of layers or objects to flow, relative to that of its neighboring layers or surrounding matrix.

Only fluids are truly viscous, so that in geology only magma can be modeled as a truly viscous medium. However, viscosity is a useful reference when dealing with certain aspects of plastic deformation. We will therefore return to viscosity of rock layers in a discussion of folding and boudinage in later chapters. Note that *non-linear viscous behavior* has been recorded experimentally for deforming hot rocks and is perhaps more applicable to rocks than linear viscosity. Nonlinear behavior in this context simply means that the viscosity changes with strain rate, as illustrated in Figure 6.8. For numerical modeling of folds, both linear and nonlinear viscosity is assumed, while theoretical modeling of boudins require nonlinear viscosity.

Viscosity is stress divided by strain rate, and is thus measured in the unit of stress multiplied by time, represented by Pa s or $kgm^{-1}s^{-1}$ in the SI system. The unit Poise was used before, where 1 Poise = 0.1 Pa s.

Plastic deformation (flow of solid rock)

Ideally, viscous materials (fluids) react to stress according to equation 6.22 no matter how small the stress may be. Under most natural (and experimental) geologic conditions a certain amount of stress is required for permanent strain to accumulate. In fact, the most important difference between fluids and solids is that solids can sustain shear stresses while fluids cannot. For rocks and other solids, elastic deformation occurs for strains up to a few percent. Beyond the *elastic limit* or the *yield stress*, permanent strain is added to the elastic strain (Figure 6.9). If the permanent strain keeps accumulating under a constant stress condition, then we have perfect *plastic deformation* (Figure 6.1 g-i). When the stress is removed after a history of elastic-plastic deformation only the plastic strain will remain (the elastic component is by definition non-permanent). Another requirement for a deformation (strain) to be called plastic is that of continuity or coherency, i.e. the material must not fracture at the scale of observation.

Plastic strain is the permanent change in shape or size of a body without fracture, accumulated over time by a sustained stress beyond the elastic limit (yield point) of the material.

Although microfractures may occur, plastic strain is generally associated with micro-scale deformation mechanisms such as dislocation movements, diffusion or twinning (Chapter 10). Because of the many mechanisms involved at the atomic level, plastic flow does not lend itself to simple physical parameters the way elastic and viscous deformation do. Instead, there are different equations or flow laws for different plastic flow mechanisms. A general example is the power-law equation on the form

$$\dot{e} = A\sigma^{n} \exp(-Q / RT) \quad (6.24)$$

where A is a constant, R is the gas constant, and T and Q are the absolute temperature and activation energy, respectively. For n=1 the material flows as a perfectly viscous fluid, and the flow is linear. For rocks this is only approximated at high temperatures. We will return to flow laws and their underlying deformation mechanisms in Chapter 10.

Perfectly plastic materials

A *perfectly plastic material*, or *Saint Venant material*, is one where the stress cannot rise above the yield stress and strain can continue to be accumulated forever without any change in the stress level (Figure 6.1h). The strength is not strain-rate sensitive: it does

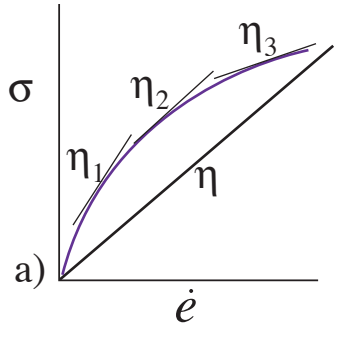

Figure 6.8 Linear (straight line) and non-linear viscous rheology in stress-strain rate space. The slope of the straight line is the viscosity (stress over strain). The non-linear curve has a gradually changing gradient, which is called the effective viscosity. The steepest gradient implies the highest viscosity, which means that it deforms relatively slowly for any given stress condition.

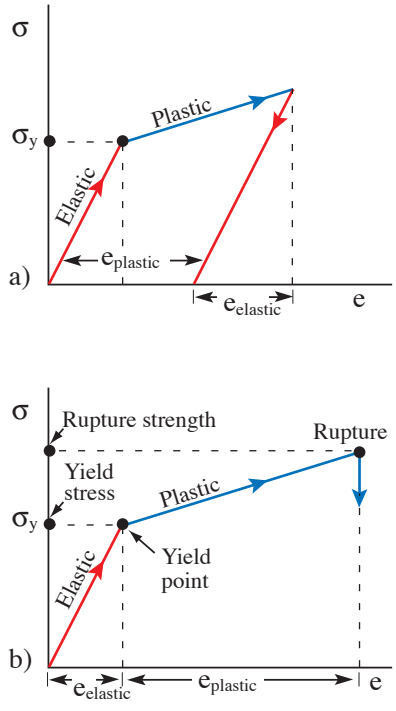

Figure 6.9 Stress-strain curve for elastic-plastic deformation. a) Elastic strain is replaced by plastic strain as the yield stress (σy) is reached. When stress is removed the elastic strain is released, and the plastic or permanent strain remains. b) In this case the stress is increased to the point where brittle rupturing occurs.

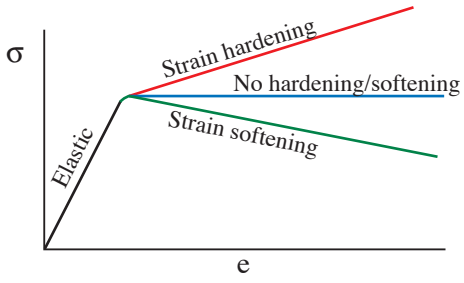

Figure 6.10 Stess-strain curve for elastic-plastic material with hardening, softening, and no hardening/softening properties.

not matter how fast you force the material to flow – the stress-strain curves will be identical. A perfectly plastic material is also incompressible. Where there is an additional component of elastic deformation, then the material is called *elastic perfect plastic* (e.g. middle curve in Figure 6.10). A mechanical analog to perfect plastic deformation is a rigid object resting on a friction surface. Force is increased without any deformation until the frictional resistance between the object and the surface (corresponding to the yield strength) is exceeded (Figure 6.1g). From this point on the force cannot exceed the frictional resistance except during acceleration, regardless of the velocity. Another example is toothpaste, which only starts flowing if you press hard enough, i.e. above the yield stress. Below the yield stress there is some elastic deformation, which is recovered when stress is removed.

Strain hardening and softening

Rocks don't generally behave as perfectly plastic materials during plastic deformation. Strain rate is likely to have an effect, and the stress level is likely to change during the deformation history. If we have to increase the applied stress for additional strain to accumulate (Figure 6.10), then we are dealing with a material science phenomenon called *work hardening*. In terms of strain, the stress necessary to deform the rock must be increased as strain increases. The rock becomes stronger or harder to deform, and we therefore often use the related term *strain hardening*.

Strain hardening is particularly apparent in metals, which can be made harder through plastic deformation. Just bend a metal wire, and then try to bend it back to its original shape. It will be difficult, because the bended part of the metal has hardened: it takes less stress to deform it next to the bend than it takes to deform the bended area. You can keep bending the wire, and the hardening is going to be more and more pronounced until it eventually breaks: strain hardening can result in a transition from plastic to brittle deformation if the level of stress is increased. In geology, strain will re-localize to an adjacent zone, which may explain why many shear zones get wider as strain accumulates (see Chapter 15)[1].

Strain hardening is related to deformation at the atomic scale. During deformation, atomic-scale defects known as *dislocations* (see Chapter 10) form and move. These dislocations intertangle and complicate the accumulation of strain. Hence, more stress is needed to drive deformation, and the result is strain hardening. Elevated temperature eases the motion of dislocations and thus reduces the effect of strain hardening. In other words, heating the bended

1 Strain hardening is also used in relation to brittle deformation structures, such as deformation bands, although it is originally defined within the context of plastic deformation.

wire makes re-bending easier.

If there is no strain hardening and the material keeps deforming without any increase in the applied force or stress, then the process is called *creep*. If, in addition, the strain rate

$$\dot{e} = \frac{de}{dt} \quad (6.25)$$

is constant, then we have *steady-state flow*. Steady-state flow may imply that dislocation movements are quick enough that strain can accumulate at a constant rate for any given stress level. The speed at which dislocations can move around in a crystal depends on differential stress, temperature and the activation energy that it takes to break atomic bonds. The relationship between dislocation-related strain and these variables can therefore be expressed in a flow law of the type portrayed in equation 6.24 (see Chapter 10).

Work softening or *strain softening* is the case when less stress is required to keep the deformation going. A geologic example is the effect of grain size reduction during plastic deformation (mylonitization). Grain size reduction makes deformation mechanisms such as grain boundary sliding more effective because of the increase in grain surface area. Other things that can lead to softening are the recrystallization into new and weaker minerals, the introduction of fluid(s) and, as already mentioned, an increase in temperature.

Strain softening and hardening is not restricted to plastic deformation. It can for instance occur during deformation of unconsolidated sand or soil, where interlocking of grains may lead to strain hardening and dilation may result in strain softening.

5.5 Combined models

Rocks and other natural materials are rheologically complex and generally do not behave as perfect elastic, viscous or plastic materials. It may therefore be useful to go one step further and combine these three types of deformations in order to describe natural rock deformation. Such combinations are commonly illustrated by means of a spring (elastic deformation), a dashpot (hydraulic shock absorber) and a rigid block that will not slide until some critical stress is exceeded (Figure 6.1 a, d and g).

We have already briefly touched upon one combined model, which is the combination of elastic and plastic deformation. This is the situation where stress and elastic strain increase until the yield point is reached, beyond which the deformation is plastic. A material that responds in this way is called an *elastic-plastic* or *Prandtl material*. The typical mechanical analog is in this case the object used to illustrate plastic material combined with a spring, where the spring is meant to represent an elastic medium (Figure 6.11a). The elastic-plastic model is commonly applied to large-scale deformation of the entire crust and the mantle.

A *viscoplastic* or *Bingham material* is one that flows as a perfectly viscous material, but only above a certain yield stress (a characteristic of plastic behavior). Below this yield stress there is no deformation at all. Both rheological experiments on lava and the actual morphology of real lava flows suggest that, over a significant range of temperatures, (liquid) silicic lava behaves like a visco-plastic fluid; that is, due to its crystal content, lava has a yield stress. Paint is a more common fluid that shows visco-plastic behavior: It takes a certain yield stress for it to flow, which prevents thin layers from running off a newly painted wall. The classical mechanical analog is a serial combination of the dashpot (a perforated piston inside a fluid-filled cylinder) and a rigid object resting on a friction surface (Figure 6.11d).

Viscoelastic models combine viscous and elastic behavior. *Kelvin viscoelastic behavior* is where the deformation process is reversible but both the accumulation and recovery of strain are delayed. It describes a material that behaves elastically on short time scales and viscously on long time scales. Viscoelastic materials can be viewed as intermediate states between fluids and solids where both the flow of a fluid and the elastic response of a solid are present. A physical model of a Kelvin viscoelastic material would be a parallel arrangement of a spring and a dashpot (Figure 6.11g). Both systems move simultaneously under the influence of stress, but the dashpot retards the extension of the spring. When the stress is released the spring will return to its original position, but again the dashpot will retard the movement. Such deformation is therefore referred to as *time-dependent*.

The constitutive equation for the Kelvin

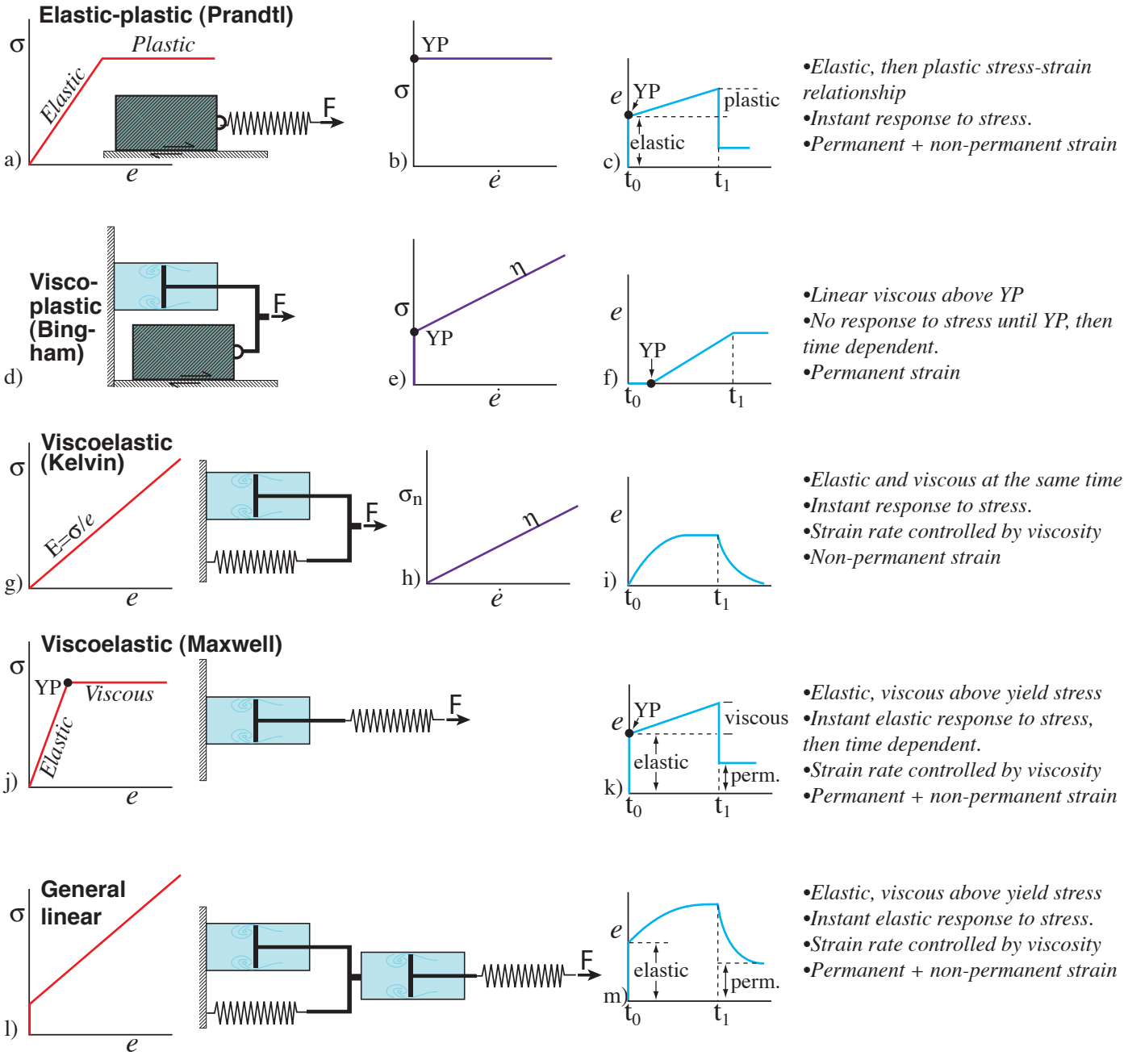

Figur 6.11 Combinations of elastic, viscous and plastic deformation illustrated by mechanical analogs (left), stress-strain (rate) curves and strain history curves (right). Perfect elastic deformation is represented by a spring, while a box with basal friction represents perfect plastic deformation. Perfect viscous deformation is represented by a dashpot. YP=yield point

viscoelastic behavior reflects the combination of viscosity and elasticity:

$$\sigma = E \cdot e + \eta \cdot \dot{e} \quad (6.26)$$

A related viscoelastic model is the *Maxwell model*. A Maxwell viscoelastic material accumulates strain from the moment a stress is applied, first elastically and thereafter in a gradually more viscous manner. In other words, its short-term reaction to stress is elastic while its long-term response is viscous, i.e. the strain becomes permanent. This model fits the mantle quite well: It deforms elastically during seismic wave propagation and viscously during mantle convection or flow related to lithospheric loading (e.g. glacial loading). The mechanical analog now consists of a serial arrangement of a dashpot and a spring (Figure 6.11j). A familiar example is the stirring of bread dough. Just a little push creates elastic deformation, while more serious stirring

creates permanent deformation. When the stirring is stopped, the dough gradually comes to rest and starts to rotate in the opposite direction due to the release of the elastic component. The constitutive equation for Maxwell viscoelastic deformation is:

$$\dot{e} = \dot{\sigma} / E + \sigma / \eta \quad (6.27)$$

Viscoelastic models are useful in large-scale models of the crust, where the elastic deformation describes its short-term response to stress and the viscous part takes care of the long-term flow.

General linear behavior is a model that more closely approximates the response of natural rocks to stress. Its mechanical analogy is shown in Figure 6.111, where the two viscoelastic models are placed in series. The first application of stress accumulates in the elastic part of the Maxwell model. Continued stress is accommodated within the rest of the model. With the removal of stress the elastic strain is recovered first, followed by the viscoelasic component. However, some strain (from the Maxwell model) is permanent.

While most of these combined idealized models predict a linear stress-strain (rate) relationship, there is no reason to assume that plastically deforming rocks follow such simple relationships during natural deformations. In fact, experimental results indicate that they do not, and a power-law (i.e. nonlinear) relationship between stress and strain rate of the form indicated in equation 6.24 with n>1 exists (curved line in Figure 6.8). This relationship characterize *nonlinear material behavior*. Nevertheless, the idealized models are useful reference models, just as deformations such as simple shear and pure shear are useful reference deformations in strain analysis.

5.6 Experiments

Experiments form the basis for much of our understanding of flow in rock. In the laboratory we can choose the medium and control physical variables such as temperature, pressure, stress conditions and strain rate. An obvious disadvantage is that we do not have enough time to apply geologic strain rates, which makes it challenging to compare laboratory results to naturally deformed rocks. The high laboratory strain rate is typically compensated for by increasing temperature, since rocks flow more readily at elevated temperatures.

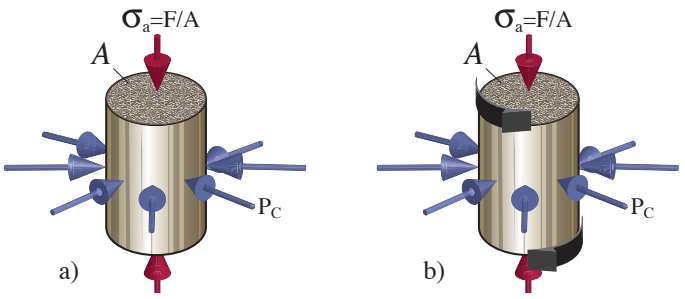

Figure 6.12 a) The standard loading configuration in triaxial rigs. The axial load σ_a and the confining pressure (P_C) are controlled independently by the experimenter. b) A configuration where a torsion is added to the axial compression and the confining pressure. This configuration allows for large shear strains to accumulate.

There are many different experimental setups, depending on the property one wants to explore and the physical conditions one wants to impose. The most common one is the triaxial deformation rig where cylindrical samples are exposed to a confining stress and a principal axial stress (P_c and σ_a in Figure 6.12a). All stresses are compressive, and the sample is shortened when the confining pressure is smaller than the axial compressive stress. If the confining pressure is larger, then the sample extends. There are thus two aspects of stress in this setup. One is the directed stress (anisotropic component), which is the applied force divided by the cross-sectional area of the cylindrical sample. The other is the confining pressure (isotropic component) which is created by pumping up the pressure in a confining gas, fluid or soft material. Confining pressures up to 1 GPa are typical, while temperatures may be up to 1400 °C and strain rates 10^{-3} to 10^{-8} s^{-1}. The stress referred to is then typically differential stress (Section 2.7). A furnace exists around the sample chamber to control the temperature of the sample during the deformation.

Besides of uniaxial or pure shear deformation, some deformation rigs can impose a rotary shear motion (shear strain) on the sample (Figure 6.12b). Most samples that have been deformed experimentally are monomineralic, such as quartzite or calcite. It is frequently assumed that the properties of single minerals such as quartz (upper crust) feldspar (crust) or olivine (mantle) control the rheological properties of various parts of the lithosphere. More data from deformation of polycrystalline samples are therefore needed.

ISOTROPIC OR HOMOGENEOUS?

These are two terms that are related, but with a significant difference. *Homogeneous* means being similar or uniform, while *isotropic* means having properties that do not vary with direction. They are used in various aspects of structural geology, for instance about strain. Homogeneous *strain* means that the state of strain is identical in any one piece of the area or volume in question. It tells nothing about the relative magnitudes of the principal strains. An isotropic strain means that the volume has been shortened or extended by the same amount in any direction. It involves no change in shape, only a change in volume. This is the *isotropic volume change* or volume strain from Chapter 3. Recall that volume can change equally much in all direction (isotropic) or preferentially in one direction (anisotropic).

Isotropic *stress* is a state where all three principal stresses are of equal magnitude. If they are not, stress can still be homogeneous if the state of stress is the same in every part of the rock. A fabric (penetrative foliation and/or lineation) can be uniform throughout a sample, in which case the rock is homogeneous. However, a *fabric* represents an anisotropy because it causes the physical properties to be different in different direction. One could envisage that sliding preferentially takes place along the foliation, or that the stress-strain relationship is different in a sample when loaded parallel and perpendicular to the foliation (Figure 5.14 a-b). Even a single, perfect crystal, which represents a homogeneous volume, can be anisotropic. This is the case with olivine, which has different mechanical properties along different crystallographic axes.

Constant stress (creep) experiments

Experiments can be sorted into those where strain rate is held constant and those where a constant stress field is maintained throughout the course of the experiment. The latter is referred to as creep experiments and involve the phenomenon called *creep*. Creep is a fairly general term used about low strain-rate deformations. Hence, it is used in geology about anything from slow down-slope movement of soil via slow accumulation of displacement along faults (brittle creep) to the slow yielding of solids under the influence of stress (ductile or plastic creep).

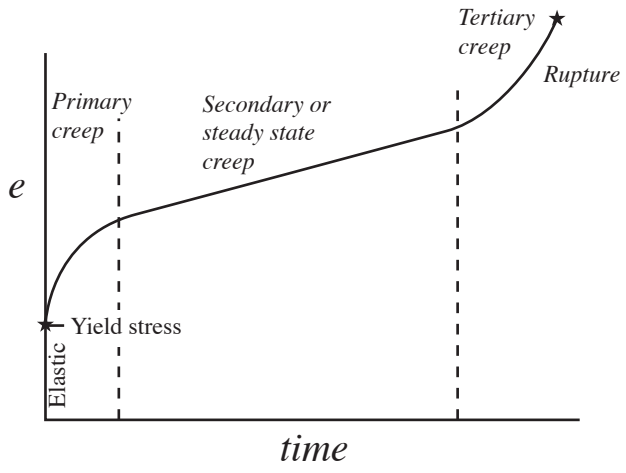

Figure 6.13 Strain-time curve for creep experiment. After initial elastic deformation, three types of creep can be defined. See text for discussion.

Plastic creep is what we are interested in here, and in the current context it is defined as follows:

Creep is the plastic deformation of a material that is subjected to a persistent and constant stress when that material is at a high homologous temperature.

Homologous temperature T_H is the ratio of a material's temperature T to its melting temperature T_m using the Kelvin scale:

$$T_H = \frac{T}{T_m} \qquad (6.27)$$

For water, with T_m = 273K, the homologous temperature at 0K (-273 °C) is 273/0=0, 273/273=1 at 273 K (0 °C), and 137/273=0.5 at 137 K (-137 °C). The homologous temperatures involved in creep processes are greater than 0.5, and creep processes becomes more active as T_H approaches 1. This is why glaciers can flow: ice deforms by creep at the high homologous temperatures of natural glaciers. The use of homologous temperature makes it possible to compare solids with different melting point. For instance, it turns out that ice and olivine behave fairly similarly at a homologous temperature of 0.95, which corresponds to -14 °C for ice and 1744 °C for olivine.

Figure 6.13 shows a generalized strain-time diagram for a creep experiment. Stress is rapidly

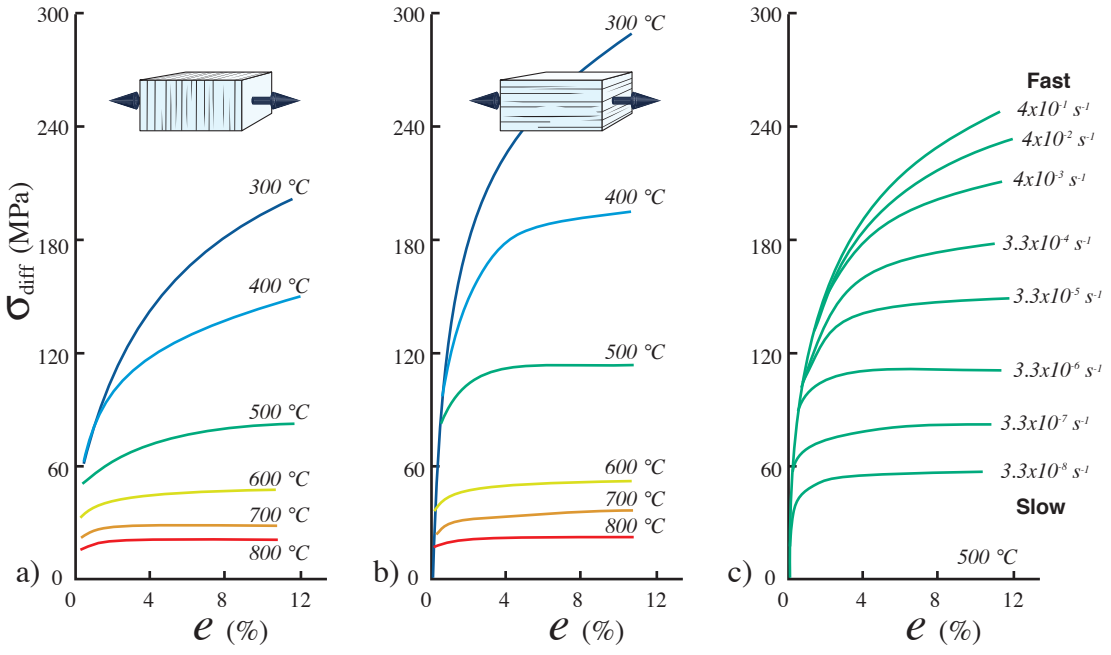

Figure 6.14 Stress-strain curves for Yule marble extended a)normal and b) parallel to the foliation. Data from Heard & Raleigh (1972). c) Stress-strain curves for Yule marble at 500 °C for a variety of strain rates. From Heard (1963).

increased to a fixed level and, after accumulation of elastic strain, creep occurs at a decreasing strain rate. This first stage of creep is called *primary or transient creep*. After some time strain accumulates more steadily and we have entered the region of *secondary or steady-state creep*. Then the *tertiary creep* stage is entered where microfracturing or recrystallization causes an increase in strain rate. This stage is terminated when a macroscopic fracture develops.

Steady-state creep is perhaps the most interesting one to structural geologists, because it appears that rocks can deform more or less steadily for extended periods of time. The constitutive equation during steady-state creep is the power law showed in equation 6.24.

Constant strain-rate experiments

During experiments where the strain rate is fixed, the sample first deforms elastically before accumulating permanent strain, i.e. the general behavior of rocks below the level of fracturing. An increase in stress is required at low temperatures in order to maintain a constant strain rate, consistent with the definition of strain hardening. For higher temperatures or low strain rates, strain does not harden and the deformation is close to steady state. A constitutive law in the form of equation 6.24 is then in effect.

5.7 The role of temperature, water etc.

An increase in *temperature* (Figure 6.14a) lowers the yield stress or weakens the rock. Think of the spring in Figure 6.1a. It can be pulled farther at room temperature than if the string is heated, before plastic (permanent deformation) occurs. At the micro-scale, a temperature increase activates crystal-plastic processes such as dislocation movements and diffusion (Chapter 10). It also lowers the ultimate rock strength, which is the (differential) stress at which the rock fractures.

Increasing the *strain rate* means increasing the flow stress level (Figure 6.14c). This means that higher stresses are required to deform a rock in the laboratory than in nature, where strain rates are lower, at the same temperature. Increasing temperature weakens the rock and therefore counteracts this effect. An increased strain rate may also mean that less plastic strain accumulates because the rock may fracture at an earlier stage. Just think about glass windows that grow thicker in their lower part over hundreds of years but almost instantaneously fracture when hit by a rock. Or glaciers that consist of slowly flowing ice that can be shattered by a swift hammer stroke. Parts

of the Earth behave in a viscous manner because of low strain rates. Increasing the strain rate also makes the rock stronger. Conversely, rocks are weaker at lower strain rates because crystal-plastic processes can then more easily keep up with the applied stress.

Increased *presence of fluids* tends to weaken rocks, lower the yield stress and enhance crystal-plastic deformation. Fluid composition may however also influence rock rheological properties.

Increasing the *confining pressure* allows for larger finite strain to accumulate before failure and thus favors crystal-plastic deformation mechanisms. In simple terms, this is related to the difficulties involved in opening fractures at high confining pressure. The effect of increased confining pressure is counteracted by any increase in pore pressure (for porous rocks), which reduces the effective stress (p. ?).

The presence of *fluids* (water) in the crystal lattice(s) may lower the strength or yield point significantly. Because of the increasing solubility of water with increasing pressure for many silicates, the effect is pressure dependent.

Non-isotropic features such as a preexisting foliation must always be considered. Figure 6.14a-b illustrates how a weak foliation in marble makes foliation-parallel extension more difficult (it takes a higher differential stress to obtain the same amount of strain). Note that the effect disappears as temperature increases.

Even for monomineralic rocks *grain size* and *crystallographic fabric* (preferred crystallographic orientation of minerals) may cause the rock to react differently, depending on the orientation of the applied forces. The anisotropy of olivine crystals is illustrated in Figure 6.15. The reaction to stress depends on the orientation of the applied forces relative to the dominant slip systems in olivine. Penetrative crystallographic fabrics may exist in the mantle, which may give the mantle a significant mechanical anisotropy that can influence location of rifting, strike-slip zones and orogeny.

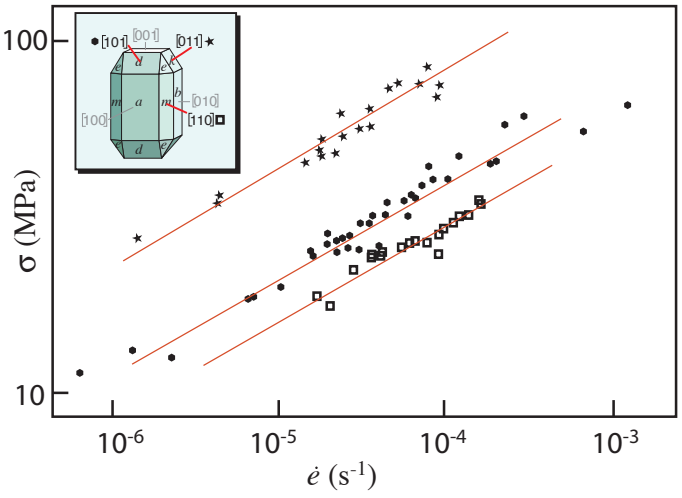

Figure 6.15 Stress-strain rate curves for dry olivine single crystals compressed in three different crystallographic directions. At any strain rate, deformation is easier for crystals shortened in the [110] direction, due to the lower strength of the (010)[100] slip system (see Chapter 10). Data from Durham & Goetze (1977).

5.8 Definition of plastic, ductile and brittle deformation

Ductile and brittle are two of the most commonly used terms in structural geology, both within and outside of the field of rheology and rock mechanics. Again we have the challenge that these terms are given different meanings by different geologists in different contexts.

In the field of rheology and rock mechanics, *ductile deformation* implies deformation without the formation of macroscopic fractures, which characterize *brittle deformation*. A *ductile material* is one that accumulates permanent strain (flows) without fracturing, at least until a certain point where its ultimate strength is exceeded. On the contrary, a *brittle material* is one that deforms by fracturing when subjected to stress beyond the yield point. Ductile materials show a classical stress-strain curve such as the one shown in Figure 6.9, and *ductile structures* are well represented in metamorphic rocks, i.e. rocks that have been deformed in the middle and lower part of the crust.

Ductile deformation also occurs in soils and unconsolidated to poorly consolidated sediments where distributed deformation rather than discrete fracturing occurs. Now the *deformation mechanisms* responsible for the ductile deformation in metamorphic rocks and loose sediments, or in high-temperature rock experiments and low-temperature soil mechanics are quite different. In the first case intracrystalline movement of point or line defects occur in the atomic lattice, as we shall see in Chapter 10. In the latter case, the mechanisms are mechanical and generally related to frictional sliding between grains and rotation of grains. Hence, both brittle (Figure 6.16) and plastic

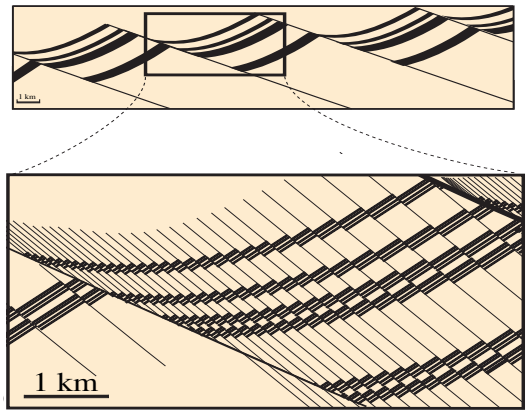

Figure 6.16 The scale-dependent nature of the ductile deformation style illustrated by a regional profile (top), where layers look continuous (ductile deformation style), and close-up where it becomes apparent that the deformation is by multiple small faults. This example is directly relevant to seismic vs. subseismic deformation.

deformation mechanisms may be involved in ductile deformation.

Plastic deformation is defined as the permanent change in shape or size of a body without fracture, produced by a sustained stress beyond the elastic limit of the material. Plasticity relates to intracrystalline deformation mechanisms and related high-temperature non-brittle mechanisms (plasticity is also used in soil mechanics about the consistency of water-rich soil, but we will exclude this use of plasticity in the current discussion). When specifically referring to such deformation mechanisms many geologists thus use the term *crystal-plastic deformation*. The use of the terms ductile and brittle may thus refer to deformation style (the way structures appear or look) or to deformation mechanisms, which may be confusing in some cases.

Ductile vs. brittle deformation styles

In a descriptive way, it is useful to distinguish between *ductile and brittle deformation styles*, where the brittle deformation style involves discrete fractures at the scale of observation (usually mesoscopic) and the ductile does not. Two closely related terms are *continuous* and *discontinuous deformation* (styles), where brittle deformation is discontinuous and ductile is continuous.

A ductile deformation style implies that preexisting structures, such as bedding, have preserved continuity at the scale of observation and that cohesion has not been lost.

A brittle deformation style displays structural discontinuities that can be related to the deformation.

According to this definition, a deformed area or volume can be ductile at one scale and brittle at another (Figure 6.16). In fact, it is hard to find structures that are not.

Ductile vs. brittle deformation mechanisms

There are many different types of mechanisms that can operate during a deformation history, depending on external and internal factors (Chapter 10). They may be grouped into brittle and plastic deformation mechanisms.

Plastic or *crystal-plastic mechanisms* occur at the atomic scale without breaking of atomic bonds but rather occur as creep processes such as dislocation migration. The term *plastic* is here used in a broad sense. In a strict sense it should be distinguished from diffusion and dissolution, which also are non-brittle deformation mechanisms. So, if you want to be very specific, there are brittle deformation mechanisms on one side and plastic, diffusion and dissolution mechanisms on the other.

Crystal-plastic deformation mechanisms result in ductile structures only.

Brittle deformation mechanisms typically generate discontinuities by means of fracturing and frictional sliding. The fracturing occurs at grain scale and above and thus may or may not be observable in outcrop or at a larger scale (Fig. 5.16a), such as that of seismic sections.

Brittle deformation mechanisms can give rise to ductile as well as brittle structures.

5.9 Rheology of the lithosphere

Rocks and minerals react differently to stress and depend on crystallographic anisotropy, temperature, presence of fluids, strain rate and pressure among other factors. Three minerals are particularly common in the lithosphere and therefore of particular interest.

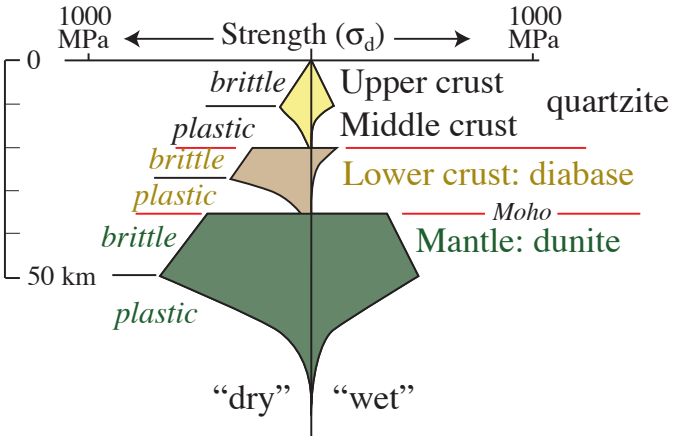

Figur 6.17 Rheologic stratigraphy through the lithosphere based on strength laws derived for quartz (quartzite), feldspar (diabase) and olivine (dunite). Note that dry rocks are considerably stronger than wet rocks. The example is based on modeling of a 35 km thick crust in an extensional regime. Based on Ter Voorde et al. (2000).

These are quartz and feldspar, which dominate the crust, and olivine which controls the rheology of the upper mantle.

Quartz deforms by brittle mechanisms up to about 300-350 °C, which correspond to crustal depths of around 10-12 km. At greater depths crystal-plastic mechanisms (creep-mechanisms) and diffusion dominate.

Feldspar, with its well-developed cleavages, is different because of the ease of cleavage cracking and the difficulty of dislocation glide and climb (crystal-plastic deformation mechanisms). It thus deforms in a brittle manner up to ~500 °C and depths of 20-30 km. However, olivine is brittle down to ~50 km depth.

The transition from the upper crust, dominated by brittle deformation mechanisms, to the deeper crust where plastic deformation dominates, is referred to as *the brittle-plastic transition* (brittle-ductile transition in some texts). Its actual depth depends on several factors, including the relative proportion of quartz and feldspar. It is generally assumed that there is enough quartz in the continental crust to control its reology. This means that even if feldspar is still brittle at 15-20 km, quartz is sufficiently represented and distributed that the crust deforms plastically already at 10-12 km. The transition is, however, also influenced by other factors. The role of fluids is commonly emphasized, and the difference between "dry" and "wet" crust is illustrated in Figure 6.17.

Figure 6.17 illustrates that the strength of the crust is at its maximum at the brittle-plastic transition. But the strength increases again as more feldspar-rich and quartz-poor mafic rocks replace quartz-rich rocks, which may commonly occur in the lower crust. A new rapid increase in strength occurs at the Moho, where the olivine-rich mantle is reached.

Because the crust is layered it is important to obtain as much information as possible about composition in order to predict the strength profile or rheological stratigraphy of the crust. Such information goes into the modeling of crustal-scale deformation, such as rifting and orogeny. The profile itself is generated by means of flow laws based on experimental work (plastic regime) and a frictional relationship known as Byerlee's law (brittle regime), which we will return to in Chapter 7. The intersection between these two laws indicates the brittle-plastic transition(s). It is also important to know that the strength of a given volume of the crust is not only controlled by factors such as temperature and composition, but also depends on the occurrence of weak shear zones and faults. Such structures tend to weaken the crust and control deformation.

---"""---

Rheology is important, particularly to understand deformation in the plastic regime. Plastic deformation mechanisms will be further discussed in Chapter 10, and structures resulting from plastic deformation will be treated in several later chapters. Before that, we will look at stress in a crustal perspective and explore the brittle aspects of rock mechanics.

Further reading:

Balmforth, N.J., Burbridge, A.S., Craster, R.V., Salzig, J. and Shen, A. 2000. Visco-plastic models of isothermal lava domes J. Fluid Mech. (2000), 403, 37–65.

Jaeger, J.C. & Cook, N.G.W., 1976. Fundamentals of rock mechanics. Chapman & Hall, London, 585 ss.

Karato, S. & Toriumi, M. (Red.), 1989. Rheology of Solids and of the Earth, 1. Oxford University Press, New York, 440 ss.

Pfiffner, O.A. & Ramsay, J.G., 1982. Constraints on geological strain rates: arguments from finite strain states of naturally deformed rocks. Journal of Geophysical Research, 87: 311-321.

Ranalli, G., 1987. Rheology of the Earth. Allen & Unwin, Boston, 366 pp.

Turcotte, D.L. & Schubert, G., 2002. Geodynamics. Cambridge University Press: 472 pp.

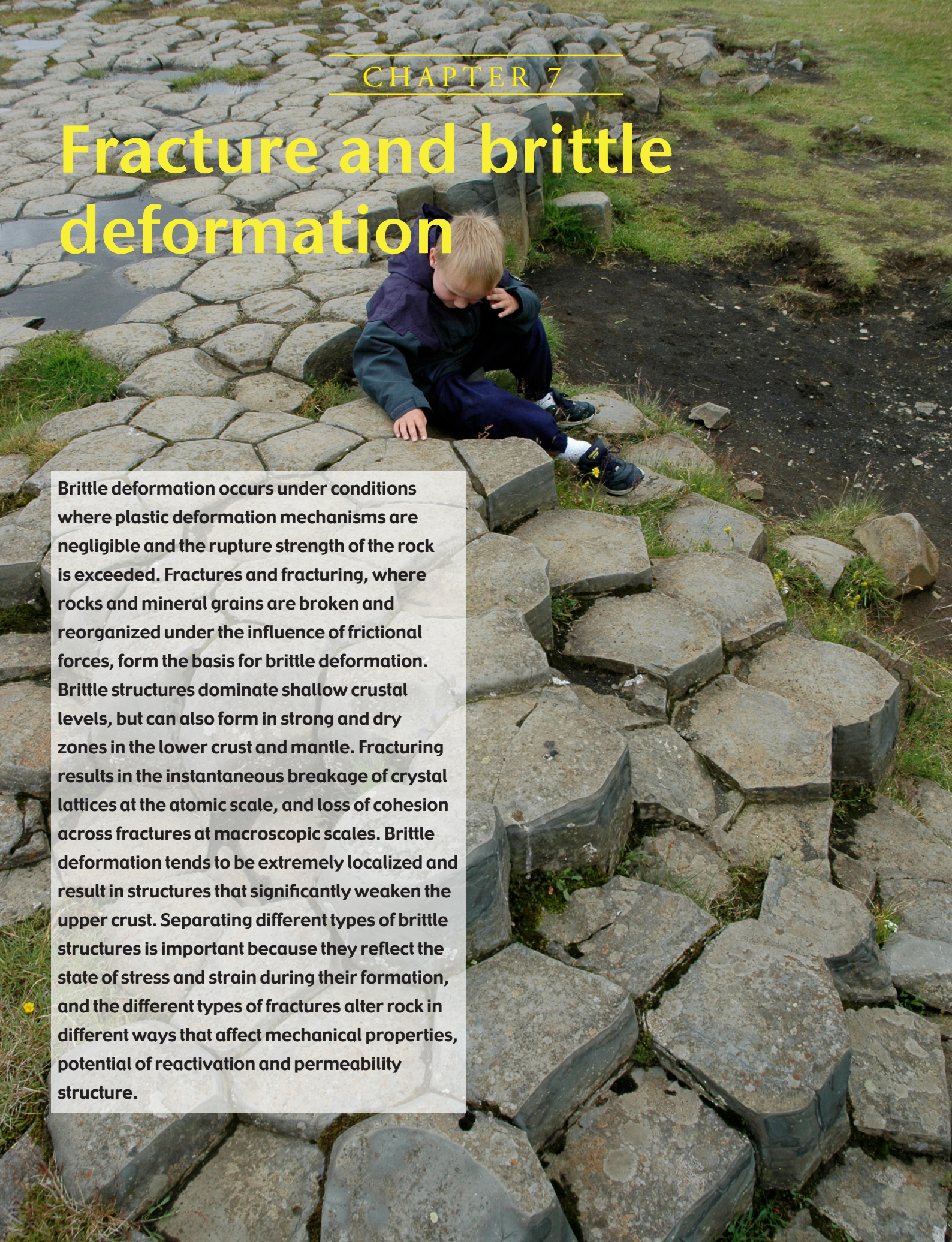

CHAPTER 7

Fracture and brittle deformation

Brittle deformation occurs under conditions where plastic deformation mechanisms are negligible and the rupture strength of the rock is exceeded. Fractures and fracturing, where rocks and mineral grains are broken and reorganized under the influence of frictional forces, form the basis for brittle deformation. Brittle structures dominate shallow crustal levels, but can also form in strong and dry zones in the lower crust and mantle. Fracturing results in the instantaneous breakage of crystal lattices at the atomic scale, and loss of cohesion across fractures at macroscopic scales. Brittle deformation tends to be extremely localized and result in structures that significantly weaken the upper crust. Separating different types of brittle structures is important because they reflect the state of stress and strain during their formation, and the different types of fractures alter rock in different ways that affect mechanical properties, potential of reactivation and permeability structure.

1.1 Brittle deformation mechanisms

Once the differential stress in an unfractured rock exceeds a certain limit, the rock may accumulate permanent strain by plastic flow, as discussed in Chapter 5. In the brittle regime[1], however, the rock deforms by fracturing once its rupture strength is reached. During brittle fracturing, grains are crushed and reorganized and strain (displacement) becomes more localized.

Structural geologists sometimes make a distinction between *intra*granular deformation, where grains fracture internally, and *inter*granular brittle deformation where fractures are much longer and cross grain boundaries. During *intergranular brittle deformation,* slip occurs along grain boundaries so that individual grains remain unfractured (Figure 7.1a). The grains translate and rotate to accommodate frictional grain boundary slip, and the whole process is called *particulate* or *granular flow*. As we shall see in Chapter 10, a different kind of non-frictional grain boundary sliding occurs in the plastic regime. In the brittle regime, grain boundary sliding is influenced by friction, and the mechanism is called *frictional sliding*. A certain friction thus needs to be exceeded for frictional sliding to occur.

The angle of repose in loose sand is controlled by the friction between individual sand grains. The higher the friction between the grains, the higher the angle of repose. In this case gravity imposes a vertical force on grain contact areas, and the shear stress will depend on the orientation of the surfaces, as discussed in Chapter 2.

Frictional sliding of grains may be widely distributed throughout a rock volume, but can also occur in millimeter to decimeter wide zones or bands. Granular flow results in a ductile shear zone where lamination can be traced continuously from one side of the zone to the other. This is a type of ductile shear zone that is governed by brittle deformation mechanisms. The word ductile is here used to describe deformation style, not deformation mechanism (see p.).

Intragranular brittle deformation occurs if the grains are "glued" together by cement, are intergrown

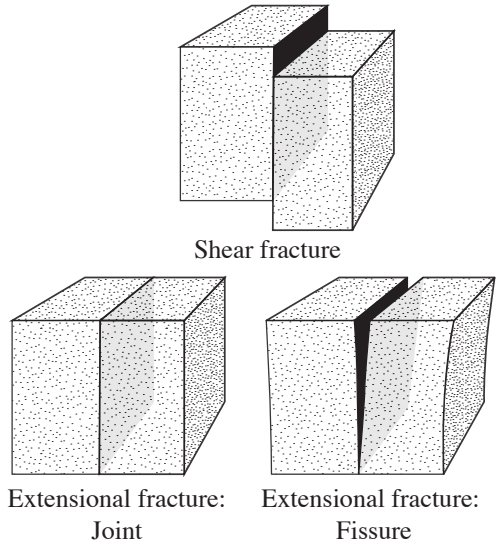

Figure 7.2 Three types of fractures.

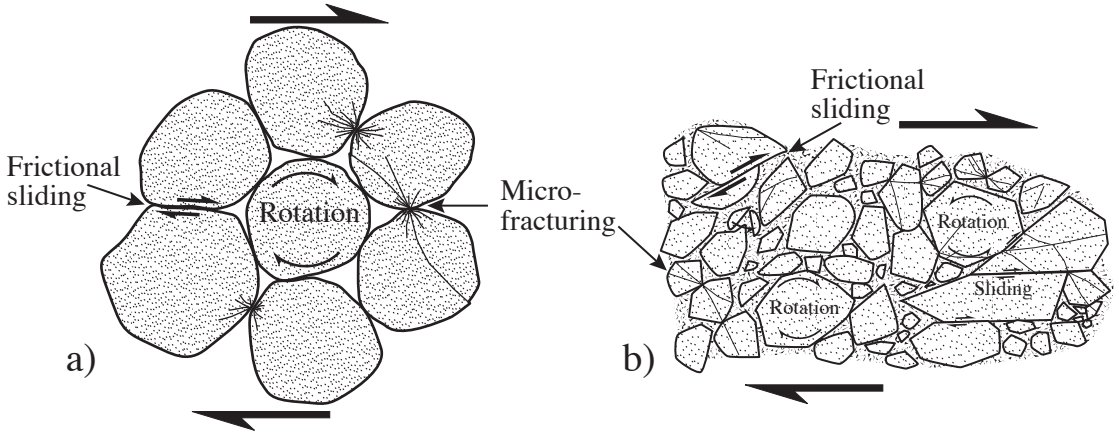

Figure 7.1 Brittle deformation mechanisms: Rigid rotation of grains, frictional sliding between grains and fracturing of grains. a) in porous rock, b) in non-porous microbreccia, where fragments rather than original grains slide, rotate and break into smaller fragments during cataclastic flow.

1 The regime where the physical conditions promote brittle deformation mechanisms such as frictional sliding along grain contacts, grain rotation and grain fracturing.

or have undergone recrystallization so that less work is required to fracture the grains than to slide them past one another. The process of fracturing and crushing grains, usually coupled with frictional sliding along grain contacts and grain rotation, is called *cataclasis*. Intense cataclasis occurs in thin zones along slip (fault) surfaces. In this case cataclasis causes extreme grain-size reduction. More moderate cataclastic deformation can occur in somewhat wider brittle or cataclastic shear zones. In this case the fragments resulting from grain crushing flow during shearing. This process is referred to as *cataclastic flow*. Cataclastic flow gives rise to deformation zones that may appear ductile at the mesoscopic scale but are governed by brittle, cataclastic deformation mechanisms at the microscale (Figure 7.1b)

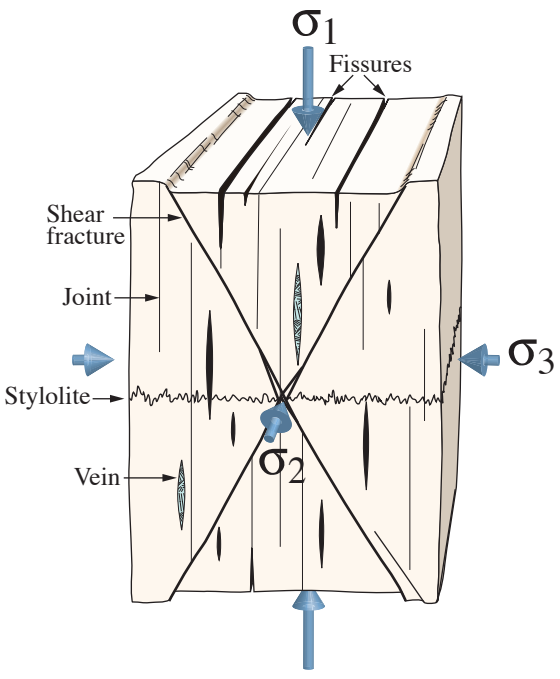

Figur 7.3 The orientation of various fracture types with respect to the principal stresses.

1.2 What is a fracture?

Strictly speaking, a fracture is any planar or subplanar discontinuity that is very narrow in one dimension compared to the other two and forms as a result of external (e.g. tectonic) or internal (thermal or residual) stress. They are discontinuities where rocks or minerals are broken, and reduction or loss of cohesion characterizes most fractures. Fractures are often described as surfaces, but at some scale there is always a thickness involved, albeit a very small one. Fractures can be separated into shear fractures (slip surfaces), opening fractures (joints), fissures and veins (Figures 7.2 and 7.3). In addition, some geologists add compaction fractures or anticracks (stylolites).

A *shear fracture* or *slip surface* is a fracture along which the relative movement is parallel to the fracture. The term "shear fracture" is used for fractures with small (mm to cm-scale) displacements, while the term *fault* is more commonly restricted to shear fractures with larger offset. The term s*lip surface* is used for fractures with fracture-parallel movements regardless of the amount of displacement and is consistent with the traditional use of the term fault.

A *joint* is a fracture with little or no macroscopically detectable displacement. Close examination reveals that most joints have a minute extensional displacement across the joint surfaces[2], and joints are therefore tension or extension fractures.

Extension fractures are filled with gas, fluids, magma or minerals. When filled with air or fluid it is called a *fissure*. Mineral filled extension fractures are called *veins*, while magma-filled fractures classify as *dikes*. Joints, veins and fissures are all referred to as extension fractures[3].

Contractional planar features (anticracks) also exist. These have contractional displacements across them and are filled with residue from the host rock. Stylolites are compactional structures, and some geologists would even regard stylolites as fractures, characterized by very irregular, rather than planar, surfaces. They do, however, define an end member in a complete kinematic fracture framework that also includes shear and extension fractures.

Rock mechanics experiments carried out at various differential stresses and confining pressures set a convenient stage for studying several aspects of fracture formation (Figure 7.4), and we will refer to experimental rock deformation on several occasions in this chapter. Similarly, numerical modeling has aided greatly to our understanding of fracture growth, particularly the field called *linear elastic fracture*

2 Some joints may show evidence of some wall-parallel slip resulting from reactivation.

3 This is the most common definition of the term joint, but some use it about any fracture (including shear fractures) with microscopic displacement, regardless of kinematics.

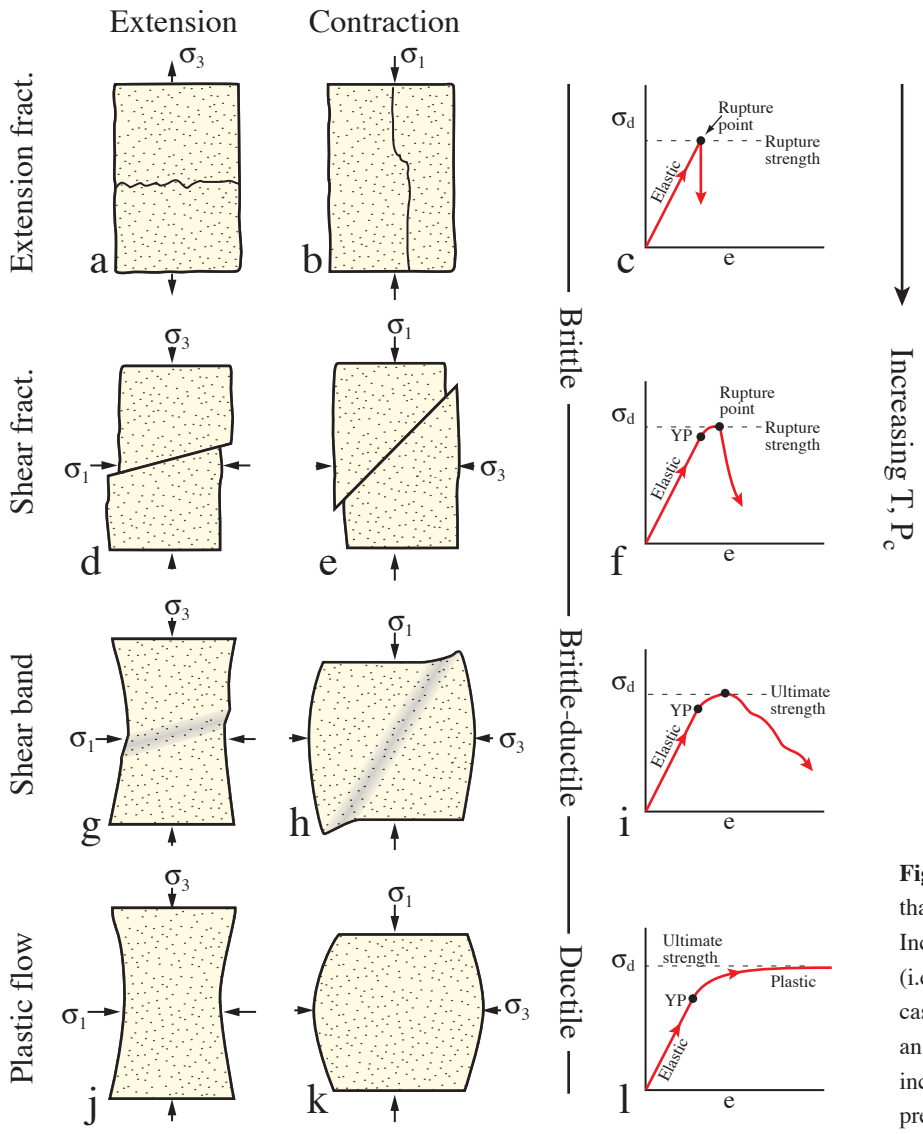

Figure 7.4 Experimental deformation structures that develop under extension and contraction. Increasing confining pressure and temperature (i.e., crustal depth) downwards. While all cases experience initial elastic deformation, an increasing degree of ductility is seen with increasing temperature (T) and confining pressure (P_c). YP=yield point.

mechanics. In the field of fracture mechanics it is common to classify the displacement field of fractures or *cracks* into three different modes (Figure 7.5). Mode I is the opening or tensile mode where displacement is perpendicular to the walls of the crack and is called *Mode I cracks* or *opening cracks*. *Mode II* represents slip (shear) perpendicular to the edge and *Mode III, slip* parallel to the edge of the crack. Mode II and III occur along different parts of the same shear fracture and may therefore be confusing to talk about Mode II and Mode III cracks as individual fractures. Combinations of shear (Mode II or III) fractures and tension (Mode I) fractures are called *hybrid fractures* or hybrid cracks. Furthermore, *Mode IV fractures* are sometimes defined for contractional features such as stylolites. The mode of displacement on fractures is an important parameter, for instance when fluid flow through rocks is an issue.

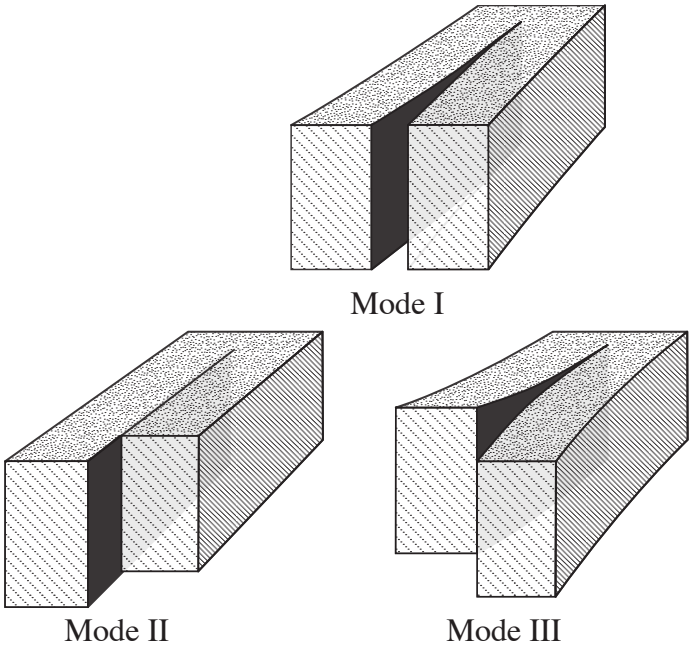

Figure 7.5 Mode I, II and III fractures.

DEFORMING ROCK IN THE LABORATORY

The mechanical properties of rocks are explored in rock mechanics laboratories, where samples are exposed to various stress fields that relate to different depths and stress regimes in the crust. Uniaxial rigs can be used to test the uniaxial compressive or tensile strength of rocks. Triaxial tests, where $\sigma_1>\sigma_2=\sigma_3$, are more common, where rock cylinders are loaded in the axial direction and the sample is confined in fluid that can be pumped up to a certain confining pressure. A typical triaxial rig can build up an axial stress of 2-300 MPa and a confining pressure of up to 50-100 MPa. Sample and fluid are commonly separated by a membrane to avoid the fluid to enter the sample and change its mechanical properties. For porous rocks or sediments it may be possible to control the pore pressure (e.g. up to 50 MPa). The distance between the pistons, i.e. the axial elongation, is monitored together with time, axial loading and confining pressure. Ringshear apperatus is used to explore the effect of large shear strain under vertical compression of up to about 25 MPa.

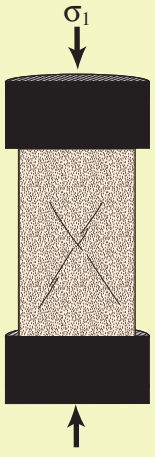

Uniaxial deformation rig, used to find the uniaxial strength of rocks. Experiments show that, in general, fine-grained rocks are stronger than coarse-grained ones, and the presence of phyllosilicates lowers the strength.

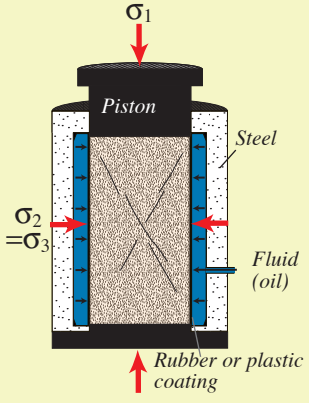

Triaxial rig. Oil pressure is pumped up in a chamber around the sample to increase the confining pressure to mimic different burial depths.

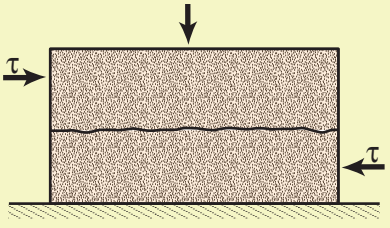

Shearbox experiment where the resistance against shear is explored. The higher the normal stress, the higher the shear stress necessary to activate the fracture. The roughness of the fracture is also important.

Ringshear apperatus, where the amount of shear strain that can be imposed on the sample is unlimited. Loose sediment is addded and processes such as clay smear and cataclasis can be studied.

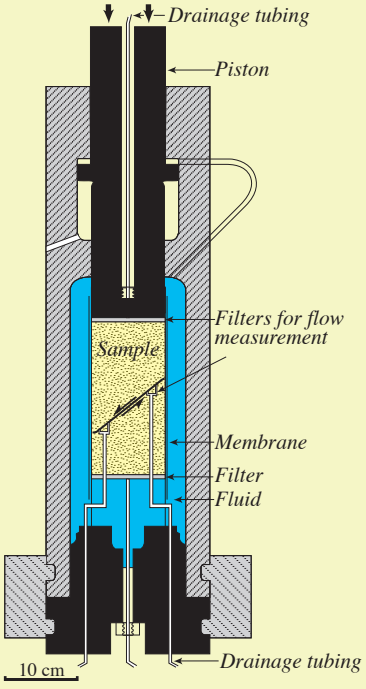

A triaxial rig where fluid (oil or water) can be pumped in and influence the behavior of an existing fracture.

1.2.1 Extension fractures

Extension fractures ideally develop perpendicular to σ_3 and thus contain the intermediate and maximum principal stresses ($2\theta=0°$, see Chapter 2). In terms of strain, they develop perpendicular to the stretching direction under tensile conditions (Figure 7.4a) and parallel to the compression axis during compression tests (Figure 7.4b). Because of the small strains generally associated with most extension fractures, stress and strain axes more or less coincide in these cases.

Joints are the most common type of extension fracture at or near the surface of the Earth and involve very small strains. Fissures are extension fractures that are more open than joints, and are characteristic of surface tension in solid (cohesive) rock (Figure 7.6). The term fissure is commonly used about long extension fractures, typically up to several kilometers long.

Extension fractures are typical for deformation under low or no confining pressure, and form at low differential stress. If extension fractures form under conditions where at least one of the stress axes is tensile, then such fractures are true *tension fractures*. Such conditions are generally found near the surface where negative values of σ_3 are more likely. They can

Figur 7.6 Fissures formed in historic times in Thingvellir, Iceland, along the rift axis between the Eurasian and Laurentian (North American) plates. The fissures are open extension fractures in basalt, but the vertical displacement (right-hand side down) indicates a connection with underlying faults.

also occur deeper in the lithosphere, where high fluid pressure reduces the effective stress (Section 7.5?). Many other joints are probably related to unloading and cooling of rocks, as indicated in the previous chapter.

1.2.2 Shear fractures

Shear fractures show slip along the fracture and typically develop at 20-30° to σ_1, as seen from numerous experiments under confined compression (Figure 7.4 c-d). Such experiments also show that they commonly develop in conjugate pairs, bisected by σ_1. Shear fractures develop under temperatures and confining pressures corresponding to the upper part of the crust. They can also form near the brittle-plastic transition, but are then characterized by a wider zone of cataclastic flow rather than by single fractures. Such shear factures result in a change in shape (Figure 7.4 e-f), which is otherwise typical for plastic deformation.

As one may expect, brittle and plastic deformation show different stress-strain curves (Figure 7.7): The more ductile the deformation, the greater the amount of plastic deformation prior to

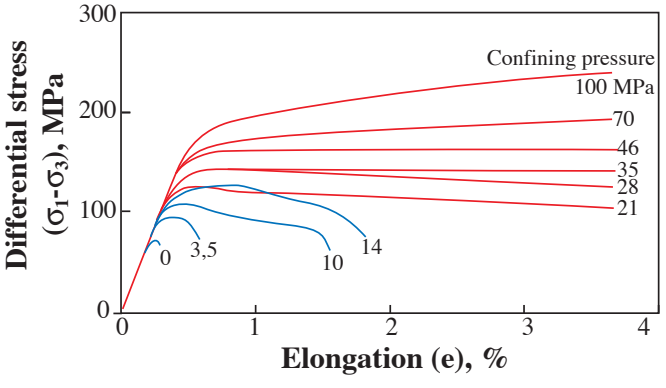

Figure 7.7 Stress-strain curves for triaxial compression of marble for a range of confining pressures. Increasing the confining pressure increases the differential stress that the rock can sustain before failure (blue curves). Over a critical confining pressure the rock retains its strength as it deforms plastically (red curves). From Paterson (1958).

fracturing. It is also interesting to note the relationship between confining pressure (depth) and stress regime (compressional or tensile) shown in Figure 7.8. The experimental data indicate that the brittle-plastic transition occurs at higher confining pressure under tension than under compression. Temperature and strain rate (?) are other important factors as discussed in previous chapters.

1.3 Failure and fracture criteria

We learned in Chapter 5 that rock response to stress depends on the level of stress or amount of accumulated strain (Figure 5.8), and on factors such as anisotropy, temperature, strain rate, pore fluid and confining pressure. In the brittle regime a deforming rock accumulates elastic strain before it ruptures (fractures) at a certain critical stress level. In the brittle-plastic transition there tends to be an intermittent phase of plastic deformation prior to failure, and the failure does not necessarily create an instantaneous through-going fracture, but rather a shear zone or shear band dominated by cataclastic flow. This contrasts to the plastic regime (Figure 7.2j-l) where strain is more broadly distributed and dominated by plastic deformation mechanisms.

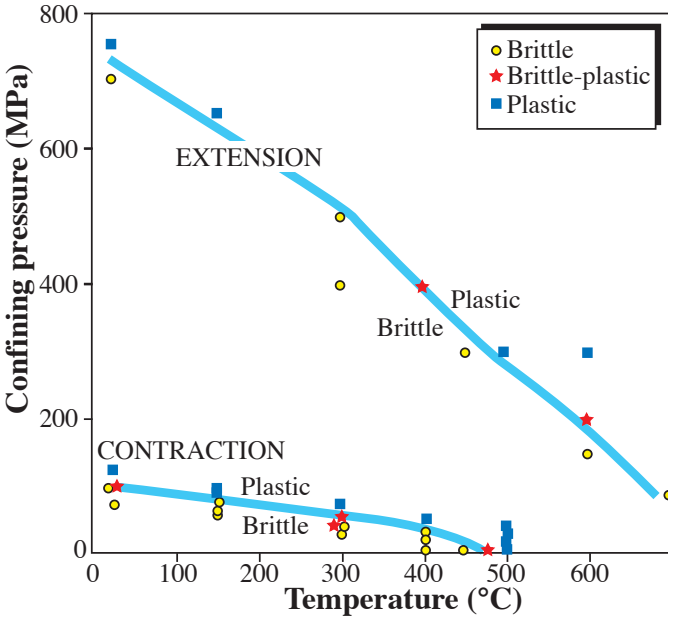

Figure 7.8 Variation of the brittle-plastic transition as a function of confining pressure and temperature for the Solenhofen limestone. From Heard (1960).

While the main focus of Chapter 5 was on

WHY SHEAR FRACTURES DO NOT FORM AT 45° TO THE LARGEST PRINCIPAL STRESS

Navier and Coulomb both showed that shear fractures do not form along the theoretical surfaces of maximum shear stress. Maximum resolved shear stress on a plane is obtained when the plane is oriented 45° to the maximum principal stress (θ=45°). This fact is easily seen from the Mohr diagram, where the value for shear stress is at its maximum when 2θ=90°. However, in this situation the normal stress σ_n across the plane is fairly large. Both σ_s and σ_n decrease as θ increase, but σ_n decreases faster than σ_s. The optimal balance between σ_n and σ_s depends on the angle of internal friction ϕ, but is predicted by Coulomb's criterion to be around 60° for many rock types. At this angle (θ=60°) σ_s is still large, while σ_n is considerably less than at θ=45°. The angle depends also on the confining pressure (depth of deformation), temperature and pore fluid and experimental data indicates that there is a wide scatter even for the same rock type and conditions.

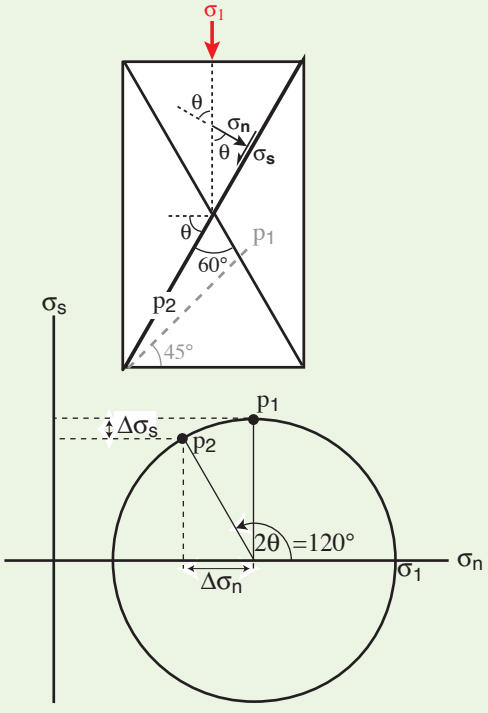

P1 is the plane of maximum resolved shear stress (2θ=90°) and forms 45° to σ_1. The plane represented by P2 is oriented at 30° to σ_1. The shear stress is still high (the difference is $\Delta\sigma_s$), but the normal stress is considerably lower ($\Delta\sigma_n$) than for P1. It is therefore easier for a fracture to form along P2 than along P1.

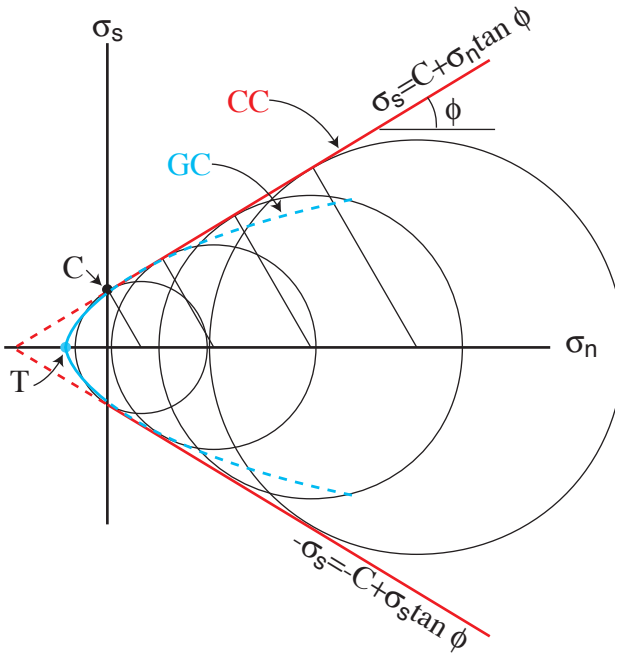

Figure 7.9 Coulumb's fracture criterion occurs as two straight lines (red) in the Mohr diagram. The circles represent examples of critical states of stress. The blue line represents Griffith's criterion for comparison. The combination of the two is sometimes used (GC in the tensile regime and CC in the compressional regime). CC=Coulomb's criterion, GC=Griffith criterion, C=the cohesive strength of the rock, T=the tensile strength of the rock.

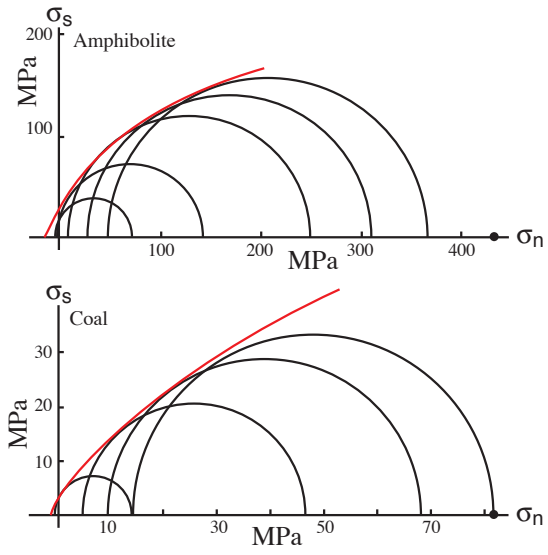

Figure 7.10 Mohr's envelope for amphibolite and coal based on triaxial tests. When the confining pressure is increased, the strength of the rock increases, and a new circle can be drawn in the figure. Note that the envelope diverges from the linear trend defined by Coulomb's criterion. From Myrvang (2001).

elastic-plastic deformation we are now focusing on the brittle part. Key questions are *when* and *how* does a rock fracture. Let us look at the first question first. For a given rock under constant temperature and constant positive confining pressure fracture depends on the differential stress (σ_1-σ_3) as well as the mean stress ((σ_1-σ_3)/2). If there is no differential stress, then the state of stress is lithostatic and there is no force pulling or pushing our rock volume in any particular direction. True, its structure could collapse and its volume decrease if it is a porous rock, but in order to make distinct fractures, differential stress is needed.

Fracture initiation requires a differential stress that exceeds the strength of the rock.

The strength of rock depends on the confining pressure or depth of burial. In the brittle, upper part of the crust, the strength is lowest near the surface and increases downwards. This is easily explored in experiments (Figure 7.7) where both confining pressure and directed axial stress are increased (Figure 5.12). In general, increasing the confining pressure makes it necessary to increase the differential stress in order to create fractures in a previously unfractured rock. In the next section we will see how this relationship is described by means of a simple relationship between the critical normal and shear stresses. The relationship is known as the *Coulomb fracture criterion for confined compression*.

1.3.1 Coulomb's fracture criterion.

At the end of the 17th century, the French physicist Charles Augustin de Coulomb found a criterion that could predict the state of stress at which a given rock under compression is at the verge of failure. The criterion considers the critical shear stress (σ_S, or τ) and normal stress (σ_n) acting on a potential fracture at the moment of failure, and the two are related by a constant tanϕ, where ϕ is called the angle of internal friction:

$$\sigma_s = \sigma_n \tan\phi \qquad (7.1)$$

The Coulomb criterion indicates that the shear stress required to initiate a shear fracture also depends on the normal stress across the potential shear plane: the higher the normal stress, the higher the shear stress

needed to generate a shear fracture. Tanϕ is commonly called the *coefficient of internal friction* μ. For loose sand it relates to the friction between sand grains and the slope angles of the sand (the angle of repose, ~30°), but for solid rocks it is merely a constant that varies from 0.47-0.7. A value of 0.6 is often chosen for μ for general calculations.

A fracture criterion describes the critical condition at which a rock fractures

Three centuries after Coulomb, the German engineer Otto Mohr introduced his famous circle in σ_S - σ_n–space, and the Coulomb criterion could conveniently be interpreted as a straight line in Mohr space, with μ representing the slope and ϕ the slope angle (note that there is also a second line representing the conjugate shear fracture on which shear stress magnitude is identical but of opposite sign).

Coulomb realized that a fracture only forms if the internal strength or cohesion C of the rock is exceeded. The complete Coulomb fracture criterion (also called Navier-Coulomb, Mohr-Coulomb and Coulomb-Mohr fracture criterion) is therefore:

$$\sigma_s = C + \sigma_n \tan\phi = C + \sigma_n \mu \qquad (7.2)$$

The constant C represents the critical shear stress along a surface across which σ_n=0. C is also called the *cohesive strength*, and has its counterpart in the *critical tensile strength* T of the rock.

The Mohr diagram provides a convenient way of interpreting the meaning of these constants (Figure 7.9). Because Equation 7.2 is the general formula for a straight line, C represents the intersection with the vertical (σ_s) axis and T denotes the intersection with the horizontal (σ_n) axis. At point C it is clear that σ_n=0, while at T, σ_s=0. As an example, loose sand has no compressive or tensile strength, which means that T=C=0 and Coulomb's fracture criterion reduces to Equation 7.1. The more the sand lithifies, the higher the C-value. However, not only will the C-value change during lithification of sand, but so also ϕ and T. In general, both C and ϕ vary from one rock type to another. For sand(stone), they both increase with increasing lithification.

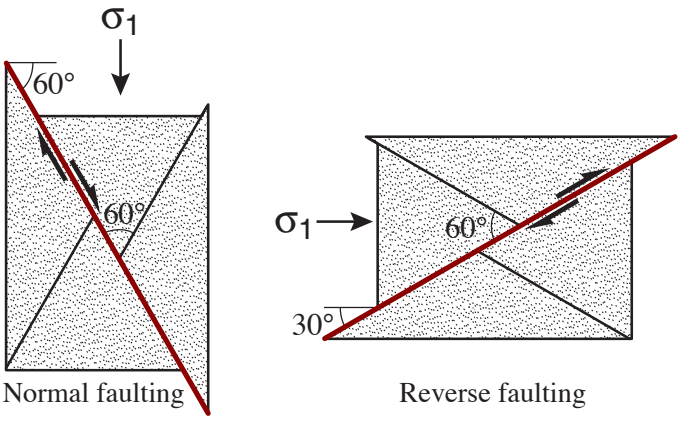

Figure 7.12 The angle between the maximum principal stress and the shear plane is commonly found to lie close to 30°. This implies that normal faults dip steeper (60°) than reverse faults (30°).

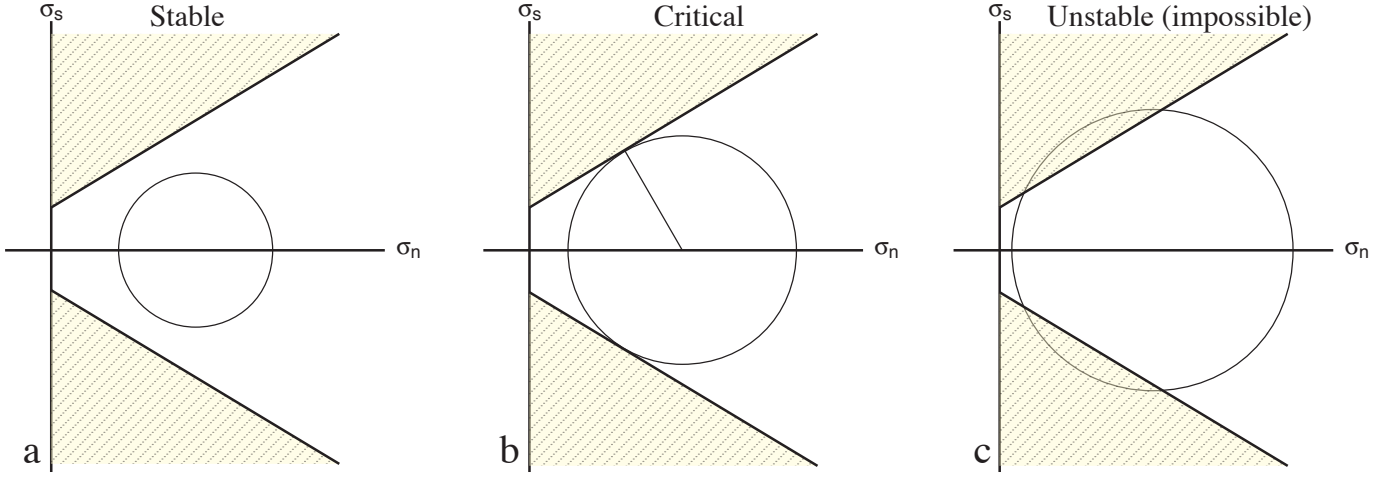

Figure 7.11 a) Stable state of stress. b) Critical situation, where the circle touches the envelope. This is when the rock is at the verge of failure, also called critically stressed. c) Unstable situation where the state of stress is higher than that required for failure. This state of stress is impossible as the rock fractures before reaching this stage.

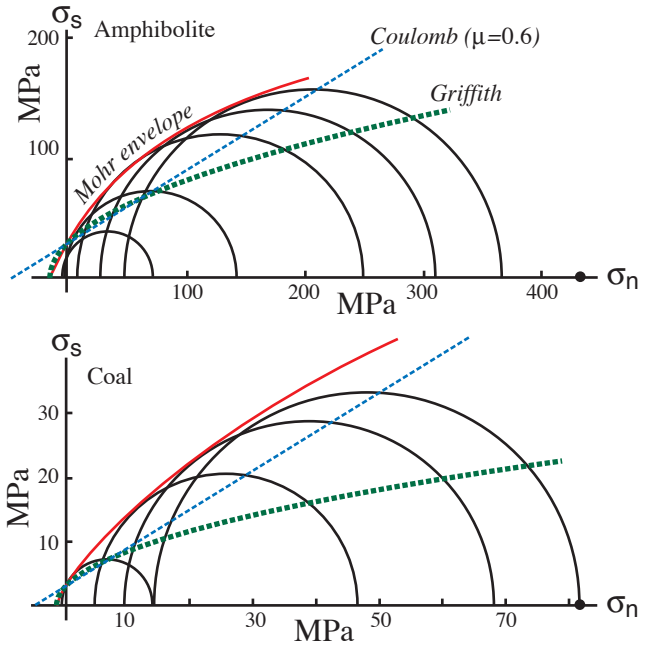

Figure 7.13 The Griffith and Coulomb fracture criteria superimposed on the experimental data presented in Figure 7.?. The criteria are placed so that they intersect the vertical axis together with the Mohr envelope. None of the criteria fit the data very well. Griffith's criteria works well for tensile stress (left of origin), but shows a too low slope in the entire compressional regime. Coulomb's criteria approaches the envelope for high confining pressure (right side of the diagram).

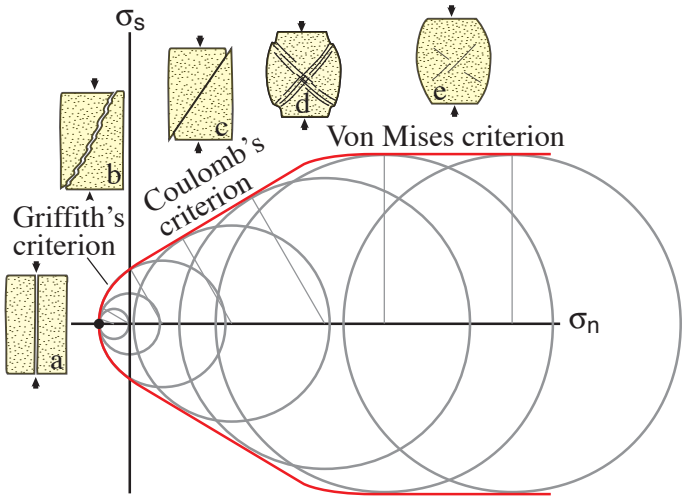

Figure 7.14 Three different fracture criteria combinied in Mohr space. Different styles of fracturing are related to confining pressure: a) Tensile fracture, b) hybride or mixed-mode fracture, c) shear fracture, d) semi-ductile shear bands, e) plastic deformation.

To see if a rock obeys Couloumb's fracture criterion and, if so, to determine C, T and μ for a given rock or sediment laboratory tests are performed. A deformation rig is generally used where the confining pressure as well as the axial load can be adjusted. The state of stress at failure is recorded and plotted in the Mohr diagram. This can be done for many different states of stress (Figure 7.9 and 7.10), and for so-called Coulomb materials the straight line that tangents the Mohr circles represents the Coulomb fracture criterion (Equation 7.2). This line is called the *Coulomb failure envelope* for the rock. Ideally, the point at which a Mohr circle touches the failure envelope represents the orientation of the plane of failure (remember the 2θ angle in the Mohr diagram), as well as the shear stress and normal stress on the plane at the moment of failure. Any Mohr circle that does not touch the envelope represents a stable state of stress (no fracturing possible; Figure 7.11a). The Coulomb failure envelope is always positive for brittle fracturing. This means that the higher the mean stress (or confining pressure), the higher the differential stress required for failure. In other words, the deeper into the brittle part of the crust, the stronger the rock, and the more differential stress is required to fracture it. Note also that the effect of the intermediate principal stress (σ_2) is ignored and that the fracture plane always contains σ_2, in agreement with Anderson's theory of faulting (Figure 6.12).

The orientation of the fracture can be expressed in terms of the angle of internal friction (ϕ) and the orientation of the fracture (θ):

$$\phi = 45^\circ - \frac{\theta}{2}, \quad (7.4)$$

or

$$\theta = 90 - 2\phi \quad (7.5)$$

Most rocks have ϕ≈30° (μ≈0.6), which means that the angle between σ_1 and the fracture, which is 90°-θ (see Figure 2.1), is around 30°. Thus, Andersonian normal and reverse faults dip at ~60° and 30°, respectively (Figure 7.12).

1.3.2 The Mohr failure envelope

Mohr's failure envelope is the envelope or curve in the Mohr diagram that describes the critical states of stress over a range of differential stress, regardless of whether it obeys the Coulomb criterion or not. The

envelope separates the stable field, where the rock does not fracture, and the unstable field, which is unachievable because fracture prevents such states of stress to occur. Each type of rock has its own failure envelope, and it is found experimentally by fracturing samples of the rock under different confining and differential stress. In some cases the Coulomb fracture criterion is a reasonably good approximation for a certain stress interval, and in other cases the envelope is clearly nonlinear (Figure 7.13). It is common for the envelope to flatten as the ductile regime is approached. In fact, the ductile regime can be approximated by a constant shear stress criterion (horizontal envelope), known as the *von Mises criterion* (σ = constant; Figure 7.14). A consequence of the non-linear shape of the envelope is that the angle between σ_1 and the failure plane decreases with increasing value of σ_3.

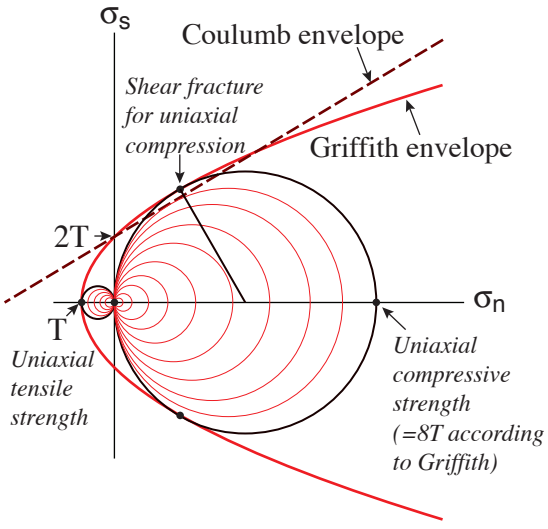

Figure 7.15 Illustration of the meaning of the terms uniaxial tensile and compressive strength in the Mohr diagram. Uniaxial means that only $\sigma_1 \neq 0$, which is obtained in a uniaxial deformation rig where the confining pressure is zero. By gradually compressing the rock sample the uniaxial compressive strength is reached when a shear fracture first form. By pulling the sample until a tension fracture forms, the uniaxial tensile strength is found. Note that the uniaxial compressive strength is much larger than the tensile strength for the same rock and conditions.

1.3.3 The tensile regime

The Coulomb criterion predicts the critical state of stress needed to create a shear fracture. Experimental data show that it does not successfully predict tension fractures. Also, the fact that it relies on the angle of internal friction, which is physically meaningless for tensile normal stress, indicates that the Coulomb criterion is inappropriate in the tensional regime. Experiments suggest that Mohr's envelope in the tensional regime is shaped like a parabola. Thus, to cover the full range of stress states in the crust, it is necessary to combine different fracture criteria, such as the parabolic failure criterion for the tensile field, Coulomb's criterion for brittle fracturing in the compressive regime, and von Mises' criterion in the plastic regime (Figure 7.14).

A particularly interesting part of Mohr's envelope is where it intersects the horizontal axis of the Mohr diagram. This point represents the critical stress at which tension fractures start to grow and is called the *critical tensile stress* T. T is found experimentally to be lower than the cohesive strength C, and varies from rock to rock. Why does T vary so much? Griffith suggested that it is related to the shapes, sizes and distribution of microscopic flaws in the deforming sample.

1.3.4 Griffith's theory of fracture

Around 1920 the British aeronautical engineer Alan Arnold Griffith extended his studies of fracture to the atomic level. He noted a large difference in theoretical strength between perfectly isotropic material and the actual strength of natural rocks measured in the laboratory. Griffith based the theoretical brittle tensile strength on the energy required to break atomic bonds. The uniaxial tensile strength of flawless rock is calculated to be around 1/10 of Young's modulus. For a strong rock this could reach ~100 GPa (Figure 5.3), which means a tensile strength of about 10 GPa (10 000 MPa). Experiments indicate that the tensile strength is closer to 10 MPa. Why this enormous discrepancy between theory and practice?

Griffith's answer was that natural rocks and crystals are far from perfect. Rock contains abundant microscopic flaws. Microcracks, voids, pore space or grain boundaries are here considered as microscopic fractures. For simplicity, Griffith modeled such flaws as strongly elliptical microfractures, now known as *Griffith (micro)cracks*. He considered the stress concentrations associated with these microfractures and the energy that it takes for them to grow and connect. He then obtained much more realistic (although not perfect) estimates of tensile strength.

In contrast to Coulomb, Griffith found a non-linear relationship between the principal stresses for a critically stressed rock. This relationship is given by the equation:

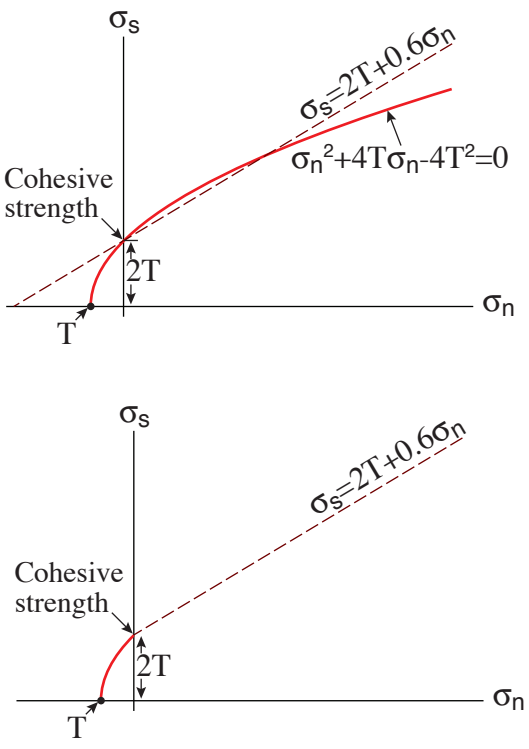

Figure 7.16 a) Comparison of the Griffith and Coulomb fracture criteria (the coefficient of internal friction is chosen to be 0.6). b) The combined Griffith-Coulomb criterion.

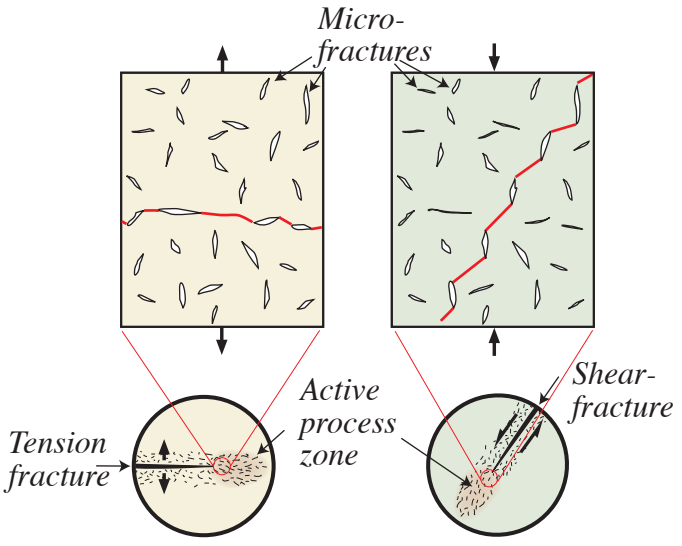

Figure 7.17 Simplified illustration of growth and propagation of extension (left) and shear fractures (right) by propagation and linkage of tensile microfractures (flaws). Propagation occurs in a process zone in front of the fracture tip. Circled figures are cm-scale views, while rectangular views illustrate the microscale structure.

$$\sigma_s^2 + 4T\sigma_n - 4T^2 = 0 \quad (7.6)$$

This can also be represented in the Mohr diagram, where it defines a parabola where the tensile strength T is the intersection with the horizontal axis. The intersection between Griffith's parabola and the vertical axis is found by setting σ_n=0 in the equation above, which gives us σ_S=2T. This value corresponds to C in Mohr's criterion. In other words, the cohesive strength of a rock is twice its tensile strength (C=2T), which is in close agreement with experimental data. We can take advantage of this new information and reformulate Coulomb's fracture criterion as:

$$\sigma_s = 2T + \sigma_n \mu \quad (7.7)$$

With this formulation it is easy to combine Coulomb's criterion for the compressional stress regime with Griffith's criterion for the tensile regime.

Griffith's important contribution is that the brittle strength of rock is controlled by randomly oriented and distributed intragranular microfractures in the rock. Microfractures with orientations close to that of maximum shear stress are then expected to grow faster than differently oriented ones, and will link and eventually form through-going fracture(s) in

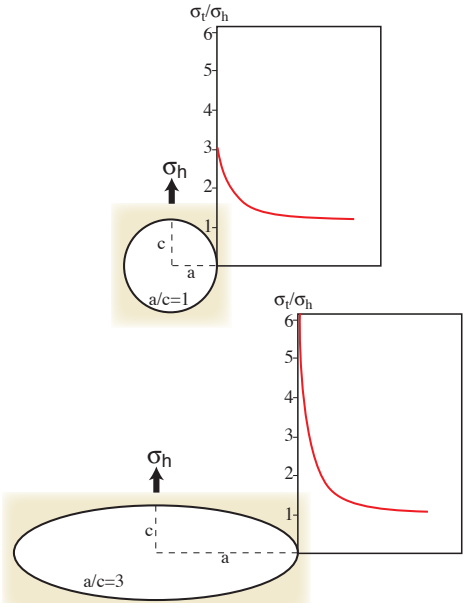

Figure 7.18 Stress concentration around a pore space or microfracture with circular and elliptic geometry in an elastic medium. Increasing the ellipticity a/c increases the stress concentration, as described in Equation 7.8. The far-field stress σ_h is tensile (negative). σ_t is the stress at the circumference of the circle and at the point of maximum curvature on the ellipse (the fracture tip point). Based on Engelder (1993).

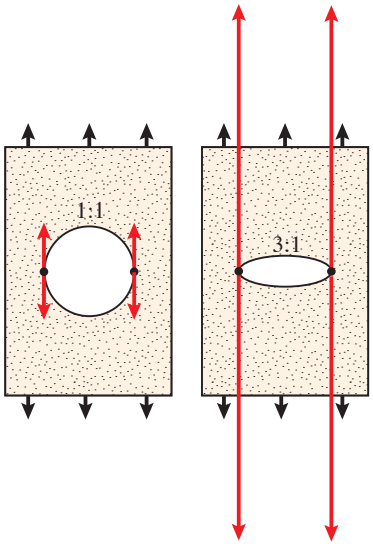

Figure 7.19 Illustration of local stress concentrations in a material with a circular and an elliptic hole. If the material is a sheet of paper it means that it will be easier to pull apart the paper with the elliptical hole. Black arrows indicate the far-field or remote stress.

the rock.

For non-porous rocks the Griffith criterion of fracture is a reasonably realistic approximation for the compressional regime as well. However, the Griffith criterion predicts that the uniaxial compressive strength should be eight times the uniaxial tensile strength (Figure 7.15), while experiments indicate that the uniaxial compressive strength of rocks is 10-50 times the uniaxial tensile strength. This discrepancy has resulted in several alternative fracture criteria. However, for porous media, such as sand and sandstone, Coulomb's criterion is quite realistic and can successfully be combined with Griffith's criterion (Figure 7.16).

1.4 Microdefects and failure

Griffith assumed that tensile fractures develop from planar microdefects or microfractures in rocks. The fracture is assumed to develop by a process where microfractures that are favorably oriented with respect to the external stress field grow and connect to form a through-going macro-fracture. Both tensile fractures (extension fractures) and shear fractures (faults) can form in this manner (Figure 7.17).

Observations indicate that microfractures occur at anomalously high frequencies near macroscopic fractures. This information suggests that microfractures form in a *process zone* ahead of a propagating macrofracture. In this zone microdefects grow and connect so that the macrofracture can grow. The process zone is in some ways similar to the frontal part of the damage zone that encloses a (macroscopic) fault, as discussed in section 8.?. Many interesting

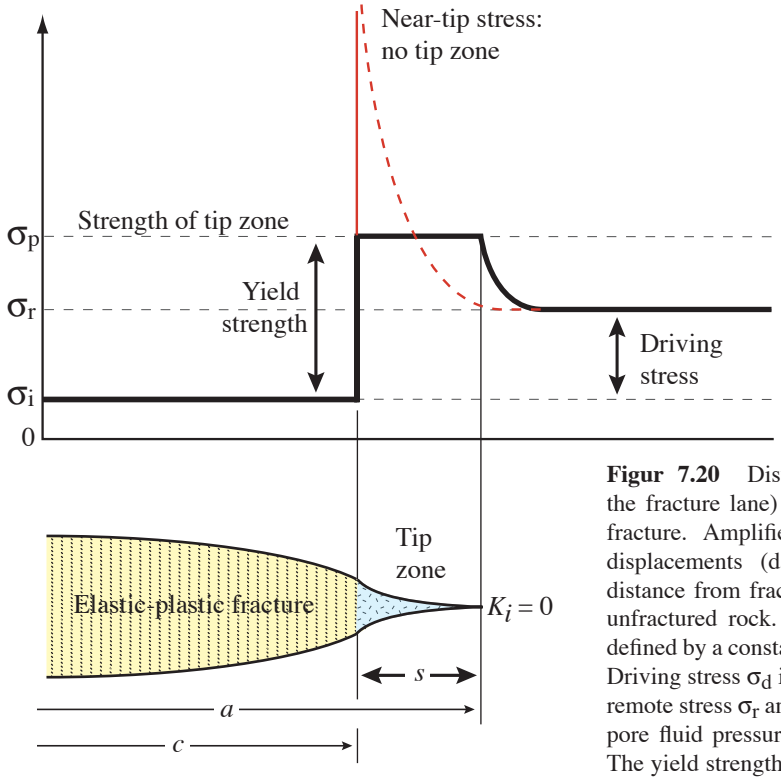

Figur 7.20 Distribution of stress (resolved on the fracture lane) near the tip of an elastic-plastic fracture. Amplified stress due to fracture wall displacements (dashed red curve) decays with distance from fracture tip to σ_r in the surrounding unfractured rock. The length s of the tip zone is defined by a constant value of yield (peak) stress σ_p. Driving stress σ_d is the difference between resolved remote stress σ_r and internal boundary value σ_i (e.g. pore fluid pressure or residual frictional strength). The yield strength is the difference between σ_p and internal boundary value σ_i.

things are going on in the process zone, such as the effect of increasing rock volume due to the growth of microfractures, which may lower the local pore pressure and strengthen the rock temporarily. But the most important aspect of microfractures is the stress concentration that occurs at their tips. This explains why they grow into macroscopic fractures.

The Griffith criterion of fracture is based on the fact that stress is concentrated at the edges of open microfractures in an otherwise non-porous medium. This makes intuitive sense, since the stress that should have been transferred across the open fracture must "find its way" around the edges. If the microfracture is a circular pore space, then the stress concentration at the edge (around the circle) will be three times the remote stress (Figures 7.18 and 7.19). The stress concentration increases if the pore is elliptical and will peak at the tip-line of the ellipse. For an elliptically shaped microfracture of aspect ratio 1:3 the local stress at the tip is seven times the remote stress. If the ellipticity is 1:100, which is more realistic for Griffith microcracks, the local stress is 200 times the remote stress. This concentration may be sufficient to break the local atomic bounds and cause growth of the microcracks. It also implies that once the microcrack starts growing, it increases its length-width ratio, which further increases the stress concentration at its tips, and continued crack propagation is promoted.

If we model the microcrack as an elliptical pore space, then the stress $-\sigma_t$ at the tip of the pore can be expressed mathematically by the relationship

$$-\sigma_t = -\sigma_h(1+(2a/c)) \quad (7.8)$$

where σ_h is the remote stress and a/c is the ellipticity (aspect ratio of the ellipse). For a circular pore space a/c=1 and $\sigma_h>0$. The stress σ_t at the tip then becomes $\sigma_t=3\sigma_h$. The elliptical model of microfractures is of course an approximation. Fractures tend to have a sharply pointed tip zone, which promotes stress concentration even further and increases the likelihood of microfracture growth (Figure 7.20).

These considerations suggest that it is likely for fractures to initiate from microdefects in the rock. It also explains why construction, ship and aerospace engineers are so concerned about microdefects and their shapes. Everything depends on whether or not the stress concentration in the tips of the microfractures is high enough to cause them to propagate. Geologists interested in rock

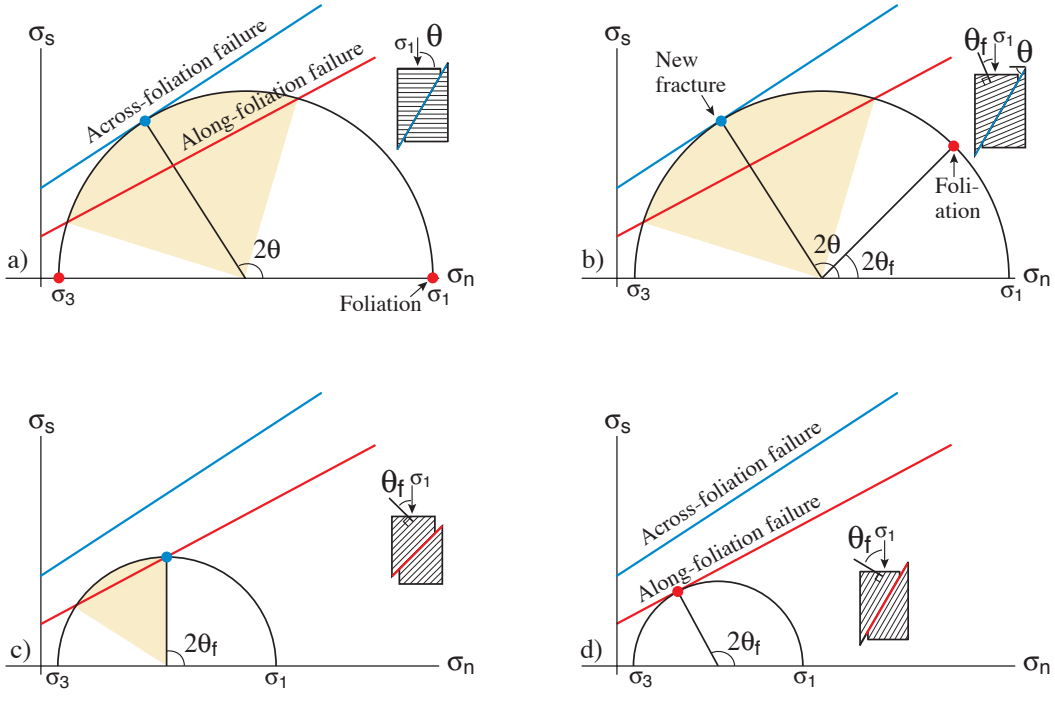

Figure 7.21 Illustration of the role of a preexisting foliation, for constant σ_3. a) σ_1 acting perpendicular to the foliation, in which case differential stress build up until the Mohr circle touches the upper envelope and across-foliationi failure occurs. Colored sector indicates the range of orientations for along-foliation failure. b) σ_1 at a high angle to the foliation, still too high for foliation-parallel failure (foliation outside the colored sector). c) σ_1 at 45° to the foliation, causing foliation-parallel failure. Sector indicates the range of foliation orientations where along-foliation failure would occur for this particular state of stress. d) The angle between σ_1 and the foliation that give failure at the lowest possible differential stress. This is the weakest direction of this particular rock.

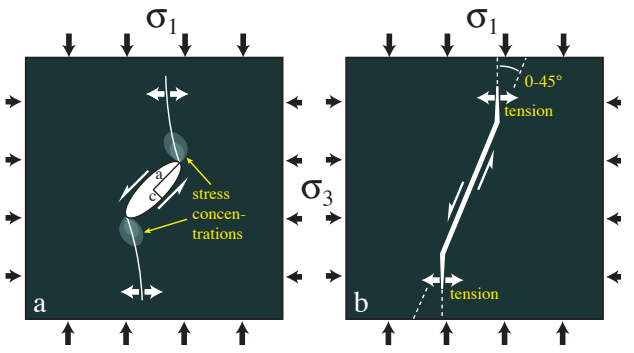

Figur 7.22 a) Griffith crack modeled as an elliptical void. Tensile stress concentrate near the crack tips (compare with Figure 7.18). b) A critically stressed Griffith crack under compression. It is oriented between 0 and 45° with respect to σ_1, depending on the ratio σ_1/σ_3. Note that tensile stress develops near the crack tips in spite of the overall compressional stress, that crack growth is accommodated by sliding along the main crack, and that the crack grows toward parallelism with σ_1.

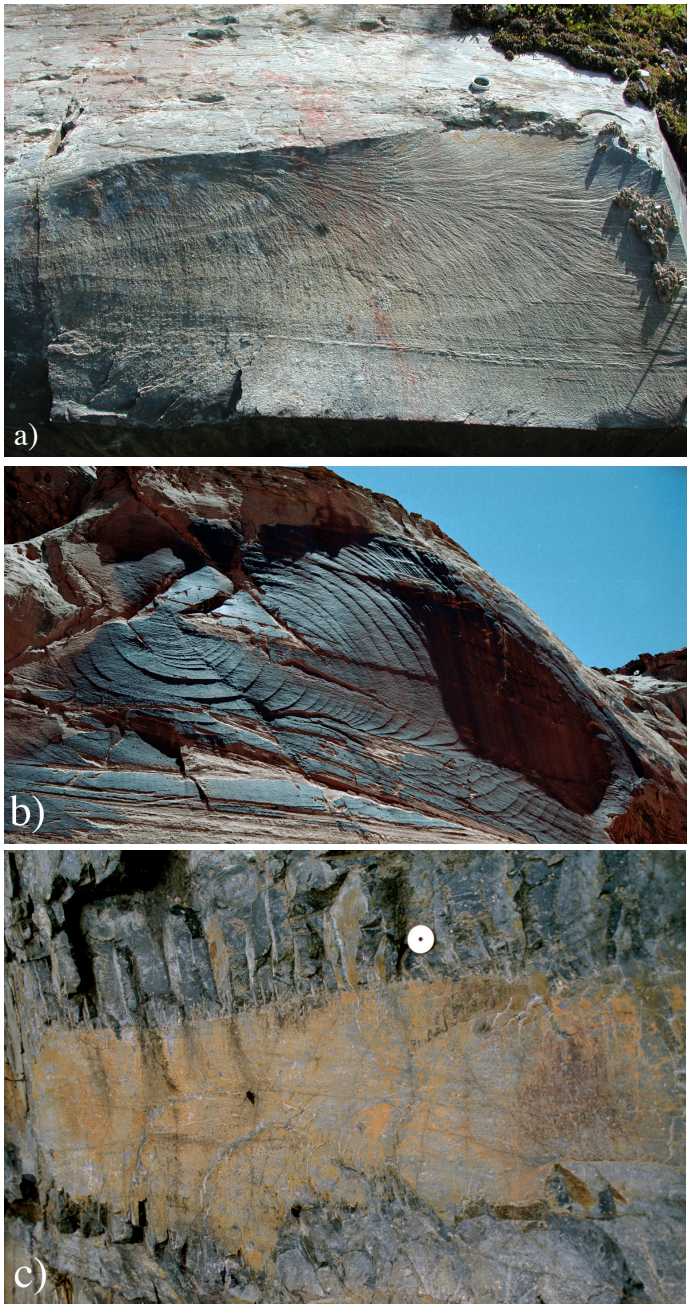

Figure 7.23 a) Arrest lines and plumose structures in meta-greywackes from Telemark, Norway. Note the faint arrest lines oriented perpendicular to the plumose hackles. b) Elliptically arranged arrest lines in the Navajo Sandstone, Utah. This sandstone is too coarse-grained for the plumose pattern to show up. c) En-echelon hackle fringes (twist hackles) along a fracture in meta-rhyolite in the Caledonides of West Norway.

mechanics sometimes talk about the driving force or *driving stress*. For tensile fractures modeled by means of linear elastic theory, the driving stress is the difference between remote stress resolved on the fracture plane and the internal pore-fluid pressure. Thus, for a tensile fracture to propagate, the driving stress must be large enough to exceed the resolved remote stress. Similarly, for closed shear fractures the driving stress (shear stress) must exceed the resisting forces, such as frictional resistance, for displacements to occur. The *stress intensity factor* K_i considers both the remote stress and the shape and length of the microfracture, and its critical value K_c is called the *fracture toughness*. The fracture toughness can thus be considered as a material's resistance against continued growth of an existing fracture. Naturally, sedimentary rocks have lower values of K_c than igneous rocks. We will not go into the details of linear elastic fracture theory in this book, but rather have a look at how temperature, fabric and sample size can have on strength.

1.4.1 Effects of fabric, temperature, stress geometry and sample size on strength

We have now seen how the presence of microscale heterogeneities in the form of microfractures reduces the strength of rock. In principle, microfractures may be distributed so that the rock is macroscopically isotropic, i.e. it has the same strength in all directions. Most rocks have an anisotropy stemming from sedimentary or tectonic fabrics such as lamination, bedding, tectonic foliation, lineation, and crystallographic fabric (preexisting fractures are treated separately below) and the difference in critical differential stress may vary by several hundred percent, depending on orientation. A rock with a planar anisotropy, such as

FRACTURE GROWTH AND WING CRACKS

One of the peculiarities of rock mechanics is the fact that, even though a deforming sample develops through-going shear fracture(s) that make an acute (~30°) angle to σ_1, shear fractures cannot grow in their own plane. Instead, a Mode I fracture forms parallel with σ_1. Such fractures are known as wing cracks or edge cracks. In three dimensions wing cracks (Mode I) will form along both the Mode II and Mode III edges of the main fracture.

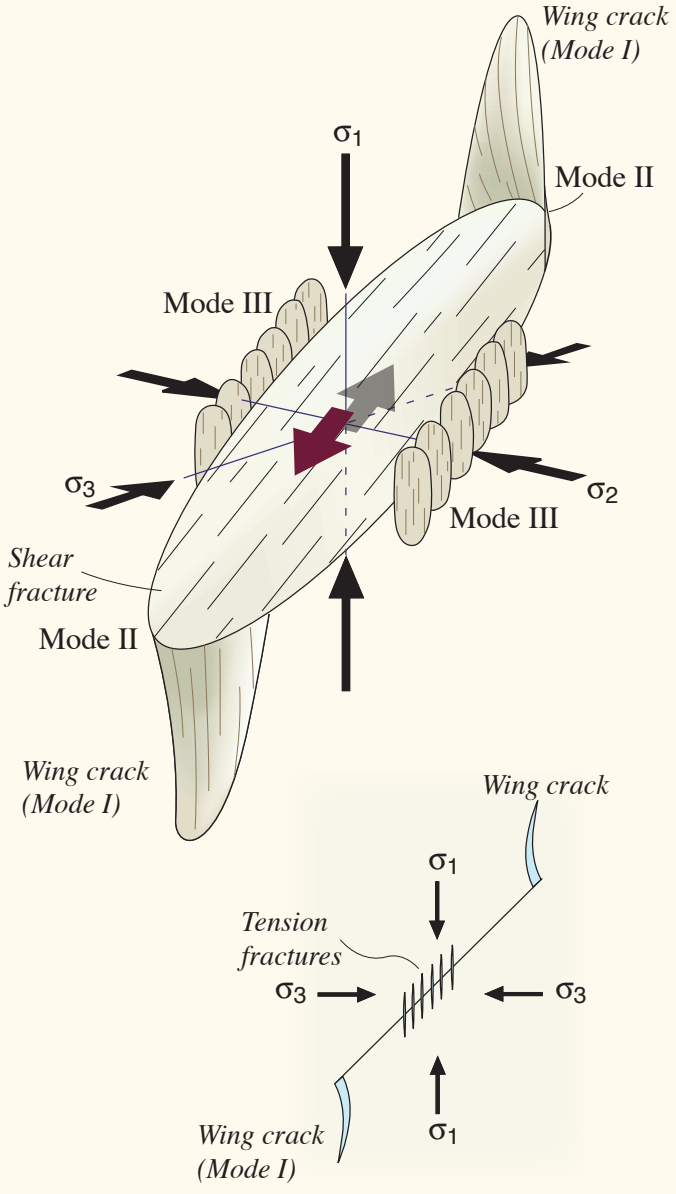

This development is in agreement with theoretical stress considerations. But how does the shear fracture propagate from this stage? The general answer is that the Mode I wing cracks are broken by a new shear fracture - a process that keeps repeating as the main fracture grows. The result is a zone of minor fractures along and around the main shear fracture, a sort of damage zone akin to that defined for faults in Chapter 8.

Based on Scholtz (1990).

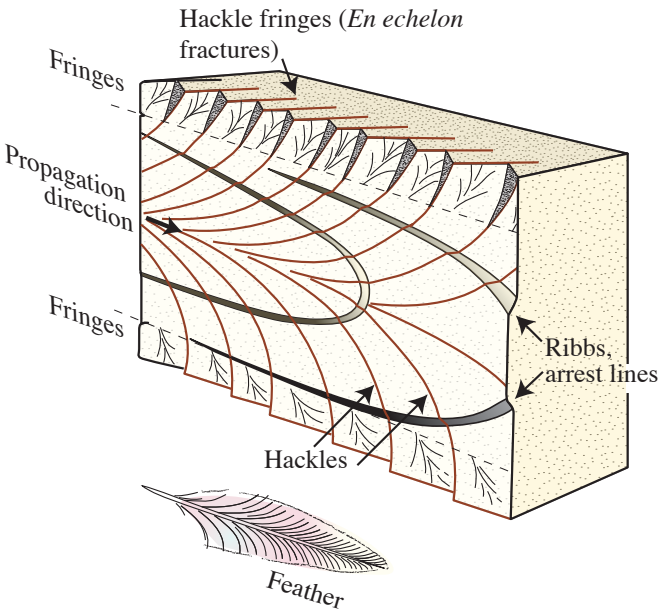

Figure 7.24 Schematic illustration of structures characteristic of joint surfaces. Based on Hodgson (1961).

a slaty cleavage, will either fail along or across the weak cleavage, depending on the orientation of the cleavage with respect to the principal stresses. In Mohr space, there will therefore be two failure envelopes (Figure 7.21). Which one is applicable depends on the orientation of the foliation.

If the foliation is oriented perpendicular (or parallel) to σ_1, then there is no resolved shear stress on the foliation and the upper envelope in Figure 7.21a applies. A shear fracture forms across the foliation at the characteristic angle of around 30° with σ_1 (i.e., $\theta \approx 60°$). Foliation-parallel extension fractures along the cleavage plane (longitudinal splitting) can develop even at low confining pressure. When the foliation is oriented closer to that typical of shear fractures in isotropic rocks, shear fractures develop along the foliation at gradually lower differential stress (Figure 7.21b-c). The orientation of the shear fracture and the strength is then controlled by the orientation of the foliation. Minimum strength is obtained where the orientation of the foliation is represented by the point where the Mohr circle touches the "along-foliation failure" on Figure 7.21d. The exact angle will depend on the weakness of the foliation, which determines the slope of the lower failure curve in Figure 7.21.

The Mohr diagram and the failure envelopes discussed above only consider confining and differential stress and do not take into consideration σ_2. Experiments show that there is a small effect

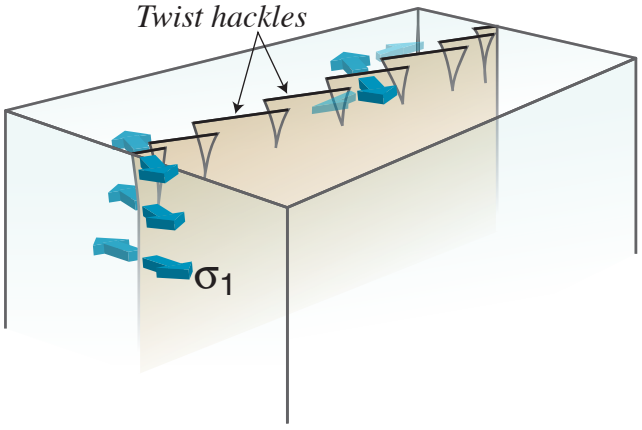

Figure 7.25 The twisting of extension fractures as they reach an interface with a mechanically different rock layer. Note the parallel twisting of σ_1 and the fractures (hackles). Compare with the hackles illustrated in Figure 7.24c.

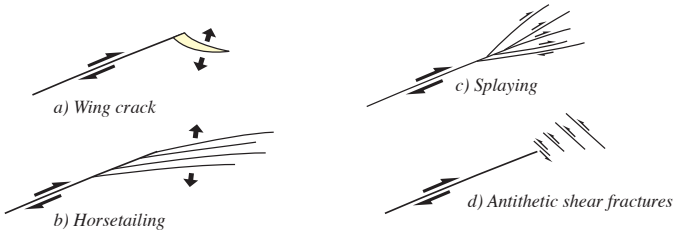

Figur 7.26 Minor fractures at the termination of fractures.

which is most pronounced when two of the stress axes are equal in size. For a vertical σ_1, the dip of the shear fracture is lowest when $\sigma_2=\sigma_1$ and highest when $\sigma_2=\sigma_3$. For foliated rocks where the foliation does not contain the intermediate principal stress axes the influence of σ_2 is greater. In this case the resolved normal and shear stress on the foliation depends on all three principal stresses.

Temperature has a major influence on rheology in the plastic regime, but its influence within the brittle regime is relatively small for most common minerals. It does however control the range of the brittle regime as increasing temperature lowers the von Mises' yield stress (lowers the yield point or the stress at which rock flows plastically).

An interesting laboratory observation is related to sample size: as the size of the sample increases, its strength is reduced. The reason for this somewhat surprising finding is that large samples contain more microfractures than do small samples. Because microfractures differ in length and shape, a large sample is likely to contain some microfractures that have a shape that causes larger stress concentrations than any of those in a smaller sample of the same rock. Hence the large sample is likely to fracture more easily than the small one.

The dependence on scale is even more pronounced at larger scales. Think of all the joints, faults and other weak structures in the crust that will be activated before the strength of the rock itself is reached. Such weak structures control the strength of the brittle crust, which means that the upper crust is not by far as strong as suggested by experimental testing of isotropic samples in the laboratory. This brings us over to another important topic; the reactivation of brittle fractures by frictional sliding.

1.4.2 Growth and morphology of fractures

Shear fractures cannot propagate in their own plane, but rather spawn new tensile cracks (wing cracks) according to Griffith's theory (Figure 7.22) or develop

Figure 7.27 Horsetailing at the termination of a shear fracture in gneiss.

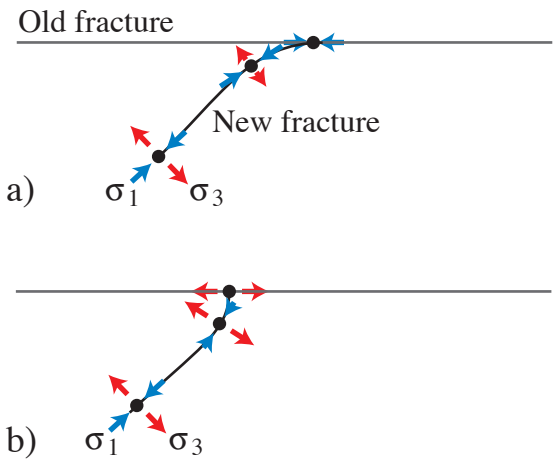

Figure 7.28 Local reorientation of fracture propagation direction in the vicinity of an existing fracture. The new fracture grows toward the preexisting one, seeking to maintain a 90° angle to σ_3. The curved geometry is caused by the rotation of the stress field around the preexisting fracture. The geometry in a) suggests that σ_1 is compressive with contraction along the preexisting fracture. If the new fracture curves against the preexisting one (b), then σ_1 and σ_3 are likely to be of similar magnitude with tension occuring along the preexisting fracture. Modified from Dyer (1988).

by activation of already existing extension fractures. In contrast, extension fractures may propagate into extensive structures. Ideally, an extension fracture will grow radially from a nucleation point so that the propagation front (tip-line) will at any point have the shape of an ellipse (Figure 7.23 a-b). The rate of propagation increases after initiation, and the joint surface gets rougher until it propagates so fast that the stress readjustments or stress oscillations at the crack tip cause it to bend. In detail, the tip bifurcates and off-plane microcracks form because of high stress and/or local heterogeneities in the tip zone. The result is long, narrow planes slightly oblique to the main fracture surface named *hackles* (Figure 7.23c), and the hackles form *plumose* (featherlike) structures. Plumose structures reflect the propagation direction along the plume axis, as shown in Figure 7.24.

Locally the main fracture may enter an area with a different stress orientation. This would typically be an interface between two rock types (e.g. bedding), in which case a series of twisted joints or *twist hackles* form in what is called the *fringe zone*. Twist hackles tend to be oriented *en echelon* because of the shear component on the main fracture locally imposed by the new orientation of σ_3. The twist hackles themselves try to orient perpendicular to σ_3, but cannot grow far in this direction because they are connected to the main fracture (Figure 7.25).

Extension fractures tend to grow in pulses. Each propagation pulse tends to end with an out-of-plane propagation with a slowing down or complete (ar)rest before the next pulse hits. Ribs are thus locations of minimum propagation velocity and form parabolic (semi-elliptic in massive rocks) irregularities sometimes referred to as *arrest lines*. Ribs are perpendicular to the plumose hackles (Figure 7.23a and 7.24) and together these structures provide unique information about the growth history of extension fractures. Plumose structures are characteristic for joints in fine-grained rocks such as siltstones, while arrest lines are also commonly seen in coarser grained lithologies such as sandstones and granites.

1.5 Fracture termination and interaction

Studies of shear fracture terminations reveal that they sometimes split into one or more fractures with new orientations. We have already looked at *wing cracks*, which are tensile fractures at the end of shear fractures (Figure 7.26a). Wing cracks are represented by one or sometimes a few tensile fractures at each end of the main fracture and are associated with rapid decrease in displacement towards the tip. In other cases a whole population of minor, typically tensile, fractures occurs in the tip zone. These are asymmetrically arranged with respect to the main fracture and referred to as *horsetail fractures* (Figures 7.26b and 7.27). If the secondary fractures in the tip zone represent a fan-shaped splaying of the main fracture, then the appropriate term is *splay*

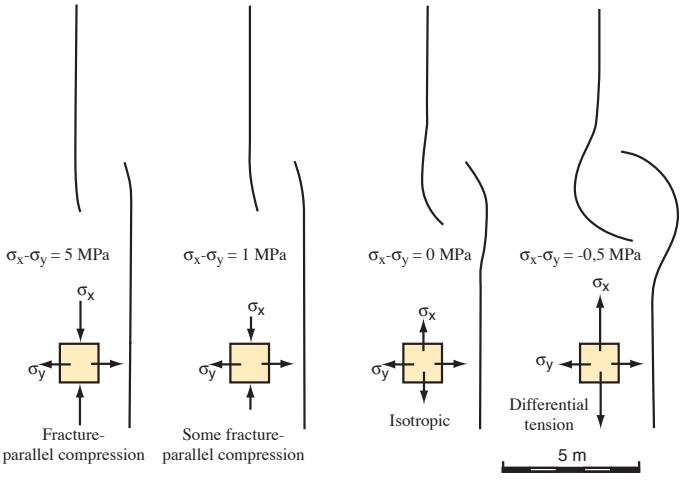

Figure 7.29 Schematic illustration of how fracture tip interaction depends on the differential stress (σ_x-σ_y) of the remote stress field. Based on Olsen and Pollard (1989) and Cruikshank et al. (1991).

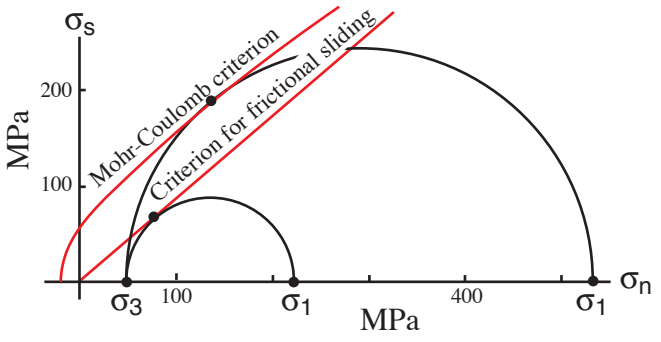

Figure 7.30 The effect of an existing fracture (plane of weakness) illustrated in the Mohr diagram. The criterion for reactivation is different from that of an unfractured rock of the same kind and the differential stress required to reactivate the fracture is considerably smaller than that required to generate a new fracture in the rock (this will also depend on the orientaiton of the preexisting fracture(s)). Based on experiments on crystalline rocks at a confining pressure of 50 MPa (ca. 4 km depth).

faults (Figure 7.26c). While splay faults are synthetic with respect to the main fault, *antithetic fractures* may also occur in the tip zone of fractures, as shown in Figure 7.26d.

Most of these tip zone fractures imply that the energy of the main fracture is distributed onto a number of fracture surfaces. This means that the energy on each fracture was reduced, which hampers continued fracture growth. The evolution of pronounced horsetail fractures or splay faults may thus "arrest" the main fracture and stop or at least pause further propagation of the fracture tip.

The stress field is perturbed around fractures in general and in the tip zone in particular. Thus, when the elastic strain fields around two fractures overlap, the local stress fields around each fracture will interfere and special geometries may develop. If a fracture grows toward an already existing one, the new fracture will curve as it "feels" the effect of the stress perturbation set up by the previous fracture (Figure 7.28). If both fractures approach each other simultaneously, they will both be affected by each other, and the degree of curvature is ideally dependent on the general state of stress (Figure 7.29).

1.6 Reactivation and frictional sliding

The Coulomb and Griffith fracture criteria, as formulated above, apply until the rock fails. One of the implications of this fact is that Anderson's theory of faulting, which again builds on Coulomb's theory, is only valid for infinitesimal fracture displacements. Once a fracture is formed it represents a plane of weakness, particularly at low confining pressure where cohesion across the fracture is lost. Renewed stress build-up is likely to reactivate existing fractures at a lower level of stress instead of creating a new fracture through the energy-demanding process of growth and linkage of minor flaws in the rock. Reactivation of fractures is a pre-requisite for major faults to develop. If this hadn't happened, the crust would have been shattered and full of small fractures with cm-scale displacements.

The orientation of a preexisting fracture with respect to the principal stresses and the friction on the fracture are the most important parameters in addition to the stress field itself (Figure 7.30). The orientation determines the resolved shear and normal stresses on the surface. In the extreme case there is no shear stress on the surface (σ_n is oriented perpendicular to the fracture), and the fracture is stuck. In other cases the friction puts a limitation on fracture reactivation potential. That local friction on the fracture is commonly referred to as the *coefficient of sliding friction* (μ_f), not the internal friction of an isotropic medium that we considered in section 7.2.

The coefficient of sliding friction is simply the shear stress required to activate slip on the fracture over the normal stress acting across the fracture:

$$\mu_f = \frac{\sigma_s}{\sigma_n} \quad (7.9)$$

In the Mohr diagram, this is a straight line (Figure 7.30), and it goes through the origin because we assume that the existing fracture has no cohesion at low confining pressure. If the fracture has a cohesive strength (C_f) the expression becomes:

$$\mu_f = \frac{\sigma_s - C_f}{\sigma_n} \quad (7.11)$$

The magnitude of C_f is usually low, and μ_f is similar for most rocks at moderate to high confining pressures (crustal depths). For low confining pressures the *surface roughness* of the fracture surface becomes important. Fault asperities resist fault slippage, and

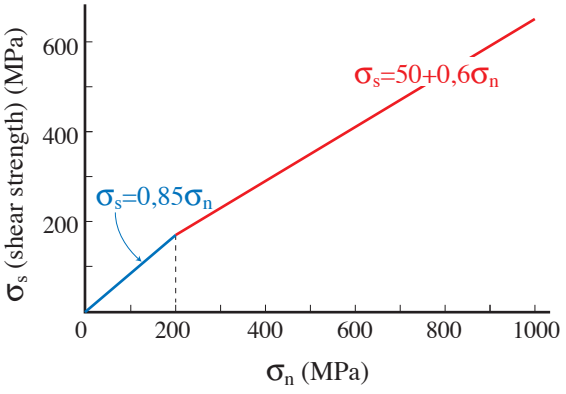

Figure 7.31 Byerlee's law is an empirical law that relates critical shear stress to normal stress. The horizontal scale is related to crustal depth (increasing to the right).

may lead to stick-slip deformation (Figure 8.34) at shallow burial depths. At deeper depths asperities are more easily dealt with and play little or no role as far as friction is concerned. After numerous experiments, Byerlee was able to define the critical shear stress at low confining pressure as:

$$\sigma_s = 0.85\sigma_n \qquad (\sigma_s < 200\,\text{MPa}) \qquad (7.12)$$

while the equation for higher confining pressure was found to be:

$$\sigma_s = 0.5 + 0.6\sigma_n \qquad (\sigma_s > 200\,\text{MPa}) \quad (7.13)$$

These equations are known as Byerlee's laws (Figure 7.31) and hold for most rocks except those that contain abundant H_2O-rich clay minerals such as montmorillonite and vermiculite.

1.7 Fluid pressure, effective stress and poroelasticity

One of the great challenges in the field of structural geology in the 20th century was to explain how gigantic thrust nappes could be transported for hundreds of kilometers without being crushed (see Chapter 16 why this was considered a problem). An important part of the explanation has to do with overpressured thrust zones, i.e. the shear zone contains fluids with anomalously high pore pressure.

This is one of several examples where fluid pressure plays an important role. We have already looked at overpressured formations in sedimentary sequences (petroleum reservoirs) in Chapter 6, where overpressure can occur if pore water in a porous and permeable formation is confined between impermeable layers. Overpressure builds up as the weight of the overburden acts on the pore pressure. An additional effect comes from the fact that water expands more quickly than rock minerals during heating. If the water cannot escape, the effect of its thermal expansion will further increase the pressure in the permeable unit.

Deeper down, metamorphic reactions release water and CO_2. This also leads to overpressure if the fluid is unable to escape along fracture networks in the generally impermeable metamorphic rocks. Mineral-filled extension fractures (veins) that occur in many low-grade metamorphic rocks are probably related to the increase of fluid pressure through fluid release due

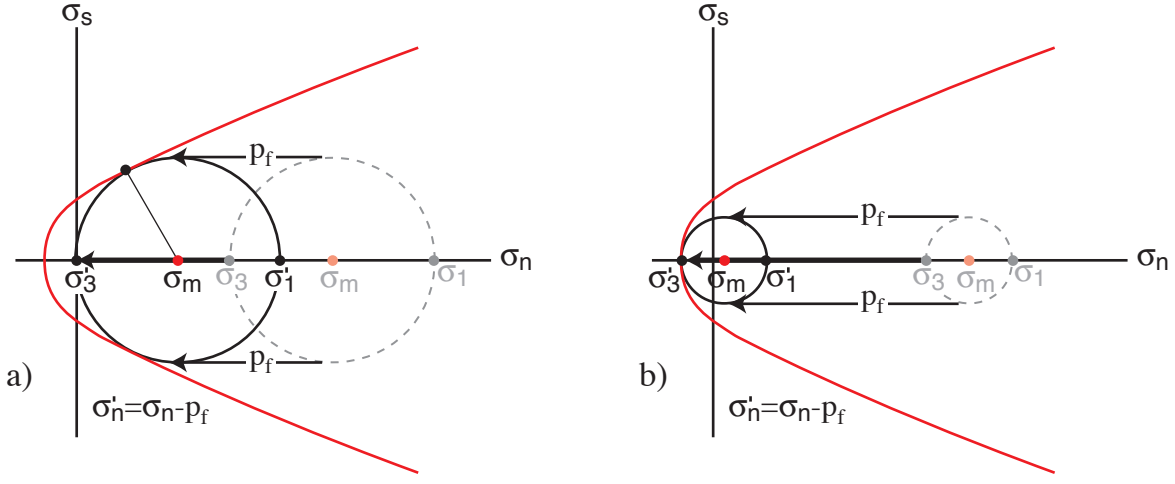

Figur 7.32 The effect of pumping up the pore fluid pressure p_f in a rock, as illustrated in the Mohr diagram. Mohr's circle is "pushed" to the left (the mean stress is reduced) and a shear fracture will form if the fracture envelope is touched while σ_3 is still positive. This will be the case if the differential stress is high. A tensile fracture forms if the envelope is reached in the tensile field as shown in b) (low differential stress).

to metamorphism. Injection of magma under pressure is also a situation where the vertical stress is balanced by fluid (magma) pressure. Finally, fluid pressure can be an important factor during fault reactivation. An increase in the fluid pressure can generate renewed movement along (or across) a fault or any other type of fracture.

The fluid pressure counteracts the normal stress resolved on the fracture, so that the resolved shear stress may be sufficient for reactivation.

Whether a new fracture forms or if an existing one is simply reactivated is controlled both by the fracture orientation relative to the principal stresses, and the effective stress.

Effective stress ($\bar{\sigma}$) is the difference between the applied or remote stress and the fluid pressure:

$$\bar{\sigma} = \sigma - p_f \qquad (7.14)$$

In three dimensions the effective stress can be expressed as:

$$\begin{bmatrix} \bar{\sigma}_{11} & \bar{\sigma}_{12} & \bar{\sigma}_{13} \\ \bar{\sigma}_{21} & \bar{\sigma}_{22} & \bar{\sigma}_{23} \\ \bar{\sigma}_{31} & \bar{\sigma}_{32} & \bar{\sigma}_{33} \end{bmatrix} = \begin{bmatrix} \sigma_{11} & \sigma_{12} & \sigma_{13} \\ \sigma_{21} & \sigma_{22} & \sigma_{23} \\ \sigma_{31} & \sigma_{32} & \sigma_{33} \end{bmatrix} - \begin{bmatrix} p_f & 0 & 0 \\ 0 & p_f & 0 \\ 0 & 0 & p_f \end{bmatrix}$$

$$= \begin{bmatrix} \sigma_{11} - p_f & \sigma_{12} & \sigma_{13} \\ \sigma_{21} & \sigma_{22} - p_f & \sigma_{23} \\ \sigma_{31} & \sigma_{32} & \sigma_{33} - p_f \end{bmatrix} \qquad (7.15)$$

or, if the principal stresses coincide with our coordinate axes:

$$\begin{bmatrix} \bar{\sigma}_1 & 0 & 0 \\ 0 & \bar{\sigma}_2 & 0 \\ 0 & 0 & \bar{\sigma}_3 \end{bmatrix} = \begin{bmatrix} \sigma_1 - p_f & 0 & 0 \\ 0 & \sigma_2 - p_f & 0 \\ 0 & 0 & \sigma_3 - p_f \end{bmatrix} \qquad (7.16)$$

Fluid pressure will weaken the rock so that deformation can occur at a lower differential stress. For porous sandstone, the pore (fluid) pressure has the following effect on the Coulomb fracture criterion:

$$\sigma_s = C - \mu(\sigma_n - p_f) \qquad (7.17)$$

An increase in pore pressure decreases the mean stress from σ_m to $\sigma_m - p_f$ while the differential stress (σ_1-σ_3) is constant (Figure 7.32).

If the effective stress is tensile (negative), i.e. if:

$$\bar{\sigma}_3 = \sigma_3 - p_f < 0 \qquad (7.18)$$

tensile fractures can form. In dry or hydrostatically pressured rocks tensile fractures can only be expected to form at very shallow depths (upper tens or hundreds of meters of the crust), but overpressure makes it possible to have tensile stress (negative σ_3) even at several kilometers depth or more, particularly where

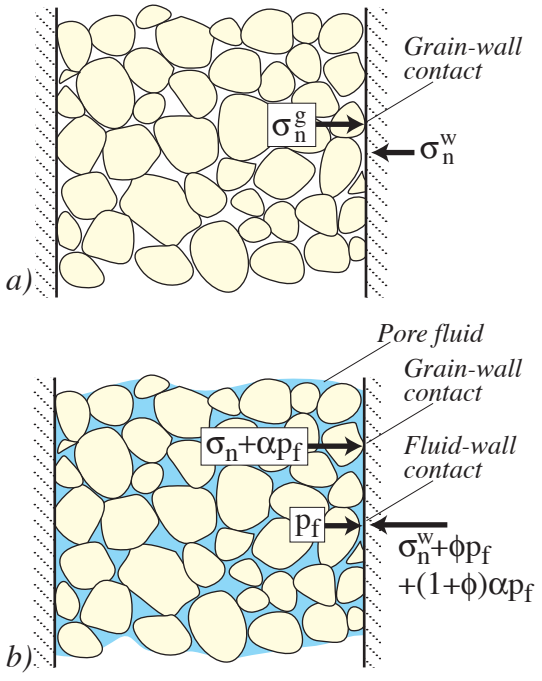

Figure 7.33 The effect of increasing the pore pressure p_f on the total stress situation in a porous rock (closed uniaxial-strain stress model). In a dry rock (a), stresses are transmitted across grain-grain or grain-wall contacts only. If pore fluid is added with a low p_f (b), then the the increase in normal stress at grain-wall contacts is smaller than the increase in pore pressure because of the absorbtion of stress by elastic deformation across the grains. This is the poroelastic effect. Modified from Engelder (1993).

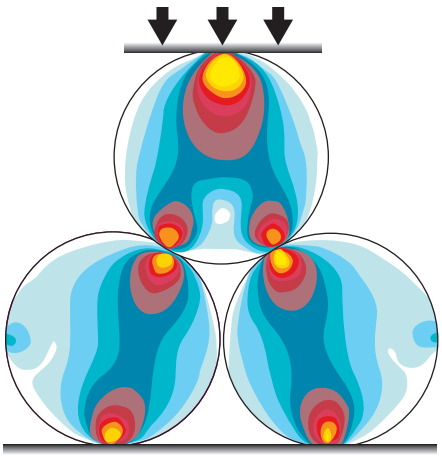

Figure 7.34 Illustration of stress concentrations at grain-grain contact areas in a porous rock or sediment. Warm colors indicate high stress. Based on Gallagher et al. (1974).

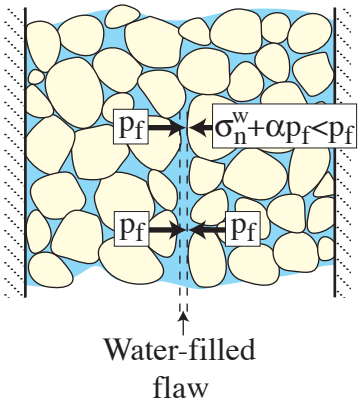

Figure 7.35 The stress situation in a flaw in a permeable porous rock. The poroelastic effect causes the stress across the grain-flaw part of the flaw walls to be less than the pore fluid pressure. Tensile stress occurs if the pore pressure gets high enough.

magmatic processes are involved.

We can rewrite Equation 7.14 so that it becomes clearer that the total stress is the sum of the effective stress and the pore pressure:

$$\sigma = \bar{\sigma} + p_f \qquad (7.19)$$

or

$$\begin{bmatrix} \sigma_{11} & \sigma_{12} & \sigma_{13} \\ \sigma_{21} & \sigma_{22} & \sigma_{23} \\ \sigma_{31} & \sigma_{32} & \sigma_{33} \end{bmatrix} = \begin{bmatrix} \bar{\sigma}_{11} & \bar{\sigma}_{12} & \bar{\sigma}_{13} \\ \bar{\sigma}_{21} & \bar{\sigma}_{22} & \bar{\sigma}_{23} \\ \bar{\sigma}_{31} & \bar{\sigma}_{32} & \bar{\sigma}_{33} \end{bmatrix} + \begin{bmatrix} p_f & 0 & 0 \\ 0 & p_f & 0 \\ 0 & 0 & p_f \end{bmatrix} \qquad (7.20)$$

To illustrate this relationship, imagine a porous and permeable sandstone (Figure 7.33) that is exposed to a uniaxial-strain reference state of stress inside a container (Figure 6.2). Let us first assume that the rock is dry and that the grains exert an average stress σ_n^w against the walls of the container. This stress is not evenly distributed along the walls but concentrated at the grain-wall contact points (Figure 7.34). The grain-wall contact stress σ_n^g depends on the area across which it is distributed and can be expressed in terms of the porosity ϕ:

$$\sigma_n^g = \left(\frac{1}{1-\phi}\right)\sigma_n^w \qquad (7.21)$$

We now fill the pores with fluid at some moderate pressure p_f, which causes the pressure against the walls to increase. The parts of the walls that are in contact with the fluid will "feel" the fluid pressure directly. At the grain-wall contact points the normal stress on the wall increases by a fraction of p_f, i.e. by a factor αp_f, where $\alpha<1$. The increase in stress against the wall, which we denote $\Delta\sigma_n$, will *not* be equal to p_f, but will be less by an amount depending on the porosity of the sandstone:

$$\Delta\sigma_n = \phi\, p_f + (1-\phi)\alpha\, p_f \qquad (7.22)$$

The factor α is known as Biot's poroelastic parameter and characterizes the poroelastic effect. But why is the stress increase less than p_f? It occurs because the cemented grain contacts are elastic. Thus, a part of the pore fluid pressure p_f is taken up by elastic deformation.

The poroelastic effect is important when considering the state of stress in sedimentary basins. It may also contribute to the formation and propagation of fractures in porous rocks (Figure 7.35). In keeping with Griffith's theory, a flaw of some kind represents a possible nucleation point for a tensile fracture. Increasing the pore pressure by an amount Δp_f gives a new pore pressure p_f that will be identical within and outside of the flaw, because the rock is permeable. At the walls between the flaw and the rock, however, the poroelastic effect (Equation 7.22) comes in to play. It tells us that the general increase in pore pressure causes the average normal stress at the rock sides of

the flaw to increase at a lower rate than in the flaw. As the pore pressure increases, at some point the fluid pressure p_f within the flaw will exceed the average normal stress exerted by the grains on the walls of the flaw. The walls are then under tension and may further separate and propagate into a larger extension fracture. The tensile stress is concentrated at the tips, and its magnitude depends on the shape of the flaw or crack according to Equation 7.8. Once the extension fracture grows, the volume (width and length) of the fracture increases and ~~hence~~ the pore pressure drops locally, and the propagation stops or pauses until the pore pressure is restored. This kind of fracture propagation history is recorded by the formation of arrest lines (Figure 7.24).

1.8 Deformation bands and fractures in porous rocks

As we have seen above, rocks respond to stress in the brittle regime by forming extension fractures and shear fractures (slip surfaces). Such fractures are sharp and mechanically weak discontinuities, and thus prone to reactivation during renewed stress build-up. At least this is how non-porous and low-porous rocks respond. In highly porous rocks and sediments, brittle deformation is expressed by related, although different, deformation structures referred to as *deformation bands*.

Deformation bands are mm-thick zones of localized compaction, shear, and/or dilation in deformed porous rocks (Figure 7.36). There are good reasons why deformation bands should be distinguished from ordinary fractures. One is that they are thicker and exhibit smaller displacements than regular slip surfaces of comparable length. Another is that, while cohesion is lost or reduced across regular fractures, many deformation bands maintain or even show increased cohesion. Furthermore, there is a strong tendency for most deformation bands to represent low-permeable bands in otherwise medium- to high-permeable rocks. Regular fractures tend to represent pathways for fluid flow in otherwise low- or unpermeable rocks. This distinction is particularly important to petroleum geologists and some hydrogeologists concerned with fluid flow in reservoir rocks. The strain hardening that occurs during the formation of many deformation bands is also in direct

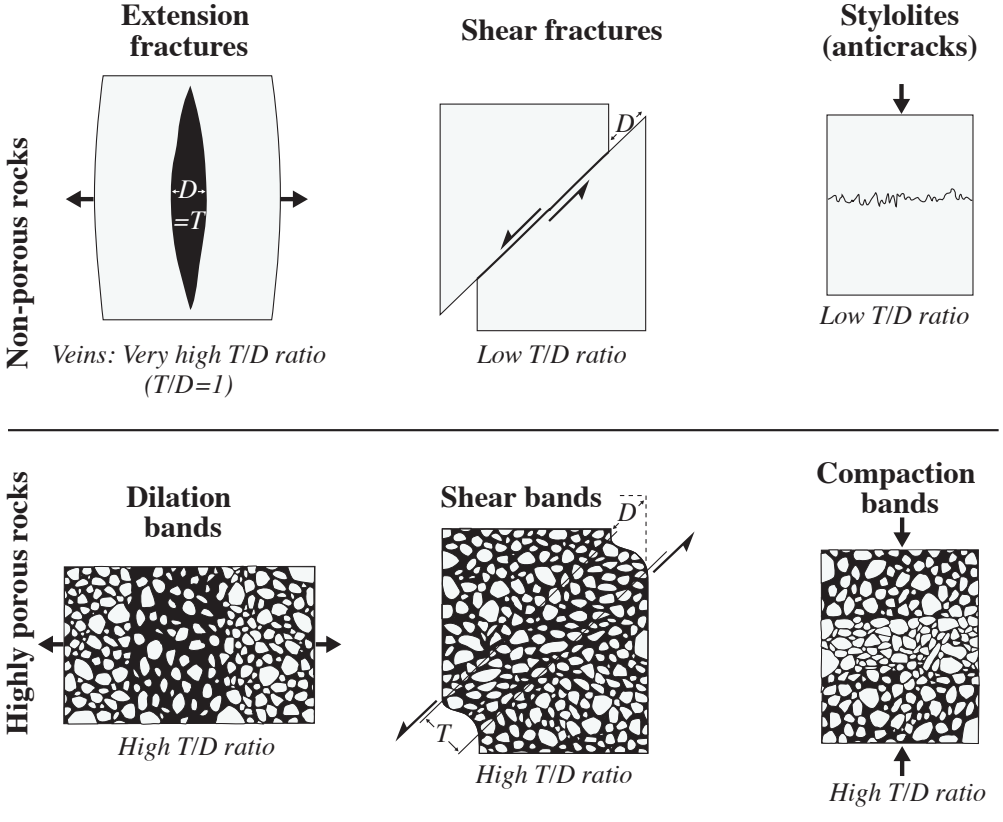

Figure 7.36 Kinematic classification of deformation bands and their relationship to fractures in low- and non-porous rocks. T=thickness, D=displacement.

contrast to the softening associated with fracturing. These differences may be of importance during the management of porous hydrocarbon and groundwater reservoirs.

The difference between brittle fracturing of non-porous and porous rocks lies in the fact that porous rocks have a pore volume that can be utilized during grain reorganization. The pore space allows for effective rolling and sliding of grains. Even if grains are crushed, grain fragments can be organized into nearby pore space.

It is primarily the kinematic freedom associated with pore space that allows the special class of structures called deformation bands to form.

1.8.1 What is a deformation band?

How do deformation bands differ from regular fractures in non-porous rocks? Here are some characteristics of deformation bands

1) Deformation bands are restricted to highly[4] porous granular media such as porous sandstones, limestones and unwelded tuff.

2) A shear deformation band is a wider zone of deformation than regular shear fractures of comparable displacement.

3) Deformation bands do not develop large offsets. Even 100 m long deformation bands seldom have offset in excess of a few centimeters, while a shear fracture of the same length tend to show meter-scale displacement.

4) Deformation bands occur as single structures, in zones, or in zones associated with slip surfaces (faulted deformation bands). This is related to the way that faults form in porous rocks by faulting of deformation band zones (see Chapter 8).

1.8.2 Types of deformation bands

Similar to regular fractures discussed above, deformation bands can be classified in a kinematic framework, where shear (deformation) bands, dilation bands and compaction bands form the end members (Figure 7.36). It is sometimes more informative to distinguish between the *mechanisms*

4 10-15% porosity or more seems to be required, although this depends also on cementation and other factors.

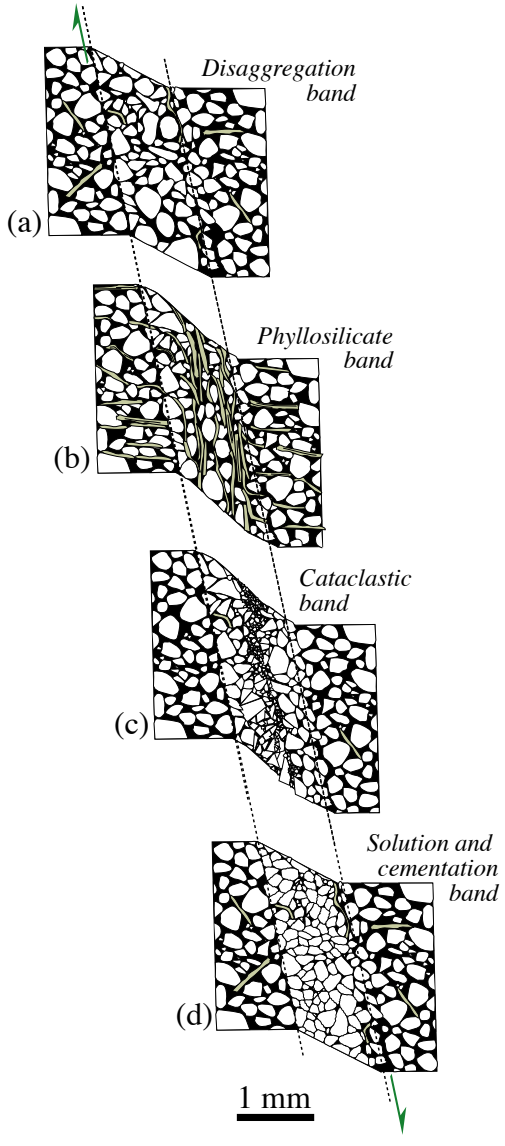

Figure 7.37 The different types of deformation bands, distinguished by dominant deformation mechanism.

operative during the formation of deformation bands. Deformation mechanisms depend on internal and external conditions such as mineralogy, grain size, grain shape, grain sorting, cementation, porosity, state of stress etc. and different mechanisms produce bands with different petrophysical properties. Thus, a classification of deformation bands based on deformation processes is particularly useful if permeability and fluid flow is an issue. The most important mechanisms are:

1) granular flow (grain boundary sliding and grain rotation)
2) cataclasis (grain fracturing)
3) phyllosilicate smearing
4) dissolution and cementation

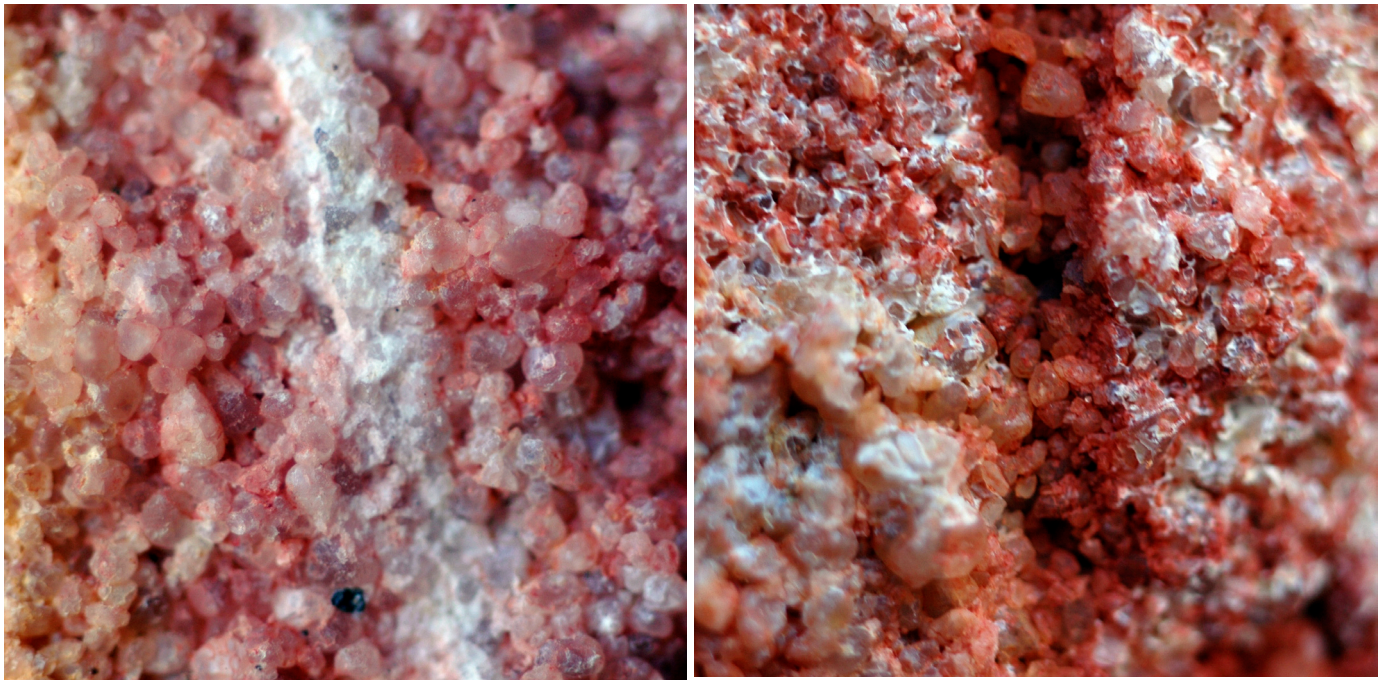

Figure 7.38 Cataclastic deformation band (left) and disaggregation band (right) in the Nubian Sandstone, Sinai. The cataclastic band represents a low-permeable structure whereas the more unusual disaggregation band has higher porosity and permeability than its host rock. Width of bands ~1 mm

A deformation band is named from the characteristic deformation mechanism, as shown in Figure 7.37.

Disaggregation bands develop by shear-related disaggregation of grains by means of grain rolling, grain boundary sliding and breaking of grain bonding cements (if there is any), a process referred to as *particulate flow* or *granular flow*. Disaggregation bands are commonly found in sand and poorly consolidated sandstones (Figure 7.38b) and form the "faults" produced in sandbox experiments. Disaggregation bands can be almost invisible in clean sandstones, but may be detected where they cross and offset laminas (Figure 7.39). Their true offsets are typically some centimeters and their thickness varies with grain size. Fine-grained sand(stones) develop ~1 mm thick bands, whereas coarser-grained sand(stones) host single bands that may be at least 5 mm thick.

Macroscopically, disaggregation bands are ductile shear zones where sand laminas can be traced continuously through the band. Most pure and well-sorted quartz sand deposits are already compacted to the extent that the initial stages of shearing involves some dilation (dilation bands), although continued shear-related grain reorganization may reduce the porosity at a later point.

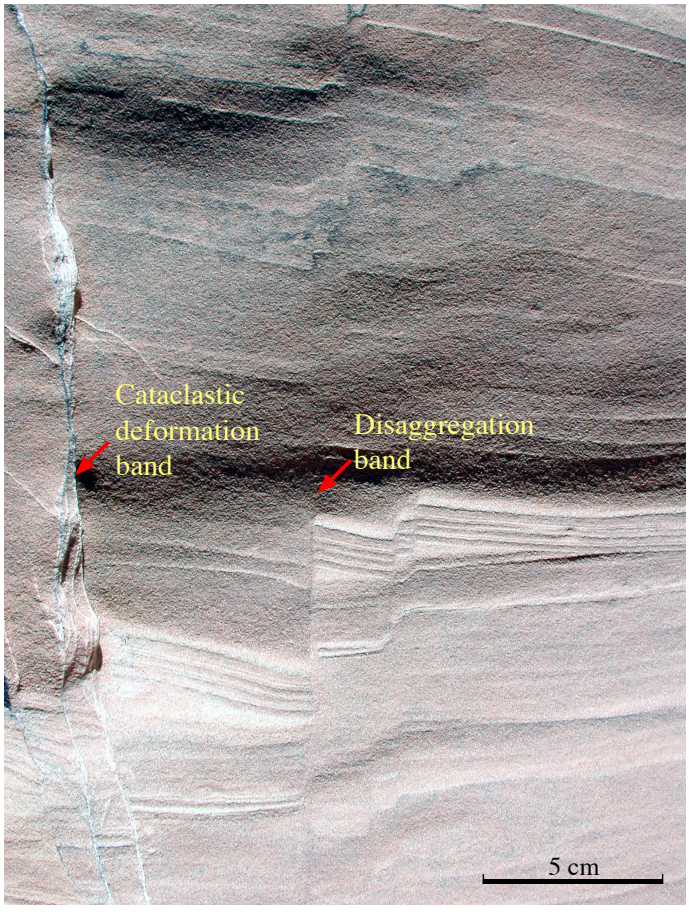

Figure 7.39 Cataclastic deformation bands and disaggregation bands in the Navajo Sandstone, Utah. Note that the disaggregation bands are almost invisible away from the marker horizons. The cataclastic bands are white due to grain crushing. It can be seen at this locality that the cataclastic bands overprint the disaggregation bands.

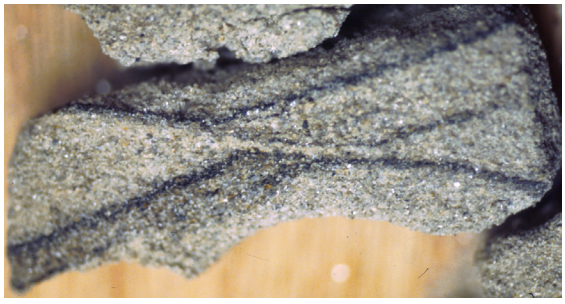

Figure 7.40 Mica-assisted deformation band in the Brent Group of the North Sea. Note the smearing of mica along the band and the similarity between the band and the lamination.

Phyllosilicate bands (also called framework phyllosilicate bands) form in sand(stone) where the content of platy minerals exceeds about 10-15%. They can be considered as a special type of disaggregation band where platy minerals promote grain sliding. Clay minerals tend to mix with other mineral grains in the band while coarser phyllosilicate grains align to form a local fabric within the bands due to shear-induced rotation (Figure 7.40). Phyllosilicate bands are easy to detect, as the aligned phyllosilicates give the band a distinct color or fabric that may be reminiscent of phyllosilicate-rich laminas in the host rock. Where the phyllosilicate content of the rock changes across bedding or lamina interfaces, a single deformation band may change from an almost invisible disaggregation band to a phyllosilicate band. Where clay is the dominant platy mineral, the band is a fine-grained, low-porosity zone that can accumulate offsets that exceed the few centimeters exhibited by other types of deformation bands. This is related to the smearing effect of the platy minerals along phyllosilicate bands that apparently counteracts any strain hardening resulting from interlocking of grains.

If the clay content of the host rock gets high enough (more than ~40% according to Fisher & Knipe 2001), the deformation structure turns into a *clay smear*. Clay smears typically show striations, meaning that they classify as slip surfaces rather than deformation bands. Examples of deformation bands turning into clay smears as they leave sand layers are common.

Cataclastic (deformation) bands form where mechanical grain breaking is a significant deformation mechanism (Figures 7.38a and 7.41).

Figure 7.41 Conjugate (simultaneous and oppositely-dipping) sets of cataclastic deformation bands in the damage zone of a fault. Note the positive relief of the deformation bands due to grain crushing and cementation. Entrada Sandstone, Utah.

These are the classical deformation bands first described by Atilla Aydin from the Colorado Plateau in the western USA. He noted that cataclastic bands consist of a central cataclastic core contained within a mantle of (usually) compacted rock. The core is characterized by grain-size reduction, angular grains and significant pore space collapse (Figure 7.42). The crushing of grains results in extensive grain interlocking, which promotes strain hardening. Strain hardening may explain the small shear displacements observed on cataclastic deformation bands (≤3-4 cm). Some cataclastic bands are compaction bands, while most are shear bands with minor compaction across them.

Cataclastic bands are mostly found in rocks that have been buried to depths of about 1.5-3 km, although evidence of cataclasis is also reported from deformation bands deformed at less than 1 km depth. Comparison suggests that shallowly formed

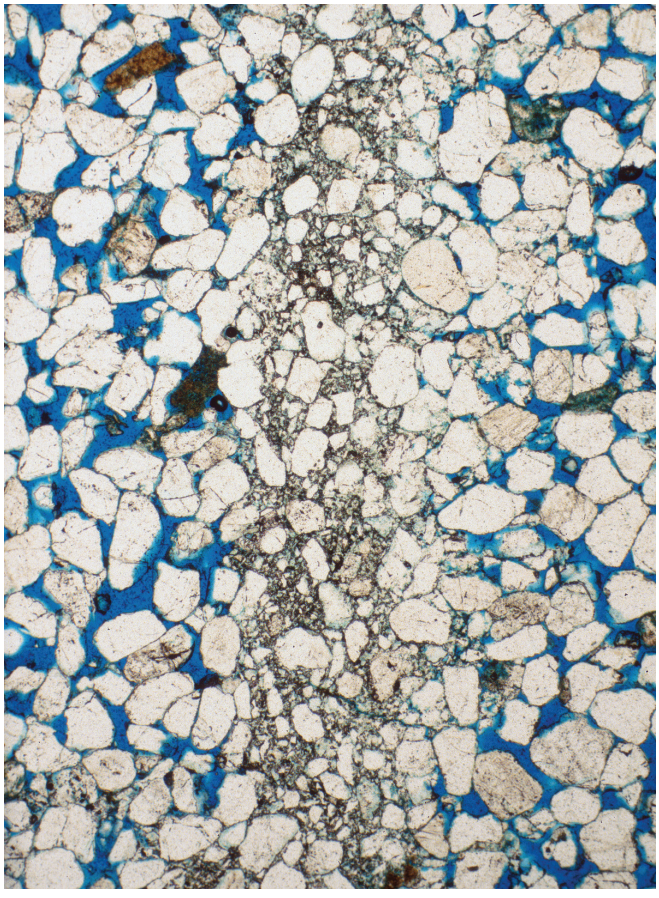

Figure 7.42 Cataclastic deformation band under the microscope. Note the reduction in grain size within the core of the band and the compaction along this zone. Blue areas indicate pore space. The band is ~1 mm wide.

cataclastic deformation bands show less intensive cataclasis than those formed at 1.5-3 km depth.

Cementation and dissolution of quartz and other minerals may occur preferentially in deformation bands because diagenetic minerals preferentially grow on the numerous fresh surfaces formed during grain crushing and/or grain boundary sliding. Such preferential growth of quartz is generally seen in deformation bands in sandstones buried >2-3 km (90 °C) and can occur during as well as long after the formation of the bands.

1.8.3 Influence on fluid flow

Deformation bands form a common constituent of porous oil, gas, and water reservoirs alike, where they occur as single bands, cluster zones or in fault damage zones (see next chapter). Although they are unlikely to form seals that can hold large hydrocarbon columns over geologic time, they can probably influence fluid flow in some cases. Their ability to do so depends on their internal permeability structure and thickness or number.

Deformation band permeability is governed by the deformation mechanisms operative during their formation, which again depends on a number of lithological and physical factors. In general, disaggregation bands show limited porosity and permeability reduction, while phyllosilicate and, particularly, cataclastic bands show permeability reductions up to several orders of magnitude. Deformation bands are thin, normally around 1 mm for each band, so the number of deformation bands (their cumulative thickness) is important.

Important is also their continuity, variation in porosity/permeability and orientation. Deformation bands tend to have a preferred orientation, for instance in damage zones, and this anisotropy can influence the fluid flow in a petroleum reservoir, particularly during water injection.

1.8.4 What type of structure forms, where and when?

Given the various types of deformation bands and their different effects on fluid flow, it is important to understand the underlying conditions that control when and where they form. A number of factors are influential, including burial depth, tectonic environment (state of stress) and host rock properties, such as degree of lithification, mineralogy, grain size, sorting, and grain shape (Table 1). Some of these factors, particularly mineralogy, grain size, rounding, grain shape and sorting, are more or less constant for a given sedimentary rock layer. They may however vary from layer to layer, which is why rapid changes in deformation band development may be seen from one layer to the next.

Other factors, such as porosity, permeability, confining pressure, stress state and cementation, are likely to change with time. The result may be that early deformation bands are different from those formed at later stages in the same porous rock layer, for example at deeper burial depths. Hence, the *sequence* of deformation structures in a given rock layer reflects the physical changes that the sediment has experienced throughout its history of burial, lithification and uplift.

The *earliest* forming deformation bands in sandstones are typically *disaggregation bands* or *phyllosilicate bands* (Figure 7.43). These structures form at low confining pressures (shallow burial)

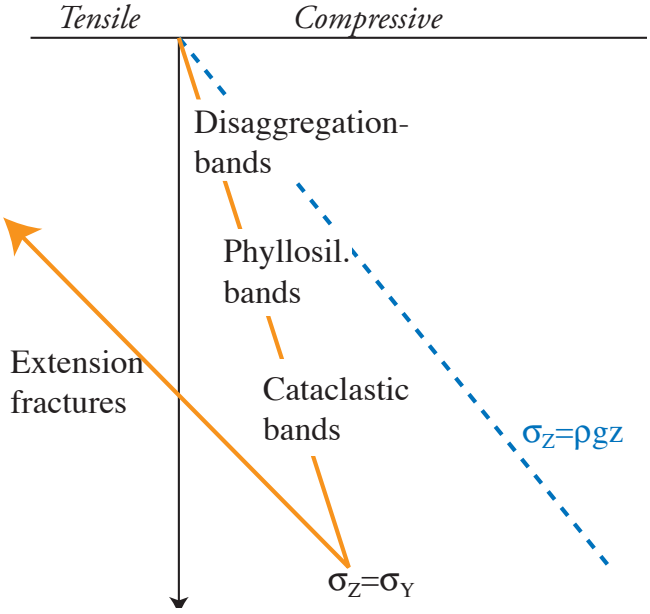

Figure 7.43 Different types of deformation bands form at different stages during burial. Extension fractures (Mode I fractures) are most likely to form during uplift. Also see Figure 6.4.

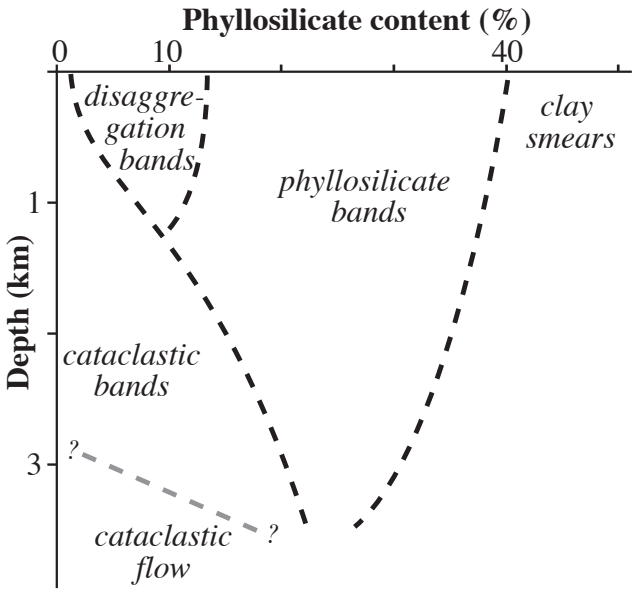

Figure 7.44 Schematic illustration of how different deformation band types relate to phyllosilicate content and depth. Many other factors influence on the boundaries outlined in this diagram, and the boundaries should be considered as uncertain.

when forces across grain contact surfaces are low and grain bindings are weak (Figure 7.44). Many early disaggregation bands are related to local, gravity-controlled deformation such as local shale diapirism, underlying salt movement, gravitational sliding and glaciotectonics.

Cataclastic deformation bands can occur in poorly lithified layers of pure sand at shallow burial depths, but are much more common in sandstones deformed at 1-3 km depth. Factors promoting shallow-burial cataclasis include small grain contact areas, i.e. good sorting and well-rounded grains, the presence of feldspar or other non-platy minerals with cleavage and lower hardness than quartz, and lithic fragments that are weaker than the majority of grains in the sediment. Quartz, for instance, seldom develops transgranular fractures under low confining pressure, but may fracture by flaking or spalling. At deeper depths, extensive cataclasis is promoted by high grain contact stresses. Abundant, well-known examples of cataclastic deformation bands are found in the Jurassic sandstones of the Colorado Plateau, where the age relation between early disaggregation bands and later cataclastic bands is very consistent.

Once the rock becomes a cohesive lithology with low enough porosity that deformation occurs by crack propagation instead of pore space collapse, then *slip surfaces*, *joints* and *mineral-filled fractures* form directly without any precursory formation of deformation band zones. This is why late, overprinting structures are almost invariably slip surfaces, joints and mineral-filled fractures. Slip surfaces can also form by faulting of low-porosity deformation band zones at any burial depth, according to the model described in the next chapter (Setion 8.?).

Joints and veins typically postdate both disaggregation bands and cataclastic bands in sandstones. The transition from deformation banding to jointing may occur as porosity is reduced, notably through quartz dissolution and precipitation. Since the effect of such diagenetically-controlled strengthening may vary locally, deformation bands and joints may develop simultaneously in different parts of a sandstone layer, but locally the general pattern appears to be deformation bands first, then faulted deformation bands (slip surface formation) and finally joints and faulted joints (Figure 7.43)

The latest fractures in uplifted sandstones tend to form extensive and regionally mappable joint sets generated or at least influenced by removal of overburden and related cooling during regional uplift. Such joints are pronounced where sandstones have been uplifted and exposed, such as on the Colorado Plateau, but are unlikely to be developed

in subsurface petroleum reservoirs unexposed to significant uplift. It therefore appears that knowing the burial/uplift history of a basin in relation to the timing of deformation events is very useful when considering the type of structures present in, say, a sandstone reservoir. Conversely, examination of the type of deformation structure present also gives information about deformation depth and other conditions at the time of deformation.

Further reading:

Fractures and fracturing

Scholz, C.H., 2002. The mechanics of earthquakes and faulting. Cambridge University Press, 496 ss.

Schultz, R.A., 1996. Relative scale and the strength and deformability of rock masses. Journal of Structural Geology, 18: 1139-1149

Segall, P. and Pollard, D.D., 1983. Nucleation and growth of strike slip faults in granite. Journal of Geophysical Research, 88: 555-568.

Reches, Z. & Lockner, D.A., 1994. Nucleation and growth of faults in brittle rocks. Journal of Geophysical Research, 99: 18159-18172.

Joints

Narr, W. & Suppe, J., 1991. Joint spacing in sedimentary rocks. Journal of Structural Geology, 13: 1037-1048.

Pollard, D.D. & Aydin, A., 1988. Progress in understanding jointing over the past century. Geol. Soc. Am. Bull., 100: 1181-1204.

Importance of fluids

Hubbert, M.K. & Rubey, W.W., 1959. Role of pore fluid pressure in the mechanics of overthrust faulting. I: Mechanics of fluid-filled porous solids and its application to overthrust faulting. Geol.Soc.Am.Bull., 70: 115-205.

Deformation bands:

Antonellini, M. & Aydin, A., 1994. Effect of faulting on fluid flow in porous sandstones: petrophysical properties. American Association of Petroleum Geologists, 78: 355-377.

Aydin, A. & Johnson, A.M., 1978. Development of faults as zones of deformation bands and as slip surfaces in sandstones. Pure appl. Geophys., 116: 931-942.

Fossen, H., Schultz, R., Shipton, Z. & Mair, K. 2007. Deformation bands in sandstone – a review. Journal of the Geological Society, London in press

Jamison, W.R., 1989. Fault-fracture strain in Wingate Sandstone. Journal of Structural Geology, 11: 959-974.

Rawling, G.C. and Goodwin, L.B., 2003. Cataclasis and particulate flow in faulted, poorly lithified sediments. Journal of Structural Geology, 25: 317-331.

Underhill, J.R. & Woodcock, N.H., 1987. Faulting mechanisms in high-porosity sandstones: New Red Sandstone, Arran, Scotland. Deformation of sediments and sedimentary rocks, 29. Geol. Soc. Spec. Publ., 91-105.

CHAPTER 8

Faults

Faults are complex and compound structures found in many geologic settings in the upper crust. They are mechanically weak, prone to become reactivated during stress build-up. Faults generally represent pathways for fluids and mineral solutions in the crust, but can seal hydrocarbon reservoirs. These structures may also represent challenges during tunnel operations and other construction work. There are thus many reasons why we should pay attention to faults.

1.1 Basic terminology

The term *fault* is used in different ways depending on the geologist and the context. A general and traditional definition would run something like:

A fault is any surface or narrow zone with visible shear displacement along the zone.

This definition is almost identical to that of a shear fracture, and some geologist use the two synonymously. Many geologists would however restrict the use of the term shear fracture to small-scale structures, reserving the term fault for structures with offset of the order of a meter or more. Others refer to shear fractures with mm to cm-scale offset as microfaults.

The thickness of a fault is another issue. Faults are often referred to as planes and surfaces. In most, if not all cases, close examination reveals that faults have a certain thickness, sometimes referred to as the fault core. However, the thickness is usually much smaller than the offset and several orders of magnitude[1] less than the fault length. Whether a fault should be considered as a surface or a zone thus largely depends on the scale of observation.

Faults of some meters or more of displacement tend to be complex zones of deformation, consisting of multiple slip surfaces, other fractures and perhaps also deformation bands. This becomes particularly apparent when considering large faults with km-scale offsets. Such faults can be considered as single faults on a map or a seismic line, but can be seen to consist of several small faults when examined in more detail. In other words, the scale dependency, which keeps haunting the descriptive structural geologist, is important here. This has lead many geologists to consider a fault as a volume of mainly brittlely deformed rock that is relatively thin in one dimension:

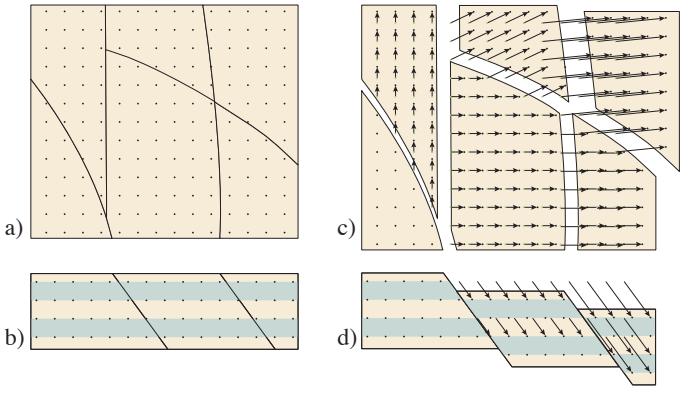

Figure 8.1 Faults appear as discontinuities not only in the field, but also on velocity or displacement field maps and profiles. The left block in the undeformed map (a) and profile (b) are fixed during the deformation. The result is abrupt changes in the displacement field across faults.

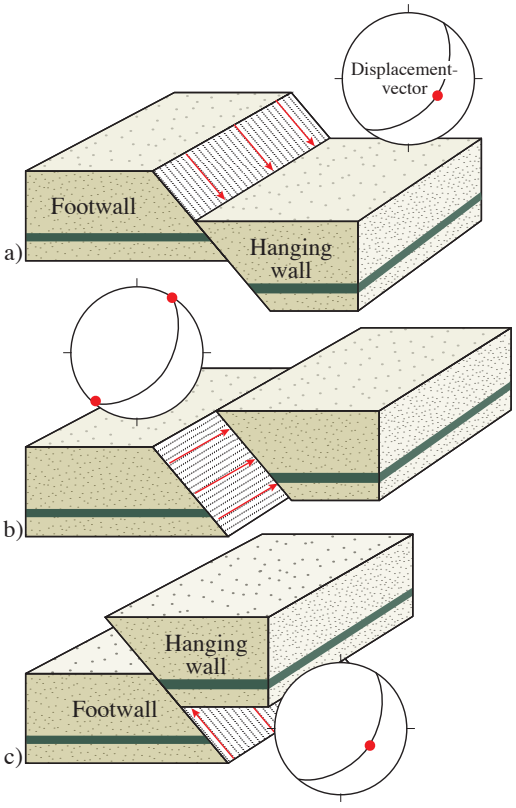

Figure 8.2 Normal (a), strike-slip (sinistral) (b) and reverse fault (c). These are end-members of a continous spectrum of oblique faults. The stereonets show the fault plane (great circle) and the displacement direction (red point).

A fault is a tabular volume of rock consisting of a slip surface or core of intense shear, and a surrounding volume of rock that has been affected by brittle deformation related to the formation and growth of the fault.

This use is particularly common in the oil industry, and the term *damage zone* applies to a significant amount of the fault volume, as discussed later in this chapter.

The term fault may also be connected to deformation mechanisms (brittle or plastic). In a very general sense, the term *fault* covers both brittle

1 By one order of magnitude less we mean ten times less.

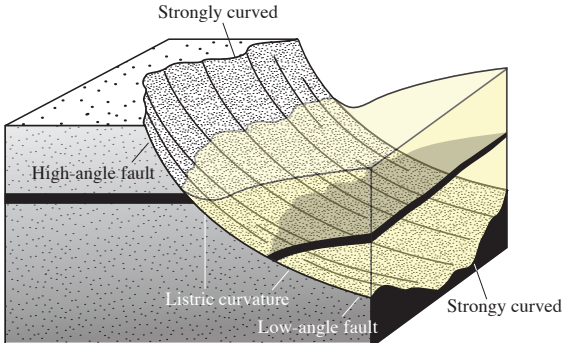

Figure 8.3 Listric normal fault showing very irregular curvature in the sections perpendicular to the slip direction. These irregularities can be thought of as large grooves or corrugations along which the hanging wall can slide.

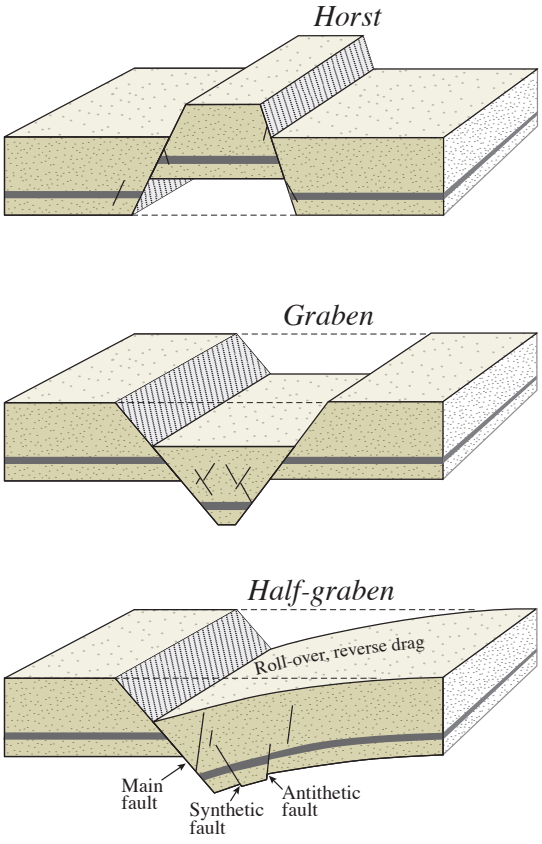

Figure 8.5 A horst, symmetric graben and asymmetric graben, also known as a half-graben. Antithetic and synthetic faults are shown. Perfectly symmetric grabens are very rare.

discontinuities and ductile shear zones dominated by plastic deformation. This is sometimes implied when discussing large faults on seismic or geologic sections that penetrate much or all of the crust[2]. In most cases, however, geologists restrict the term fault to slip or shear discontinuities dominated by brittle deformation mechanisms. This opens for yet another definition of a fault:

A fault is a discontinuity with wall-parallel displacement dominated by brittle deformation mechanisms.

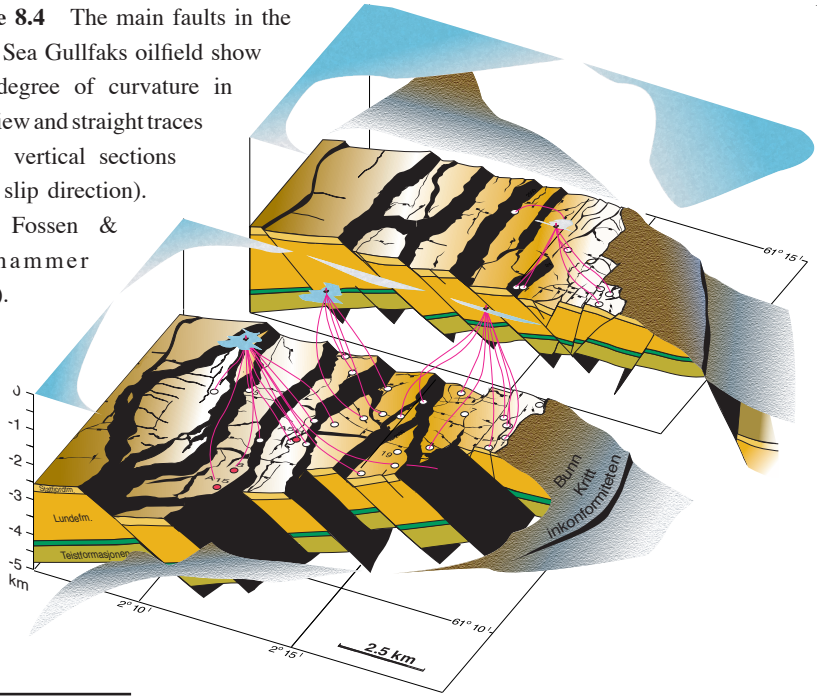

Figure 8.4 The main faults in the North Sea Gullfaks oilfield show high degree of curvature in map view and straight traces in the vertical sections (main slip direction). From Fossen & Hesthammer (2000).

By discontinuity we are here relating to layers, i.e. faults cut off rock layers and make them discontinuous. Also the velocity and displacement field are discontinuous across a fault. A kinematic definition, particularly useful for experimental work and GPS-monitoring of active faults is therefore needed (Figure 8.1):

A fault is a discontinuity in the velocity or displacement field associated with deformation

If we are observing an ongoing deformation, such as a sandbox experiment, or are performing a numerical experiment, then the velocity field can be calculated by comparing small increments of deformation. If we are comparing the

2 Where it is necessary to be specific about micromechanisms, the term *brittle fault* can be used.

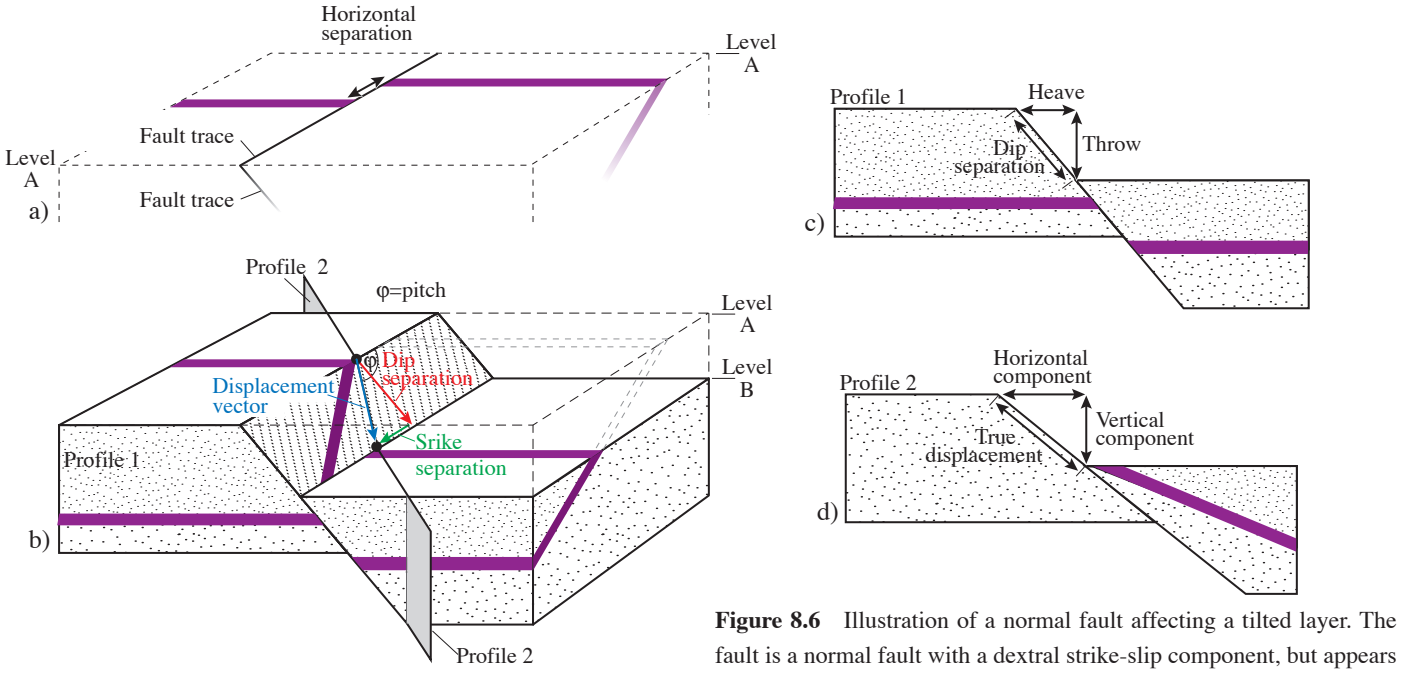

Figure 8.6 Illustration of a normal fault affecting a tilted layer. The fault is a normal fault with a dextral strike-slip component, but appears as a sinistral fault in map view (a). c) and d) show profiles perpendicular to fault strike (c) and in the (true) displacement direction (d).

initial and final stages, then abrupt changes in the displacement field can show us where the faults are located.

As mentioned in the previous chapter, faults differ from shear fractures because a shear fracture cannot simply expand in its own plane into a larger fault. In order to make a fault it is necessary to create a complex process zone with numerous small tension fractures, some of which link to form the fault slip surface while the rest is abandoned[3]. This means that even on the microscale a fault is not a single plane. Only at a somewhat larger scale do they appear as surfaces or thin zones of discontinuity.

1.1.1 Geometry of faults

Non-vertical faults separate the *hanging wall* from the underlying *footwall* (Figure 8.2). Where the hanging wall is lowered relative to the footwall, the fault is a *normal fault*. The opposite case, where the hanging wall is upthrown relative to the footwall, is a *reverse fault*. If the movement is lateral, i.e. in the horizontal plane, then the fault is a strike-slip fault. Strike-slip faults can be sinistral (left-lateral) or dextral (right-lateral) (from the latin words sinister and dexter, meaning left and right, respectively).

Although some fault dip values are more common than others, with strike-slip faults typically occurring as steep faults and reverse faults commonly having lower dips than normal faults, the full range from vertical to horizontal faults is found. If the dip angle gets less than 30° the fault is called a *low-angle fault*[4], while *steep faults* dip steeper than 60°. Low-angle reverse faults are called *thrust faults*, particularly if the movement on the fault is tens of kilometers or more.

A fault that flattens downward is called a *listric fault* (Figure 8.3). Downward-steepening faults are sometimes called antilistric. The terms ramps and flats are used about alternating steep and subhorizontal portions of the fault surface. For example, a fault that varies from steep to flat and back to steep again has a *ramp-flat-ramp geometry*.

Irregularities are particularly common in the section perpendicular to the fault slip direction. For normal and reverse faults this means curved fault traces in map view (Figure 8.4). Irregularities in this section cause no conflict during fault slippage as long as the axes of the irregularities coincide with the slip vector. Where irregularities also occur in the

3 alternatively, faults may form by reactivation of joints, which are extension fractures that can propagate into long structures by in-plane propagation; see Chapter 7

4 Some make the distinction at 45° rather than 30°.

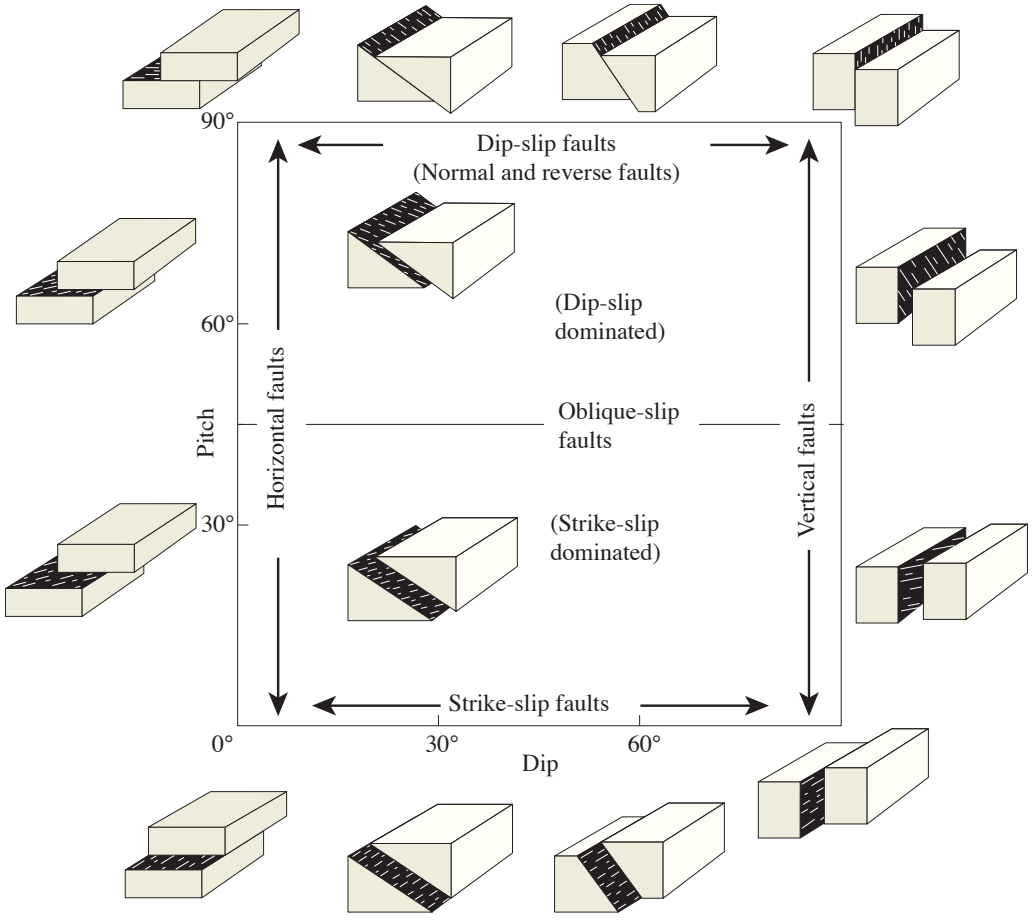

Figure 8.7 Classification of faults based on the dip of the fault plane and the pitch, which is the angle between the slip direction (displacement vector) and the strike. Based on Angelier (1994).

slip direction, the hanging wall and/or footwall must deform. For example, a listric normal fault typically creates a hanging-wall rollover (see Chapter 20).

The term *fault zone* traditionally means a series of subparallel faults or slip surfaces close enough to each other to define a zone. The width of the zone would depend on the scale of observation – it can be some centimeters or meters in the field but could be on the order of a kilometer or more when studying large-scale faults such as the San Andreas Fault. The term fault zone is now also used about the cataclastically deformed volume of rock associated with an outcrop-scale fault, comprising what is known as the inner high-strain fault core and the surrounding lower-strain damage zone.

Two separated normal faults dipping toward each other create a down-faulted block known as a *graben* (Figure 8.5). Normal faults dipping away from each other create an up-faulted block called a *horst*. The largest faults in a study area, called *master faults*, are associated with minor faults that may be antithetic or synthetic. An *antithetic fault* dips towards the master fault, while a *synthetic fault* dips against the master fault (Figure 8.5). These expressions are relative and only make sense when minor faults are related to specific larger-scale faults.

1.1.2 Displacement, slip and separation

The vector connecting two points that were connected prior to faulting indicates the local *displacement vector* or *net slip direction*[5] (Figure 8.1). Ideally, a strike-slip fault has horizontal slip direction while normal and reverse faults have slipped in the dip direction (oppositely directed displacement vectors). In practice, the total slip that we observe is the sum of the individual displacement or slip vectors. The individual slip event (earthquakes) may have had different slip

5 Displacement (vector) and slip (vector) are used synonymously in this chapter.

directions. We are therefore back to the difference between deformation *sensu stricto*, which relates the undeformed and deformed states, and deformation history. We could look for traces of the slip history by searching for such things as multiple striations. We will return to these kinds of fault surface structures in the next chapter.

A series of displacement (net slip) vectors over the slip surface gives us the total *displacement* or *slip field* on the surface. Striations, kinematic indicators (Chapter 8) and offset of layers provide the field geologist with information about direction, sense and amount of slip. Many faults show some deviation from dip-slip and strike-slip faults in the sense that the net slip vector is oblique. The degree of obliquity is given by the *pitch* (also called *rake*), which is the angle between the strike of the slip surface and the slip vector (striation), and the fault is called an oblique-slip fault (Figure 8.7).

Unless we know the net slip or displacement vector we may be fooled by the offset portrayed on an arbitrary section through the faulted volume, be it a seismic section or an outcrop (Figure 8.5a). The apparent displacement that is observed is called the (apparent) *separation*. *Horizontal separation* is the separation of layers observed across a fault on a horizontal exposure or map (Figure 8.5a), while the *dip separation* is that observed along the fault trace in a vertical section (Figure 8.5c). In a vertical section the dip separation can be decomposed into the horizontal and vertical separation. These are more commonly referred to as the *heave* (horizontal component) and *throw* (Figure 8.5c). Only a section that contains the true displacement vector shows the true displacement or total slip on the slip surface (Figure 8.5d).

A fault that affects a layered sequence will, in three dimensions, separate each surface (stratigraphic interface) so that two fault cut lines appear (Figure 8.8). If the fault is non-vertical and the displacement vector is not parallel to the layering, then a map of the faulted surface will show an open space between the two cutoff lines. The width of the open space, which will not have any contours, is related to both the fault dip and the dip separation on the fault. Further, the opening reflects the heave (horizontal separation) seen on vertical sections across the fault (Figure 8.8).

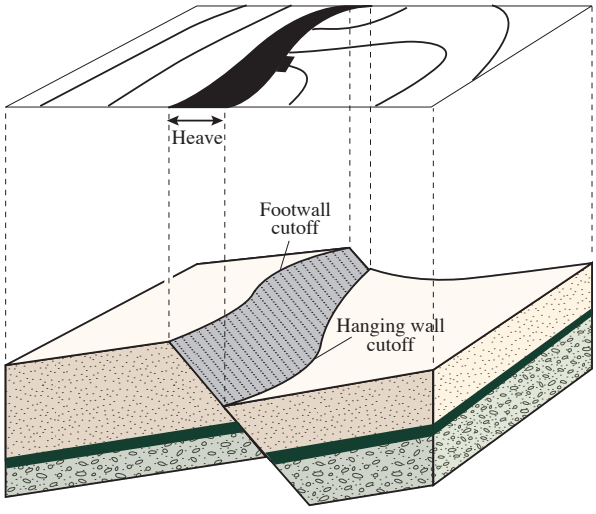

Figure 8.8 The relationship between a single fault, a mapped surface and its two cutoff-lines. Such *structure contour maps* are used extensively in the oil industry where they are mainly based on seismic reflection data.

1.1.3 Stratigraphic separation

Drilling through a fault results in either a *repeated* or *missing section* at the *fault cut* (point where the wellbore intersects the fault). For vertical wells it is simple: normal faults omit stratigraphy while reverse faults cause repeated stratigraphy in the well (Figure 8.9a). For deviated wells where the plunge of the well bore is less than the dip of the fault, repetition is seen across normal faults, as shown in Figure 8.9b. The common term for the separation seen in wells is *stratigraphic separation*. Stratigraphic separation, which is the most accurate measure of fault slip obtainable from a subsurface oil field, is equal to the fault throw only if the strata are horizontal. Most faulted strata are not horizontal, and the throw must be calculated or constructed.

1.2 Fault anatomy

Faults drawn on seismic or geologic sections are usually portrayed as single lines of even thickness. In detail, however, faults are rarely simple surfaces or zones of constant thickness. In fact, most faults are complex structures consisting of a number of structural elements that may be hard to predict[6]. Because of the

6 We are here using the term fault in the modern sense, where it includes the complexities associ-

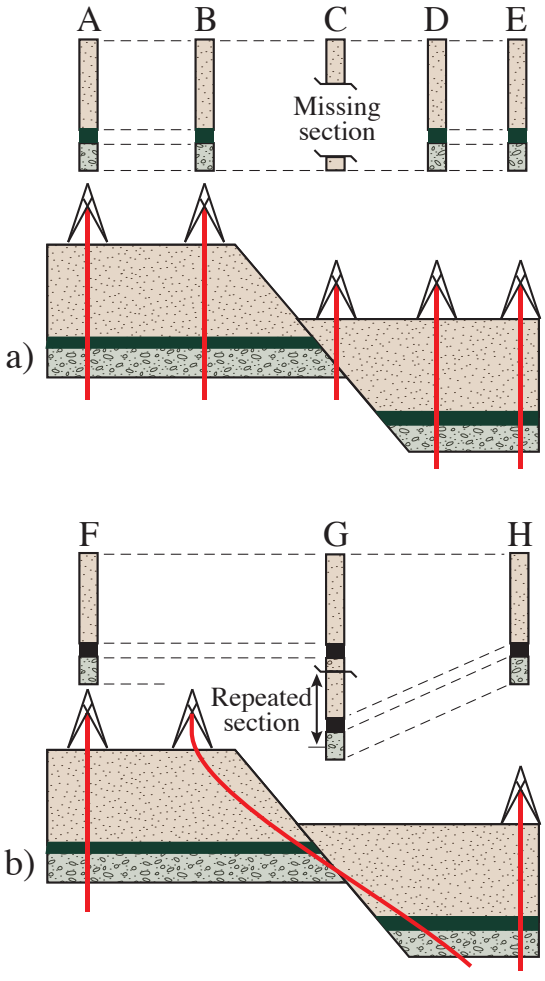

Figure 8.9 Stratigraphic separation for normal faults. a) Missing section in vertical wells always indicate normal faults (excluding stratigraphic changes). b) Repeated section, normally associated with reverse faults, is seen for normal faults if the fault is steeper than the wellbore. The opposite is the case for reverse faults (not shown).

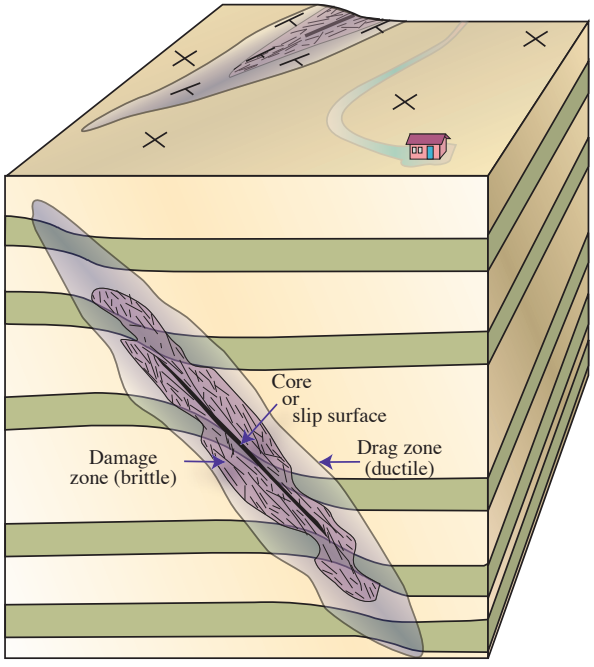

Figure 8.10 Simplified anatomy of a fault.

variations in expression along, as well as between faults, it is not easy to come up with a simple and general description of a fault. In most cases it makes sense to distinguish between the central *fault core* or slip surface and the surrounding volume of brittlely deformed wallrock known as the *fault damage zone* (Figure 8.10).

The fault core can vary from a simple slip surface or mm-thick cataclastic zone through a zone of several slip surfaces to an intensely sheared zone up to several meters wide where only remnants of the primary stratigraphic, igneous or metamorphic structures are preserved. In crystalline rocks, the fault core can consist of practically non-cohesive *gouge* where clay minerals have formed at the expense of feldspar and other primary minerals. In other cases, hard and flinty *cataclasites* constitute the fault core, particularly for faults formed in the lower part of the brittle upper crust. Various types of *breccias*, cohesive or non-cohesive, are also found in fault cores. In extreme cases friction causes crystalline rocks to melt locally and temporarily, creating a glassy fault rock known as *pseudotachylyte*.

In soft, sedimentary rocks fault cores typically consist of non-cohesive smeared-out layers. In some cases soft layers such as clay and silt may be smeared

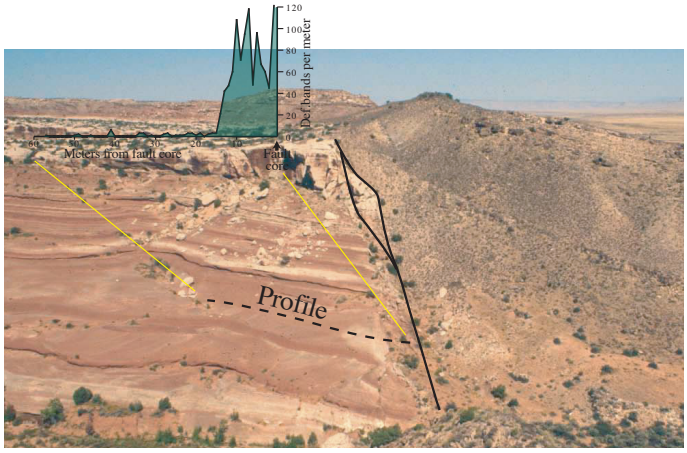

Figure 8.11 Damage zone in the footwall to a normal fault with ~200 m throw. The footwall damage zone is characterized by a fracture frequency diagram based on measurements of the number of fractures per meter. The dipping hanging-wall layers reflect a wide hanging-wall drag zone. A fault lens is seen in the upper part of the fault.

ated with fault initiation and growth.

FAULT ROCKS

When fault movements alter the original rock sufficiently it is turned into a (brittle) fault rock. There are several types of fault rocks, depending on lithology, confining pressure (depth), temperature, fluid pressure, kinematics etc. at the time of faulting. It is useful to distinguish between different types of fault rocks, and to separate them from mylonitic rocks formed in the plastic regime. Sibson (1977) suggested a classification based on his observation that brittle fault rocks are generally non-foliated, while mylonites are well foliated. He further made a distinction between cohesive and non-cohesive fault rocks. Further subclassification was done based on the relative amount of large clasts and fine-grained matrix. Sibson's classification is descriptive and works well if we add that also cataclastic fault rocks may show a foliation in some cases. Its relationship to mechanism is also clear, since mylonites, which result from plastic deformation mechanisms, are clearly separated from cataclastic rocks in the lower part of the diagram.

Fault breccia is an unconsolidated fault rock consisting of less than 30% matrix. If the matrix-fragment ratio gets higher, the rock is called a *fault gouge*. A fault gouge is thus a strongly ground down version of the original rock, but the term is sometimes also used about strongly reworked clay or shale in the core of faults in sedimentary sequences. These unconsolidated fault rocks form in the upper part of the brittle crust. They are conduits of fluid flow in non-porous rocks, but contribute to fault sealing in faulted porous rocks.

Pseudotachylyte consists of dark glass or microcrystalline, dense material. It forms by localized melting of the wall rock during frictional sliding. Pseudotachylyte can show injection veins into the sidewall, chilled margins, may contain inclusions of the host rock and may show glass structures. It typically occurs as mm-to cm-wide zones that make sharp boundaries to the host rock. Pseudotachylytes form in the upper part of the crust, but can form at large crustal depths in dry parts of the lower crust.

Crush breccias are characterized by their large fragments. They all have less than 10% matrix and are cohesive and hard rocks. The fragments are glued together by cement (typically quartz or calcite) and/or by microfragments of mineral that have been crushed during faulting.

Cataclasites are distinguished from crush breccias by their lower fragment-matrix ratio. The matrix consists of crushed and ground down microfragments that form a cohesive and often flinty rock. It takes a certain temperature for the matrix to end up as a flinty medium and most cataclasites are thought to form at 5 km depth or more.

Mylonites are not strictly fault rocks (although they were in Sibson's original classification), and are subdivided based on the amount of large, original grains and recrystallized matrix. Mylonites are well foliated and commonly also lineated and show abundant evidence of plastic deformation mechanisms rather than frictional sliding and grain crushing. They form at greater depths than cataclasites and other fault rocks; above 300 °C for quartz-rich rocks. The end member of the mylonite series, blastomylonite, is a mylonite that has recrystallized after the deformation has ceased (postkinematic recrystallization). It therefore shows equant and strain-free grains of approximately equal size under the microscope, with the mylonitic foliation still preserved in hand samples. Plastic deformation and mylonites are treated further in Chapters 10 and 15.

Pseudotachylyte with injection vein formed in granitic gneiss near Bergen, Norway.

		Non-foliated	Foliated	
Incohesive		Fault breccia (>30% visible fragments)		
		Fault gouge (<30% visible fragments)	Foliated gouge	
Cohesive		Pseudotachylyte		
		Crush breccia (fragments > 5 mm) Fine crush breccia (fragments 1-5 mm) Crush microbreccia (fragments < 1 mm)		<10%
	Cataclasites (Grain size reduction by cataclastic mechanisms)	Protocataclasite	Mylonite series (Grain size reduction by plastic def. mechanisms): Protomylonite	10-50%
		Cataclasite	Mylonite	50-90%
		Ultracataclasite	Ultramylonite	>90%
			Grain size increase by recrystalliz.: Blastomylonite	

% Matrix

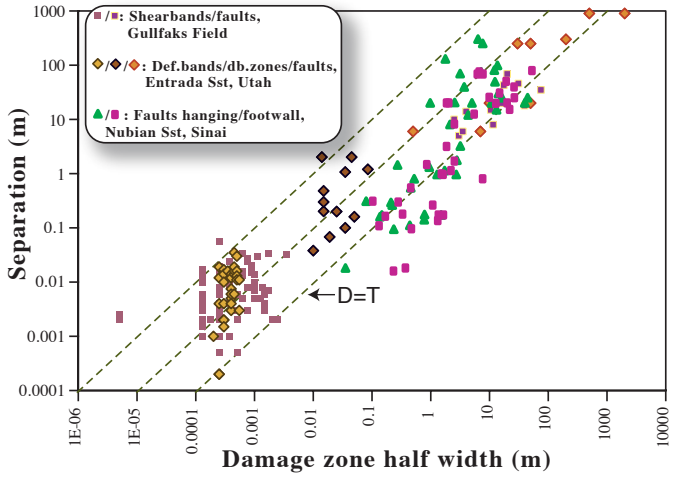

Figure 8.12 Damage zone thickness (T) plotted against separation (D) for faults in porous sandstones. Note logarithmic axes. Sinai data from Beach et al. (2000).

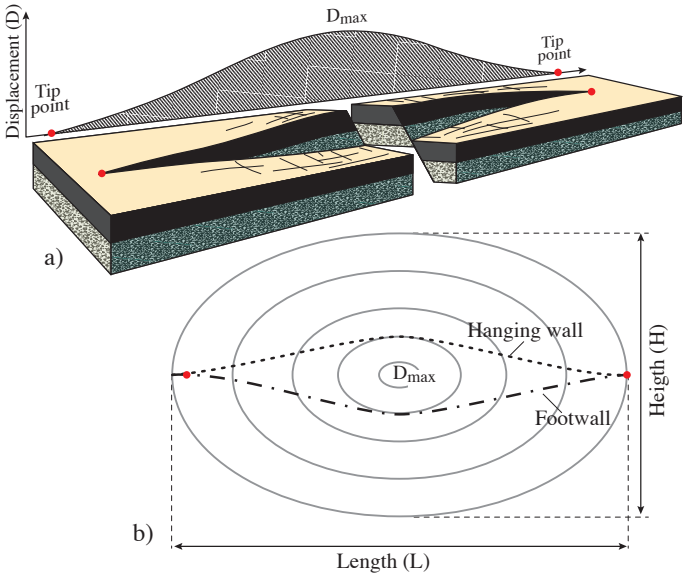

Figure 8.13 a) Schematic illustration of an ideal, isolated fault. The displacement profile indicates maximum displacement near the center. b) The fault plane with displacement countours. Stipled lines are the hanging wall and footwall cutoff lines and the distance between them indicates the dip separation (displacement if the movement is dip-slip).

out to a continuous membrane which, if continuous in three dimensions, may greatly reduce the ability for fluids to cross the fault. In general, the thickness of the fault core shows a positive increase with fault throw, although variations are great even along a single fault within the same lithology.

The damage zone is characterized by a density of brittle deformation structures that is higher than the background level. It envelops the fault core, which means that it is found in the tip zone as well as on each side of the core (Figure 8.11). Structures that are found in the damage zone include various deformation bands, shear fractures, tension fractures and stylolites.

The width of the damage zone can vary from layer to layer, but similar to the fault core there is a positive correlation between fault size (throw) and damage zone thickness. Figure 8.12 shows that the variation for a given fault throw is around two orders of magnitude (i.e., a factor of 100), which means that predicting fault size from damage zone thickness or vice versa is not going to yield a very accurate estimate.

Layers are commonly deflected (folded) around faults, particularly in faulted sedimentary rocks. The classical term for this behavior is *drag*, which is used here as a purely descriptive or geometric term. The drag zone can be wider or narrower than the damage zone, and can be completely absent. The distinction between the damage zone and the drag zone is that drag is an expression of continuous or ductile fault-related strain, while the damage zone is by definition restricted to brittle deformation. They are both part of the total strain zone associated with faults. In general, soft rocks develop more drag than stiff rocks.

1.3 Displacement distribution

It is sometimes possible to map displacement variations along a fault in the field in the horizontal or vertical direction. In both cases most faults show a maximum displacement in the central part of the fault trace, gradually decreasing towards the tips (Figure 8.13). The shape of the displacement profile may vary from linear to bell-shaped or elliptic. Displacement profiles are sometimes classified into those that have a well-defined central maximum (Peak-type) and those that have a wide, central part of fairly constant displacement (plateau-type). Examples are shown in Figure 8.14.

It may be hard to collect enough displacement data from a single fault to obtain a good picture of the displacement distribution on the fault surface. However, British coalmine data and high-quality seismic data have made it possible to contour

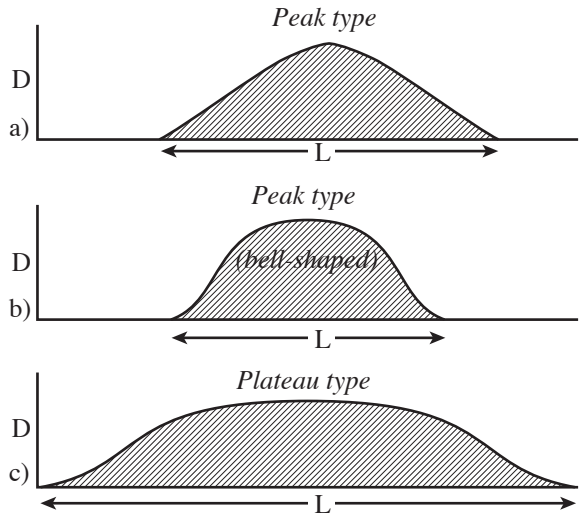

Figure 8.14 Types of displacement (D) profiles along faults.

displacement on a number of faults. The results show that the displacement is generally greatest in the central part of single, isolated faults, gradually decreasing towards the tip line – a conclusion that is consistent with the field observations mentioned in the previous paragraph. These observations also support the idealized model where an isolated fault has an elliptic tip line and elliptical displacement contours (Figure 8.15 and 8.16). The elliptical model can also be applied to extensional fractures, where the displacement vectors are perpendicular to the fracture. It should be emphasized that this simple elliptical model is meant to describe an isolated fault in an isotropic medium. In most cases faults interact and occur in layered sequences, which complicates this simple model.

1.4 Identifying faults in an oil field setting

It is in many cases crucial to correctly identify and collect information about faults in petroleum exploration and production. We will here consider different sources of data that give information about faults in an oil field in an extensional setting, but the same principles can be applied to contractional and strike-slip regimes.

1.4.1 Seismic data

Interpretation of seismic data is the most common

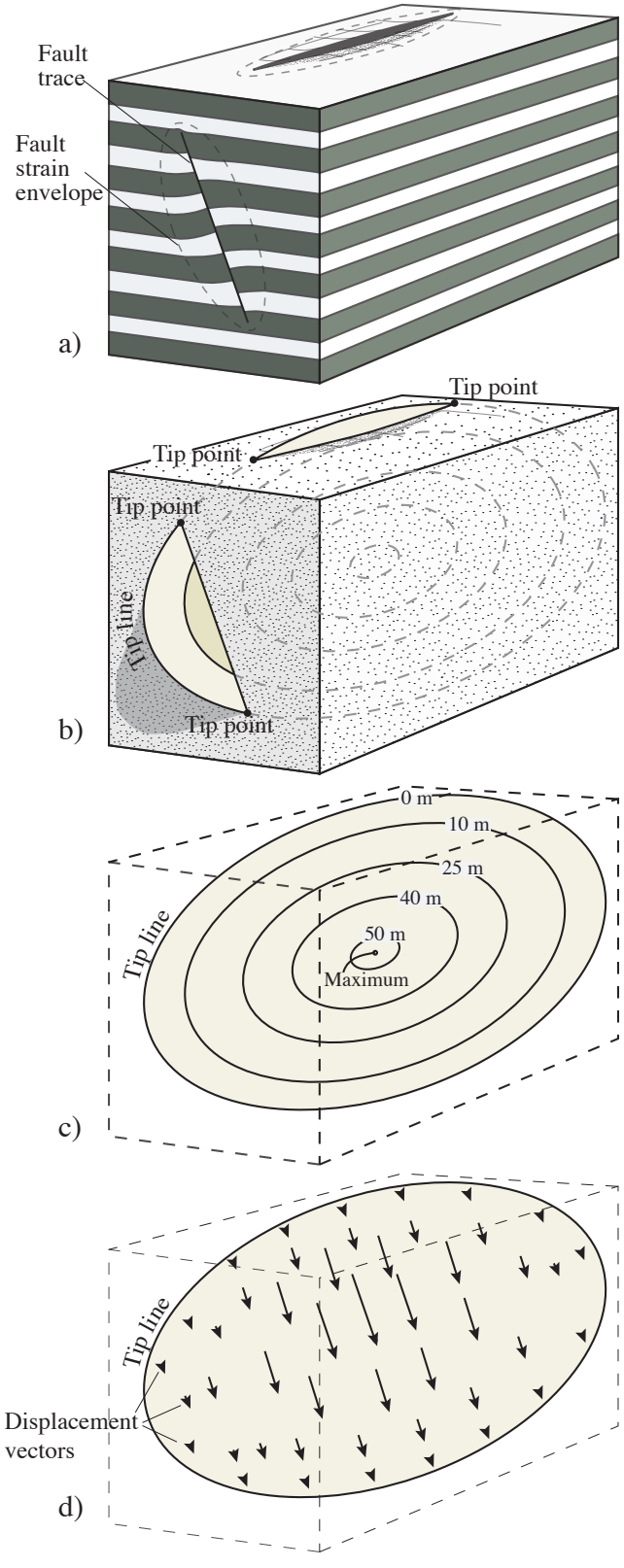

Figure 8.15 Geometric aspects of an isolated fault. The fault trace is the intersection between the fault surface and an arbitrary surface (outcrop, seismic line) (a). The end points of the fault trace are called tip points (b). They lie on the tip line, which is the zero-displacement line that outlines the fault (c). Displacement increases towards the center of the fault. This can be expressed in terms of displacement contours (c) or displacement vectors (d).

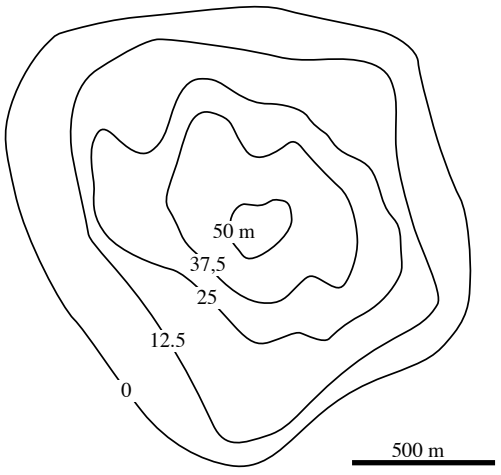

Figure 8.16 Displacement countours for a fault interpreted from high-resolution seismic data from the Gulf of Mexico. Modified from Childs et al. (2003).

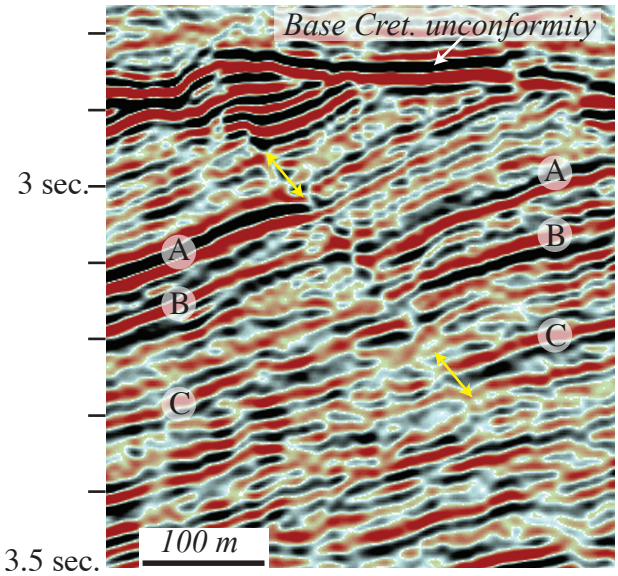

Figure 8.17 A fault imaged on seismic data (arrows). The dip separation is identified by the discontinuity of reflectors. 3D seismic from the Visund Field, North Sea.

way of identifying and mapping faults in the subsurface. Identification of faults depends on the presence of mappable seismic reflectors. Discontinuous reflectors indicate fault locations, and the dip separation is estimated by correlation of seismic reflectors across the fault (Figure 8.17).

Seismic data has a limit in resolution that varies from dataset to dataset, but it is usually difficult or impossible to identify faults with throw less than 15-20 meters even on high-quality 3D seismic data sets. Complications along faults, such as fault lenses and fault branching, may be difficult to resolve on seismic data alone. Where available, well information is used to constrain the seismic interpretation.

3D data represent a cube of data (Figure 8.18) where faults and reflectors can be interpreted in any direction, including on horizontal sections (time slices). This gives a unique possibility to interpret the three-dimensional geometry of faults and fault populations.

Basin-scale faults and fault arrays are more readily identified on regional 2D lines. Some 2D lines are deep-seismic lines which image the deep parts of the crust and the upper mantle (Figure 1.6).

1.4.2 Fault cut and well log correlation

Faults along the wellbore are typically identified by means of stratigraphic correlation. As shown in Figure 8.9, reverse and normal faults cause repetition and omission of stratigraphic section, respectively. Knowledge of the stratigraphy from other wells in the area forms the basis for this type of fault identification. The size of the faults identifiable by this method depends on the characteristic stratigraphic markers, the number of and distance to other wells in the area, sedimentary facies variations and the orientation of the well. The identification of the *fault cut* (fault location in the wellbore) also depends on characteristic signatures on the well logs. Cores are generally not available, and standard logs such as gamma ray logs, density logs, neutron logs and resistivity logs are used for stratigraphic well correlations. Faults with stratigraphic separation down to 5 meters are detectable in the Brent Group of the North Sea where the density of wells is high (Figure 8.19).

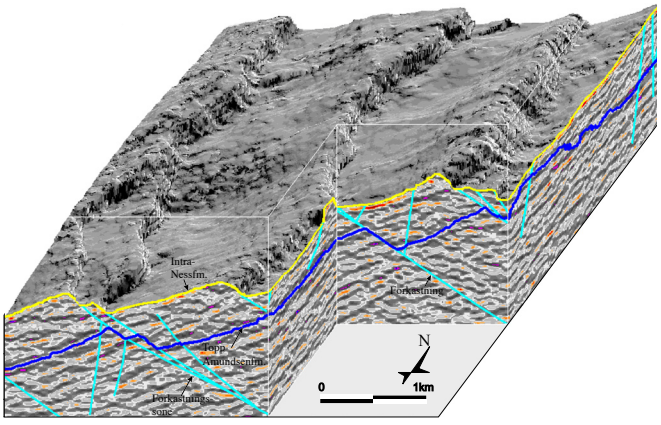

Figure 8.18 Faults as they may appear in a seismic data cube. Data from the Gullfaks Field. From Hesthammer & Fossen (1997).

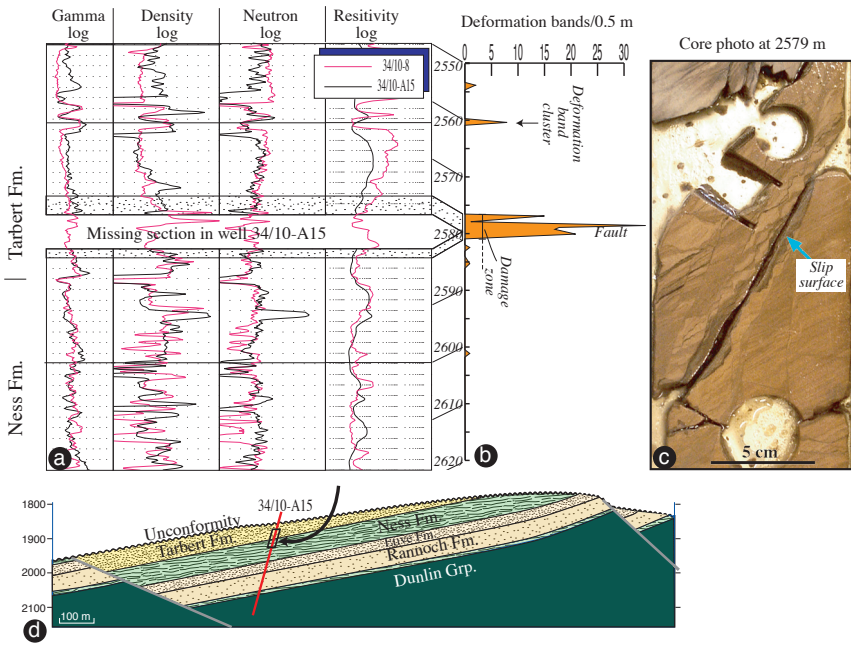

Figure 8.19 Fault separation detected by log correlation with a neighboring well. The complete log in well 8 is shown in red, and the correlation gives a missing section of ~6 m in well A15. The damage zone (orange) was estimated from core inspection to be a few meters wide. Based on Fossen & Hestshammer (2000).

1.4.3 Dipmeter data and borehole images

Microresitivity is measured continuously along the wellbore by the three or more (usually 16) electrodes of a dipmeter tool. The responses from the different electrodes are correlated around the borehole in narrow depth intervals to fit a plane. The planes are generally bedding or lamination, but may also represent deformation bands or fractures.

Orientations (usually given by dip and dip azimuth) are plotted in dipmeter diagrams. For structural analysis, separating dip azimuth and dip into individual plots and compressing the vertical scale can be advantageous, as shown in Figure 8.20. Faults can then be identified in at least three different ways. The first is to look for sudden changes in dip or dip azimuth. These occur where a fault separates two blocks in which the layering is differently oriented – a fairly common situation across many faults. An example is seen between the 17 and 31 m faults in Figure 8.20.

Another characteristic feature is the presence of local intervals with rapid but progressive changes in dip and/or dip azimuth. Such anomalies are known as cusps (Figure 8.21). Cusp-shaped dip patterns indicate fault-related drag in many cases. Stratigraphic log correlation indicates 9 m missing section in the example shown in Figure 8.21.

The third characteristic is the appearance of anomalous orientations that may stem from fractures or deformation bands in the damage zone or from the main slip surface itself. The high dip values at the locations of the faults in Figure 8.20 may be examples of this.

It is now common to create a (almost) continuous microresistivity image of the borehole based on the resistivity data from more sophisticated

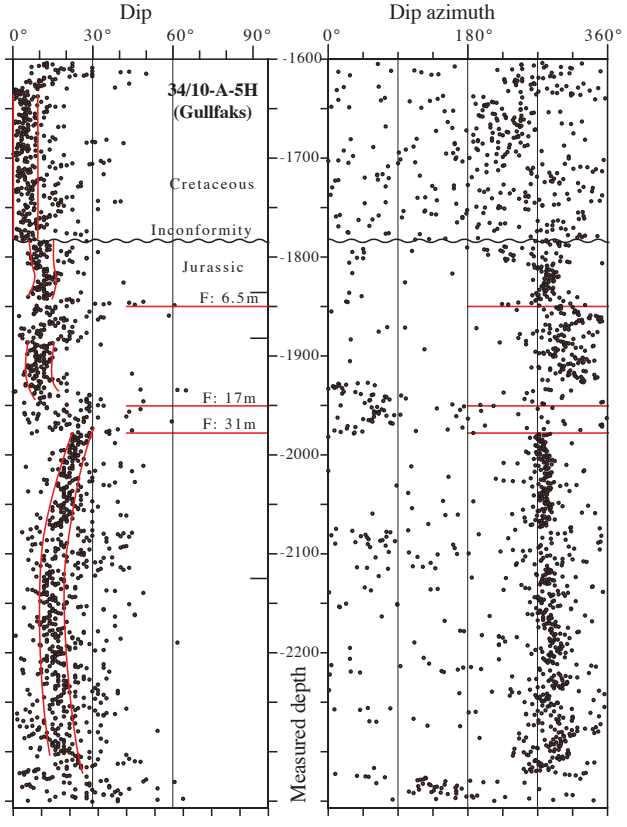

Figure 8.20 Dipmeter data from the Gullfaks Field, where dip and dip azimuth (dip direction) are plotted against the depth measured along the wellbore. Faults identified by stratigraphic correlation (missing section) are indicated. Based on data in Hesthammer (1999).

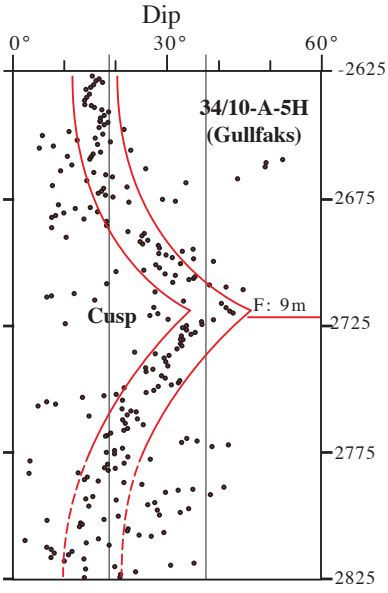

Figure 8.21 Dipmeter data (dip against depth) showing a classical cusp geometry related to drag around a minor fault. Data from the Gullfaks Field (well 34/10-C-3).

tools, such as FMI ("Formation MicroImager"). This tool measures microresistivity by means of a few hundred electrodes. The result is a continuous image of the wall that is reminiscent of an actual picture of the rock. Such images are analyzed at workstations where bedding and structural features are interpreted.

1.4.4 Core information

Only a small percentage of the drilled section in a reservoir will be cored, and one may find that only exceptionally are faults and fractures present in the core material. The main reason is that brittle tectonic deformation is scarce away from faults, and drillers are reluctant to cut cores across faults because of the risk of jamming and potential pressure problems. Furthermore, some cored fault rocks may be so non-cohesive that they fall apart to form what is known as *rubble zones*. However, successfully cored faults and damage zones represent valuable information. Such samples allow for microscopic studies and permeability measurements. Furthermore, the width and nature of the damage zone, and sometimes even the fault core, can be estimated. Figure 8.22 shows an example of a core through a fault with 6 m missing section. The central slip surface (very thin core) and shear fractures in the damage zone are visible.

The orientation of faults and fractures in cores can be measured if the core is oriented. Usually it is not, and its orientation must be reconstructed based on knowledge of bedding orientation from dipmeter data or seismic data. Cores are usually split in the direction of maximum dip, and this direction is found from dipmeter or seismic data. The method thus works for dipping layers only and is not very accurate.

1.5 The birth and growth of faults

1.5.1 Fault formation in non- and low-porous rocks

Faults in rocks with low or no porosity may grow from shear fractures, which according to the Griffith theory form from microfractures or so-called Griffith-fractures. According to Griffith's model the microfractures can expand in their own planes. However, more recent research has shown that shear fractures cannot expand in their own planes, meaning that they have to change orientation with respect to the principal stresses in order to grow. Hence, they curve and form wing cracks or related cracks across which there is tension (p.). Experiments show that a phase of intense microfracturing occurs prior to fracture initiation or propagation. Once the density of microfractures reaches a critical level, the main fracture expands by linkage of favorably oriented microfractures. The zone of microfractures (and mesofractures) ahead of the fracture tip zone is called the *frictional breakdown zone* or the *process zone*.

To make a fault, a number of small shear fractures, tension fractures and hybrid fractures must form and connect. The incipient fault surface is irregular, which leads to grinding and microfracturing of the walls. A thin core of brecciated or crushed rock typically forms.

Figure 8.22 1 m long core section across a minor (6 m missing section) fault in the Gullfaks Field. Holes are from plugs sampled for permeability analysis.

During fault growth, new fractures form in the walls next the fault core. Hence, most faults have a well-defined *core* of intense cataclastic deformation and a surrounding *damage zone* of less intense fracturing.

Natural rocks are not isotropic, and in many cases faults form along preexisting mesoscopic weaknesses in the rock. Such weaknesses can be layer interfaces or dikes, but the structures that are most likely to be activated as faults are joints (and, of course, preexisting faults). This is so because joints tend to be very weak and almost planar structures with low or no cohesion and with even (low friction) surfaces. Joints may also form surfaces many tens of meters or more in length and/or height, because as extension structures they have had the freedom to expand in their own plane. Faults formed by faulting of joints inherit some of the features of the original joints. If it forms by frictional sliding on a single, extensive joint, the initial fault tends to be a sharp slip surface with almost no fault core and with (almost) no damage zone. If slip accumulates, however, the fault outgrows the joint and links with other joints in the vicinity of its tip zone. The damage zone then thickens, and the fault core may grow.

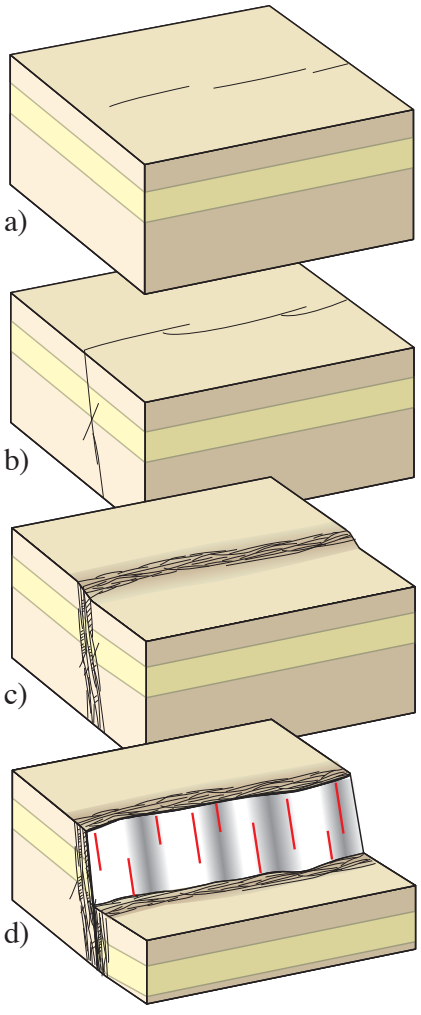

Figure 8.23 The general model for fault formation in porous sandstone. a) Individial deformation bands, b) linking of bands, b) the formation of a deformation band zone, and c) faulting of the zone.

1.5.2 Fault formation in porous rocks

In highly porous rocks and sediments, fault growth follows a somewhat different path. The difference has to do with the presence of pore space, which gives the grains a unique opportunity to reorganize. If the grains in a sandstone are weakly cemented together, then the grains will reorganize by rotation and frictional grain boundary sliding (translation) during deformation. In other cases grains can also break internally. In either way, the deformation is likely to localize into narrow zones or bands to form structures are known as *deformation bands*. Different types of deformation bands are discussed in the previous chapter (Section 7.5).

Field observations, as well as experimental and numerical work, show that deformation proceeds by sequential formation of new deformation bands adjacent to the initial one (Figure 8.23). This means that at some point it is easier to form a new band next to the existing one than to keep shearing the primary band. The result is a *deformation band zone*, and this development is commonly explained in terms of strain hardening. Strain hardening is thought to be related to the loss of porosity in the band and is most pronounced where grains are crushed (cataclastic bands). Note the difference between process zones in non-porous and highly porous rocks: The process zone in non-porous rocks *weakens* the host rock and increases porosity by the formation of cracks. In high-porosity rocks the deformation bands in the process zone in many cases *harden* the rock and reduce porosity.

Once a certain number of deformation bands have accumulated in the deformation band zone, porosity is greatly reduced, and a slip surface can grow. Slip surfaces nucleate in small patches that propagate, link up, and ultimately form through-going slip surfaces. Slip surfaces are mechanically weak structures and accumulate meters of slip or more. Mature, through-going slip surfaces are commonly associated with a thin (mm-thick) zone

of ultracataclasite, which may be considered as the local fault core. The surrounding population of deformation bands represents the fault damage zone.

1.5.3 The damage zone

The growth of deformation bands and/or ordinary fractures prior to the formation of a through-going slip surface has implications for our understanding of the damage zone. The moment the slip surface (fault) forms, the enclosing zone of already existing structures will become the damage zone. Once the fault is established, the process zone in front of the fault tip also forms part of the damage zone, moving ahead of the fault tip as the fault expands (Figure 8.24). In a porous rock, this zone is likely to consist of deformation bands. Because of the way that faults form in porous rocks by faulting of a deformation band zone (Figure 8.23), the length of the deformation band process zone tends to be longer than the process zone seen in many non-porous rocks. This is particularly true if the deformation bands are cataclastic, in which case the process zone can be several hundred meters long.

If the structures of the damage zone form ahead of a propagating fault tip, then the damage zone should be built up of fractures and deformation bands that formed in the process zone, i.e. structures that are slightly older than the local slip surface. A consequence of this assumption would be that the width and strain of a damage zone is independent of fault displacement. Empirical data (Figure 8.12) shows that this is not the case, even though the fault (slip surface) represents the weakest part of the rock,

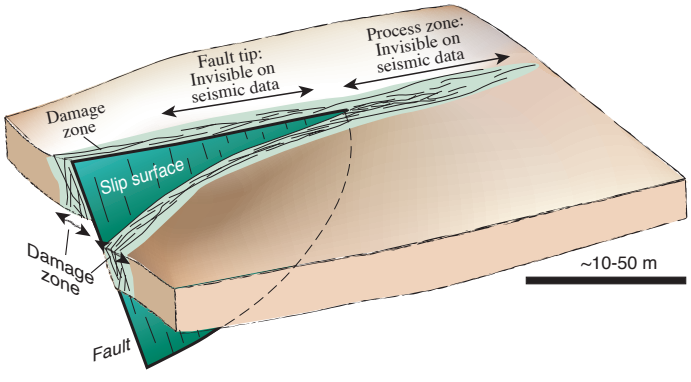

Figure 8.24 A fault is contained within a damage zone, which means that there is a (process) zone ahead of the tip where the rock is "processed" prior to fault propagation. The process zone may potentially contribute to compartmentalization of petroleum reservoirs.

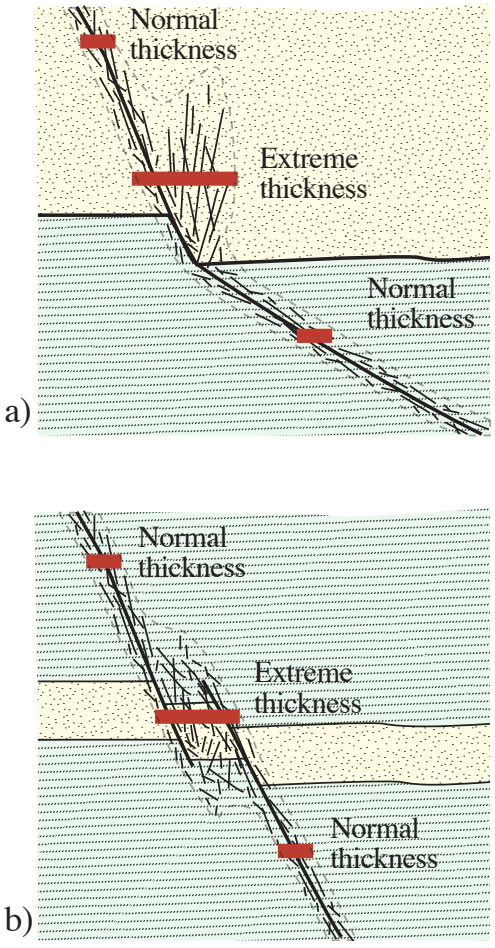

Figure 8.25 Variations in the thickness of damage zones related to a) change in dip and b) linkage. In these situations, minor structures are added to the damage zone until the fault cuts through the complex zone along a straighter path.

and should be reactivated without the creation of more side-wall damage. The answer is simply that faults are not perfectly planar structures, nor do they expand within a perfect plane. Faults are irregular at many scales because the rocks that they grow in are both heterogeneous and anisotropic. Faults may bend as they meet a different lithologic layer or as they link with other faults (Figure 8.25).

The structures in the damage zone form prior to, during and after the local formation of the slip surface (fault).

If the fault is temporarily or locally planar and smooth, then there may be periods during which displacement accumulate without any deformation of the wall rocks, i.e. without any widening of the damage zone. Then there may be times or places where fault linkage occurs or places where fault

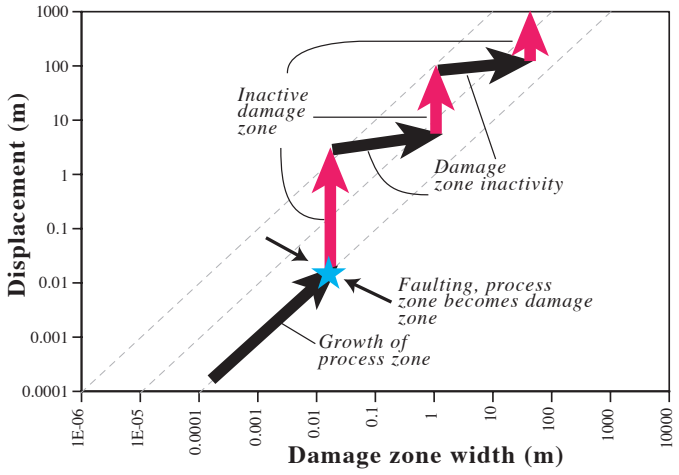

Figure 8.26 Schematic illustration of how a damage zone can grow periodically. The first stage is the growth of the process zone. Once the fault forms, the process zone becomes the damage zone and slip occurs smoothly for a while (red arrow) until complications lock the fault and causes renewed growth of the damage zone (3). This repeats itself as the fault grows. The result is considerable scatter of fault data in fault displacement-damage zone width diagrams.

bends or lenses cause rapid growth in damage zone width. Eventually, complications such as bends and links are cut through so that the fault recovers to a more planar structure. Thus, the growth of damage zones may to some extent be temporal and local (Figure 8.26), which contributes to the scatter seen in Figure 8.12.

1.5.4 The ductile drag zone

Drag is best defined as any systematic change in the orientation of layers or markers around a fault. It must also be genetically related to the evolution of the fault. In practice this means that the anomalous orientation of the layers must be confined to the near vicinity of the fault. How big this volume can be is less clear. If one includes such structures as rollovers, also called reverse drag structures, they may be up to several kilometers long on the hanging-wall side (considerably less on the footwall side) for large listric faults. More commonly, the term drag is used about zones some meters or tens of meters wide.

Figure 8.27 Drag of layers of siltstone and sandstone along vertical fault located along the left margin of the picture. Colorado National Monument, USA.

Drag is permanent continuous deformation of layers around a fault by means of brittle deformation mechanisms, directly related to the formation and/or growth of the fault.

Drag is seen in layers that are soft enough to deform ductilely in the upper, brittle part of the crust. It is therefore most commonly seen in faulted sedimentary sequences (Figure 8.27). Furthermore, drag can form in any tectonic regime. The kinematic requirement is that the angle between the slip vector of the fault and the layering is not too small. Because layering tends to be subhorizontal in sedimentary rocks, drag is most commonly associated with normal and reverse faults and less commonly developed along strike-slip faults. Folds also develop in subhorizontal layers along strike-slip faults (see Figure 18.11), but these are not drag folds. Thus, we may want to add another characteristic of drag folds: their fold axes must make a high angle to the displacement vector of the fault.

There are two geometrically different types of

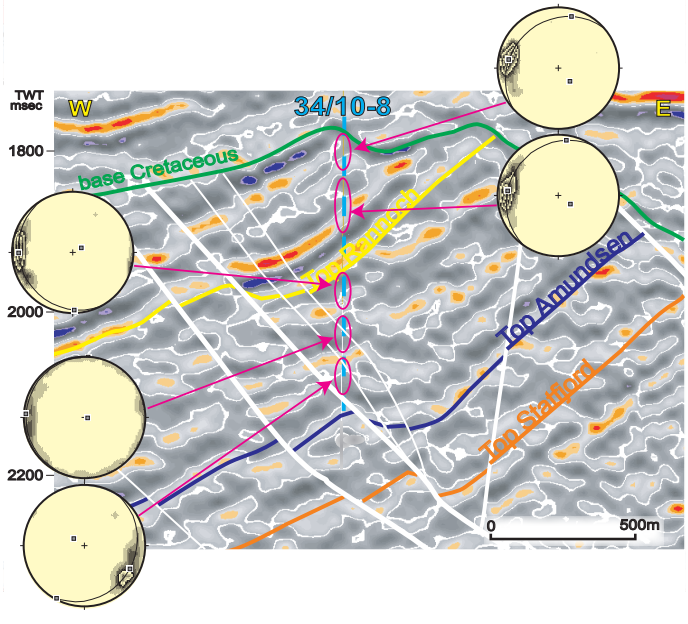

Figure 8.28 Dipmeter data collected along a vertical North Sea well. Stereonets show dip azimuth of layering in selected intervals. A change from left- to right-dipping layers is consistent with the normal drag portrayed by the seismic reflectors. Also note that the drag zone widens upward, consistent with the trishear model.

SUBSEISMIC FAULTS

Ductile or brittle? As mentioned before, these terms depend on the scale of observation. Consider the large-scale drag in the hanging wall of large normal faults. When imaged on a seismic sections (or from a far distance), the layers may appear continuous and the deformation can be described as being ductile. There could still be lots of subseismic faults, because what appears to be continuous layers may be signals that are smeared out to continuous reflectors during the data processing. Two different cases are shown. In one case a series of antithetic subseismic faults affect the layers, in the other the faults are synthetic with respect to the main faults. Since the faults are too small to be imaged seismically, the two seismic images are identical. But the true dip is different in the two cases. Core data and perhaps dipmeter data will give the true dip. If the difference between dip determined from cores or dipmeter data is significant, then it is likely that subseismic faults occur. If the dip determined from cores is the same as the seismic dip, then the deformation is microscopic, perhaps by granular flow (typical for sediments that were poorly lithified at the time of deformation).

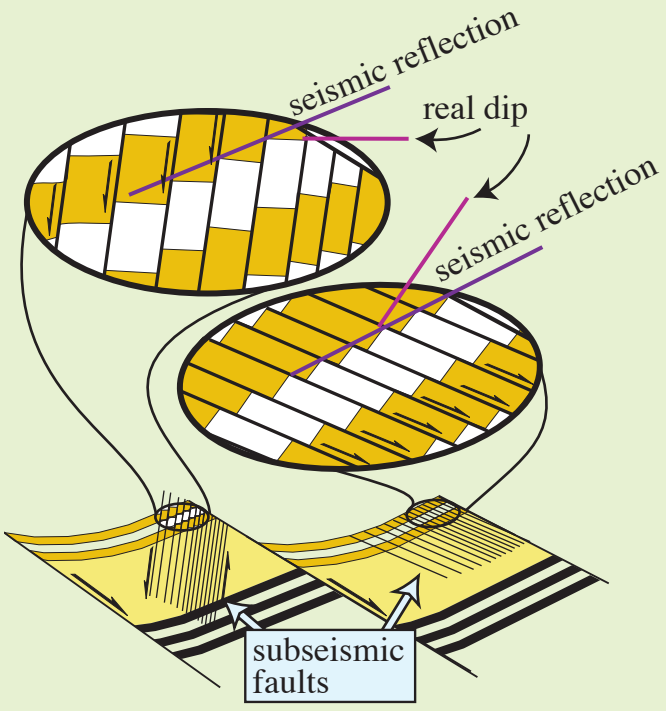

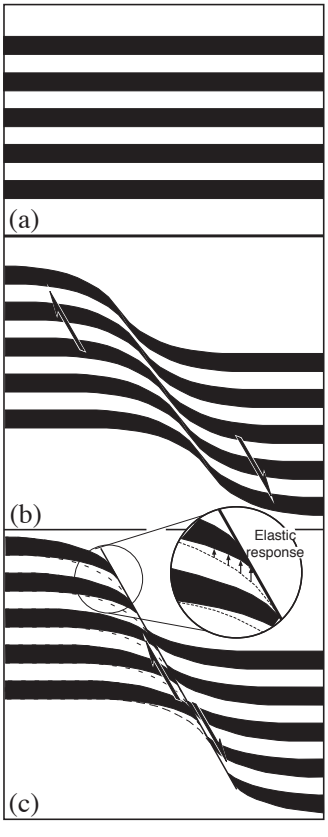

Figure 8.29 Simple shear model for normal drag development. The width of the drag zone is constant along the fault.

drag: normal drag and reverse drag. *Normal drag* is the shear zone-like geometry where layers flex towards parallelism with the fault (Figure 8.28). Normal drag involves displacement, so that the total offset is the sum of the ductile normal drag and the discrete fault displacement. *Reverse drag* is used about the opposite case, where layers that are concave in the slip direction. The fold defined by a roll-over structure on the hanging-wall side of listric normal faults is reverse drag. Both normal and reverse drag occur along faults, depending on the local fault geometry.

It was originally thought that drag was the result of friction along the fault during fault growth. The idea then changed to that of flexuring of the layers prior to fault formation. The latter model seems to fit many examples of drag. This model is in many ways similar to that of damage zone development: in both cases layers are deformed in the wake of the fault tip. The difference is that the folding is ductile down to the scale of a hand sample, meaning that it does not involve mesoscopic fracturing or deformation band formation. That is at least true in the early stages. As the folds tighten and strain accumulates, fractures and deformation bands also form, and the damage zone is established. However, the structures in the damage zone are small enough to be neglected as we consider the overall geometry of the drag fold zone[7].

The geometry of a drag fold contains information about how it formed. A drag fold in

7 Note that the damage zone is the zone of fractures (including deformation bands) around the fault, and is not directly related to the ductile drag zone.

TRISHEAR

The trishear method, first published by Eric Erslev around 1991, models the ductile deformation in a triangular area in front of a propagating fault tip. The hanging wall side of the triangle moves with a constant velocity above a fixed footwall and the apical angle of the triangle is chosen. The triangle is symmetric with respect to the fault and the velocity vector is identical for all points located

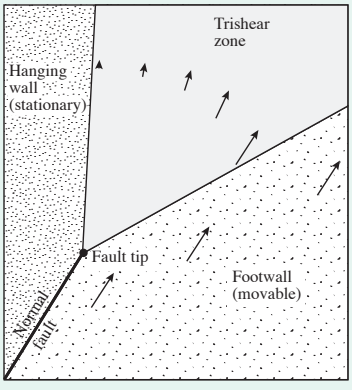

along any ray originating at the fault tip. Across the zone the velocity increases towards the hanging wall, Also, the direction of the velocity vector changes gradually towards parallelism with the hanging wall, as shown in the figure. We choose the apical angle of the trishear zone, the fault dip and amount of slip, and the ratio of propagation to slip (P/S ratio). P/S=0 means that we fix the triangular zone to the footwall. P/S=1 means fixing the zone to the hanging wall. In most cases it is more realistic with P/S>1. Trial and error will give the geometry that most closely matches your field observations or seismically imaged structure. With a trishear program we can model the ductile deformation in front of a propagating fault tip and the resulting drag along the fault in a surprisingly realistic manner.

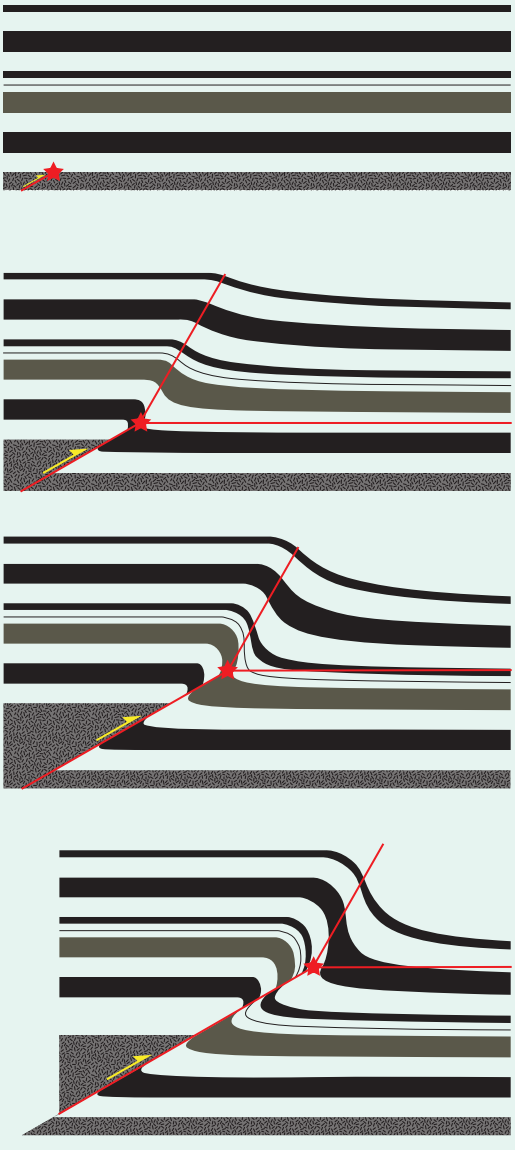

Trishear model of a reverse fault affecting an overlying sedimentary sequence. P/S=1.5. Star indicates the fault tip at each stage.

which the layers have the same geometry along the fault (constant width of drag zone) can conveniently be modeled by simple shear. In fact, the structure is a simple shear zone (Chapter 15) with a fault discontinuity in its central part (Figure 8.29).

In many other cases the drag zone is upward-widening, and a different kinematic model must be applied. A popular model is called *trishear*. In this model strain is distributed in a triangular or fan-shaped zone of active deformation ahead of the fault tip (Figure 8.30). This zone moves through the rock as the fault propagates, and no further folding occurs once the fault has cut through the layers. The width of the triangular deformation zone varies from case to case, but in all cases the drag zone widens upsection. This method seems to work particularly well in places of reactivated basement faults that grow into overlying sedimentary strata. Many examples of such structures are found in the uplifts on the Colorado Plateau and in the Rocky Mountains foreland in Wyoming and Colorado, where the fold structures are commonly referred to as *forced folds*.

Folds that form ahead of a propagating fault tip are called *fault propagation folds*. Thus, many drag folds are *faulted fault propagation folds*. However, drag can also form or become accentuated in the

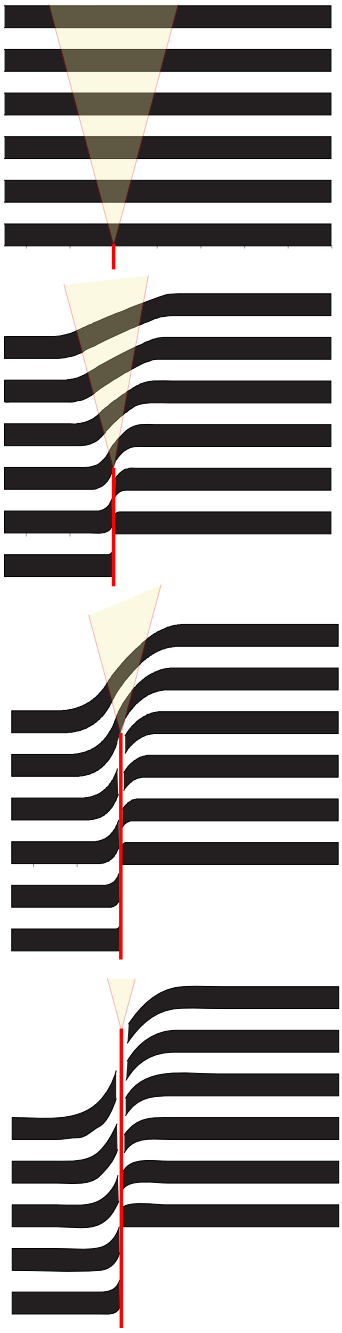

Figure 8.30 Trishear modeling of normal drag development. In this model the drag zone widens upwards.

walls of an already existing fault. Just like the damage zone, fault drag can develop due to locking of the fault at fault bends, vertical fault links and other complications that can increase the friction along faults. The effect of non-planar fault geometry is discussed in the last chapter of this book and the development of normal drag between two overlapping fault segments is illustrated in Figure 8.31. The latter mechanism can take drag to the point where the rotated layer, which typically is a clay or shale, forms a membrane or smear along the fault.

Drag can form both ahead of the fault tip and in the walls of an active fault.

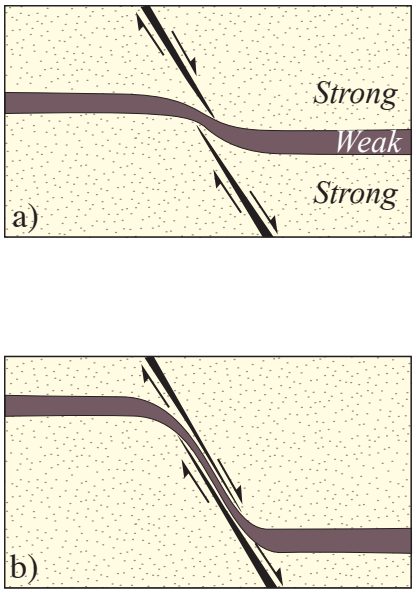

Figure 8.31 Normal dragging of mechanically weak layer (e.g. clay) between two overlapping fault segments.

1.5.5 Drag, deformation mechanisms and the damage zone

Drag can occur by granular flow, particularly in poorly lithified sediments. Granular flow leaves little or no trace of the deformation except for the rotation of layering or modification of sedimentary structures. In consolidated sedimentary rocks grains may start to fracture, and the mechanisms becomes distributed cataclastic flow. The mechanisms are the same that operate in the different deformation bands discussed in the previous chapter, but the deformation during drag folding is less localized and strain is considerably lower. There is however a strain gradient towards the fault, as shown in Figure 8.32.

Fractures or deformation bands typically occur in drag zones. In such cases the density of fractures or deformation bands increases toward the fault, as shown in Figure 8.33. The appearance of mesoscopically mapable fractures or deformation bands indicates that we are in the damage zone. Where drag folds are well developed the drag zone tends to be wider than the damage zone, although the opposite situation also occurs.

Some faults, particularly in metamorphic rocks, show drag-like folding of the layering similar to that shown in Figure 8.29. A closer examination of many

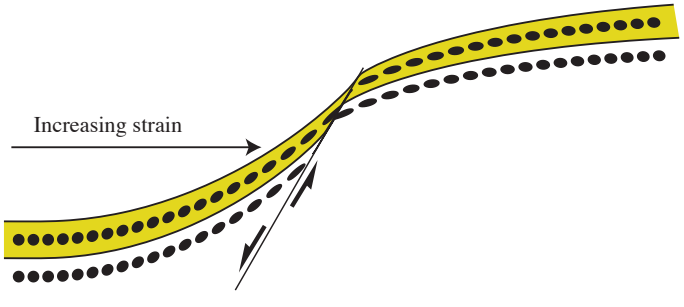

Figure 8.32 Strain ellipses portraying the relation between layer orientation and strain. Generated by means of the trishear program FaultFold (R. Almendinger 2003).

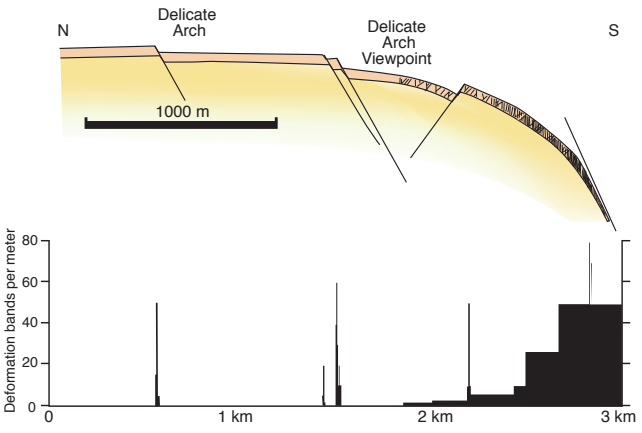

Figure 8.33 Folding of layers adjacent to a fault is an expression of off-fault strain. Where the folded layers were originally horizontal, a direct relationship can be etablised between their dip and strain. The strain can be accommodated by granular flow, deformation bands, tension fractures, and/or small faults. The graph indicates a correlation between deformation band density and dip of layering in this example from Arches National Park. Modified from Antonellini & Aydin (1995).

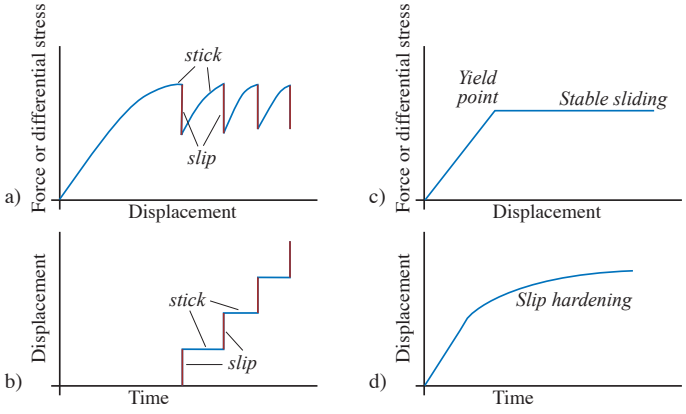

Figure 8.34 Idealized graphs illustrating the difference between stick-slip and stable sliding. a) and b) stick-slip graphs, c) ideal stable sliding and d) stable sliding with slip hardening.

such "drag" folds reveal that they are controlled by plastic deformation mechanisms and are thus shear zones around faults that can have formed in a variety of ways, mostly around the brittle-plastic transition. We do not consider such fold structures as drag folds, although geometrically the similarity can be striking.

1.5.6 Fault growth and seismicity

Once a fault surface is established it will represent a mechanically weak structure that is likely to fail again during renewed stress build-ups. Faults grow by two mechanisms. The most common one is called *stick-slip*, where slip accumulates at very sudden *seismic slip* events, separated by periods of no slip (Figure 8.34). Stress builds up between the slip events until it exceeds the frictional resistance of the fault. This is the model used to understand earthquakes: the result of the "slip" is an earthquake whose magnitude is related to the amount of energy released during the stress drop. In terms of strain, this is related to the amount of elastic strain that is released as the fault moves.

The other way for faults to accumulate slip is by *stable sliding* or *aseismic slip*. Ideally, displacement accumulates at a constant rate during stable sliding (Figure 8.34 a). Some laboratory experiments show that a gradually increasing force is needed for slip to continue. This effect is called *slip hardening* (Figure 8.34d) and is related to damage of the slip surface during deformation.

Several factors control whether fault displacement accumulates gradually or by sudden slip events. Rock experiments indicate that stable sliding is more likely when the normal stress across the fault is small, which means that stable sliding is more common in the uppermost part of the brittle crust than deeper down. Low-angle faults along overpressured layers in a sedimentary sequence would also be likely to experience stable sliding even at several kilometers depths because overpressure reduces the effective normal stress across the fault (see p.).

Lithology is another important factor: porous sediments and sedimentary rocks are more likely to deform by stable sliding than are low-porous crystalline rocks. In particular, stick-slip is favored in low-porosity quartz-rich siliceous rocks while clay promotes stable sliding. Clay-bearing incohesive fault gouge in the fault core has some of the same effect as claystone: thick and continuous zones of clay gouge promote stable sliding. The fact that gouges tend to represent pathways for fluid flow may add to their ability to slide in a stable fashion.

Close to the brittle-plastic transition, elevated temperatures introduce plastic deformation mechanisms that also promote stable sliding. Stick-slip deformation is of minor importance in the plastic regime, which means above ~300 °C for granitic rocks.

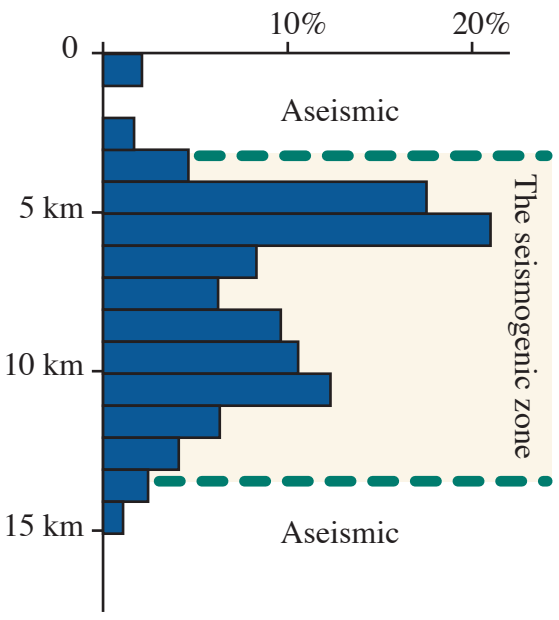

Figure 8.35 Distribution of earthquake in the crust beneath Parkfield, California (CHECK). The distribution is characteristic for the continental crust away from subduction zones. From Marone & Scholz (1988).

In summary, we could say that in the very top of the crust (upper kilometer or two), earthquakes are expected to be rare because of low normal stresses, weak and unconsolidated fault cores (gouge) and, at least in sedimentary basins, weak and porous rocks in general. Below this depth one would expect abundant seismic or stick-slip activity until the brittle-plastic transition is reached. This is exactly what earthquake data indicate, and the zone is called the *seismogenic zone* (Figure 8.35).

Typically, a single fault in the seismogenic zone shows evidence of both stick-slip and stable sliding. While seismic events may be responsible for the majority of total displacement accumulated over time, slow, *aseismic*[8] "creep" is found to occur between *seismic* events. There is also a need for small *postseismic* adjustments that may or may not be seismic.

Fault slip and displacement accumulation are commonly discussed in terms of seismicity and seismic slip behavior. It is important to realize that a single earthquake is unlikely to add more than some meters of displacement. A quake of magnitude 6.5-6.9 that activates a 15-20 km long fault gives no more than one meter of maximum displacement. Only the largest earthquakes can generate offsets of 10-15 m. This has a very important implication:

A fault with a kilometer displacement must be the product of hundreds if not thousands of earthquakes

It is worth noting that the accumulation of such displacements would take thousands or millions of years, depending on the local displacement rate. Throw rates for faults can be found by dating layers that are offset and measure their displacements. Average displacement rates of around 1-10 mm/y have been published for major faults in tectonically active areas.

Large faults tend to slip along a restricted part of their total fault surface. The total displacement distribution for a large fault is therefore the sum of displacements contributed by individual slip events (earthquakes) (Figure 8.36). While it seems clear that single slip events produce more or less elliptical displacement contours, as shown in Figure 8.16, the finite displacement distribution from a large number of slip events (earthquakes) is more difficult to predict or understand. The *characteristic earthquake model* assumes that each slip event is equal to the others in terms of slip distribution and length. The location of the displacement maximum is however shifted for each slip event. The *variable slip model* predicts that both the amount of slip and length varies from event to event, while the *uniform slip model* considers the slip at a given point to be the same in each slip event (the area varies). We will not go into the details of these models here, but simply state that displacement accumulation results in a displacement maximum near the middle of the fault, gradually off toward the tips, as shown in Figure 8.13.

1.6 Growth of fault populations

Faults grow from microfractures or deformation band zones and accumulate displacement over time as deformation proceeds. Faults tend to nucleate many places within a regionally deforming rock volume. Hence, faults tend to occur as *fault populations*. In general, many faults in a population

8 *Seismic* means sudden energy release and displacement accumulations by means of earthquakes. *Aseismic* means gradual displacement accumulation without the generation of earthquakes.

soon become inactive and thus remain small. Others reach an intermediate stage before dying, while a few grow into long faults with large displacements. Faults are unlikely to grow as individual structures for a long time. As they grow, they are likely to interfere with nearby faults. Growth by linkage is a very common mechanism that creates some of the most interesting and important structures in faulted regions (Figures 8.37 and 8.38).

1.6.1 Fault interference and relay structures

In a population where faults grow in length and height, faults and their surrounding stress/strain fields will locally interfere. Let us consider two faults whose tips approach each other during growth. Before the tips have reached each other (but after their strain fields have started to interfere) the faults are said to *underlap* (Figure 8.39a). Once the tips have passed each other, the faults are *overlapping* (Figure 8.39b-c). Under- and overlapping faults are said to be *soft-linked* as long as they are not in direct physical contact. Eventually the fault tips may link to form a *hard link* (Figure 8.39d).

Underlapping faults "feel" the presence of a neighboring fault tip in the sense that the energy required to keep the deformation going increases. The propagation rate of the fault tips in the area of underlap is thus reduced, which causes the displacement gradient to increase. This results in an asymmetric displacement profile, where the maximum is shifted toward the overlapping tip (Figure 8.40; t_1).

This asymmetric displacement distribution gets more pronounced as

Figure 8.37 Extension fracture population along the edge of a paved road. Each of the fractures have grown from microfractures and have reached a variety of sizes. The pavement is now more or less saturated with fractures, implying that additional strain will accommodate by coalsescense of existing fractures rather than by the nucleation of new ones.

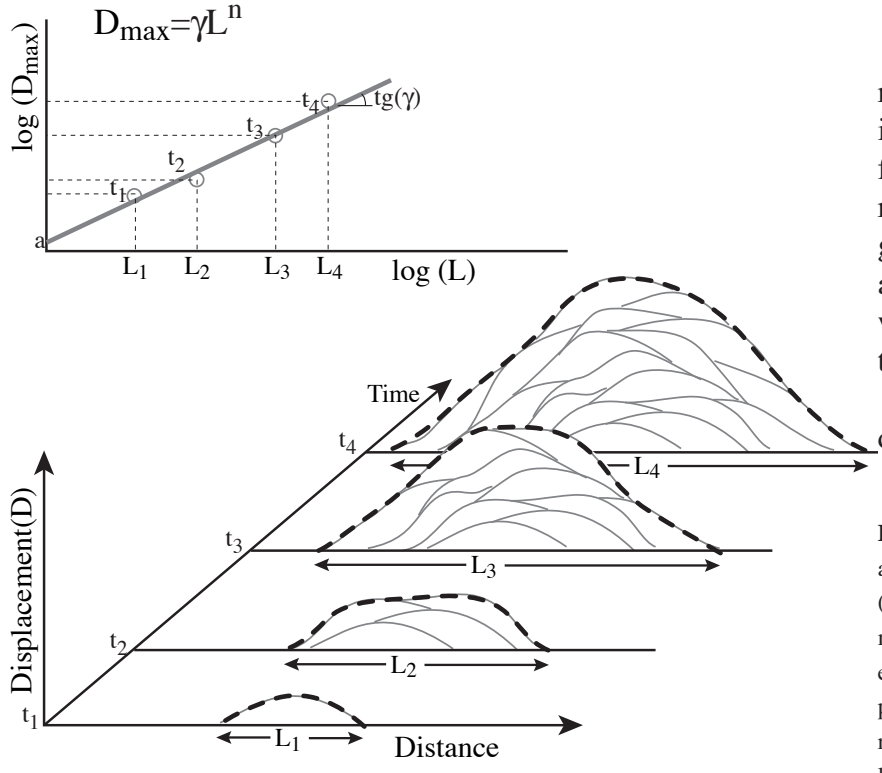

Figure 8.36 Schematic illustration of displacement accumulation through repeated slip events (earthquakes). Each event results in up to a few meters of displacement. In this model, repeated slip events form a bell-shaped cumulative displacement profile that resembles that of a single slip event. The result of this model is a straight line in a logarithmic length-displacement diagram.

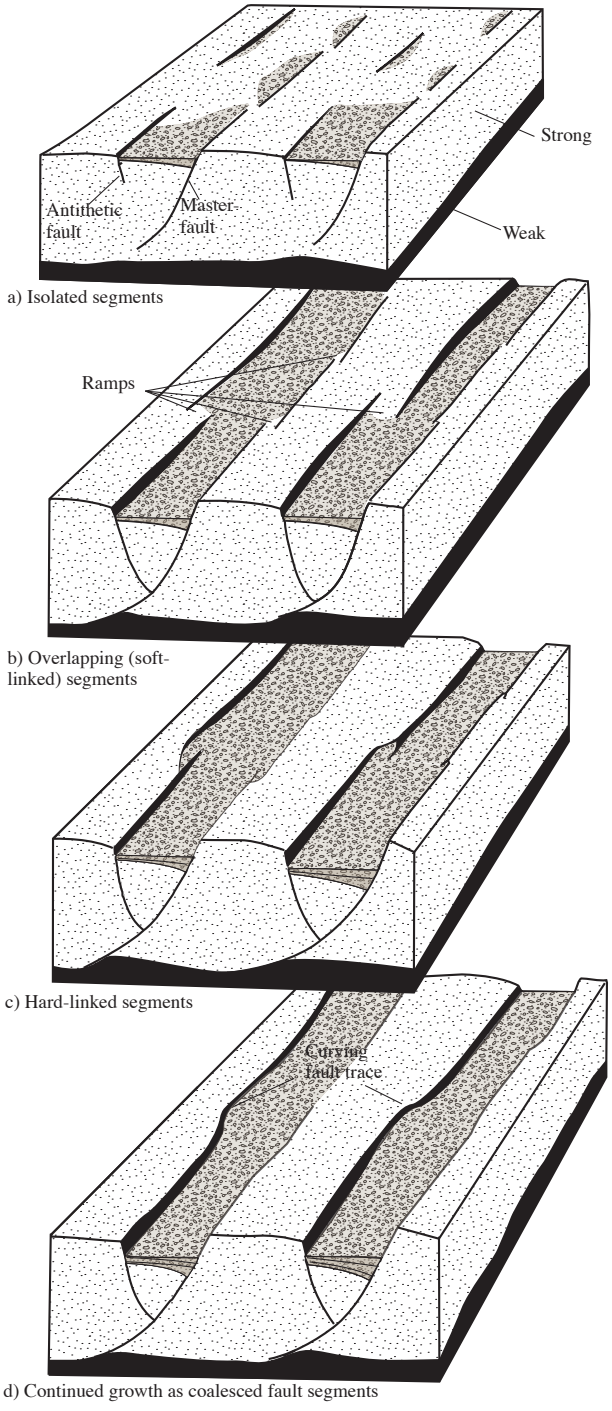

Figure 8.38 Simplified model for the development of a fault population in Canyonlands, Utah. The faults develop from isolated fractures into long faults through the formation and destruction of relay ramps. Based on Trudgill and Cartwright (1994).

the faults overlap, and if the layers in the overlap zone are subhorizontal they become folded. The folding is a result of ductile displacement transfer (relay) from one fault to the other and is directly related to the high displacement gradients in the overlapping tip zones. If the fault interference occurs perpendicular to the slip direction, which for normal and reverse faults means in the horizontal direction, and if the layering is subhorizontal, then the folding is well expressed in the form of a ramp-like fold. The fold itself is called a *relay ramp* and the entire structure is known as a *relay structure* (Figure 8.39c and 8.41).

The ramp is a fold that may contain extension fractures, shear fractures, deformation bands and/or minor faults depending on the mechanical rock properties at the time of deformation. Eventually the ramp will break to form a *breached relay ramp*. The two faults are then directly connected and an

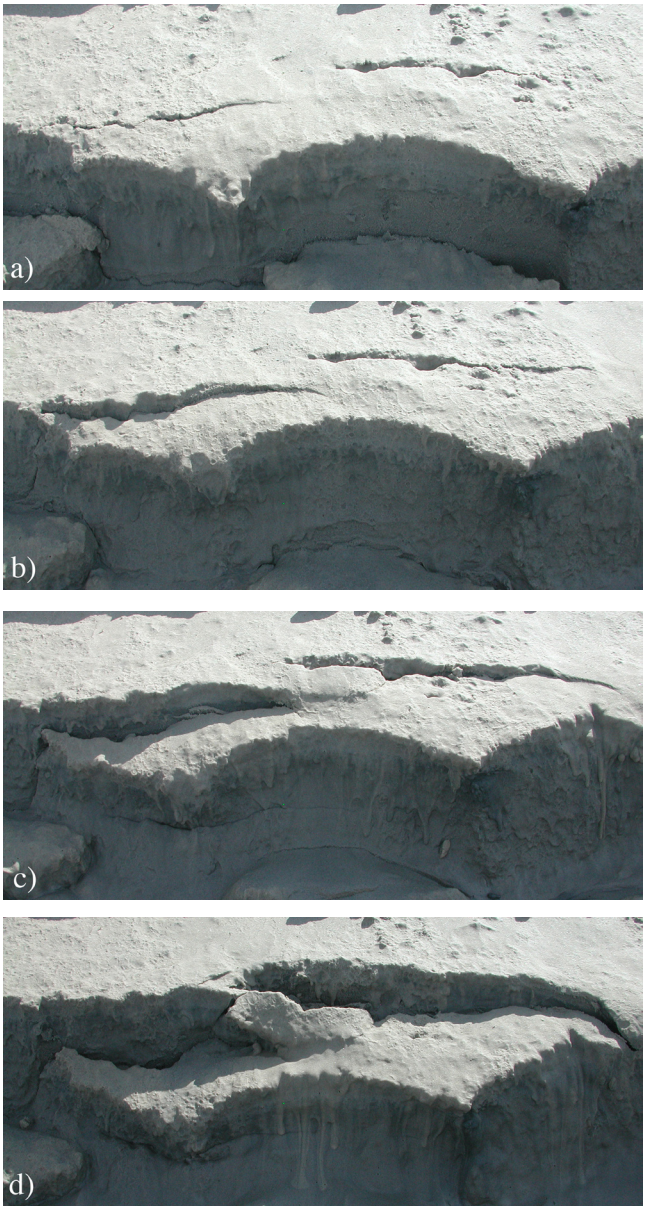

Figure 8.39 The development of curved fault systems in unconsolidated sand (beach geology!). Two isolated fractures (a) overlap (b-c) to form a relay ramp that eventually becomes breached (d). Faults were initiated by splashing water on the sand. The width of each picture is ca. 50-60 cm.

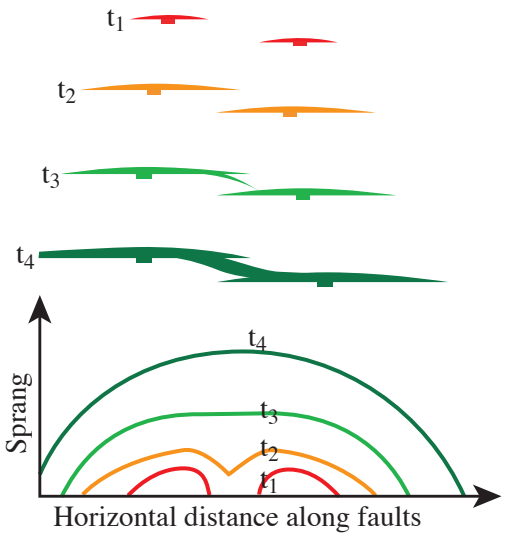

Figure 8.40 Illustration of the change in displacement along two faults that overlap and coalesce. The upper part shows the two segments in map view at four different times (t_1-$t_)$ during their growth history). The lower part shows the displacement profile at the four different stages.

associated with an abnormally wide damage zone.

Upon breaching there will be a displacement minimum at the location of the relay structure. The total displacement curve along the fault will therefore show two maxima, one on each side of the relay structure (Figure 8.40). As the deformation proceeds and the fault accumulates displacement, the displacement profile will approach that of a single fault, with a single, central maximum. However, the link is still characterized by the wide damage zone and a step in the horizontal fault trace. If the fault mapping is based on seismic data, a sudden change in strike may be the only indication of a breached ramp (Figure 8.42). Such steps are therefore very important as they may hint on the locations of both breached and intact relay ramps.

Bends and jogs of faults in map view are very common on many scales. Figure 8.39 shows the development of a non-planar fault in sand. The final fault can be seen to be the result of interaction between individual fault segments through the creation and breaching of relay ramps. The curved fault pattern seen in map-view is very similar to that displayed by much larger faults, such as the northern North Sea faults shown in Figure 8.43 and the Wasatch Fault in Utah (Figure 8.44). It seems likely that these large faults formed by fault linkage as portrayed in Figure 8.39.

It is clear that ramps come in any size and stage of development. It is important to understand that relay ramps and overlap zones are formed and destroyed continuously during the growth of a fault population.

1.6.2 Interference along the slip vector

Faults grow both in the direction normal and parallel to the slip direction and therefore interfere in both the vertical and horizontal directions (Figure 8.45). For simplicity we will here consider dip-slip faults, which means that we will be looking at the vertical

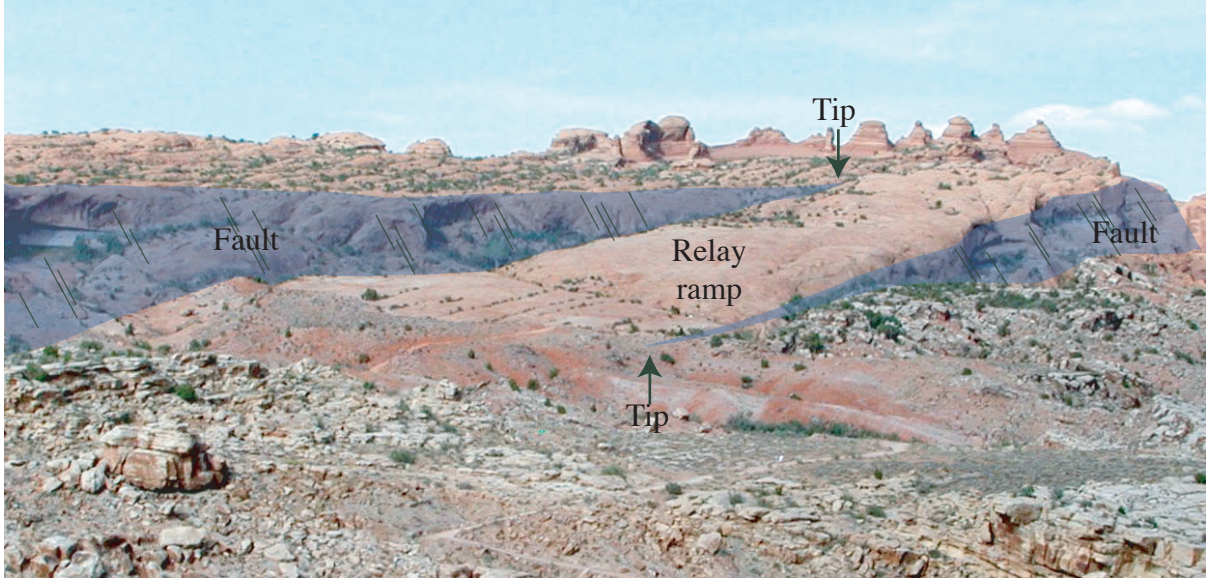

Figure 8.41 Relay ramp formed between two overlapping fault segments in Arches National Park, Utah. There is a higher density of deformation bands within the ramp than away from the ramp.

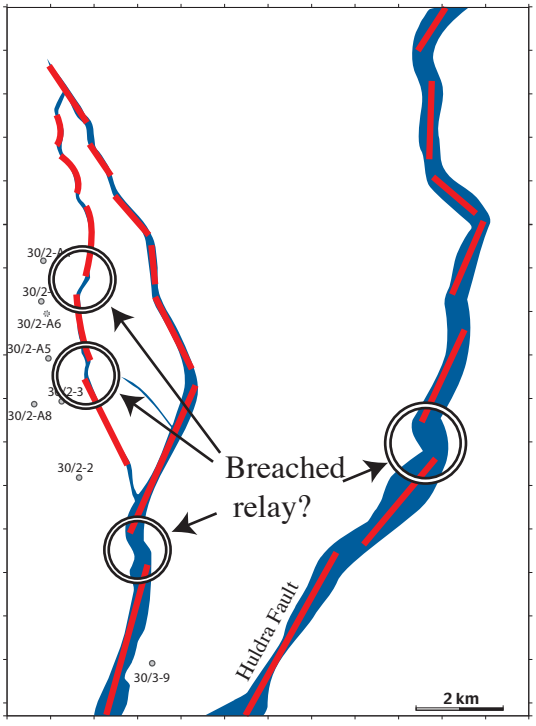

Figure 8.42 Normal faults from a North Sea oil field (map view). Locations of sudden changes in strike may represent broken relay zones or locations of relay ramps that are of subseismic size or overlooked by the seismic interpreter. From Fossen et al. (2003).

section[9]. Relay structures are most commonly recognized and described in map view, but this is simply because they are easier to observe in map view. High vertical sections are less common than large horizontal exposures, and the continuity of good seismic reflectors in the horizontal direction makes it easier to map relays in map view than in the vertical direction. It takes a whole package of good reflectors to identify and map vertical overlap zones on seismic sections. There is therefore a good chance that vertical relay zones are underrepresented in seismic interpretations.

Faults initiate after a certain amount of strain that depends on their mechanical properties (Young's modulus etc.). Strong rock layers start to fracture while weak rocks still accumulate elastic and ductile deformation. As these fractures grow into faults, they will interfere and connect. In many cases sandstones become faulted before shales. The process is similar to that occurring in map view, except that the angle between the displacement vector and the layering is different. We do not get ramps as shown in Figure 8.41, but rotation of layers as shown in Figure 8.46. The rotation depends on fault geometry and how the faults interfere.

Restraining overlap zones (Figure 8.46a-c) are, in this connection, overlap zones with shortening in the displacement direction. In principle, volume reduction may accommodate the deformation within the zone. More commonly, however, the layers within the overlap zone get rotated as shown in Figure 8.46c.

Releasing overlap zones (Figure 8.46d-e) are zones where the fault constellation and sense of displacement cause stretching within the overlap zone. Weak layers such as shale or clay layers are rotated within releasing overlap zones. If the overlap zone is narrow, such weak layers can be smeared along the fault zone (Figure 8.31 and 8.47). Field observations show that this is a common mechanism for the formation of clay smear in sedimentary sequences, but usually on too small scale to be detected from seismic data. Such structures may cause faults to be sealing with respect to fluid flow, which may have important implications in petroleum

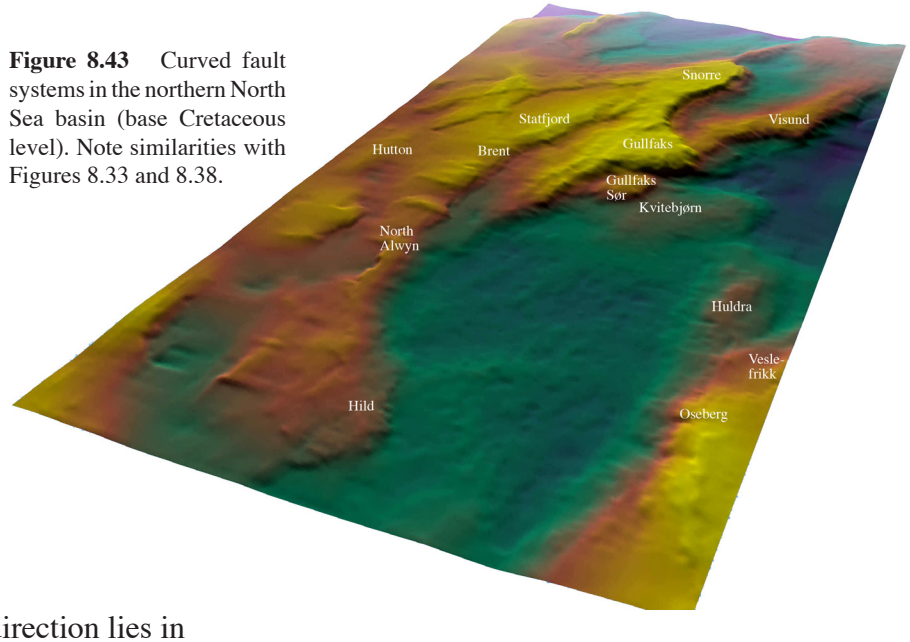

Figure 8.43 Curved fault systems in the northern North Sea basin (base Cretaceous level). Note similarities with Figures 8.33 and 8.38.

9 For strike-slip faults the slip direction lies in the strike direction of the fault. This case is specifically considered in Chapter 19.

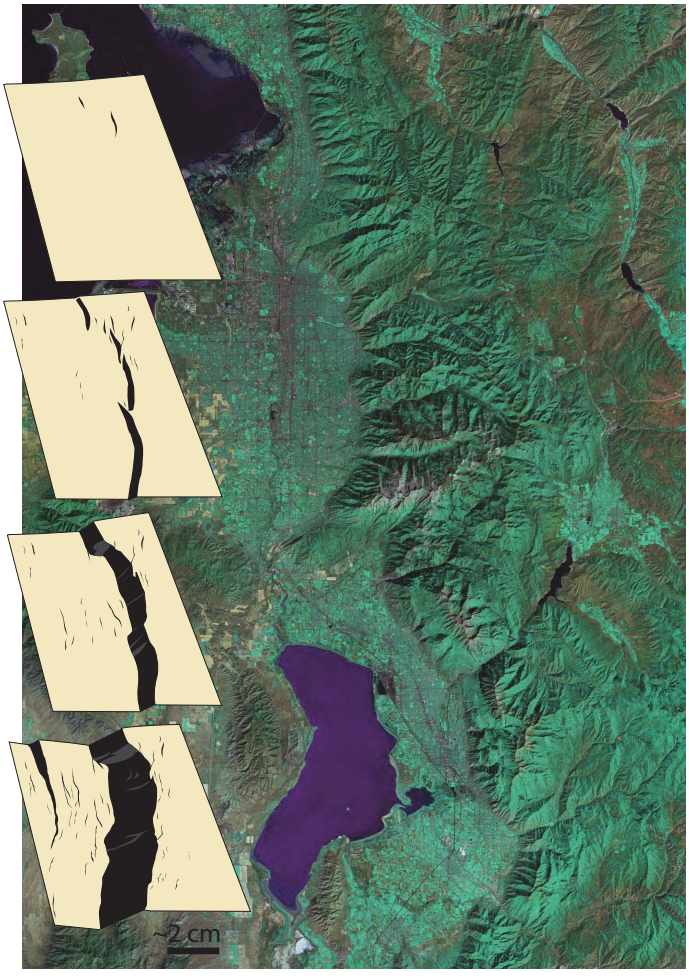

Figure 8.44 **The** Wasatch fault zone, which separates the Wasatch Mountains in the east from the Basin-and-Range region in the west. Note the curved fault geometry, indicating a history of segment linkage. Similar geometries developed at four stages of a plaster extension experiment are shown.

or groundwater reservoirs.

1.6.3 The control of lithology on fault growth

Layering or *mechanical stratigraphy* is important as fault populations develop in layered rocks. The timing of fault formation in the different layers is one aspect, and the way that faults form (ordinary fracturing vs. faulting of deformation band zones) is another. Mechanical stratigraphy simply implies that the rock consists of layers that respond mechanically differently to stress, i.e. they have different strengths and different Young's moduli (E). In simple terms, some layers, such as clay or shale, can accommodate a considerable amount of ductile strain, while other layers, such as limestone or cemented sandstone, fracture at much lower amounts of strain. The

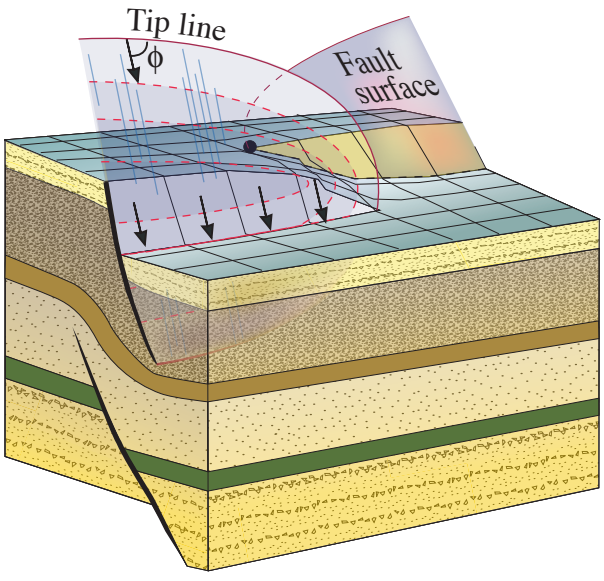

Figure 8.45 Faults interfere in both the horizontal and vertical directions as they grow. In both cases displacement is transferred from one fault to the other, and layers between the overlapping tips tend to fold into ramps or drag folds. From Rykkelid og Fossen (1992).

result is that, in a layered sequence, fractures or deformation bands initiate in certain layers while adjacent layers are unaffected or less affected by such brittle structures (Figure 8.48).

So long as the deformation band or fracture grows within a homogeneous layer, a proportionality exists with respect to length, height and maximum displacement. This is illustrated in Figure 8.49a, where the fracture or deformation band has not reached the upper and lower boundaries of the layer. Once the fracture touches the layer boundaries (Figure 8.49b) it is called a *vertically constrained fracture*, and the fracture will only expand in the horizontal direction. This means that the fracture gets longer and longer while its height remains constant, i.e. its eccentricity increases. In fact, its shape is likely to become more rectangular than elliptical.

The moment a fracture is constrained, its area increases only by layer-parallel growth, and its displacement/length (D/L) ratio gets lower than what it was during its unconstrained growth history. In simple terms, the reason is that displacement scales with fracture area, and since the fracture area only increases along its length, the length has to increase at a faster rate relative to displacement.

Eventually, if the fracture keeps accumulating displacement, it will break through the bounding

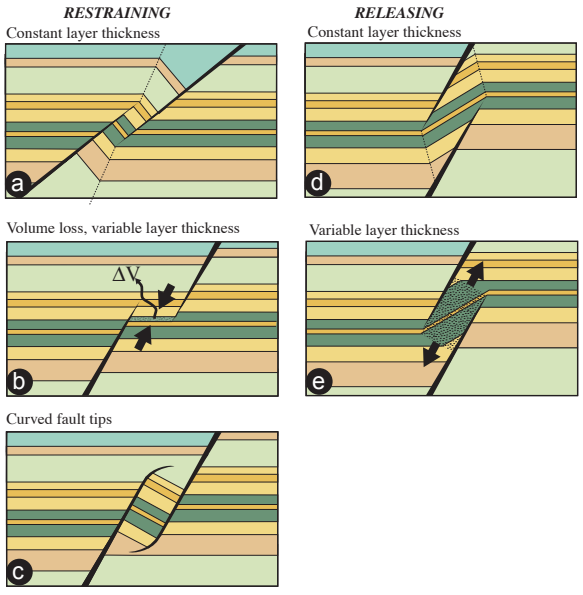

Figure 8.46 Different types of vertical overlap zones (horizontal layering). a) Contractional or constraining type where constant layer thickness implies marked reverse drag. b) Contraction compensated for by local dilation. c) Contractional structures where the fault tips bend towards each other give a marked drag. Extensional or restraining zones with constant (d) and variable (e) layer thickness give normal drag. Based on Rykkelid & Fossen (2002).

interface and expand into the overlying/underlying layers (Figure 8.49c). The D/L relation will then return to its original trend (Figure 8.49d). The same development is seen for deformation bands in sandstone-shale sequences. At a critical point the deformation band cluster in the sandstone is cut by a

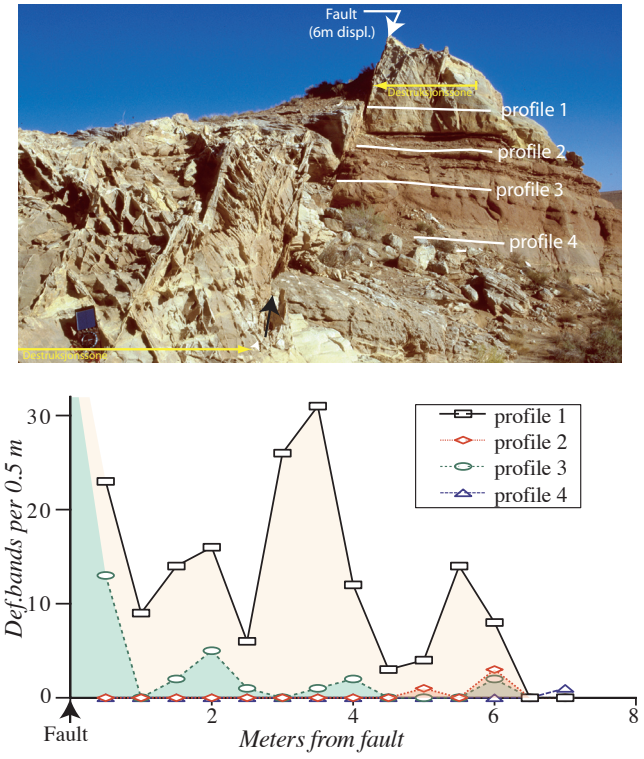

Figure 8.48 Distribution of deformation bands in the footwall to a fault with 6 m displacement. The frequency is considerably higher in the clean, highly porous sandstone (Scan 1) than in the more fine-grained layers (Scans 2 and 3). It is also lower in the thin sandstone layer (Scan 4). San Rafael Desert, Utah.

slip surface (fault) which extends into the over and/or underlying shale.

Figure 8.47 Overlapping faults where a shale is caught in the overlap zone between two faults and smeared along the faults. Moab, Utah.

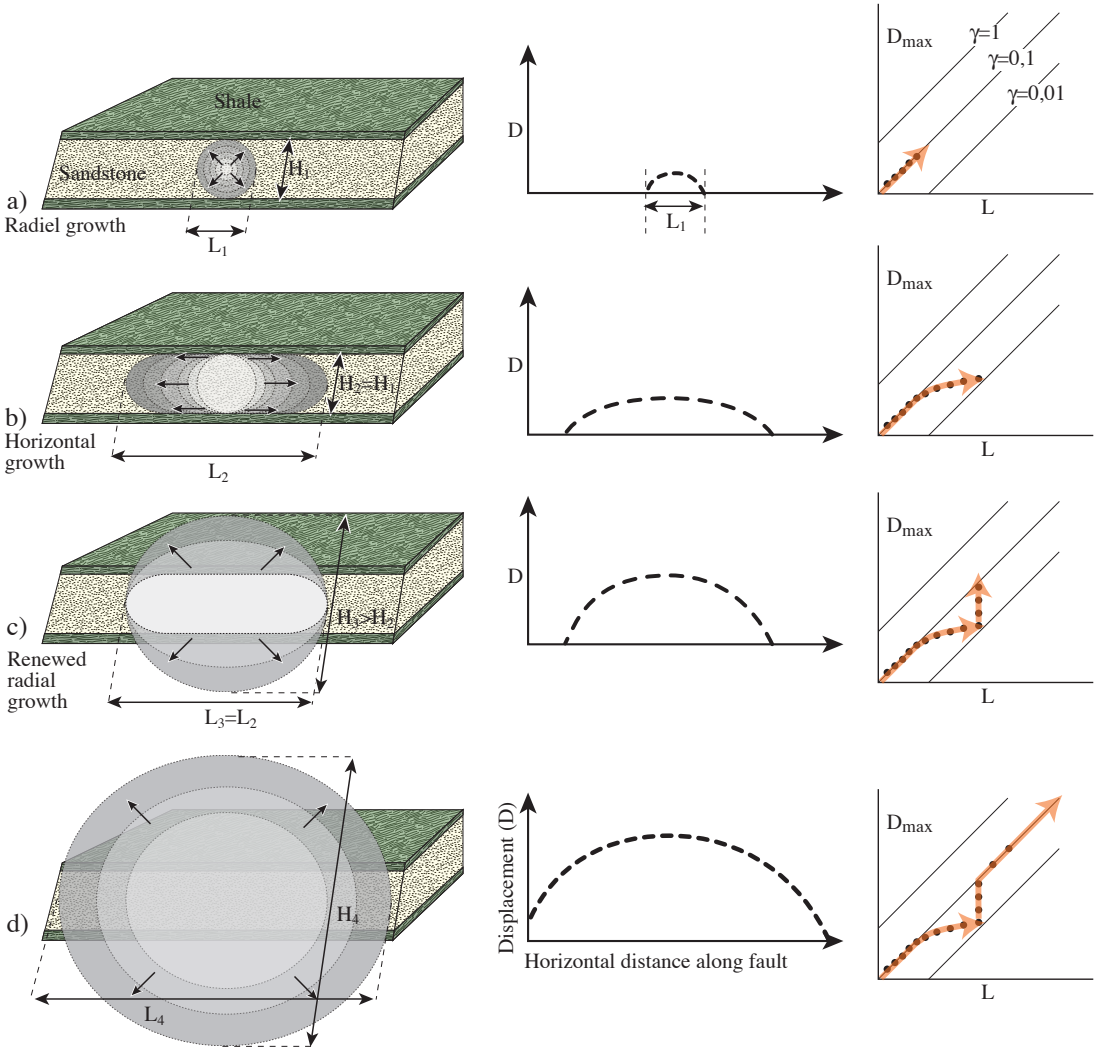

Figure 8.49 Growth of a fault in a layered sequence, with displacement profile and Displacement-Length evolution shown to the right (logarithmic axes). The fault nucleates in the sandstone layer (a) with a normal displacement profile and expands horizontally when hitting the upper and lower boundaries (b). A relatively long or plateau-shaped displacement profile evolves. At some point the fault breaks through the under/overlying layers (c) and starts growing in the vertical direction again. The displacement profiles regains a normal shape. Such litihological influence on fault growth causes scatter in D-L diagrams.

1.6.4 D-L relations during fault growth

The maximum displacement (D_{max}) along a fault is a function of the fault's eccentricity (ellipticity: length/height or L/H ratio) and the strength (driving stress) of the rock (Figure 7.20). L is commonly plotted against D_{max} in a logarithmic diagram as shown in Figure 8.50. Straight lines in such diagrams indicate an exponential or *power-law* relation between D and L that can be expressed as

$$D_{max}=\gamma L^n$$

Fractures that grow such that D and L are proportional, i.e. $D_{max}=\gamma L$, define straight, diagonal lines in the logarithmic diagram with slope γ (n=1). Field data seem to plot along diagonal lines, although with a considerable amount of scatter (Figure 8.50). Some populations of cataclastic deformation bands do however show lower slopes (n<1). This may be related to their sensitivity to mechanical stratigraphy, as discussed in the previous section. Mechanical stratigraphy occurs at different scales, from meter-scale beds up to the thickness of the entire brittle crust. Hence, it is thought that the effect repeats itself to some degree at different scales, causing some of the scatter seen in Figure

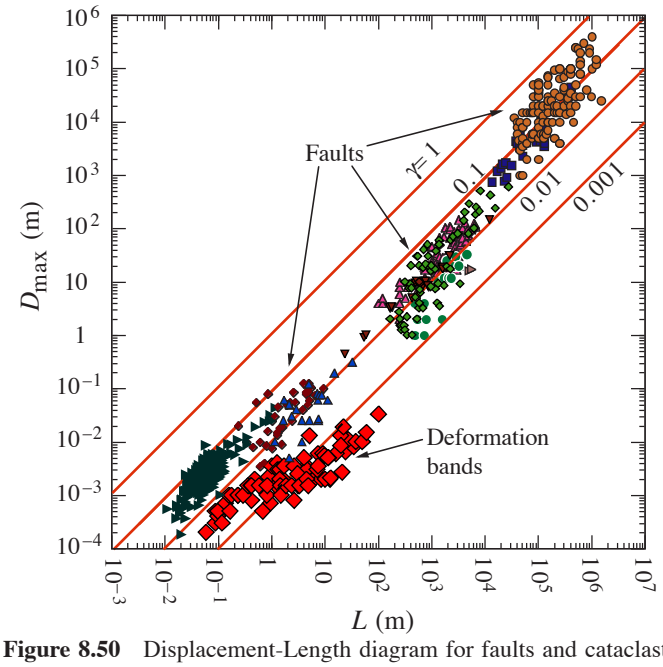

Figure 8.50 Displacement-Length diagram for faults and cataclastic deformation bands. Faults from a number of localities and settings are plotted. The deformation bands show a clear deviation from the general trend in that they are longer than predicted from their displacement. Modified from Schultz & Fossen (2002).

8.50[10]. The relation between D and L can be of interest in several cases, for instance where the displacement is known from well information or seismic data, and the total length of the fault is to be estimated. However, the scatter of data makes predictions unreliable.

1.7 Faults, communication and sealing properties

Faults may affect fluid flow in many cases. Faults in non-porous or low-porous rocks are generally conduits of fluids. In other words, target damage zones when drilling for water in non- or low-porous rocks.

In highly porous rocks, faults more commonly act as baffles to fluid flow. In a petroleum reservoir setting it is important to distinguish between their effect over geologic time and their role during production. Some faults are sealing over geologic time (millions of years) and can stop and trap considerable columns of oil and gas. Some faults that are not sealing over geologic time may still hinder fluid flow during production of an oil or gas field (over days or years). The ability for faults to affect fluid flow is commonly referred to as fault *transmissibility* or *transmissitivity*. Fault transmissibility is influenced by the nature of the damage zone, but is mostly controlled by the thickness and properties of the fault core.

1.7.1 Juxtaposition

The lithological contact relations along a fault are essential when it comes to its effect on fluid flow in a porous reservoir. Where sand is completely juxtaposed against shale, the fault is

RELAY RAMPS IN PETROLEUM RESERVOIRS

Relay ramps can be important features in a petroleum reservoir. In the context of exploration, ramps can cause communication (migration of oil) across a fault that is elsewhere sealing. During production, relay ramps may represent pathways for water, oil or gas and cause pressure communication between otherwise isolated

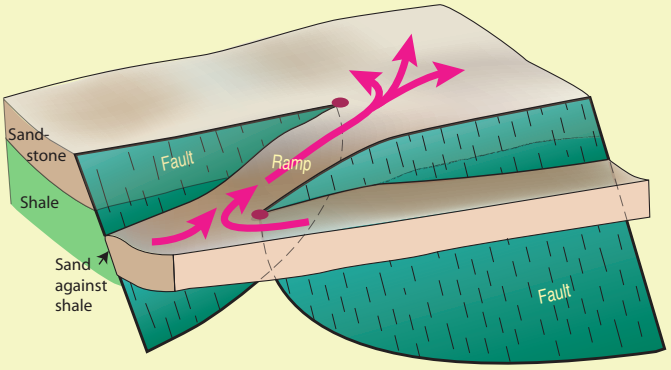

fault blocks. Relay ramps may contain abundant subseismic structures, depending on their stage of maturity. They will generally have a wide damage zone that may cause problems to wells placed in the zone. Both breached and intact ramps are easily interpreted as sudden bends in the fault trace. The kinks can represent the interpreter's smoothing of an intact ramp around or below seismic resolution, or a breached ramp. Unbreached and "newly" breached ramps may show a displacement minimum in the ramp area that may be detectable from seismic data.

10 Another source of scatter is the growth of faults by linkage, as discussed in section 8.6.1.

sealing regardless of the properties of the fault itself. However, where sand is juxtaposed against sand, the transmissibility of the fault is solely controlled by the physical properties of the fault core and the fault damage zone. These properties are again controlled by the amount of smearing of fine-grained material along the fault, the fault core thickness, the deformation mechanisms within the core and in deformation bands and any other fractures surrounding the core.

1.7.2 Cataclasis

Cataclasis in the fault core reduces grain size and therefore reduces porosity and permeability. Cataclasis is promoted by deep (>1 km) burial depths, low phyllosilicate content, well-sorted grains and low pore-fluid pressure. Cataclasis can create a cataclasite or ultracataclasite so dense that it will potentially stop fluid flow across the fault even if there is high-permeable rock on each side of the fault. Cataclasis also occurs in deformation bands in the damage zone, and the more deformation bands, the larger their effect on fault transmissibility during production. The effect of cataclastic (and other) deformation bands is probably negligible in most cases when it comes to sealing capacity over geologic time.

1.7.3 Diagenetic effects

Diagenetic changes that occur after or during the faulting process can change the mechanical and petrophysical properties of the fault rock significantly in some cases. The most important change is probably caused by dissolution and precipitation of quartz, which can turn the fault rock into a non-permeable □quartzite□. Quartz dissolution and cementation is a problem at temperatures above ~90 °C (3 km). In many basins, such as the North Sea, quartz cementation occurred much later than the faulting as the sediments were buried during post-rift subsidence. Quartz and other minerals may be preferentially deposited in faults because of the reactant surfaces that form during faulting due to the scratching and breaking of grains. In addition, fluids can easily move along faults in some cases, increasing the flux of silica-bearing fluids. Calcite cementation in faults is also fairly common, but is thought to form less continuous structures.

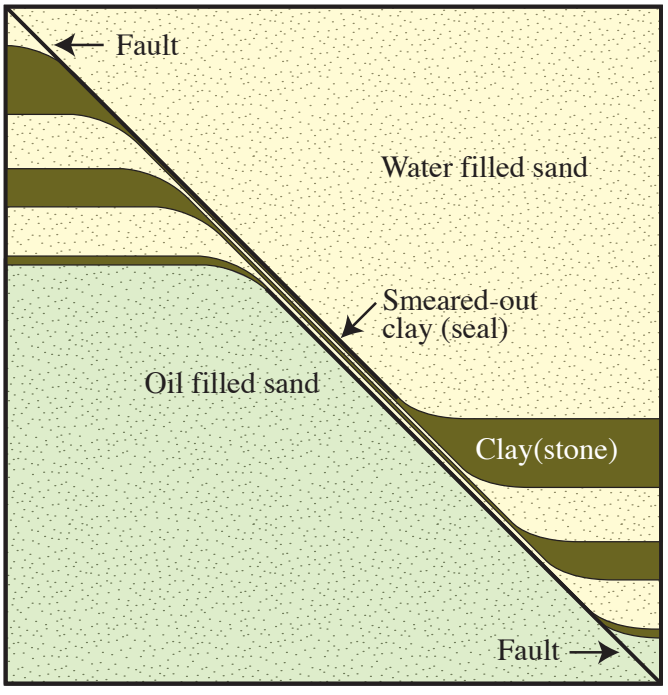

Figure 8.51 Principal sketch showing how clayrich layers can be smeared out along a fault to form a seal or barrier for fluid flow. In this example the oil-filled sandstone is not in communication with the higher water-filled sandstone because of the impermeable clay membrane. Note that for the fault to be sealing, the membrane must be continuous also in the third direction for as far as the two sands are in contact.

1.7.4 Clay and shale smear

Layers of clay or shale can be smeared along the fault during the fault movement (Figure 8.51). Clay and shale are more ductile than sand and sandstone in most cases; field observations and experimental results alike show that clay can smear and seal faults. For this to happen there must be clay or shale layers in the faulted sequence. The more clay or shale layers there are, the larger the chance of smearing. A common mechanism is the smearing of clay or shale between two *vertically overlapping fault segments*, as shown in Figure 8.47. A less common mechanism is *injection*, where abnormally high pressures in clay layers cause *clay injection* along the fault core. *Clay abrasion*, where clay is tectonically eroded from clay-rich layers along the fault and incorporated into the fault core, is a third mechanism that contributes to clay smearing.

The likelihood of smearing increases with increasing amount of clay, i.e. with the number of

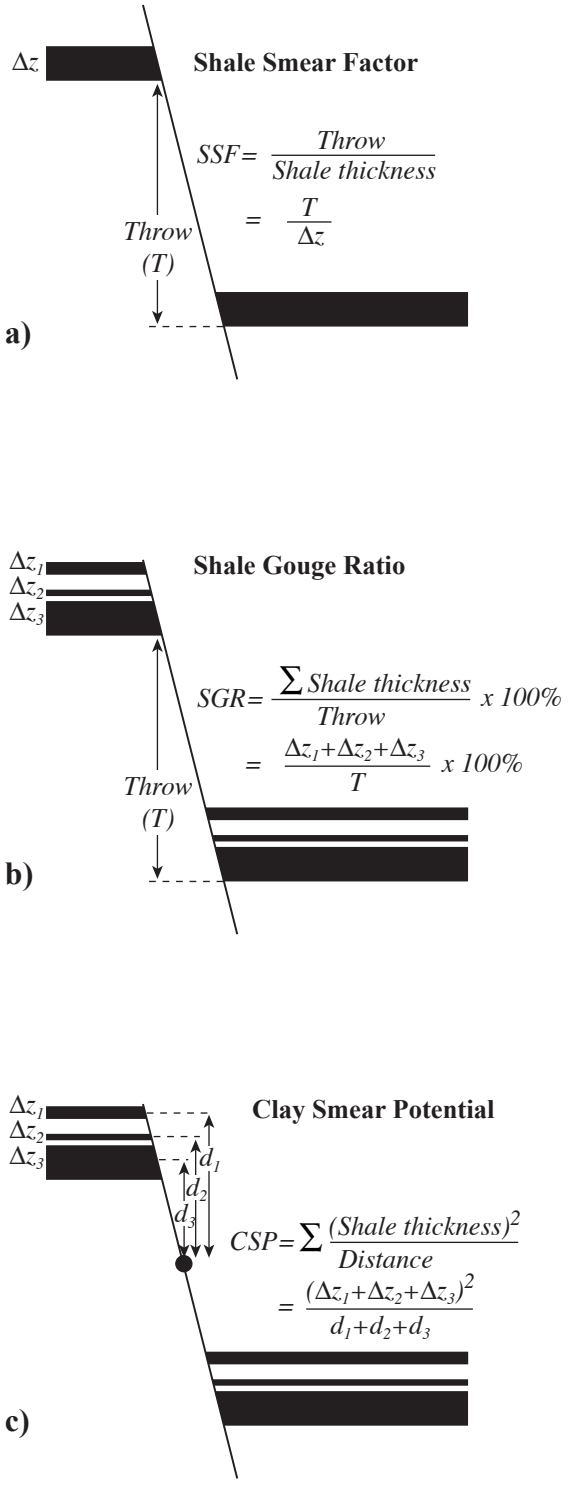

Figure 8.52 Three algorithms for estimating the likelihood of smear on a fault.

clay layers and their thicknesses, and decreases with increasing fault displacement. The more displacement, the higher the probability that the seal is discontinuous and the fault is leaky. If the discontinuity of the seal is local and small, it may still reduce the flow rate across the fault.

There is a need to put numbers on the clay smearing potential of faults. In the simple case where there is a single clay or shale layer and a single fault (Figure 8.52), then the Shale *Smear Factor* (SSF) gives the ratio between fault throw T[11] and the thickness of the shale or clay layer (Δz):

$$SSF = \frac{T}{\Delta z} \quad (8.1)$$

This puts a number to the local probability of smear, and the number will vary along the fault as displacement and perhaps also the layer thickness change. For SSF>7 the fault is considered to be transparent (non-sealing). Obviously, there are other factors that influence on the sealing capacity of a fault, so this number gives a simplistic estimate only.

In cases where there is more than one clay or shale layer the contribution of each must be included. This ratio, the percentage of clay or shale in the slipped interval, is known as*"Shale Gouge Ratio"* (SGR) and is the sum of shale bed thicknesses over the fault throw:

$$SGR = \frac{\sum \Delta z}{T} \cdot 100\% \quad (8.2)$$

A high SGR value indicates high sealing probability. There is a realistic chance that the fault is sealing when the SGR-value exceeds 20%, and the probability increases with the SGR. The probability would also depend on the mechanical properties of the shale or clay layers at the time of deformation, which should be taken into consideration in each case. In general, shallow burial promotes smearing while deep burial involves a higher risk of a leaky seal.

Clay smear can also be characterized by estimating the *clay smear potential* (CSP). CSP relates to how far a clay or shale layer can be smeared before it breaks and becomes discontinuous:

11 Displacement would have been a better parameter to use than throw, but throw is a popular term among petroleum geologists…

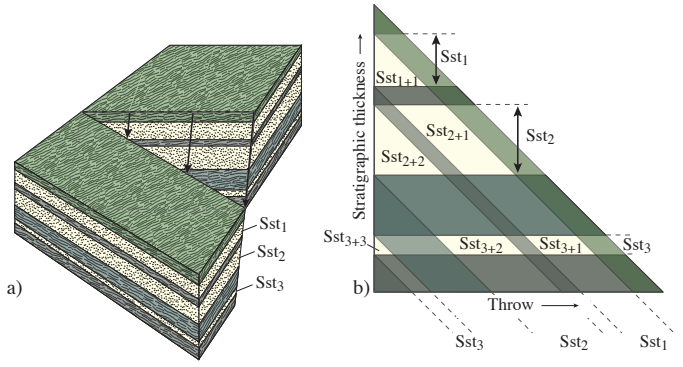

Figure 8.53 The concept of triangle diagram construction. A synthetic fault with a linearly increasing displacement is considered (a). In the block diagram the layers on the upthrown side are horizontal while they are dipping on the opposite side. This is carried over to the triangular diagram to the right (b). Because the displacement increases from zero on the left hand side, different lithologic contact relations occur in different parts of the diagram. Areas of sand-sand and sand-clay contact can easily be found.

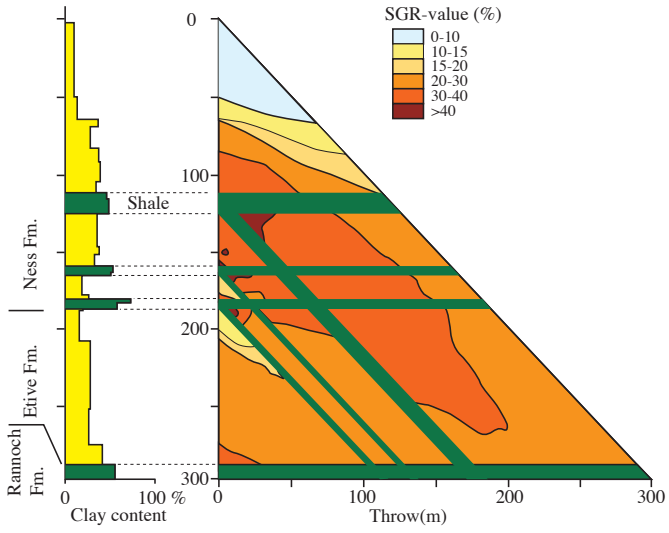

Figure 8.54 SGR-values can be added to the triangle diagram, as for this example from the North Sea Brent Group (stratigraphy shown to the left). The SGR-value is calculated for different points in the diagram and contoured. High SGR-values means high sealing factor. The diagram shows that the sealing probability is highest where there are clay layers and where the displacement is relatively small. Based on Høyland Kleppe (2003).

$$CSP = \sum \frac{\Delta z^2}{d} \qquad (8.3)$$

where d is the distance from the source (clay) layer and Δz represents the individual thickness of each clay or shale layer.

Coal can also be smeared along faults if it is mixed with clay. However, pure coal normally behaves brittlely when faulted. Even sand can be smeared along faults when in a poorly consolidated state. Sand smearing at shallow depths may improve communication across faults, but is rarer than shale smear.

1.7.5 Triangle diagrams

Lithology and displacement are, as emphasized above, important factors in the estimation of the sealing properties of faults. These factors can be combined and visualized in a *triangle diagram* (Figure 8.53). The local stratigraphy is plotted along the vertical axis and extended parallel to the other two sides so that they gradually separate. This is in effect similar to what happens along a fault, where layer separation increases with increasing displacement. In the diagram, horizontal stratigraphic layers represent the hanging wall layers, while the dipping layers represent the footwall. Layer separation and fault displacement increase as we move to the right in the diagram, and we can read off the contact relations for any given value of fault displacement. The different lithologies (layers) in the diagram are colored. For a sand-shale sequence different colors indicate sand-sand, sand-shale and shale-shale juxtaposition. Furthermore, for each point in the diagram one or more of the parameters SGR, SSF and CSP can be calculated and the triangular diagram can be colored to illustrate the variation in, for example, SGR (Figure 8.54).

”””

While faults may look simple when portrayed as simple lines on geologic maps and interpreted seismic sections, more detailed considerations reveal that they are complicated structures composed of a number of structures at various scales. Although our understanding of faults and related structures has increased significantly over the last couple of decades, much research remains before we reach the point at which we can predict or model their geometries and properties based on input such as tectonic regime, lithology and burial depth. Before leaving the upper, brittle portion of the crust we will look at how kinematic information can be extracted from fault populations and how this information reflects the deformation and state of stress during

their formation.

Further reading:

Petroleum oriented:

Allmendinger, R. 1993. Aydin, A., 2000. Fractures, faults, and hydrocarbon entrapment, migration and flow. Marine and Petroleum Geoology, 17: 797-814.

Fossen, H. & Hesthammer, J., 1998. Structural geology of the Gullfaks Field, northern North Sea. In: M.P. Coward, H. Johnson & T.S. Daltaban (eds.), Structural geology in reservoir characterization. Geological Society, London, Special Publications, 127: 231-261.

Steen, Ø., Sverdrup, E. & Hanssen, T.H. (Red.), 1998. Predicting the distribution of small faults in a hydrocarbon reservoir by combining outcrop, seismic and well data. In: Jones, G., Fisher, Q.J. and Knipe, R.J. (eds.), Faulting, fault sealing and fluid flow in hydrocarbon reservoirs. Geological Society, London, Special Publications, 147: 27-50.

Yielding, G., Walsh, J. & Watterson, J., 1992. The prediction of small-scale faulting in reservoirs. First Break, 10: 449-460.

Displacement variations

Barnett, J.A.M., Mortimer, J., Rippon, J.H., Walsh, J.J. & Watterson, J., 1987. Displacement geometry in the volume containing a single normal fault. American Association of Petroleum Geologists Bulletin, 71: 925-937.

Ferill, D.A. & Morris, A.P., 2001. Displacement gradient and deformation in normal fault systems. Journal of Structural Geology, 23: 619-638.

Hull, J., 1988. Thickness-displacement relationships for deformation zones. Journal of Structural Geology, 4: 431-435.

Walsh, J.J. & Watterson, J., 1989. Displacement gradients on fault surfaces. Journal of Structural Geology, 11: 307-316.

Walsh, J.J. & Watterson, J., 1991. Geometric and kinematic coherence and scale effects in normal fault systems. In: Roberts, A.M., Yielding, G. and Freeman, B. (eds.), The geometry of normal faults. Geological Society Special Publication, 56: 193-203.

Dipmeterdata, drag and fault-related folding

Bengtson, C.A., 1981. Statistical curvature analysis techniques for structural interpretation of dipmeter data. American Association of Petroleum Geologists, 65: 312-332.

Erslev, E.A., 1991. Trishear fault-propagation folding. Geology, 19: 617-620.

Fault geometry and lithology

Benedicto, A., Schultz, R.A. & Soliva, R., 2003. Layer thickness and the shape of faults. Geophysical Research Letters, 30: 2076.

Jackson, J. & McKenzie, D., 1983. The geometrical evolution of normal fault systems. Journal of Structural Geology, 5: 472-483.

Fault linkage

Childs, C., Watterson, J. & Walsh, J.J., 1995. Fault overlap zones within developing normal fault systems. Journal of the Geological Society, 152: 535-549.

Childs, C., Nicol, A., Walsh, J.J. & Watterson, J., 1996. Growth of vertically segmented normal faults. Journal of Structural Geology, 18: 1389-1397.

Larsen, P.-H., 1988. Relay structures in a Lower Permian basement-involved extension system, East Greenland. Journal of Structural Geology, 10: 3-8.

Means, W.D., 1989. Stretching faults. Geology, 17: 893-896.

Peacock, D.C.P. & Sanderson, D.J., 1994. Geometry and development of relay ramps in normal fault systems. American Association of Petroleum Geologists Bulletin, 78: 147-165.

Rykkelid, E. and Fossen, H., 2002. Layer rotation around vertical fault overlap zones: observations from seismic data, field examples, and physical experiment. Marine and Petroleum Geology, 19: 181-192.

Damage zone

Shipton, Z.K. & Cowie, P., 2003. A conceptual model for the origin of fault damage zone structures in high-porosity sandstone. Journal of Structural Geology, 25: 333-344.

Caine, J.S., Evans, J.P. & Forster, C.B., 1996. Fault zone architecture and permeability structure. Geology, 24: 1025-1028.

Kim, Y.-S., Peacock, D.C.P. & Sanderson, D.J. 2004. Fault damage zones. Journal of Structural Geology 26: 503–517.

Fault sealing and clay smear

Clausen, J.A., Gabrielsen, R.H., Johnsen, E. & Korstgård, J.A., 2003. Fault architecture and clay smear distribution. Examples from field studies and drained ring-shear experiments. Norwegian Journal of Geology, 83: 131-146.

Hesthammer, J. & Fossen, H., 2000. Uncertainties associated with fault sealing analysis. Petroleum Geoscience, 6: 37-45.

Hesthammer, J., Bjørkum, P.A. & Watts, L.I., 2002. The effect of temperature on sealing capacity of faults in sandstone reservoirs. American Association of Petroleum Geologists Bulletin, 86: 1733-1751.

Knipe, R.J., 1992. Faulting processes and fault seal. In: Larsen, R.M., Brekke, H, Larsen, B.T. and Talleraas, E. (eds.), Structural and tectonic modelling and its application to petroleum geology. NPF Special Publication, Elsevier, Amsterdam, 325-342.

Knott, S.D., 1993. Fault seal analysis in the North Sea. American Association of Petroleum Geologists Bulletin, 77: 778-792.

Manzocchi, T., Walsh, J.J. & Yielding, G., 1999. Fault transmissibility multipliers for flow simulation models. Petroleum Geoscience, 5: 53-63.

Faults and seismic data

Hesthammer, J. & Fossen, H., 1997. The influence of seismic noise in structural interpretation of seismic attribute maps. First Break, 15: 209-219.

Fault strain

King, G. & Cisternas, A., 1991. Do little things matter? Nature, 351: 350.

Marrett, R. & Allmendinger, R.W., 1992. Amount of extension on “small” faults: an example from the Viking Graben. Geology, 20: 47-50.

Reches, Z., 1978. Analysis of faulting in three-dimensional strain field. Tectonophysics, 47: 109-129.

Fault rocks

Sibson, R., 1977. Fault rocks and fault mechanisms. Journal of the Geological Society, 133: 191-213.

Other

Horsfield, W.T., 1977. An experimental approach to basement controlled faulting. Geologie en Mijnbouw, 56: 363-370.

Peacock, D.C.P., Knipe, R.J. & Sanderson, D.J., 2000. Glossary of normal faults. Journal of Structural Geology, 22: 291-305.

Fault displacement rates

Roberts, G.P., and Michetti, A.M., 2004, Spatial and temporal variations in growth rates along active normal fault systems: an example from The Lazio – Abruzzo Apennines, central Italy: Journal of Structural Geology, v. 26, p. 339-376.

Morewood, N.C., and Roberts, G.P., 2002, Surface observations of active normal fault propagation: implications for growth: Journal of the Geological Society, v. 159, p. 263-272.

CHAPTER 9

Kinematics and paleostress in the brittle regime

Populations of faults, slip surfaces and extension fractures contain important information about the deformation history and strain field. Even the stress field at the time of fracturing can be explored if some fundamental assumptions are made. Some of these assumptions may seem unrealistic when dealing with naturally deformed rocks. However, in most cases where they can be tested against independent observations these stress inversion methods seem to give reasonable results. It is of fundamental importance to be able to determine the displacement vector and sense of movement (kinematics) of faults, and to distinguish between different generations or movement. Hence, kinematic analysis is important in field-based studies of brittle deformation.

1.9 Kinematic criteria

The true finite displacement vector on a fault surface can be found directly where a point in the hanging wall can be connected to an originally neighboring point in the footwall. Such points can be faulted fold hinges or other recognizable linear structures that intersect with the fault surface. Unfortunately, such points are rarely found. In most cases we are pleased if we can correlate layers or seismic reflectors from one side to the other. If the fault surface is exposed in the field we would use the lineation on the fault surface to estimate the orientation and length of the displacement vector. The assumption is typically made that the lineation on the fault surface represents the displacement direction. It may, however, be that the lineation only records the last part of the deformation history, i.e. the last slip event(s), and that earlier slip events have been overprinted by this structure. Careful searching for multiple, overprinting lineations is therefore called for when collecting fault slip data in the field.

In other cases it is not even possible to correlate stratigraphy or marker horizons from one side of the fault to the other. We do not have any information about the size of the fault (although the width of the damage zone and fault core may give us some hints), and we do not even know whether the fault movement was reverse or normal, sinistral or dextral. Again the lineation on the fault surface is useful, but we need to apply independent kinematic criteria in order to determine the sense of slip. Many such criteria exist, although many of them tend to be unequivocal. Hence, as many kinematic criteria as possible must be combined for kinematic analysis in these cases.

1.9.1 Mineral growth and stylolites

Fault surfaces are seldom perfectly planar structures. Kinematic structures may form where geometric irregularities occur in the slip direction. Where an irregularity causes local contraction, contractional structures such as stylolites and ”cleavage” may be found (Figures 9.1 and 9.2).

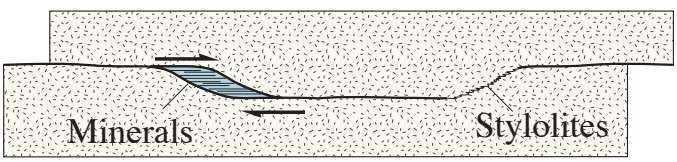

Figure 9.1 Irregularities along a fault can result in room for mineral growth (opening mode) or shortening where stylolites or compactional structures form. The localization of such structures relative to the local fault geometry gives reliable information about the sense of slip.

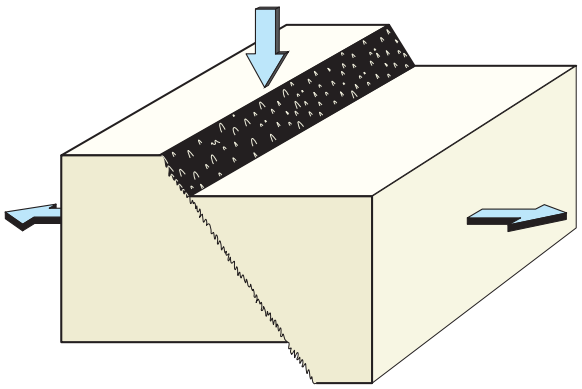

Figure 9.2 Faults with a component of shortening across the fault surface can result in pressure solution and stylolite formation in limestone and marble. Linear stylolitic structures sometimes form, called slickolites. Slickolites form a lineation that parallel the movement direction quite precisely.

Conversely, differently oriented irregularities may cause extension and opening of voids where mineral growth takes place (Figure 9.1). A study of the relation between fault surface geometry and the occurrence of contractional versus extensional structures may reveal the sense of slip with a high degree of confidence.

1.9.2 Subsidiary fractures

Small fractures developed along a fault or slip surface may show geometric arrangements that carry information about the sense of slip on the fault. These small fractures have been given different names depending on their orientations and kinematics (Figure 9.3). *T-fractures* are simply the name often used for small extension fractures in this setting. They may be open but are more commonly mineralized with quartz or carbonates and do not show striations. The orientation of T-fractures with respect to the main or average slip surface or *M-surface* characterizes the sense of slip. If the M-surface is oriented horizontally, T-fractures will dip around 45° in the slip direction (Figure 9.3).

A set of shear fractures, known as *P-fractures*, is sometimes seen to dip in the opposite direction. With M still being horizontal, these make low angles to M and kinematically correspond to low-angle ”reverse” or ”thrust faults”. In this setting Riedel shear fractures or *R-fractures* represent low-angle normal ”faults” while R’*-fractures* correspond to antithetic reverse faults that make a high angle to M. Riedel fractures tend to be more common than R’ and P, but they all exist and their local kinematics as well as their orientation with respect to M reveal the sense of movement on the main structure. T-structures are perhaps the most reliable of these, because it is easy to distinguish from

the various shear fractures.

Jean-Pierre Petit separated the various structures that one may see along fault surfaces as T, P and R-criteria, where the letters T, P and R indicate the dominating subordinate fracture element of the structure. *T-criteria* comprise extension fractures (T) that intersect the striated fault slip surface (M). In cross section T and M tend to form an acute angle of intersection pointing against the slip direction, as shown in Figure 9.3a. The intersections may also occur as curved structures pointing toward the direction of slip (Figure 9.3b). Such structures resemble glacial chatter marks that form when flowing ice plucks pieces off fairly massive bedrock such as quartzite or granite.

P-criteria are dominated by P-fractures and may occur together with T-fractures (Figure 9.3c). P-surfaces are not as well striated as R- and M-fractures, and they are characterized by their low angle to M. Situations where undulations of the main slip surface create a systematic pattern with striations on the side facing the movement of the opposite wall (contractional side) and no striations on the lee (extensional) side (Figure 9.3d) can also be regarded as P-criteria.

R-criteria, which is the most commonly used type of kinematic criterium, are based on the acute angle between R and M (Figure 9.3e and f). The lines of intersection between R and M show a high (close to 90°) angle to the striae on M. Curved, lunate fractures are also common (Figure 9.3f). Faults with small offsets may not have developed a through-going slip or M-surface, in which case the fault may be defined by en-echelon arranged R-fractures (Figure 9.3g), and sometimes also R'-fractures. The R-fractures are then closely arranged and striations are not well developed.

1.9.3 Ploughing, mineral growth and slickensides

Asperities or relatively hard objects (rock fragments, pebbles or strong mineral grains) on one side of a fault surface may mechanically plough grooves or *striations* into the opposing wall. Material in front of the object is being pushed aside, while a lunate opening occurs on the lee side, typically filled with material from the opposite wall. A ridge may sometimes be found ahead of the object, as shown in Figure 9.4.

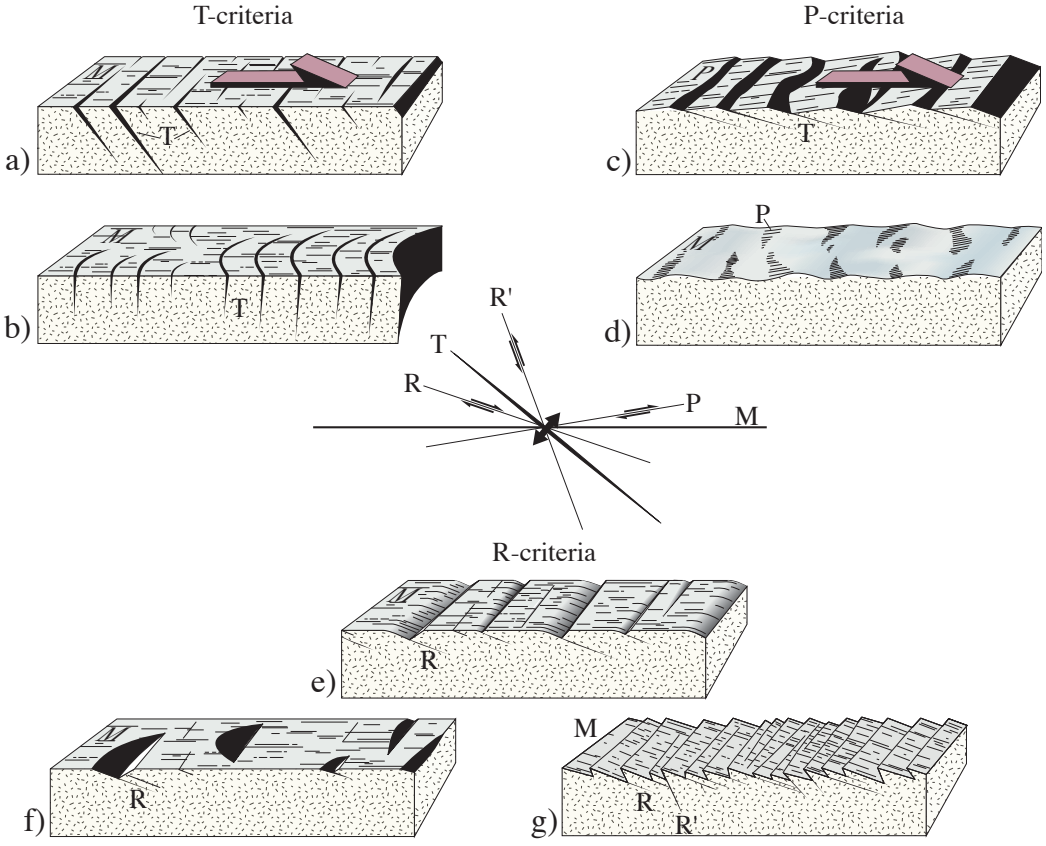

Figure 9.3 Kinematic criteria along a fault with subordinate fractures or irregularities. The criteria are related to the general nomenclature used for fractures in a shear system in the brittle regime (R, R', P, T and M fractures). M = the average slip surface (fault), T = tension fractures, R = Riedel shears. Identification of the type of subordinate fracture helps interpret the movement on the fault. Based on Petit (1987).

The lunate opening soon evolves into a groove whose length ideally corresponds to the movement of the hard object relative to the rest of the wall. At least that's what we would like to think. But there are many examples of cm-scale offsets causing decimeter- or even meter-long striations. Hence, there must be other mechanisms at work than just physical carving. One explanation is that some striations are *corrugations* that did not form purely as frictional grooves. These are linear structures that formed at the initial stage of fracture growth and may be polished and striated as slip accumulates. The result may be long and well-developed striae on slip surfaces that have very small (cm or even mm-scale) offsets. Hence, small-scale fault corrugation structures do *not* necessarily reflect the amount of slip on the surface. Striations are typically found on (but not restricted to) polished slip surfaces called *slickensides*, where the striations are known as *slickenlines*.

In addition to frictional striations, minerals may crystallize on the lee side of asperities (irregularities), thus revealing the sense of slip. When minerals crystallize as fibers, the orientation of the fibers tends to be close to the slip direction. It is commonly found that minerals precipitated on fault slip surfaces are subsequently affected by renewed slip. It is therefore common to see slickenlines developed on deformed mineral fill along fault surfaces. Lineations related to fractures are further discussed in Chapter 13.

1.10 Stress from faults

Fault observations used in paleostress analysis include the local strike and dip of the fault surface, the orientation of the lineation (usually given by its rake or pitch) and the sense of movement. When such data are collected for a fault population it is in principle possible to obtain information not only about strain but also about the orientation of the principal stresses (σ_1, σ_2 and σ_3) and their relative magnitudes (i.e. the shape of the stress ellipsoid). Paleostress methods hinge on several assumptions. The most basic is that the faults in question formed in the same stress field. Others are that the rocks are fairly homogeneous and that the structures did not rotate significantly since they were initiated.

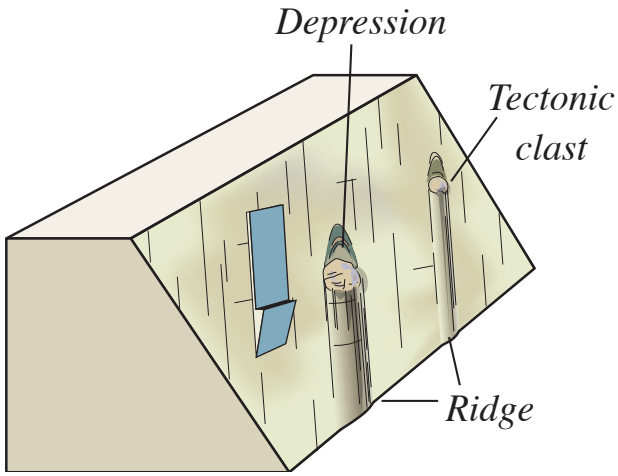

Figure 9.4 Pointed asperities or tectonic clasts sitting on fault surfaces may form lunate depressions on the lee side and and ridges on the opposite side. Such lineations are called groove-mark lineations.

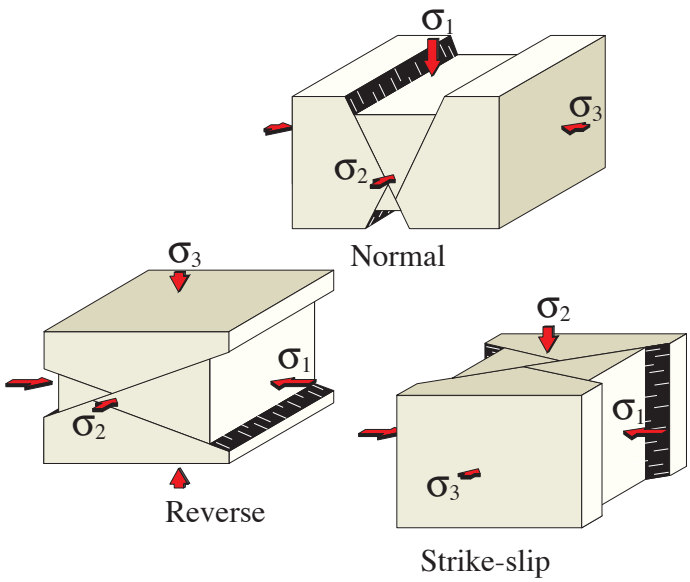

Figure 9.5 Conjugate shear fractures and their relation to stress according to Anderson's conditions for planar strain. Note that the acute angle is bisected by σ_1 and the two fractures intersect along σ_2.

1.10.1 Conjugate sets of faults

A simple case of deformation is *plane strain*[1] expressed in terms of conjugate fault systems. A conjugate system has two sets of oppositely dipping faults where the lineations are perpendicular to the line of fault intersection (Figure 9.5). The sense of slip is complementary on the two sets, and the angle between the two sets should be constant. According to Coulomb's fracture criterion, which tells us that faults or shear fractures form at an angle to σ_1 that is controlled by the internal friction of the rock, the angle between the two sets should be consistent with the mechanical properties of the rock (and the pore fluid pressure) at the time of deformation. More importantly, conjugate

1 Do not confuse stress with strain here. There are always three stress axes (even for plane strain), although no strain occurs along the intermediate principal strain axis.

sets should develop symmetrically about the principal stresses for both normal, reverse and strike-slip faults (Figure 9.5). According to the Andersonian theory of faulting (p. ?), the slip direction or lineation would be in the dip direction (reverse and normal faults) or in the strike direction (strike-slip faults). Hence, conjugate faults and their striations reveal the orientations of the principal stresses. In some cases we may find that the principal stresses deviate somewhat from the horizontal/vertical directions predicted by Anderson, which may indicate that the area has been tilted since the time of deformation or that the stress field was rotated or refracted through this volume of rock. As mentioned in Chapter 6, such deviations can occur near large and weak faults or joint zones.

Two conjugate sets of faults indicate plane strain (Figure 9.6 a-b), and the strain axes are found by plotting the fault sets in a stereonet (Figure 9.6c). The orientation of the principal stress axes can be inferred based on the assumption of isotropic rheology, constantly oriented stress field and negligible rotation of the fault blocks. In fact, we can draw a parallel between conjugate sets observed in rock mechanics experiments and their angular relation to the principal stresses.

In other cases fault systems may contain more than two conjugate sets. A simple case is shown in Figure 9.6 d-e, where two genetically related pairs of fractures coexist. This constellation is referred to as *orthorhombic* based on its symmetry elements. Again, the strain axes are easily found from stereoplots, and the stress axes can be inferred (Figure 9.6e).

1.10.2 Complex fault populations

Conjugate fault sets do occur in nature, particularly in rocks that have experienced a single phase of brittle deformation. In most cases, however, fracture patterns show more complicated arrangements. Furthermore, fracture populations are likely to get reactivated through time, and we would like to know something about how an already existing fracture population will respond to a given new stress field.

This is not a trivial thing to predict in detail, but there are some important statements that can be made. The most important one is the fact that planes (fractures) oriented perpendicular to one of the three principal stresses will not slip. This is reasonable since there is no shear component in this situation (σ_s=0). For any other orientation $\sigma_s \neq 0$ and frictional sliding (slip) will occur if σ_s exceeds the frictional resistance against slip. It seems reasonable to make the assumption that slip on a surface will occur in the direction of maximum resolved shear stress. If the largest shear stress is in the dip direction we will get

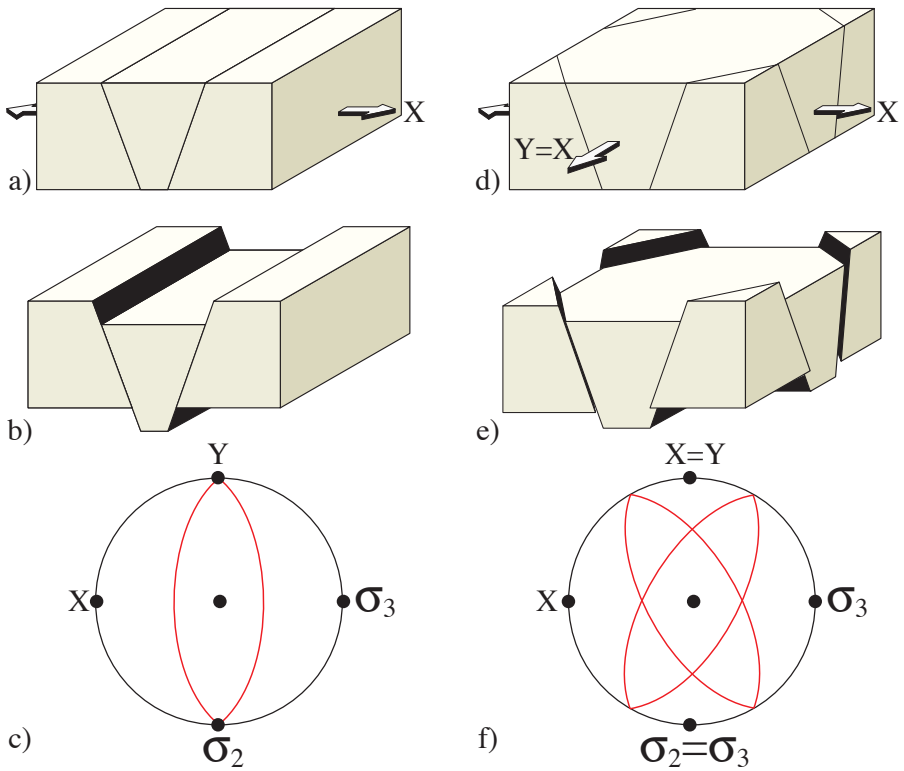

Figure 9.6 A single pair of dip-slip conjugate fault sets (a-c) form in plane strain, while multiple sets require 3D strain (d-f). The patten shown in e) is called orthorombic from its high degree of symmetry. In these idealized cases the principal stresses and strains are parallel.

normal or reverse faults. If the maximum shear stress vector is horizontal, strike-slip faulting results. Any other case results in oblique-slip movements. This assumption is known as the *Wallace-Bott hypothesis*:

Slip on a planar fracture can be assumed to occur parallel to the greatest resolved shear stress.

The hypothesis implies that the faults are planar, fault blocks are rigid, block rotations are negligible and that the faults formed during the same phase of deformation under a uniform stress field. Clearly, these are simplifications. For example, intersecting faults have the potential to locally perturb the stress field. On the other hand, empirical observations and numerical modeling suggest that the deviations are relatively small in most cases, suggesting that the Wallace-Bott hypothesis is a reasonable one. Building on these simple assumptions we can measure a fault

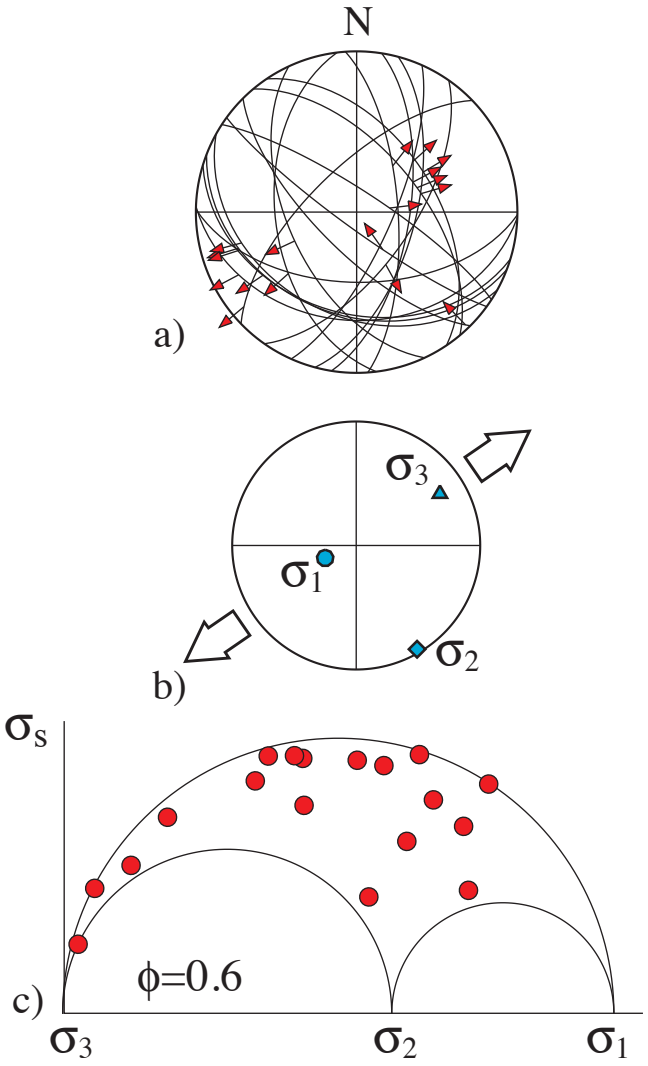

Figure 9.7 a) Actual fault data, shown by great circles (fault surfaces) and arrows (lineations) on an equal area lower hemisphere plot. b) Principal stresses found from stress inversion. c) The data plotted in the dimensionles Mohr-diagram, indicating a relation between the principal stresses (ϕ =0.4).

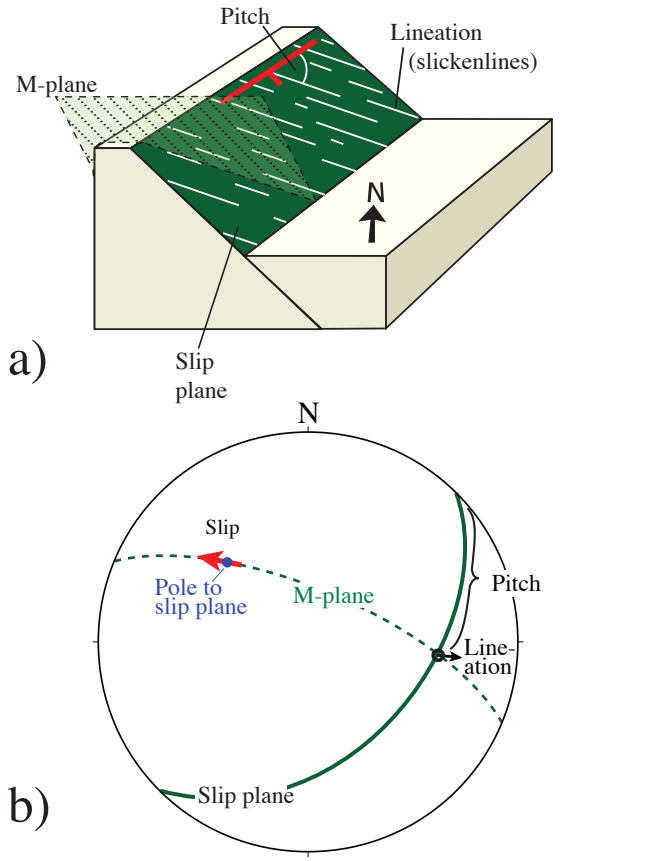

Figure 9.8 **a)** Schematic illustration of pitch as measured on a fault surface. b) The pitch plotted in a stereonet (lower hemisphere, equal area). This projection also shows how the tangent-lineation is found for a known slip plane (as shown in a) and its lineation (striation) by plotting a plane (the movement or M-plane) that contains the lineation and the pole to the slip plane. The tangent-lineation (red arrow) is the arrow drawn tangential to the M-plane at the pole to the slip plane. Its direction describes the movement of the footwall relative to the hanging wall, in the present case a normal movement, where the footwall moves up to the W.

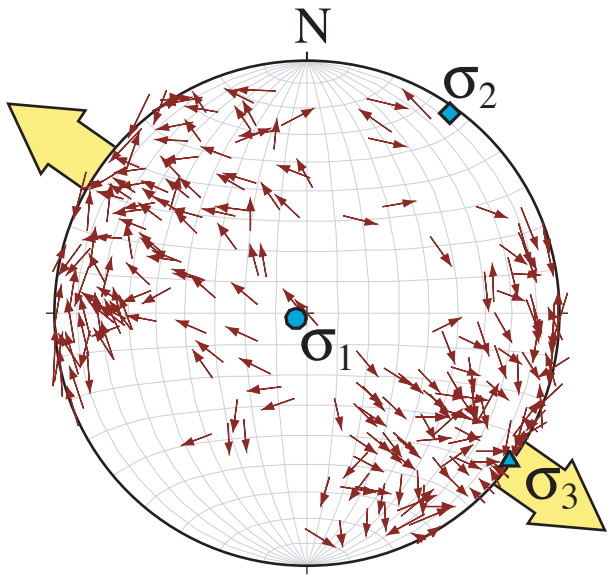

Figure 9.9 Tangent-lineation diagram for fault data from basement gneisses west of Bergen, Norway. σ_1 can be defined, but the ϕ-value, which in principle is found by comparing with the next figure, is difficult to define. This is quite common and is partly due to limited variation in fault orientations.

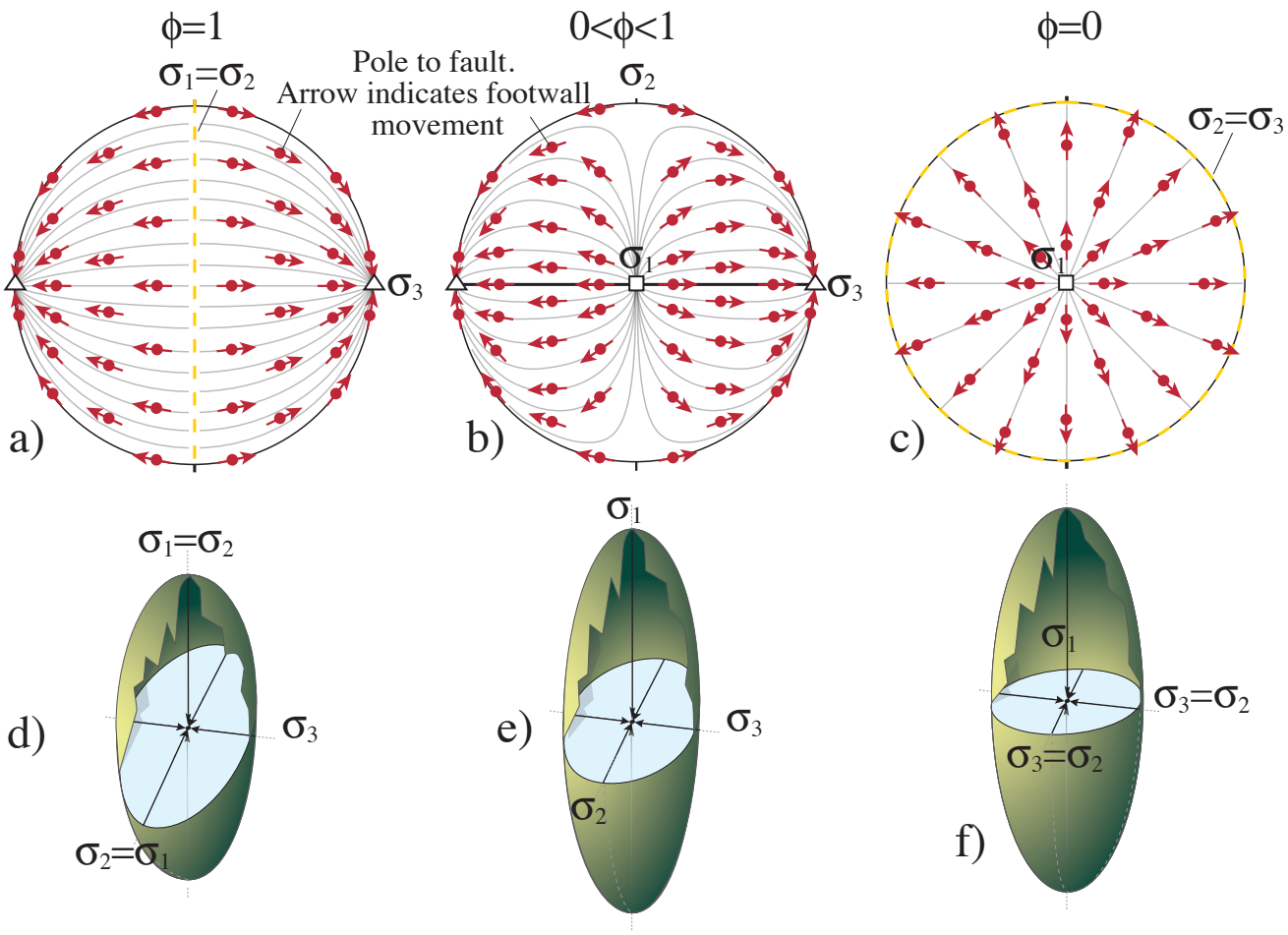

Figure 9.10 a-c) Stereographic projection of poles to faults (points). Arrows indicate footwall versus hanging wall movements. The pattern emerges by considering faults with different orientation, and the assumption is made that the movement is parallel to the direction of maximum shear stress on each surface. The pattern depends on the ratio between the principal stresses, expressed by ϕ. By plotting field data in these diagrams one can obtain an estimate for the orientation of the principal stresses and ϕ. The geometry of the strain ellipsoid is shown (d-f). Based on Twiss & Mores (1992).

population with respect to fault orientation, lineations and sense of slip and use these data to calculate the orientation and relative size of the stress axes. The methods used for this purpose are known as stress inversion techniques.

1.10.3 Paleostress from fault slip inversion

While the absolute values of the principal stresses are unachievable in most cases, their relative magnitude, i.e. the shape of the stress ellipsoid, can be estimated from fault population data. For this purpose we use the stress ratio

$$\phi=(\sigma_2-\sigma_3)/(\sigma_1-\sigma_3) \quad (9.1)$$

where $0\leq\phi\leq1$. The ratio ϕ is also called R^2. ϕ=0 for a prolate stress ellipsoid, where $\sigma_2=\sigma_3$ (uniaxial compression). ϕ=1 implies that $\sigma_1=\sigma_2$, and the stress ellipsoid is oblate (uniaxial tension). We use this ratio to express the stress tensor, which in the coordinate system defined by the principal stresses is:

$$\begin{bmatrix}\sigma_1 & 0 & 0\\ 0 & \sigma_2 & 0\\ 0 & 0 & \sigma_3\end{bmatrix} \quad (9.2)$$

An isotropic stress component can be added to the stress tensor, and they can be multiplied by a constant without changing the orientation and shape of the stress ellipsoid. The stress tensor that contains this

2 Note that R is defined as 1-ϕ by some authors.

information is known as the *reduced stress tensor*, which is here expressed in terms of two constants *k* and *l*, where k=*l*/(σ_1-σ_3) and *l*=-σ_3:

$$\begin{bmatrix} \sigma_1 + l & 0 & 0 \\ 0 & \sigma_2 + l & 0 \\ 0 & 0 & \sigma_3 + l \end{bmatrix} \begin{bmatrix} k & 0 & 0 \\ 0 & k & 0 \\ 0 & 0 & k \end{bmatrix} = \begin{bmatrix} 1 & 0 & 0 \\ 0 & \phi & 0 \\ 0 & 0 & 0 \end{bmatrix} \quad (9.3)$$

Adding the constant *l* to each principal stress is the same as adding an isotropic stress. Furthermore, multiplying the axes by the constant *k* means contracting or inflating the stress ellipsoid while maintaining its shape.

While the full stress tensor contains six unknowns, the reduced tensor contains only four unknowns, represented by ϕ and the orientation of the principal stresses. In other words, the reduced stress tensor gives us the orientation and shape of the stress ellipsoid. While we have discussed how stress influences slip on fractures (by causing slip in the direction of the maximum resolved shear stress), the inverse problem where the (reduced) stress tensor is calculated from slip data is more relevant to paleostress analysis.

By inversion of fault slip data we mean reconstructing the orientation and shape of the stress ellipsoid based on measured fault slip data.

Because the reduced stress tensor has four unknowns we need data from at least four different fault surfaces to find the tensor. The tensor that fits all the data is the tensor we are looking for. However, because of measuring errors, local stress deflections, rotations etc., we are searching for the tensor that best fits the fault slip data. We therefore collect data from more than four slip surfaces, usually 10-20 or more. This gives many more equations than unknowns, and a statistical model is applied that minimizes the errors.

The calculations are done by a stress inversion program, of which several are available. The results are presented in stereoplots that show the orientations of the principal stress axes, and in dimensionless Mohr-diagrams that suggest the relative sizes of the principal stresses (Figure 9.7). During the calculation of the reduced stress tensor there may be remaining data that do not fit in during the calculations. These may be treated separately to see if they together define a second tensor that may relate to a separate tectonic event. A safer way to distinguish between subpopulations is to use field criteria such as cross-cutting relations and characteristic mineral phases on slip surfaces.

A geometric way of extracting stress from fault slip data is to construct *tangent-lineation diagrams*. This is done by plotting each fault plane and its lineation, the M-plane, which contains the pole to the fault plane and the lineation, and by drawing an arrow tangent to the M-plane at this pole (Figures 9.8 and 9.9)[3]. The direction of the arrow reflects the movement of the footwall relative to the hanging wall. When differently oriented slip surfaces are plotted, the resulting pattern reveals both the orientations and the relative magnitudes (ϕ) of the principal stress axes (Figure 9.10). Clearly, many data points from faults with a variety of orientations are required to obtain a reliable result.

Paleostress analyses need to be treated with care for several reasons. One is the fact that they heavily depend on our ability to identify fault populations formed under a stress field that is constant during the history of faulting. Another is that the stress field needs to be uniform. We know that fault interaction, as well as any mechanical layering, tends to perturb the stress field, so this assumption is likely to be an approximation only. Outputs from paleostress analyses have to be interpreted in the light of these facts and additional locality-specific circumstances.

1.11 A kinematic approach to fault slip data

Because the paleostress method based on inversion of fault slip data relates stress and slip based on the Wallace-Bott hypothesis and several assumptions that clearly are not met in full in practical examples, some geologists prefer a purely kinematic approach where strain and strain rate rather than stress are treated. Graphically the method consists of plotting the fault planes and corresponding slip-related lineations in a stereoplot (Figure 9.11). Based on the orientation and sense of slip, a P- and T-axis are found for each fault plane. These axes are symmetry axes of the contractional and extensional quadrants. They are perpendicular to each other and are contained in the plane that is perpendicular to the fault plane. This plane also contains the lineation (slip direction). Furthermore, P and T make 45° to the fault plane

3 Software, such as FaultKin, does this for you, but we should understand what the program does to our data.

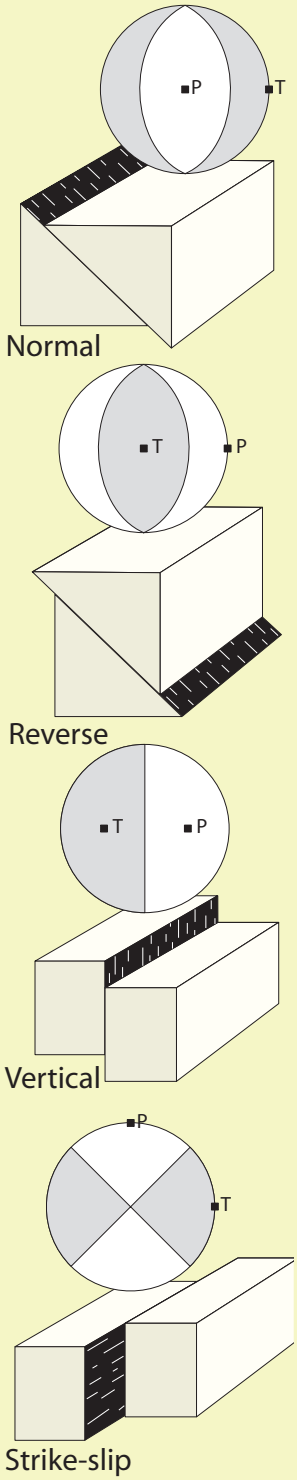

FOCAL MECHANISMS AND STRESS

A so-called *fault-plane solution* is found by mapping the distribution of P- or S-waves around the hypocenter of an earthquake. The actual fault plane and its complementary, orthogonal theoretical shear plane (together called nodal planes) are plotted as stereographic projections based on the principle that the sense of slip (normal, reverse etc.) on a fault controls the distribution of seismic waves. The nodal planes are found by using observations of the first P-wave movement at various seismic stations, i.e. whether they are compressive or tensile. The planes are plotted as stereographic projections, and the result is the well-known "beach-ball"-style projections shown to the left. Information about the first arrivals (compressive P or tensile T) from several seismologic observatories is used to construct and constrain the orientations of the nodal planes and their senses of movement, known as the focal mechanism. The quadrants are separated by the fault plane and the complementary nodal plane, and the P- and T-axes are plotted in the middle of the quadrants. As shown to the left, different "beach balls" indicate different focal mechanisms or sense of fault movement.

Which of the two nodal planes actually represents the fault plane is unknown from seismic data alone, unless aftershock analysis is involved. Only the P- and T-axes are known. P and T are *not* identical to σ_1 and σ_3, although this erronious assumption is too commonly made. With a crust full of weak structures many earthquakes must be expected to result from reactivation of preexisting fractures. There is therefore no precise relation between fault orientation and the stress field. However, we know that σ_1 must lie in the P field, and σ_3 in the T-field. Thus, observations from multiple earthquakes on variously oriented faults gives a distribution of data that increases our chances of a good estimate of the stress axes. In principle we can use stress inversion to estimate the principal stresses.

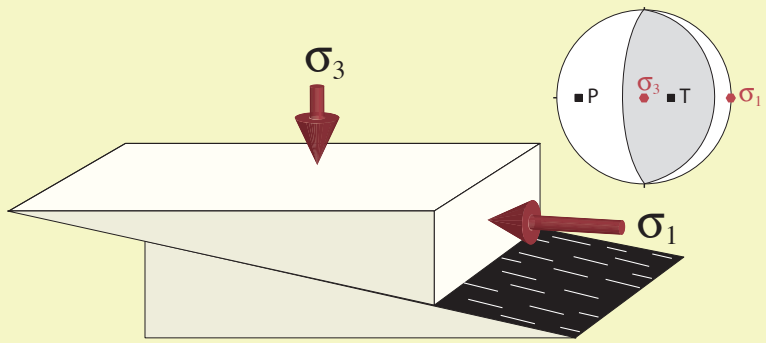

Example where the principal stresses and the P- and T-axes are not identical. A low-angle thrust fault is activated with a vertical σ_3 and a horizontal σ_1. Since P and T always bisect the nodal planes the principal stresses and the P- and T-axes will only coincide if the fault is oriented at 45° to σ_1.

(Figure 9.11). The position of T and P depends on the fault movement sense (normal, reverse, sinistral or dextral).

A pair of P and T-axes is found for each fault in the fault population. For fault populations with a distribution in fault orientations we end up with a distribution of P- and T-axes. Ideally, they should be separated by two orthogonal surfaces, which are fitted to the plot. Y (the intermediate strain axis) is represented by the line of intersection between the planes, while Z and X are located in the middle of the P- and T-fields, respectively (Figure 9.11c). This gives the orientation of the stress (or strain) axes – the magnitude can only be approached by adding information about displacement and area of each fault. Also the kinematic method is quickly done by means

of a computer program, and in most cases it can be shown that the strain axes found by this method are very similar to the stress axes found by inversion of slip data as described in the previous section. The kinematic method also relies on a uniform strain field and separation of slip information generated during different phases of deformation.

1.12 Contractional and extensional structures

While analyses of fault slip data are concerned with shear fractures and faults, contractional and extensional structures are also useful for stress or strain rate considerations. Contractional structures, also known as anticracks, are found as solution seams or stylolites in some (mostly) brittlely deformed rocks. In general, such structures represent small strains with little or no rotation. A close connection between stress and strain axes can therefore be expected in many cases. The same is the case with low-strain extension structures such as veins and joints. While contractional structures tend to form perpendicular to σ_1, extensional fractures form perpendicular to σ_3. The combination of contraction and extension structures is particularly valuable, and when occurring in faulted rocks these structures can be used in or compared to the results of stress-inversion methods.

A related kinematic method involves the reconstruction of walls displaced during dike intrusion. Magma overpressure during intrusion may cause fracturing of the surrounding rock, into which magma flows to form dikes. In the presence of a significant tectonic stress, the fractures and thus the dikes are oriented perpendicular to σ_3. In most cases, however, the rock contains preexisting fractures that will be filled with magma. Fractures with an orientation close to perpendicular to σ_3 will preferentially open, but in order to estimate strain and stress we have to look for points on each side of the dike that once were adjacent

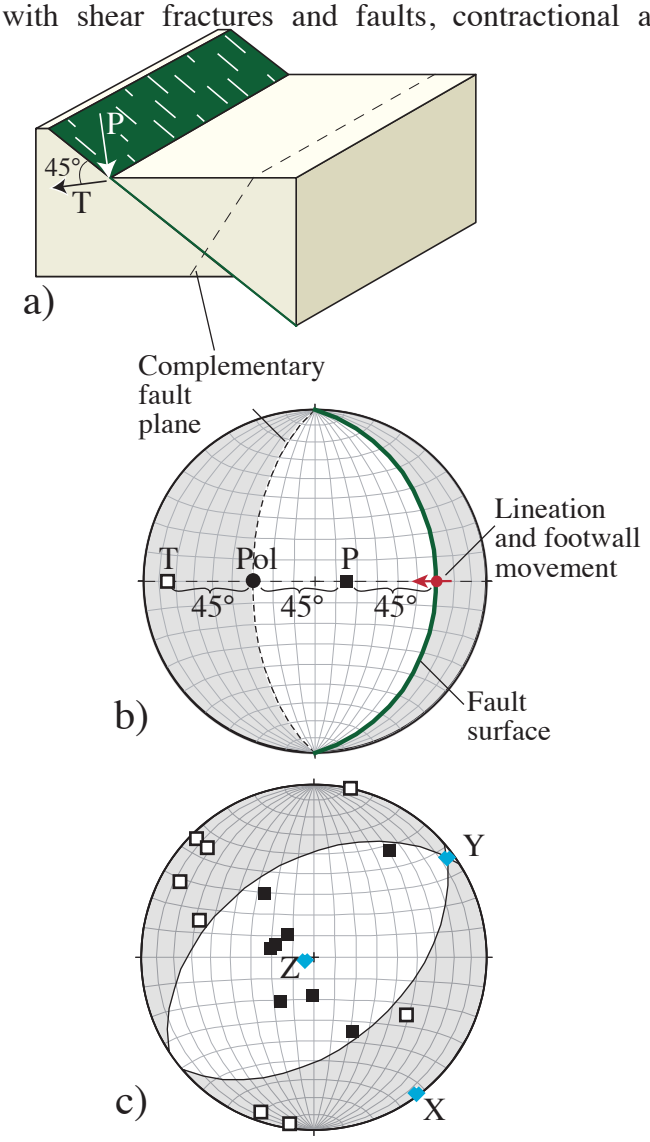

Figure 9.11 Kinematic analysis of fault data. a) a simple normal fault. b) Plot of the fault, the lineation and the sense of movement. The complementary shear plane oriented 90° to the fault is shown (pole). The T- and P-axes bisect these two planes. c) Data from 16 faults with different orientations. Each of the faults is plotted as illustrated in b). Ideally, the P- and T-axes will plot within two sectors separated by two mutually orthogonal planes. If they do not, then the conditions are not fulfilled; they may for example have formed in two different stress fields. 16 data points are a minimum, but indicate a NW-SE stretching and vertical shortening, i.e. an extensional regime.

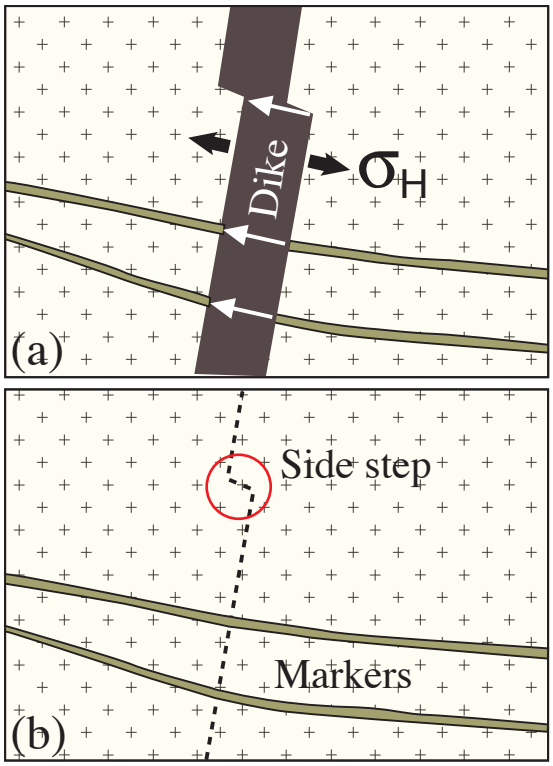

Figure 9.12 Reconstruction of a horizontal section (a) to the situation prior to dike intrusion (b). Arrows can be drawn between points that once were neighbors to find displacement vectors. For small strains these vectors approximate σ_H.

to each other. Such points can be corners where dikes step sideways (Figure 9.12). In these cases displacement vectors can be constructed by drawing connecting lines between separated corners, as shown in Figure 9.13. Older structures that were separated by dikes can also be used, such as veins, older dikes, fold hinges and steeply dipping layers. In these cases we observe strain (the local extension direction), but because of the small displacements usually involved it is reasonable to correlate horizontal extension with σ_H. Assuming that the vertical stress is a principal stress axis, $\sigma_H=\sigma_3$. It is the local stress that is found, and it is not uncommon to find that dikes rotate in the vertical direction into a fringe-like geometry such as shown in Figure 9.14. Such geometries indicate that the σ_H changes direction in the vertical direction, similar to fringe zones around fractures (Figure 7.23).

---”””---

There are other methods to find the orientation of stress in the upper crust. In particular you should be aware that deformation twins in calcite can be used. This is also low-strain deformation, which is characteristic for all paleostress methods. Once strains get higher, particularly in non-coaxial settings, rotation of structures occur, and stress-strain relations tend to get complicated. In all cases, one should be aware of the fact that stress can only be deduced from strain patterns and never observed directly. Some assumption must always be made to go from strain observations to stress. It is therefore wise to maintain some humility when extracting paleostress information from deformation structures in rocks.

Figure 9.13 Side-stepping dike intrusion, well suited for stress determination. The corners were connected prior to the intrusion, and the extension direction, which can be assumed to be close to the minimum principal stress, is found by connecting the corners. Permian dike along the shoulder of the North Sea rift system.

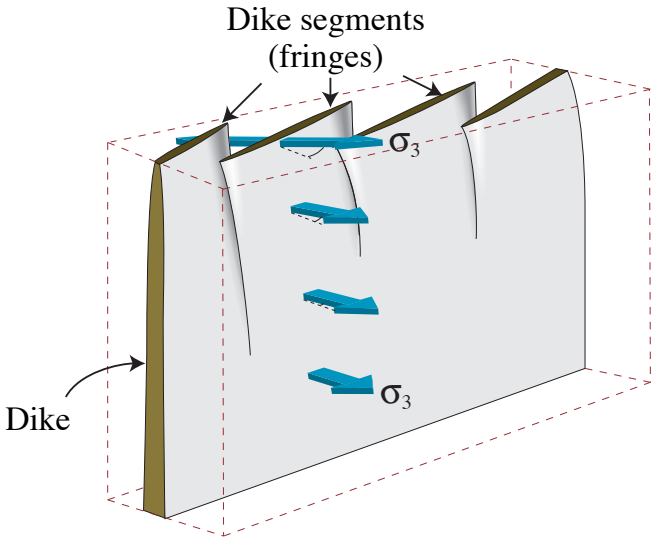

Figure 9.14 En echelon dike system that are connected at depth – one of Anderson's popular interpretations published in 1951. Anderson interpreted this phenonemon as the result of an upward rotation of σ_3 towards the surface during magma intrusion.

Further reading:

Anderson, E.M., 1951. The dynamics of faulting. Oliver & Boyd, Edinburgh, 191 ss.

Sense of slip

Petit, J.-P., 1987. Criteria for the sense of movement on fault surfaces in brittle rocks. Journal of Structural Geology, 9: 597-608.

Stress and strain from fault populations

Angelier, J., 1994. Fault slip analysis and palaeostress reconstruction. P.L. Hancock (Eds.), Continental deformation. Pergamon Press, Oxford, England, 53-100.

Cashman, P.H. & Ellis, M.A., 1994. Fault interaction may generate multiple slip vectors on a single fault surface. Geology, 22: 1123-1126.

Etchecopar, A., Vasseur, G. and Daignieres, M., 1981. An inverse problem in microtectonics for

the determination of stress tensors from fault striation analysis. Journal of Structural Geology, 3: 51-65.

Marrett, R. & Allmendinger, R.W., 1990. Kinematic analysis of fault-slip data. Journal of Structural Geology, 12: 973-986.

Stress from extension and contraction structures

Dunne, W.M. & Hancock, P.L., 1994. Paleostress analysis of small-scale brittle structures. P.L. Hancock (Red.), Continental deformation. Pergamon press, 101-120.

Fry, N., 2001. Stress space: striataed faults, deformation twins, and their constraints on paleostress. Journal of Structural Geology, 23: 1-9.

Jolly, R.J.H. and Sanderson, D.J., 1995. Variation in the form and distribution of dykes in the Mull swarm, Scotland. Journal of Structural Geology, 17: 1543-1557.

Valle, P., Færseth, R.B. & Fossen, H., 2002. Devonian-Triassic brittle deformation based on dyke geometry and fault kinematics in the Sunnhordland region, SW Norway. Norsk Geologisk Tidsskrift, 82: 3-17.

The relation between stress and strain

Marrett, R. & Peacock, D.C.P., 1999. Strain and stress. Journal of Structural Geology, 21: 1057-1063.

Twiss, R.J. & Unruh, J.R., 1998. Analysis of fault slip inversions: do they constrain stress or strain rate? Journal of Geophysical Research, 103 (B6): 12,205-12,222.

Watterson, J., 1999. The future of failure: stress or strain? Journal of Structural Geology, 21: 939-948.

CHAPTER 11

Folds and folding

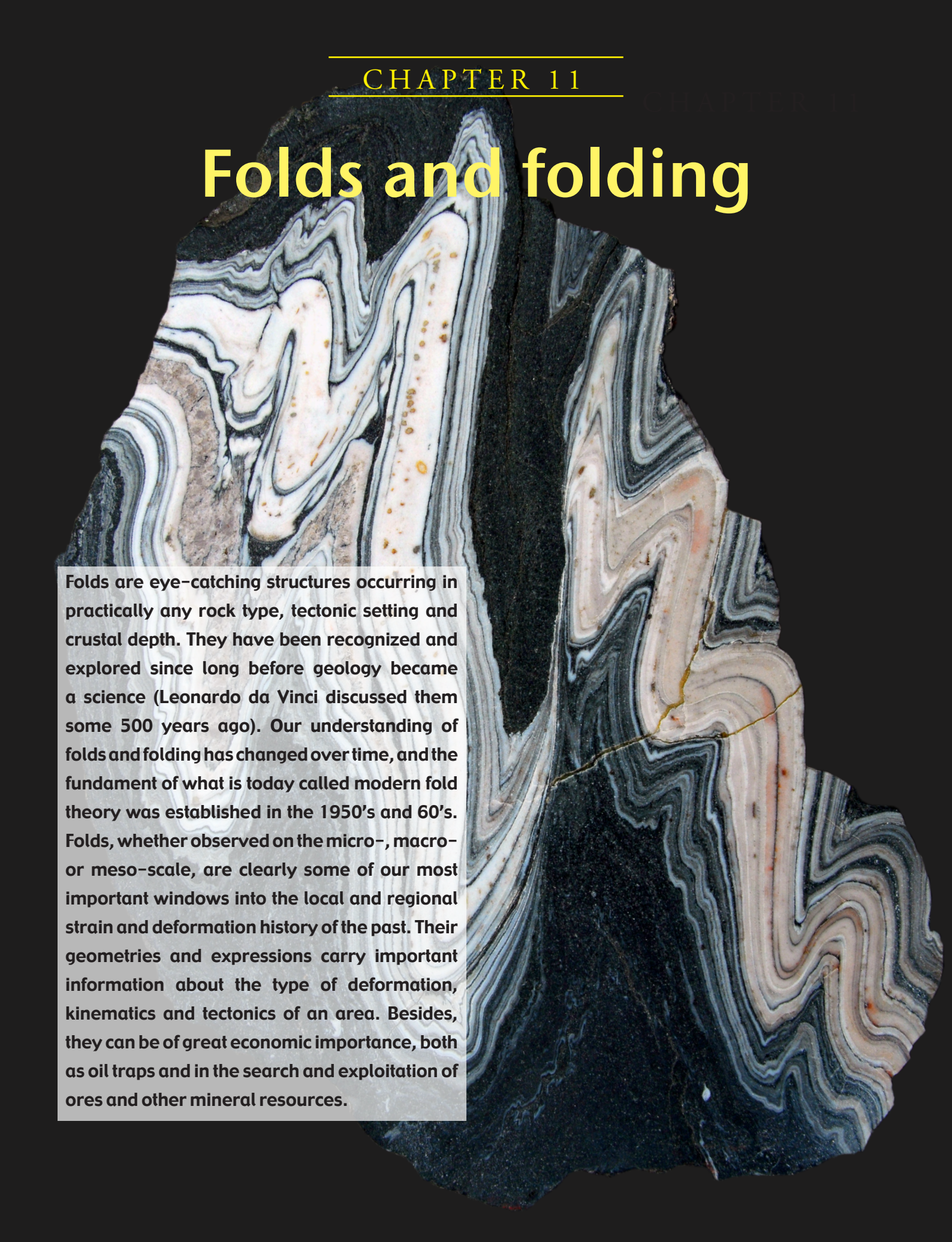

Folds are eye-catching structures occurring in practically any rock type, tectonic setting and crustal depth. They have been recognized and explored since long before geology became a science (Leonardo da Vinci discussed them some 500 years ago). Our understanding of folds and folding has changed over time, and the fundament of what is today called modern fold theory was established in the 1950's and 60's. Folds, whether observed on the micro-, macro- or meso-scale, are clearly some of our most important windows into the local and regional strain and deformation history of the past. Their geometries and expressions carry important information about the type of deformation, kinematics and tectonics of an area. Besides, they can be of great economic importance, both as oil traps and in the search and exploitation of ores and other mineral resources.

1.1 Geometric description

We can learn much about folds and folding by performing controlled physical experiments and numerical simulations, but modeling must always be rooted in observations of naturally folded rocks. Before going into a discussion about how folds form we need to be able to describe their geometry and occurrence accurately.

1.1.1 Single fold structures

A fold is, as shown in Figure 11.1, made up of a *hinge* that connects two usually differently oriented *limbs*. The hinge may be sharp and abrupt, but more commonly the curvature of the hinge is gradual, and a *hinge zone* is defined. The point of maximum curvature of the folded layer is located in the hinge zone and is called the *hinge point*. Hinge points are connected in three dimensions by a *hinge line*. The hinge line is commonly found to be curved, but where it appears as a straight line it is called the *fold axis*.

The *axial surface*, or *axial plane* when approximately planar, connects the hinge lines of a folded layered rock. The *axial trace* of a fold is the line of intersection of the axial surface with the surface of observation (e.g. the surface of an outcrop or a geologic section). The axial trace connects hinge points on this surface. Note that the axial surface does not necessarily bisect the limbs (Figure 11.2b).

Folds with straight hinge lines are *cylindrical* (Figure 11.3a). A cylindrical fold can be viewed as a partly unwrapped cylinder where the axis of the cylinder defines the *fold axis*. At some scale all folds are non-cylindrical, since they have to start and end somewhere, but the degree of cylindricity varies from fold to fold. In many cases folds look cylindrical at a certain scale of observation, for instance in an outcrop (Figure 11.4). Such cylindricity has important characteristics that can be taken advantage of. The most important is that the poles to a cylindrically folded layer define a great circle, and the pole (π-axis) to that great circle defines the fold axis (Figure 11.5a).

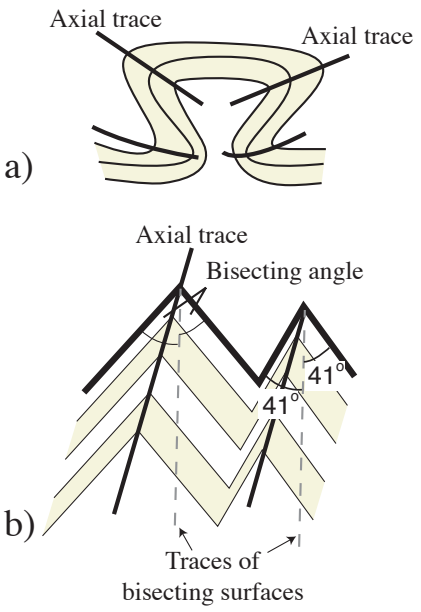

Figure 11.2 a) Boxfolds have two sets of axial surfaces. b) The bisecting surface, i.e. the surface dividing the interlimb angle in two, is not necessarily identical to the axial surface.

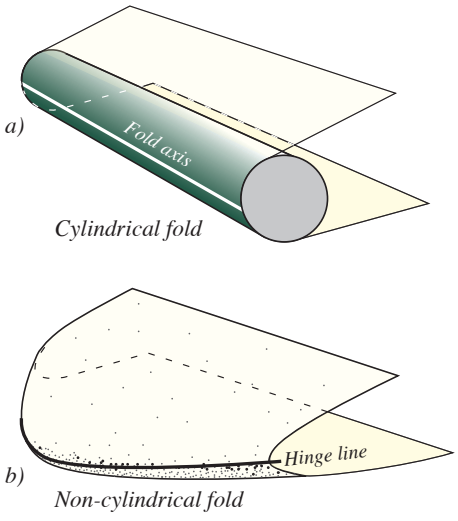

Figure 11.3 Cylindrical and non-cylindrical fold geometries.

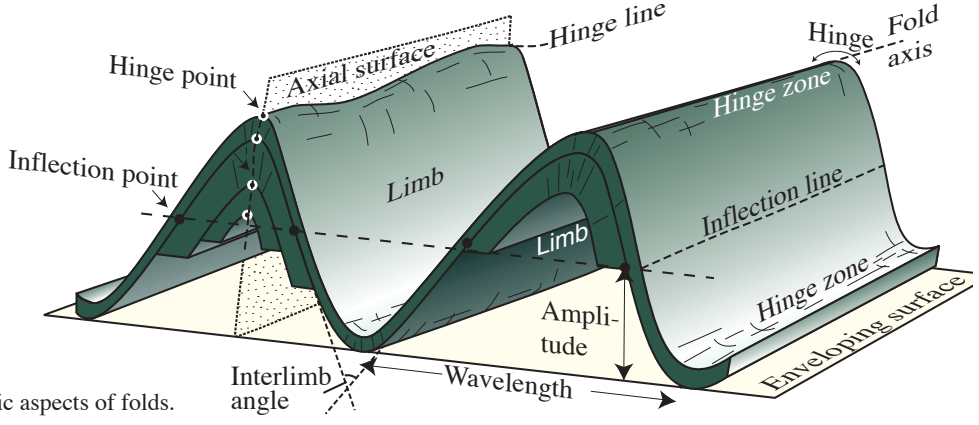

Figure 11.1 Geometric aspects of folds.

Figur 11.4 Cylindrical folded granite dike in amphibolite.

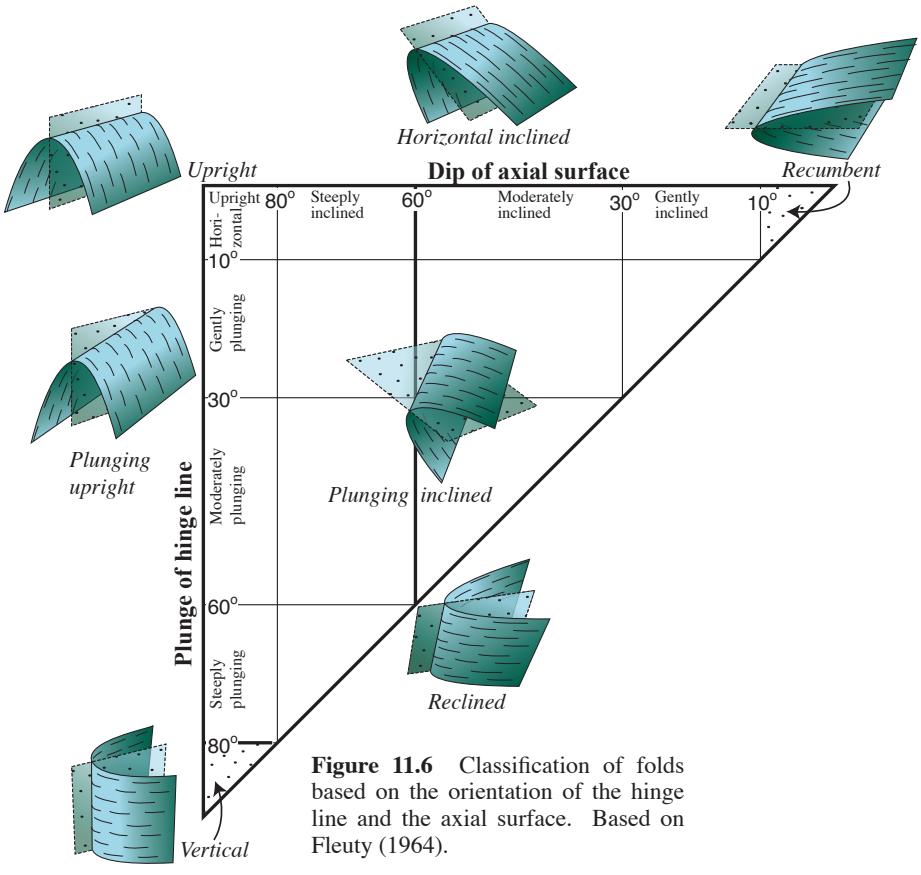

Figure 11.6 Classification of folds based on the orientation of the hinge line and the axial surface. Based on Fleuty (1964).

When great circles are plotted instead of poles, the great circles to a cylindrically folded layer will cross in a common point representing the fold axis, in this case referred to as the β-axis (Figure 11.5b). This method can be very useful when mapping folded layers in the field but also works for other cylindrical structures, such as corrugated fault surfaces.

A fold is described by the orientation of its axial surface and hinge line (Figure 11.6). Furthermore, folds can be characterized by their opening or *interlimb angle*, which is the angle enclosed by its two limbs. Based on this angle folds are separated into gentle, open, tight and isoclinal (Figure 11.7).

Most of the folds shown in Figure 11.6 are *antiforms*. An antiform is a structure where the limbs dip down and away from the hinge zone, whereas a *synform* is the opposite, trough-like shape (Figure 11.8b-c). Where a stratigraphy is given, an antiform is called an *anticline* where the rock layers get younger away from the axial surface of the fold (Figure 11.8e). Similarly, a *syncline* is a trough-shaped fold where layers get younger toward the axial surface (Figure 11.8d). Returning to Figure 11.6, we can have upright or plunging synforms as well as antiforms. We can even have recumbent synclines and anticlines, because their definitions are related to stratigraphy and younging direction. The terms recumbent and vertical antiforms and synforms have no meaning.

Imagine a tight to isoclinal recumbent fold being refolded during a later tectonic phase. We now have a set of secondary synforms and antiforms. The younging direction across their respective axial surfaces will depend on whether we are on the inverted or upright limb of the recumbent fold, as shown in Figure 11.8h.

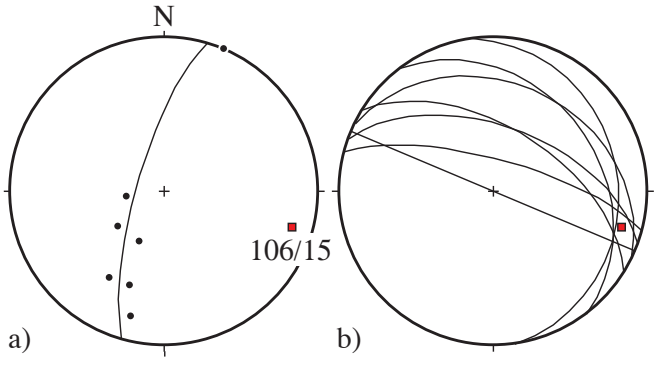

Figure 11.5 Measurements of bedding around a folded conglomerate layer. a) Poles to bedding plot along to a great circle. The pole to this great circle (π-axis=106/15) represents the fold axis. b) The same data plotted as great circles. For a perfectly cylindrical fold the great circles should intersect in the point (β-axis=106/15) representing the fold axis. Data from a natural fold (Fossen 1988).

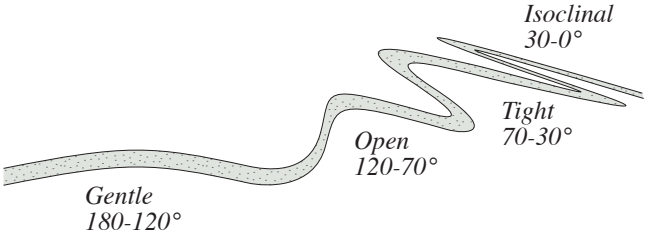

Figure 11.7 Fold classification based on interlimb angle.

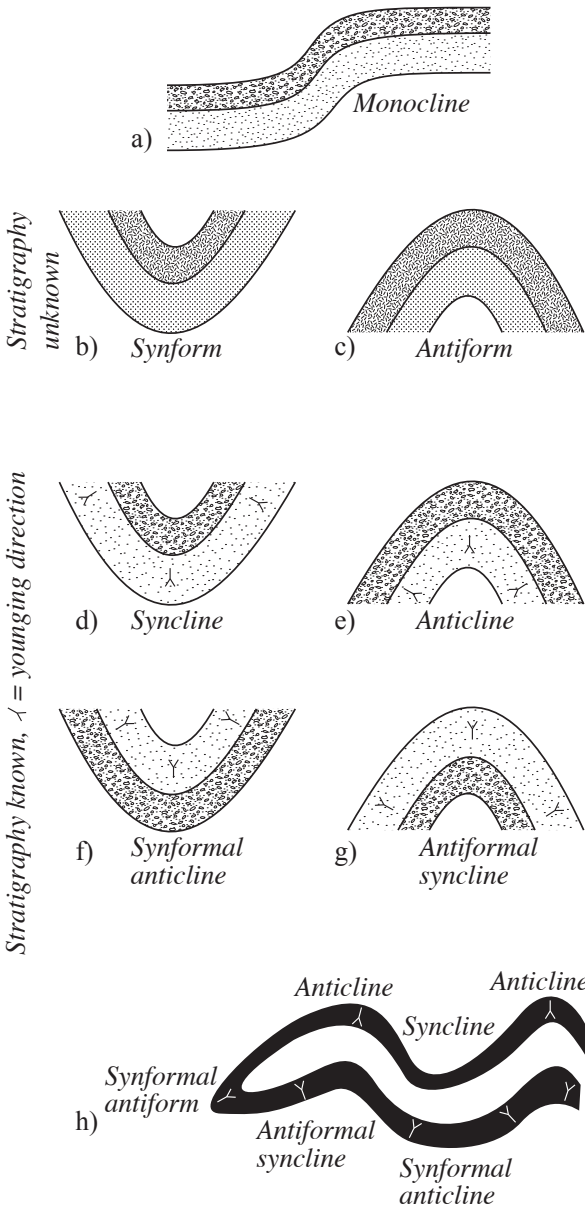

Figure 11.8 Basic fold shapes. The bottom figure illustrates how various types of syn- and antiforms may occur in a refolded fold.

We now need new terms, synformal anticline and antiformal syncline, to separate the two cases (Figure 11.8f-g). A *synformal anticline* is an anticline because the strata get younger away from its axial surface. At the same time, it has the shape of a synform, i.e. it is synformal. Similarly, an *antiformal syncline* is a syncline because of the younging direction, but it has the shape of an antiform. Technically, a synformal anticline is the same as an anticline turned upside down, and an antiformal syncline looks like an inverted syncline. Confused? Remember that these terms only apply when mapping in polydeformed stratigraphic layers, typically in orogenic belts.

As already stated, most folds are non-cylindrical. A non-cylindrical upright antiform is sometimes said to

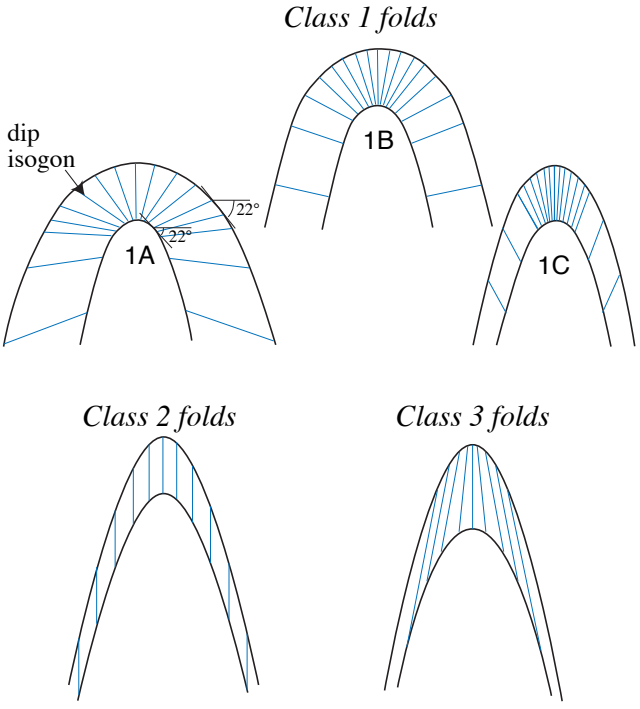

Figure 11.9 Ramsay's (1967) classification based on dip isogons. Dip isogons are lines connecting points of identical dip for vertically oriented folds.

be *doubly-plunging*. Large doubly-plunging antiforms can form attractive traps of oil and gas – in fact they form some of the worlds largest oil traps. When the non-cylindricity is pronounced, the antiform turns into a *dome*. Similarly, a strongly non-cylindrical synform is called a *basin*.

A *monoclinal fold* is a fold with only one (dipping) limb and is mostly used about map-scale structures related to reactivation of underlying faults or

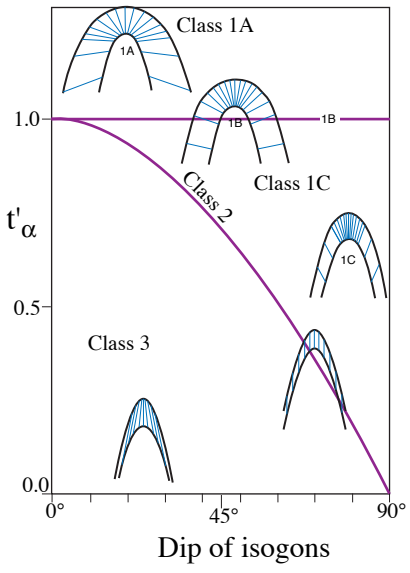

Figure 11.10 Fold classes plotted in a diagram where normalized layer thickness is plotted against dip of the folded surface. t'_α is the local layer thickness divided by the layer thickness in the limb.

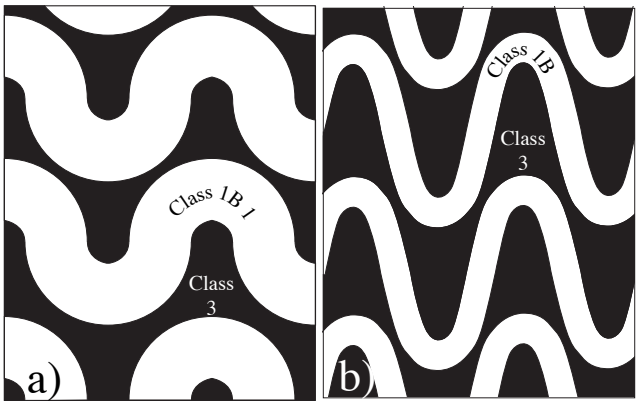

Figure 11.11 Alternating class 1B and 3 folds are commonly seen in folded layers. Competent layers exhibit class 1B geometry.

differential compaction of the subsurface. (Figure 11.8a)

Some folds have layers that maintain their thickness through the fold, while others show thickened limbs or hinges. These, and related features, were explored by the British geologist John Ramsay, who classified folds geometrically by means of *dip isogons*. By orienting the fold so that its axial trace becomes vertical, lines or dip isogons can be drawn between points of equal dip on the outer and inner boundaries of a folded layer. Dip isogons portray the difference between the two boundaries and thus the changes in layer thickness. Based on dip isogons, folds can be classified into three main types (Figures 11.9 and 11.10):

Class 1: Dip isogons converge downward. The inner (lower) arc is tighter than the outer one.
Class 2 (*similar folds*, also called *shear folds*): Dip isogons parallel the axial trace. The shape of the inner and outer arcs are identical.
Class 3: Dip isogons diverge downward. The outer arc is tighter than the inner one.

Class 1 folds are further subdivided into classes 1A, B and C, where 1A folds are characterized by thinned hinge zones, 1B folds (also called *concentric* or *parallel folds*; Figure 11.11) have constant layer thickness, while 1C folds have slightly thinned limbs. Class 2 and, particularly, class 3 folds have more pronounced thin limbs and thickened hinges.

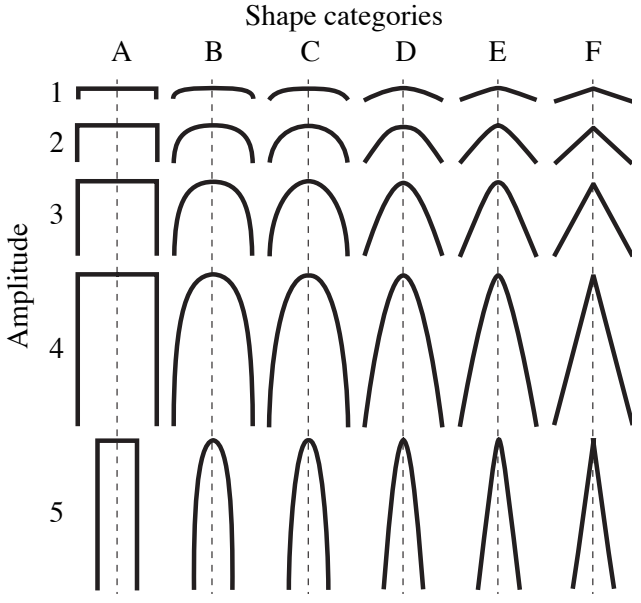

Figure 11.13 Fold classification based on shape. From Hudleston (1973).

Folds are also classified according to shape. A spectrum of shapes is found, from angular chevron folds (Figure 11.12a), via circular or concentric folds, to box-folds. Box-folds are special in that they have two hinge zones and two sets of axial surfaces (Figure 11.2).

Folds do not necessarily show the regularity of mathematical functions as we know them from simple classes of algebra. Nevertheless, simple harmonic analysis (Fourier transformation) has been applied in the description of fold shape. A matematical function is then fitted to a given folded surface (layer interfaces), and the form of the Fourier transformation useful to geologists is:

$$f(x) = b_1 \sin x + b_3 \sin 3x + b_5 \sin 5x \ldots \quad (11.1)$$

This series converges rapidly, so it is sufficient to

Figure 11.12 a) Chevron folds (angular folds) in micaceous metasediment, b) S-fold in mylonitic gneisses, and c) Z-fold.

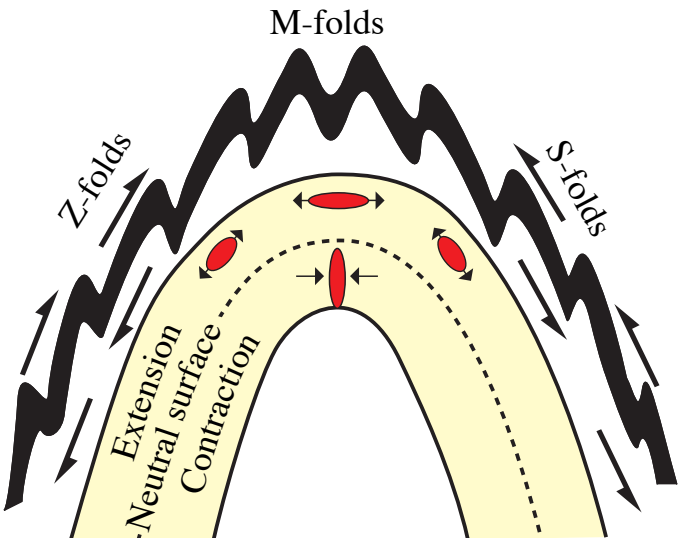

Figure 11.14 Z- M- and S-folds may be related to lower-order folds, in which case they provide information about the geometry of the large-scale fold.

consider only the first coefficients, b_1 and b_3, in the description of natural folds. Based on this method Peter Hudleston prepared the visual classification system for fold shape shown in Figure 11.13.

1.1.2 Fold systems

Folds usually come in groups or systems, and although folds may be quite non-systematic, neighboring folds tend to show a common style, especially where they occur in rows or trains. In these cases they can, akin to mathematical functions, be described in terms of wavelength, amplitude, inflection point and a reference surface called the *enveloping surface*. The enveloping surface is the surface or line tangent to individual hinges along a folded layer, as shown in Figure 11.1.

Folds can be symmetric or asymmetric in cross section and form M-folds (symmetrical) or S- and Z-folds (asymmetrical, see Figures 11.12 and 11.14). Fold systems consisting of folds with the same symmetry (Z or S) have a certain *vergence*. Consider the sense of displacement of the upper limb relative to the lower one when determining the vergence (Figure 11.15). Fold vergence is important in structural analysis:

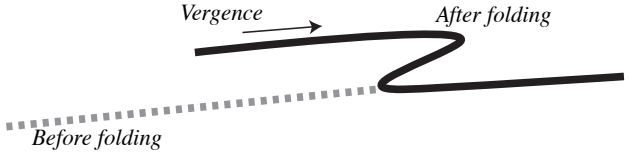

Figure 11.15 The concept of fold vergence. This fold is right-verging.

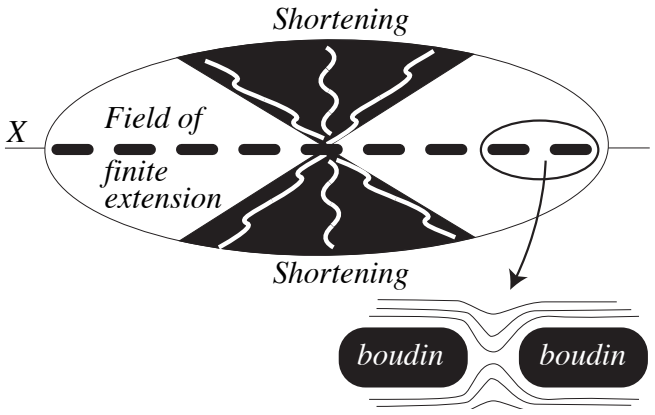

Figure 11.16 Fold vergence in relation to the strain ellipsoid for coaxial deformation, Note that folds can also occur between boudins in the field of finite extension.

1) If a fold system represents parasitic (second-order) folds on a larger synformal or antiformal structure, such as shown in Figure 11.14, then their (a)symmetry indicates their position on the large-scale structure. They can therefore be used to map out related first-order structures that may not be directly visible in the field.

2) If asymmetric folds are unrelated to any lower-order structure and located in a shear zone, the asymmetry may give information about the kinematics (sense of movement) in the zone (such analyses should be used together with independent kinematic indicators; see Chapter 15).

3) The (a)symmetry of folds may reflect strain and the orientation of the strain ellipse (Figure 11.16). In general, layers that are parallel to ISA_3 (see Chapter 3) will develop symmetric folds. This picture is more complicated for simple shear and other non-coaxial deformations, since layers that are parallel to ISA_3 at one moment will have rotated away from this position at the next.

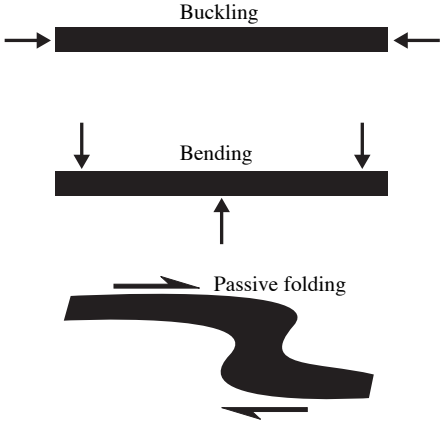

Figure 11.17 The relation between how force is applied and fold mechanisms.

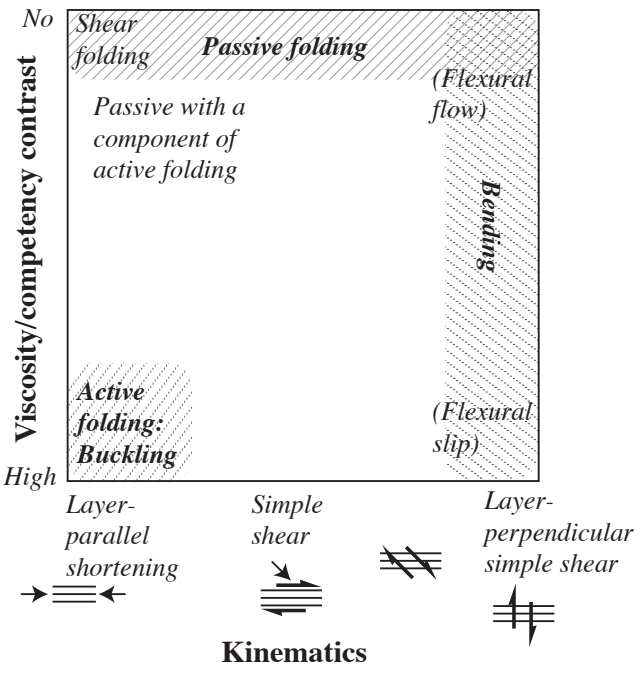

Figure 11.18 Classification of fold mechanisms with respect to viscosity contrast and kinematics.

1.2 Folding – mechanisms and processes

Folds can form in many different ways by means of different mechanisms. There are different ways to separate the different fold mechanisms, but a common one is to distinguish between active folding, passive folding and bending (Figures 11.17 and 11.18).

1.2.1 Active folding

Active folding or *buckling* is a process that can initiate when a layered rock is shortened parallel to the layering (Figure 11.19). If an isotropic rock layer has perfectly planar and parallel boundaries and perfectly parallel with a constantly oriented σ_1, then it will shorten without folding even though there is a viscosity contrast between the layer and the host rock. However, if there are small irregularities on the layer interfaces, then these irregularities can grow to form buckle folds with a size and shape that depend on the thickness of the folded layer and its viscosity contrast with its surroundings.

Buckling or active folding implies that there is layer parallel shortening and a viscosity contrast involved.

Buckling of single layers

Buckling of single, competent layers in a less competent (viscous) matrix (Figure 11.19) is relatively easy to explore. Single-layer folds formed by buckling have the following characteristics:

1) The fold wavelength-thickness ratio (L/h) is constant for each folded layer if the material is mechanically homogeneous and if they were deformed under the same physical conditions. Such folds are often called *periodic folds*. If the layer thickness varies, then the wavelength is changed accordingly (Figure 11.20).
2) The effect of the folding disappears rapidly (about the distance corresponding to one wavelength) away from the folded layer.
3) The folds in the competent layer approximate class 1B folds (constant layer thickness). If there are two or more folded competent layers then the incompetent layers in between are folded into class 1A and class 3 folds (Figures 11.11 and 11.21). The cusp (pointed) hinges point to the more competent layers.
4) The outer part of the competent layer is stretched

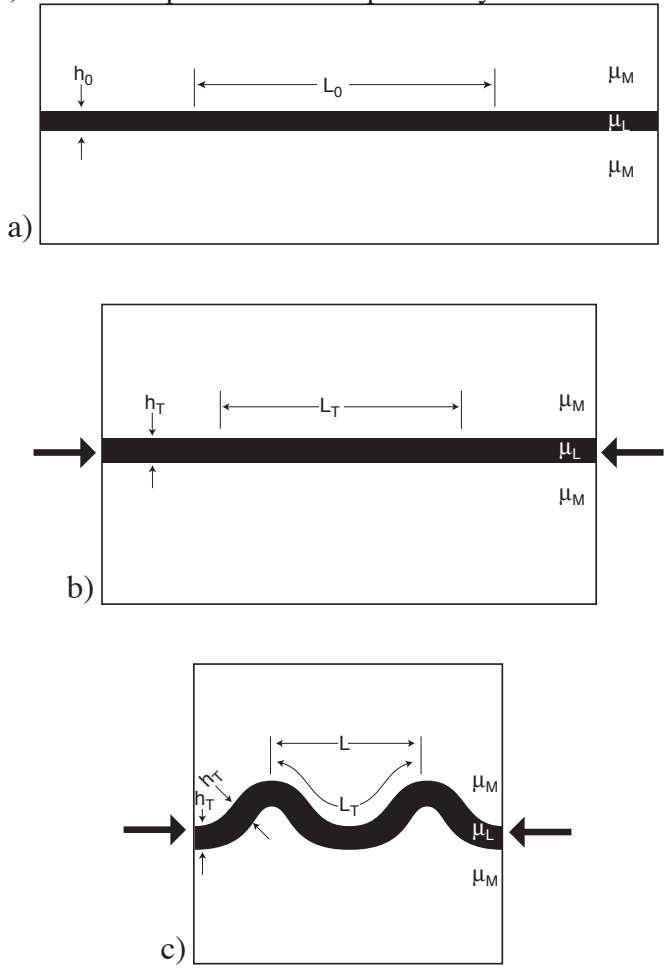

Figure 11.19 Buckling of a single layer. L_0 is the original length that is changed into L_T after initial shortening (a-b) while μ_L and μ_M are layer and matrix viscosities, respectively. h_0 is the original layer thickness (a) which increases to h_T during the initial thickening phase (b). L is the wavelength while L_T is the arc length. Based on Hudleston (1986).

Figure 11.20 Two folded layers of different thickness. The upper and thinner one shows a smaller dominant wavelength than the lower one.

Figure 11.21 Extension fractures (veins) in the outer arc of folded competent layers. Varanger, Northern Norway.

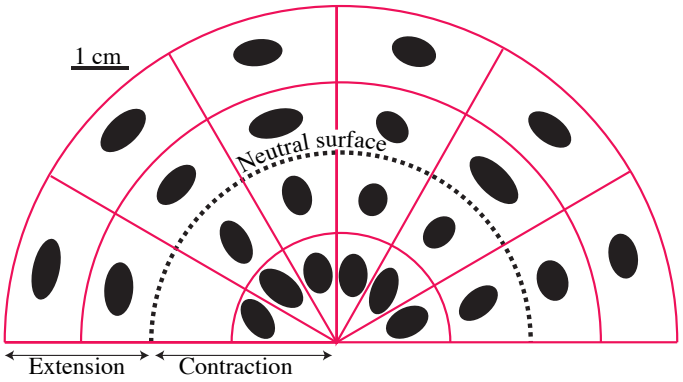

Figure 11.22 Strain distribution in the hinge zone of a folded limestone layer in shale. Outer-arc stretching is separated from inner-arc shortening by a neutral surface. From Hudleston & Holst (1984).

while the inner part is shortened. The two parts are typically separated by a *neutral surface* (Figure 11.22). Note that layer-parallel shortening, which always takes place prior to folding, can reduce or eliminate the outer extensional zone.

5) The normal to the axial surface or axial cleavage indicate the direction of maximum shortening (Z).

If the layers are Newtonian viscous, and disregarding any layer-parallel shortening, then the relation between wavelength and thickness is given by:

$$L_d/h = 2\pi(\mu_L/6\mu_M)^{1/3} \qquad (11.2)$$

μ_L and μ_M are the viscosities of the competent layer and the matrix, respectively, while L_d is the dominant wavelength and h the layer thickness. Experiments and theory show that homogeneous shortening (T) occurs initially, together with the growth of irregularities into very gentle and long-amplitude fold structures. When the most accentuated folds achieve opening angles around 160-150°, the role of layer-parallel shortening decays. From that point on the folds grow without any significant increase in layer thickness. Equation 11.2 can be expanded to include layer-parallel thickening:

$$L_{dT}/h_T = 2\pi(\mu_L/6\mu_M(T+1)T^2)^{1/3} \qquad (11.3)$$

L_{dT} is here the revised expression of the dominant wavelength, while h_T is the thickness when layer-parallel shortening (thickening) is taken into account. The factor T is identical to the strain ratio X/Z, or $1+e_1/1+e_3$.

The viscosity contrast $\mu_L/6\mu_M$ can be estimated (formulas not shown here) by measuring the average length of the folded layer over one wavelength and h_T for a fold population. In addition, the layer-parallel shortening T in the competent layers must be estimated.

Buckling has been modeled under the assumption of linear or Newtonian viscosity (Equation 5.23). It is likely that most rocks show non-linear rheological behavior during plastic deformation, which has consequences for the buckling process. A power-law rheology is then be assumed (Equation 5.24), where the exponent n>1. The higher the n-exponent, the quicker the fold growth and the less the layer parallel shortening T. Many natural folds show low T-values, and, together with low L/h ratios (L/h<10), this indicates a non-linear rheology. However, the

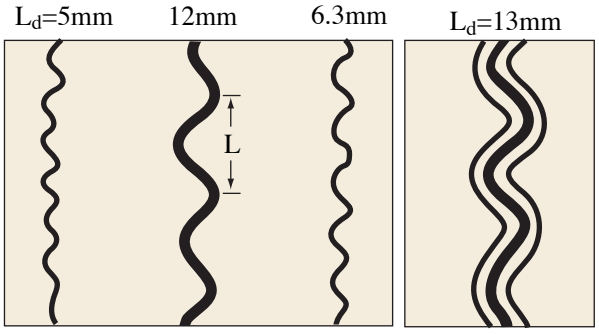

Figure 11.23 Folding of multilayered rocks. When far apart the layers act as individual layers (left). The closer they get, the more they behave as a single layer with thickness larger than that of the thickest of the individual layers. Based on experiments by Currie et al. (1962).

differences between the results from viscous and power-law rheology models are not great.

Multilayer folding

L_d/h is significantly less for multilayer than for single layer buckling. Where two thin layers get close they will behave more like a single layer whose thickness is the sum of the two thin layers (Figure 11.23). Where we have alternating thick and thin layers the thin layers will start to develop folds first (Figure 11.24 a-b). At some point also the thick layers will start to fold (with longer wavelength) and control the process. The result is relatively large folds controlled by thick layers together with small, second-order folds formed earlier in the process (Figure 11.24c). An example is shown in Figure 11.25.

Buckling of layers can be modeled by different mechanisms. The simplest ones are known as orthogonal flexuring and flexural slip and flow. We will briefly review these fundamental models. Just remember that these are idealized, end-member models and that natural folding generally involves a component of several of them.

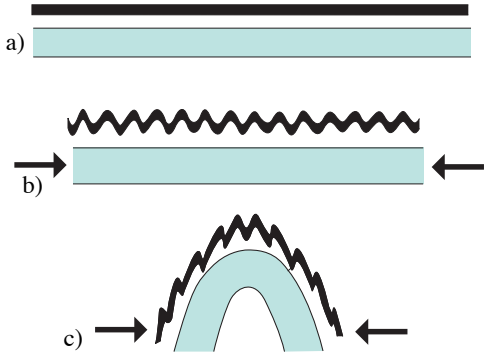

Figure 11.24 Illustration of how folding initiates in thin layers. Once the thicker layer starts to fold, the smaller folds in the thin layer becomes parasitic and asymmetric as they become deformed by flexural flow.

1.2.2 Flexural slip and flexural flow

Flexural slip is slip along layer interfaces or very thin layers during folding. Flexural slip "experiments" are carried out daily all over the world when paperback books or phone directories are bent. During this process slip occurs between individual paper sheets. It is a prerequisite that the deforming medium is layered or has a strong mechanical anisotropy. In nature, the anisotropy could be mica-rich thin layers in a quartzite or mylonite, or thin shale layers between thicker sandstone or limestone beds in sedimentary rocks. Flexural slip can occur in the middle crust where plastic deformation mechanisms would be involved, but flexural slip is perhaps more common where sedimentary strata are folded in the upper crustal brittle regime. In the latter case bedding surfaces act like faults, and slickenlines will sometimes be developed on the slipped surfaces, as shown in Figure 11.26a. Maximum slip occurs at the inflection points

Figure 11.25 Buckled multilayers. Note how the largest folds affect the entire layer package.

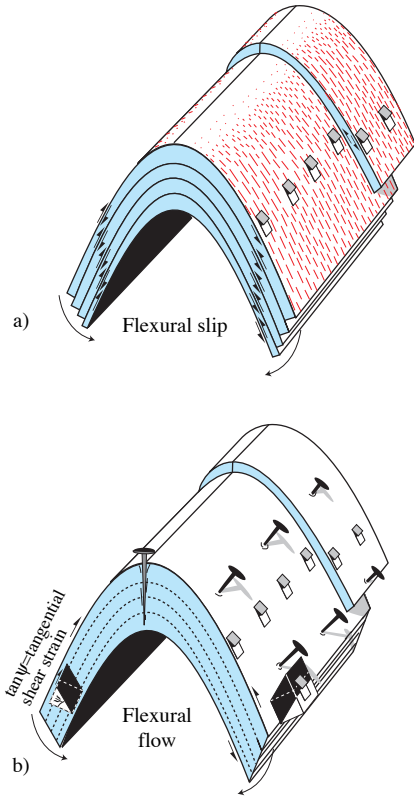

Figure 11.26 a) Flexural slip, showing opposite sense of slip on each limb, decreasing towards the hinge zone. b) Flexural flow, where fold limbs are being sheared. Ideally, layer thickness is preserved. Thickened hinges are commonly found in natural folds, indicating that flow other than by layer-parallel simple shear is involved.

and dies out towards the hinge line, where it is zero. The sense of slip is opposite on each limb, and the slip is consistent relative to the hinges. For an upright fold in sedimentary layers, slip is always towards the anticline hinge and away from the syncline hinge (Figure 11.26a).

In cases where strain is more evenly distributed in the limbs in the form of shear strain, as is more commonly the case in the plastic regime, flexural slip turns into the closely related mechanism called *flexural flow*. In this case the shear strain is directly related to the orientation (rotation) of the layers, as shown in Figure 11.26b: the higher the rotation, the higher the shear strain. For originally horizontal layers folded into an upright fold, shear strain is directly related to dip ($\gamma = \tan(\text{dip value})$). In general, the shear strain is zero in the hinge line and the axial surface, and the sense of shear is opposite on each side of the fold (Figure 11.26b). This results in a characteristic strain distribution in the fold. For example, the neutral surface separating extension from contraction, typical for many buckle folds, is not found in pure flexural-flow folds. Flexural flow produces identical strain in the

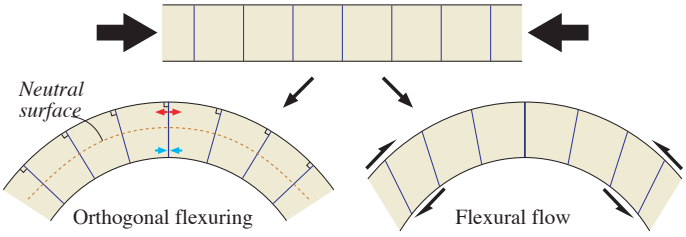

Figure 11.27 Layer-parallel shortening resulting in orthogonal flexuring and flexural flow. Note what happens to the originally orthogonal lines.

inner and outer part of a fold, but strain increases away from the hinge. Note that evidence for a combination of orthogonal flexuring (see below) and flexural flow or slip is commonly found in buckle folds, in which case a neutral surface generally exists.

Pure flexural folds are perfect class 1B folds. We can estimate the amount of layer-parallel shortening for such folds by measuring the length of any of the folded layers. This layer has maintained its original length because it was the shear plane throughout the folding history. The presence of additional mechanisms changes this opportunity.

1.2.3 Orthogonal flexuring

Orthogonal flexuring or tangential longitudinal strain is a deformation type with its own specific conditions: all lines originally orthogonal to the layering remain so throughout the deformation history. The result is stretching of the outer part and shortening of the inner part of the folded layer. The long axis of the strain ellipse is therefore orthogonal to bedding in the outer part of the layer and parallel to bedding in the inner part, as shown in the folded limestone layer in Figure 11.22. Figure 11.27 shows a comparison between flexural flow and orthogonal flexuring.

A neutral (no strain) surface separates the outer extended and inner contracted part of the folded

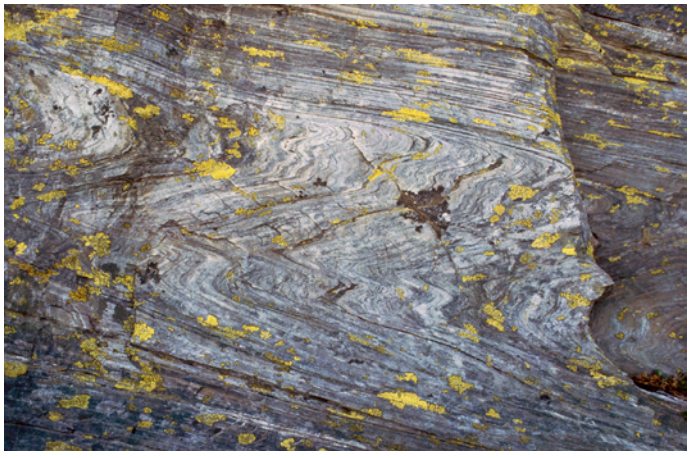

Figure 11.28 Passive (class 2) folding of quartzite in a Caledonian mylonite zone.

layer. During the folding history, the neutral surface moves inward towards the core of the fold, which can result in contraction structures overprinted by extension structures.

Pure orthogonal flexuring is only possible for open folds. When folds get tighter, the conditions of orthogonal flexuring becomes harder and harder to maintain, and flexural slip or flow may gradually take over. Evidence for orthogonal flexuring is typically found in stiff, competent layers that are resistant to ductile deformation. Some newer works have simplified the definition of orthogonal flexuring to a mechanism resulting in outer-arc contraction and an inner-arc extension. By getting rid of the requirement of orthogonality, the model gets more general and embraces many more natural examples.

1.2.4 Passive folding

Passive folding is typical for rocks where passive flow occurs, i.e. where the layering exerts no mechanical influence on folding. In these cases the layering only serves as a visual expression of strain. Perfectly passive folds are class 2 (similar) folds, and passive folds that are associated with simple shear are called *shear folds*.

Examples of passive folding are found where layers enter shear zones or elsewhere are affected by heterogeneous simple shear. Drag folds along faults (Chapter 8) are examples typical for the brittle regime. Passive folds are frequently found in mylonite zones, particularly in quartzites (Figure 11.28) where the mechanical effect of layering is negligible. Thus, passive folds form under heterogeneous simple shear (Figure 11.29), but can also form under heterogeneous pure shear (Figure 11.30), in which case they should not be referred to as shear folds.

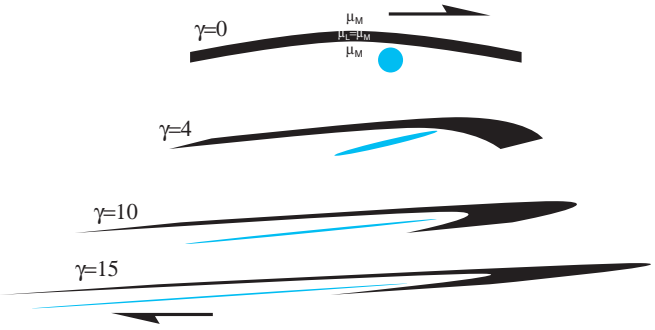

Figure 11.29 Formation of class 2 fold by simple shearing of a non-planar layer. No viscosity contrast is involved.

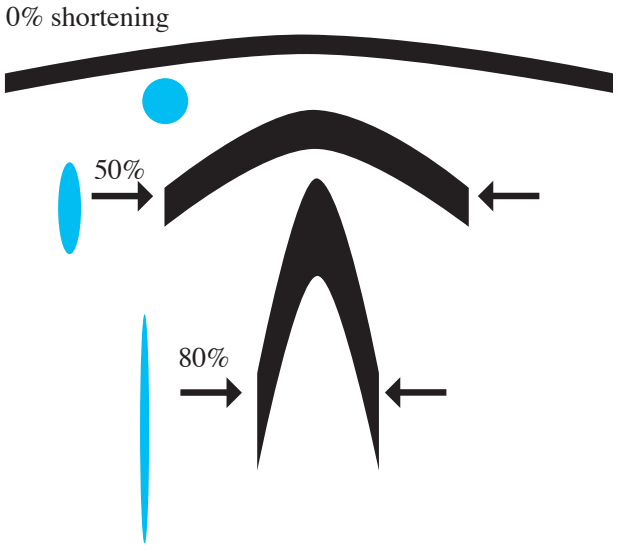

Figure 11.30 Class 2 fold formed by pure shearing of non-planar layer. No viscocity contrast.

1.2.5 Bending

Bending occurs when forces act *across* the layers at a high angle (Figure 11.17), unlike buckle folds where

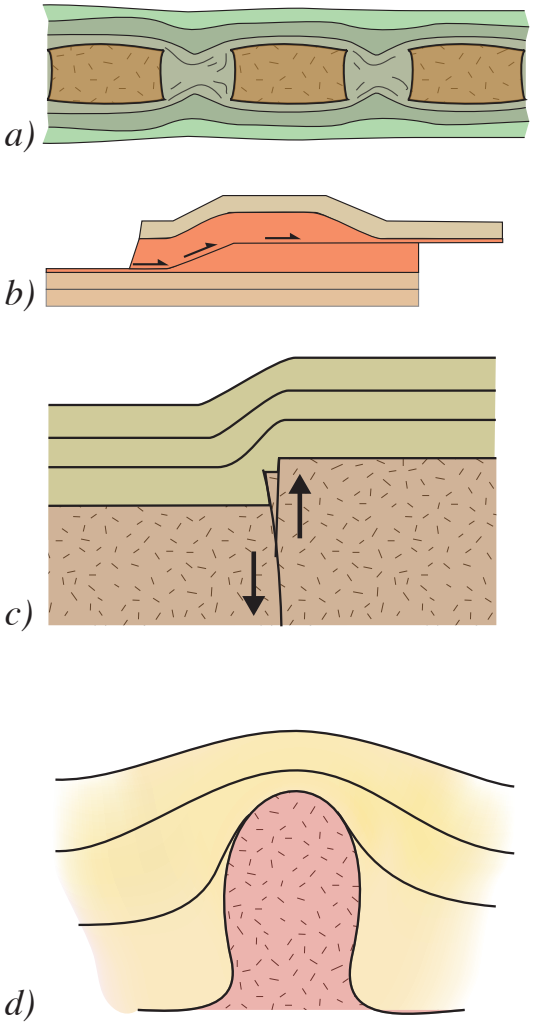

Figure 11.31 Examples of bending in various settings and scales. a) between boudins. b) above thrust ramps, c) above reactivated faults, and d) above shallow intrusions or salt stocks or ridges.

the main force acts parallel to layers. In fact, most folds caused by bending can be regarded as passive or passive shear folds in which layers are extended rather than shortened during bending. Any mechanical contrast has therefore only limited influence on the resulting fold structure, although boudinage may occur internally in the fold limbs. Bending has been studied in great detail by engineers because of its importance in the field of construction engineering.

There are many examples of bending:

-Fault-bend folds, where thrust sheets are bent as they move over a ramp structure (Figure 11.31b) (see Chapter 16).

-Bending or flexuring of sedimentary sequences over reactivated faults. Numerous examples of this exist where basement fault become reactivated and affect the overlying soft sedimentary layers (Figure 11.31c).

-Differential compaction, where a layer compacts more in one area than in another due to different degrees of compaction of the underlying layers. This is very common in postrift-deposits in sedimentary basins.

-Bending of rock layers above a pluton or a salt diapir (Figure 11.31d).

-Around or between boudins (Figure 11.31a and 11.32).

Both orthogonal flexuring, flexural slip and flexural flow are mechanisms that can occur during bending of layers.

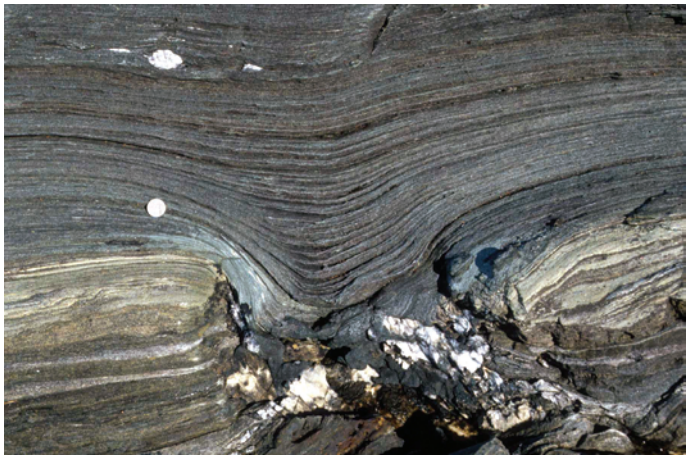

Figure 11.32 Passive folding of layers between boudins.

1.2.6 Kinking

Kink bands and *kink folds* are common in well-laminated rocks rich in phyllosilicate minerals. Kink bands are cm- to dm-wide zones or bands with sharp boundaries across which the foliation is abruptly rotated. Wider zones are more commonly referred to as kink folds. Geometrically kink bands and kink folds are asymmetric Class 2 folds. They are relatively low-temperature plastic deformation structures where there is no slip along the foliation (no flexural slip). Like chevron folds they have no hinge zone, but there are significant differences between the two. One is that chevron folds commonly deform by flexural slip. Another is that chevron folds initiate with their axial surface perpendicular to σ_1, while kink bands are oblique to σ_1. Furthermore, kink bands may develop in conjugate sets (Figure 11.33), in which case σ_1 bisects the sets as shown in Figure 11.34. Conjugate kink bands or kink folds are also called box folds, conjugate kinks or conjugate folds. When kink bands

FOLD OVERLAP STRUCTURES

Individual folds can overlap and interfere. Just like faults (Chapter 8), they initiate as small structures and may interact through the formation of overlap or relay structures. Fold overlap structures were first mapped in thrust and fold belts, particularly in the Canadian Rocky Mountains, and many of the fundamental principles of fault overlap structures come from the study of fold populations.Fold overlaps are zones where strain is transferred from one fold to another. Relay ramps form, and the rapid variations in offset that characterize fault overlap zones correlate to rapid changes in amplitude along folds in these zones.

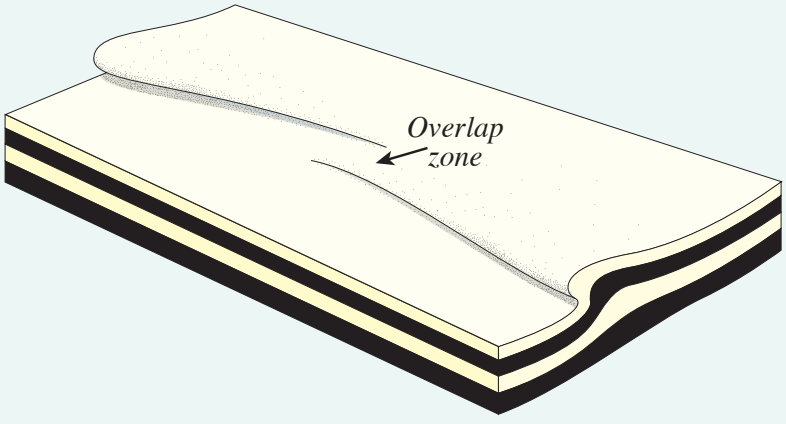

Figure 11.33 Conjugate kink bands in mylonitized anorthosite gabbro, Bergen Arcs.

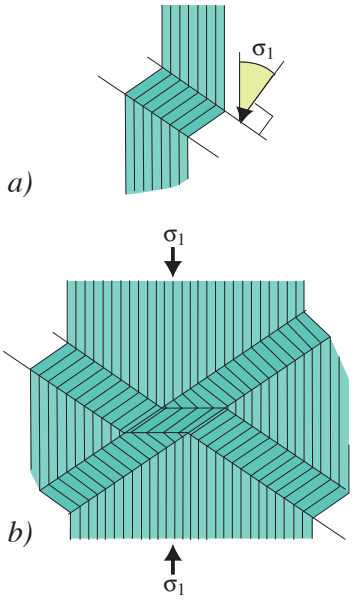

Figure 11.34 The orientation of σ_1 is only vaguely indicated by the orientation of a single set of kink bands (a). For conjugate sets σ_1 can be determined more presicely.

occur as single sets, σ_1 is known to be oblique to the band, but its precise orientation is unknown.

It is a general principle that stress can only be estimated from strain when the amount of strain is modest. Conjugate kink bands generally involve small strains, which justifies their link to stress. However, kink folds can rotate during the deformation history if strain keeps accumulating, and the result may be the formation of chevron folds.

1.3 Fold interference patterns

In areas affected by two or more deformation phases ~~we may find that~~ folds may be superimposed on each other. In such cases of fold interference we may find simple or complex patterns of folding that depend on the orientations of the two fold sets. John Ramsay distinguished between three main patterns (Figures 11.35 and 11.36). Type 1 is the classical dome-and-basin structure, Type 2 is the so-called boomerang-type (Figure 11.37), and Type 3 has been described as the hook-shaped type. Interference patterns typically arise from the overprinting of a second phase of deformation on an earlier set of deformation structures, but can also be the result of non-steady-state flow, where the orientation of the ISA locally or regionally changed during the course of the deformation. There is also a Type 0 pattern defined by two identical, but temporally separate fold systems. The result of Type 0 interference is simply a tighter fold structure. Type 1 patterns can also be the result of a single phase of heterogeneous non-coaxial deformation, or by amplification of preexisting irregularities (Figure 11.38). These extremely non-cylindrical folds are often called sheath-folds. In general it is useful to

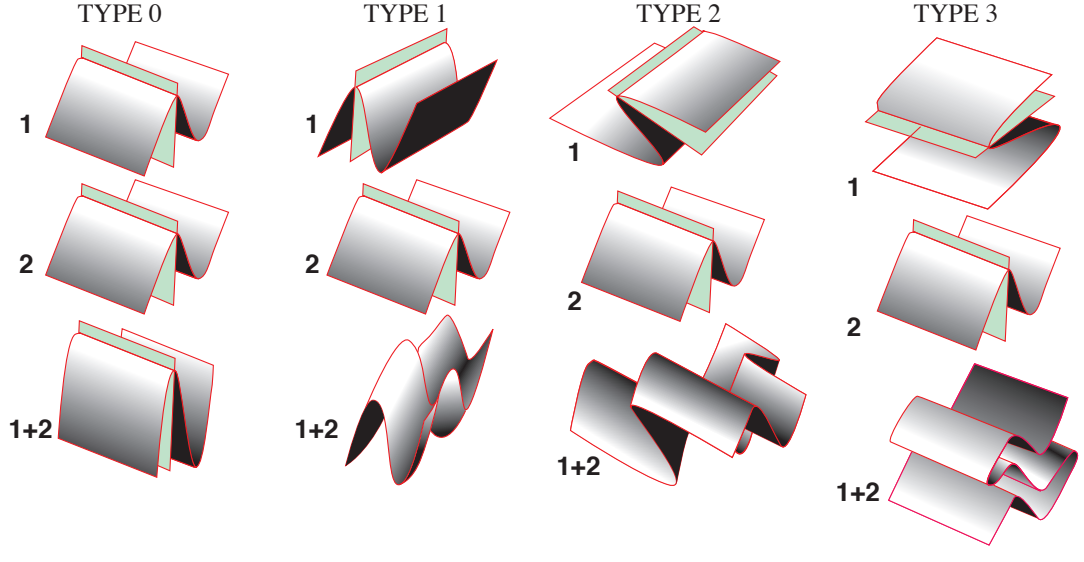

Figure 11.35 Principal types of fold superposition. Based on Ramsay (1967).

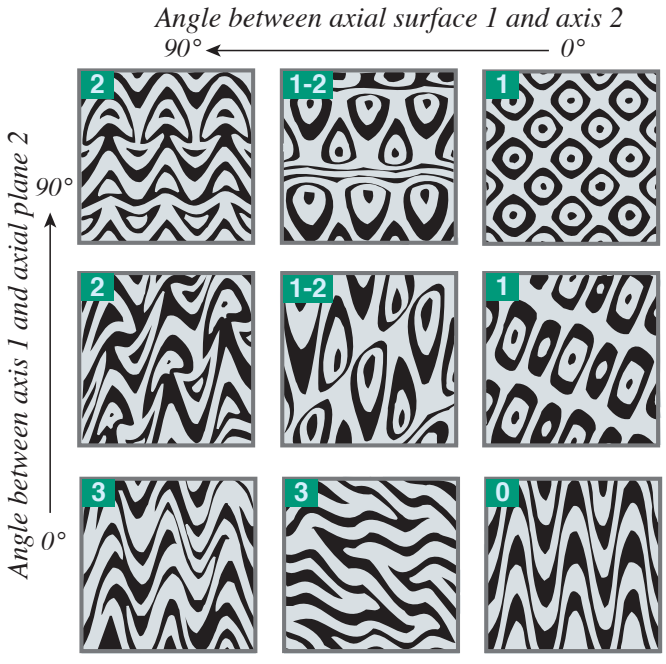

Figure 11.36 Fold interference patterns of cylindrical folds, classified according to the relative orientations of fold axes and axial planes. The patterns are numbered 0-3. Based on Ramsay & Huber (1987).

be able to recognize the geometric relations between different fold phases by use of the patterns depicted in Figure 11.36.

1.4 Folds in shear zones

In high-strain shear zones or mylonite zones folds form and grow continuously during shearing. Folding can occur where layers initially occur in the contractional field or where layers are rotated into this field due to irregularities in the zone. Such folds can be regarded as passive if the mechanical contrast between layers is negligible, or active if a significant viscosity contrast exists. Whether a fold is active or passive can be addressed by geometric analysis, since passive folds are Class 2 and active folds Class 1 and 3 folds (Figures 11.9 and 11.10).

At high strains the foliation in a shear zone will, in principle, be almost parallel to the shear plane. It will still be in the extensional field, but a modest perturbation of the layering can easily cause it to enter the contractional field. The result is a family of folds that verge in accordance with the sense of shear. This sort of rotation can occur around tectonic lenses or heterogeneities (see Figure 15.23) or by a slight rotation of the ISA due to a change in the stress field or rotation of the shear zone.

If the hinge lines of the folds lie in the shear plane they will remain in this position. In practice, however, hinge lines will initiate at an angle to the shear plane and rotate towards parallelism with the shear direction. Open folds with hinge lines that make a high angle to the transport direction (Figures 11.38a

DUCTILE FOLDING IN THE BRITTLE REGIME

Most folds are the result of plastic flow in the middle and lower crust, but folding can also occur at shallower depth. They may form where gravitational instabilities or dewatering cause deformation of unconsolidated sediments. Folding of buried porous sediments is particularly common where pore fluid pressure is high (overpressure). Folds in sediments are often found to be very non-cylindrical, somewhat similar to noncylindrical folds found in some mylonitic rocks. They do not however develop axial planar cleavage so commonly asfolds formed under metamorphic conditions. They are also confined to special layers where the layers above and below may be untouched by the folding.

Folds formed in unconsolidated or poorly consolidated sediment (Varanger, Norway).

Figure 11.37 Type 2 interference pattern in folded quartz schist.

and 11.39) are therefore thought to have experienced less shearing than those that are tighter with hinge lines closer to the transport direction (Figure 11.38c). This rotational behavior of fold hinges in non-coaxial flow has been used to explain why many high-strain shear zones contain folds with hinges subparallel to the lineation. Extensive rotation of hinges may result in so-called *sheath folds*, where the hinge line is subparallel to the lineation for the most part, except for their noses where the hinge line abruptly changes orientation (Figure 11.38c). Sections through sheath

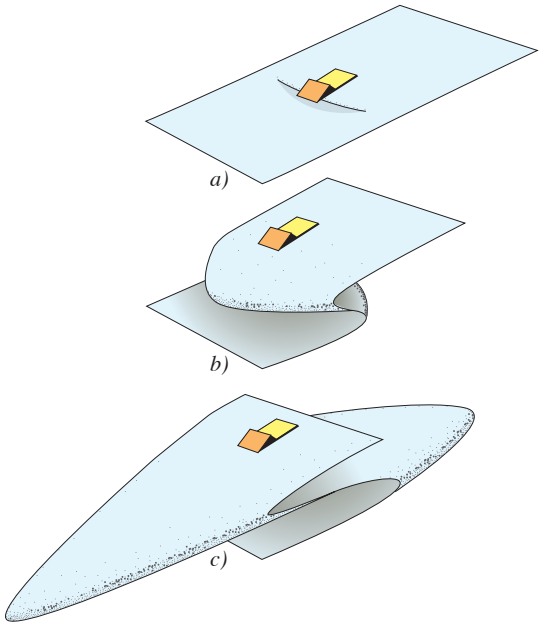

Figure 11.38 Development of sheath folds (highly non-cylindrical folds) by amplification of a pre-existing irregularity. Note that it takes high shear strains to form sheath folds by simple shear. Shear strain increases from a) to c).

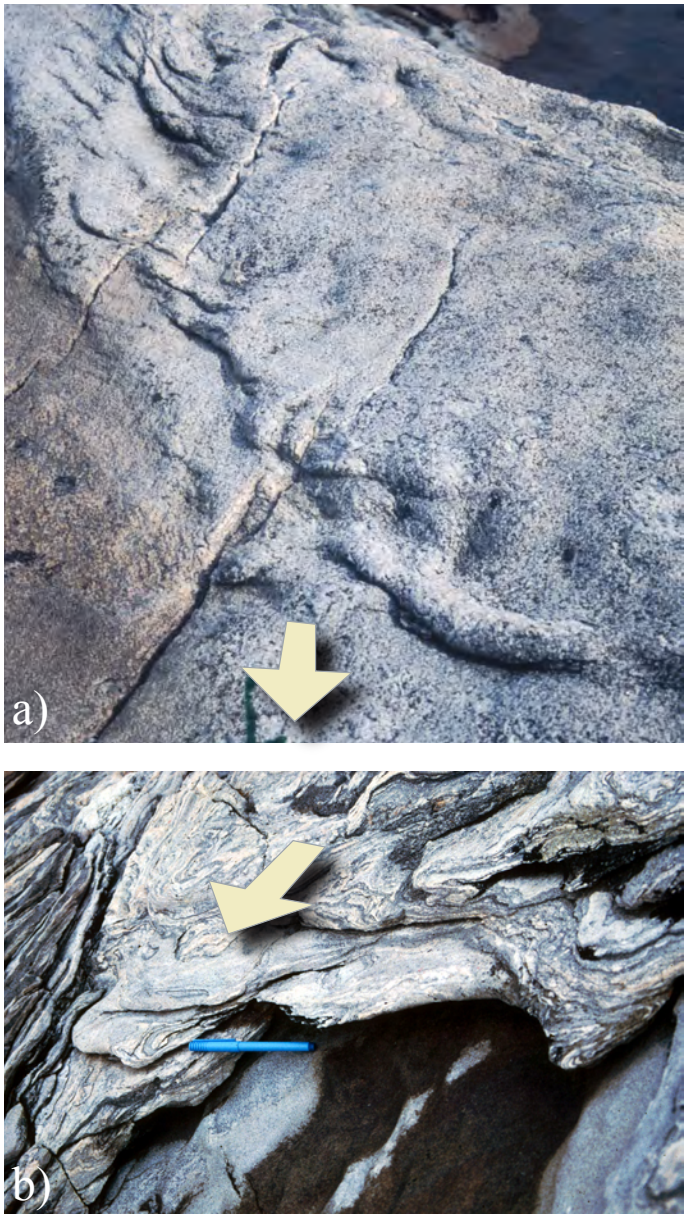

Figure 11.39 a) Early-stage folds in Caledonian shear zone. Hinge lines make a high angle to the lineation and transport direction (arrow). b) More mature stage of folding in the same shear zone. Hinge lines are highly curved and refolded, oriented both parallel, oblique and orthogonal to the transport direction (arrow).

folds resemble Type 1 fold interference patterns, but are formed during a single event of shearing (not necessarily a during a pure simple shear).

Folds in shear zones can also form in other ways. The foliation may be perpendicular to the shear zone walls, which is the case in many steep strike-slip shear zones (Chapter 18). Folds form with hinge lines oblique to the zone. The obliquity depends on the vorticity number of the zone and on the exact orientation of the layering relative to the shear zone.

Examples of such folds are found along the San Andreas Fault in California.

1.5 Folds in the upper crust

While most of the folds discussed above and seen in nature formed in the plastic regime in the crust, folds also form in the upper crust. Gravity-conrolled soft-sediment deformation of sand create non-cylindrical folds are recorded, for example, on unstable delta slopes or continental slopes. Soft-sediment folds are also associated with mud diapirs. *Fault propagation folds* forming ahead of a fault tip also occur in unmetamorphosed and even unconsolidated sediments and sedimentary rocks in the upper part of the crust. Deflection of layers around a fault, known as *drag*, is another example of fault-related folds. Hanging-wall folds controlled by fault geometry is yet another. These structures are covered in Chapters 8, 16 and 19. Most of these shallow-crustal structures have in common that they are formed by brittle deformation mechanisms and that they are not associated with axial plane cleavages.

---”””---

Folds in metamorphic rocks are closely associated with cleavage and to some extent also lineations. We will there fore proceed with a look at these structures.

Further reading:

General

Donath, F. A. and Parker, R. B., 1964, Folds and Folding: Geological Society of America Bulletin, v. 75, p. 45-62.

Hudleston, P.J., 1986. Extracting information from folds in rocks. Journal of Geological Education, 34: 237-245.

Johnson, T.E., 1991. Nomenclature and geometric classification of cleavage-transected folds. Journal of Structural Geology, 13: 261-274.

Ramsay, J.G. & Huber, M.I., 1987. The techniques of modern structural geology: folds and fractures, 2. Academic Press, London.

Folds in shear zones

Bell, T.H. & Hammond, R.E., 1984. On the internal geometry of mylonite zones. Journal of Geology, 92: 667-686.

Cobbold, P.R. & Quinquis, H., 1980. Development of sheath folds in shear regions. Journal of Structural Geology, 2: 119-126.

Platt, J.P., 1983. Progressive refolding in ductile shear zones. Journal of Structural Geology, 5: 619-622.

Fossen, H. & Holst, T.B., 1995. Northwest-verging folds and the northwestward movement of the Caledonian Jotun Nappe, Norway. Journal of Structural Geology, 17(1): 1-16.

Harris, L.B., Koyi, H.A. & Fossen, H., 2002. Mechanisms for folding of high-grade rocks in extensional tectonic settings. Earth-Sciences Review, 59: 163-210.

Krabbendam, M. & Leslie, A.G., 1996. Folds with vergence opposite to the sense of shear. Journal of Structural Geology, 18: 777-781.

Skjernaa, L., 1989. Tubular folds and sheath folds: definitions and conceptual models for their development, with examples from the Grapesvare area, northern Sweden. Journal of Structural Geology, 11(6): 689-703.

Vollmer, F.W., 1988. A computer model of sheath-nappes formed during crustal shear in the Western Gneiss Region, central Norwegian Caledonides. Journal of Structural Geology, 10: 735-745.

Buckling

Biot, M.A., 1961. Theory of folding of stratified viscoelastic media and its implications in tectonics and orogenesis. Geological Society of America Bulletin, 72: 1595-1620.

Hudleston, P. & Lan, L., 1993. Information from fold shapes. Journal of Structural Geology, 15: 253-264.

Sherwin, J.-A. & Chapple, W.M., 1968. Wavelengths of single layer folds: a comparison between theory and observation. American Journal of Science, 266: 167-179.

Fold geometry

Bell, A.M., 1981. Vergence: an evaluation. Journal of Structural Geology, 3: 197-202.

Stabler, C.L., 1968. Simplified fourier analysis of fold shapes. Tectonophysics, 6: 343-350.

Mechanisms and processes

Bobillo-Ares, N.C., Bastida, F. & Aller, J., 2000. On tangential longitudinal strain folding. Tectonophysics, 319: 53-68.

Hudleston, P.J., Treagus, S.H. & Lan, L., 1996. Flexural flow folding. Does it occur in nature?

Geology, 24: 203-206.
Ramsay, J.G., 1974. Development of chevron folds. Geological Society of America Bulletin, 85: 1741-1754.
Tanner, P.W.G., 1989. The flexural-slip mechanism. Journal of Structural Geology, 11: 635-655.

Strain in folds

Holst, T.B. & Fossen, H., 1987. Strain distribution in a fold in the West Norwegian Caledonides. Journal of Structural Geology, 9: 915-924.
Hudleston, P.J. & Holst, T.B., 1984. Strain analysis and fold shape in a limestone layer and implications for layer rheology. Tectonophysics, 106: 321-347.
Ramberg, H., 1963. Strain distribution and geometry of folds. Bulletin of the Geological Institution of the University of Uppsala, 42: 1-20.
Roberts, D. & Strömgård, K.-E., 1972. A comparison of natural and experimental strain patterns around fold hinge zones. Tectonophysics, 14: 105-120.

Folds in extensional settings

Chauvet, A. & M. Séranne, 1994. Extension-parallel folding in the Scandinavian Caledonides: implications for late-orogenic processes. Tectonophysics 238: 31-54.

Fletcher, J.M., Bartley, J.M., Martin, M.W., Glazner, A.F. & Walker, J.D., 1995. Large-magnitude continental extension: an example from the central Mojave metamorphic core complex. Geological Society of America Bulletin, 107: 1468-1483.

CHAPTER 12

Foliation and cleavage

Foliation and cleavage are terms that cover any tectonic planar structure that penetrates rock. They go hand in hand with folds and lineations and form the most common type of structures in the crust. Their wide occurrence makes them particularly useful: where strain markers may be missing, a foliation can give us useful information about strain. Its angular relation with bedding or other layering may reveal the location relative to large-scale folds in a poorly exposed area. The occurrence of foliations can give important information about sense of movement in non-coaxial deformation regimes. Cleavage and foliations also create slates and schists that are of significant economic importance in many parts of the world.

A. Heim (1878)

1.1 Basic concepts

1.1.1 Fabric

In structural geology the term *fabric* is used to describe penetrative and distributive components of the rock bodies (Figure 12.1). It can be composed of platy or elongate minerals with a preferred orientation. Examples include mica flakes in a mica schist or actinolite needles in an actinolite schist.

A fabric is built of minerals that *penetrate* the rock at the scale of a hand sample, and not a single foliation surface or thin zone. The distance between the elements that constitute a fabric is typically less than about a decimeter, which excludes a series of faults or small shear zones as fabric elements in the traditional sense of the term.

A fabric is penetrative, meaning that newly-grown minerals that are restricted to a fault or joint surface do not form a fabric.

A variety of objects in rocks, such as minerals, mineral aggregates, conglomerate pebbles etc., can be arranged in different ways and thereby give rise to different kinds of fabrics. It is useful to make a distinction between random fabrics, linear fabrics and planar fabrics. A *linear fabric* is characterized by elongate elements with a preferred orientation. A *planar fabric* contains tabular or platy minerals or other "flat" objects with a common orientation. A planar fabric needs not be planar in the mathematical sense – the planar structures or elements are commonly seen to bend around rigid objects or may be affected by subsequent folding. In fact, *curviplanar fabric* would be a more appropriate term in some cases. A *random fabric* is one where its elements show no preferred orientation (more commonly developed in sedimentary and igneous rocks).

All rocks, magmatic, sedimentary and metamorphic alike, ~~can~~ show a fabric, but fabrics

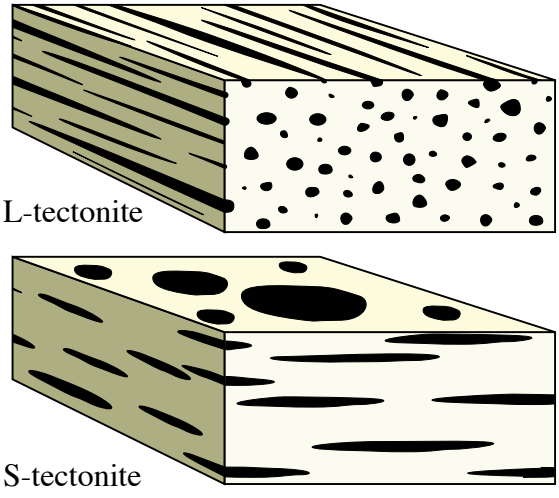

Figure 12.1 Fabric is a configuration of objects penetrating the rock. Linear objects form L-fabrics (above) while planar objects constitute S-fabrics. The rocks are known as L- and S-tectonites, respectively.

are particularly well developed in strongly deformed metamorphic rocks referred to as tectonites. In such rocks the fabrics are named according to the shape and organization of the fabric elements. Rocks that show a marked linear fabric are called *L-tectonites*, and those showing a pronounced planar fabric are called *S-tectonites* (Figure 12.1). *L-S tectonites* is the term used about deformed rocks that contain both a linear and a planar fabric. A close connection between fabric and the shape of the strain ellipse has been suggested for strongly deformed metamorphic rocks: L-fabrics indicate constrictional strain, L-S fabrics relate to plane strain and S-fabrics are the signature of flattening strain (see Chapter 3.?).

1.1.2 Foliation

Foliation (derived from the latin word *folium*, meaning leaf) is generally used for any fabric-forming planar or curviplanar structure in a metamorphic rock, but may also include primary sedimentary bedding or magmatic layering. A distinction is

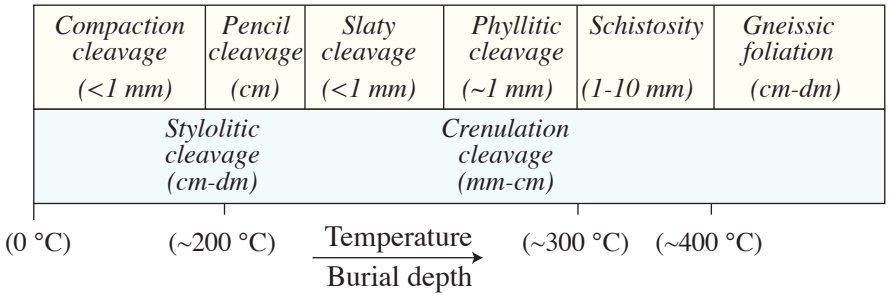

Figure 12.2 Schematic overview of important cleavage and foliation types, arranged according to burial depth or temperature and with an indication of the spacing of foliation domains. Temperatures indicated are very approximate.

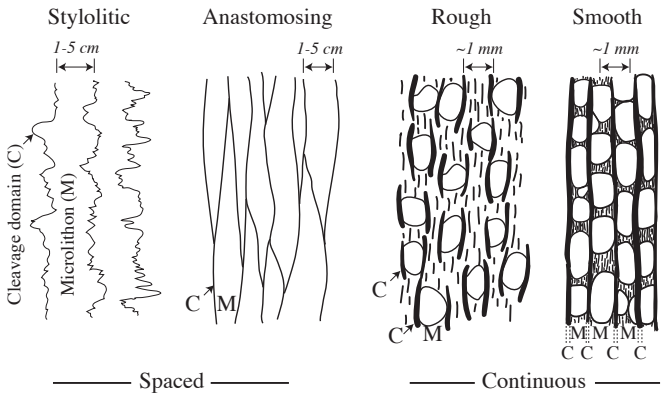

Figure 12.3 Disjunctive cleavage types. Stylolitic (limestones) and anastomosing (sandstones) cleavage are usually spaced, while continuous cleavages in more fine-grained rocks are separated into rough and smooth variants, where the rough cleavage can develop into the smooth version. All disjunctive cleavages are domainal, and the cleavage domains (C) are separated by undeformed rock called microlithons (M).

usually made between *primary foliation*[1] or structures (in sedimentary and magmatic rocks) and *secondary foliation* (such as axial planar cleavage). Secondary foliations are *tectonic foliations* if they form as a result of tectonic stress. Foliation resulting from compaction is an example of a secondary foliation that is not tectonic. In structural geology we tend to restrict the term to planar structures formed by deformation (Figure 12.2).

A foliation is a planar *fabric*. This means that a single surface, such as a fault or a joint, will not form a foliation. Even if parallel fractures should be distributed throughout a hand sample they may lack the cohesion that is a second characteristic of foliations. Although rocks typically split preferentially along the foliation, force is required to overcome that cohesion.

Foliation separate layers with differences in grain size or that contain parallel oblate clasts in a conglomerate, recrystallized tabular grains with a uniform orientation, platy minerals arranged into mm-thick zones or domains, densely distributed cohesive microfractures and microfolds (crenulations).

1.1.3 Cleavage

The term *cleavage* refers to the ability of a rock to split or cleave into more or less parallel surfaces. Cleavage is a subgroup of foliation – not all foliated rocks split preferentially along the foliation. Cleavage is found in low-grade (greenschist facies and lower) or barely metamorphic rocks, and in micaceous gneisses or schists in the form of late stage crenulation cleavage.

Both cleavage and foliation are penetrative at the scale of a hand sample, but the spacing of the planar elements varies. If the distance is greater than 1 mm and distinguishable in hand sample as individual surfaces or zones it is designated as *spaced cleavage* (Fig. 12.3). If the distance is less than 1mm, then the structure is a *continuous cleavage*. Naturally, continuous foliated rocks split into thinner slices or flakes than do rocks with spaced foliations.

1.1 Relative age terminology

The Austrian geologist Bruno Sander introduced around 1930 the designation S for foliations. Foliations in a given outcrop or area that can be shown to be of different ages are designated S_n, where the suffix n indicates the relative age. Primary foliations, such as bedding or magmatic layering, are referred to as S_0. The oldest secondary foliation is designated S_1, the second one S_2 and so on (Figure 12.4). Foliations are commonly related to folds, in which case the designation for folds (F) and foliations (S) share suffixes. For example, folds related to the first foliation (S_1) in a rock are referred to as F_1 etc. Similarly, the deformation phases are named D_1, D_2 etc.

1.2 Cleavage development

There are many types of cleavages and a rich terminology is available. To efficiently deal with cleavages and foliations it is useful to constrain the discussion to the crustal depth (temperature) and lithology of the rock in question. We will here consider the most common

Figure 12.4 Two generations of foliations in metagabbro in a Caledonian ophiolite fragment. The primary magmatic layering (S_0) has been reworked into a shear-related foliation (S_1) during Caledonian shearing.

1 Many geologists do not subscribe to such a wide use of the term, and using the term primary planar structures is safer.

types of foliation that develop during deformation in a prograde metamorphic development, i.e. when a rock is buried to progressively deeper depths.

1.2.1 *Early modification of primary structures*

The first secondary foliation forming in sedimentary rocks is related to their compaction history. Reorientation of mineral grains and collapse of pore space result in accentuation and reworking of the primary foliation (bedding). For a clay or claystone, the result is a shale with a marked *compaction cleavage* (Figure 12.5). For limestone, and in some cases also sandstones, pressure solution results. Pressure solution, which in this case is temperature rather than pressure or stress controlled, and therefore better termed dissolution, produces clay-rich subhorizontal and irregular seams where quartz or carbonate has been dissolved. The seams are known as pressure solution seams, and the foliation is called a *pressure solution cleavage* or, more correctly, just *solution cleavage*. The spacing of the seams may be several centimeters, and the cleavage is therefore a spaced cleavage. The compaction cleavage in a shale is however a continuous cleavage. These non-tectonic cleavages are regarded as S_0 foliations.

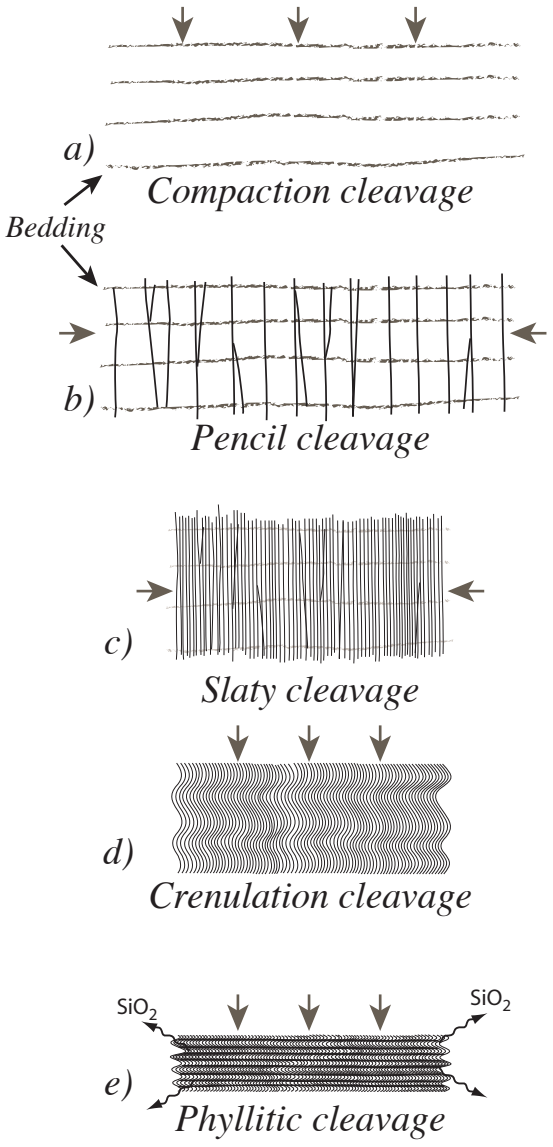

Figure 12.5 Possible history of cleavage development in a mudstone.

1.2.2 *Early tectonic development and disjunctive cleavage*

A tectonic foliation can result if a sedimentary rock is exposed to tectonic stress. If σ_1 is horizontal, a vertical cleavage forms. A new pressure solution cleavage can form in limestones (and sometimes in sandstones). This cleavage will generally make a high angle to S_0.

PENCIL CLEAVAGE AND STRAIN

The development of pencil cleavage can be represented in the Flinn plot as shown below. Step I involves compaction during burial. The flattening strain involved causes the path along the horizontal axis. Compaction is completed at stage 1. Horizontal tectonic shortening (Step II) then re-deforms the strain ellipse into a prolate geometry (stage 2). Pencil structures are now formed. If the deformation continues (Step III), then the Z-axis becomes vertical and the vertical tectonic cleavage starts to dominate. Strain eventually becomes oblate again (stage 3) and further deformation causes a vertical stretching lineation to develop (stage 4).

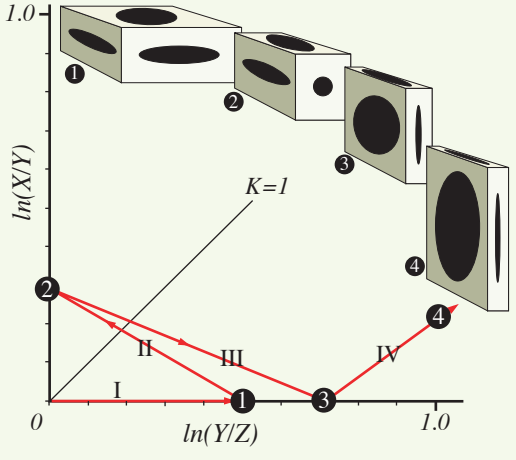

FRACTURE CLEAVAGE

Fracture cleavage (spaced cleavage) is sometimes used about closely spaced fractures in unmetamorphosed or very low grade metamorphic rocks, particularly limestones and sandstones. Fracture cleavage sometimes form by fracturing of pre-existing cleavage planes. Ordinary cleavage forms by contraction perpendicular to the cleavage planes. Fracture cleavage, as defined here, involves extension across the cleavage. They are therefore better classified as small-scale fracture arrays in many cases.

Shear fractures can also occur close and systematically enough that they resemble cleavage. This type of "cleavage" is very restricted, typically to fault cores and fault damage zones damage zones. There are additional uses of the term fracture cleavage in the literature, and it is wise to avoid this term to avoid confusion.

Slaty cleavage turning in to a spaced disjunctive cleavage in the fine-grained sandstone above. The latter could be termed a fracture cleavage because of the fracturing along the pressure-solution seams.

Right-dipping subparallel fractures in sandstone near the Bartlett Fault, Utah, resembling a cleavage in the unmetamorphosed Entrada Sandstone.

Shales react to stress by *reorientation* of clay minerals. At some point the secondary cleavage will be as pronounced as the primary one, and clay minerals will be equally well oriented along S_1 and S_0. The shale will now fracture along both S_1 and S_0 into pencil-shaped fragments, which explains why the cleavage is known as *pencil cleavage*. Pencil cleavage also occurs where two tectonic cleavages develop in the same rock due to local or regional changes in the stress field. This type of pencil cleavage is associated with some thrust ramps, formed close in time during the same phase of deformation (Figure 12.6).

Figure 12.6 Pencil cleavage formed during thin-skinned thrusting of shale in the Caledonian foreland. Fornebu, Oslo.

If the tectonic shortening persists, it will eventually dominate over the compactional cleavage. More and more clay grains become reoriented into a vertical position while quartz grains experience dissolution. Microfolding of the clay grains may also occur. The result is a continuous cleavage that totally dominates the structure and texture of the rock. The rock is now a *slate* and its foliation is known as *slaty cleavage*.

The formation of slaty cleavage occurs while the metamorphic grade is very low, so that recrystallization of clay minerals into new mica grains hardly takes place. However, a close look at a well-developed slaty cleavage reveals that a change has taken place in terms of the distribution of the minerals. There are domains dominated by quartz and feldspar, known as *QF-domains*, that separate *M-domains* rich in phyllosilicate minerals. The letters Q, F and M relate to quartz, feldspar and mica, and this structure is

Figure 12.7 Phyllitic cleavage bears similarities with crenulation cleavage when viewed under the microscope. The difference is that the crenulations are invisible to the naked eye. In this case a phyllitic cleavage dies out towards a folded competent lamina.

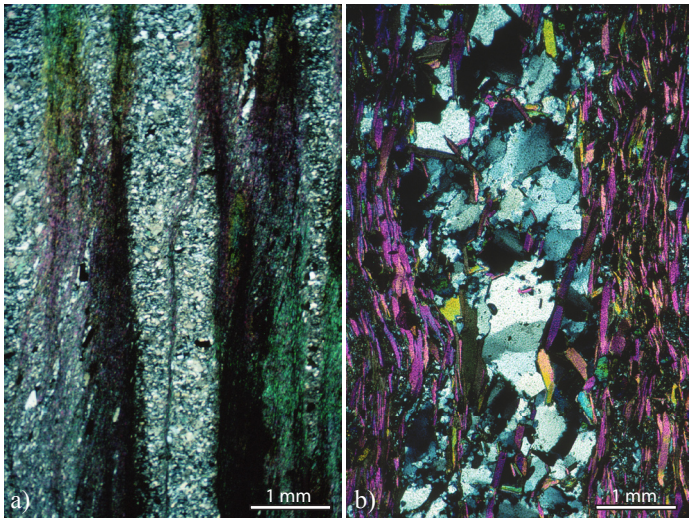

Figure 12.8 a) The rock on the left has barely entered the greenschist facies and shows a phyllitic cleavage. b) This cleavage formed higher into the greenschist facies, showing very well-developed QF- (middle) and M-domains and coarser grain size.

clearly visible under the microscope, i.e. the domains are considerably thinner than 1 mm. The QF-domains are typically lozenge- or lens-shaped while the M-domains form narrower, enveloping zones. As shown below, many types of cleavages and foliations show a domainal structure, and they can all be referred to as *domainal cleavages*.

It was earlier thought that slaty cleavage forms by grain rotation alone. We now know that so-called wet diffusion or pressure solution must be involved in order to produce the domainal structure that characterizes slaty cleavage. Grains of quartz and feldspar are dissolved perpendicular to the orientation of the cleavage and achieve lensoid shapes (disk shapes in three dimensions). Where this happens, phyllosilicates are concentrated and M-domains form.

The term *disjunctive cleavage* (Figure 12.3) is commonly used about early tectonic domainal cleavage in previously unfoliated rocks such as mudstones, sandstones and limestones. The term disjunctive implies that it cuts across rather than crenulating (folding) preexisting foliations.

1.2.3 Greenschist facies – from cleavage to schistosity

New mica minerals grow at the expense of clay minerals in shales and slates when they enter the field of greenschist facies metamorphism. A *phyllite* forms and the cleavage changes into a *phyllitic cleavage* (Figure 12.7). The new mica minerals grow with their basal plane more or less perpendicular to the Z-axis of the strain ellipsoid, and more or less perpendicular to σ_1. The new-formed mica grains are thus parallel and the phyllitic cleavage is established. The cleavage is still a continuous one, and the development of QF- and M-domains is more pronounced than for slaty cleavage. The domainal cleavage becomes better developed because dissolution (wet diffusion) accelerates with increasing temperature (Figure 12.8).

When the original claystone reaches upper greenschist facies and perhaps lower amphibolite facies, the mica grains grow larger and become easily visible in hand sample. At the same time, the foliation gets less planar, wrapping around quartz-feldspar aggregates and strong metamorphic minerals such as garnet, kyanite and amphibole. The foliation is no longer called a cleavage but a *schistosity*, and the rock is a *schist*.

Schistosity is also found in quartz-rich rocks such as quartz schists and granites. Here the thickness of M and QF-domains is on the mm- or even cm-scale and they appear more regularly and planar than for micaschists. This is why quartz schists and sheared granites split so easily and can be used for various

building purposes. In summary, while wet diffusion (solution) and grain reorientation dominated the formation of slaty cleavage, increased recrystallization controls the formation of schistosity.

1.2.4 Secondary tectonic cleavage (crenulation cleavage)

An already established foliation can be affected by a later cleavage (S_2 or higher) if the stress field changes during the deformation or due to a later deformation phase. Because cleavages tend to form perpendicular to the maximum shortening direction (X), a new cleavage will form that overprints the preexisting one(s). In many cases this occurs by folding the previous foliation into a series of microfolds, in which case the cleavage is called a *crenulation cleavage*. A crenulation cleavage is thus a series of microfolds at the cm-scale or less with parallel axial surfaces (Figure 12.9). Depending on the angle between the existing foliation and the secondary stress field, the crenulation cleavage will be symmetric or asymmetric. A *symmetric crenulation cleavage* has limbs of equal length, while an *asymmetric crenulation cleavage* is composed of small, asymmetric folds that may be S- or Z-folds.

Crenulation cleavage through which the earlier foliation can be traced continuously is known as *zonal crenulation cleavage*. In the opposite case, where there is a sharp discontinuity between QF- and M-domains, the cleavage is called a *discrete crenulation cleavage*. The M-domains are here thinner than the QF-domains and mimic microfaults. Discrete and zonal crenulation cleavages can grade into each other within a single outcrop.

Crenulation cleavage is restricted to lithologies with a pre-existing well-developed foliation that at least partly is defined by phyllosilicate minerals. It is commonly seen in micaceous layers while absent in neighboring mica-poor layers. There is a natural connection between the domainal thickness of the affected foliation and the wavelength of the new crenulation cleavage: thicker domains produce longer crenulation wavelengths. This is the same relationship between layer thickness and wavelength that was explored in Chapter 11, where the viscosity contrast was shown to be important. A close connection is also seen between crenulation cleavage and folding, as discussed in the next section (Figure 12.10).

We can find any stage of crenulation cleavage development, from faint crenulation of foliations to intense cleavage development where recrystallization and pressure solution has resulted in a pronounced domainal QF-M-structure. In the latter case the original foliation can be almost obliterated in hand sample although usually observable under the microscope. Progressive evolution of crenulation cleavage is accompanied by progressive shortening across the cleavage, and eventually a crenulation cleavage can transform into a phyllitic foliation.

Figure 12.9 Asymmetric crenulation cleavage affecting well-foliated metasediments. The cleavage is discrete in the middle, micaceous layer, while it is zonal and more weakly developed in the more quartz-rich adjacent layers.

Figure 12.10 Crenulation cleavage affecting the phyllitic cleavage shown in Figure 12.8a. The crenulation cleavage is seen to be axial planar to dm-scale folds. Photo: Ø.J. Jansen.

Figure 12.11 Discrete cleavage in phyllite, axial planar to mesoscopic folds. Joma area, Central Norwegian Caledonides.

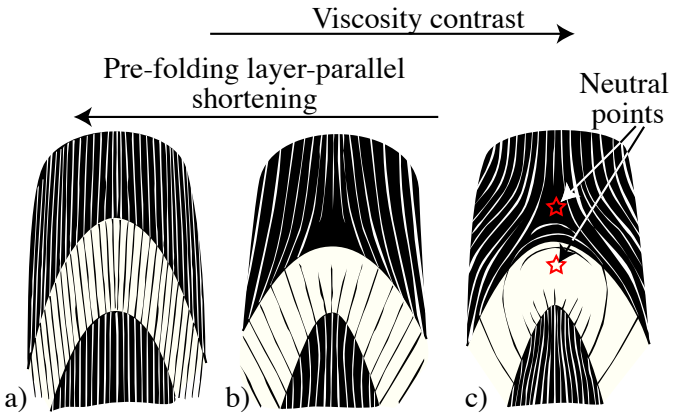

Figure 12.13 Different cleavage patterns in and around the hinge zones of folded competent layers. The amount of layer-parallel shortening prior to the folding is important, together with the viscosity contrast. Based on Ramsay & Huber (1987).

1.3 Cleavage, folds and strain

1.3.1 Axial planar cleavage

A close geometric relation between cleavage and folds is seen in most cases, and it is clear that the two form simultaneously (Figure 12.11). Geometrically a cleavage splits the fold more or less along the axial surface, particularly near the hinge zone. Where a cleavage parallels the axial surface, the cleavage is called *axial planar cleavage*. Interestingly, if we study the cleavage-fold relations in detail we may see a difference in orientation between the axial plane and the cleavage. In fact, the orientation of the cleavage may be seen to vary from layer to layer. The variations occur across layers of contrasting competence or viscosity and the phenomenon is called *cleavage refraction*. The higher the contrast in competency, the more pronounced the refraction.

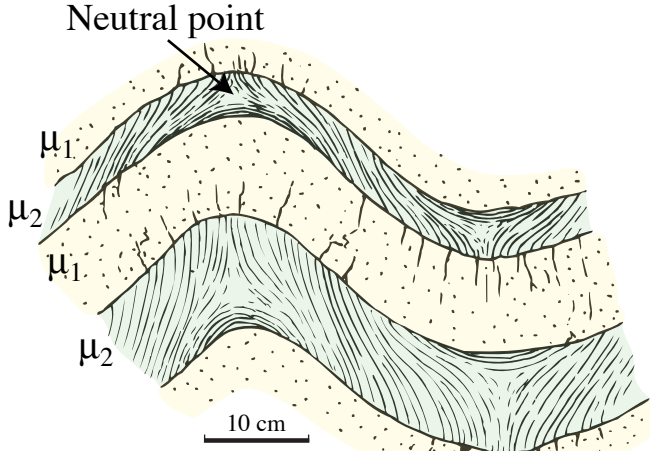

Figure 12.12 Folded sand-shale layers. Non-planar cleavage in the shale reflects variations in the orientation of the local X-Y plane. Note that there is no cleavage at the neutral points. Compare witih the next figure. Redrawn from Roberts & Strömgård (1972).

Cleavage can also form a variety of patterns in the hinge zone. David Roberts mapped such patterns in the Caledonian nappes in Finnmark, North Norway (Figure 12.12) and showed how the patterns can be reproduced in the laboratory. In general, the cleavage is oriented perpendicular to the shortening axis, i.e. it represents the XY-plane of the strain ellipsoid. As shown in the examples from Finnmark and other places, the cleavage can disappear in two points in the hinge zone. One of these points is located in the competent layer and the other in the incompetent layer. The two points where cleavage vanishes are called *neutral points*.

The example shown in Figure 12.12 is not unique, but it is more common to see a continuous cleavage through alternating competent and incompetent layers, as shown in Figure 12.13a, or to see cleavage being developed in the incompetent layer only. The explanation lies in the early deformation history, as the resulting pattern is sensitive to the amount of layer-parallel shortening prior to cleavage formation. More specifically, the cleavage will be continuous if it is already well developed at the onset of folding. The result is illustrated in Figure 12.13a. If, on the other hand, the layer starts to fold before the cleavage is established, then the pattern shown in Figure 12.13c will emerge.

Field investigations show that at least some cleavage refraction is characteristic when layers of contrasting competence are folded. The refraction is most easily explained by a difference in shear strain (γ) between competent and incompetent layers (Figure 12.14). In this model the strain ellipse at the interface between a competent and incompetent layer

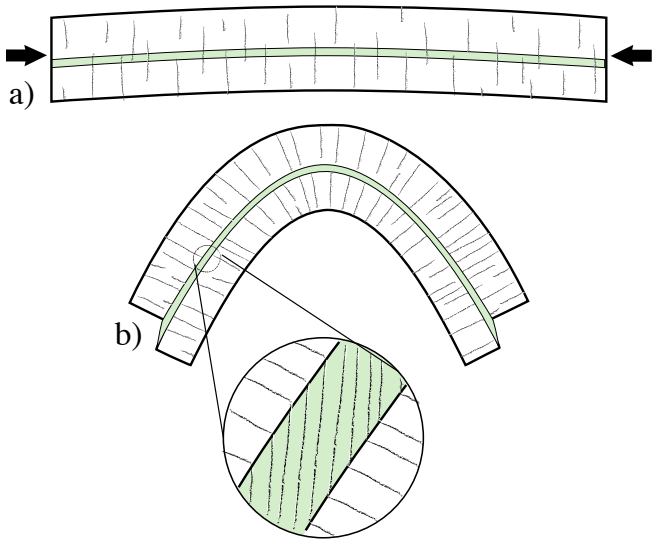

Fiure 12.14 Cleavage refraction caused by localized shear in incompetent layers on fold limbs (flexural shear).

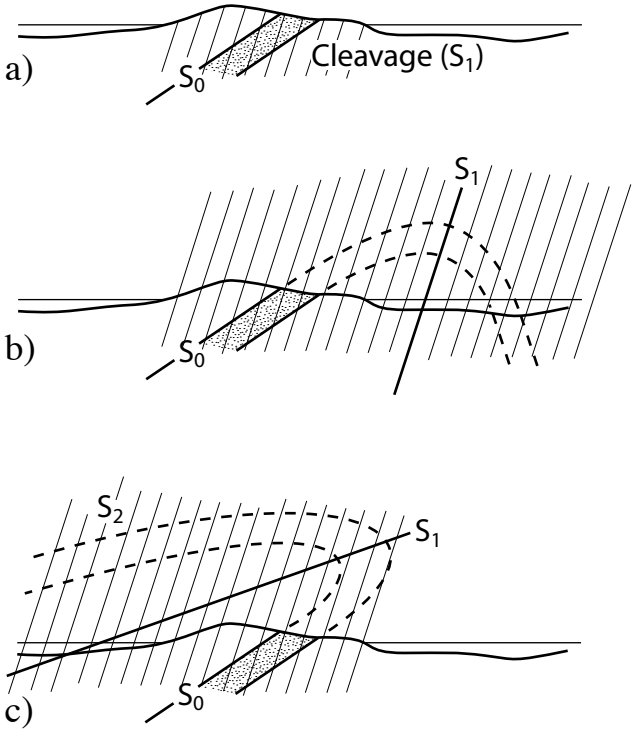

Figure 12.15 a) Mapped cleavage-layering relation in an area. b) Interpretation of a large-scale fold based on the assumption that the cleavage is related to such a fold. If the fold has a completely different geometry (c), then the fold and the cleavage formed at different times.

is common to the strain ellipsoids in both layers, as shown in Figure 12.14.

The angular relation between cleavage and layering is also related to the position on the overall fold structure (Figure 12.15). In spite of its tendency to show some refraction, cleavage has a fairly consistent orientation across a fold, while the attitude of the folded layers change systematically. As shown in Figures 12.15a and b the fold geometry can easily be constructed (qualitatively) from observations of the cleavage-layering relation from only a single locality. Clearly this method assumes a genetic relationship between the cleavage and the folding. Later cleavage that is unrelated to the folding can also occur in a polydeformed area, in which case the angular relations tell nothing about the large scale fold geometry (Figure 12.15c).

1.3.2 Strain

Cleavage formed at low metamorphic grades, i.e. slaty cleavage and in part crenulation cleavage and phyllitic cleavage, are generally assumed to represent the X-Y or flattening plane. Knowing the orientation of the X-Y plane of the strain ellipsoid is very useful information when conducting structural analysis of a region.

Next we will turn to the shape of the strain ellipsoid. In general, volume loss (dilation) is an important component of cleavage-related strain. At low temperature and shallow burial depths compaction cleavage forms in sediments involving a 30-40% reduction in volume. Pressure solution-dominated cleavages in limestones may involve an even larger loss of volume. Rocks with a well-developed slaty cleavage typically show evidence of 50-75% shortening across the cleavage (Figure 12.16). How do we know? Fortunately, strain markers such as the reduction spots in some shales (spheres in three dimensions) are well preserved. When deformed, these reduction spots change from circles to ellipses that represent sections through the local strain ellipsoid (Figure 4.1). Fossils with known original shape or geometry can also be used to estimate strain in cleaved (meta)sedimentary rocks.

Cleavages approximate the X-Y plane of the strain ellipsoid and are characterized by substantial volume loss.

In principle shortening perpendicular to cleavage is compensated by stretching in the plane of cleavage (through pure shear or axially symmetric flattening, see

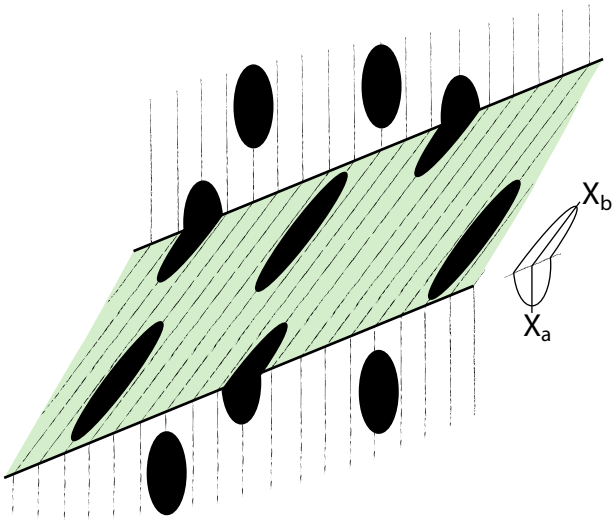

Figure 12.16 Strain associated with cleavage refraction (assuming no slip along layer interfaces). The strain must be compatible across the interfaces, i.e. strain ellipses must fit together as shown. In this situation, the only deformation possible is simple shear and/or volume change across the layering.

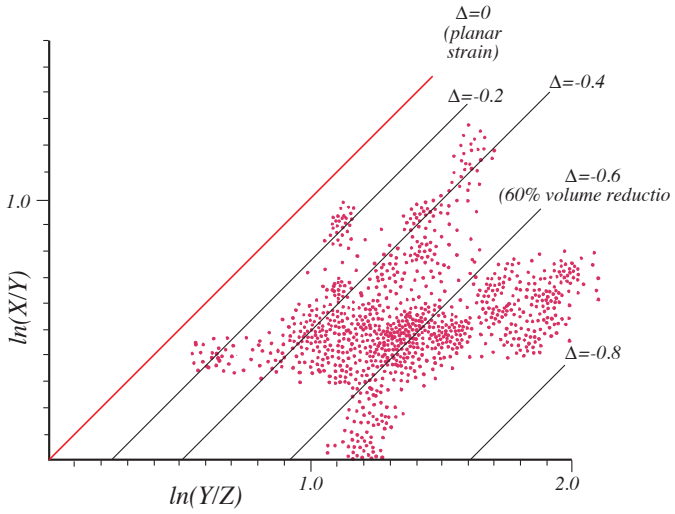

Figure 12.17 Strain data from slates with well-developed slaty cleavage. The data fall completely within the field of flattening. Δ is the volume loss factor from Chapter 3. Data from Ramsay & Wood (1973).

Figure 3.13). The effect of such flattening depends on the role of pressure solution. If pressure solution (wet diffusion) is a prominent deformation mechanism, which it often turns out to be, then the shortening may be uncompensated for in the X-Y plane, and oblate shapes result. Significant loss of volume has been documented by a number of studies (Figure 12.17), which shows that diffusion of material out of the rock is an important mechanism during cleavage formation[2]. While physical compaction may be important in the formation of compaction cleavage in porous rocks, wet diffusion becomes more important as temperature increases.

Pressure solution (wet diffusion) is responsible for the oblate strain ellipsoids associated with cleavage formation.

Phyllitic cleavage and the foliation in schists can be influenced by simple shear deformation. They are not always the result of pure coaxial shortening. Furthermore, so-called shear bands that may look similar to axial plane cleavages can develop. Shear bands do not relate directly to the strain ellipsoid but provide important information about the sense of vorticity, as discussed in Chapter 15.

2 Alternatively, the dissolved material would be precipitated in the QF-domains, which does not appear to be the case to any great extent in most cases.

1.3.3 Transected folds

In many cases the axial surface has more or less the same orientation as the axial plane cleavage, but not always. In some cases there is a marked difference between cleavage and axial surface (Figure 12.18), even where the folding and the cleavage are genetically related and where there is no refraction due to rheologically contrasting layers. In such cases the cleavage transects not only the axial surface but also the hinge line or axis of the fold (Figure 12.18). Such cleavage is called *transecting cleavage*, and the folds are referred to as *transected folds*.

The extensive slate belts of Wales and the Scottish Southern Uplands exhibit classical examples of transected folds. The obliquity is systematic in these regions, with the cleavage being rotated

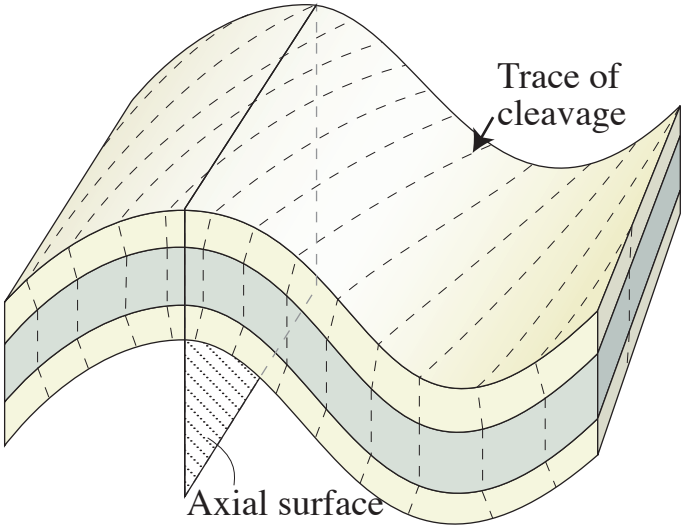

Figure 12.18 Cleavage transecting the axial surface of at transected fold.

clockwise relative to the fold axis, as shown in Figure 21.18. There is more than one explanation for this phenomenon, but most involve simple shear with or without additional pure shear. The systematic mismatch between the axial planes and cleavage in the British Caledonides has been explained by sinistral transpression (see Chapter 18). In such a tectonic regime folds and cleavages will rotate during the deformation and a slight time difference between the onset of folding and cleavage formation can result in transected folds. However, transected folds can also form in coaxial deformations in the case of non-steady-state flow, i.e. where the ISA rotates relative to the deforming rock.

1.4 Foliations in quartzites, gneisses and mylonite zones

Mica-bearing quartzites develop a foliation known as *schistosity*. There are not enough phyllosilicates to make the continuous cleavages seen in slates and phyllites, or the wavy foliation seen in micaschists, but the impure quartzite or *quartz schist* will split neatly into cm- to dm-thick slabs typically used for pavements or other building purposes. The splitting is mainly due to parallel phyllosilicates that impose an anisotropy to the rock. A pure quartzite will never develop a well-defined schistosity because there are no phyllosilicate minerals to become reoriented and concentrated. A shape fabric formed by flattening of individual quartz grains can give the rock some anisotropy, but not as strongly as in quartz schist. Pure quartzites preserve a *quartzitic banding* from variations in grain size or color variations, commonly

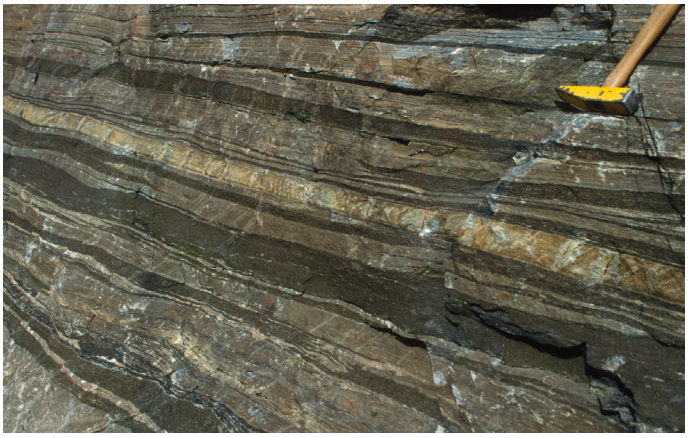

Figure 12.19 Gneissic banding, formed during shearing of a heterogeneous intrusive complex. High strains are required to reach this stage of transposition.

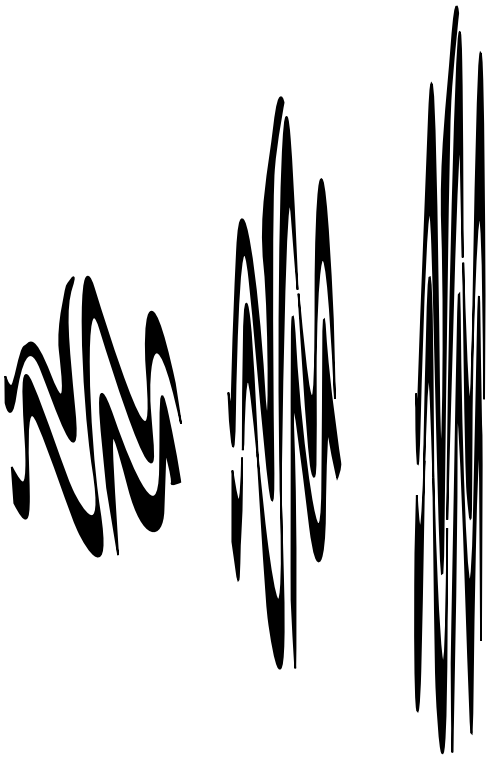

Figure 12.20 Example of transposition by horizontal shortening and vertical extension. The result is a banded rock with intrafolial and perhaps isolated fold hinges.

portraying tight to isoclinal similar folds where strain is high.

Granites and other quartzofeldspathic rocks poor in phyllosilicate minerals do not develop cleavage as easily as most other rocks. Significant time and energy is required to reorganize and collect those few mica grains in a granite under lower greenschist facies conditions[3]. Many magmatic rocks also have a high feldspar/quartz ratio. Feldspars require considerably higher temperature than quartz to deform plastically and lack the mobility of quartz in wet diffusion.

This does not mean that there is no foliation in deformed magmatic rocks. In some cases we can see a spaced cleavage in coarse grained, magmatic rocks. The spacing between the mica-enriched domains may well be several centimeters. At high strains granites and other magmatic rocks will develop a foliation from reorientation and flattening of minerals and mineral aggregates. In many cases this process can be related to non-coaxial deformation, in contrast to the coaxial deformations that seem to be responsible for cleavages in many slates and phyllites. The foliation in magmatic rocks is called *schistosity* or *gneissic banding* rather than cleavage (Figure 12.19).

Gneissic banding commonly results from a

3 Phyllosilicates can also grow as secondary minerals at the expense of feldspar (and H_2O) in some cases.

Figure 12.21 Mylonitic foliation formed by shear-related plastic grain-size reduction of a granitic rock. The domains are much finer than the banding in Figure 12.17.

transposition process, in which case it can be called a *transposition foliation* consisting of a *transposed layering*. By transposition we mean a process where earlier structures, including dikes, veins and single or multiple foliations, are rotated and flattened into almost complete parallelism (Figure 12.20). Both coaxial and non-coaxial deformation can result in a transposed foliation if strain is high.

Even if there are no preexisting planar structures in our magmatic rock, high strain, and particularly high non-coaxial strain, may result in a *mylonitic foliation*. Mylonitic foliations are related to transposed layering and gneissic banding, but the distance between the foliation domains is smaller, typically on the mm- or cm-scale (Figure 12.21). This is related to the high strains involved; high strains flatten objects and thin layers. Mylonite zones are typically found in shear zones or thrust zones that involve large (km-scale or more) displacements. Mylonites and mylonitic shear zone structures are discussed in more detail in Chapter 15.

---***---

Foliations are extremely common in deformed rocks. Because foliations form perpendicular or at a high angle to the shortening direction, they give us important strain information where regular strain markers are absent. Furthermore, there are many types of foliations that relate not only to lithology, but which reflect the temperature or depth of burial during deformation. Foliations should always be devoted close attention in deformed metamorphic rocks.

Further reading:

Beutner, E. & Charles, E., 1985. Large volume loss during cleavage formation, Hamburg sequence, Pennsylvania. Geology, 13: 803-805.

Cosgrove, J.W., 1976. The formation of crenulation cleavage. Journal of the Geological Society, 132: 155-178.

Dieterich, J.H., 1969. Origin of cleavage in folded rocks. Americal Journal of Science, 267: 155-165.

Engelder, T. & Geiser, P., 1979. The relationship between pencil cleavage and lateral shortening within the Devonian secion of the Appalachian Plateau, New York. Geology, 7: 460-464.

Goldstein, A., Knight, J. & Kimball, K., 1999. Deformed graptolites, finite strain and volume loss during cleavage formation in rocks of the taconic slate belt, New York and Vermont, U.S.A. Journal of Structural Geology, 20: 1769-1782.

Gray, D.R. & Durney, D.W., 1979. Crenulation cleavage differentiation: implications of solution-deposition processes. Journal of Structural Geology, 1: 73-80.

Hanmer, S.K., 1979. The role of discrete heterogeneities and linear fabrics in the formation of crenulatons. Journal of Structural Geology, 1: 81-91.

Johnson, T.E., 1991. Nomenclature and geometric classification of cleavage-transected folds. Journal of Structural Geology, 13: 261-274.

Mancktelow, N.S., 1994. On volume change and mass transport during the development of crenulation cleavage. Journal of Structural Geology, 16: 1217-1231.

Ramsay, J.G. & Huber, M.I., 1983. The techniques of modern structural geology: Strain analysis, 1. Academic Press, London, 307 ss.

Ramsay, J.G. & Woods, D.S., 1973. The geometric effects of volume change during deformation processes. Tectonophysics, 16: 263-277.

Robin, P.-Y., 1979. Theory of metamorphic segregation and related processes. Geochemica et Geochemica Acta, 43: 1587-1600.

Siddans, A.W.B., 1972. Slaty cleavage - a review of research since 1815. Earth-Science Reviews, 8:

205-212.
Sorby, H.C., 1853. On the origin of slaty cleavage. New Philo. J. (Edinburgh), 55: 137-148.
Swager, N., 1985. Solution transfer, mechanical rotation and kink-band boundary migration during crenulation-cleavage development. Journal of Structural Geology, 7: 421-429.
Treagus, S.H., 1983. A theory of finite strain variation through contrasting layers, and its bearing on cleavage refraction. Journal of Structural Geology, 5: 351-368.
Treagus, S.H., 1988. Strain refraction in layered systems. Journal of Structural Geology, 10: 517-527.
Wood, D.S., 1974. Current views of the development of slaty cleavage. Annual Reviews of Earth Science, 2: 1-35.
Worley, B., Powell, R. & Wilson, C.J.L., 1997. Crenulation cleavage formation: evolving diffusion, deformation and equilibration mechanisms with increasing metamorphic grade. Journal of Structural Geology, 19: 1121-1135.

CHAPTER 13

Lineations

Linear structures often go hand in hand with planar structures in deformed rocks. Since their first presentation on a printed map in 1888 by the Norwegian geologist Hans Reusch, it has been clear that lineations contain important information about strain as well as kinematics. In this context it is important to distinguish between the different types of linear structures, because they have different meanings and implications, depending on their settings and relationships with other structures.

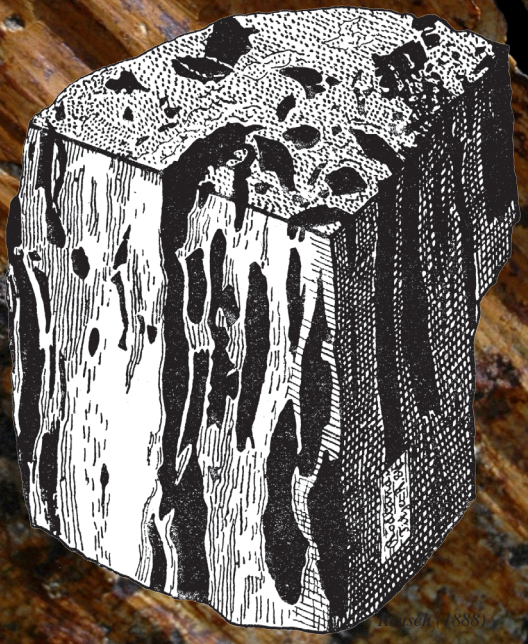

1.1 Basic terminology

Lineation is a term used to describe linear elements that occur in a rock. A large number of non-tectonic or *primary linear structures* occur in both undeformed and deformed rocks. Ropy lava, flow lineations and columns in columnar basalts in igneous rocks and long axes of aligned non-spherical pebbles, groove marks and aligned fossils in sedimentary rocks are some examples. In our context the term lineation is used for linear structures resulting from deformation, although primary structures may also be involved, such as in the formation of S_0-S_1 intersection lineations (see below). *Tectonic linear structures* include elongated physical objects, such as strained mineral aggregates or conglomerate pebbles, lines of intersection between two sets of planar structures, and geometrically defined linear features such as fold hinge lines and crenulation axes. A distinction is made between *penetrative lineations*, which build up a linear fabric or L-fabric, *surface lineations*, which are restricted to a surface (e.g. slickenlines), and non-physical, *geometric lineations* such as fold axes.

Lineations are generally distinguished from the related term *lineament*, which is used for linear features at the scales of topographic maps, aerial photos, satellite images or digital elevation models. Lineaments may be related to planar structures such as fractures and foliations that intersect the surface of the Earth.

1.2 Lineations related to plastic deformation

Penetrative lineations (Figure 13.1) are found almost exclusively in rocks deformed in the plastic regime. Where the lineation forms a fabric that dominates an S-fabric, the rock can be classified as an *L-tectonite*. A strong L-fabric usually plots in the constrictional field of the Flinn diagram (Figure 3.?), i.e. X>>Y≥Z. A combination of a foliation (S-fabric) and a penetrative lineation (L-fabric) is more common, and is located closer to the diagonal in the Flinn diagram. A rock with a combined L- and S-fabric is referred to as an LS-tectonite.

1.2.1 Mineral lineations

A penetrative linear fabric is typically made up of aligned elongate minerals. Amphibole needles in an amphibolite are a common example. The alignment reflects recrystallization reorientation during deformation, but can also arise from a solution/precipitation process. Precipitation of quartz in pressure shadows or *strain shadows* may also facilitate minerals or mineral aggregates to grow in a preferred direction.

Cataclasis, pressure solution and recrystallization all contribute to a change in shape of minerals during deformation. Ideally, if a mineral aggregate had a spherical shape at the onset of deformation, its shape after deformation would represent the strain ellipsoid. In practice, the original shape is unknown so that the final shape only gives us a qualitative impression of the shape of the strain ellipsoid. Nevertheless, deformed mineral aggregates in gneisses have been used for strain analysis, although the difference in viscosity between the aggregates and their surroundings may add uncertainty to the results. In cases where the initial shape is known and the competency contrast is small, such analyses are particularly useful. Deformed conglomerates or oolites are examples of rocks where linear shapes can quantitatively be related to strain (see Chapter 4). These and other lineations formed by the shape of deformed objects are named *stretching lineations* (Figure 13.2). Stretching lineations are extremely common in plastically deformed rocks.

Fibrous minerals also form lineations where

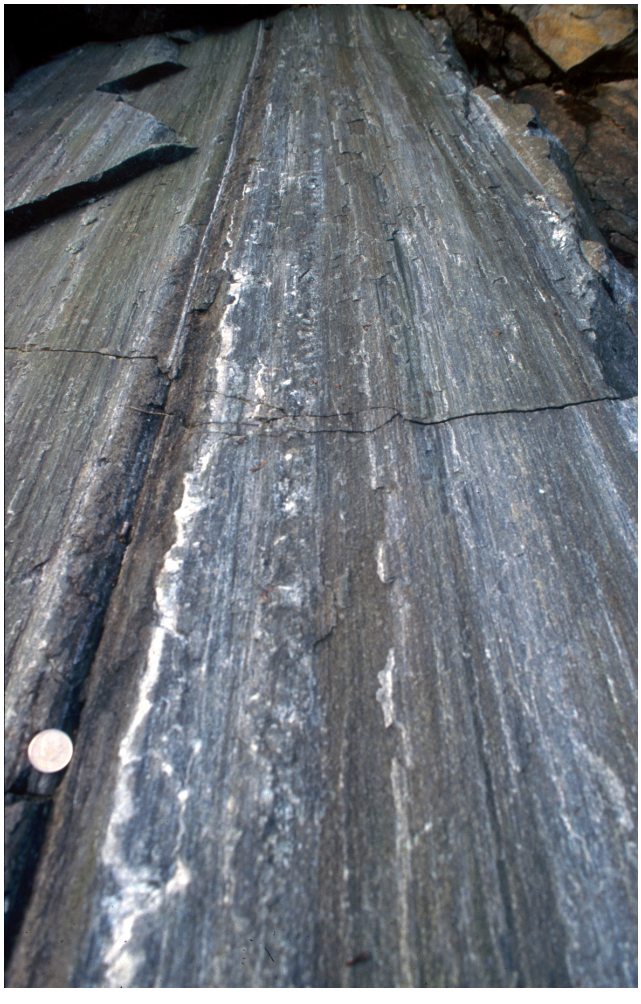

Figure 13.1 Mineral lineation in gneiss.

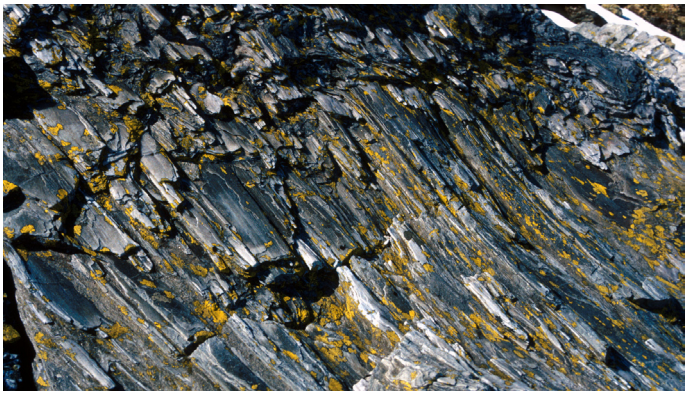

Figure 13.2 Stretching lineation in quartzite conglomerate. The long axes of the pebbles are dipping to the right. The Bergsdalen Nappes, West Norway Caledonides.

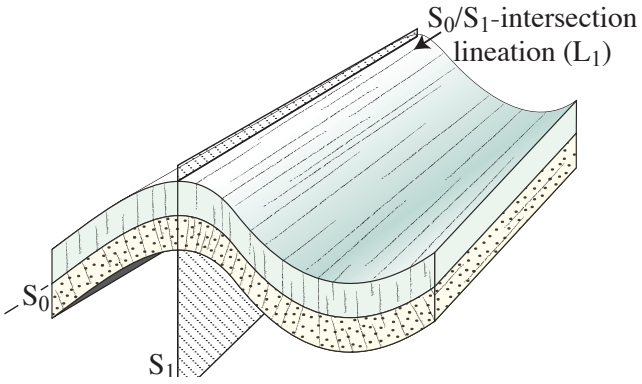

Figure 13.3 Intersection lineations appearing on bedding or foliation surfaces that are intersected by a later foliation.

they have grown in a preferred direction, and usually define the stretching direction or ISA_1. Referred to as *mineral fiber lineation*, they commonly indicate the stretching direction during fiber growth. Fiber lineations can form in veins in unmetamorphosed sedimentary rocks, particularly in overpressured mudstones, but also in veins and associated with porphyroclasts in low-grade metamorphic rocks. Fibers do not grow if temperature gets higher than those of middle greenschist facies conditions. Thus, mineral fibers form in the brittle and low-T plastic regimes.

Rodding describes elongated mineral aggregates that are easily distinguished from the rest of the rock. Quartz rods are common in micaschists and gneisses where striped quartz objects occur as rods or cigars in the host rock. Rods are often considered as stretching lineations, but are commonly influenced by other structure-forming processes. They may represent isolated fold hinges, or be related to boudinage or mullion structures (see below), or to deformed veins with an originally elongated geometry.

1.2.2 Intersection lineations

Many deformed rocks host more than one set of planar structures. A combination of bedding and cleavage is a common example. In most cases multiple sets of planar structures intersect. The line of intersection is regarded as a lineation and bears the name *intersection lineation*. Where the first tectonic cleavage (S_1) cuts the primary layering or bedding (S_0), the resulting intersection lineation (L_1) appears on the bedding planes, as shown in Figure 13.3. Intersection lineations formed by the intersection of two tectonic foliations are also common. In most cases intersection lineations are related to folding, with the lineation running parallel to the axial trace and the hinge line (Figure 13.4). Note that for transected folds (Figure 12.16) there will be an angle between the intersection lineation and the axial trace.

In some cases an intersection lineation can be seen only locally in a deformed rock. In most cases, however, their frequency and distribution is large enough that the lineation can be considered penetrative (Figure 13.4).

1.2.3 Fold axes and crenulation lineations

Fold axes are generally regarded as linear structures, despite being theoretical lines related to the geometrical shape of the folded surface. Some rocks have a high enough density of parallel fold axes that they constitute a fabric. This is often the case with small-scale folding or crenulation of phyllosilicate-rich metamorphic rocks, known as *crenulation lineations*. Crenulation lineations are simply composed of numerous mm- to cm-scale fold hinges of low-amplitude folds. They is commonly seen in multiply deformed phyllites, micaschists and in micaceous layers in quartz-schists, mylonites and gneisses. Crenulation lineations are closely associated with intersection lineations but are different in that they are constituted by fold hinges identifiable to the naked eye.

During folding of layered rocks crenulation cleavages and crenulation lineations form at an early stage, while larger folds form later on during the same process. It is therefore of interest to compare the early-formed crenulation lineations with the subsequent fold axes in order to explore how the layers rotated relative to the stress field. We are already familiar with the concept of transected folds, where a crenulation lineation is expected to make an oblique angle to the fold axis (Figure 12.5).

Figure 13.4 Intersection lineation in quartz schist between two foliations in the Caledonian nappes of West Norway. The lineation is parallel to the hinges of minor folds.

1.2.4 Boudinage

Boudins are competent rock layers that have been stretched into segments. Individual boudins are generally much longer in the third dimension (perpendicular to the common section of observation) and thus define a lineation. Boudins form where the X-axis of the strain ellipsoid is significantly larger than Y. Chocolate-tablet boudins (see next chapter) can form when X≈Y.

When occurring in folded layers, boudins typically appear on the limbs of the fold with their long axes oriented in the direction of the fold axis (Figure 13.6). In general, boudinage structures are most easily recognized in sections that make a high angle to the X-axis and are best shown in a section that contains X. Because of this fact they may be difficult to recognize as linear features in deformed rocks. It is also true that boudins are restricted to competent layers and therefore more restricted in occurrence than most other lineations. They are nevertheless

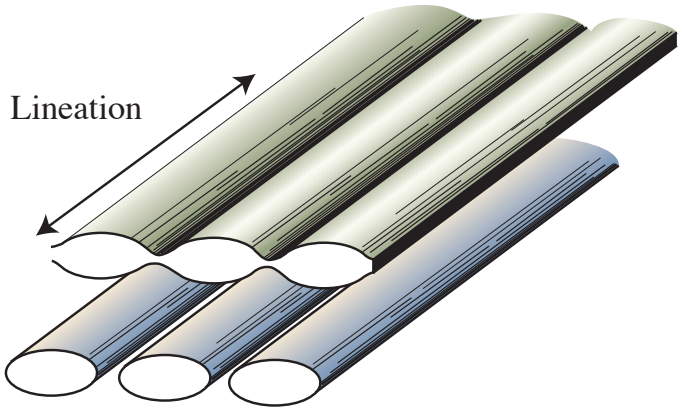

Figure 13.5 Cylindrical pinch-and-swell structures (above) and boudines represent linear elements in many deformed rocks.

important enough structures to deserve a full (next) chapter.

1.2.5 Mullions

Mullion is the name that structural geologists use for linear deformation structures that are restricted to the interface between a competent and an incompetent rock[1]. The viscosity contrast must be significant for mullions to form, and their cusp shapes always point into the more competent rock, i.e. the one with the higher viscosity at the time of deformation (Figure 13.7). Such mullions are closely related to buckle folds in the sense that their formation is predicted by a contrast in viscosity, they form by layer-parallel shortening, and their characteristic wavelength is related to the viscosity contrast. But they differ from buckle folds by having shorter wavelengths and they are restricted to a layer interface. A common place to find mullion structures in metamorphic rocks is at

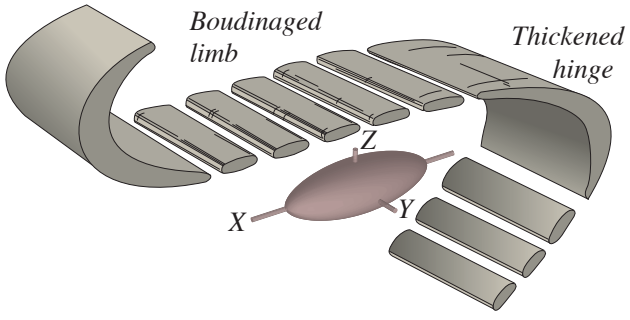

Figure 13.6 Common connection between folding and boudinage. The fold hinges are thickened while the limbs are extended and boudinaged. The strain ellipse is indicated.

1 Note that the term mullion has been used in several different ways in the literature, ranging from striations on fault surfaces (fault mullions) to those formed in extension as well as contraction.

the boundary between quartzite and phyllite or schist. Mullions are also common on the surface of quartz pods in micaschists.

1.2.6 Pencil structures

The formation of *pencil structures* occurs as a result of discrete interference between compaction cleavage and a subsequent tectonic cleavage, or between two equally developed tectonic cleavages, as discussed in Chapter 12. Pencil structures have a preferred orientation and form a lineation in unmetamorphosed and very low-metamorphic rocks.

1.3 Lineations in the brittle regime

Some lineations occur only on fracture surfaces. They are not fabric-forming elements and are more characteristic of the brittle regime in the upper crust. These lineations form by mineral growth in extension fractures, as striations ~~are~~ carved on the walls of shear fractures and faults, by intersections between fractures and by primary geometries that form during fracture formation.

Mineral lineations in the brittle regime tend to be restricted to *fiber lineations* (Figure 13.8). These lineations are minerals that have grow in a preferred direction on fractures. The growth of minerals on fractures usually requires opening mode or extension. Furthermore, the minerals must grow in a preferred direction for a lineation to be defined. Minerals such as quartz, antigorite, actinolite, and anhydrite commonly occur fibrous on fractures.

Mineral fibers are found in many extensional or Mode I fractures, as shown in Figure 13.9. The orientation of the fibers is commonly taken to represent the extension direction. Curved fibers are sometimes seen, implying that the extension direction has changed during the course of deformation or that shear has occurred after the formation of the fibers.

Even though extension is involved in the formation of fibrous mineral lineations, this does not imply that such lineations are restricted to extension fractures. Because of the irregular shapes of most shear fractures, a component of extension may locally occur and minerals may grow as the walls separate (Figure 13.10). The mineral fibers grow on the lee side of steps or other irregularities, precipitated from fluids circulating on the fracture network. Thus, the sense of slip is detectable from the relation between fiber growth and fracture geometry.

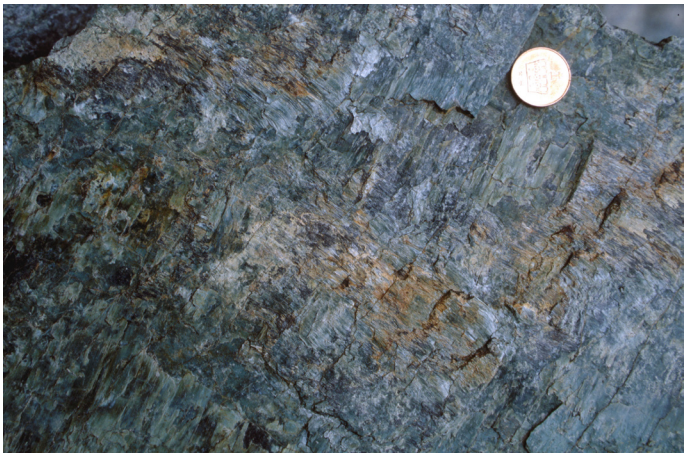

Figure 13.8 Two perpendicular sets of mineral lineations on a fault surface in serpentinite. The two directions indicate movements under two different stress fields. Leka Ophiolite, Scandinavian Caledonides.

Striations or *slickenlines* are lineations found on shear fractures and form by physical abrasion of hanging-wall objects into the footwall or vice versa (Figure 13.11 and 12). The smooth and striated slip surface itself is called a *slickenside*. Slickensides tend to be shiny, polished surfaces coated by a ≤1 mm thick layer of crushed, cohesive fault rock. Hard objects or asperities can carve out linear tracks or grooves known as *fault grooves*. The term groove lineation can be used for this type of slickenlines. Such mechanically formed slickensides may show similarities with glacially striated surfaces. Close examination of many slickensided slip surfaces reveals that they are formed on mineral fill or that they actually are fiber lineations. There are thus two principal types of slickenlines; those that form by mechanical abrasion (striations) and those formed by fibrous growth (slip fiber lineations).

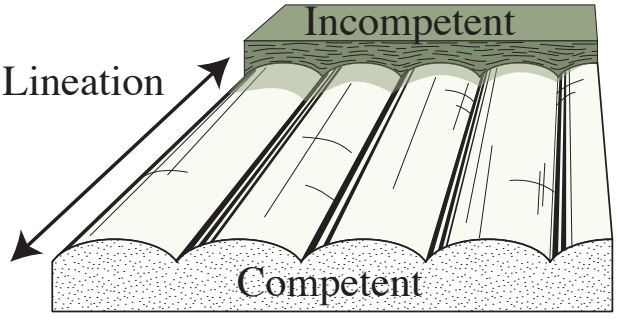

Figure 13.7 Mullion structures form lineations at the interface between rocks of significantly different competence (viscosity).

Figure 13.9 Fiber lineation (talk) in extension fracture where the fibers have grown perpendicular to the fracture walls as the fracture opened. Evidence of mild shearing parallel to the fracture is seen.

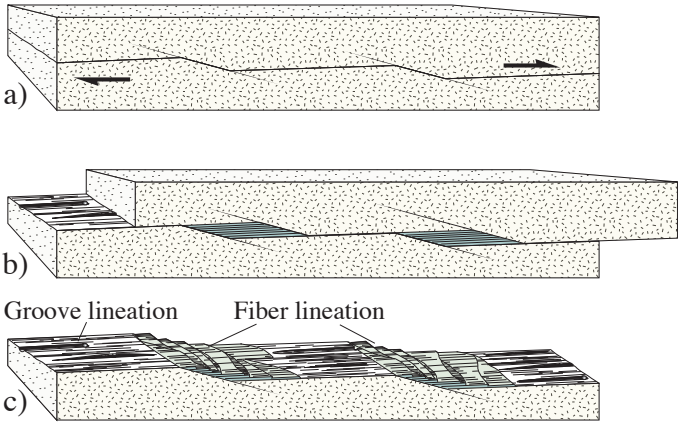

Figure 13.10 Formation of fiber lineation in irregular shear fractures. a) Early stage. b) Final stage. In c) the upper wall is removed for inspection. Groove lineations (striations) are found on surfaces that have not opened during faulting.

Figure 13.11 Slickensides with slickenlines, formed by cataclastic shearing of epidote on a post-Caledonian normal fault in the Precambrian of West Norway.

Minerals may grow during the movement history of a fault, and it is not uncommon to find a combination of fiber lineations and striations, where both the wall rock and the new-formed minerals are subjected to mechanical abrasions and thus show striations.

Geometric striae relate to the initial irregular shape of a shear fracture. Such irregularities may have a preferred orientation or axis in the slip direction and appear as a lineation on an exposed wall. A special type of geometric striae is the cigar-shape seen on the walls of deformation band clusters, as portrayed in Figure 13.13. Geometric striae and physical striae or slickenlines commonly coexist.

Intersection lineations are found on fractures where the main slip plane is intersected by secondary fractures such as Riedel fractures or tension fractures. The lines of intersection typically (but not necessarily) form a high angle to the slip direction, in marked contrast to striae and mineral lineations that tend to parallel the slip direction.

Finally, we mention a type of lineation that is typical for deformed limestones. It forms perpendicular to pressure solution seams where shortening occurs across the fracture surface and are composed of tubular structures known as stickolites. These structures tend to point in the direction of contraction and slickolites are thus a kind of lineation that is kinematically different from the other lineations discussed above.

Figure 13.12 Striated fault surface separating limestone from sandstone. Lunar-shaped grooves that indicate the sense of slip (normal with a slight dextral component) are associated with competent fragments in the limestone breccia (also see Fig. 9.?). Riedel-fractures in the footwall intersects the striated fault surface, adding a gently left-dipping intersection lineation to the striated fault surface. Moab Fault, Utah.

Figure 13.13 Lineations in a zone of deformation bands. The lineation points down dip and is an expression of the cigar-shaped geometry of the undeformed rock between the deformation bands. Entrada Sandsone, San Rafael Desert, Utah.

1.4 Lineations and kinematics

1.4.1 Fault-related kinematics

Lineations are important structures for understanding the sense of movement on individual slip surfaces as well as the kinematics of fault populations. Fiber lineations, slickenlines and so-called geometric lineations give good indications of the movement, although a reliable determination of the sense of movement may require additional information. To distinguish normal from reverse movements or sinistral from dextral slip requires detailed information about fracture morphology relative to mineral growth, second-order fracture geometry, and correlation of markers across the slip surface or observation of drag adjacent to the fault. The traditional method of ”feeling” the sense of slip from moving your hand in either direction is in itself an unreliable method because that typically records “last movement”. Always identify the secondary structures or lineations that give rise to differences in friction and use their relative orientations to determine sense of slip.

It is common to find two or more sets of linear structures on a single slip surfaces (Figure 13.8). Different sets record different movements at different times, implying that the stress field changed between different slip events or moving block encountered a change in fracture pattern or lithologic character. In some cases the growth history and composition of minerals on such fractures can be used to reveal the relative timing of movement events. Multiple fault lineations may indicate local changes in the stress field during a single deformation event or may represent movement during two distinct regional stress fields.

1.4.2 Lineations and kinematic axes in the plastic regime

Lineations are common structures in plastic shear zones and mylonite zones, including extensional shear zones, strike-slip zones, or mylonites associated with thrust nappes. Recognized as containing important kinematic information as early as the 19th century, the burning question whether such lineations form parallel or perpendicular to the general movement direction continued into the mid-1900’s. By 1950 the Austrian geologist Bruno Sander set the scene with his focus on coordinate systems and symmetry. He defined three orthogonal axes, *a*, *b* and *c*, where the *a*-axis was defined as the transport direction and *c* being perpendicular to the shear plane (Figure 13.14). The issue was: do lineations and fold axes parallel the kinematic *a*- or *b*-axis? Sander and his school insisted that lineations indicate the *b*-direction. Sander’s theory was that the plane of symmetry in a deformed rock must contain the *a*-axis, while the *b*-axis is oriented perpendicular to this plane. Others, such as the British geologist E.M. Anderson and the Norwegian geologist Anders Kvale, opposed ~~to~~ Sander’s view. In the Norwegian Caledonides as elsewhere the stretching lineation was found to be parallel with the regional transport direction, and was also parallel to many fold axes. Anderson, Kvale and others thus concluded that the lineation in most cases is parallel to the *a*-axis. This is the view that soon became generally accepted.

The concept of kinematic axes was soon abandoned and replaced by strain axes that relate

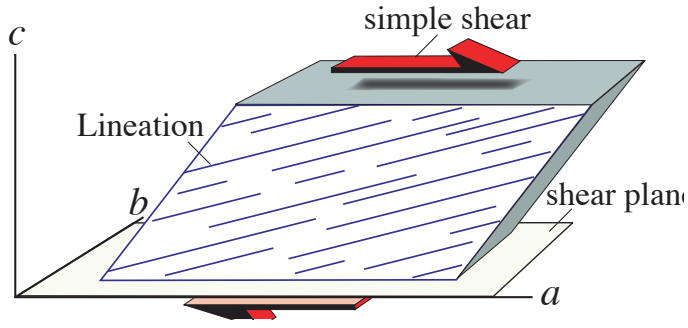

Figure 13.14 The stretching lineation and its relation to Sander's kinematic axes for simple shear. The lineation rotates towards the kinematic *a*-axis (the shear or transport direction) by increasing strain.

to the shear zone walls or other suitable planes of reference. For simple shear, the lineation lies in Sander's *a*-*c* plane, or the X-Z plane of the strain ellipsoid as it rotates from its initial position at 45° to the shear plane towards the shear direction (i.e. the kinematic *a*-axis; Figure 13.14). The lineation thereby has an orientation that depends on strain. For very high strains the lineation approximates the *a*-axis. For a thrust or penetratively deformed thrust nappe, this means that the trend of the lineation indicates the direction of transport[2].

Transport directions give somewhat less meaning when dealing with pure shear, but even in this case a transport of material in a fixed direction can be predicted. Just think of a soft thrust nappe collapsing by pure shear above a rigid basement. A consistently arranged stretching lineation is expected. For perfect pure shear the lineation will be parallel to the pure shear zone. Hence, the lineation becomes a perfect *a*-lineation in Sander's nomenclature. For other types of deformation, such as transtension, the lineation can be found to be oblique to the shear direction no matter how intense the deformation may be (see Chapter 18). In fact, it may even change orientation in quite dramatic ways.

More general deformations, such as oblique combinations of pure and simple shear (where the shear plane and the pure shear flattening plane are mutually oblique), can give a whole range of lineation orientations. These may become quite complicated, but it is important to realize that the implications of lineation orientation depends on the type of deformation, be it is simple shear, pure shear, or some combination of the two. The connection between lineation patterns and strain also tells us that the lineation pattern holds information about strain. A radial lineation pattern generated by three-dimensional gravitational collapse, as shown in Figure 16.27, suggests that the deformation is far from planar. Consistent linear patterns are however rather common, and because simple shear appears to dominate many shear zones with consistent linear patterns, the assumption that the lineations indicate the transport direction provide a very useful working hypothesis.

1.4.3 Other types of lineations

Stretching lineations are often the easiest type of lineations to resolve when transport direction is the issue. *Fold axes*, *crenulation lineations* and *intersection lineations* can be trickier. Such lineations may be results of a later, superimposed deformation that has little or nothing to do with the formation of the structures from an earlier major deformation. However, they may be useful in cases where different types of lineations form during the same deformation as the foliation that they affect. This is sometimes the case in mylonites, where foliation is continually folded and new cleavages are formed repeatedly during the process of mylonitization.

In some cases the fold axes make a high angle to the stretching and mineral lineation. Hence, two sets

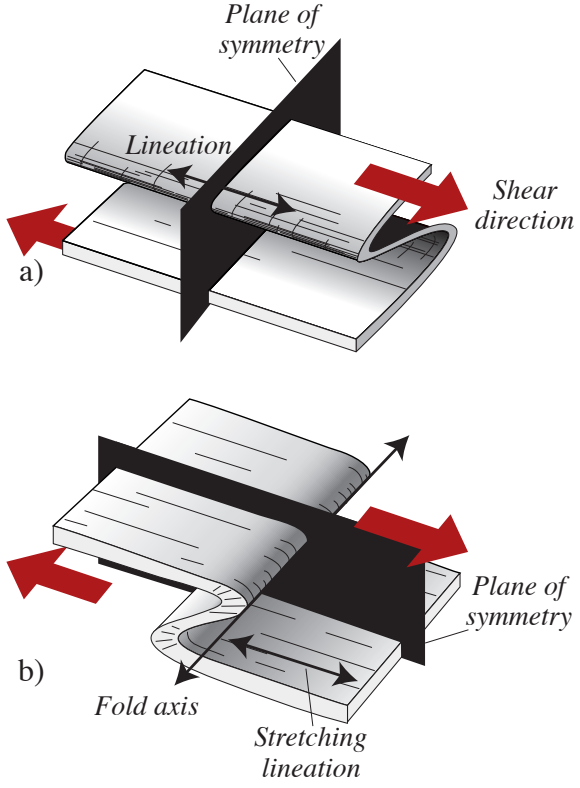

Figure 13.15 Folds and symmetry. Folds may have axes that are parallel as well as perpendicular to the stretching lineation. Using the concept of symmetry to estimate the transport direction is clearly not a reliable approach when dealing with folds.

2 There will be two possible directions, and kinematic structures or regional correlations are necessary to determine the actual direction .

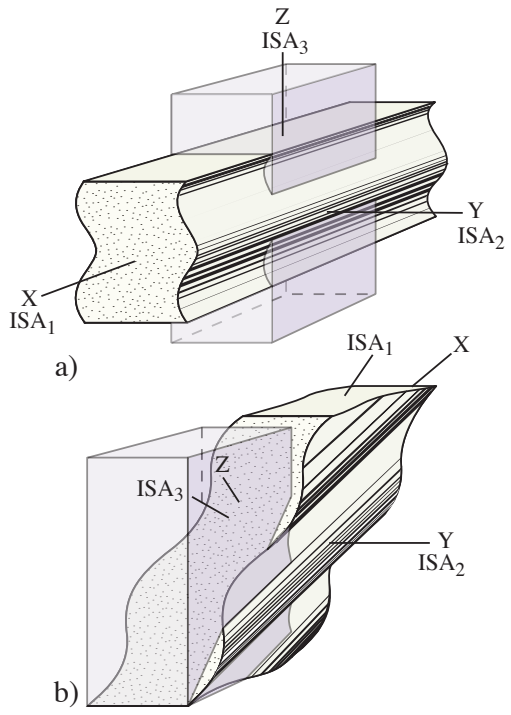

Figure 13.16 Folds and stretching lineations formed under pure shear (top) and simple shear (bottom). In both cases the fold axes and stretching lineation become subparallel (perfectly parallel for pure shear, subparallel for simple shear). Based on Rykkelid (1987).

of non-parallel lineations occur (Figure 13.15a). In some high-strain tectonites fold axes and intersection lineations are more or less parallel to the stretching and mineral lineation (Figure 13.15b and 13.16). Fold axes that parallel other lineations were still considered a problem in the middle of the 20th century. Today we have a set of reasonable explanations for parallel fold axes and other lineations. Rotation of fold hinges due to high shear strain is one. Others include the formation along lenses strongly elongated in the stretching direction, by local strike-slip movements related to local adjustments in heterogeneous tectonites, or by amplification of originally non-planar structures (Chapter 11).

---***---

Lineations are important because of their close relation to kinematics or movement directions and considered with the foliation(s) that contain them provide significant information about the deformation history. Boudinage, often considered as a lineation, is another structure that deserves closer attention, and will be treated in the following chapter.

Further reading:

Cloos, E., 1946. Lineation. Geological Society of America Memoir, 18: 122p.

Ellis, M.A. & Watkinson, A.J., 1987. Orogen-parallel extension and oblique tectonics: the relation between stretching lineations and relative plate motions. Geology, 15: 1022-1026.

Kvale, A., 1953. Linear structures and their relation to movements in the Caledonides of Scandinavia and Scotland. Quaternary Journal of the Geological Society, 109: 51-73.

Lin, S. & Williams, P.F., 1992. The geometrical relationship between the stretching lineation and the movement direction of shear zones. Journal of Structural Geology, 14: 491-498.

McLelland, J.M., 1984. The origin of ribbon lineation within the southern Adirondacks, U.S.A. Journal of Structural Geology, 6: 147-157.

Petit, J.-P., 1987. Criteria for the sense of movement on fault surfaces in brittle rocks. Journal of Structural Geology, 9: 597-608.

Ridley, J., 1986. Parallel stretching lineations and fold axes oblique to a shear displacement direction - a model and observations. Journal of Structural Geology, 8: 647-653.

Sander, B. 1930. Gefügekunde der Gesteine. Springer-Verlag, Vienna.

Sanderson, D.J., 1973. The development of fold axes oblique to the regional trend. Tectonophysics, 15: 55-70.

Sander, B. 1948. Einführung in die Gefügekunde der Geologischen Körper, vol. 1. Springer-Verlag, Vienna.

Sander, B. 1950. Einführung in die Gefügekunde der Geologischen Körper vol. 2. Springer-Verlag, Vienna, 352 p.

Shackleton, R.M. & Ries, A.C., 1984. The relation between regionally consistent stretching lineations and plate motions. Journal of Structural Geology: 111-117.

Skjernaa, L., 1980. Rotation and deformation of randomly oriented planar and linear structures in progressive simple shear. Journal of Structural Geology, 2: 101-109.

Tanaka, H., 1992. Cataclastic lineations. Journal of Structural Geology, 14: 1239-1252.

Turner, F. J. & Weiss, L. E. 1963. Structural analysis of metamorphic tectonites. McGraw-Hill, New York.

Williams, G.D., 1978. Rotation of contemporary folds into the X direction during overthrust processes in Laksefjord, Finnmark. Tectonophysics, 48: 29-40.

CHAPTER 14

Boudinage

In the plastic regime, layers tend to fold when shortened. Similarly, layers that are being stretched can be divided into individual pieces known as boudins. Classical boudinage is therefore the counterpart of buckling. Both structures form where there is a viscosity contrast where the competent layer is buckled or extended. Extension of layers is increasingly likely during progressive rock deformation, because layers tend to rotate into the field of extension. Later phases of deformation may shorten these layers, turning them into folded or crenulated rocks. However, the originally extensional nature of the layering is commonly found preserved, for instance in the form of folded boudins.

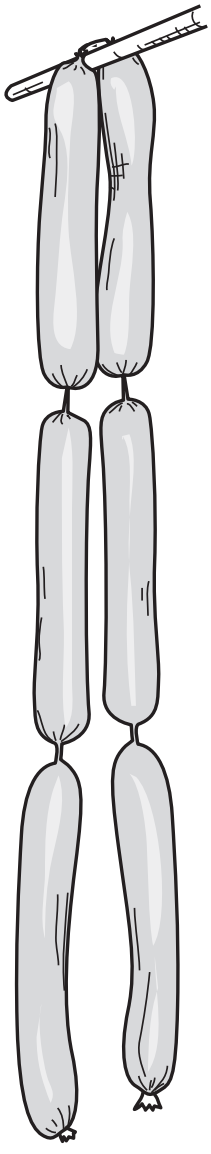

1.1 Boudinage and pinch-and-swell structures

Boudins (from the French word for sausage) are extensional structures formed by layer-parallel extension. *Boudinage* is the process that leads to the formation of boudins from originally continuous layers.

Classical boudins form where single competent layers are extended into separate pieces through plastic, brittle or a combination of plastic and brittle deformation mechanisms (Figure 14.1). The boudinaged layer is located in a rock matrix that deforms plastically. The boudins are separated by brittle extension fractures, by shear fractures, or by ductile shear zones that are restricted to the boudinaged layer.

Boudins are more or less regularly shaped rectangular fragments formed by stretching of competent layers or foliations.

There are also examples of regularly spaced areas of thinning in many extended competent layers without the separation into isolated fragments or boudins. Such structures are called *pinch-and-swell structures*. Pinch-and-swell structures are structures where the boudin-like elements are barely connected, as shown in Figure 14.2b. Both regular boudins and pinch-and-swell structures are controlled by temperature, strain rate and viscosity contrast or foliation development. High temperature promotes plastic deformation mechanisms also in the most competent layer. A high viscosity contrast and strain rate promotes fracturing of competent layers. These parameters will also affect the geometry of the boudins.

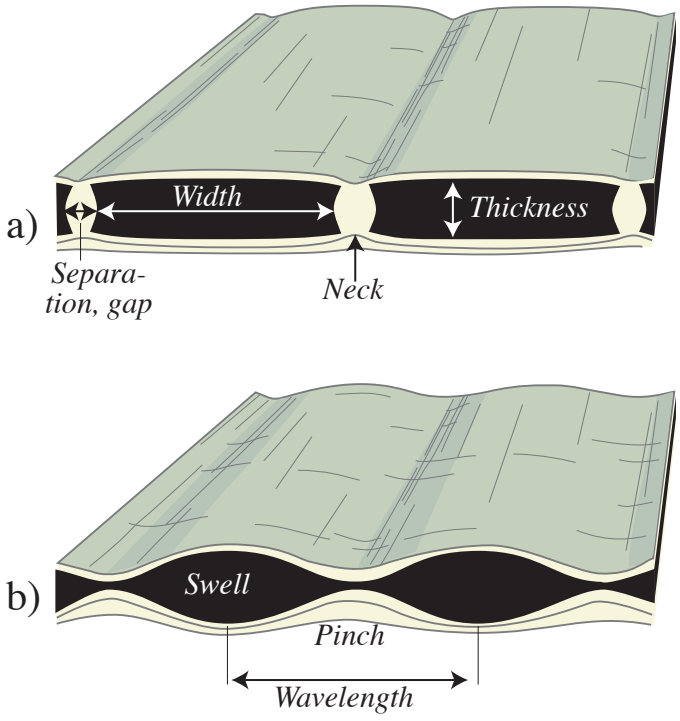

Figure 14.2 a) Descriptional terminology of boudins and pinch-and-swell structures.

1.2 Geometry, viscosity and strain

A boudin has ~~a certain~~ *thickness* and *width,* and boudins have a measurable *separation* (Figure 14.2a). Experiments show that thick layers develop wider boudins than thin layers, just as thick buckled layers show longer wavelengths than thin layers (Figure 10.20). During boudinage a competent layer is broken up into more and more boudins until a characteristic width/thickness or *aspect ratio* is reached. Further stretching only increases the separation, not the aspect ratio. Typical aspect ratios fall in the range 2-4 (Figures 14.3 and 14.4). The ratio is comparable to the characteristic wavelength of buckle folds.

The separation is the distance between the boudins. Unlike the aspect ratio, the separation is

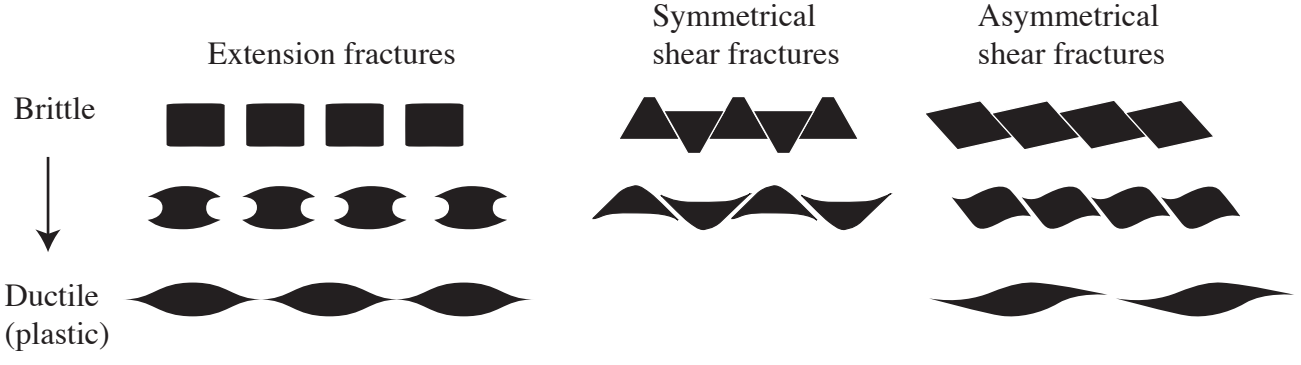

Figure 14.1 The geometry of boudins is largely controlled by whether boudins are separated by extension or shear fractures, and on the influence of plastic versus brittle deformation mechanisms. Asymmetric boudins may indicate non-coaxial deformation.

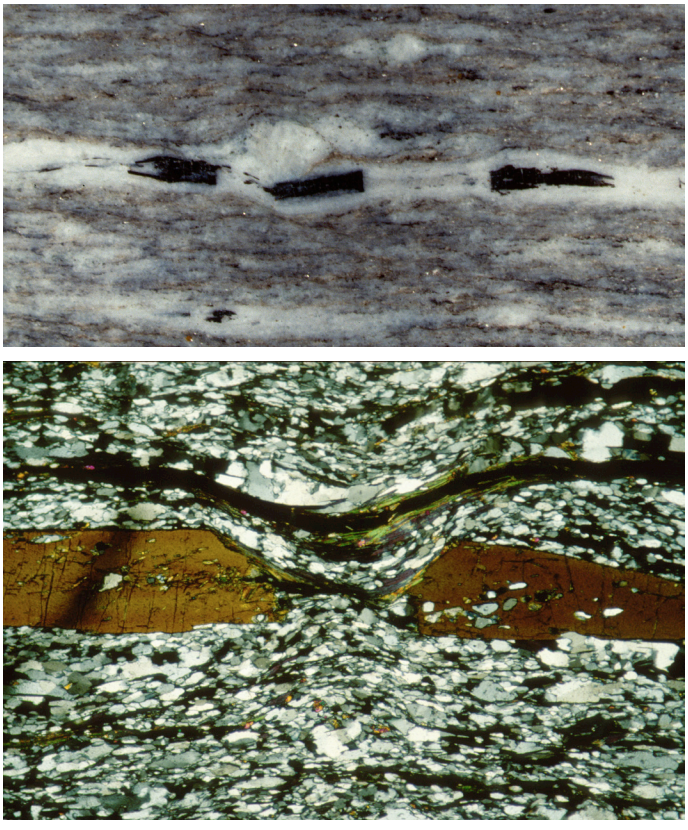

Figure 14.3 Boudinage on the microscale. Top: boudinaged amphibole crystals as seen in hand sample. Crystals are 2 mm thick. Bottom: boudinaged amphiboles as seen in thin section. This amphibole is 1 mm thick.

independent of the viscosity contrast between the boudinaged layer and its adjacent layers. Instead it depends mostly on strain, more specifically on the amount of layer-parallel extension. Separation is therefore more variable than the aspect ratio of boudins.

Hans Ramberg extended competent layers in a less competent matrix in the laboratory. He found that the competent layers were subdivided into boudins or pinch-and-swell structures. He also realized that the strongest or most competent layers formed the most rectangular boudins (Figure 14.5a-b). Less competent layers developed pinch-and-swell structures (Figure 14.6). Ramberg's experiment tells us that the shape of boudins reflects the viscosity contrast in the rock during deformation. Well-rounded corners (Figure 14.7) indicate that the margins of the boudins deformed predominantly by plastic deformation mechanisms, similar to the neighboring layer. In some cases we can see plastic deformation of one margin only, as shown in Figure 14.5d. Experiments tell us that the viscosity contrast is different along the two margins, being least where the plastic deformation (and rounded corners) occurs.

Numerical modeling has shown that the stress concentration is largest at the corners of boudins. This explains why the corners are the first parts of the boudins to be deformed. Where this stress concentration results in deformation of the boudins, *barrel-shaped boudins* may result (Figure 14.7).

Ramberg and later workers carried out theoretical analyses that indicate that the tensile stress causing

Figure 14.4 Rectangular boudins, formed by stretching of a granite dike in metasediments. Cross-cutting relations are preserved between the dike margins and the foliation, showing that the dike rotated anticlockwise relative to the foliation. Hydrothermal deposition of quartz in the gaps between the boudins is a common feature in boudinaged felsic rocks. Photo: E. Rykkelid.

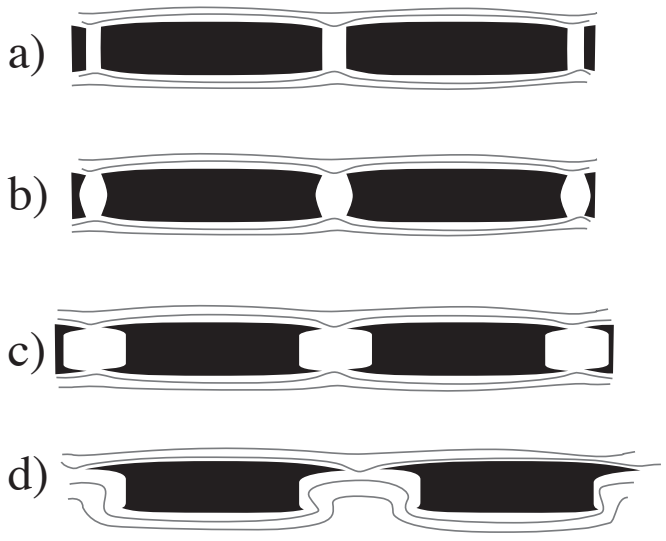

Figure 14.5 Different types of boudin-geometries, all involving extensional fracturing. a) Rectangular, b) weak plastic component, c) marked plastic component along margins, d) pronounced plastic component along upper margin, almost absent along lower margin. This indicates that the viscosity contrast is higher along the lower margin.

boudinage increases from the corners towards the central part of the boudin margin. This means that long boudins have higher tensile stress in their central parts than short boudins. The subdivision of early-formed boudins thus continues until the tensile stress in the middle of the boudin falls below a critical value, which occurs when the boudins become shorter than some critical length. The critical length has been passed when the boudin is so short that the tensile stress is smaller than the tensile strength of the material. This model also explains why individual boudins from the same layer do not have exactly the same length (Figure 14.8).

Figure 14.6 Boudinage structures in amphibolite layers (metamorphosed basaltic dikes) in quartz schist, Kalak Nappe, northern Norway Caledonides. The deformation is strongly influenced by plastic deformation. Photo: Steffen Bergh.

Pinch-and-swell structures have even larger similarities with buckle folds than boudins. In cases where the viscosity contrast is significant, the mathematical relationship between the dominant wavelength (L_d) and thickness (h) can be directly applied. The relationship is given by Biott's classical formula

$$L_d/h = 2\pi(\mu_L/6\mu_M)^{1/3}$$

where L_d/h represents the length/thickness aspect ratio of the structures. Pinch-and-swell structures can also form when the viscosity contrast is small (by a mechanism known as resonance folding), but then the L_d/h values tend to fall in the range 4-6.

Buckle folds can form in both non-linear (Newtonian) and linear media. However, pinch-and-swell structures only form in media with non-Newtonian properties. This restriction is an important reason why folds are more abundant than pinch-and-swell and boudin structures in deformed rocks. Folds can also form by passive mechanisms, in rocks with layers with little or no viscosity contrast.

1.3 Asymmetric boudinage and rotation

Until this point we have regarded boudins as symmetrical structures. *Asymmetric boudins* (Figures 14.1, 14.8 and 14.9) are also commonly found in deformed metamorphic rocks. Asymmetric boudins are separated by shear fractures or shear bands (small-scale shear zones) that tend to die out once they leave the boudinaged layer. If the boudinaged layer behaves in a brittle manner during deformation, then the differential stress or strength of the competent layer will determine whether shear fractures or extension fractures form. Extension fractures form when $(\sigma_1 - \sigma_3) < 4T_0$, where T_0 is the tensile strength of the rock layer.

Figure 14.7 Plastic deformation of the margins of boudins. Proterozoic gneiss, Haugalandet, SW Norway.

Figure 14.8 Boudinaged granitic layer in gneiss. The asymmetric boudins have fairly similar, but not identical lengths. According to theory, boudinage continues until all of the boudins have a length shorter than some critical value. Sinistral sense of shear.

Boudins separated by shear fractures are sometimes pulled apart without much rotation or shear (Figure 14.10 a-b). These boudins parallel the surrounding foliation, and the shear fractures will open in an extensional mode. This behavior is typically seen in migmatitic gneisses where amphibolitic layers, for example, are pulled apart and the new-formed space (volume) is filled with melt or new minerals.

Where boudins are offset by shear structures, significant *rotation* of the boudins occurs (Figure 14.10c-d). This process resembles the domino model, discussed in Chapter 17, which works as well for systems of asymmetric boudins as for rotated fault blocks in extensional settings (Figure 17.3). The rotation keeps the boudins aligned with the general foliation of the rock.

Rotated asymmetrical boudins can also form by rotation of symmetrical boudins during non-coaxial deformation. Experiments show that layer-parallel simple shear causes rotation of already existing boudins. But in what direction will the boudins rotate? In simple terms, short and competent boudins rotate as rigid objects synthetic to the direction of shear[1]. Long boudins, i.e. boudins with high aspect ratios, will rotate against the direction of shear. Whether a boudin rotates anti- or synthetically with respect to the sense of shear thus depends on the shape or aspect ratio of the boudin (Figure 14.11). However, it also depends on the type of flow (W_k), the presence or absence of a foliation in the boudins, whether slip occurs along its margins, whether extensional fractures or shear bands separate the boudins, and the viscosity contrast at the time of deformation. In general, the larger the competency contrast, the more rigid the boudins, and rigid objects rotate more easily with the shear sense. Shear band separation causes back-rotation of the boudins antithetically (the domino effect of the previous paragraph). The effect of foliation is

Figure 14.9 Asymmetric boudins in amphibolitic gneiss. The boudins are separated by shear fractures in the amphibolite. The fractures turn into ductile shear zones outside of the boudins and rapidly die out. Sinistral sense of shear.

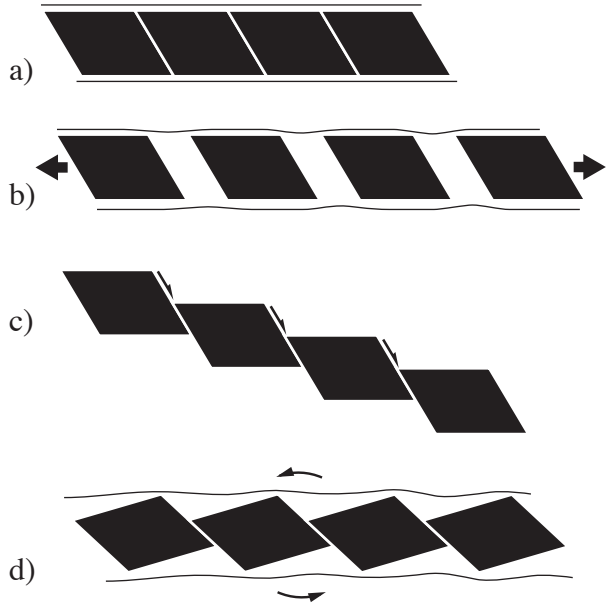

Figure 14.10 Asymmetric boudins can form by extension across shear fractures (a-b), or by a combination of shearing along shear fractures and boudin rotation.

1 This means that if the sense of shear is clockwise, the rotation of the boudins will always be clockwise.

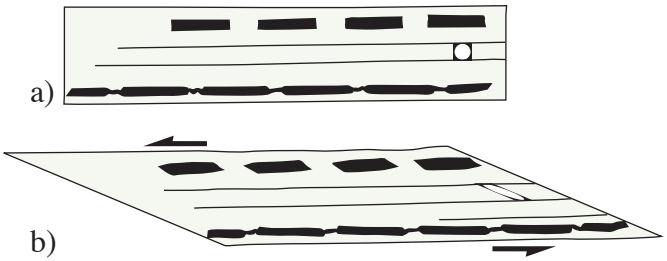

Figure 14.11 Experimental study of the effect of boudin aspect ratio during shearing. Short boudins rotate synthetic to the sense of shear while long boudins back-rotate. Based on Hanmer (1986).

discussed in the next section. Field observations show that most (but not all) boudins rotate against the sense of shear, as shown in Figure 14.12 and Figures 14.8-9.

An additional factor often overlooked is the orientation of the boudinaged layer prior to deformation. So far we have implicitly assumed that it was about parallel to the extension direction, which does not necessarily have to be the case. We know that boudins form in the field of instantaneous stretching. Figure 14.13 shows how a layer can rotate from a high angle towards parallelism with the flattening X-Y plane during a coaxial deformation history. Rigid objects rotate slower than the general foliation, causing an asymmetry to develop. Experiments show that the more quadratic the boudins, the larger the difference in rotation between boudins and the foliation. If the coaxial deformation continues far enough, the difference will decrease, but the process typically stops before subparallelism is reached.

What about non-coaxial deformation? It is impossible to decide from the observation of a single occurrence of rotated boudins whether the deformation is coaxial or non-coaxial. Rotated boudins can result from either or both coaxial and non-coaxial deformations. However, the degree of coaxiality can sometimes be estimated where we have multiple layers with different initial orientations.

1.4 Foliation boudinage

In the discussion above we considered the boudinage of individual layers – boudinage in the classical sense. They do not have to be isolated layers. In the same way that layers can get close enough to interfere during buckling, adjacent layers can interfere during boudinage. The result is boudins with thickness greater than that of individual layers. In many cases highly deformed rocks have a penetrative foliation rather than competent layers. That foliation may be thought of as layering at the microscale, and may develop structures known as foliation boudinage. Foliation boudins are one or more orders of magnitude thicker than the microlayering represented by the foliation but do in many ways resemble classical boudins.

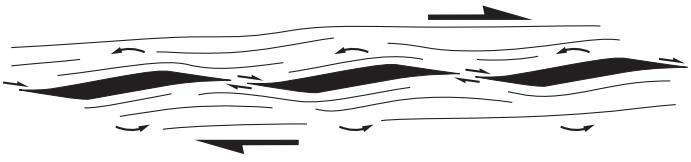

Figure 14.12 Typical sense of rotation of boudins during simple shear. The rotation is "against" the sense of shear, sometimes referred to as back-rotation.

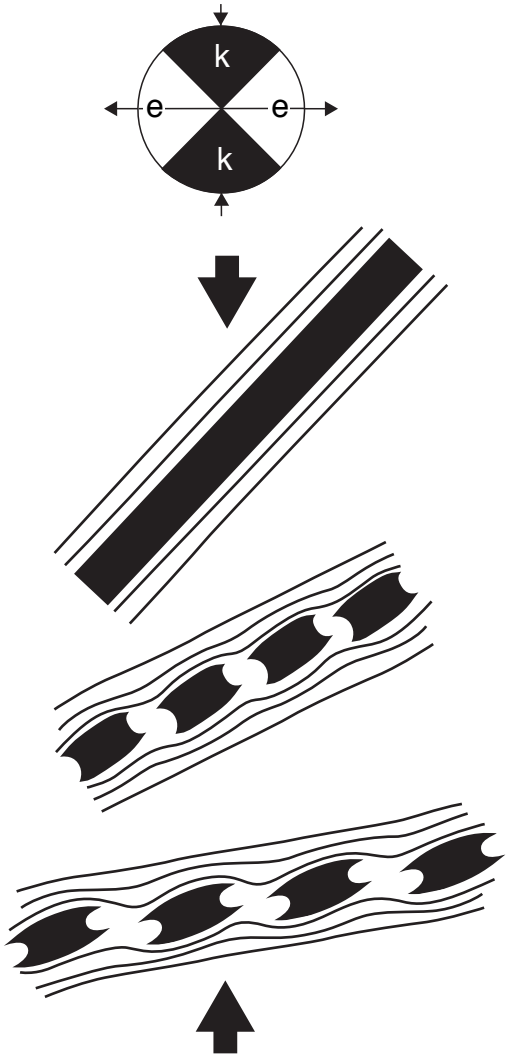

Figure 14.13 Asymmetric boudins forming in pure shear in a layer that is originally oblique to the plane of flattening.

Symmetrical foliation boudins are separated by tension fractures. The fractures are filled with quartz or other hydrothermal minerals, and/or by flow of adjacent rock layers (Figure 14.14). The foliation within the boudin is typically pinched towards the

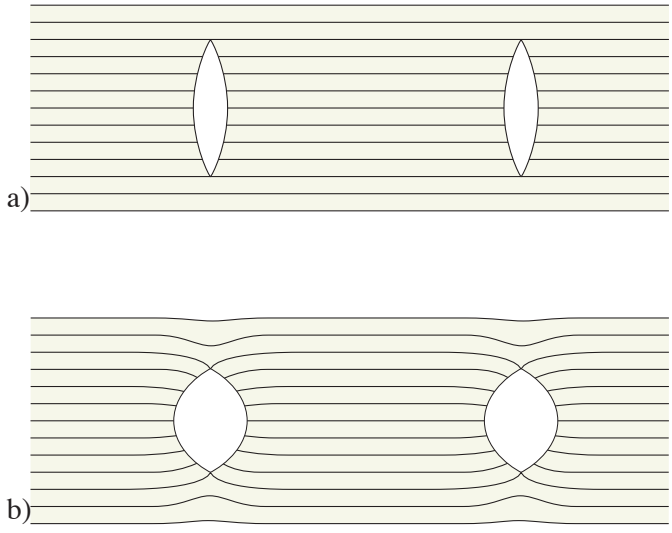

Figure 14.14 The principle of symmetric foliation boudinage. a) Formation of tension fractures. b) vertical closing and horizontal opening of the fractures. Based on Platt & Vissers (1980).

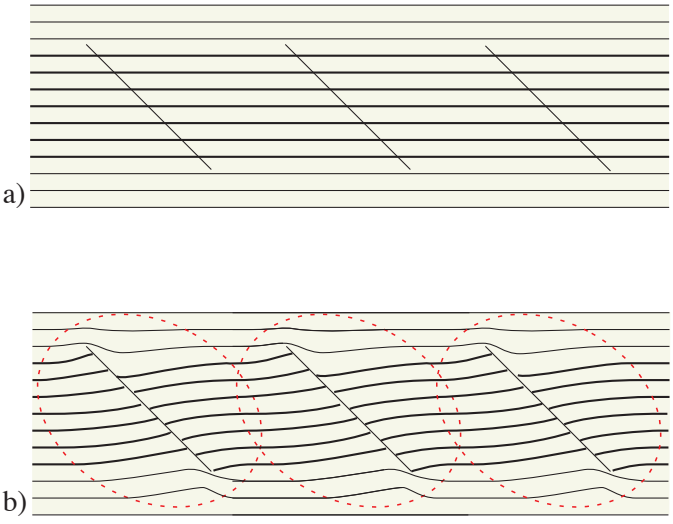

Figure 14.16 Formation of asymmetric foliation boudinage. a) Formation of shear fracture. b) Movement along the shear fractures (shear bands) causing rotation of the foliation between the fractures. Inspired by Platt & Vissers (1980).

extension fracture (Figure 14.15). The fracture itself can be quite irregular, giving the impression that the foliation in the area has been torn.

Asymmetrical foliation boudins (Figure 14.16) are separated by brittle shear fractures or by ductile shear bands showing relative movement along the fractures/bands. Mineral fill is less common than for symmetrical foliation boudins. Asymmetrical foliation boudins are found on many scales. They are found as single or conjugate sets and have many similarities with the type of shear bands discussed in Chapter 15. Similar to shear bands, they are reliable kinematic indicators when only one set of shear fractures or shear bands is developed. They are more reliable than classical boudins because no significant viscosity contrast exists between the boudins and the surrounding rock. The effect of rigid body rotation, which promotes synthetic rotation, is thus eliminated. Instead, the rotation is controlled by the geometrically necessary rotation of the foliation around a shear fracture or shear band of limited length, as shown in Figure 14.16.

Figure 14.15 Symmetric foliation boudinage in amphibolite facies gneisses.

The strong foliation that develops in many tectonites is generally considered to make foliation-parallel extension difficult. This probably explains why foliation boudinage is common in well-foliated rocks. The foliation "tears", which allows for some more extension. Foliation boudinage is therefore a type of structure that develops at a relatively late stage of deformation, after the foliation is well developed.

1.5 Boudinage and the strain ellipse

Boudins are usually observed in sections close to the X-Z section of the finite strain ellipsoid. All of the figures shown so far represent this section. However, the third direction is also important because it contains important information about the related strain field (Figure 14.17). It may be challenging to get three-dimensional control in the field, but we should also look for evidence of strain in the Y-direction.

Boudins commonly show rod-like geometries, so that sections perpendicular to the X-Z section shows neither boudinage nor folding of the layer. The boudins are arranged like railroad crossties or sleepers (Figure 14.17b) with no shortening or extension along their long axes. Thus strain can be assumed to be close to planar with the Y-axis of the strain ellipsoid oriented along the long axes of the boudins (Figure 14.17b).

If the layers are boudinaged in two directions (Figure 14.17a and Figure 14.18) stretching is impled in two directions, i.e. flattening strain. If the extension can be shown to be equal in the two directions we have

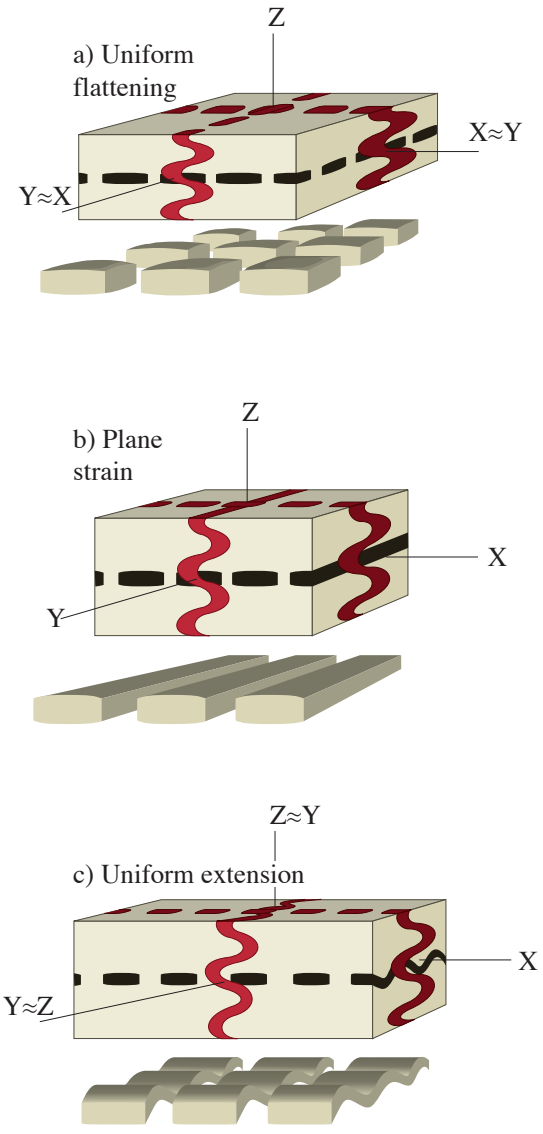

Figure 14.17 The relation between boudinage geometry and strain geometry. Typically folds and boudins occur in differently oriented layers, but a single layer may show boudin structures in one section and folds in another if strain is constrictional.

evidence for uniform flattening, i.e. an oblate strain ellipsoid, where X>>Y=Z. This pattern of boudinage is called *chocolate tablet boudinage*.

In more rare cases layers can be found to be boudinaged in one direction and folded in the other, as shown in Figure 14.17c. This tells us that the layer is shortened in one direction within the layer and extended in the other. This is what we would expect if deformation is close to uniform stretching (Figure 3.?).

These structures should not be confused with boudinaged folds or folded boudins (p. ?). Boudinaged folds form when layers rotate from the field of shortening into that of extension. Folded

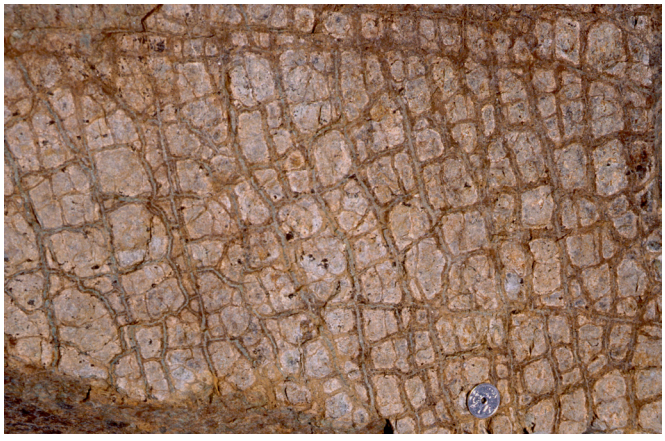

Figure 14.18 Chocolate tablet boudinage, i.e. boudinage in two directionss indicates two directions of finite extension, or flattening strain. From the Leka Ophiolite, Central Scandinavian Caledonides.

boudins (Figure 14.19) do not form in a single, steady-state deformation because layers rotate from the shortening field into the extensional field, and never the opposite. Folded boudins can however form in a single deformation where the foliation is perturbed by tectonic lenses or other heterogenetities in the deforming volume. Hence, before using folded boudins as evidence for multiphase deformation, other possibilities must be evaluated.

1.6 Really large-scale boudinage

Seismic images of the lower crust tend to portray conjugate sets of dipping reflectors, which is somewhat different from the patterns seen in the middle and upper crust. The conjucate sets are commonly interpreted as shear zones between lens-shaped portions of less-deformed lower-crustal rock. They occur at the 100-meter to kilometer scale. Seismic noise can generate similar patterns so that such images are not unambiguous. However, the study

Figure 14.19 Folded boudins cannot form under a single phase of deformation unless the ISA changes orientation during the deformation (non-steady state deformation). Folded boudins therefore indicate either non-steady state deformation or multiple phases of deformation.

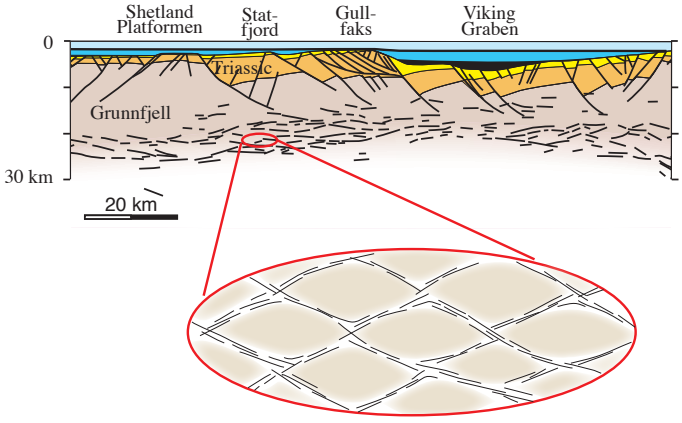

Figure 14.20 Lower crustal structures as seen on deep-seismic lines are sometimes interpreted as large-scale boudins and related to vertical shortening. Based on Odinsen et al. (2000).

of exposed pieces of lower-crustal rocks gives some support to the interpretation that large-scale boudinage structures occur in the lower crust. They may not be considered classical boudinage per se, but they are similar enough to be mentioned in this context. The patterns are consistent with vertical shortening and lateral extension (pure shear) and are particularly characteristic for the lower crust beneath rift systems or other areas of extension (Figure 14.20).

Boudinage of the lower and middle crust can also occur at even larger scale, where the entire middle crust is parted into boudin-like elements (Figure 14.21). A considerable amount of extension is needed to boudinage the crust in this manner.

Further reading:

Ghosh, S.K., 1988. Theory of chocolate tablet boudinage. Journal of Structural Geology, 10: 541-553.

Hanmer, S., 1986. Asymmetrical pull-aparts and foliation fish as kinematic indicators. Journal of Structural Geology, 8: 111-122.

Lacassin, R., 1988. Large-scale foliation boudinage in gneisses. Journal of Structural Geology, 10: 643-647.

Lloyd, G.E., Ferguson, C.C. & Reading, K., 1982. Boudinage structure: some interpretations based on elastic-plastic finite element simulations. Journal of Structural Geology, 3: 117-128.

Mandal, N. & Karmakar, S., 1989. Boudinage in homogeneous foliated rocks. Tectonophysics, 170: 151-158.

Platt, J.P. & Vissers, R.L.M., 1980. Extensional structures in anisotropic rocks. Journal of the Geological Society, 2: 397-410.

Ramberg, H., 1955. Natural and experimental boudinage and pinch-and-swell structures. Journal of Geology, 63: 512-526.

Ramsay, J.G., 1967. Folding and fracturing of rocks. International series in the earth and planetary sciences. McGraw-Hill, New York, 568 pp.

Sengupta, S., 1983. Folding of boudinaged layers. Journal of Structural Geology, 5: 197-210.

Smith, R.B., 1975. Unified theory on the onset of folding, boudinage, and mullion structure.

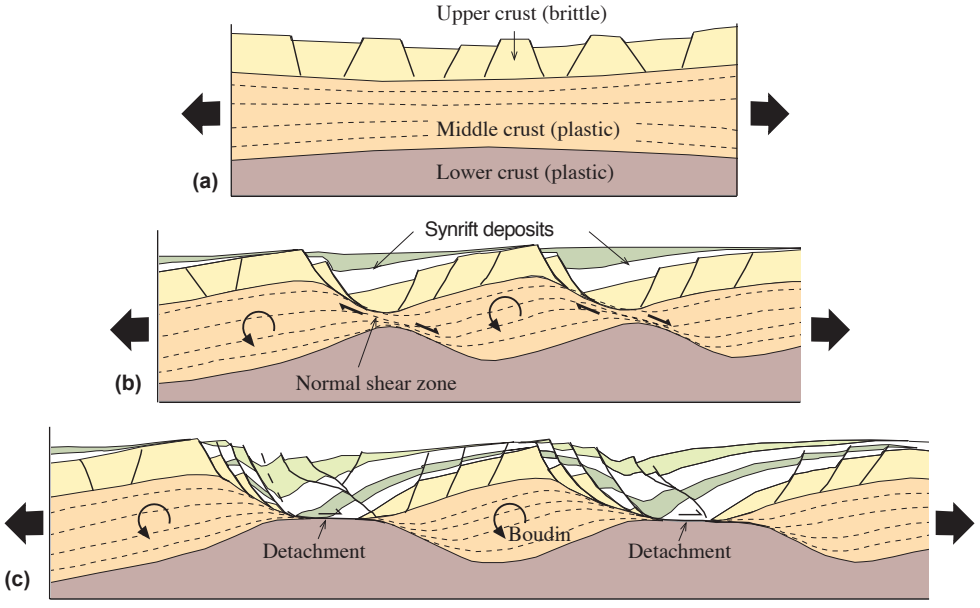

Figure 14.23 Idealized model showing how the middle crust can be extended by asymmetric boudinage. From Harris et al. (2002).

Geological Society of America Bulletin, 86: 1601-1609.

Strömgård, K.E., 1973. Stress distribution during formation of boudinage and pressure shadows. Tectonophysics, 16: 215-248.

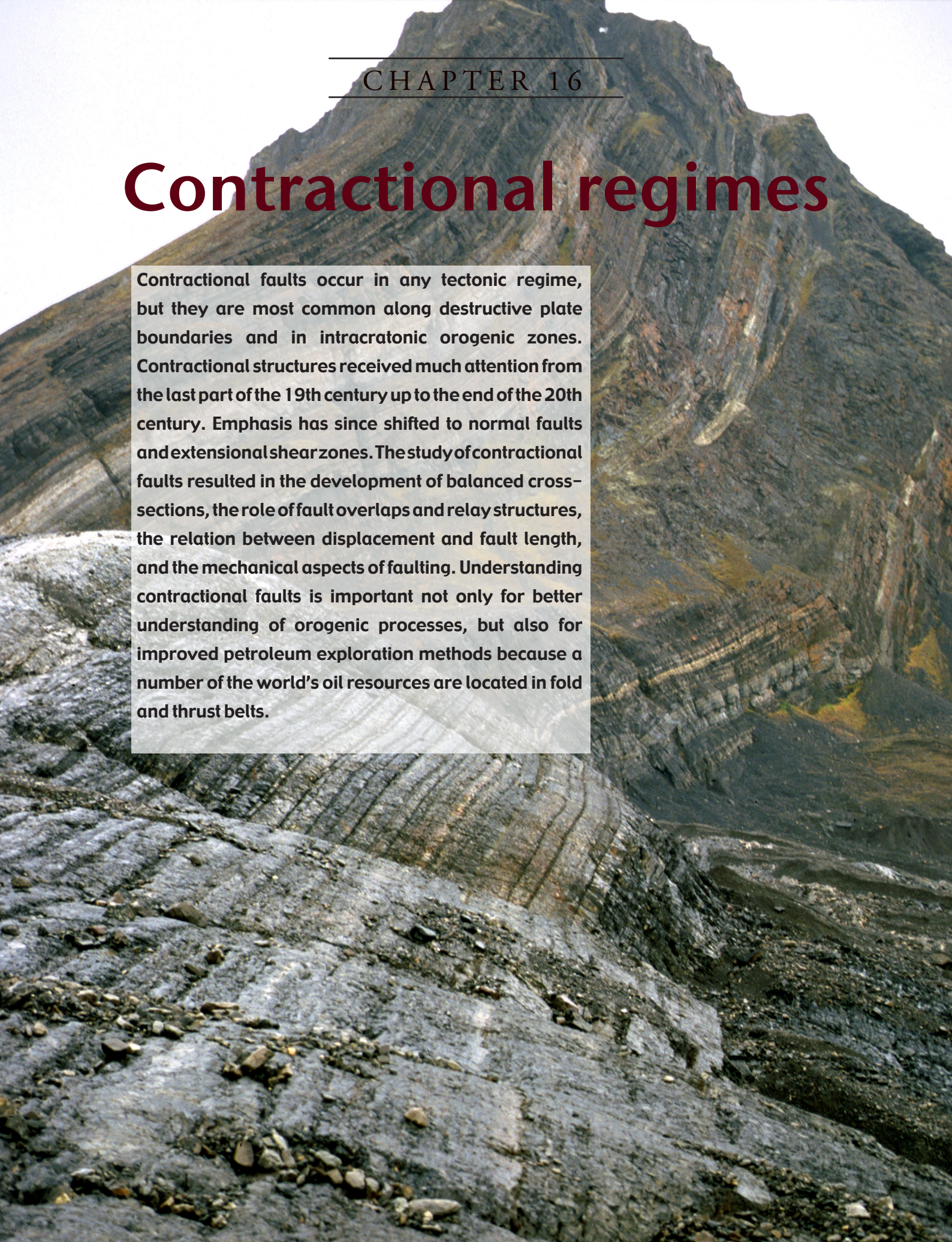

CHAPTER 16

Contractional regimes

Contractional faults occur in any tectonic regime, but they are most common along destructive plate boundaries and in intracratonic orogenic zones. Contractional structures received much attention from the last part of the 19th century up to the end of the 20th century. Emphasis has since shifted to normal faults and extensional shear zones. The study of contractional faults resulted in the development of balanced cross-sections, the role of fault overlaps and relay structures, the relation between displacement and fault length, and the mechanical aspects of faulting. Understanding contractional faults is important not only for better understanding of orogenic processes, but also for improved petroleum exploration methods because a number of the world's oil resources are located in fold and thrust belts.

1.1 Introduction

Contractional deformation structures form when rocks are shortened by tectonic or gravitational forces. Consider a layered volume of rock being shortened in the direction of the layering, as shown in Figure 16.1. A number of micro- and macrostructures may result. Shortening can be accommodated by volume loss (Figure 16.1b) through the formation of dissolution seams (stylolites), solution along grain contacts or by physical compaction. A pure shear response can be envisioned where horizontal shortening is compensated by vertical thickening perpendicular and where layers maintain their orientation (Figure 16.1c) or buckle (Figure 16.1d). Finally, shortening can result in contractional faults (Figure 16.1e), commonly in association with folds. These are the main focus of this chapter.

Contractional faults cause shortening of the crust or of some reference layer, such as primary bedding. These are accomplished by *reverse faults* and *thrust faults*. Reverse faults are steeper than thrust faults (steeper than 30°[1]) and usually do not accumulate the large displacements seen in thrusts, but there is a gradual transition between the two. Such faults can occur at any scale, from the microscale to regional orogenic belts and subduction zones.

Contractional faults also embrace normal and strike-slip faults that shorten a reference layering. This occurs where reverse faults have been rotated and overturned into apparent normal faults, or where normal faults dip at a lower angle than the reference layering, as shown in Figure 16.2. Such faults are less common, and typically occur on the outcrop scale. However, contractional normal faults are not rare. Remember: it is all a matter of reference and scale. In the following we use the Earth's surface as the reference, i.e. assume that contractional faults are reverse and thrust faults only, unless otherwise stated.

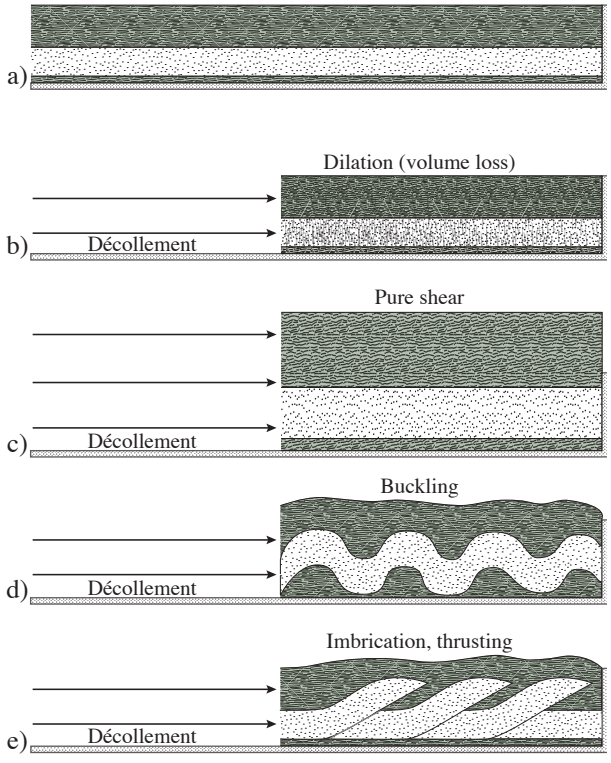

Figure 16.1 Shortening of layers can result in a wide range of strain regimes and structures: b) dilation and cleavage formation, c) pure shear without folding, d) buckling, e) imbrication.

1.2 Thrust faults

1.2.1 Nappe terminology

A *thrust* is a low-angle fault or mylonite zone where the hanging wall has been transported over the footwall. The movement should be predominately dip-slip. It has been suggested that the term thrust be reserved for horizontal displacements (heaves) in excess of 5 km, but the term is also deliberately used for outcrop-scale low-angle reverse faults. For thrust faults developed in rocks that are younging upwards or with upwards decreasing metamorphic grade, the following is true:

Thrust faults bring older rocks on top of younger rocks, and rocks of higher metamorphic grade on top of rocks of lower metamorphic grade.

According to this statement, both or either stratigraphy or metamorphic grade can be used to identify and map thrusts. Stratigraphic control is thus very important in the mapping of thrust faults in–foreland fold and thrust belts. It should however be noted that the premises on which this statement is based are not always fulfilled. In cases where the rocks have been deformed by previous deformation phase(s), or where the deformation history is complex, exceptions to this general statement can occur.

Figure 16.2 Contractional faults that at the same time are normal faults. They are contractional because they shorten or contract the layers that they affect.

1 Some geologists makes the distinction at 45° dip.

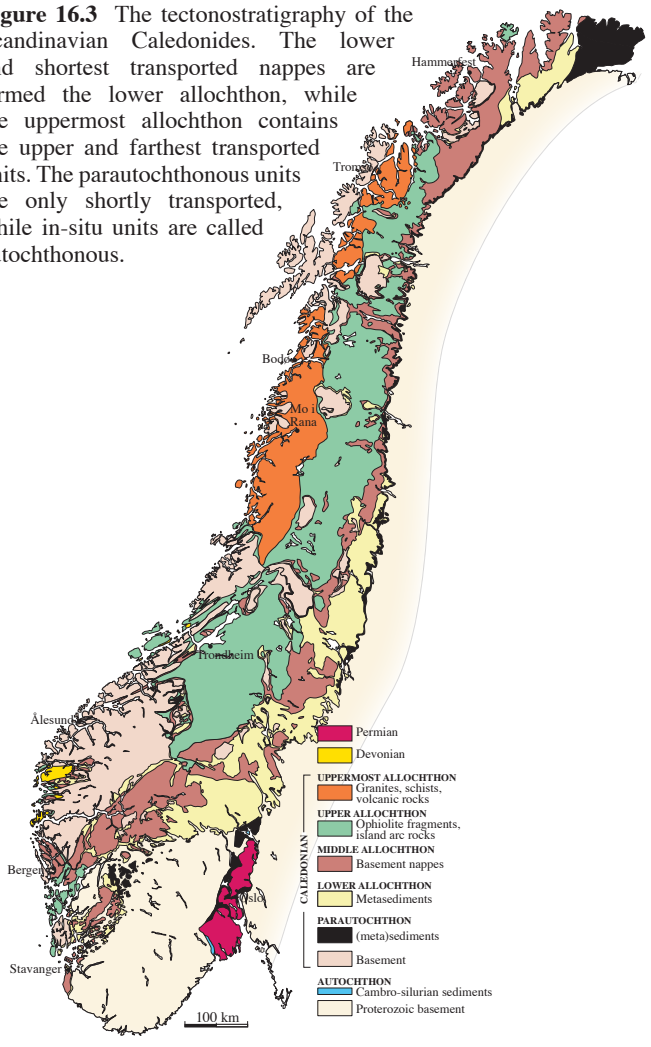

Figure 16.3 The tectonostratigraphy of the Scandinavian Caledonides. The lower and shortest transported nappes are termed the lower allochthon, while the uppermost allochthon contains the upper and farthest transported units. The parautochthonous units are only shortly transported, while in-situ units are called autochthonous.

Figure 16.4 Duplex structure in dolomitic sandstones near Ny-Ålesund, Svalbard, formed during Tertiary contraction. Note S-shaped horses and floor and roof thrusts. Photo: Steffen Bergh.

A thrust separates the substrate from a *thrust nappe*. Thrust nappes are characteristic of contractional orogens such as the Caledonian-Appalachian orogen and the Alps. Thus, when referring to the orientations and directions of structures within thrust nappes, one commonly refers to the hinterland or foreland. The hinterland is the area in the central portion of the collision zone, and the foreland is the marginal (usually continentward) part.

Although some thrust nappes occur as single units, they commonly contain a number of internal sheets, each separated by another thrust fault. The smallest units in a thrust nappe are referred to as horses, as discussed in more detail in the next section. All of these thrust units are thin relative to their length and width. A collection of thrust nappes that share common lithological and/or structural features are referred to as a *nappe complex*.

A thrust nappe is bounded by a basal fault known as a *sole thrust* or *floor thrust* and an overlying *roof thrust*. In the common case of stacked nappes, the roof thrust of one nappe may serve as the floor thrust for one above. However, the shallowest of a stack of thrust nappes may be limited upwards by a free erosion surface. The lowermost sole thrust, the one that separates the entire stack of thrust nappes from a less deformed or undeformed basement, is also called a *décollement* – a term that is also used for similar low-angle extensional faults and for faults or shear zones of uncertain sense of movement.

Nappes exposed at the surface can be discontinuous because erosion has selectively removed some parts while others have been spared. An erosional remnant of a nappe is called a *klippe* (German terminology). Similarly, an erosional ”hole” through a nappe that exposes the underlying rock unit or nappe is called a *window* or *fenster* (German for window). By comparing rocks in nappes with those of the underlying and unthrusted basement it is possible to determine whether the nappes belong to the same unit and probably transported for only a short distance, or whether they are completely different and far-travelled. There is a special terminology for these relations. Starting at the bottom, the basement is called *autochthonous*[2]. Slices of basement and perhaps its sedimentary cover thrust only a few kilometers or so are called *parautochthonous*. Ideally, parautochthonous units are easily correlated with the basement rocks. Above the locally-derived parautochthonous unit(s) are the *allochthonous*[3] units. These units have been transported from areas that originally were many tens or hundreds of kilometers away. There may be many allochthons or allochthonous units in a nappe pile, and, as has been done formally in the Scandinavian Caledonides (Figure 16.3), they may be subdivided

2 Derived from greek, generally meaning “formed or originating in the place where found”.

3 Allochthonous is derived from greek, where ”allo” means “different” and ”chthon” means “ground”.

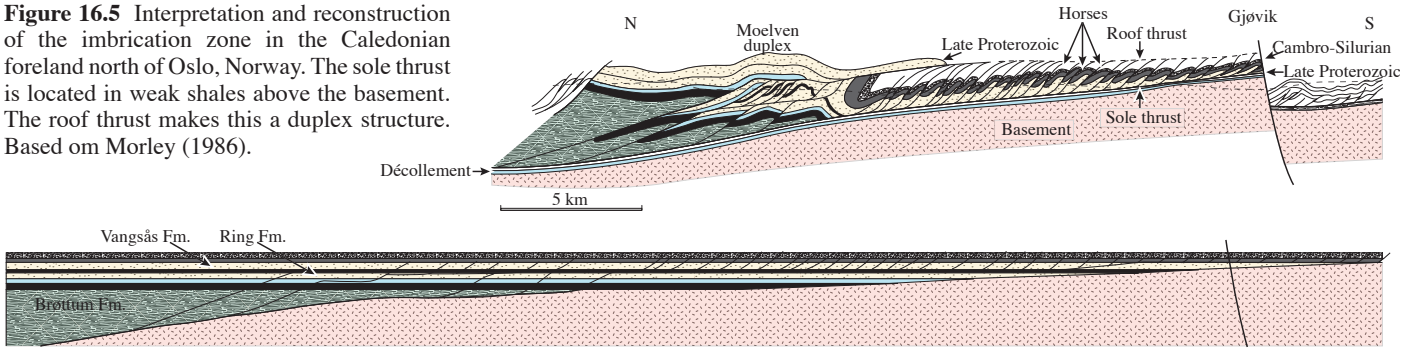

Figure 16.5 Interpretation and reconstruction of the imbrication zone in the Caledonian foreland north of Oslo, Norway. The sole thrust is located in weak shales above the basement. The roof thrust makes this a duplex structure. Based om Morley (1986).

into the lower, middle, upper and uppermost allochthons

1.2.2 Fault geometries

Contractional faults in the foreland of an orogenic zone typically form *imbrication zones* (Figures 16.4 and 16.5). An imbrication zone is a series of similarly oriented reverse faults that are connected through a low-angle floor thrust. If, in addition, a roof thrust bounds the zone upwards, then the complete structure is called a *duplex structure* (Figures 16.6 and 16.7). A duplex consists of *horses* that are arranged piggy-back, similar to the cards in a tilted card deck (Figure 16.5). The horses typically have an S-shaped geometry in the vertical profile (Figure 16.6), and they tend to dip towards the hinterland (the central part of the orogen). Horses can however be folded, faulted and rotated during the thrusting history so that their primary geometries and orientations become modified.

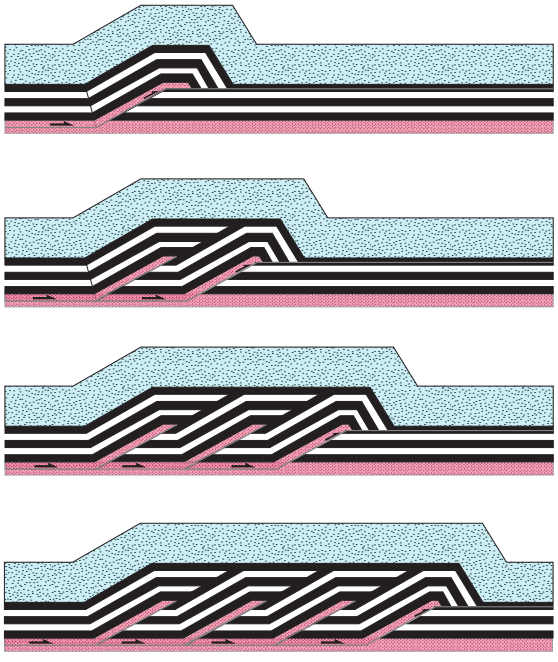

Figure 16.6 Development of a duplex. Note the characteristic double kink-fold in the frontal horse.

In very low-grade or non-metamorphic sedimentary sequences deformed in the brittle regime the steep ramp-segments of imbrication zones likely form first. They form in the strongest or most competent layers which fracture first during layer-parallel shortening. You can visualize this by thinking of what would happen if you compressed a sequence consisting of one or more chocolate plates in jelly. The chocolate would soon break and then the faults would link along the jelly. That is about what happens in a limestone-shale sequence during layer-parallel shortening. The combination of two flat thrusts at different stratigraphic levels connected through a steeper reverse fault (ramp) is referred to as a *flat-ramp-flat fault*[4]. Ramps may also give rise to thrusts or reverse faults with displacement opposite to the

Figure 16.7 Micro-scale thrust structures and related folds (thin section). These structures, including roof thrusts, floor thrusts and horses, are similar to those found at much larger scale. Tertiary thrust zone in Carboniferous shales, Isfjorden, Svalbard. Picture is 2 cm wide. Photo: Steffen Bergh.

4 The same terminology is used for normal faults.

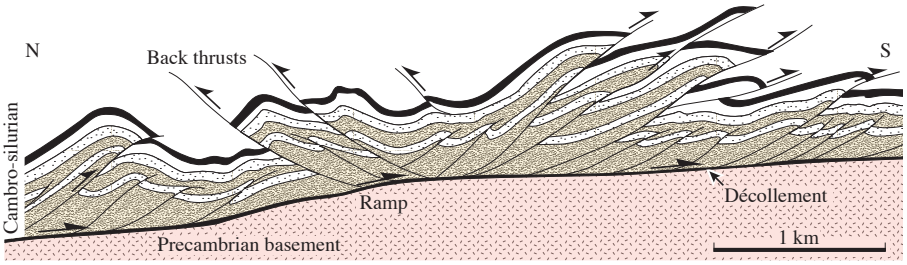

Figure 16.8 Back thrusts generated above a ramp in the sole thrust. The main thrusting direction is toward the right (south). North of Oslo, Norway. Based on Morley (1986)

general sense of displacement. Such *back-thrusts* form as the result of geometric complications in ramp locations (Figure 16.8).

Kinematically, an imbrication zone transfers slip from one stratigraphic layer to a higher one toward the foreland. The lower horizontal décollement or floor thrust yields some of its displacement to each of the individual horse-bounding faults. At the top, displacement is "collected" by the roof thrust. Hence, the floor thrust terminates if all of the displacement is transferred to the roof thrust, as seen in Figure 16.9.

Many ramps strike more or less perpendicular to the transport direction and are called *frontal ramps* in thrust terminology. Frontal ramps show dip-slip movements with striations in the dip direction. However, ramps may also be oblique to the transport direction (Figure 16.10). Such *oblique ramps* are oblique slip faults formed with a combination of dip-slip and strike-slip motion. Ramps that form parallel to the movement direction of the thrust sheet are known as *lateral ramps*. Many lateral ramps are found to be steep or vertical, and are really strike-slip faults that connect frontal ramp segments. The fact that they transfer slip from one frontal ramp to another has also qualified them to the name *transfer faults*. Another term used about this type of fault is *trear-fault*.

As in any other fault system, thrust faults are connected into three-dimensional networks. Where a fault splits into two we have a *branch point* (Figure 16.11) or, in three dimensions, a *branch line*. Branch lines enclose tectonic units (thrust nappes or horses) unless the thrust fault dies out as a blind thrust fault. The part of the branch line that delimits the unit in the front is called the *leading branch line*, while the one in the rear end is called the *trailing branch line*.

Branch points and branch lines can occur at outcrop scale, for example in an imbrication zone, but can also be found on a regional scale. It has been suggested that the orientation of branch lines can be used to constrain the movement direction of individual nappes. This is based on the assumption that ramps are predominantly frontal and lateral; oblique ramps are less common.

1.2.3 Foreland and hinterland

The style of deformation in a contractional regime depends on the lithologies involved and the depth at the time of deformation. In orogenic belts there is a distinction between structures formed in the marginal *foreland* area and the more central *hinterland* area.

In the foreland the classical imbrication and duplex structures structures described above are more common. We find these structures in the sedimentary sequence covering the underlying basement. In

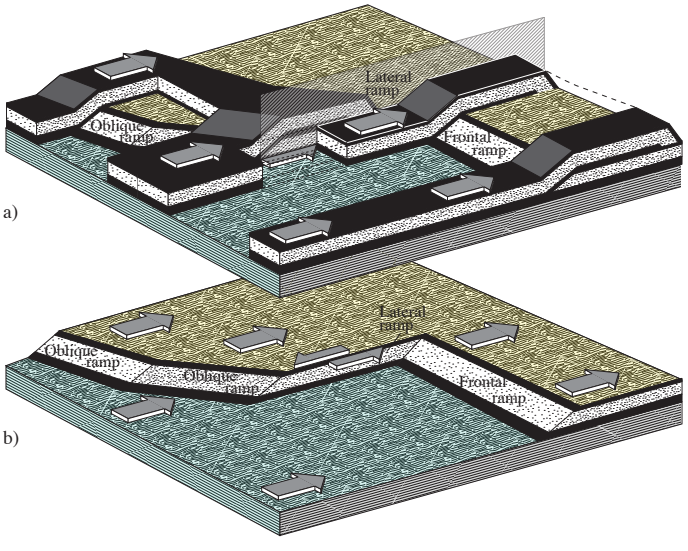

Figure 16.10 Various thrust ramps and their geometries. a) Some of the hanging wall strata included. Here, the ramps appear as folds. b) Hanging wall removed.

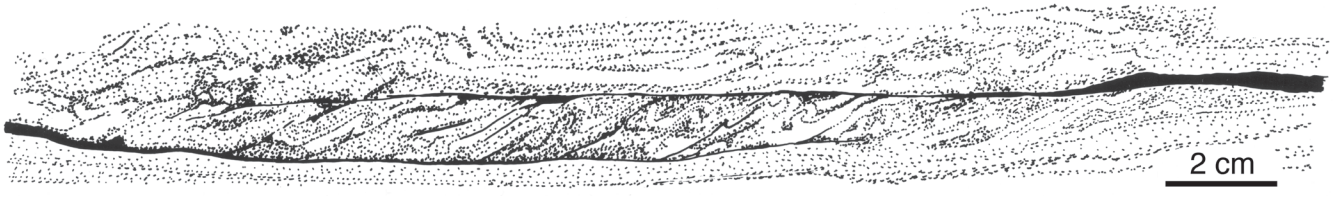

Figure 16.9 Imbrication zone formed in the overlap zone between two mica-rich layers (black) in mylonitic gneiss. The zone formed as displacement on the lower mica-rich layer was transferred to the upper one. From Rykkelid & Fossen (1992).

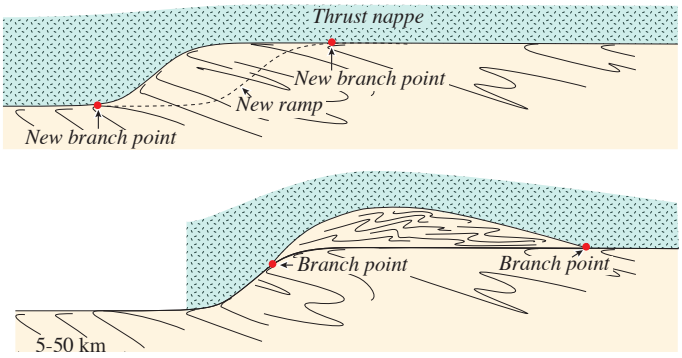

Figure 16.11 Formation of a new thrust nappe at a ramp. Branch points are indicated.

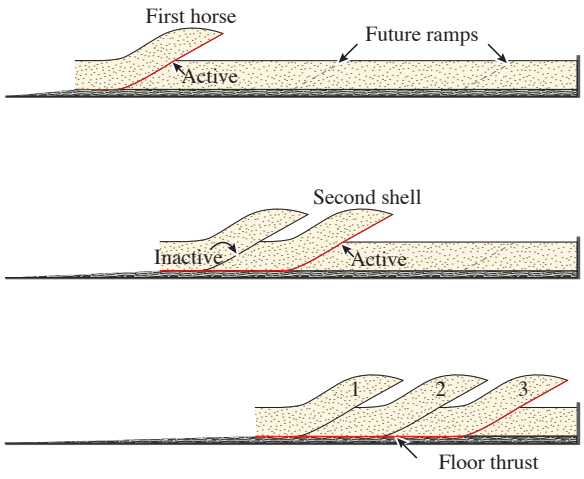

Figure 16.13 The "standard" formation of an imbrication zone, known as "in sequence thrusting". The horses get younger towards the foreland (right) in this model. Deviations from this model are known as "out of sequence thrusting".

the Alpine example shown in Figure 16.12, the foreland-style is exemplified by the Jura Mountains, where Jurassic-Cretaceous sediments are folded and imbricated. A section through a part of the Caledonian foreland structures is illustrated in Figure 16.5, showing extensive imbrication and duplex formation. In both cases the basement is practically undeformed and separated from the shortened sedimentary cover by a basal sole thrust or décollement. It is the classical example of *thin-skinned* tectonics and is characteristic for deformed foreland areas. The style of deformation is simple compared to more internal parts of collision zones, with a stratigraphic control that enables correlation across faults.

In the *hinterland* the basement is also involved, and the style is therefore referred to as *thick-skinned*. Thrust nappes in the hinterland can therefore be much thicker than those in the foreland and include metamorphic and magmatic rocks. In the interpretation of the Alpine orogen shown in Figure 16.12, the entire lower crust is imbricated. Another characteristic is the occurrence of island-arc or outboard terranes, thrust onto the continental margin from oceanic terranes during convergent plate movements. Hinterland nappes can vary from internally undeformed to penetratively deformed. Where they are penetratively folded they may be referred to as *fold nappes*. Nappes with an intense or mylonitic internal fabric are called *mylonite nappes*.

At a large scale in an orogenic zone the basement is thrust under a wedge-shaped stack of thrust nappes. The orogenic wedge thickens and lengthens over time, as fragments of the down-going crust are sliced off and incorporated within the allochthonous units and as oceanic rock units are added. The rest of the basement is transported deeper into the subduction zone and undergoes high-grade metamorphism and related deformation. Hinterland-structures therefore tend to form at greater depths than foreland-structures, a fact that favors plastic shear zones and plastic deformation in general. There is of course deformation going on at shallow levels in the hinterland-zone as well. These are however influenced by extensional faulting and are typically removed by erosion in old orogenic belts.

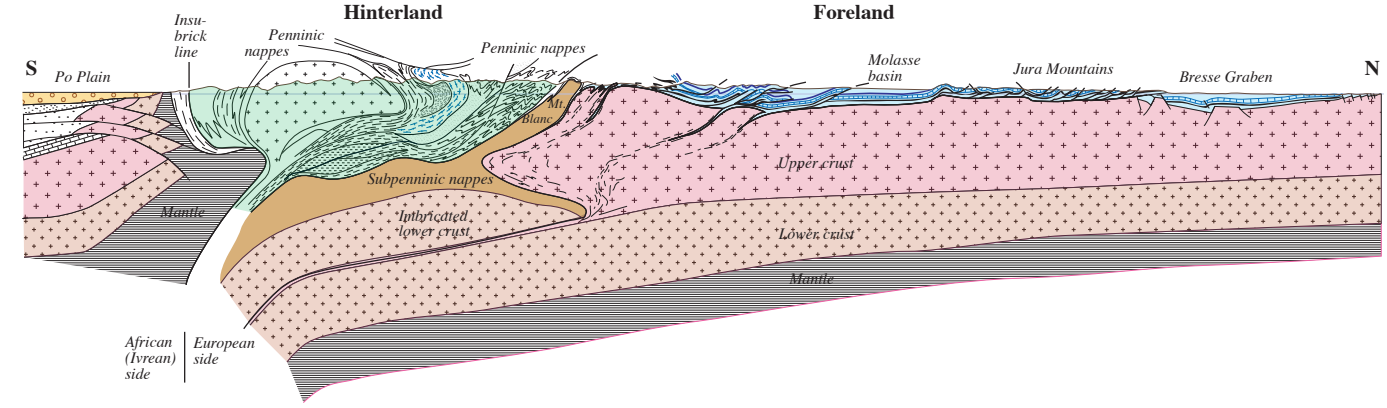

Figure 16.12 Cross-section through the Alps, showing the thin-skinned foreland deformationi in the north (left) and the more pervasive and complicated deformation in the hinterland. Imbrication of the lower crust is indicated, based on seismic information. Based on Schmid & Kissling (2000).

THE MOINE THRUST ZONE

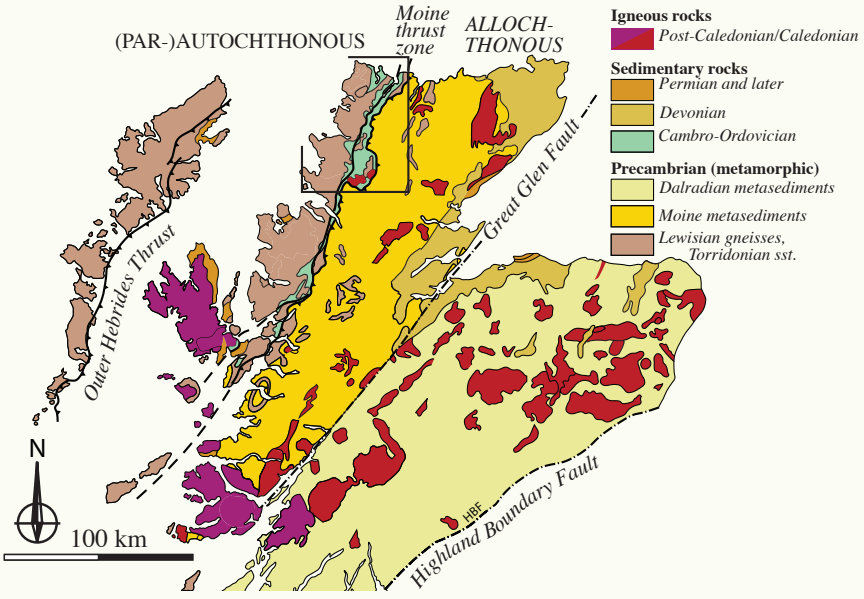

The Caledonian Moine thrust zone in the NW Scottish Highlands has become a classic area of thrust tectonics. Here, a large unit of late-Proterozoic metasediments (the Moine and Dalradian rocks) were thrust northwestward above Archaean basement (the Lewisian) and its sedimentary cover. Some 100 km of overthrusting lead to the formation of imbricate structures, duplexes, mylonites and many other structures and fault rocks typically associated with major thrusts. The first ideas about thrusting arose during geologic mapping in the last half of the 19th century. The mapping showed that old rocks (detached basement gneisses) were resting on younger ones (Cambro-Ordovician sediments), an observation that called for the concept of thrust tectonics. Stratigraphy was key to the mapping of the Moine thrust zone. In particular, the Cambro-Ordovician stratigraphy is easily recognized in the area and has made it possible to map out very impressive duplex structures throughout the thrust zone. The recognition and balancing of duplex structures was inspired by the mapping of such structures in the Canadian Rocky Mountains in the 1970-80's.

A very sharp thrust contact between Precambrian gneisses and underlying Cambrian quartzite in the Moine thrust zone.

Sliver of Lewisian basement thrust above Cambrian sedimentary layers. Older rocks resting on younger ones, as seen here, is a classical feature in thrust and nappe regions.

In addition to the Moine thrust zone, the Outer Hebrides Thrust, Great Glen Fault and Highland Boundary Fault are fundamental Scottish structures. These are Precambrian faults that have been reactivated both before, during and after the Caledonian orogeny. Reactivation of preexisting faults is a characteristic feature of orogenic belts.

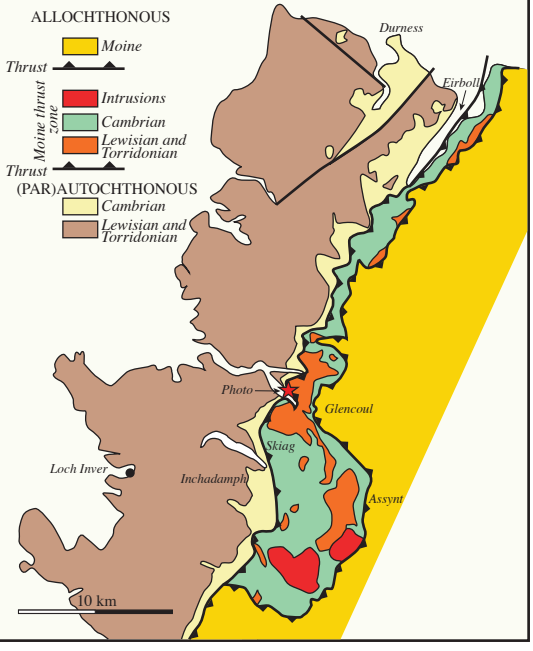

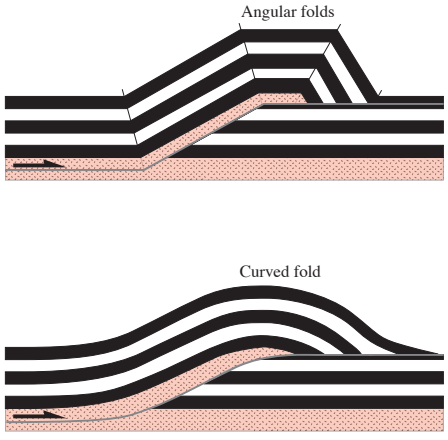

Figure 16.14 Ramp- and fold geometry are connected: angular ramps give angular folds, while rounded ramps give rounded folds.

1.3 Ramps, thrusts and folds

The temporal development of imbrication zones can vary, but the model that is regarded as normal is shown in Figure 16.13. Here, the individual sheets or horses are formed in sequence, so that successively younger faults form in the direction of thrusting. This foreland-directed progression of duplexes and imbricate zones is called in-sequence thrusting. The foreland-most ramp or thrust is the youngest one and carries the other horses on its back toward the foreland. In-sequence thrusting enables the zone of contractional deformation to expand in the foreland direction. Thrust faults that do not follow this systematic pattern of expansion are said to be *out of sequence*. Out of sequence thrusting can influence the overall geometry of a duplex or imbrication zone and complicate stratigraphic relations.

Tectonic horses in duplexes form by the successive formation of ramps in competent layers. Hence stratigraphy controls both the location and sizes of tectonic horses: the thicker the competent layers, the larger the horses. Furthermore, weak layers control the location of décollements.

The largest duplexes or imbrications are found in the hinterland where basement is involved. Here, large parts of the crust, perhaps even the entire crust, can be imbricated. The identification of such large-scale duplexes relies on deep-seismic data, whereas small-scale structures can be seen in outcrop (Figure 16.4) or even in thin-section (Figure 16.7).

1.3.1 Fault-bend folds

The moment a ramp is established and the hanging wall starts climbing above it, the hanging-wall layers are deformed into a fault-bend fold. The geometry of the fold reflects the geometry of the ramp. Angular ramps produce angular folds (kink folds), while more gently curved ramps result in less angular folds (Figure 16.14). The relation between ramp and fold geometry is simple enough that they can be modeled by means of simple computer programs. Knowing the fold geometry one can construct the ramp geometry and vice versa.

An interesting aspect of the deformation history associated with fault-bend folds is that the hanging wall layers first are bent to accommodate the ramp. Then as they pass the ramp they are restored to their original, usually horizontal, orientation (Figure 16.15). The layers are thus deformed twice over a short transport distance. In this sense the ramp is an area in which hanging-wall layers are "processed" before transported toward the foreland at a higher stratigraphic level. It is also interesting that while the

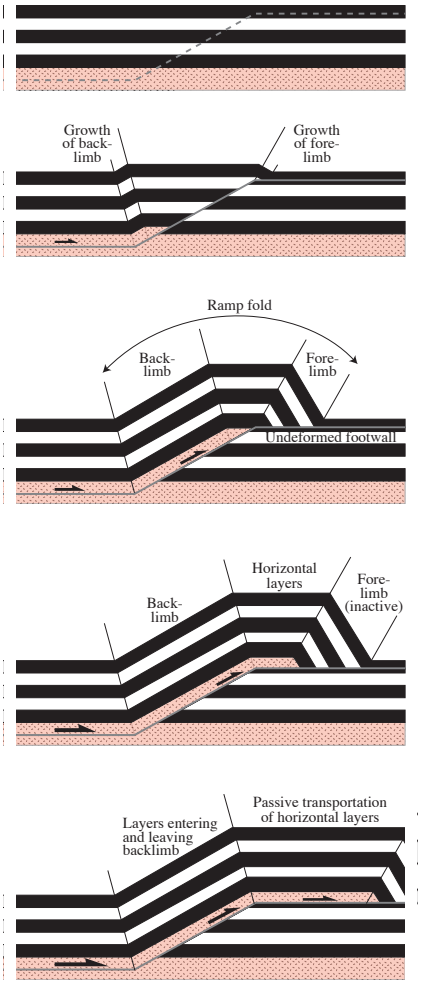

Figure 16.15 Development of a fault-bend fold. Note that layers are rotated to become hinterland-dipping in the ramp region and then rotated back to horizontal as they leave the ramp. Alson note that the forelimb is inactively transported towards the foreland (right).

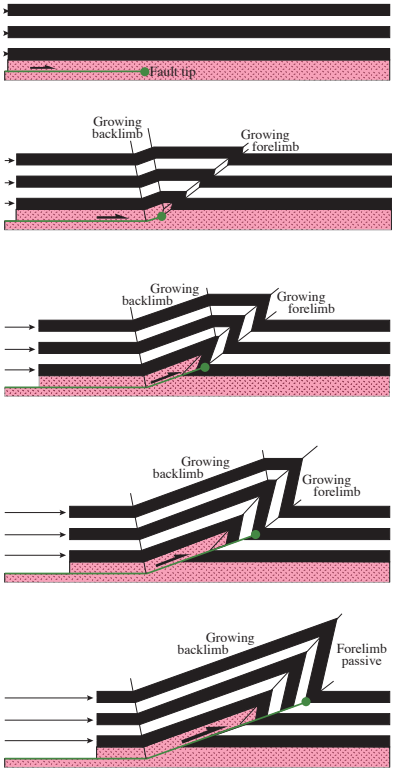

Figure 16.16 Progressive development of a fault-propagation fold.

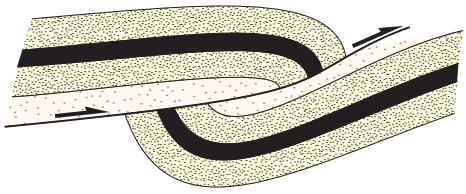

Figure 16.17 Layers commonly show drag near thrust and reverse faults. This type of drag may form where a fault cuts through a fault propagation fold. The ductility of the layers and the geometry of the ramp determine the final fold geometry.

fault-bend fold is stationary, the fold in the trailing edge of the horse or sheet is passively transported toward the foreland.

1.3.2 Fault-propagation folds

Like normal and strike slip faults, reverse and thrust faults generally have a brittle process zone and a ductile fold zone around their tips. The fold zone is particularly well developed for many thrust faults and has therefore received much attention. The fold associated with the fault tip is a *fault-propagation fold* – a name originally applied to the particular type of fold that develops ahead of a propagating thrust,

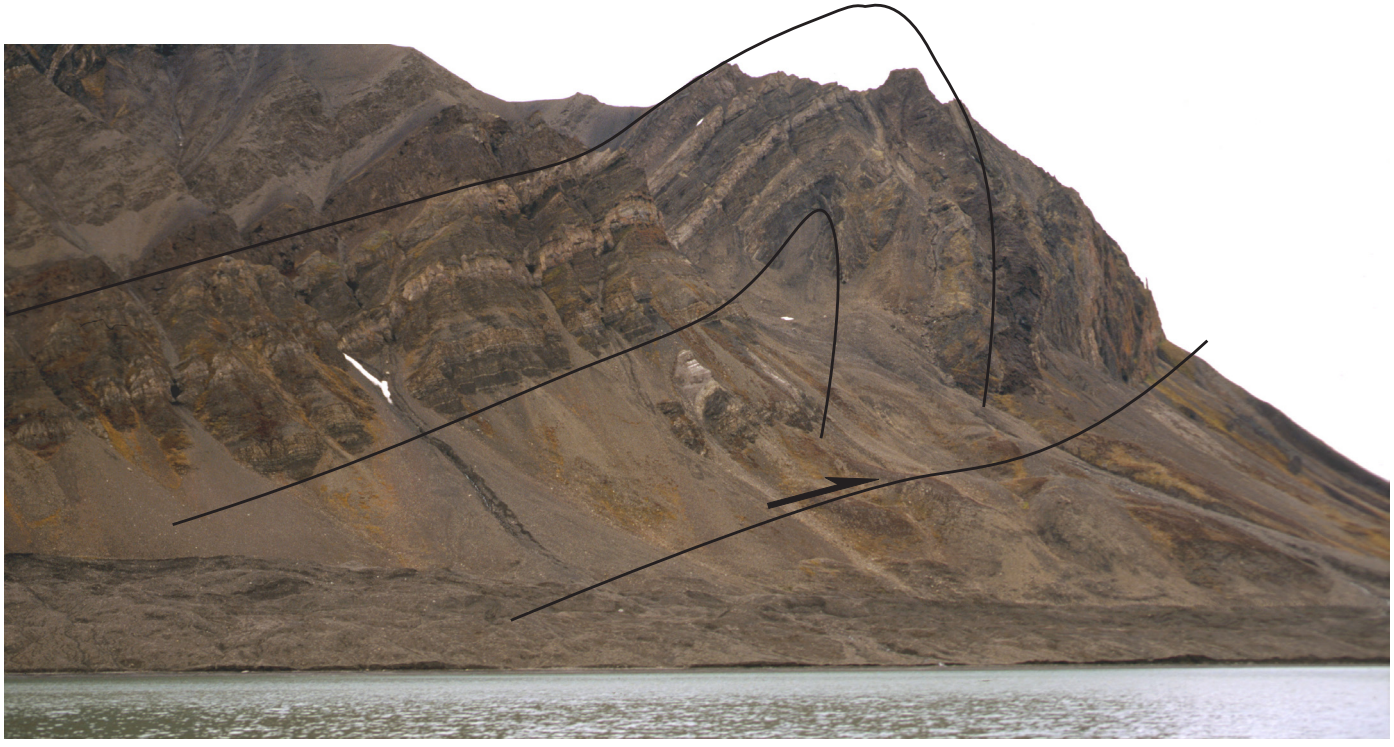

Figure 16.18 Fault-propagation fold in the Tertiary thrust and fold belt in Mediumfjellet, Svalbard.

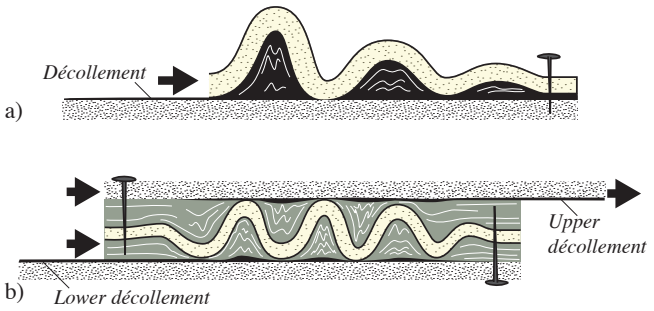

Figure 16.19 a) Detachment folds develop above a décollement (detachment) during shortening. b) a related type of folds forms between two décollements when displacement is transferred upward in the direction of transport.

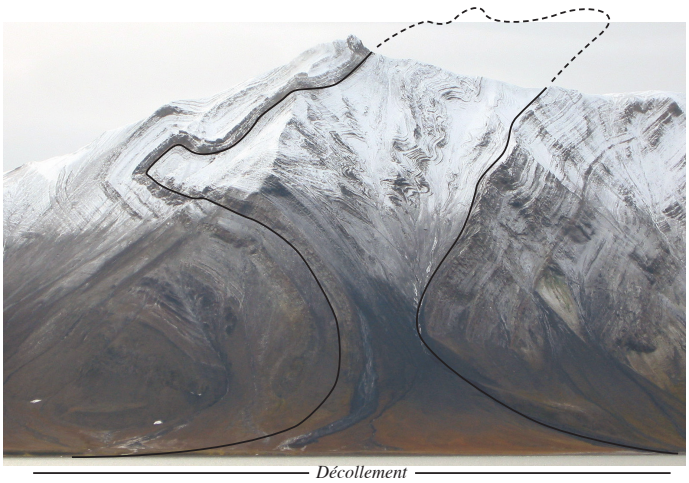

Figure 16.20 Large-scale detachment folding related to the Tertiary thrust and fold belt in Spitsbergen. The detachment is located below sea level. Photo: Mina Aase.

but which can also be used more generally for folds forming in front of any propagating fault tip. Fault-propagation folds differ from fault-bend folds and other folds in that they move with the fault tip as the tip propagates. A fault-bend fold on the other hand is located at the ramp and remains stationary. Fault-bend folds also tend to have steeper, commonly overturned layers in the forelimb.

Classical fault-propagation folds form in subhorizontal strata where faults propagate up-section[5]. A simple model for the formation of such a fault-propagation fold is shown in Figure 16.16. Keeping layer-thickness constant allows for simple construction of the fold geometry as a function of displacement gradient, fault dip and fault geometry. An asymmetric foreland-verging fold is the result.

Unless deformation ceases, the fault will break through the fault-propagation fold. The result may be drag folds along the fault. Thrust faults tend to break through the lower syncline, creating high-angle relations between the fault and the hanging-wall layers (Figures 16.17 and 16.18).

1.3.3 Detachment folds

Fault bend folds form at ramps, and fault-propagation folds form where faults propagate across the layering. However, there is another type of folds that can form where slip is solely along the layering. This type of folds, known as *detachment folds* or *décollement folds*, forms where layers above a detachment shorten more than their substrate. In fact, the substrate is commonly found to be undeformed, and the situation is the one portrayed in Figure 16.19a. Detachment folds tend to develop above very weak layers, such as (overpressured) shales or evaporites.

5 For a fault-propagation fold to form the fault has to cross the layering. Otherwise, deformation occurs only by layer-parallel slip or shear.

As the folds form by buckling, the weak layer locally flows to accommodate the geometrical difference between the flat décollement and the folded layer(s). The main reason why they are more common in contractional regimes is because of the many layer-parallel décollement in such settings.

Detachment folds are generally upright, with boxfold geometry and oppositely-dipping axial surfaces (Figure 16.20). A strong viscosity contrast between the folded layer and its surroundings promotes the formation of a series of buckle folds ("a train"). The offset along the detachment shows a gradual decrease toward the foreland, and may terminate as a blind fault. A special type of detachment-controlled folds sometimes develops where offset is transferred from one weak layer to a higher one (Figure 16.19b). In principle, this is similar to what happens at thrust ramps, but in some cases competent layer(s) between the two levels deform by buckling rather than by imbricate faulting and duplex formation. Vertical transfer of displacement may reflect weak layer pinch outs, as seen in Figure 16.19b.

Classical detachment folds are upright, but can be overturned due to distributed simple shear. The detachment folds in the Jura Mountains in the Alpine foreland area (Figure 16.12) is the classic example. Here, the competent folded layers are limestone overlying evaporites. Detachment folds may also occur on smaller scale and in different lithologies, as shown in the mylonitic gneisses in Figure 16.9 and the unconsolidated glacifluvial sediments in 16.21.

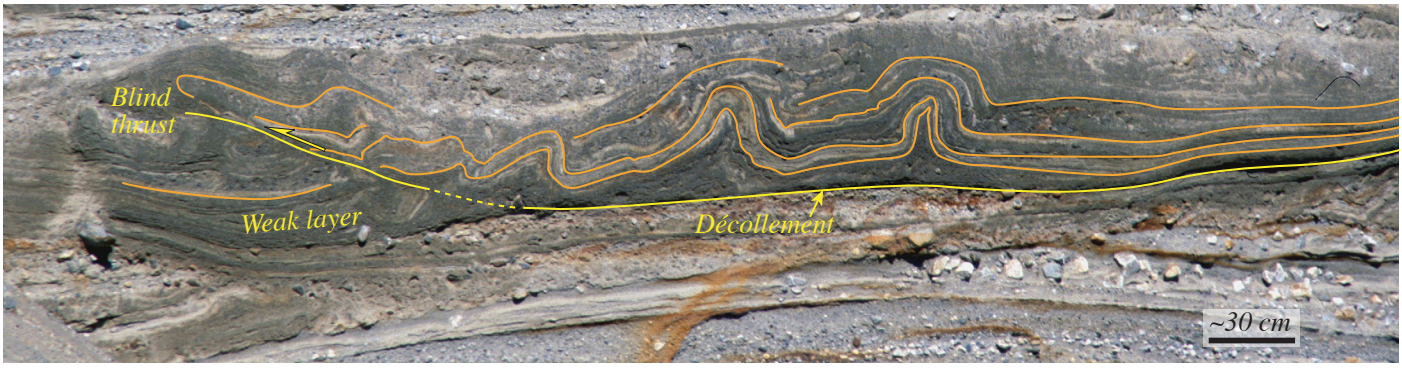

Figure 16.21 Detachment folds formed by a glacier advancing over non-consolidated delta deposits at the end of the last Quaternary glaciation in West Norway.

1.4 Orogenic wedges

1.4.1 The wedge model

Fold and thrust belts show an overall wedge-shaped geometry in cross-section, thinning towards the foreland. Such tectonic wedges occur in mountain ranges and above subduction zones, particularly in front of island-arc complexes. Sometimes just the low-metamorphic foreland-section is considered, in other cases the entire section from the foreland to the hinterland is emphasized. Both tend to show a wedge-shaped geometry.

The formation of tectonic wedges is commonly compared to the build-up of a wedge-shaped pile of snow or sand in front of a snowplow or bulldozer (Figure 16.22). At shallow crustal levels, where brittle deformation mechanisms dominate, the shape of the wedge depends not only on the force applied and gravity, but also on 1) the friction along the basal thrust or décollement, 2) the internal strength or frictional coefficient of the material within the wedge, and 3) any erosion at the surface of the wedge (Figure 16.23a). In principle the wedge model is independent of the actual size of the wedge, so that as the wedge grows in length by frontal imbrication it will also deform internally to maintain a stable shape.

The basal friction is a major controlling factor in the wedge model. The lower the basal friction, the lower and longer the wedge. In orogenic wedges the basal friction is controlled by the properties of the relatively weak basal décollement. The décollement commonly consists of lithologies rich in phyllosilicates, but elevated fluid pressure may be even more important. This is particularly true in subduction zones where the décollement zone acts as a conduit for fluids released from wet sediments and, in the metamorphic zone, recrystallization and dehydration reactions. A uniform frictional coefficient is commonly applied in simple models, while a gradual variation that leads to a curved slope of the wedge may be more realistic. In the snowplow analog: when the basal friction increases, i.e. if the toe part locks up because of irregularities

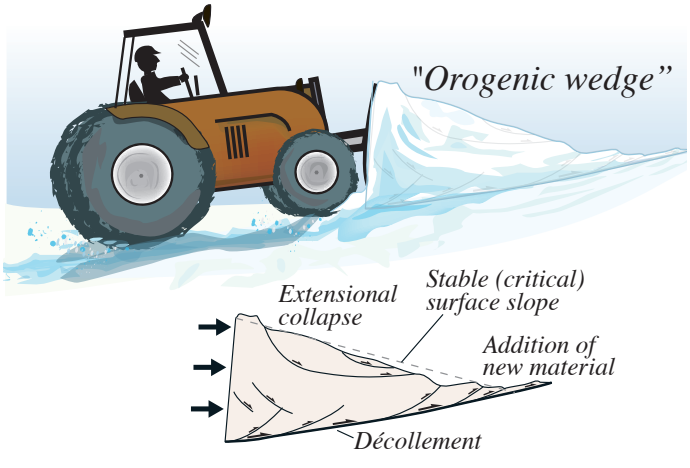

Figure 16.22 The creation and evolution of orogenic wedges are in many ways similar to the accretion of a snow or soil wedge in front of a bulldozer.

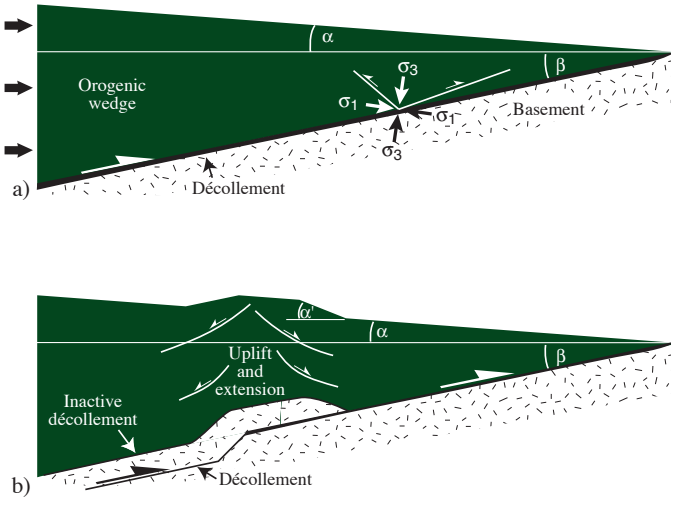

Figure 16.23 a) Principles of an orogenic wedge. There is a close connection between the orientation of the décollement, its friction, the applied force at the end, gravity and the internal strength or rheological properties of the wedge. b) The incorporation of a basement slice (known as tectonic underplating) generates uplift and instability. Consequently, the wedge responds by thinning through normal faulting.Hence, normal faults can form in an orogenic wedge in addition to reverse faults dipping toward and away from the hinterland.

THRUST NAPPES – MECHANICALLY IMPOSSIBLE?

The bulldozer model was rejected for a while in favor of gravity driven models because of mechanical considerations: How can enormous thrust nappes be pushed horizontally or up-hill for tens or hundreds of kilometers without being internally crushed? Simple mechanical calculations tell us that the nappes will crush or fold at the initial stage. Hubbert & Rubey resolved the issue in a classical work from 1959, where they emphasized the importance of pore pressure in the basal thrust zone. Overpressure close to lithostatic pressure considerably decreases the push that is needed to move the nappe. High fluid pressure (P_f) in the décollement zone decreases the effective normal stress σ_n by an amount P_f. Using Mohr-Coulomb's fracture criteria the shear stress on the décollement then becomes:

$$\sigma_s = C - (\sigma_n - P_f)\,\mu$$

Others have pointed out the importance of the fact that the nappe does not move as a rigid block. Instead, the movement occurs by the accumulation of numerous small slip events, either in the form of earthquakes or as episodes of creep. The analogy used to explain this type of movement is the way a caterpillar moves (study one if you do not know). In this way, the frictional resistance that has to be overcome becomes much smaller than by simultaneous slip on the entire basal thrust.

at the subsurface, more force is needed and snow or sand piles up to a higher wedge with a steeper slope.

The stress within the wedge must everywhere be identical to the strength of the material being deformed, i.e., the stress must be critical at every point in the wedge. This is why the orogenic wedge model is referred to as the critical taper or *critical wedge model*. Wherever the stress gets higher, the material will immediately deform until equilibrium is regained. In mathematical models Coulomb's fracture criterion is used to model critical wedges, which is particularly relevant for shallow (upper crustal) wedges or parts of wedges. Such models are known as *Coulomb wedges*. Larger and deeper orogenic wedges are controlled by plastic flow laws, and simple wedge models for viscous and plastic media have been developed (Figure 16.24).

Erosion at the surface of the wedge will lower the surface slope and make the wedge unstable. The result is for the wedge to grow in height by internal redistribution of material. In practice, this means reverse faulting and perhaps folding until the stable surface slope. During this process rocks move vertically through a combination of surfacial erosion and related wedge deformation to bring metamorphic rocks (closer) to the surface in an orogenic belt.

The characteristic stable wedge geometry is achieved when the wedge is everywhere at the critical angle and on the verge of collapse. Material is accumulated in the front through imbrication and the formation of duplex structures, as described in the previous sections of this chapter. In shallow wedges the subsurface remains undeformed. In the hinterland region of a large orogenic wedge, however, basement blocks may be incorporated, leading to reorganization of the décollement zone and its frictional properties, and to vertical growth of the wedge (Figure 16.23b). This growth causes the wedge to thicken locally, creating a slope instability that again results in local thinning by extensional deformation. The thinning occurs in the upper part of the wedge by normal faulting, while the top-to-the foreland sense of movement along the

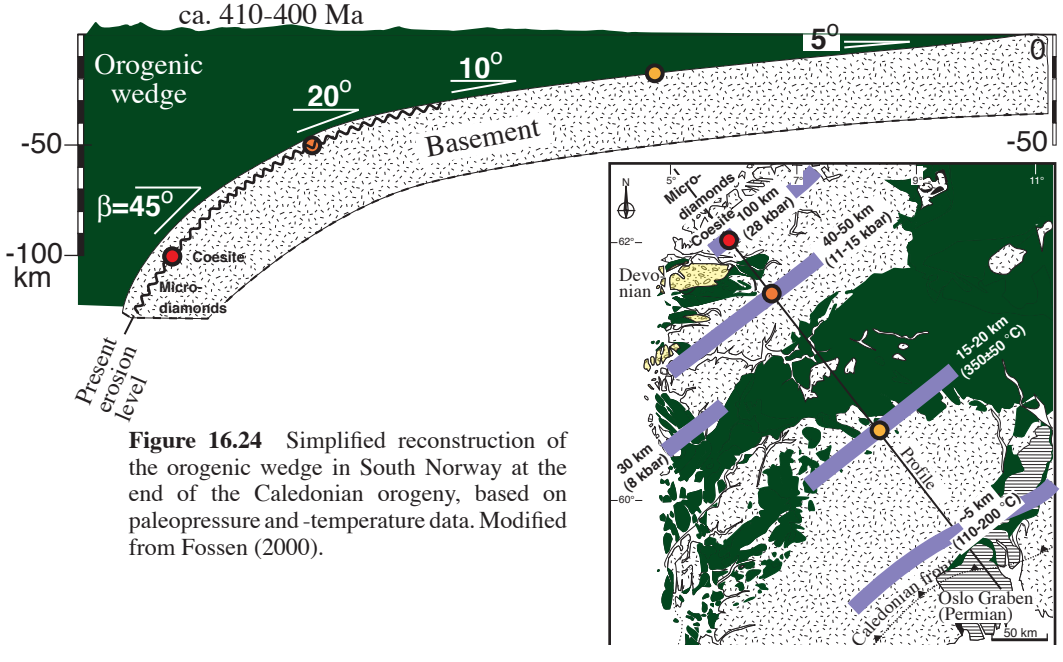

Figure 16.24 Simplified reconstruction of the orogenic wedge in South Norway at the end of the Caledonian orogeny, based on paleopressure and -temperature data. Modified from Fossen (2000).

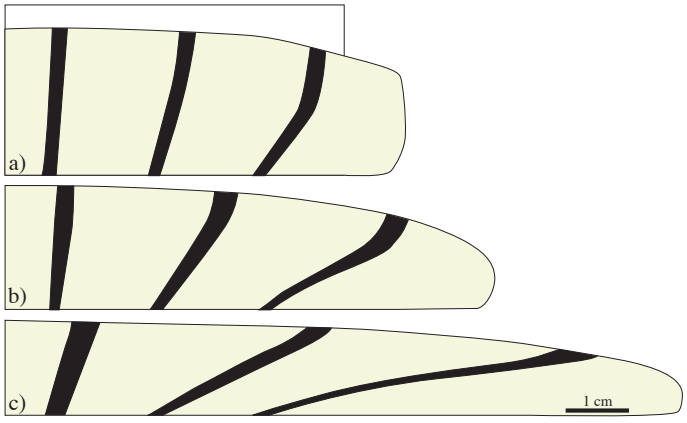

Figure 16.25 Experimental simulation of gravitational spreading of a thrust nappe or nappe stack. Note that most of the spreading occurs by flow of the upper part, while the basal part shows little or no movement. Together with the distortion of the originally vertical markers this indicates a significant component of simple shear. However, the change in height and length in the shear (horizontal) direction reveals a pure shear component. The deformation is therefore subsimple shear. Based on Ramberg (1981, p. 224).

décollement zone continues simultaneously.

1.4.2 Gravitational models

The wedge or bulldozer model is not the only model that has been suggested to explain deformation in contractional orogens. Other models use gravity as the dominant driving force just as much as the "push from behind". As an orogenic belt develops, the highest mountains develop in the central part. Gravity becomes important when the hinterland reaches elevations where thrust nappes move gravitationally (Figure 16.25). The Tibetan plateau in the Himalayan mountain chain is a modern example. The first variant of the gravitational model assumed that thrust faults formed as rock units, i.e. thrust nappes, slid down from the elevated hinterland. This model is sometimes referred to as the gliding model (Figure 16.26a).

The *gliding model* was popular in the 1950-60's, particularly in the Alps where many of the well-mapped thrust faults dip towards the foreland. However, seismic imaging of active orogenic belts show that the décollement always dips toward the hinterland. The present foreland-dip in the Alps is thus likely a late modification. The gliding model is therefore not applicable to major thrusts, but can still be applicable on a smaller scale at shallower level in contractional zones.

Gravitational collapse is a term now associated with normal faults rather than with reverse and thrust faults. Gravitational collapse in contractional zones occurs when the thickened crust collapses because it is not strong enough to support its own weight.

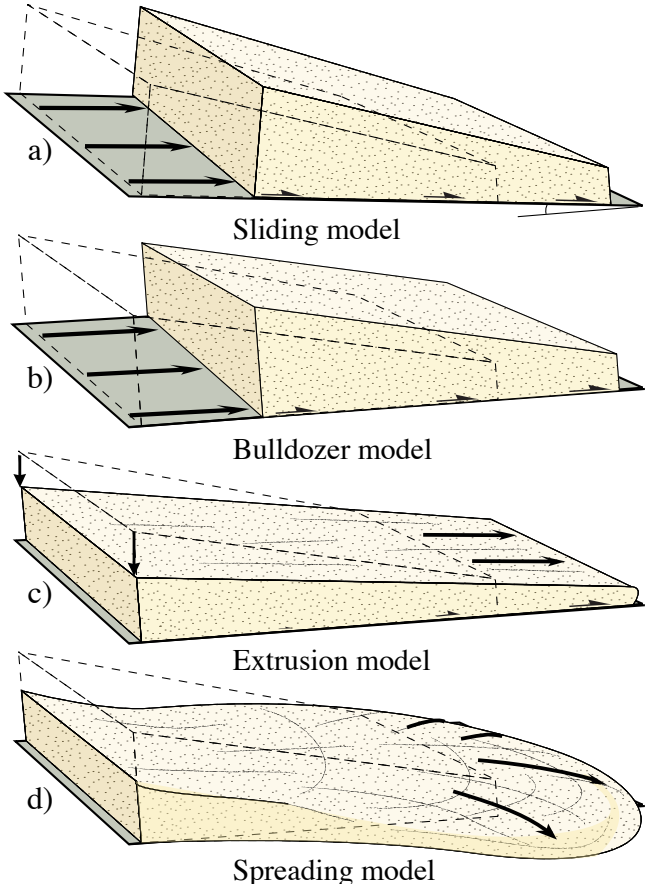

Figure 16.26 Various models for nappe translation. Sliding (a) requires a foreland-dipping décollement while the other models do not. a) and b) are rigid translations, driven by gravity (a) and a push from behind (b). c) and d) are also gravity driven, differing by boundary conditions (whether material is constrained on the sides or not). Combinations of these models are possible.

This may be related to weakening related to heating and magmatic intrusion. A popular model calls on delamination of the lower and densest portion of the lithosphere. Removal of the dense root causes uplift of the lithosphere, which again promotes gravitational collapse (see Figure 17.21). The collapse may result in new-formed normal faults or shear zones, or reactivation of existing thrusts as low-angle extensional faults (Figure 17.6).

In principle, gravitational collapse can push thrust nappes towards the foreland. This may occur as the orogenic wedge thins and extends towards the foreland. The process shares many similarities with that of glaciers, whose flow is also gravity driven. When the material in the wedge only extrudes toward the foreland, perpendicular to the orogenic front, the model is called an *extrusion model* (Figure 16.26c). However, if the elevated area spreads out in a more or less radial pattern it is referred to as a *spreading model* (Figure 16.26d). Both of these models can be

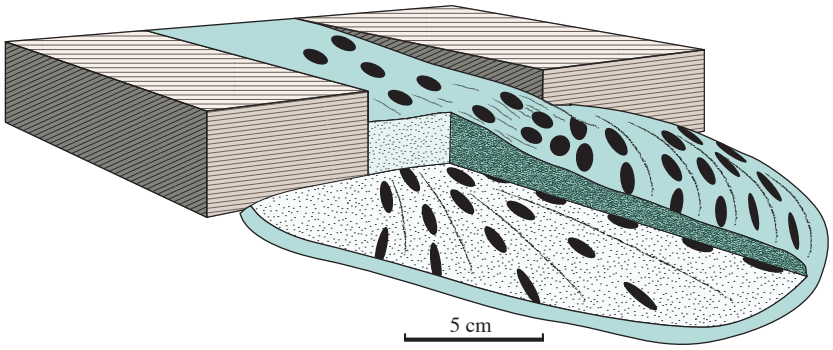

Figure 16.27 The spreading model explored in the laboratory. The deformation between the two boxes is extrusion. Once the material leaves the constraining boxes, spreading generates radial strain patterns that are different in the lower and upper parts of the material. Ellipses indicate strain. Based on Merle (1989).

simulated in the kitchen using dough, which is weak enough that it collapses and spreads out. Spreading freely it flows in a radial pattern, but constrained by two sidewalls it extrudes in a pure-shear manner. These mechanisms can also be modeled more sophistically in the laboratory (Figure 16.25 and 16.27) or numerically. Hans Ramberg explored this type of deformation in his famous laboratory in Uppsala and later numerically on a computer. One of the interesting aspects of such collapse is that the entire wedge or nappe pile is thinned, compensated by lateral extension. In these models the thrust is passively formed as a consequence of spreading over a rigid basement (Figure 16.26b), and the displacement increases towards the foreland. Technically it dies out somewhere in the hinterland.

The extrusion and spreading models have implications also for the strain and deformation history. The vertical thinning and lateral extension of the wedge is a significant component of coaxial deformation throughout much of the wedge. Pure shear to subsimple shear dominate the simple extrusion model, and three-dimensional coaxial deformation characterize radial spreading. The spreading model gives a radial distribution of the X-axis of the finite strain ellipsoid, with different patterns in the upper and lower parts (Figure 16.27). Both the shape and orientation of the strain ellipsoid should therefore be investigated when considering models of nappe transport. Curved thrust fronts could be another indication of gravitational spreading.

Many nappes, such as the Jotun Nappe of the Scandinavian Caledonides, show little or no internal deformation above the intense non-coaxial deformation along their bases. Spreading or extruding nappes must be weak enough to deform internally, which requires a certain temperature and mineralogy. Quartz-rich nappes would, for example, be more likely to collapse than would feldspar-rich nappes at temperatures in the range of 300-500 °C. Although alternative interpretations exist, pervasive deformation of quartzite and the famous quartzitic Bygdin Conglomerate beneath the rigid and feldspar-rich Jotun Nappe was explained in terms of extrusion by the geologist Jake Hossack.

Further reading:

Bombolakis, E.G., 1986. Thrust-fault mechanics and origin of a frontal ramp. Journal of Structural Geology, 8: 281-290.

Boyer, S.E. & Elliott, D., 1982. Thrust systems. American Association of Petroleum Geologists Bulletin, 66: 1196-1230.

Braathen, A., Bergh, A.G. & Maher, H.D., 1999. Application of a critical wedge taper model to the Tertiary transpressional fold-thrust belt on Spitsbergen, Svalbard. GSA Bulletin, 111: 1468-1485.

Butler, R.W., 1982. The terminology of structures in thrust belts. Journal of Structural Geology, 4: 239-245.

Butler, R. W. H. 2004. The nature of “roof thrusts” in the Moine Thrust Belt, NW Scotland: implications for the structural evolution of thrust belts. Journal of the Geological Society 161: 1-11.

Coward, M.P., 1983. The thrust and shear zones of the Moine thrust zone and the NW Scottish Caledonides. Journal of the Geological Society, 140: 795-811.

Coward, M.P. & Kim, J.H., 1981. Strain within thrust sheets. In: McClay, K.R. & Price, N. J. (Eds.), Thrust and Nappe Tectonics. Geological Society Special Publications, 9: 275-292.

Dahlen, F.A., 1990. Critical taper model of fold-and-thrust belts and accretionary wedges. Annual Reviews Earth Planetary Science, 18: 55-99.

Elliot, D., 1976. The motion of thrust sheets. Journal of Geophysical Research, 81: 949-963.

Erslev, E.A., 1991. Trishear fault-propagation folding. Geology, 19: 617-620.

Fossen, H., 2000. Extensional tectonics in the Caledonides: synorogenic or postorogenic? Tectonics, 19: 213-224.

Fyfe, W. & Kerrich, R., 1985. Fluids and thrusting. Chemical Geology, 49: 353-362.

Gee, D., 1978. Nappe emplacement in the Scandinavian Caledonides. Tectonophysics, 47: 393-419.

Geiser, P.A., 1988. Mechanisms of thrust propagation: some examples and implications for the analysis of overthrust terranes. Journal of Structural Geology, 10: 829-845.

Hossack, J.R., 1983. A cross-section through the Scandinavian Caledonides constructed with the aid of branch line maps. Journal of Structural Geology, 5: 103-111.

Hossack, J.R., Garton, M.R. & Nickelsen, R.P., 1985. The geological section from the forland up to the Jotun thrust sheet in the Valdres area, south Norway. In:Sturt, B.A. & Gee, D.G. (eds.) The Caledonide orogen - Scandinavia and related areas. John Wiley & Sons Ltd, Salisbury, 443-456.

Hossack, J.R. & Cooper, M.A., 1986. Collision tectonics in the Scandinavian Caledonides. M.P. Coward & A.C. Ries (Red.), Collision tectonics. Geological Society Special Publications, 19, 287-304.

Hubbert, M.K. & Rubey, W.W., 1959. Role of fluid pressure in mechanics of over-thrust faulting. Geological Society of America Bulletin, 70: 70-205.

McClay, K. & Price, N.J. (eds.), 1981. Thrust and nappe tectonics. Geological Society Special Publications 9.

Mitra, G. & Wojtal,S. (red.), 1988. Geometries and mechanisms of thrusting, with special reference to the Appalachians. Geological Society of America Special Paper 222, 236 pp.

Moore, J.C., Cowan, B. & Karig, D.E., 1985. Structural styles and deformation fabrics of accretionary complexes. Geology, 13: 77-78.

Morley, C.K., 1986. Vertical strain variations in the Osa-Røa thrust sheet, North-western Oslo Fjord, Norway. Journal of Structural Geology, 8: 621-632.

Morley, C.K., 1994. Fold-generated imbricates: examples from the Caledonides of Southern Norway. Journal of Structural Geology, 16: 619-631.

Price, R.A., 1981. The Cordilleran foreland thrust and fold belt in the southern Canadian Rocky Mountains. In: M.P. Coward and K.R. McClay (eds.), Thrust and Nappe Tectonics. Spec. Publs geol. Soc. Lond., pp. 427-448.

Ramberg, H., 1977. Some remarks on the mechanism of nappe movement. Geol. För. Stockholm Förh., 99: 110-117.

Sanderson, D.J., 1982. Models of strain variations in nappes and thrust sheets: a review. Tectonophysics, 88: 201-233.

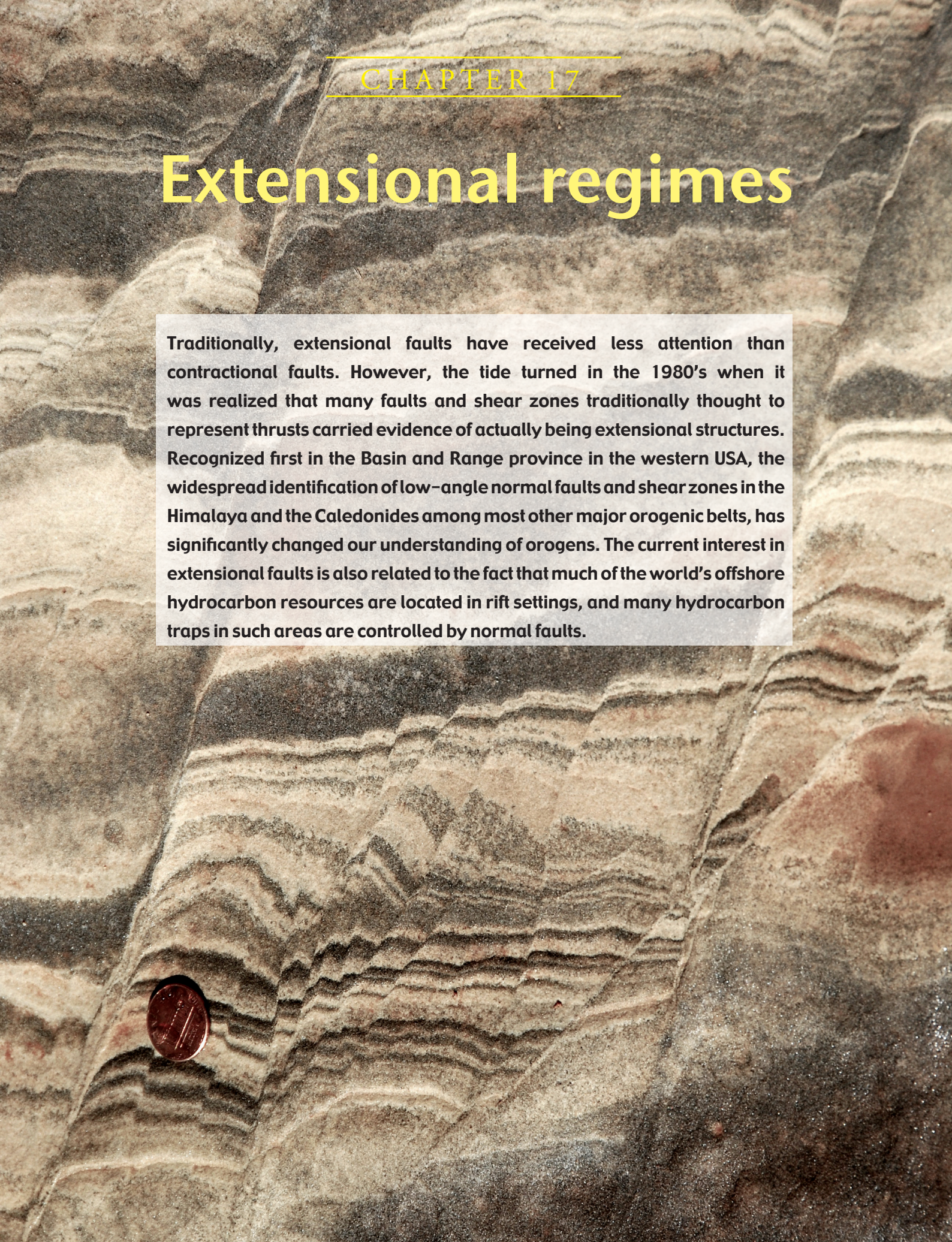

CHAPTER 17

Extensional regimes

Traditionally, extensional faults have received less attention than contractional faults. However, the tide turned in the 1980's when it was realized that many faults and shear zones traditionally thought to represent thrusts carried evidence of actually being extensional structures. Recognized first in the Basin and Range province in the western USA, the widespread identification of low-angle normal faults and shear zones in the Himalaya and the Caledonides among most other major orogenic belts, has significantly changed our understanding of orogens. The current interest in extensional faults is also related to the fact that much of the world's offshore hydrocarbon resources are located in rift settings, and many hydrocarbon traps in such areas are controlled by normal faults.

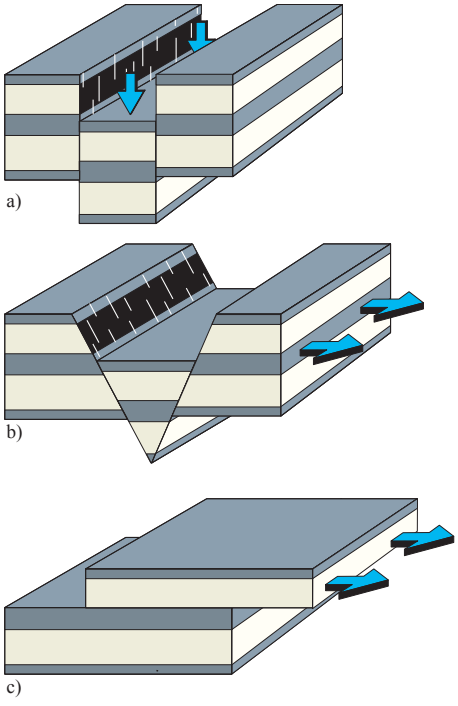

Figure 17.1 Using the surface of the Earth as a reference, extensional faults (b) are the spectrum of faults between vertical (a) and horizontal (c) faults. Note that vertical and horizontal faults are neither extensional nor contractional.

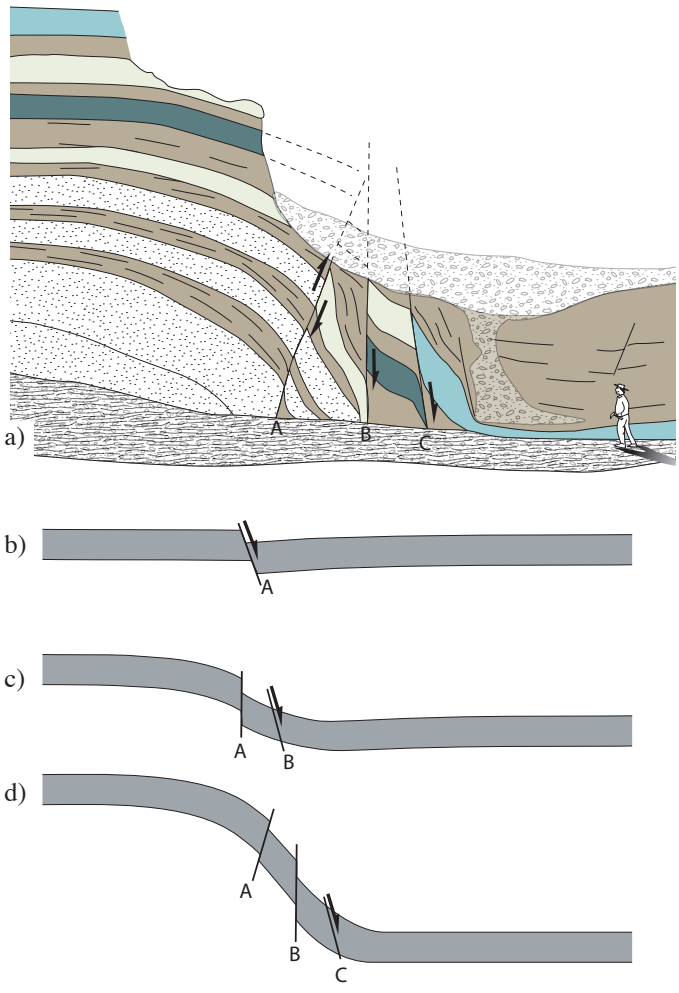

Figure 17.2 a) Reverse faults and normal faults coexisting in a folded layer along a fault. Both the reverse and normal faults are extensional faults because they extend the layers. The reverse faults probably formed as normal faults before being rotated during the folding. San Rafael Desert, Utah.

1.1 Introduction

Extensional faults cause extension of the crust or some reference layering in deformed rocks. At regional and large scales, the crust itself is that reference. If the distance between two points on the surface of the earth is increased during deformation, then extension occurs in that direction. But this can also occur across a strike-slip fault, depending on the positions of the two points. So, we have to evaluate extension perpendicular to the strike of the fault(s). This is the principal extension direction across an extensional fault (Figure 17.1b). The opposite is true for contractional faults.

For smaller faults, the term extensional faults can be used for faults that extend a given reference layer, independent of the orientation of the layering itself. In this sense, reverse faults can be extensional faults as long as the reference layer is extended by the faults (Figure 17.2). It is therefore useful to specify a reference surface like, for example, the terms crustal extension or layer-parallel extension.

A reverse fault can be an extensional fault if a tectonic or sedimentary layering is used for reference.

Fault dip is also important. Vertical faults imply neither extension nor shortening of the crust (Figure 17.1a). More generally, faults that are oriented perpendicular to a layer do not stretch or shorten the layer. Horizontal (or layer-parallel) faults represent the other end member: they neither shorten nor extend the layering per se (Figure 17.1c). Layer-parallel faults occur as flat portions (flats) of both extensional faults and contractional faults.

1.2 Systems of extensional faults

Both high- and low-angle extensional faults are common. In fact, they commonly coexist. A simple explanation for very steep faults is that they

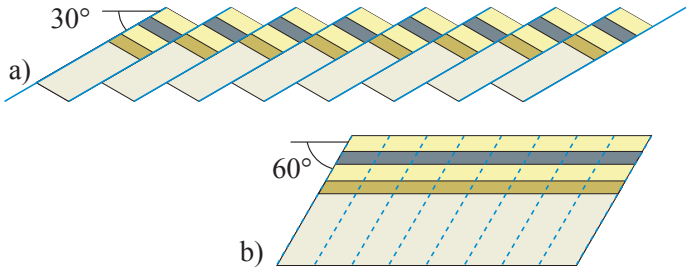

Figure 17.3 Rigid domino-style fault blocks can be restored by rigid rotation until layering is horizontal. a) Layers and faults dip in oppposite directions. b) Restoration by 30° rotation and removal of displacement.

THE RIGID DOMINO MODEL:

- No block-internal strain
- Faults and layers rotate the same amount
- All faults dip the same amount (parallel)
- Faults have equal offset
- Layers and faults have constant dip (planar)
- All blocks rotate at the same time and rate

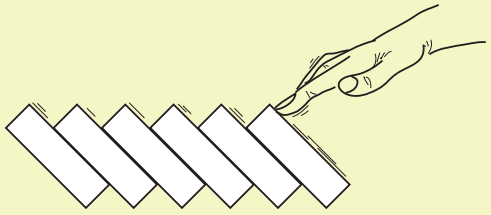

represent reactivated joints. Recall that joints are close to vertical because they form perpendicular to σ_3, which tends to be horizontal in the upper crust. Similarly, many low-angle normal faults have been interpreted as reactivated thrust faults. At the same time, experiments and field observations indicate that both high and low angle extensional faults can form under a single phase of extension without the use of preexisting zones of weakness. In particular, faults can rotate from initial high-angle faults to low-angle structures, although low-angle faults are also thought to form directly without much rotation.

1.3 Rotation by the rigid domino model

Sections through a rifted portion of the crust typically show a series of rotated fault blocks. The sense of rotation is easily estimated from the dip direction of the rotated layers. The fault blocks are commonly arranged more or less like domino bricks or similar to overturned books in a not quite full bookshelf (Figure 17.3). Kinematically the domino model requires the domino blocks to be bounded by a listric (curved) fault (Figure 17.4). If not, space problems arise between the domino blocks and the undeformed area. A smaller or more distributed space problem still exists between the base of the blocks and the substrate. This problem can be solved if a mobile medium, such as clay or evaporite underlies the domino system, or if the volume is filled with magma. Where the blocks are large enough to reach the brittle-plastic transition in the crust, then the problem can be solved by plastic flow of the subsurface rocks.

The ideal domino model assumes that the fault blocks are rigid, i.e. internally unstrained. If this requirement is met, then restoration of a geologic section in the extension direction is easy, as shown in Chapter 20. The blocks are then simply back-rotated until the layering becomes horizontal, and displacement is removed.

.

1.4 The soft domino model

Fault blocks seldom behave as rigid objects, and certainly not in rift systems with relatively weak if not unconsolidated sediments. Besides, we have already seen (Chapter 8) that faults occur in populations where size tends to be distributed according to a power law (Figure 8.?). In fact, the rigid domino model requires all faults to be of equal length and displacement,

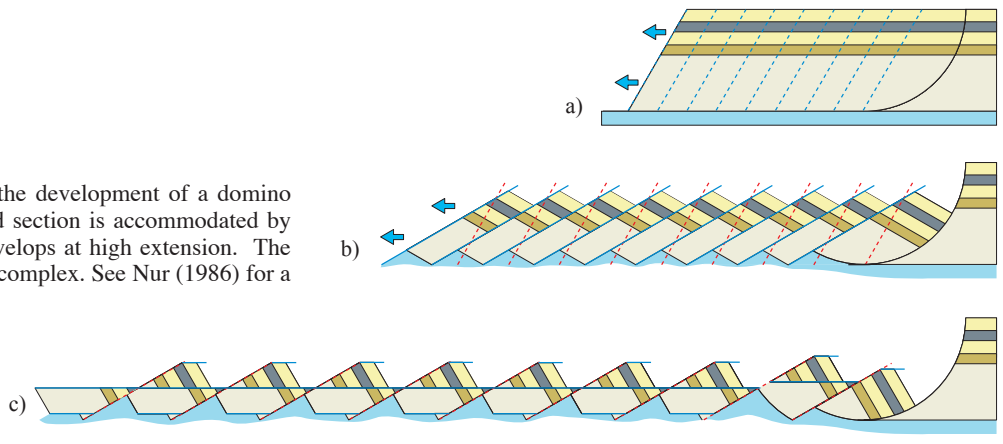

Figure 17.4 Schematic illustration of the development of a domino system. a) The transition to undeformed section is accommodated by a listric fault. b) A new set of faults develops at high extension. The resulting fault pattern can become quite complex. See Nur (1986) for a more detailed description.

and not showing any displacement gradient. Natural observations, numerical modeling and experiments alike show that systems of rotated fault blocks have experienced block-internal deformation and that displacement varies along faults and from fault to fault.

Because of these facts, a *soft domino model* permits internal strain to accumulate within blocks. The amount of extension through simple back-rotation of blocks and comparing to the present section no longer applies. A representative model for the internal fault-block deformation must be chosen. A ductile simple shear deformation is an easy approach, but we will save this discussion for the last chapter.

1.5 Why do domino systems form?

Extension of the crust can either result in a more or less symmetric horst-and-graben system or in a domino system of the types discussed above. The total extension and crustal thinning may be the same, but the fault arrangement depends on the way the rocks respond to the deformation, i.e. how strain is accommodated in the crust (Figure 17.5). Clearly, one of the most important factors that promotes the development of asymmetric domino-style fault systems is the presence of a weak low-angle layer or structure. This can be an overpressured formation, a mobile clay(stone), a salt layer or a preexisting fault that is prone to be reactivated. Conversely, the absence of such a weak layer or structure favors a more symmetrical horst-and-graben system. Some experiments suggest that if such a weak horizon or décollement has a regional dip, then domino-style faults are more likely to dip in the same direction (Figure 17.6).

1.6 Multiple fault sets in domino systems

If a domino system is exposed to very high extension, then the faults will rotate so far away from their initial orientation that a new set of faults forms (Figure 17.4). This happens when the shear stress along the first faults decreases below the critical shear stress of the deforming rock, which depends on the

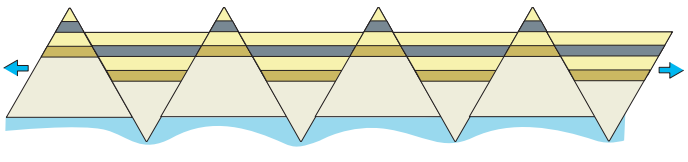

Figure 17.5 The alternative to domino-style stretching is the development of horst-graben systems. This deformation style is, ideally, symmetric and an overall pure shear strain.

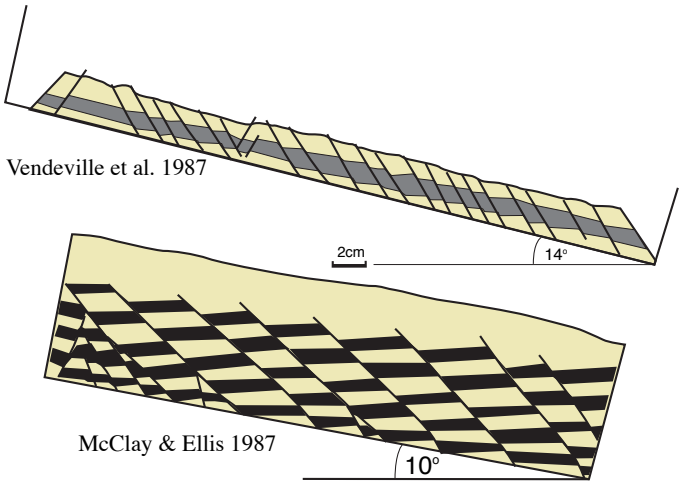

Figure 17.6 Sandbox experiments where the base of the model is tilted prior to extension. The tilting may be the cause for the uniform dip and dip direction of the faults.

strength of the rocks and of the mechanical properties of the faults. For realistic values it can be shown that new faults are expected after 20-45° rotation. The new faults will cut the old ones and rotate the rocks further, while the old faults are inactivated. Examples that this model actually works are reported from areas of high crustal extension, such as in the Basin and Range province in the western USA.

1.7 Low-angle faults and core complexes

Low-angle faults were originally mapped in fold and thrust belts only, and with few exceptions normal faults were considered to be high-angle structures, typically with dips around 60°. Field mapping in the Basin and Range province in the 1970´s, and later in many other parts of the world, revealed the fact that extensional low-angle faults are fairly common (Fig. 17.7). Seismic images have strengthened this view, as have numerical and physical modeling.

1.7.1 The problem with low-angle normal faults

Low-angle extensional faults represent a mechanical challenge. In the general case where σ_1 is vertical, the formation of such faults would be mechanically infeasible for ordinary rock types. The unlikely reactivation of preexisting low-angle faults in the upper crust, combined with the observation that few low-angle faults are seismically active, calls for alternative explanation. The most natural explanation is that low-angle faults are rotated normal faults with

THE GULLFAKS DOMINO SYSTEM

The North Sea Gullfaks oil field consists of a domino system limited by a eastern horst complex. The domino system consists of 4-6 main blocks, each subdivided by smaller faults. Well data show that a large number of subseismic faults and fault-related structures exists, including a large population of deformation bands. Furthermore, the dipping layering shows a systematic westward decrease in dip within each block. Therefore, a perfect rigid domino model does not work. If the blocks are backrotated rigidly so that the layering becomes horizontal on average, the faults only obtain a 45° dip. This is lower than the ~60 ° fault dip expected from the mechanical considerations in Chapter 6. The discrepancy can be explained by internal fault block strain.

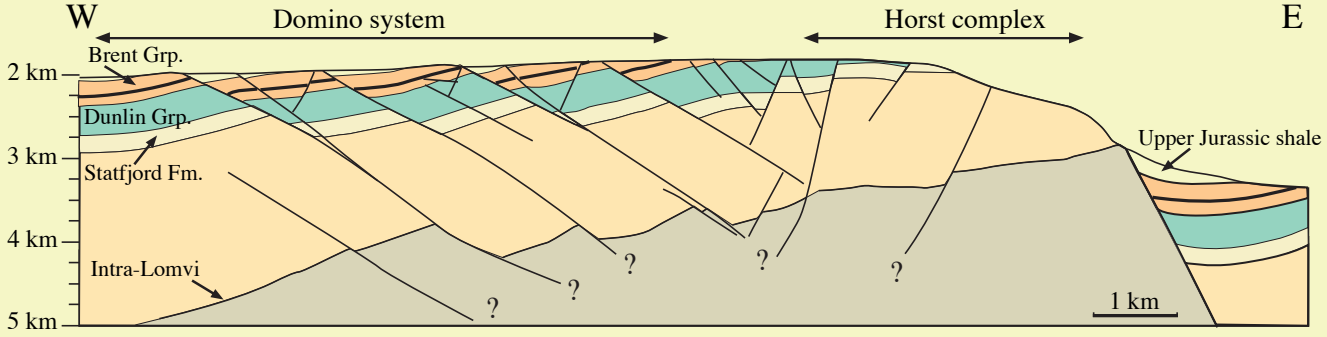

steeper initial dips.

1.7.2 Rotated normal faults

The model that gained popularity towards the end of the 1980's involves extension at the scale of the entire crust. The isostatic effects of extension require that base of the model is mobile – a parameter that is unaccounted for in physical experiments where the base of the model is fixed.

Figure 17.8 illustrates the principle of the model. A listric normal fault forms in the upper crust, flattening along a weak zone near the brittle-plastic transition. The hanging wall to the weak zone or detachment is sometimes referred to as the *upper plate*, while the footwall is the *lower plate*. After a certain amount of extension a new fault forms in the hanging wall, while the first fault is inactivated. Inactivation is partly due

Figure 17.7 The low-angle fault underneath the Hornelen Devonian basin in the Scandinavian Caledonides separates Devonian sandstones and conglomerates from mylonitic rocks of the Nordfjord-Sogn Detachment. Photo: Vegard V. Vetti.

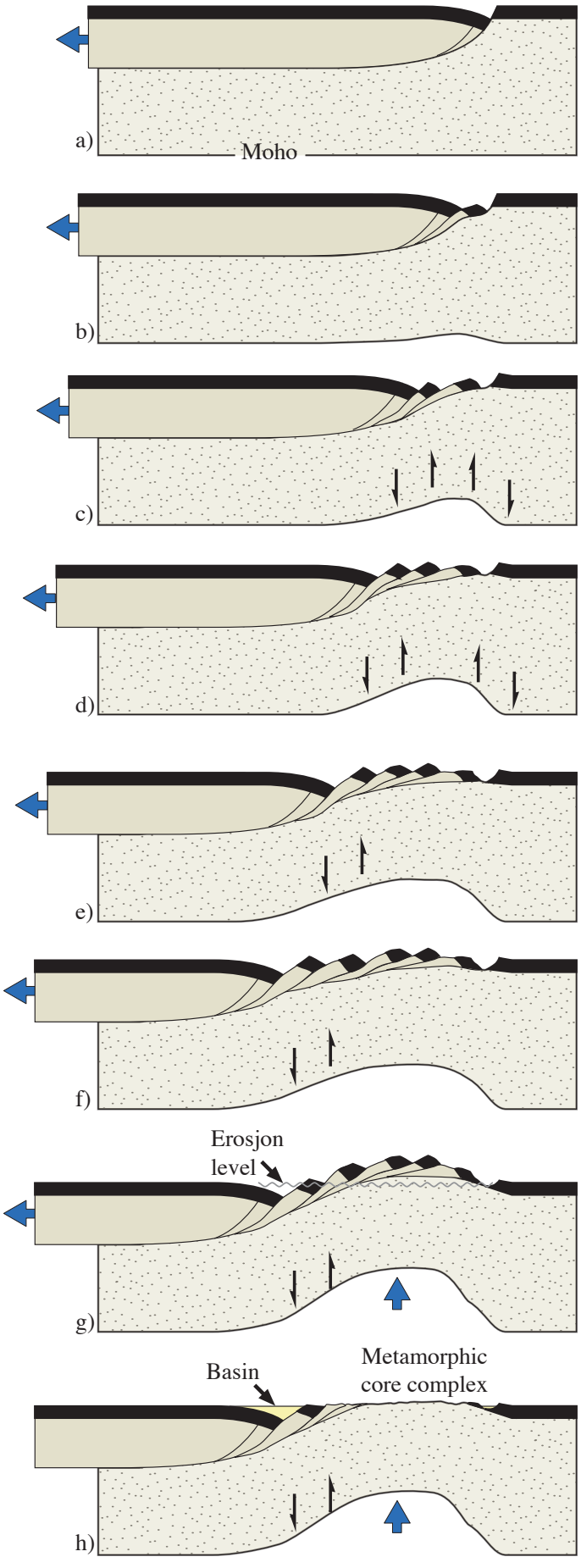

to isostatic uplift of the thinned portion of the crust. This uplift rotates the original fault to the point where it gets mechanically favorable to create a new fault in the hanging wall. This process repeats itself until a series of rotated domino-style blocks and related half grabens are established. In this model, the steepest fault will be the youngest and active fault (compare geometry of these with horses in a thrust duplex).

Note that these domino-style fault blocks are different than those of the classical domino model because they develop at different times. The model is thus an example of how a domino-style fault block array can arise by a process that does not comply with the ideal domino model.

1.7.3 Rolling hinges and metamorphic core complexes

The model shown in Figure 17.8 involves simple shear deformation of the lower and middle crust. During this deformation, the upper crust is thinned and Moho is elevated. Erosion of the uplifted fault complex in the upper plate adds to this effect and eventually leads to exposure of lower plate rocks. The deformation in the upper plate is brittle, but the shearing along the horizontal detachment is initially plastic. However, this deformation takes on a more brittle character as the detachment is uplifted. Eventually, when the detachment is exposed it will appear as a core of metamorphic and mylonitic rocks overprinted by brittle structures in a window through upper plate rocks (Figure 17.8h). The lower plate rocks in this window are referred to as a *metamorphic core complex* and such core complexes were first mapped and described in the Basin and Range region in Arizona and Nevada. Similar complexes have been found in many other parts of the world, including the Alps and the Scandinavian Caledonides (Figure 17.9).

A closer look at Figure 17.8 reveals that the vertical shear on the footwall (right) side of the figure gradually ceases. The oppositely directed shear on the hanging-wall side remains active underneath the active part of the fault system, moving in the hanging-wall direction. If we consider the crustal flexure as a fold, then the hinge zone is seen to move or roll in the hanging-wall direction during the course of the extensional development. This effect has led to the name the *rolling hinge model*.

Figure 17.8 Development of a metamorphic core complex during crustal-scale extension and isostatic compensation. Note how new wedge-shaped fault blocks successively get torn off the hanging wall. Also note how isostatic compensation is accommodated by means of vertical shear. Based on Wernicke and Axen (1988).

THE MAGNET HIGH

Magnet High is the name given to a rotated fault block in the northernmost part of the North Sea. The elevated crest collapsed in the latest Jurassic, and the faults seem to have been deformed into a ramp-flat-ramp geometry. This situation reflects the early stage of the development of a metamorphic core complex, as shown in Figure 17.8.

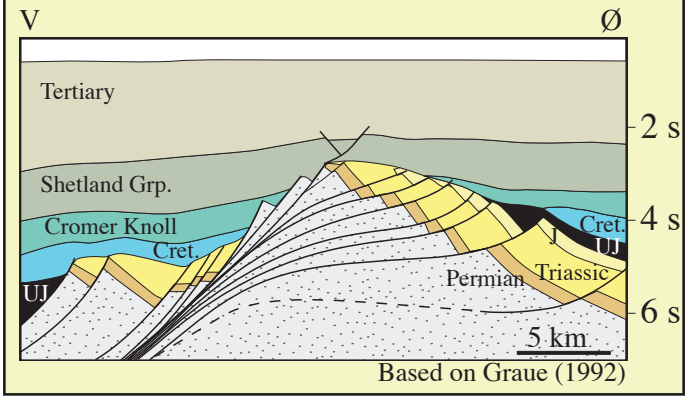

1.7.4 Direct formation of low-angle faults

While models involving rotation of high-angle normal faults to low-angle extensional faults are popular, some low-angle extensional faults form with low initial dips. A characteristic feature of such faults is that they cut high-angle faults, contrary to what the models in Figures 17.8 and 17.4 show. This type of extensional faulting has been produced in experimental work, as shown in Figure 17.10.

There must of course be a reason for a low-angle fault to take over the extension. Such a reason could perhaps be that the high-angle faults lock up, but it is more likely to be caused by a subhorizontal zone of weakness. In undeformed sedimentary sequences overpressured shales or evaporite layers represent anomalously weak layers along which an extensional fault may flatten. In previously deformed rocks, preexisting faults or shear zone may create the anisotropy that causes the formation of a low-angle extensional fault. Thrust faults are low-angle structures that commonly are reactivated under extension, for instance when the stress conditions change at the end of an orogeny. In fact, it seems to be the rule rather than the exception that orogenic belts contain low-angle normal faults or extensional shear zones that have formed by reactivation of thrusts.

1.8 Ramp-flat-ramp geometries

We have already seen how extensional faults can have a listric geometry. Another geometry that is particularly common for large-scale extensional faults is the combination of two ramps linked by a subhorizontal segment. Such *ramp-flat-ramp geometries* generate extensive hanging-wall strain because the hanging wall must adjust to the fault geometry during fault movements.

A series of wedge-shaped fault blocks may develop above the ramp-flat-ramp fault, where the faults either die out upward or reach the surface (see the hanging wall to fault 6 in Figure 17.11 and Figure

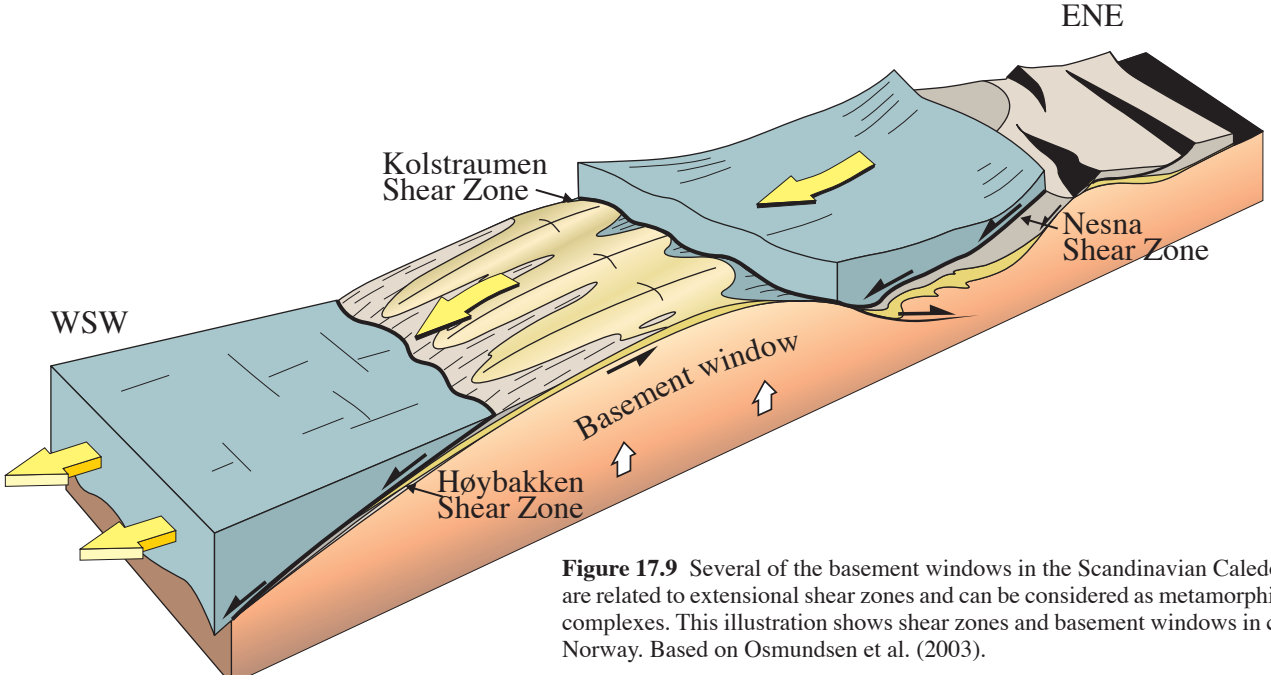

Figure 17.9 Several of the basement windows in the Scandinavian Caledonides are related to extensional shear zones and can be considered as metamorphic core complexes. This illustration shows shear zones and basement windows in central Norway. Based on Osmundsen et al. (2003).

17.12). A series of such faults or fault blocks are called an extensional *imbrication zone*, similar to the use of the term in the contractional regime. A related type of extensional structure is a series of lenses that together form an extensional *duplex*. Extensional duplexes have floor- and roof faults similar to contractional duplexes.

A horst complex is commonly seen to develop

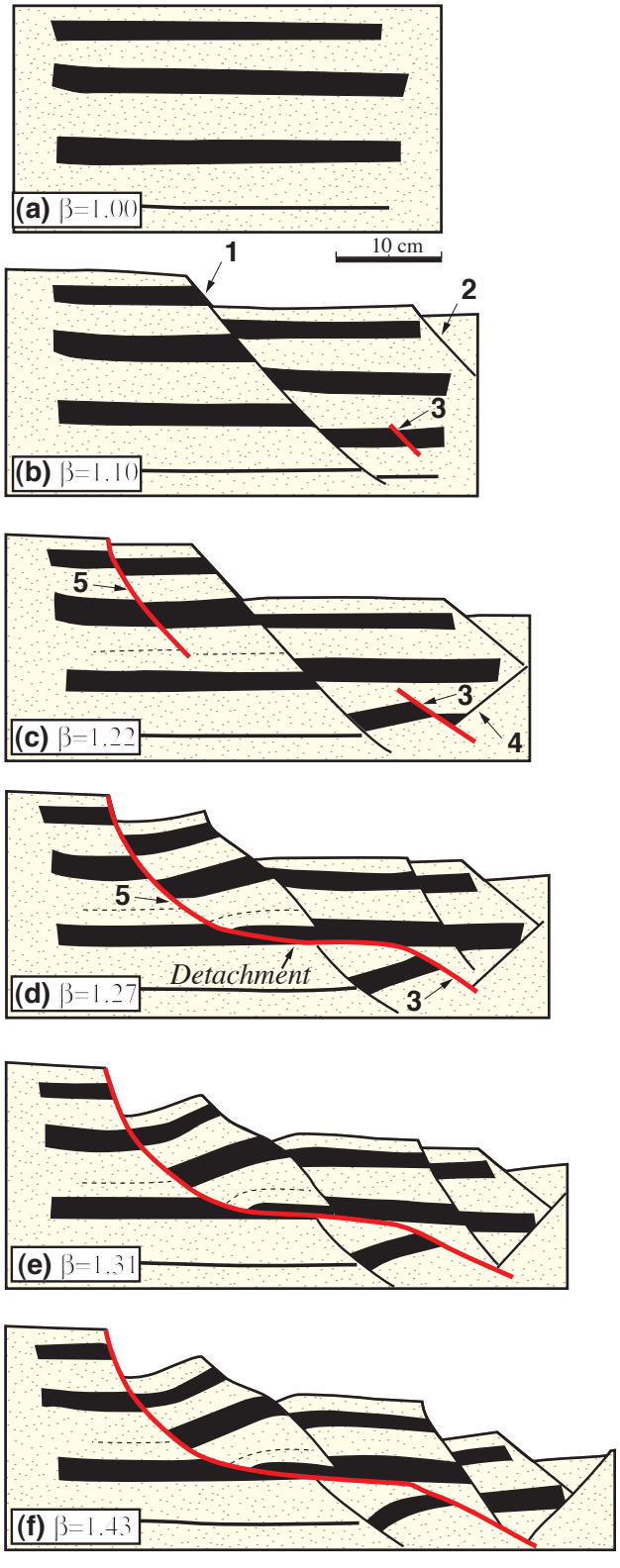

Figure 17.10 Plaster experiment showing how a low-angle fault can form at a relatively late stage during an extensional deformation history. Note that the late fault (red) cuts preexisting high-angle faults and that a horst is about to establish above the flat fault segment. From Fossen et al. (2000).

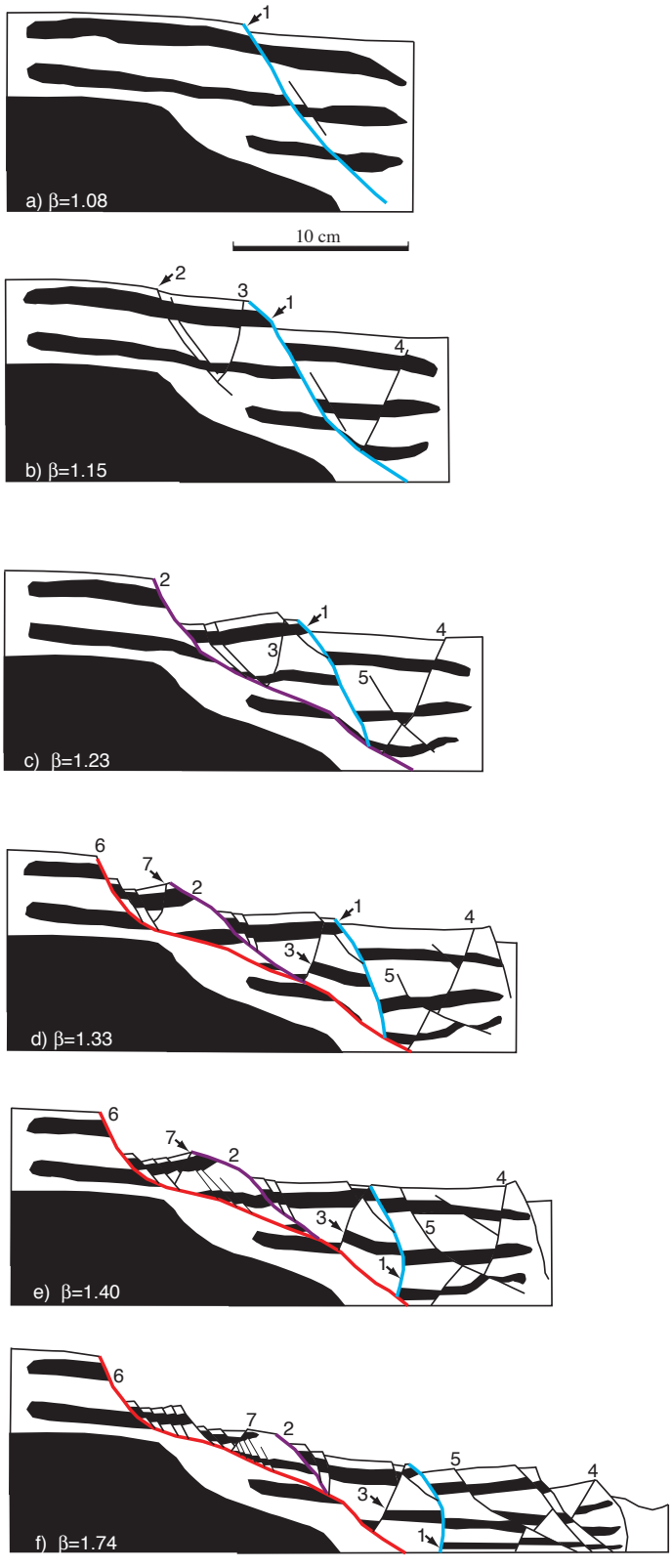

Figure 17.11 Footwall collapse as seen in a plaster experiment. Note how new faults sequentially form in the footwall at the same time as the dip of the controlling fault is reduced.

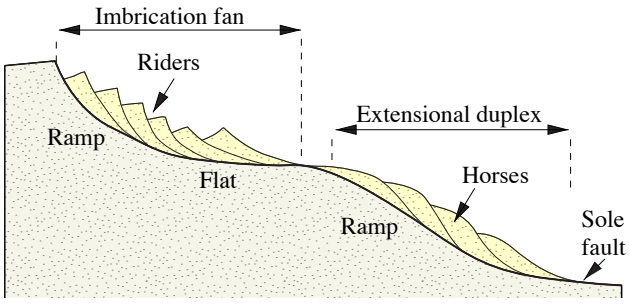

Figure 17.12 Extensional imbrication and duplex structures. The hanging wall is not drawn. Conceptual diagram based on Gibbs (1984).

above the flat in experiments (Figure 17.11) and in rift systems such as the North Sea (box – the Gullfaks system). Domino-style fault arrays commonly develop behind the horst as the footwall collapses. In Figure 17.11 the development of a horst complex is repeated. The first horst is defined by faults 1 and 3, and the second by faults 2 and 7.

1.9 Footwall collapse

Footwall collapse is the process where new faults successively form in the footwall, as seen in Figure 17.11. After the formation of fault 1 a new synthetic fault (2) forms in its footwall. At a later stage fault 6 forms farther into the footwall, and the result is a complex fault array in the hanging wall to the youngest of the main faults, i.e. fault 6. Footwall collapse is common where huge fault blocks form and rotate in rift systems, and the elevated crests of these blocks collapse under the influence of gravity and tectonic forces. In some cases gravity itself causes gravitational collapse of the footwall. Slumping on curved fault surfaces results, creating complex stratigraphical relationships that are a challenge in petroleum exploitation (Figure Statfjord Field?).

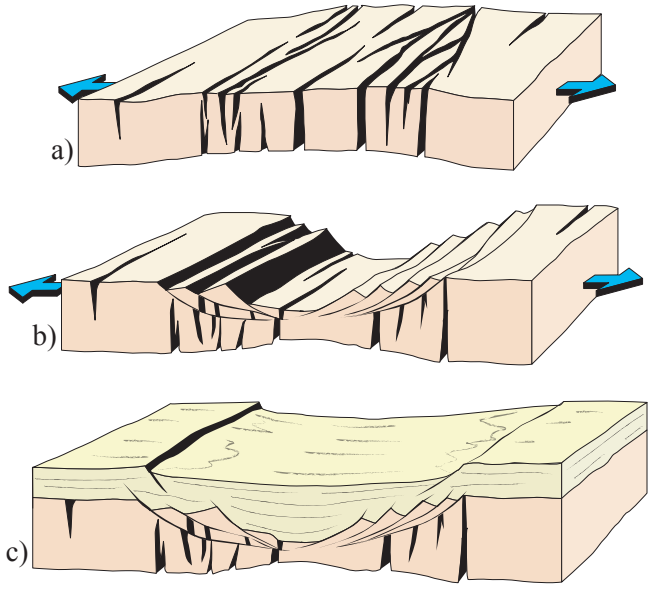

Figure 17.13 Three stages in rift development. a) Early tension creating or rejuvenating deep-going fractures. Strain is low at this stage. Magma locally fills the deep fractures. b) The stretching phase, during which major fault complexes and arrays form. c) Post-rift subsidence and sedimentation. Based on Gabrielsen (1986).

1.10 Rifting

A rift forms where the crust is pulled apart by tectonic forces. There can be several factors leading to the formation of a rift, and two end-member models are known as the active and passive rifting models. In the *active model*, the rift is generated by a rising hot mantle material or *plumes* in the asthenospheric mantle. The result is a rift dominated by magmatism and not necessarily so much extension. In the *passive model*, the rift forms because of tension generated by extensional plate-tectonic movements. Passive rifts tend to form along zones of inherited weakness in the lithosphere, such as reactivated contractional structures from former orogenic zones.

Many natural rifts tend to contain components of both of these models. In a somewhat simplified case, initial rifting may result from large-scale doming of the crust (Figure 17.13a). Steep fracture systems form at this stage, and may reach deep enough to promote magma generation and intrusion form the mantle. The following and main stage is the stretching stage, where the crust is vertically thinned and laterally extended (Figure 17.13b). Major faults and fault blocks form during this stage. Once stretching has come to a halt, the final subsidence stage is reached (Figure 17.13c). The crust cools, the basement is deepened and postrift sediments are deposited. Faults are mostly limited to those formed by differential compaction.

The extensional development of a rift is reflected by its sedimentary record. The *prerift* sequence is the sedimentary package deposited prior to extension. The syn-rift sequence are constituted of sediments deposited during the rifting. *Synrift* sediments show thickness and facies variations across growth faults, and hanging-wall thickening and footwall thinning or non-deposition is characteristic. The *post-rift* sequence is controlled by the geometry of fault blocks and subsidence after cessation of extension.

1.11 Half-grabens and accommodation

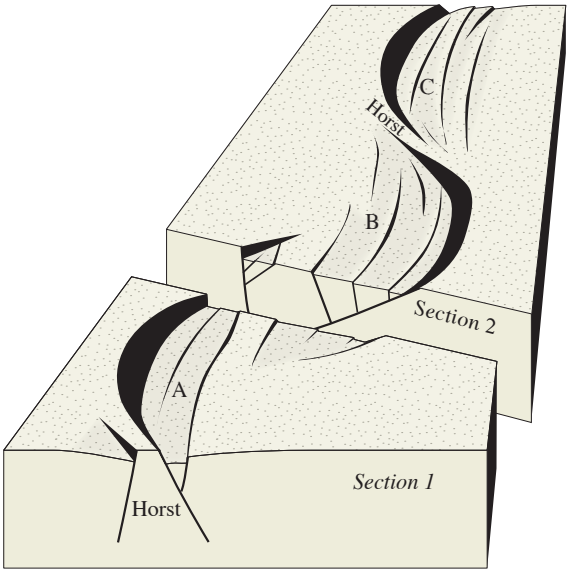

Figure 17.14 Rift system with differently dipping master faults. This type of rift is composed of interfering and overlapping half-grabens. The overlaps were called accommodation zones by Rosendahl and coworkers in the 1980's, based on observations from the East African Rift. Different types of half-graben arrangement occur. Accommodation zones may contain horsts (section 1) or grabens (section 2).

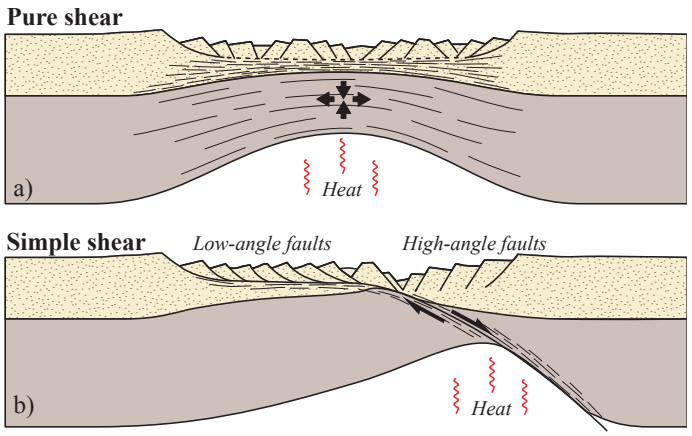

Figure 17.15 Two idealized models for crustal extension and rifting. The pure shear model is symmetric, with maximum heat underneath the middle of the rift. The simple shear model is dominated by a generally low-angle shear zone that produces an asymmetry on the rift.

zones

A feature of rift systems that was first explored in the East-African rift system in the Lake Tanganikya area is the development of a rift from a series of oppositely dipping half grabens. Each half-graben has a curved, half-moon shaped geometry and where one ends another, typically oppositely dipping graben, takes over. Depending on the arrangement of the grabens and secondary faults in their hanging walls, basinal highs (horsts) or lows (grabens) may form (Figure 7.14). The term accommodation zone is sometimes used specifically for this type of half-graben overlap structure.

1.12 Pure and simple shear models

Crustal stretching in rift zones is sometimes discussed in terms of the pure shear and simple shear models (Figures 17.15 and 17.16). The pure shear model is also called the McKenzie model, and the simple shear model is sometimes referred to as the Wernicke model, named after the authors who published the respective models in the 1970's and 80's. In the *pure shear model*, which is the older of the two, the total contribution of individual faults in the rift creates a symmetric thinning of the crust. The overall strain is pure shear, and horizontal extension is balanced by vertical thinning. The lower crust is thinned by plastic deformation mechanisms, while the upper crust deforms by brittle faulting.

While the pure shear model is overall symmetric by nature, the *simple shear model* results in an asymmetric rift. The term simple shear is used because this model is controlled by a dipping detachment fault or shear zone that transects the crust and possibly the entire lithosphere. This detachment involves a localized shear strain that is significant enough that the model is referred to as the simple shear model. The two sides of a rift controlled by a dipping detachment are geometrically different, as is the thermal structure. In the pure shear model the highest temperature gradient is found underneath the middle of the basin, while it is typically offset in the simple shear model. This has consequences for uplift and subsidence patterns, and different variations of the simple shear model yield different results.

1.13 Stretching estimates, fractals and power law relations

The amount of extension or stretching across a rift can be found in several different ways. Geologic profiles based on deep seismic profiles showing the thinning of the crust can be used. If area conservation is assumed, i.e. no material transport in or out of the section and no assimilation of crustal material by the mantle, then restoring the section to the point where the crustal thickness is constant and equal to that of the present rift margins gives an estimate of the extension.

A purely structural method of estimating the amount of extension is the summing of fault heaves along a reference horizon across the rift. If block

rotation is modest, the sum should equal the extension along the section. There is, however, typically a mismatch between the strain estimate obtained from summing fault heaves and that calculated from area balancing. In all cases the sum of heaves gives lower stretching estimates. In some cases the two estimates differ by a factor of two. Why this discrepancy?

One possibility is that the lower part of the rifted crust may be assimilated by the mantle. Hence, the assumption of area conservation does not hold and extension is overestimated. The fault displacement model may be flawed by the fact that subseismic faults and ductile deformation structures, or structures that are too small to appear on the geologic section from which fault heaves are summed, are ignored. So how do we correct for the contribution of subseismic faults?

It may sound like faults that are too small to appear on a seismic line or geologic section would not make much of a difference anyway. However, if the number of small faults is large, they may sum up to a significant amount of extension. This was explored in the 1980's and 1990's, and it was then realized that the distribution of fault offsets (or heaves) in many fault populations varies systematically according to a power law relation. The method is to collect fault displacement data from seismic lines, geologic maps and outcrops, and plot them in cumulative plots with logarithmic axes. Fault offset is measured along a chosen horizon on parallel seismic lines or geologic profiles and sorted on a spreadsheet. The offset values are then plotted along the horizontal axis and the cumulative number along the vertical axis. In practice, this means plotting the largest offset first with cumulative number 1, the second largest offset with cumulative number 2 and so on. Alternatively, the cumulative number per kilometer can be plotted along the vertical axis. In the latter case, the frequency is portrayed, i.e. how frequent faults with a given offset statistically occur in the given profile direction.

Several cumulative fault offset plots show

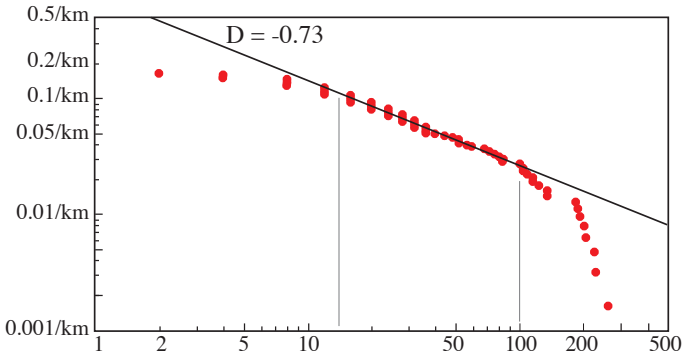

Figure 17.17 Log-log plot of fault displacement against cumulative number (normalized against length). The data define a fairly straight line in the central part. Undersampling of small and large faults explains the deviationfrom the straight line at each end. Data from the Gullfaks Field. From Fossen & Rørnes (1996).

a straight segment, which implies a power law distribution. A power law or self-similar relation implies that the data plot along a straight line in the log-log diagram. Mathematically this can be described by the expression

$$N = aS^{-D} \quad (17.1)$$

where S is displacement, throw or heave, N is the cumulative number of fault offsets and a is a constant. The exponent D describes the fractal dimension or slope of the straight line. Since we are working in log-log space it makes sense to rewrite the expression as

$$\log N = \log a - D \log S \quad (17.2)$$

which is the equation for a straight line with slope –D. The exponent D describes the relation between the number of small and large offsets. A large D value implies that there is a large number of small faults for each large fault. Hence, the larger the D-value, the more strain is accumulated by small faults, and

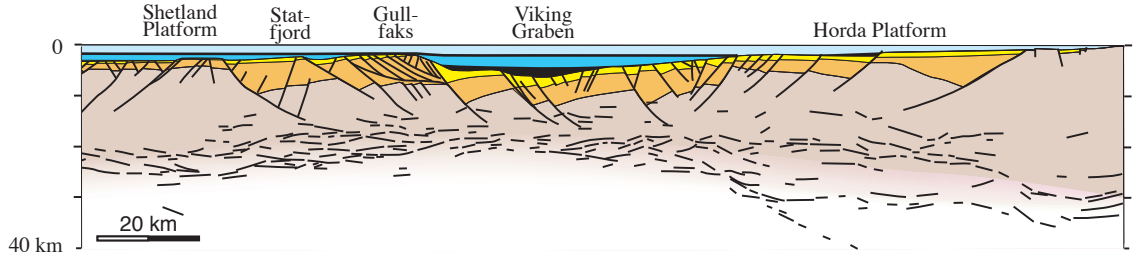

Figure 17.16 Section based on a deep seismic line across the northern North Sea. This section has been interpreted in terms of pure shear as well and simple shear and may be considered to contain elements of both models. Based on Odinsen et al. (2000).

FRACTALS AND SELF-SIMILARITY

A fractal is a geometric form that can be divided into smaller parts where each part has a form corresponding to the larger one. Fractals are called self-similar, meaning that one or more of their properties repeat at different scales. This goes for many properties of geological structures, such as faults and folds, although they may not be fractal as a whole. For example, large folds may consist of lower-order folds with corresponding shape, which again may consist of yet smaller folds of the same shape. Or a fracture set as seen from a satellite image may look like a field observation or thin-section fracture pattern from the same area. They will not be identical, but at some scales (e.g. 100 km above the surface, at the surface and under the microscope) they may look similar. This is why a scale often needs to be added to pictures of geological structures.

Special properties or sizes of fracture polulations are usually considered. In one dimension the fault offset is such a size. If the distribution of offset values from a fault population defines a straight line in a log-log plot, as shown in Figure 17.17, then the offsets are *self similar*. This means that for a randomly chosen fault offset there is always a fixed number of faults with 1/10th of the chosen offset. So, for each fault with 1 km displacement there will be, for example, 100 faults with 100 m offset. For each fault with 100 m offset there will be 100 faults with 10 m offset and so on. The relation is described by the exponent D (Equation 17.2). In two and three dimensions self-similarity and fractal dimensions can be applied to fault length and other geometrical aspects of faults. Fractal theory has many applications in geology and it is useful to know its mathematical basis and geological applications.

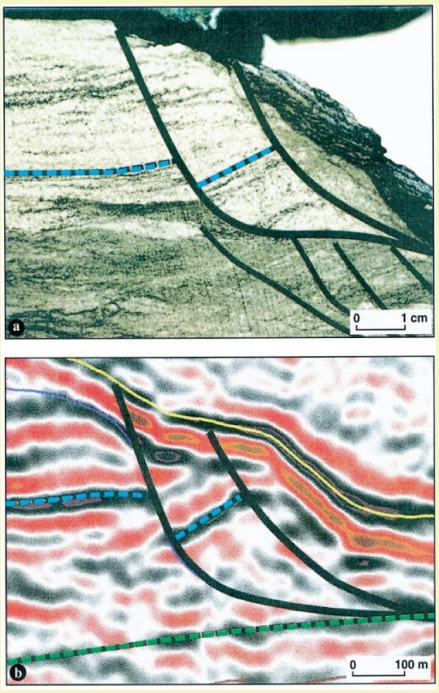

Structures on a) cm-scale (core) and b) 100 m scale, both from the North Sea Statfjord Field. The two structures look very similar and illustrate the concept of self-similarity as applied to fault geometry. From Hesthammer & Fossen (1999).

the larger the error involved in extension estimates where small faults are left out. Common D-values are 0.6-0.8.

Real data seldom define a perfectly straight line in cumulative log-log diagrams. However, a central straight segment is sometimes found (Figure 17.17), with curved segments at each end. The truncation is caused by underrepresentation of faults with very small offsets (the problem of resolution) and underrepresentation of faults with large offsets (the profiles do not always intersect the largest faults). The straight segment can be extended to small fault offsets (upwards to the left in Figure 17.17), but at some point this relation is bound to break down. This could occur as discrete deformation is accumulated by deformation bands rather than faults, or when approaching the grain size of the deformed rock.

Mesozoic extension across the northern North Sea rift is estimated to almost 100 km by balancing the crustal area (crustal thinning). Summing fault heaves

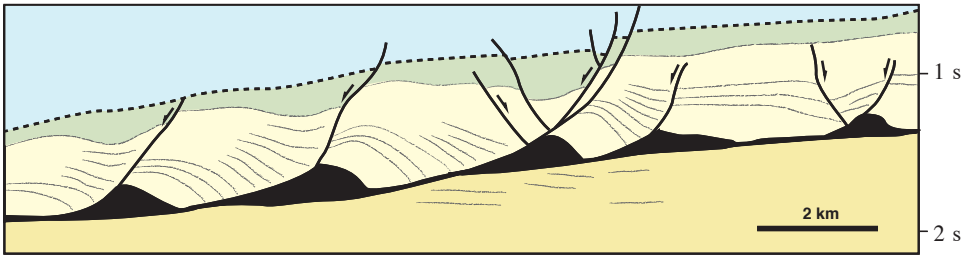

Figure 17.18 Gravity-driven syn-sedimentary extension above a low-angle detachment in the Kwanza Basin on the passive West African continental margin (Angola). Fault blocks are sliding on a thin and weak salt layer and are therefore detached from the substrata. The salt is flowing plastically and accommodates area problems caused by the fault block rotation. Modified from Duval et al. (1992).

from regional seismic line interpretations indicate an extension of about 50 km. It has been shown that much, if not all, of this difference can be accounted for by subseismic faults, if the power law relation can be extrapolated down to small subseismic faults.

1.14 Passive margins and oceanic rifts

If a continental rift is extended far enough, the crust will break and be replaced by oceanic crust. A *passive margin* then occurs on each side of the rift, which is now located in oceanic crust. In the Viking Graben in the northern North Sea, stretching related to the late Jurassic-early Cretaceous rift phase is around 150% (β=1.5). Stretching beyond 1.5 would result in initial magmatism and volcanism, and close interaction between faulting and magmatism until oceanic crust initiates (at a stretching factor around 3).

Little seismic activity occurs in passive margins. Fault movement is mostly gravity driven, resulting not only in slumping but also large-scale extensional fault systems soled on weak layers of salt or clay (Figure 17.18).

While passive continental margins gradually subside and become covered by clastic sediments, tectonic activity along the oceanic rift is very common. One of the main differences between continental and oceanic rifts is the much more extensive addition of magma in the latter. Hot magma and thin crust cause the rift to be a positive (elevated) structure with a deeper central graben. The potential energy represented by the relatively high rift elevation is partially released by means of listric normal faults that dip away from the rift axis. Low-angle detachments with normal sense of movement are described from mid-oceanic ridges, together with metamorphic core complexes that are geometrically and kinematically similar to those found in areas of continental extension. However, our knowledge of the structural geology along oceanic ridges is hampered by their inaccessibility, but new accumulation of high-quality deep-ocean data, both direct observational and indirect ocean bottom seismometer, is giving new information of the structural processes along oceanic ridges.

1.15 Orogenic extension and orogenic collapse

Extension is by no means limited to rift zones and passive margins. Impressive extensional faults and shear zones are common in active mountain belts

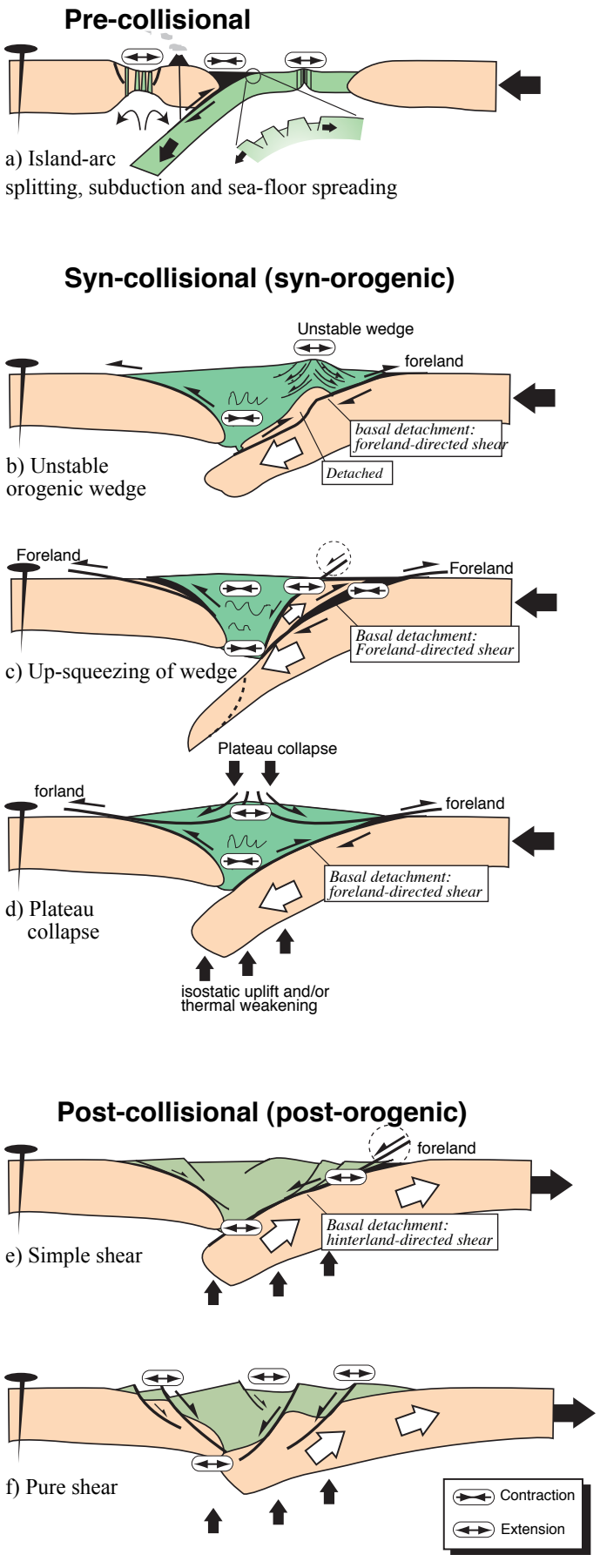

Figure 17.19 Different types of extension connected with an orogenic cycle. Modified from Fossen (2000).

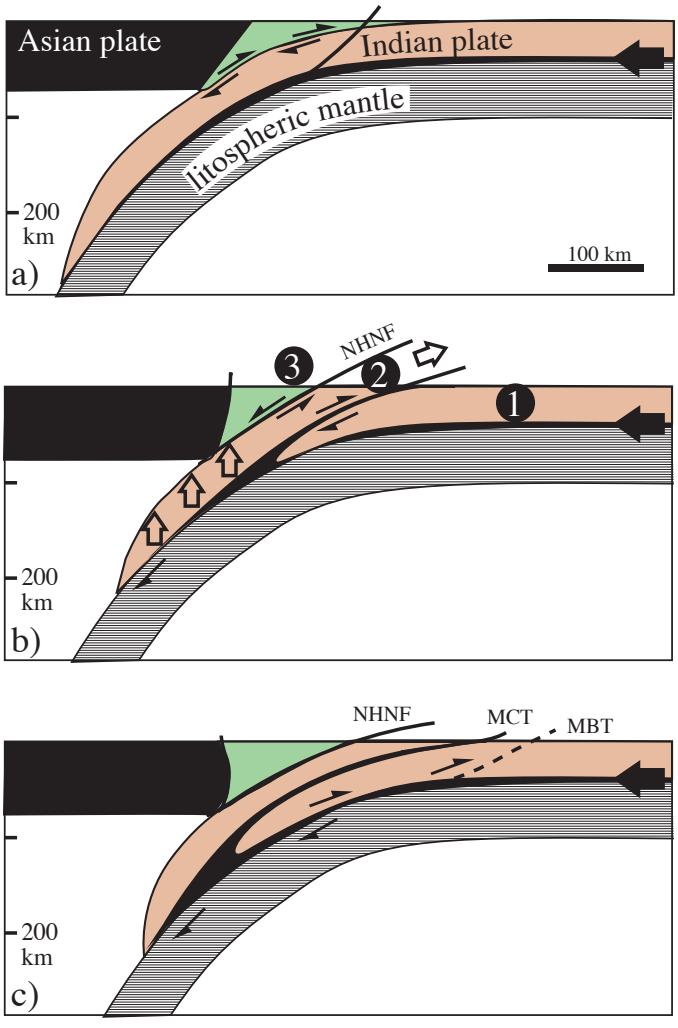

Figure 17.20 Model of the formation of a major normal fault (NHNF) in the Himalayan orogen. A slice of the continental crust is detached and uplifted by a combination of compression and bouyancy. The slice (2) is underlain by a thrust and overlain by a normal fault. Based on physical modelling by Chemenda (1995). NHNF=North Himalaya Normal Fault, MCT=Main Central Thrust, MBT=Main Boundary Thrust.

and in orogenic zones where plate convergence has ceased.

Orogeny is one of several stages in the Wilson cycle. In other words, orogenic belts are often built on older divergent plate boundaries or rifts, and they typically rift again at a later stage. In the early stages of a typical orogenic cycle where an ocean exists between two converging continents, back-arc rifting is the common extensional component (Figure 17.19a). Stretching also occurs in the upper part of the oceanic crust where it enters the subduction zone under the island arc. This stretching is a large-scale example of outer arc extension of buckled layers discussed in Chapter 11.

Later, as the continents collide, extensional faults and shear zones may form in the orogenic wedge where the wedge becomes unstable, as discussed in the previous chapter. If a large basement slice is incorporated, the wedge thickens excessively and responds to this instability by creating normal faults or shear zones (Figure 17.19b). Applied to the active Himalayan orogen, a model describes the detached basement slice as relatively low density, so that it may rise bouyantly with the formation of a thrust fault on its lower side and a normal fault on its upper side (Figure 17.19c). A wedge-shaped slice in a contractional regime can also contribute to its ascent. Figure 17.20 outlines this model in greater detail.

A third model for synconvergent extension examines changes in the thermal structure of the lower crust and the lithospheric mantle. During a continent-continent collision crustal material is subducted and heated. Heating weakens the crust, potentially to the point where it collapses under its own weight along extensional faults and shear zones (Figure 17.19d).

Even though the subducting lithospheric plate is gradually warmed up, it will remain cooler than the surrounding lithospheric mantle for a significant time interval. Cooler and denser lithosphere may detach and sink into the underlying mantle. This process may be aided by the transformation of minerals to phases with denser molecular structures, particularly the

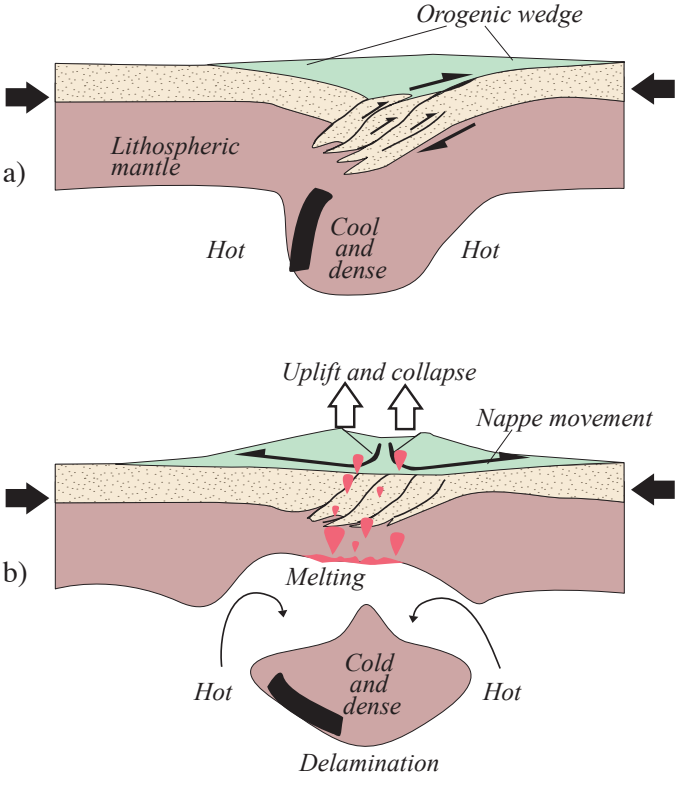

Figure 17.21 The delamination model for synorogenic collapse of orogens. The cold and dense root sinks into the mantle, causing uplift of the lithosphere and high-level transport of rocks from the hinterland towards the foreland. Extension is limited to the upper part of the crust, and the sense of shear on the basal thrust is toward the foreland. Based on Fossen (1993).

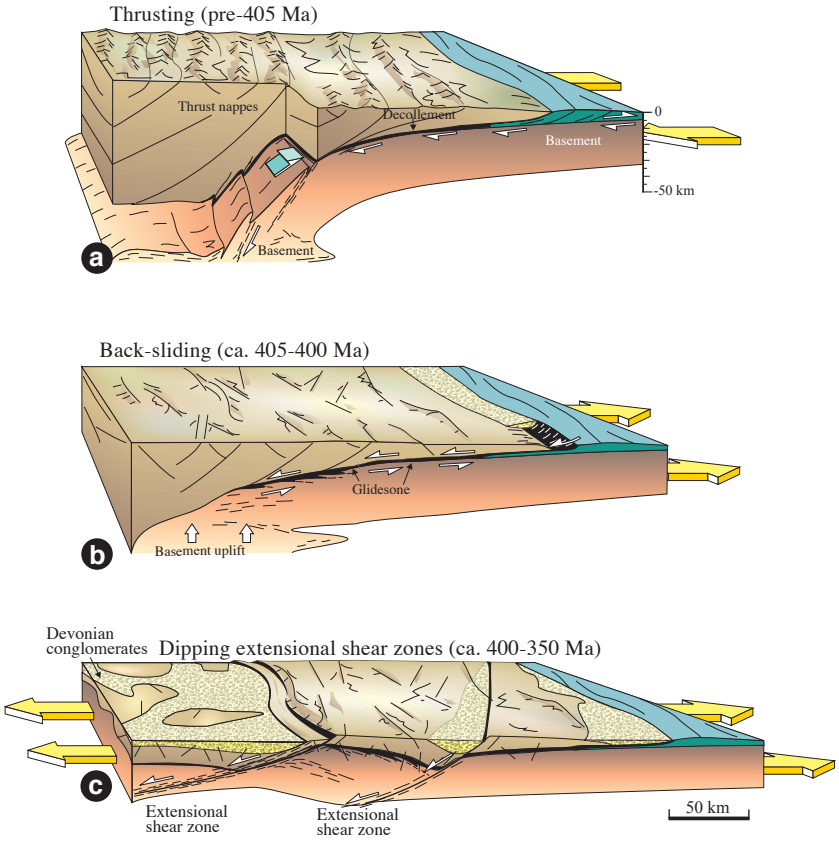

Figure 17.22 The development of low-angle extensional faults and shear zones in the southern Scandinaviann Caledonides. a) Emplacement of nappes during plate convergence. b) Back-sliding of the orogenic wedge, causing reversal of the sense of shear along the basal detachment. c) Formation of hinterland-dipping shear zones and faults that cut both the thrusts and the basement. Based on Fossen (2000).

transformation of mafic rocks to eclogite. Detachment results in orogenic uplift (Figure 17.19d), and the likelihood of orogenic collapse becomes significant. This model is called the *delamination model* (Figure 17.21) and results in more rapid heating of the orogenic root, partial melting and increased magmatic activity.

1.16 Postorogenic extension

Throughout the divergent history of an orogenic belt, the sense of movement on the basal thrust is always toward the foreland. Once the sense of shear is reversed and the orogenic wedge moves towards the center of the collision zone, the orogen kinematically enters the divergent or postorogenic stage. At this stage extensional deformation dominates at all crustal levels. One mode of postorogenic extensional deformation involves reversal of the basal thrust and higher-level thrusts within the orogenic wedge (Figures 17.19e and 22b). Such reactivation of basal thrust zones can cause the formation of metamorphic core complexes, as described in the previous chapter.

A second mode of extension is the formation of hinterland-dipping shear zones cutting through the crust. This occurs after the hinterland has been uplifted due to tectonic thinning and erosion, making continued shearing along the basal detachment less favorable. Instead, new hinterland-dipping shear zones and faults develop (Figures 17.19f and 22c). These shear zones typically affect the entire crust and transect and further rotate the reversed basal thrust. Well-developed examples of such structures have been interpreted in the Scandinavian Caledonides.

Further reading:

Jackson, J. & McKenzie, D., 1983. The geometrical evolution of normal fault systems. Journal of Structural Geology, 5: 472-483.

Wernicke, B. & Burchfiel, B.C., 1982. Modes of

extensional tectonics. Journal of Structural Geology, 4: 105-115.

Orogenic collapse and extension

Andersen, T.B., Jamtveit, B., Dewey, J.F. & Swensson, E., 1991. Subduction and eduction of continental crust: major mechanisms during continent-continent collision and orogenic extensional collapse, a model based on the Norwegian Caledonides. Terra Nova, 3: 303-310.

Braathen, A. et al., 2000. Devonian, orogen-parallel, opposed extension in the Central Norwegian Caledonides. Geology, 28: 615-618.

Dewey, J.F., 1987. Extensional collapse of orogens. Tectonics, 7: 1123-1139.

England, P.C. & Houseman, G.A., 1988. The mechanics of the Tibetan plateau. Royal Soc. Lond. Phil. Trans., 326, series A: 301-320.

Fossen, H. & Rykkelid, E., 1992. Postcollisional extension of the Caledonide orogen in Scandinavia: structural expressions and tectonic significance. Geology, 20: 737-740.

Hartz, E. & Andresen, A., 1995. Caledonian sole thrust of central East Greenland: a crustal-scale Devonian extensional detachment? Geology, 23: 637-640.

Houseman, G. & England, P., 1986. A dynamical model of lithosphere extension and sedimentary basin formation. Journal of Geophysical Research, 91(B1): 719-729.

Wheeler, J. & Butler, R.W.H., 1994. Criteria for identifying structures related to true crustal extension in orogens. Journal of Structural Geology, 16: 1023-1027.

Rotated normal faults and metamorphic core complexes

Brun, J.P. & Choukroune, P., 1983. Normal faulting, block tilting, and décollement in a stretched crust. Tectonics, 2: 345-356.

Buck, W.R., 1988. Flexural rotation of normal faults. Tectonics, 7: 959-973.

Davis, G.H., 1983. Shear-zone model for the origin of metamorphic core complexes. Geology, 11: 342-347.

Fletcher, J.M., Bartley, J.M., Martin, M.W., Glazner, A.F. & Walker, J.D., 1995. Large-magnitude continental extension: an example from the central Mojave metamorphic core complex. Geological Society of America Bulletin, 107: 1468-1483.

Lister, G.S. & Davis, G.A., 1989. The origin of metamorphic core complexes and detachment faults formed during Tertiary continental extension in the northern Colorado river region, U.S.A. Journal of Structural Geology, 11: 65-94.

Malavieille, J. & Taboada, A., 1991. Kinematic model for postorogenic Basin and Range extension. Geology, 19: 555-558.

Nur, A., Ron, H. & Scotti, O., 1986. Fault mechanics and the kinematics of block rotations. Geology, 14: 746-749.

Scott, R.J. & Lister, G.S., 1992. Detachment faults: Evidence for a low-angle origin. Geology, 20: 833-836.

Wernicke, B. & Axen, G.J., 1988. On the role of isostasy in the evolution of normal fault systems. Geology, 16: 848-851.

Wernicke, B., 1985. Uniform-sense normal simple shear of the continental lithosphere. Canadian Journal of Earth Sciences., 22: 108-125.

Extensional faults in overall contractional regimes

Burchfiel, B.C. et al., 1992. The south Tibetan detachment system, Himalayan orogen: extension contemporaneous with and parallel to shortening in a collisional mountain belt. Geological Society of America Special Paper, 269: 48 ss.

Platt, J.P., 1986. Dynamics of orogenic wedges and the uplift of high-pressure metamorphic rocks. Geological Society of America Bulletin, 97: 1037-1053.

Rift systems

Angelier, J., 1985. Extension and rifting: the Zeit region, Gulf of Suez. Journal of Structural Geology, 7(5): 605-612.

Gabrielsen, R.H., 1986. Structural elements in graben systems and their influence on hydrocarbon trap types. A.M.e.a. Spencer (Red.), Habitat of Hydrocarbons in the Norwegian continental shelf, Norwegian Petroleum Society. Graham & Trotman, 55-60.

Gibbs, A.D., 1984. Structural evolution of extensional basin margins. Journal of the Geological Society, 141: 609-620.

Graue, K., 1992. Extensional tectonics in the northernmost North Sea: rifting, uplift, erosion and footwall collapse in Late Jurassic to Early Cretaceous times. A.M. Spencer (Red.), Generation, accumulation and production of Europe's hydrocarbons II. Springer-Verlag, Berlin, 23-34.

Roberts, A. & Yielding, G., 1994. Continental extensional tectonics. P.L. Hancock (Red.), Continental deformation. Pergamon Press,

223-250.

The pure and simple shear models for rifting

McKenzie, D., 1978. Some remarks on the development of sedimentary basins. Earth and Planetary Science Letters., 40: 25-32.

Kusznir, N.J. & Ziegler, P.A., 1992. The mechanics of continental extension and sedimentary basin formation: a simple-shear/pure shear flexural cantilever model. Tectonophysics, 215: 117-131.

Accommodation zones

Rosendahl, B.R., 1987. Architecture of continental rifts with respect to East Africa. Annual Review of Earth and Planetary Science, 15: 445-503.

CHAPTER 18

Strike-slip, transpression and transtension

Strike-slip faults constitute an important class of faults that have been studied for more than 100 years. They first received attention in California, Japan and New Zealand, where very long strike-slip faults with considerable displacement intersect the surface of the Earth. They are known for their close association with earthquakes, particularly the San Andreas Fault in California. Understanding such faults and the tectonic regimes in which they occur is therefore of great public as well as academic interest. Many strike-slip zones involve a component of perpendicular shortening or extension. The result is known as transpression and transtension – three-dimensional deformations that link strike-slip, extensional and contractional regimes.

Photo: Aykut Barka

1.1 Introduction

Strike-slip faults are faults where the displacement vector is parallel to the strike of the fault and thus parallel to the surface of the Earth (Figure 18.1). Strike-slip faults are typically steeper and more planar than other faults, at least they appear so in map view. Curvatures and geometric irregularities also occur along strike-slip faults, but more commonly in the vertical than in the horizontal section, perpendicular to the displacement vector. However, curvatures in map view do occur and have important implications for the structures associated with strike slip faults. Strike-slip faults occur on all scales, and represent some of the longest and most famous faults in the world. The San Andreas fault is one of the more famous strike-slip faults.

A strike-slip fault can be *sinistral* (left-lateral) (Figure 18.2) or *dextral* (right-lateral) and ideally involves no vertical movement of rocks. While the extent of reverse and normal faults is strongly limited by the thickness of the crust, strike-slip faults can extend around the entire globe and can accumulate an infinite amount of displacement in principle. Such strike-slip faults have never been found, but the idea illustrates the fact that strike-slip faults can accumulate large displacements. For this reason, strike-slip faults such as the Great Glen fault in Scotland, the Tornquist Zone in Europe and the Billefjorden Fault in Spitsbergen have been assigned hundreds of kilometers of lateral displacements.

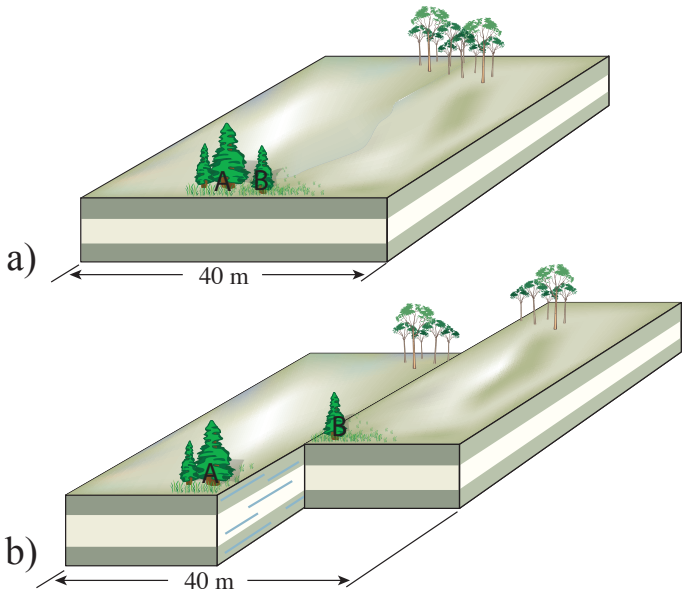

Figure 18.1 Strike-slip faults offset in the strike direcetion of the fault, i.e. parallel to the surface of the Earth.

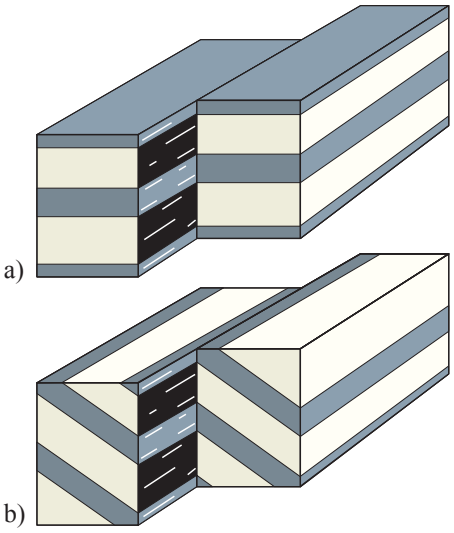

Figure 18.2 Pure strike-slip faults show no offset in any section if layers are horizontal (a) or strike parallel to the fault (b). They can therefore be difficult to identify from seismic data alone.

1.2 Transfer faults

Strike-slip faults have several different kinematic roles and are accordingly given different names. *Transfer faults* are strike-slip faults that transfer displacement from one fault to another. In general, any kind of fault that is connected to at least one other fault is involved in displacement transfer, but the term is used specifically for a particular type of strike-slip fault whose tips terminate against other faults or extension fractures. Transfer faults are therefore bounded and cannot grow freely, implying that their displacement increases relative to their length.

Transfer faults occur on all scales and they connect a range of structures. They can connect open

Figure 18.3 Sinistral transfer fault between two extension fractures. Path to Delicate Arch, Utah.

or mineral-filled extension fractures (Figure 18.3), veins, dikes, normal faults of the same (Figure 18.4a) or opposite (Figure 18.5) dip directions, oblique faults, reverse faults (Figure 18.4b) and more. At larger scale, transfer faults connect continental rift axes where they typically are associated with a change in dip ~~for large rift faults~~. In mid-oceanic ridges, oceanic ridge valleys are shifted along transfer faults. When oceanic transfer faults first were discovered in the 1960's they were given the name *transform faults* (Figure 18.6).

Transform faults are large (km-scale or longer) strike-slip faults that segment plates or form plate boundaries. The term was first used about the many transfer faults that define plate boundaries or offset mid-ocean ridges (Figure 18.7a). In other places they connect mid-ocean ridges to destructive plate boundaries (island arcs; Figure 18.7b), or they connect two segments of a destructive plate boundary (Figure 18.7c). Transform faults that define plate boundaries can get very long. The most famous example is the 1200 km long *San Andreas Fault* in California, which represents a transform fault along the boundary between the North American and Pacific plates. Large transform faults are actually fault zones rather than simple faults. The San Andreas Fault constitutes a number of more or less parallel faults of various lengths in a ~100 km wide zone. Folds also occur along this zone, together with reverse and normal faults. We will come back to these later in this chapter. For now we emphasize the fact that, among the many faults in the zone, usually only one is active at any given time. In this sense, a fault zone such as the San Andreas Fault is different from most active plastic shear zones where the deformation is going on in all or at least a significant portion of the zone.

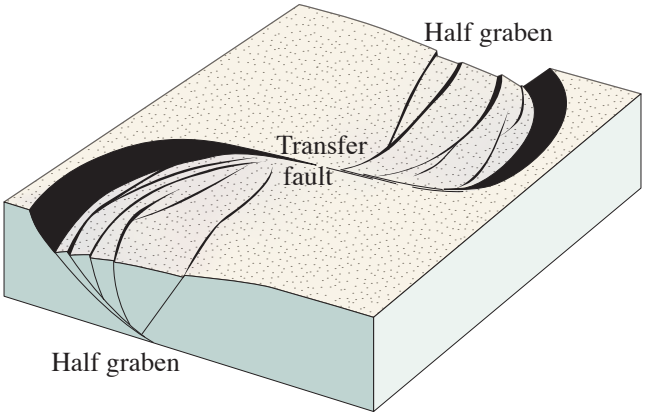

Fig. 18.5 Strike-slip faults that connect half grabens of opposite polarity are a kind of transfer faults. Such transfer faults are common in rifts such as the East-African rift system, the North Sea rift and the Rio Grande rift.

1.3 Transcurrent faults

Transcurrent faults are strike-slip faults that have free tips, i.e. they are not constrained by other structures. Their free tips move so that the fault length increases as displacement accumulates. Such strike-

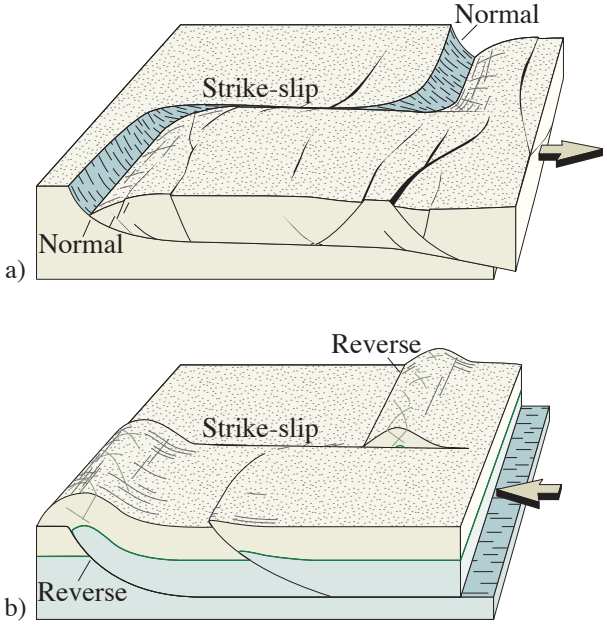

Figure 18.4 Strike-slip movements can occur along lateral ramps in both extensional and contractional settings. Such strike-slip faults are transfer faults and can attain significant offsets and little or no along-strike variation in displacement. In each end the transfer faults are connected to extensional or contractional faults.

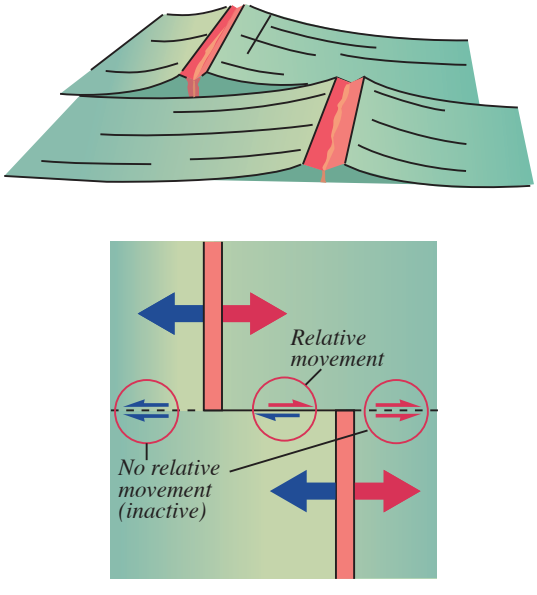

Figure 18.6 Transform fault from a mid-ocean ridge (perspective and map view). The fault is only active between the ridge segments (except for minor vertical ajustments). The offset is constant along the active part of the fault, and its length grows at a rate that is directly proportional to the spreading rate.

slip faults thus follow a normal displacement-length relationship (Figure 8.12). Free strike-slip faults form within plates and are therefore *intraplate faults*. In contrast, transforms that occur along plate boundaries are *interplate faults*. Transcurrent faults can be expected to meet and interfere with other faults at some point during their growth history, but they will never have the special kinematic role that transform faults have.

Long strike-slip faults intersect the surface of the Earth. At depth they may terminate against structures such as thrust faults, extension faults and subduction zones (Figure 18.8), or they may penetrate the brittle-plastic transition and continue downward as steep plastic shear zones.

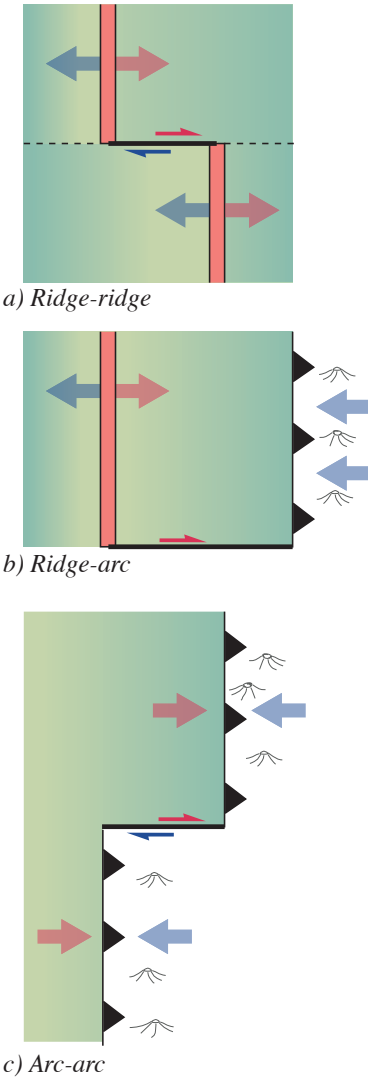

Figure 18.7 Transform faults are strike-slip faults connected by plate boundaries. a) Fault between two mid-ocean spreading ridge segments. b) Transform fault connecting a rift segment and an island arc/subduction zone. c) Fault displacing a destructive plate boundary. The length of the fault increases in a), is constant in b) and increases or decreases in c), depending on the relationship between the spreading rate and the subduction rate.

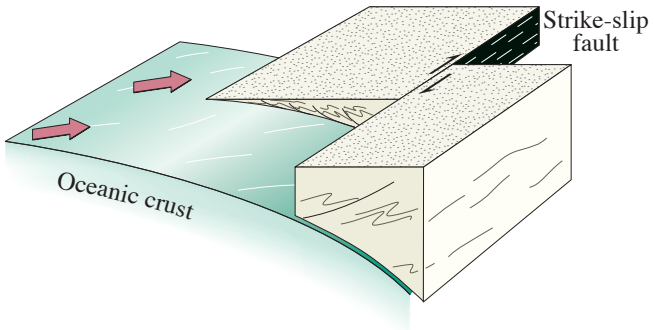

Figure 18.8 Strike-slip fault rooted in a subduction zone with an oblique subduction vector. This model has been applied to the San Andreas Fault where the oceanic plate is the Pacific Plate and the detached block is the Salina block.

1.4 Development and anatomy of strike-slip faults

1.4.1 Single faults (simple shear)

Strike-slip faults form when individual parts of the crust move at different rates along the surface of the Earth. Just like normal and reverse faults, strike-slip structures are complex when viewed in detail. Several secondary structures are associated with strike-slip faults, and experiments have helped us explore some of the most important ones. Riedel's clay experiments from the early 1900's are the most famous. He used two stiff wooden blocks covered by a clay layer (Figure 18.9). The blocks were slid past one another, and stress was transferred to the overlying clay, which deformed progressively.

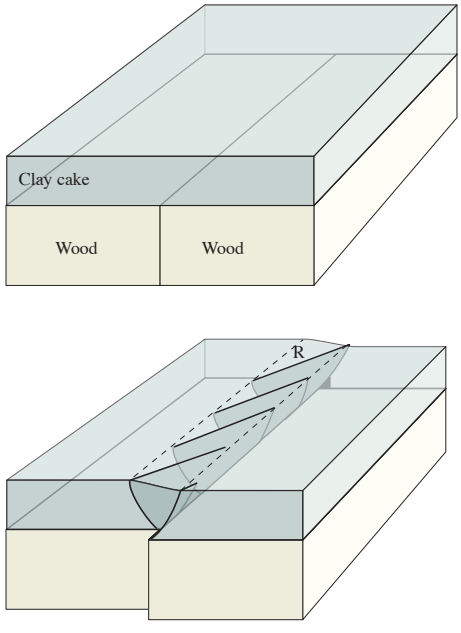

Figure 18.9 Physical model with two wooden blocks underneath a clay layer. Note the geometry of the R-fractures and the upward expansion of the shear zone.

HOW DO LONG STRIKE-SLIP FAULTS FORM?

Rock mechanics considerations tell us that when a shear fracture forms, the stress field in the tip regions will generate local tension fractures, so-called wing cracks. This was first shown by cutting a straight fracture in a plastic plate and then impose a stress field as shown in the figure. How then can strike-slip faults of up to several hundred kilometers long form?

It has been suggested that faults form from extension fractures or joints that already are long. But not as long as hundreds of kilometers. Such lengths must be achieved by linking of reactivated joints. The model requires a separate phase of extension and jointing prior to strike-slip faulting, which makes strike-slip faulting a two-phase history of deformation. An alternative is that the faults use other weak structures. If joints and faults do not already exist, then dikes and steep layering or foliations may be used. Some of these structures are much longer than joints, and strike-slip faults can more easily form as long structures without the formation of wing cracks that lock up the fault.

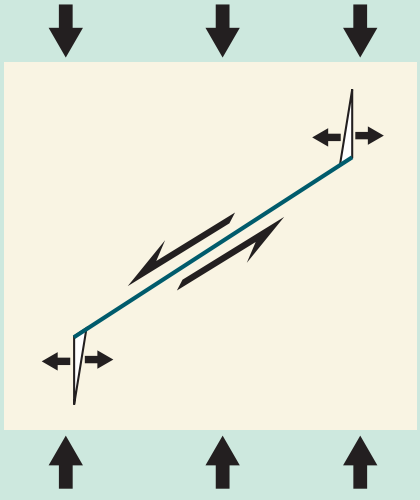

Riedel soon realized that the clay layer did not develop a clean, single fault but a wide deformation zone comprised of an array of small fractures . These subsidiary fractures are classified based on their orientation and sense of slip relative to the trend of the overall strike-slip zone. The first sets of fractures

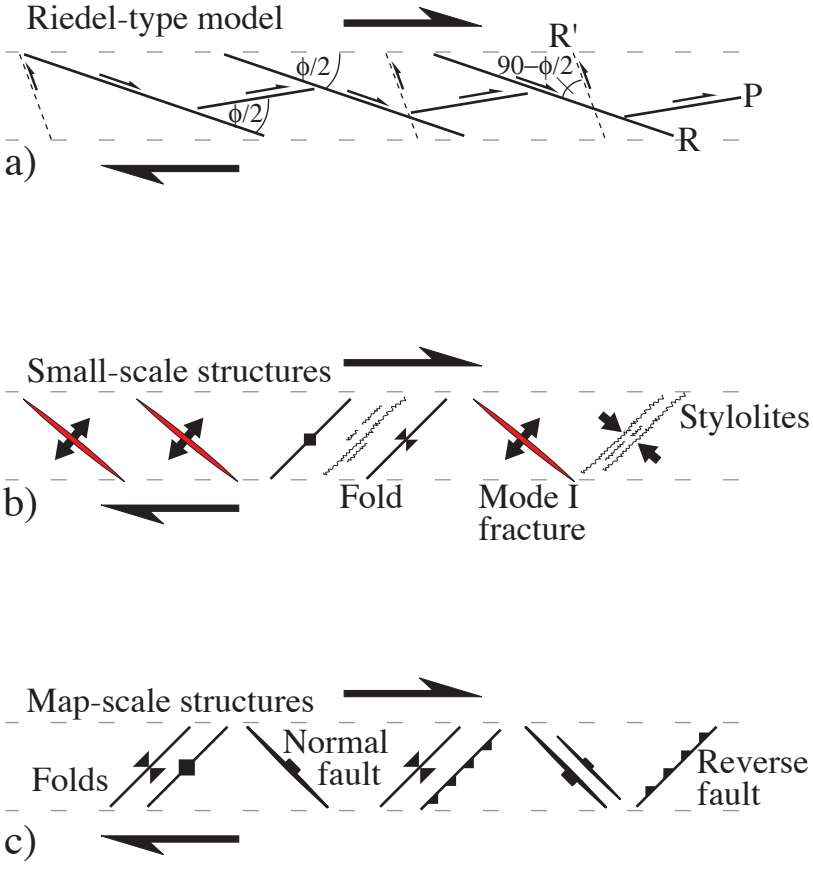

Figure 18.10 Structures formed by dextral strike-slip motion. a) Riedel-model where R and R' are synthetic and antithetic Riedels. P-shears are secondary and connect R and R' surfaces. ϕ=the angle of internal friction. b) Other small-scale structures that can form along a strike-slip zone. c) Large-scale structures.

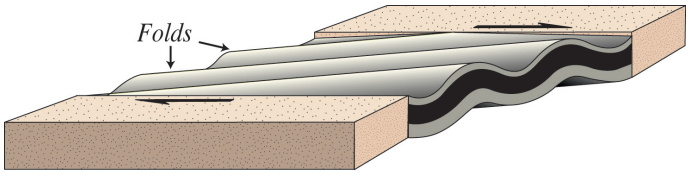

Figure 18.11 Folds formed by strike-slip movement in a wide deformation zone where the layering is horizontal. Note that the axial traces and fold axes form an acute angle with the shear zone.

to form are shear fractures. One set, known as R-fractures or R-shears[1] (Riedel shears), make a low angle with the overall shear zone and show the same sense of slip. Another set is made up of R'-fractures are antithetic fractures that make a high angle to the zone, as shown in Figure 18.9. Although they commonly occur together, R-fractures are more common than R' fractures, and R' fractures only rarely develop significant offsets. A third set of shear fractures are known as P-fractures or P-shears. These usually develop after the development of R-fractures (Figure 18.10a). The development of P-fractures is probably related to temporal variations in the local stress field along the shear zone as offset accumulates.

In addition to the brittle R, R' and P-fractures, (ex)tension or T-fractures can occur (Figure 18.10b). In the shear zone setting represented by Riedel's clay model, T-fractures will form perpendicular to the maximum instantaneous strain axis (ISA_1). For large strike-slip zones, normal faults will show the same strike orientation as T-fractures. Folds can also develop (Figures 18.10b-c and 18.11), typically before deformation is localized into discrete faults. The axial traces of the folds are initially at a high (~90°) angle to the minimum instantaneous stretching axis (ISA_3), provided that the layering is more or less horizontal. Dipping layers can also be folded in strike-slip zones, but the relationship between the ISA and the fold axes is more complicated. Other contractional structures, such as stylolites and reverse faults, can also form in strike-slip zones (Figures 18.10b-c). These will have approximately the same orientation as the fold axes.

A simple folding experiment can be carried out by performing a simple shear movement with your two hands and a piece of fabric. Folds form immediately at an angle to the shear direction – the direction of most rapid stretching of the fabric and rotate as the shearing proceeds.

1.4.2 Conjugate strike-slip faults (pure shear)

Strike-slip faults may occur as simple structures or in zones of more or less parallel fault strands. However, strike-slip faults can also form as conjugate sets, implying that they were active at about the same time under the same regional stress field (Figure 18.12).

Conjugate strike-slip faults fit well into both Anderson's model and Coulomb's fracture criterion. In this model, the acute angle between the two sets is bisected by σ_1 and the angle itself is determined by the internal friction of the rock. Kinematically, such faults result from pure shear in the horizontal plane, where shortening in one direction is compensated by orthogonal extension in the other. In this ideal model no extension or contraction occurs in the vertical direction.

The most famous large-scale example of conjugate strike-slip faults is the fault system on the north side of the Himalaya (Figure 18.13). Here the Indian continent moves towards the Eurasian continent, and some of the convergent movements are accommodated by a series of active strike-slip faults. Strike-slip faults in this region accommodate lateral transport of material away from the collision zone, and shortening perpendicular to this zone. The physical model shown in Figure 18.13 illustrates the idea. This model implies that the area north of the collision zone is weaker than the stiff Indian plate.

1.4.3 Fault bends and stepovers

In sections containing the displacement vector (e.g, map view) ideal strike-slip faults are perfectly straight. However, even the simplest experimental models produce structures that are oblique to the

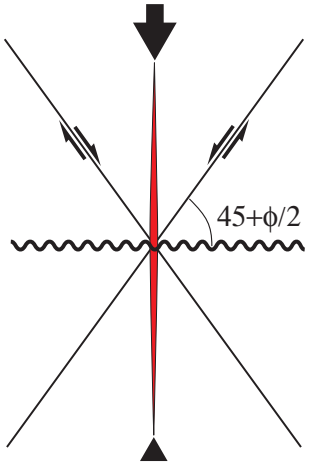

Figure 18.12 Conjugate pure shear model for the formation of strike-slip faults. The orientation of extension fractures (vertical) and stylolites (horizontal) are indicated. The model assumes that both sets are active more or less at the same time.

1 The term R-*shear* is not in keeping with good use of the word shear, but is used so extensively that we accept the use in these cases. The correct term would be R-shear fractures or just R-fractures.

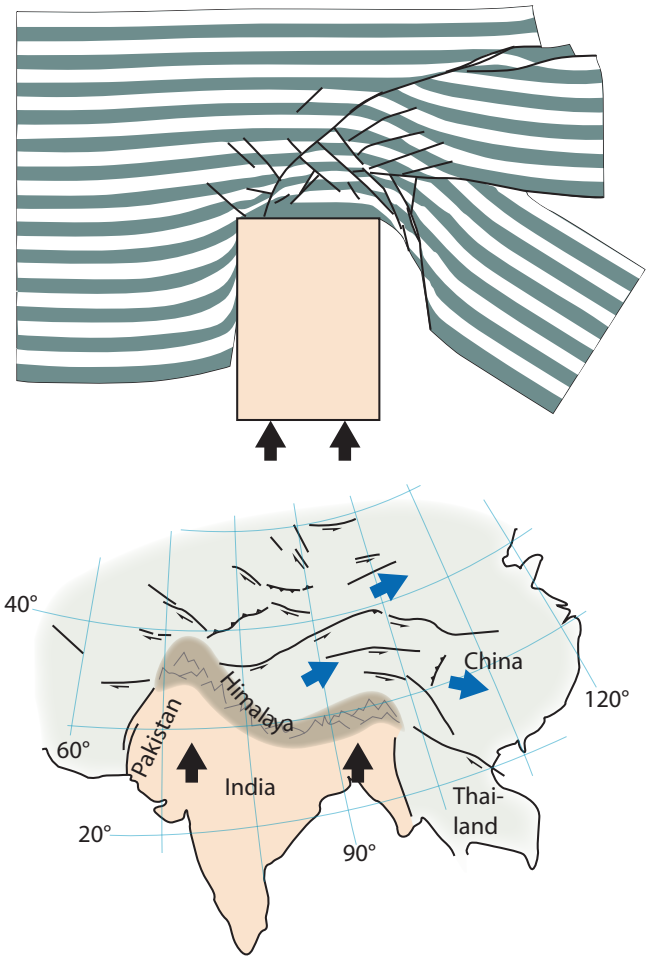

Figure 18.13 Formation of strike-slip faults in front of a stiff indenter. Two sets of faults, which can be considered conjugate, form while material is extruded sideways. The model is thought to represent an analogue to what is going on in the area north of the Himalaya. The experiment is described byTapponnier et al. (1986).

general trend of the fault (Figure 18.10). Natural strike-slip faults show geometrical irregularities as a consequence of irregularities generated by linkage of fault segments, as seen in Figures 18.9 and 18.10a[2]. When individual fault segments overlap and link, a local deviation from the general fault trend is established in the form of a *fault stepover* or *fault bend*. Contractional or extensional structures form in such bends, depending on the sense of slip on the fault relative to the sense of stepping (Figure 18.14).

Contractional structures include stylolites, cleavages, folds and reverse faults, and they form in *restraining bends*. Subparallel reverse or oblique-slip contractional faults bounded by the two strike-slip segments can form and are called *contractional strike-slip duplexes*. On a large scale, restraining bends are recognized as areas of positive relief. After some time the contractional structures are likely to be transected by a new and straighter fault strand. The strain hardening within the restraining bend is then reduced or eliminated, although some irregularities may remain. The new fault in the restraining zone is likely to develop from P-shears.

Releasing bends produce extensional structures such as normal faults and extension fractures. Extensional fractures are common in mesoscale releasing bends, while faults with a normal slip component tend to dominate larger scale examples. Series of parallel extensional faults bounded on both sides by strike-slip faults, as shown in Figure 18.14, are called *extensional strike-slip duplexes*. Normal faults generate negative structures, i.e. basins that can be filled with sediments at various scales (Figures 18.15 and 16). Over time the basin will lengthen as new normal faults form. The Dead Sea is such a basin, created in an overlap zone between two strike-slip transforms. Such basins are called *pull-apart basins*.

1.4.4 Seismic imaging and flower structures

Reflection seismic data provide information about strike-slip faults in depth. Pure strike-slip faults

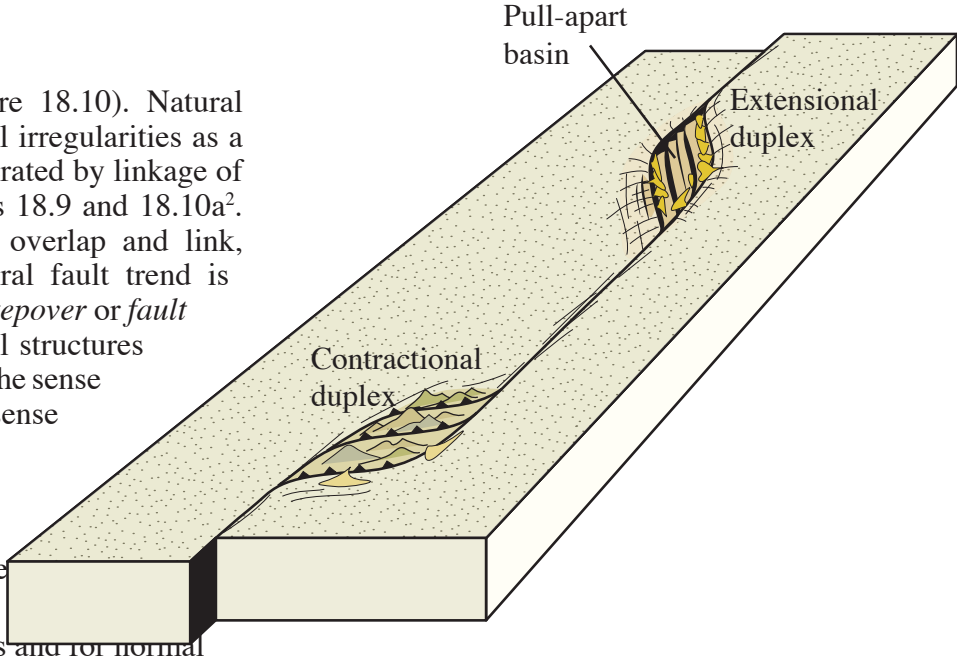

Figure 18.14 Extensional duplex (transtension) and contractional duplex (transpression) developed at bends or stepovers along a strike-slip fault system. Large-scale examples may lead to basin formation and local orogeny.

2 It is linkage in the slip dire geometric complications, which is strike directionfor strike-slip faults and for normal and the dip direction for extensional and contractional faults.

SIDEWAYS IN SPITSBERGEN

Several straight faults transect Svalbard in the N-S direction. They show many of the characteristics of strike-slip faults, including straight fault traces and steep dips. Most geologists agree that they have acted as strike-slip faults, primarily with a dextral sense of slip. The Billefjorden Fault is the most conspicuous one. In the 1960's the British geologist W. Brian Harland assigned hundreds of kilometers to this fault. He also connected this fault to the Great Glen Fault in Scotland – an interpretation that not everybody fully accepts.

It is now clear that at various times and under changing stress fields, the Billefjorden Fault has acted in a normal as well as reverse sense. This is a characteristic feature of strike-slip faults. The result is a complex fault zone that may be difficult to interpret.

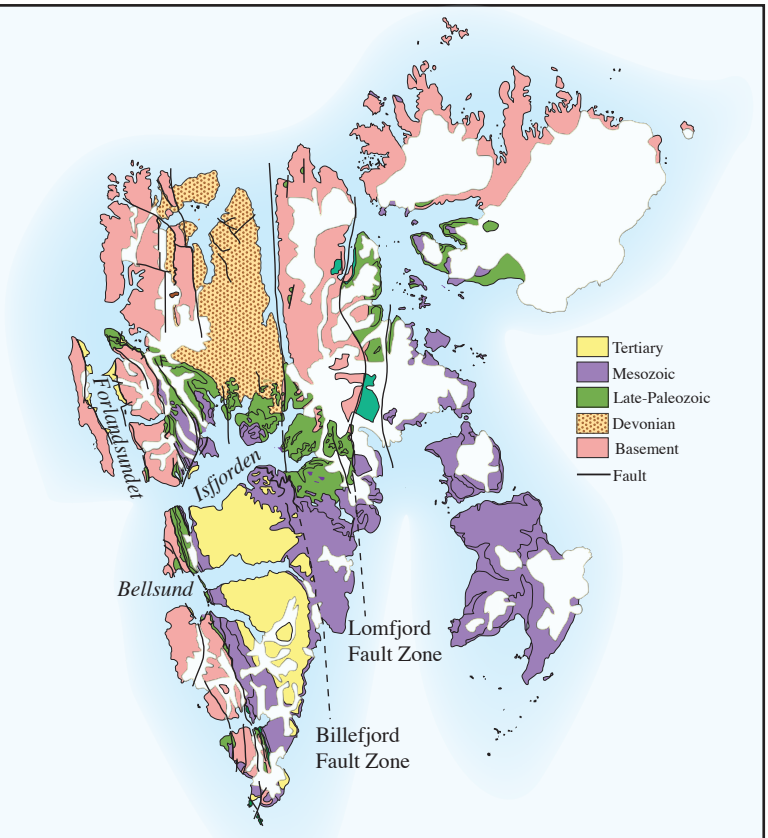

can be difficult to detect from seismic data alone, not only because most are too steep to set up reflections, but also because horizontal layers or layers striking parallel to the fault show no displacement in the vertical direction (Figure 18.2). The clue is then to look for restraining and releasing bends, where vertical movements are associated with normal faults, reverse faults or folds. A characteristic feature of such bends is their tendency to split and widen upward. These structures are called *flower structures*. Flower structures that are associated with restraining bends are called positive, and those associated with releasing bends are called negative flower structures (Figure 18.17).

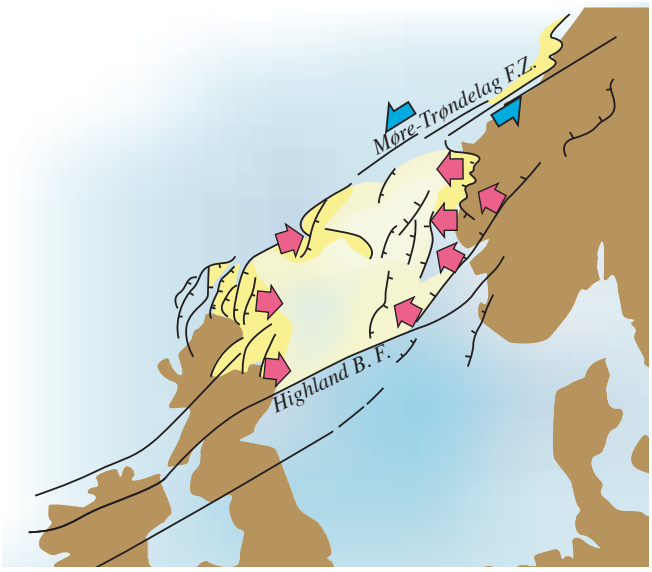

Figure 18.15 An interpretation of the Devonian deposits in the northern UK and SW Norway as forming in a pull-apart system (transtensional overlap) between two strike-slip faults. Based on Séranne et al. (1991).

Strike-slip faults thus bifurcate and widen toward the surface, particularly in restraining and releasing bends. One reason for this may be the changes in the mechanical properties near the surface. While a fault is generally much weaker than its surroundings, less consolidated and perhaps more jointed layers occur near the surface. In this setting it is easier to form multiple faults.

1.5 Transpression and transtension

We have seen that bends in strike-slip faults can produce local components of contraction or extension. The type of deformation occurring in such bends is referred to as transpression and transtension. These modes of deformation do not have to be restricted to fault bends – they can dominate the full length of the strike-slip fault if the fault (or shear zone) is not purely strike-slip (simple shear). It contains an additional component of shortening or extension perpendicular

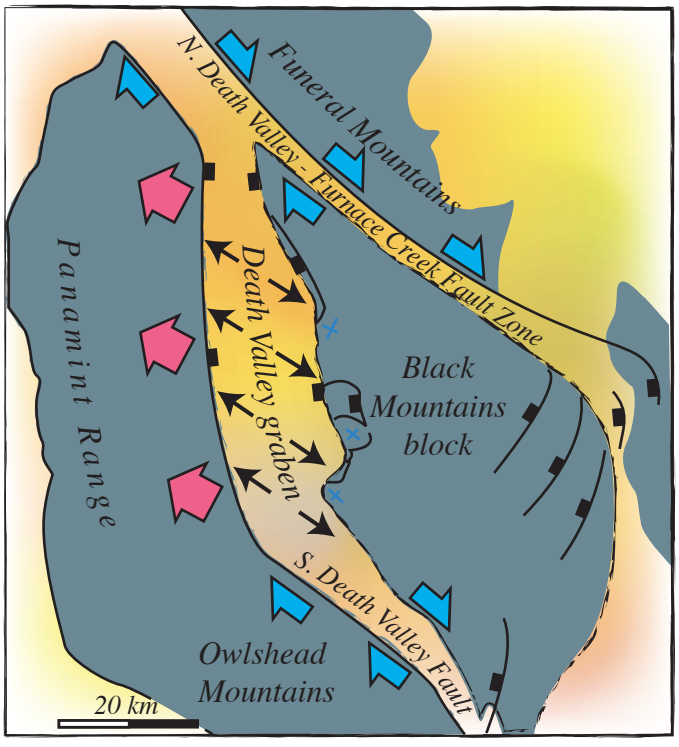

Figure 18.16 Death Valley, which locally reaches below sea level, is a pull-apart basin in a transtensional system. Based on Wright et al. (1974).

to the fault plane.

In general, transpression is the spectrum of combinations of strike-slip and pure contraction (Figure 18.18), and transtension is the combinations of strike-slip with extension. In other words;

Transpression (transtension) is the simultaneous combination of strike-slip motion along a shear zone or fault, combined with perpendicular shortening (extension).

For a vertical shear zone of finite width, transpression and transtension can be modeled quite simply. The strike-slip component is a horizontal simple shear displacement along a vertical plane while the shortening can be modeled as a coaxial deformation with horizontal shortening and vertical and/or lateral extension. Let us make the coaxial component a pure shear with vertical extension (Figure 18.19). This is the simplest mathematical model proposed for transpression, first presented by Sanderson and Marchini in 1984. Using the deformation theory from Chapter 3, the simultaneous application of the two components can be represented by the deformation matrix

$$D = \begin{bmatrix} 1 & \Gamma & 0 \\ 0 & k & 0 \\ 0 & 0 & k^{-1} \end{bmatrix} = \begin{bmatrix} 1 & \dfrac{\gamma(1-k)}{\ln(k^{-1})} & 0 \\ 0 & k & 0 \\ 0 & 0 & k^{-1} \end{bmatrix} \quad (18.1)$$

The matrix is three-dimensional because the pure and simple shear components act in two perpendicular planes. γ is the simple shear or strike-slip component, while the k-value determines the amount of shortening or extension across the zone. For k=0.7 the zone is thinned 30% and we have transpression. For k=1.2 the thickness of the zone is increased by 20% and the deformation is transtensional. As always, once we have established a deformation matrix we can find the orientation and shape of the strain ellipse, Wk and ISA, and by using incremental matrixes we can calculate rotation patterns of passive lines and planes. Let us use this opportunity to explore some aspects of transpression and transtension

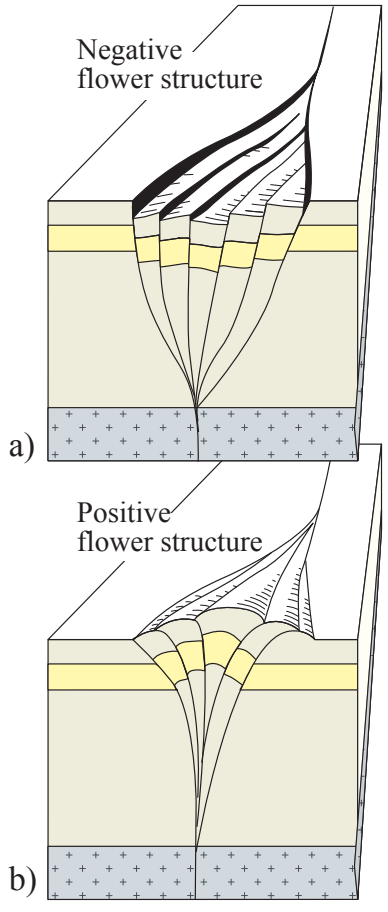

Figure 18.17 Principal features of a) negative and b) positive flower structures.

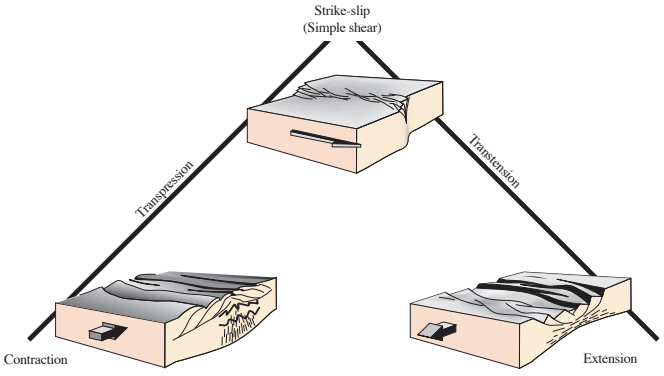

Figure 18.18 Transpression and transtension connect contraction, strike-slip and extension.

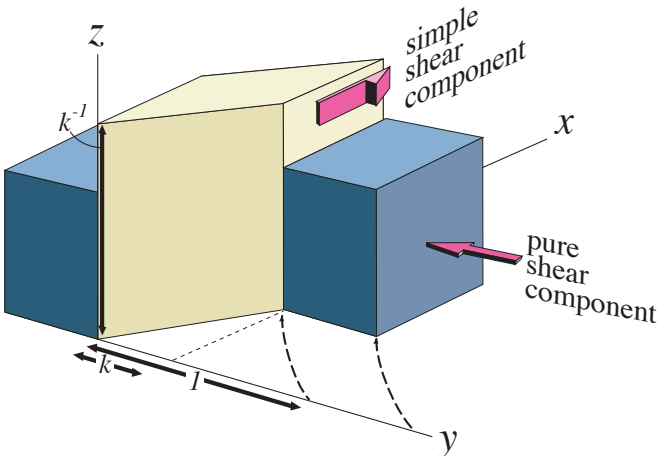

Figure 18.19 Sanderson and Marchini's (1984) simple model for transpression.

1.5.1 Strain ellipsoid

Using the deformation matrix (Equation 18.1) it can be shown that for our model transpression results in oblate ellipsoids (flattening) while transtension generates prolate ellipsoids (Figure 18.20 fig21). The long axis X of the strain ellipsoid is horizontal for transtension, and vertical for transpression with a strong pure shear component. However, for some transpressional deformations where the pure shear factor is not too strong (Wk<0.81), Y is initially vertical and X horizontal before the two switch places (Figure 18.21 fig 20). The switch occurs when the deformation path hits the horizontal axis in the Flinn diagram. A similar switch between Y and Z occurs for transpression.

The orientation of the longest axis of the strain ellipse in the horizontal plane, be it X or Y, can be found using the equation

$$\theta' = \tan^{-1}[(\lambda - \Gamma^2 - 1)/k\Gamma]. \qquad (18.2)$$

Her θ' is the angle between the longest horizontal axis and the vertical shear zone. Knowing the strain ratio R in the horizontal section, we can estimate W_k by means of Figure 18.22a.

1.5.2 Linear structures

We just noted that the lineation in a zone of transpression is oblique to the shear zone by an angle θ', or vertical in some cases. We sometimes have lines and planes that will rotate more or less passively during the deformation history. Using matrix premultiplication (Section 3.22) and small strain increments we can calculate how lines and planes rotate during progressive deformation. We will here focus on lines, although plane rotations can be explored in the same way. Lines of different initial orientations outline different paths for any given deformation type, as illustrated in the stereonets on Figure 18.23 (left). For simple shear (perfect strike-slip shear zone) lines rotate along great circles (Figure 18.23, W_k=1). For pure shear (W_k=0) a symmetric pattern emerges. For transtension the paths are controlled by the oblique flow apophysis, and lines will eventually end up parallel to this apophysis (Figure 18.23). This means that deforming linear structures will concentrate at an orientation oblique to the shear zone and the shear direction. In our model the angle α between the apophysis and the shear zone will be:

$$\alpha = \tan^{-1}[(\ln k)/\gamma]. \qquad (18.3)$$

The angularity will be qualitatively similar but

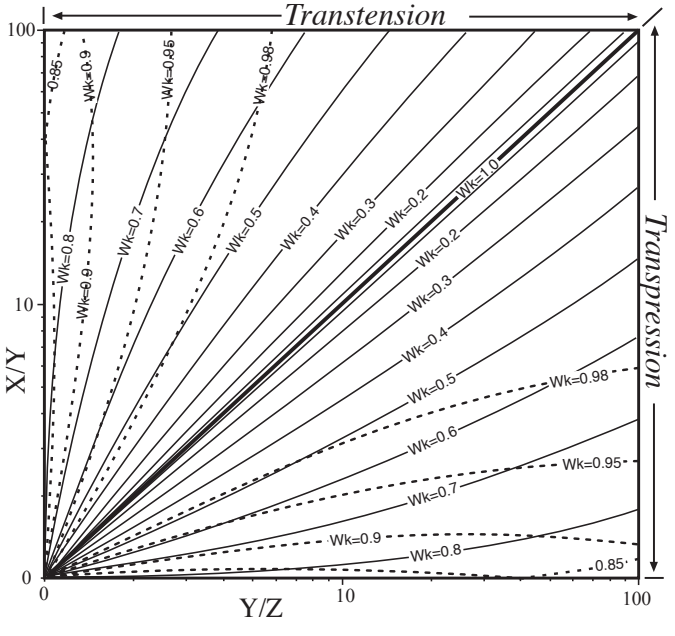

Figure 18.20 Flinn diagram where constant Wk paths are shown. From Fossen & Tikoff (1993).

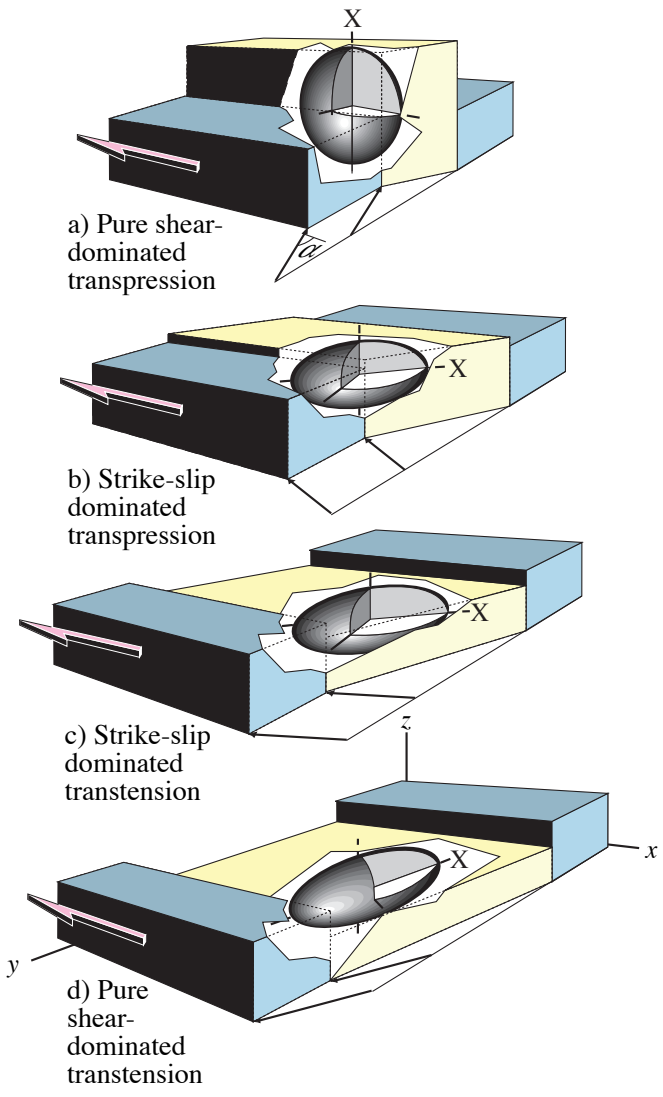

Figure 18.21 The orientation and shape of the finite strain ellipsoid for the four classes of transpression/transtension discussed in the text. From Fossen et al. (1994).

not identical to the obliqueness of the stretching lineation (eq. 18.2). Hence, using the lineation to determine the transport direction is not presicely correct in transtension zones. In practice, if we can identify a strain gradient, e.g. from the low-strained margin toward the center of the zone, then the rotation pattern can be compared to the theoretical patterns shown in Figure 18.23, and the type of transpression or transtension can be found. If strain data can be added, then Figure 18.20 can also be used.

It is important to understand that the simple model for transpression and transtension referred to above is only one of many possible models. Not all strike-slip shear zones are vertical, and lateral extrusion as well as vertical extension can occur. Nevertheless, the simple model shown in Figure 18.19 illustrates that transpression can involve vertical transport of rock, which at large scale in combination with erosion brings metamorphic rocks to the surface.

1.6 Strain partitioning

Natural rocks tend to be anisotropic and heterogeneous. Sandstone, limestone and shale react differently to deformation, as do alternating layers of micaschist and granitic gneiss. In general, the simple shear component is most easily accommodated in the weakest layers, while the rest of the zone is left with the pure shear component. In other words, the total strain is partitioned between layers of different mechanical properties (Figure 18.24). This strain partitioning is merely a selective distribution of strain components within the total deformation zone.

What does this have to do with strike-slip, transpression and transtension? It turns out that partitioning of the pure and simple shear components of transpression and transtension is common, and it can be seen from the microscale to the scale of orogenic belts (Figures 18.25 and 18.8). At mesoscale and mapscale the result can be zones where strain and fabrics can be quite different.

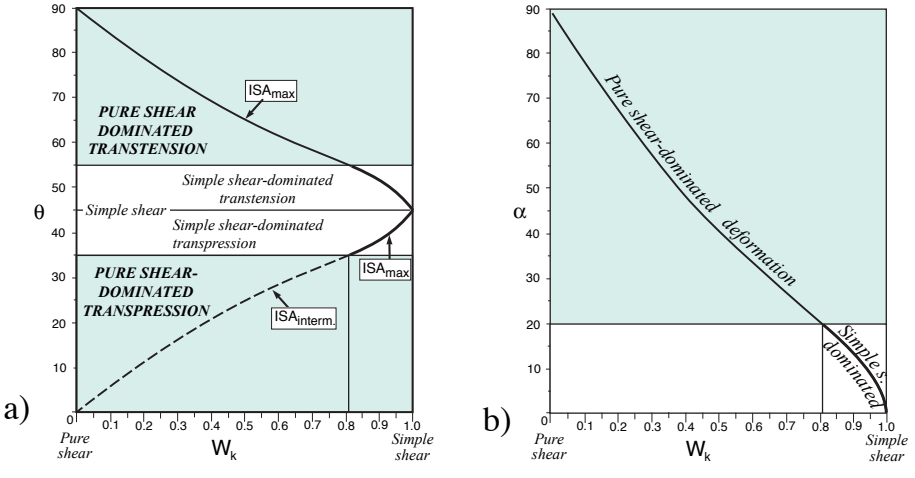

Figure 18.22 a) The connection between Wk and the angle θ between the maximum horizontal instantaneous stretching axis and the shear zone. b) The relation between α (the orientation of the oblique flow apophysis) and Wk (for both transpression and transtension). From Fossen & Tikoff (1993).

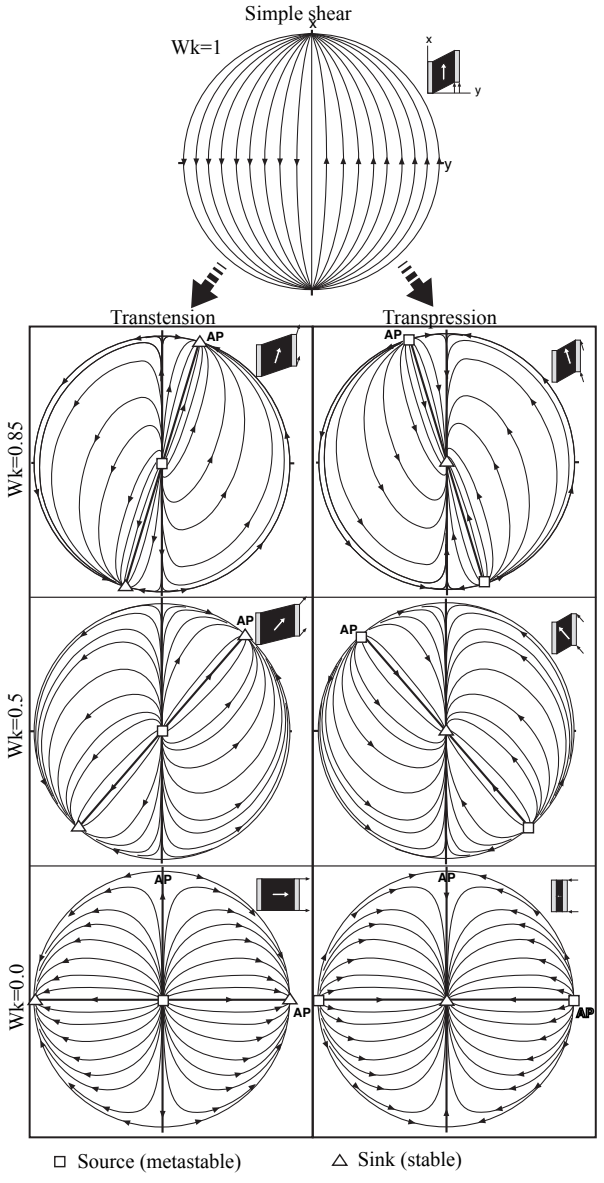

Figure 18.23 Rotation patterns for passive linear structures. From Fossen et al. (1994).

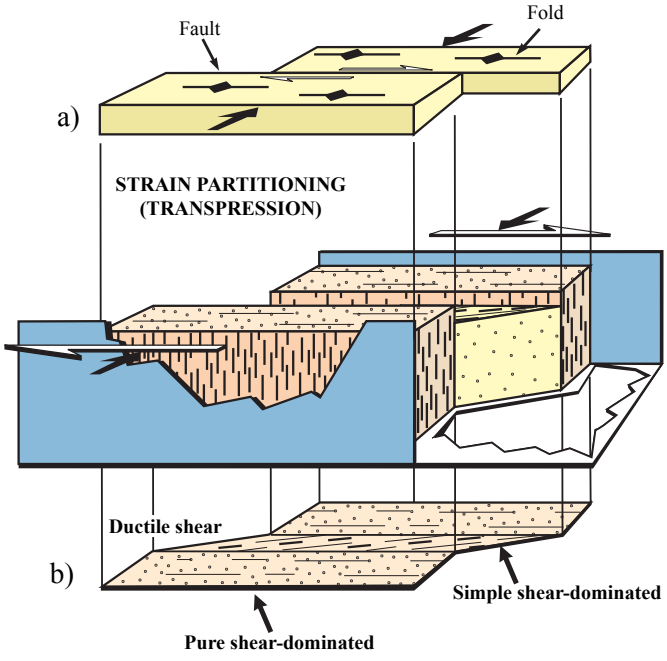

Figure 18.24 Illustration of straion partitioning in a zone of transpression. Some blocks experience mostly simple shear, while other are pure shear-dominated. At high crustal levels the simple shear zone is reduced to one or more faults.

1.6.1 Plate margins and large-scale strain partitioning

Transpression and transtension are common deformation types along plate margins and are now recognized from current and paleo-plate margins from all over the world. While relative plate movements are seldom perfectly strike-slip (conservative). if we know the movement vector of one plate relative to the other, then we also know the orientation of the oblique horizontal flow apophysis: they are identical (Figure 3.22). This very useful fact can be used to model structures in deformation zones along plate boundaries.

Strain partitioning along strike-slip dominated plate boundaries involves a balance between the amount of strike slip or simple shear on one hand, and the amount of shortening or extension on the other. For a transpressional margin, the more simple shear localized to weak zones, the more pure shear must be accommodated by adjacent rocks. The San Andreas fault system, generally regarded as a strike-slip zone, is in fact a transpressional zone because the plate vector makes a 5° angle with the plate margin in Central California (Figure 18.25). From this information alone it can ~~be calculated or~~ seen from Figure 18.22b that Wk=0.985 and the deformation is very close to simple shear (strike slip), ~~but not quite~~. ISA_1 is oriented at 42.5° to the plate margin. However, because so much of the simple shear component is taken up by strike-slip faults, the domains between the faults receive a significant amount of horizontal shortening (pure shear). This explains why ISA_1 (and σ_1) is not oriented at 42.5° but at a much lower angle to the plate margin in these domains. It also explains why folds with axes almost parallel to the faults exist in the pure-shear dominated domains. Even young, open folds are oriented at 6-12° to the plate margin, while a strike-slip or simple shear deformation predicts that they be closer to 45°. Strain partitioning is therefore an important concern in many strike-slip zones and plate margins.

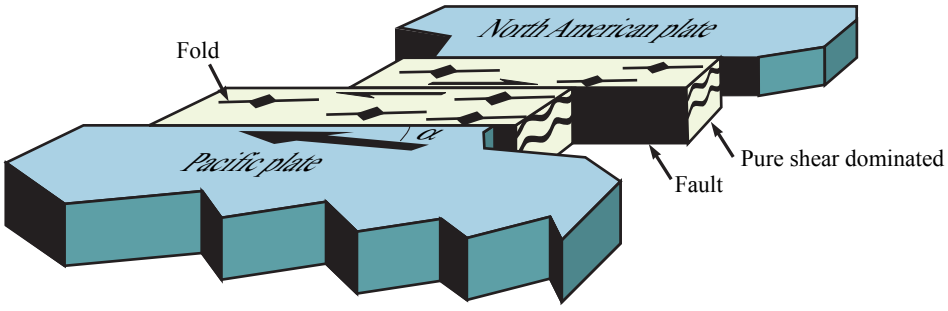

Figure 18.25 Schematic illustration of the San Andreas fault system in California. The angle α between the two flow apophyses is only 5°, but most of the simple shear is released along the faults so that pure shear dominates the volume between the faults. That's why the fold axes are subparallel to the faults.

---###---

Strike-slip zones are often more interesting where components of coaxial strain and/or geometrical complications occur. Although there are many more models of transpression and transtension that can be explored and they can be made incredibly complex, simple models based on map pattern and field detail can explain many important features, generate additional questions while contribute to further understanding of these interesting structures.

Further Reading:

Aydin, A. & Nur, A., 1982. Evolution of pull-apart basins and their scale independence. Tectonics, 1: 91-105.

Fossen, H., Tikoff, T.B. & Teyssier, C.T., 1994. Strain modeling of transpressional and transtensional deformation. Norsk Geologisk Tidsskrift, 74: 134-145.

Harding, T.P., 1976. Predicting productive trends related to wrench faults. World Oil, June 1976: 64-69.

Jones, R.R., Holdsworth, R.E., Clegg, P., McCaffrey, K. & Travarnelli, E., 2004. Inclined transpression. Journal of Structural Geology, 26: 1531-1548.

McClay, K. & Dooley, T., 1995. Analogue models of pull-apart basins. Geology, 23: 711-714.

Oldlow, J.S., Bally, A.W. & Lallemant, G.A., 1990. Transpression, orogenic float, and lithospheric balance. Geology, 18: 991-994.

Peacock, D.C.P., 1991. Displacements and segment linkage in strike-slip fault zones. Journal of Structural Geology, 13: 1025-1035.

Peacock, D.C.P. & Sanderson, D.J., 1995. Strike-slip relay ramps. Journal of Structural Geology, 17: 1351-1360.

Robin, P.-Y.F., 1994. Strain and vorticity patterns in ideally ductile transpression zones. Journal of Structural Geology, 16: 447-466.

Sanderson, D. & Marchini, R.D., 1984. Transpression. Journal of Structural Geology, 6: 449-458.

Sylvester, A.G., 1988. Strike-slip faults. Geological Society of America Bulletin, 100: 1666-1703.

Tikoff, B. & Greene, D., 1997. Stretching lineations in transpressional shear zones: an example from the Sierra Nevada Batholith, California. Journal of Structural Geology, 19: 29-39.

Tikoff, B. & Peterson, K., 1998. Physical experiments of transpressional folding. Journal of Structural Geology, 20: 661-672.

Tikoff, B. & Teyssier, C.T., 1994. Strain modeling of displacement-field partitioning in transpressional orogens. Journal of Structural Geology, 16: 1575-1588.

Treagus, S.H. & Treagus, J.E., 1992. Transected folds and transpression: how are they associated? Journal of Structural Geology, 14: 361-367.

Westaway, R., 1995. Deformation around stepovers in strike-slip fault zones. Journal of Structural Geology, 17: 831-846.

Wilcox, R.E., Harding, T.P. & Seely, D.R., 1973. Basic wrench tectonics. American Association of Petroleum Geologists, 57: 74-96.

Woodcock, N.H. & Schubert, C., 1994. Continental strike-slip tectonics. In: Hancock, P.L. (ed.), Continental deformation. Pergamon Press, 251-263.

CHAPTER 19

Balancing and restoration

Restoring a geologic section or map can be a very useful exercise. It attempts to link the present deformed stage to the undeformed stage. It requires that the section or map is balanced, else restoration will not be feasible. There must be a balance between the deformed section, the restored section and the interpretation. Such exercises were first performed for geologic sections from areas of contraction, but are now also commonly applied to extensional areas. Balancing and restoration provides critical constraints on the development of reasonable interpretations, although they give no guarantee that the interpretation is correct.

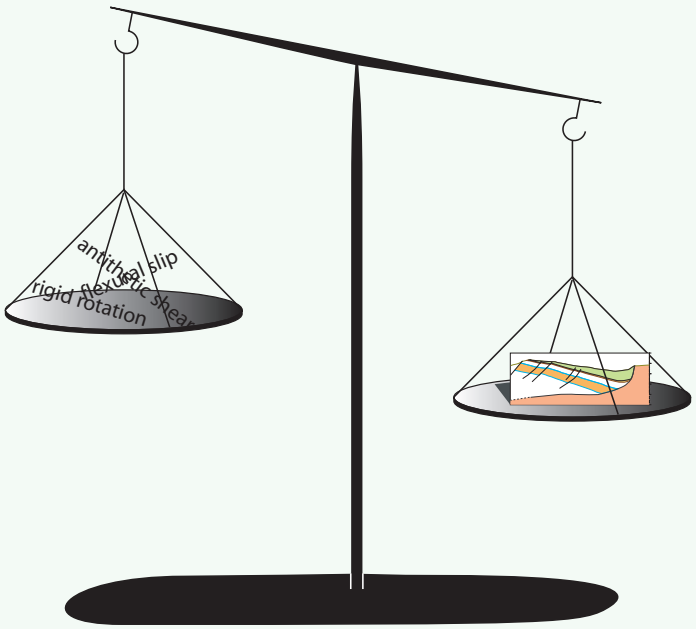

1.1 Introduction

Geologic data always contain enough uncertainties to support several different interpretations, some of which are more likely than others[1]. Our choice of explanation will depend on the quality of the data, our geologic knowledge and experience, and the time and resources available to work on the data. Balancing is a method that tests the realism of our sections and maps.

Balancing adjusts a geologic interpretation so that it not only seems reasonable, but also restorable to the pre-deformation situation. Restoration involves taking a section or map and works back in time to undeform or retrodeform the rocks. In terms of the deformation theory discussed in Chapter 3 this is the same as applying the resiprocal or inverse deformation matrix D^{-1}, except that the deformation does not have to be a linear transformation. One must decide whether the type of deformation, is dominated by rotation, translation and some sort of simple shear, flexural flow, or some combination. By applying reciprocal versions of these deformations the deformed section or map should be retrodeformed to a section without overlaps and gaps, without fault offsets (except for possible earlier phases) and for sedimentary layers, to unfolded, horizontal layers. Only when we have demonstrated that a geologic section can be restored to a likely pre-deformational stage can it be said to be balanced.

A geologic section is not proven balanced until the restored version is presented.

Technically, one is not initially interested in the deformation history or sequence of deformation events. Only the deformed and undeformed stages are considered. One can thus isolate different components of the deformation, such as rigid rotation, fault offset (block translations) and internal deformation of fault blocks (ductile deformation). It is also possible to start with an undeformed model and deform it until reaching something that looks like the interpreted section. This is not called balancing, but *forward modeling*.

There are several reasons why balancing and restoration is increasingly used. They help assure that the interpreted section or map is realistic and provide support for strain estimates as, for example, determining the amount of extension or shortening along a cross section. In the 1960's Dahlstrom and coworkers applied this tool to reconstruct sections in the Canadian Rocky Mountains prior to contraction, and calculated the amount of contraction involved. Later the same principles were used in areas of extension, such as the Basin and Range province and the North Sea rift. The Scottish geologist Alan Gibbs was one of the first to apply the principles of restoration to vertical sections from the North Sea rift.

A perfectly balanced section or map is not necessarily correct, but is likely to be more correct than a section that cannot be balanced.

So far we have talked about balancing and restoration of maps and profiles only. In fact, restoration and balancing can be done in one, two and three dimensions. One-dimensional restoration is known as line restoration, two-dimensional restoration is most commonly applied to cross sections, while three-dimensional restoration and balancing takes into account possible movements in all three dimensions.

1.2 One-dimensional restoration

The simplest form of restoration is to reconstruct how a mapped line was oriented and located before the deformation. The line could be the trace of bedding or some other geologic contact in a geologic section, typically an interpreted seismic marker on a seismic section through a faulted region. Boudinaged beds or linear features are other examples.

Preferentially we seek to study sections that contain the displacement vector or the maximum and/or minimum principal axes of the strain ellipsoid. For most contractional and extensional regimes, subhorizontal traces of layers fulfill this condition provided that the section contains the extension or contraction direction. A direct estimate of the amount of contraction or extension is the outcome of the restoration. In the following we shall consider a series of fault blocks separated by discrete faults.

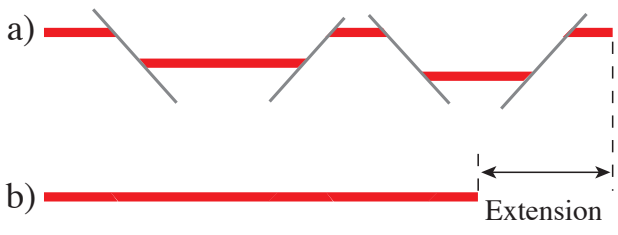

Figure 19.1 The concept of one-dimensional restoration where the marker is horizontal. In this case the line segments can be moved along the fault traces until they form a continuous layer. The extension is found by comparing the undeformed and the deformed state.

1 Ockham's Razor suggests that the less complicated interpretation is often more likely the correct one. Sometimes called the "Law of Parsimony"

CONDITIONS FOR BALANCING OF CROSS SECTIONS

- The interpretation is geologically sound
- The deformation is plane strain
- The section is in the direction of tectonic transport
- The choices of deformation (vertical shear, rigid rotation etc) must be reasonable and based on our general knowledge of deformation in the given tectonic setting
- The result must be geologically reasonable, based on independent observations and experience

1.2.1 Constant length restoration

The simplest form of line restoration assumes that the line's initial length is the same as its length after deformation. It has been extended or shortened only through the formation of separations or overlaps. This principle is called *constant length restoration* or balancing and is a useful first approach when a quick restoration is needed.

Constant length restoration works well when our layer has the same orientation before and after deformation, as shown in Figure 19.1. It is then an easy task to restore the line segments into a continuous horizontal line. The difference in length between the restored and the deformed state gives an estimate of extension (or contraction).

If the line (layer) was rotated during deformation we have to restore it to its original horizontal orientation. Rigid rotation of each line segment is the easiest approach. When the deformed line segments are curved, rigid body rotation cannot restore the line. The length of line segments is then likely to have changed from the undeformed to the deformed stage, and *variable-length restoration* must be considered.

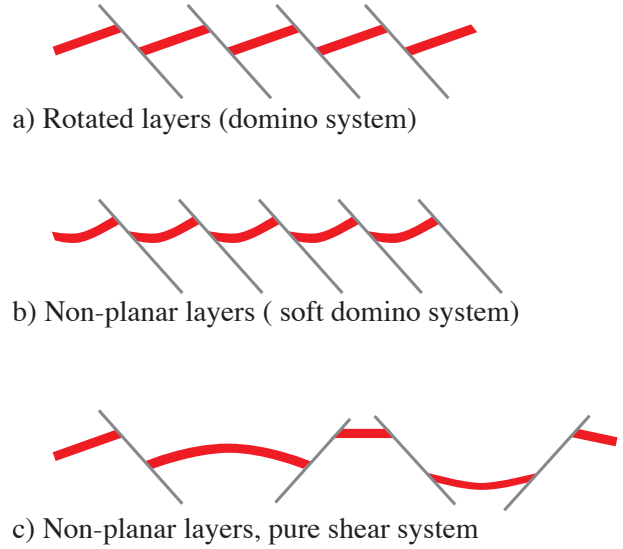

Figure 19.2 **a)** Rotated layers can be restored by rigid rotation and removal of fault displacement if layers are unfolded. b) and c) Folded layers must be restored by a penetrative (ductile) deformation such as vertical or inclined shear.

1.2.2 Variable length restoration

Non-planar layers (Figure 19.2) have changed from their original horizontal orientation and planar geometry[2]. The layers have experienced ductile or continuous deformation at the scale of observation. In most cases this implies a change in the length of the profiles, which in extensional regimes generally means extension of the layers. If the extension is small, then constant-length balancing may be an acceptable approximation. If not, some assumptions have to be made about the ductile deformation, i.e. continuous deformation between or away from faults.

A common assumption is that layers have been stretched and folded by simple shear. Heterogeneous vertical shear, where particles (e.g., sand grains) move along vertical lines, is the simplest model. Antithetic

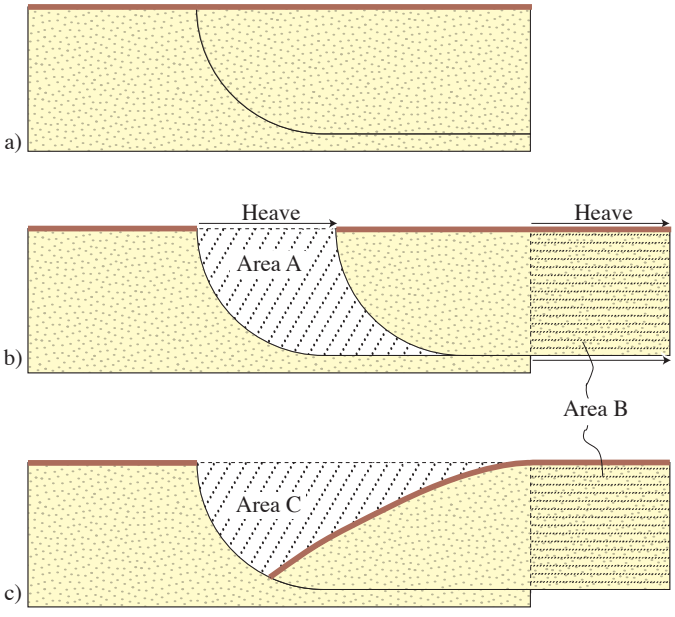

Figure 19.3 Constant area balancing of the hanging wall to a listric fault. Areas A, B and C must be identical for the section to balance. Note that the length of the layer increases in the hanging wall.

2 This could also be the case with planar layers, but it is more obvious if the deformed layers are curved

and synthetic shear are alternative models. We will return to this below.

Other assumptions that have been used to model deformation of the hanging wall of non-planar faults include constant displacement along the master fault and constant fault heave. We have already seen how displacement can be expected to vary along faults. Although these assumptions may work geometrically, they are geologically unsound except for very special cases. The use of different assumptions provides alternative explanations and highlights the uncertainties involved.

1.3 Two-dimensional restoration

Two-dimensional restoration involves restoration of two or more horizons or layers as well as the faults and folds that they portray. Some principles of section restoration are already touched upon in Chapter 16 and an example is given in Figure 16.5.

1.3.1 Preservation of area versus length

Most sections are restored using the assumption that the cross-sectional area and layer length is the same before and after deformation. Preservation of layer length is particularly useful during balancing of simple sections in fold- and thrust belts. In a contractional regime layer-parallel simple shear is common, localized to weak layers or along layer interfaces. Layer-parallel shear preserves both bed length and area. Even if layers start to fold, layer-parallel shear is realistic in the form of flexural slip or flexural shear. These are realistic fold mechanisms that preserve both layer length and area.

In extensional regimes layer-parallel shear is less common, although it may occur. Simple shear across the layering, such as distributed vertical shear, is a better approximation. This type of deformation changes the layer length, but preserves area. That is why the assumption of constant area in extensional regimes is more realistic than that of preservation of bed length, particular where deformation is associated with listric extensional faults (Figure 19.3).

1.3.2 The effect of compaction

Constant area implies that area is conserved even though the shape of a given area may change during deformation. However, compaction, which is dilation by vertical shortening, may occur during as well as after tectonic deformation. Its effect is significant for shallow deformation of porous rocks. Growth faults in sand-shale sequences are an extreme example. In this case the fault dip decreases downward as a result of compaction (Figure 19.4).

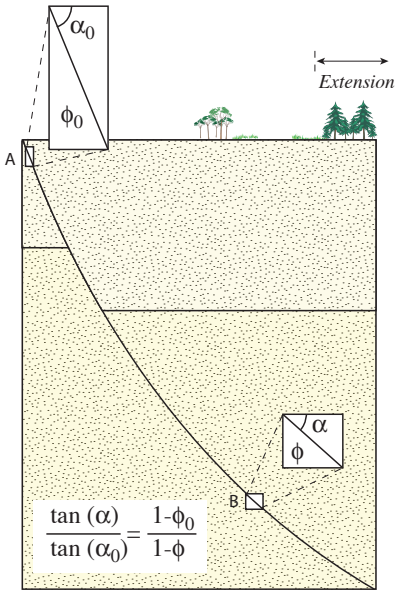

Figure 19.4 The effect of compaction on the geometry of synsedimentary faults (growth faults). The fault dip gets lower at depth because of higher cumulative compaction. Knowledge of the original porosity can be used to calculate the original fault dip at any point along the fault. ϕ_0 is typically around 0.4 (40%) for sandstone and 65-70% for clay. Note that there may be other reasons why some faults flatten with depth.

Compaction also has a geometric effect on faults in a sedimentary sequence. When faults get buried, their upper parts of the faults compact more than their lower parts. This effect changes an initially planar fault into a gently antilistric geometry (Figure 19.5).

Additionally, sand compacts less than mud and clay. Clay has an initial porosity close to 70%, while that of sand is around 40%. So if a fault forms in a recently deposited sand-clay sequence, subsequent compaction will give the fault a lower dip in the more compacted clay layers than in sand layers.

There is also the effect of differential compaction on each side of a fault. If the offset on a fault becomes

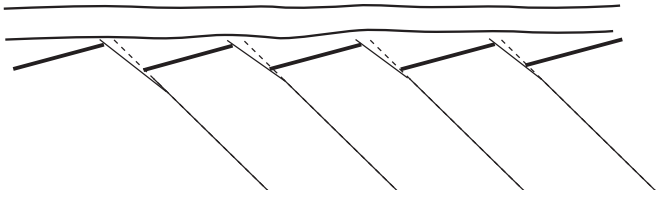

Figure 19.5 Post-tectonic compaction is largest in the upper part of a sedimentary sequence. The reduction of the dip of the faults will therefore be greater in the shallow part. An initially straight fault wil therefore flatten towards the top due to differential compaction.

WHAT DOES VERTICAL AND INCLINED SHEAR REALLY MEAN?

The disributed or ductile deformation of layers in a deformed section can be modeled in many ways. It is convenient to use simple shear, and the variables are shear strain and the inclination of the shear plane, referred to as the *shear angle*. At the scale of a seismic or geologic section, we may not be able to see the deformation structures that make a layer look non-planar. The structures may be sumseismic faults, deformation bands, extension fractures or microscale reorganization structures. Hence, the deformation is ductile at our scale of observation, and their effects are modeled by simple shear.

It is sometimes claimed that the orientation of small faults in the hanging wall represent a guide to the choice of shear angle. The two figures below show hanging walls with small-scale faults that are mostly synthetic to the main fault. However, their arrangements call for antithetic shear, as shown by yellow arrows. These examples illustrate the difficulty involved in using small faults to determine the shear angle.

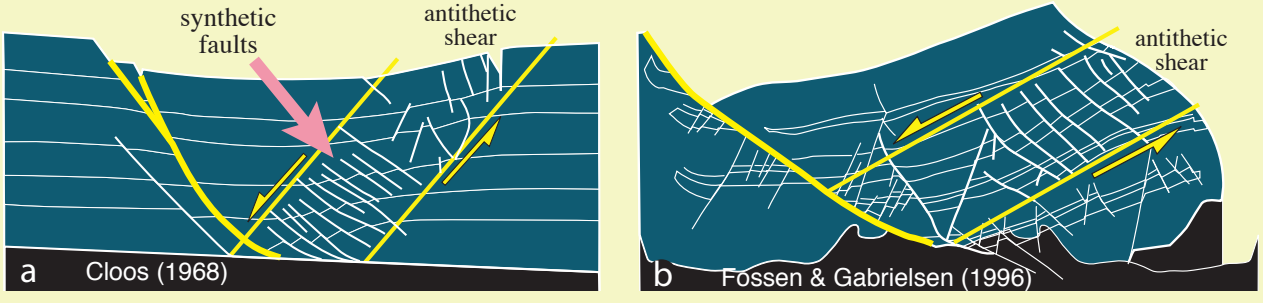

large, say some hundred meters or more, then the hanging wall layers will compact more than those in the adjacent footwall, simply because the footwall layers have already been compacted to a larger extent or are crystalline rocks. For dipping extensional faults, the result is a hanging wall syncline, as shown in Figure 19.6.

Most balancing programs utilize compaction curves for various lithologies that remove the effect of compaction during restoration.

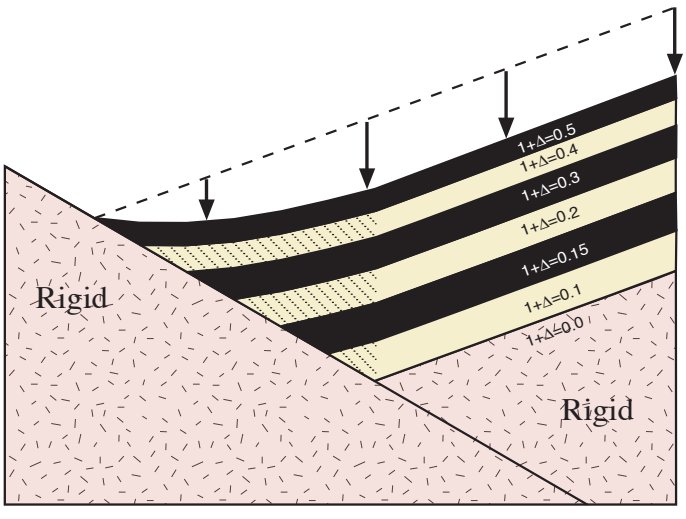

Figure 19.6 If the hanging wall compacts more than the footwall, a compaction syncline arises. In the example shown here the hanging wall is assumed to be rigid while hanging-wall layers compact from 50% in the topmost layer down to 10% in the lower layer above the rigid basement.

1.3.3 Shear angle and trishear

Constant area-deformation of the hanging wall of a listric fault was first modeled by means of vertical shear. This is sometimes referred to as the Chevron method, named for the oil company that first utilized the method. Vertical shear involves no extension or shortening in the horizontal direction, but individual layers will be extended, rotated and thinned.

It was soon realized that the hanging-wall shear deformation could deviate from vertical. Both antithetic (shear plane dipping against the main fault) and synthetic shear were evaluated. The differences between the two are illustrated in Figure 19.7. Choosing the right shear angle is not easy, and we commonly have to try and fail before making the choice. It seems that antithetic shear with a shear angle of around 60° works well in many deformed hanging walls above listric faults. Vertical shear may be more realistic when considering large parts of the crust. Synthetic shear works in cases where faults steepen downward (antilistric faults, Figure 19.8).

Synthetic shear also applies where a hanging-

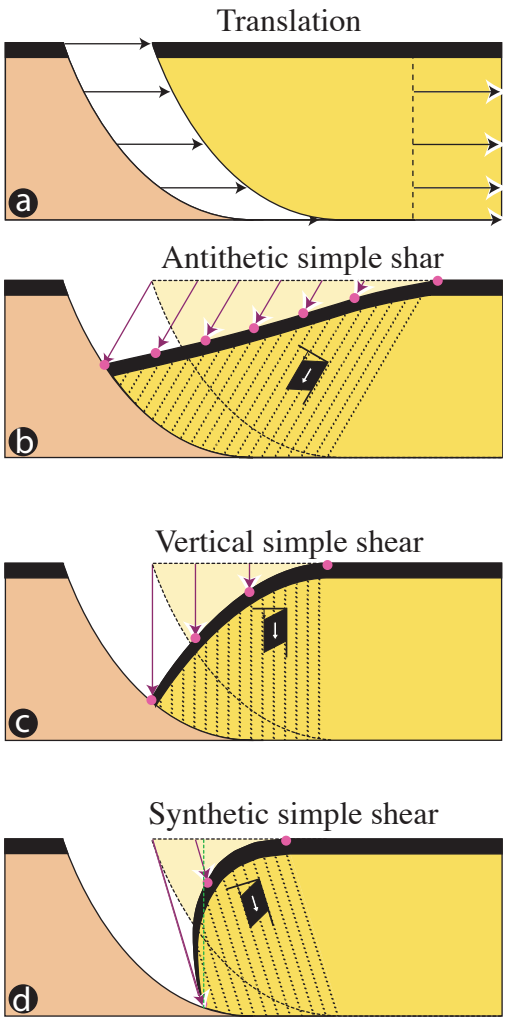

Figure 19.7 a) Deformation of the hanging wall above a listric fault. a) Pure translation. b-d) Antithetic, vertical and synthetic shear. Note the different hanging-wall geometries and the fact that the shear only affects the left part of the hanging wall.

wall syncline is developed, as shown in Figure 19.9. However, in cases where the syncline widens upward, trishear (p. ?) may be a more realistic alternative (Figure 19.10). Trishear has no fixed shear angle, but represents a mobile triangular deformation zone. The zone is located in front of the fault tip and is considered a ductile process zone. Trishear is an interesting model that explains local drag structures and folding of layers around faults, but is not applicable to entire regional sections, as is vertical or inclined shear. However, it is possible to combine general vertical shear throughout a cross section and apply local trishear to certain faults within that section.

1.3.4 Finding fault geometry from hanging-wall layers

At shallow levels in rift systems it is common

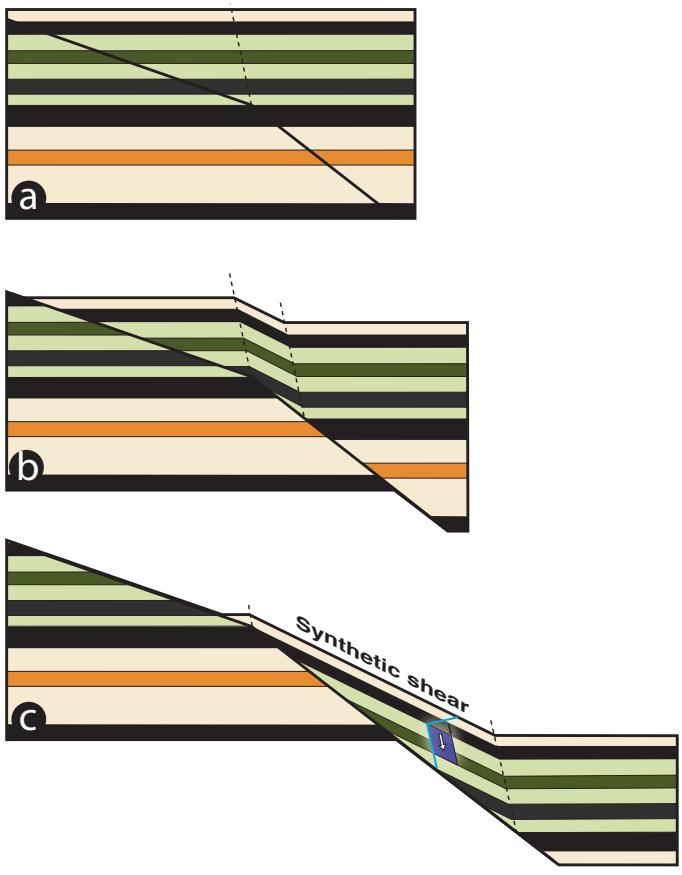

Figure 19.8 Local synthetic shear in the hanging wall to a normal fault. The simple shear is related to the downward steepening of the fault.

to see reflectors in seismic sections offset by a fault, while the fault geometry at depth remains unclear, but the direct relationship between fault geometry and layer geometry provides important insight. Where the hanging wall reflectors are curved, the fault is also likely to be curved. Hence, we can use the shape of the layers to calculate the shape of the fault and, in the case of a roll-over structure, to estimate the depth to the detachment.

There is a direct relationship between fault

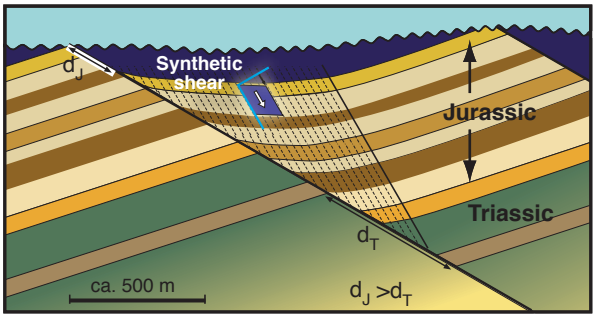

Figure 20.9 Example of synthetic shear, used to model the hanging wall synclines in soft domino systems of the North Sea. Based on Fossen & Hesthammer (1998b).

geometry and hanging-wall deformation for non-planar faults

We do, however, need to choose a model for hanging-wall deformation, and the result will be different for synthetic, vertical and antithetic shear angles. Vertical shear gives a deeper detachment than antithetic shear (Figure 19.11), but the amount of extension involved will be greater for antithetic shear. If, in some cases, we have information from both hanging-wall and fault geometries, we can find the shear angle that balances the section. For most antithetic cases, a 60° shear angle is commonly found, supporting antithetic shear as a reasonable assumption.

1.3.5 Restoration in map view

A mapped horizon that has been affected by extensional faulting is portrayed as a series of isolated fault blocks, by contractional faulting as overlapping fault blocks, or a combination of both. If we consider a case of extensional faulting (Figure 19.12a), the separation between the blocks reflects the amount of extension. It is reminiscent of a jigsaw puzzle, and the restoration involves putting the pieces back to their pre-deformational positions (Figure 19.12b).

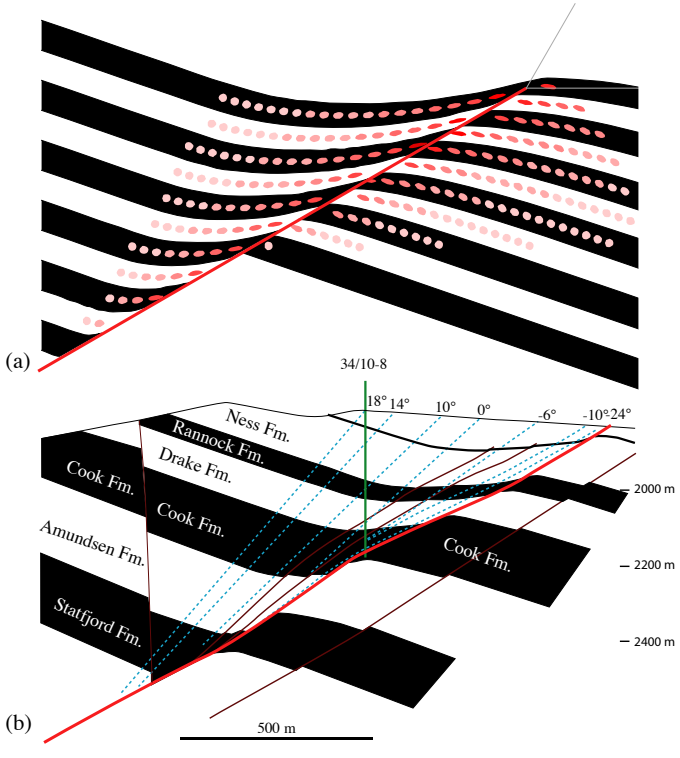

Figure 19.10 (a) Trishear applied to a gently dipping normal fault that has propagated up-section. A hanging-wall syncline forms, similar to the one shown in Figure 19.9. b) Example from the Gullfaks Field, North Sea, constrained by seismic and well data.

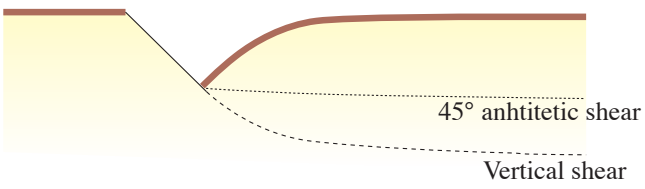

Figure 19.11 Example of a curved hanging wall layer. The shape of the layer reflect the fault geometry at depth. However, the choice of shear angle influences the estimated fault geometry. The difference is here illustrated for antithetic and vertical shear. From White et al. (1986).

The goal is to restore the "puzzle" to the state where the amount of "openings and overlaps" is minimized, either manually or by computer. If the blocks involve no internal deformation and the layering is horizontal, reconstruction is relatively simple.

Under other, more realistic, situtations, where layers are planar but not horizontal, rigid-body rotation of the blocks may be necessary. If layers are non-planar, then the surface should be unfolded or additional errors may be introduced. The choice of strain model may not be easy—are points on the surface to be projected back to the horizontal plane by oblique or vertical shear? If constant surface area is assumed, a flexural slip fold model is implied – are the curvatures involved small enough that they can be neglected? In spite of these potential inaccuracies, the outcome is often still quite useful in the final interpretation.

Map restoration provides abundant useful information. The displacement field emerges by connecting the locations of points before and after deformation, (Figure 19.12c). The orientation of displacement vectors allows the distinction between plane and non-plane strain (parallel displacement vectors vs. diverging vectors, respecitvely) and an assessment of the influence of gravity during deformation. Additionally, if non-plane strain, area will not be conserved in any cross section through the deformed volume, and cross-sections will not balance. If the strain is plane, then sections chosen for cross-section balancing must be oriented parallel to the displacement vectors.

Some important outcomes from map restoration include the following. Relative movement of points on each side of faults will give the local displacement vector of the fault (Figure 19.12d). The nature of slip (dip slip, oblique slip, strike-slip etc.) on faults is thereby revealed and the amount of rotation of blocks about the vertical axis also emerges from map restoration (Figure 19.12e). The amount of strain in any horizontal direction will also be apparent. Finally, the gap and/or overlap areas provides an idea about

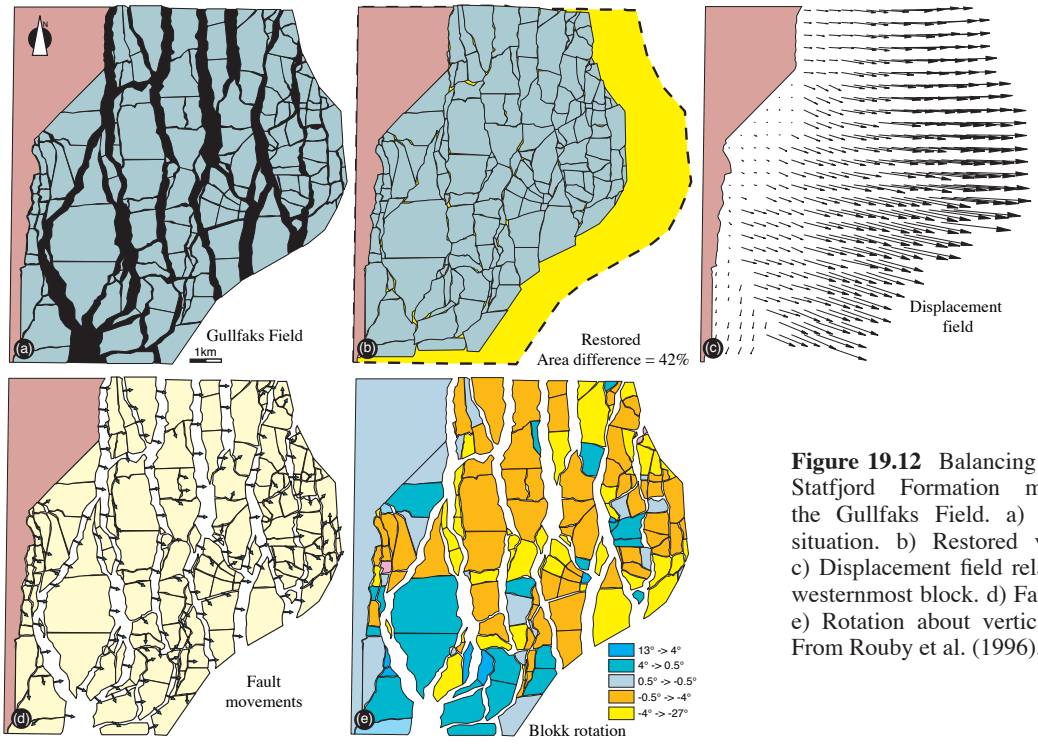

Figure 19.12 Balancing of the Statfjord Formation map of the Gullfaks Field. a) Present situation. b) Restored version. c) Displacement field relative to westernmost block. d) Fault slip. e) Rotation about vertical axis. From Rouby et al. (1996).

the consistency of the restoration and reliability of the interpretation.

1.4 Reconstruction in three dimensions

Map restoration is sometimes described three-dimensionally. However, true three-dimensional restoration involves volume, and means simultaneous map-view and cross section restoration. Fault blocks are considered as three-dimensional objects that can be moved around and deformed internally, but not independent of each other. Three-dimensional restoration is inherently difficult, and is beyond the scope of this book.

Each surface is mathematically treated as a mesh of triangles or other polygons that can be deformed. Using vertical shear, it is like holding a handful of pencils that connect different surfaces, where each pencil is free to move a slightly different amount than its neighbors. The advantage of three-dimensional restoration is the opportunity to account for both planar and non-planar strain. Of the many inherent problems, the many choices involved and the time required to set up and run make simpler forms of restoration preferred. They may not be as accurate, but they provide very important information without involving too much work.

Further reading:

Dahlstrom, C.D.A., 1969. Balanced cross sections. Can. J. Earth Sci., 6: 743-757.

Gayer, R.A., Rice, A.H.N., Roberts, D., Townsend, C. & Welbon, A., 1987. Restoration of the Caledonian Baltoscandian margin from balanced cross-sections: the problem of excess continental crust. Transactions of the Royal Society of Edinbourgh: Earth Sciences, 78: 197-217.

Gibbs, A.D., 1983. Balanced cross-section construction from seismic sections in areas of extensional tectonics. Journal of Structural Geology, 5(2): 153-160.

Hossack, J.R., 1979. The use of balanced cross-sections in the calculation of orogenic contraction: a review. Journal of the Geological Society, 136: 705-711.

de Matos, R.M.D., 1993. Geometry of the hanging wall above a system of listric normal faults - a numerical solution. American Association of Petroleum Geologists, 77: 1839-1859.

Morley, C.K., 1986. The Caledonian thrust front and palinspastic restorations in the southern Norwegian Caledonides. Journal of Structural Geology, 8: 753-766.

Morris, A.P. & Ferrill, D.A., 1999. Constant-thickness deformation above curved normal faults. Journal of Structural Geology, 21: 67-83.

Mount, V.S., Suppe, J. & Hook, S.C., 1990. A forward modeling strategy for balancing cross sections. American Association of Petroleum Geologists,

74: 521-531.

Nunns, A., 1991. Structural restoration of seismic and geologic sections in extensional regimes. American Association of Petroleum Geologists, 75: 278-297.

Rouby, D., Fossen, H. & Cobbold, P., 1996. Extension, displacement, and block rotation in the larger Gullfaks area, northern North Sea: determined from map view restoration. American Association of Petroleum Geologists, 80: 875-890.

Rouby, D., Xiao, H. & Suppe, J., 2000. 3-D Restoration of complexly folded and faulted surfaces using multiple unfolding mechanisms. American Association of Petroleum Geologists Bulletin, 84: 805-829.

Rowan, M.G., 1993. A systematic technique for sequential restoration of salt structures. Tectonophysics, 228: 331-348.

Westaway, R. & Kusznir, N., 1993. Fault and bed "rotation" during continental extension: block rotation or vertical shear? Journal of Structural Geology, 15: 753-770.

Winterfield, C.V. & Oncken, O., 1995. Non-plane strain in section balancing: calculation of restoration parameters. Journal of Structural Geology, 17: 447-450.

Withjack, M.O. & Peterson, E.T., 1993. Prediction of normal-fault geometries - a sensitivity analysis. American Association of Petroleum Geologists, 77: 1860-1873.

Woodward, N.B., Boyer, S.E. & Suppe, J., 1989. Balanced geological cross-sections: An essential technique in geological research and exploration. Short course in geology, AGU, 6: 132 s.

Woodward, N.B., Gray, D.R. & Spears, D.B., 1986. Including strain data in balanced cross-sections. Journal of Structural Geology, 8: 313-324.

CHAPTER ??

Salt tectonics

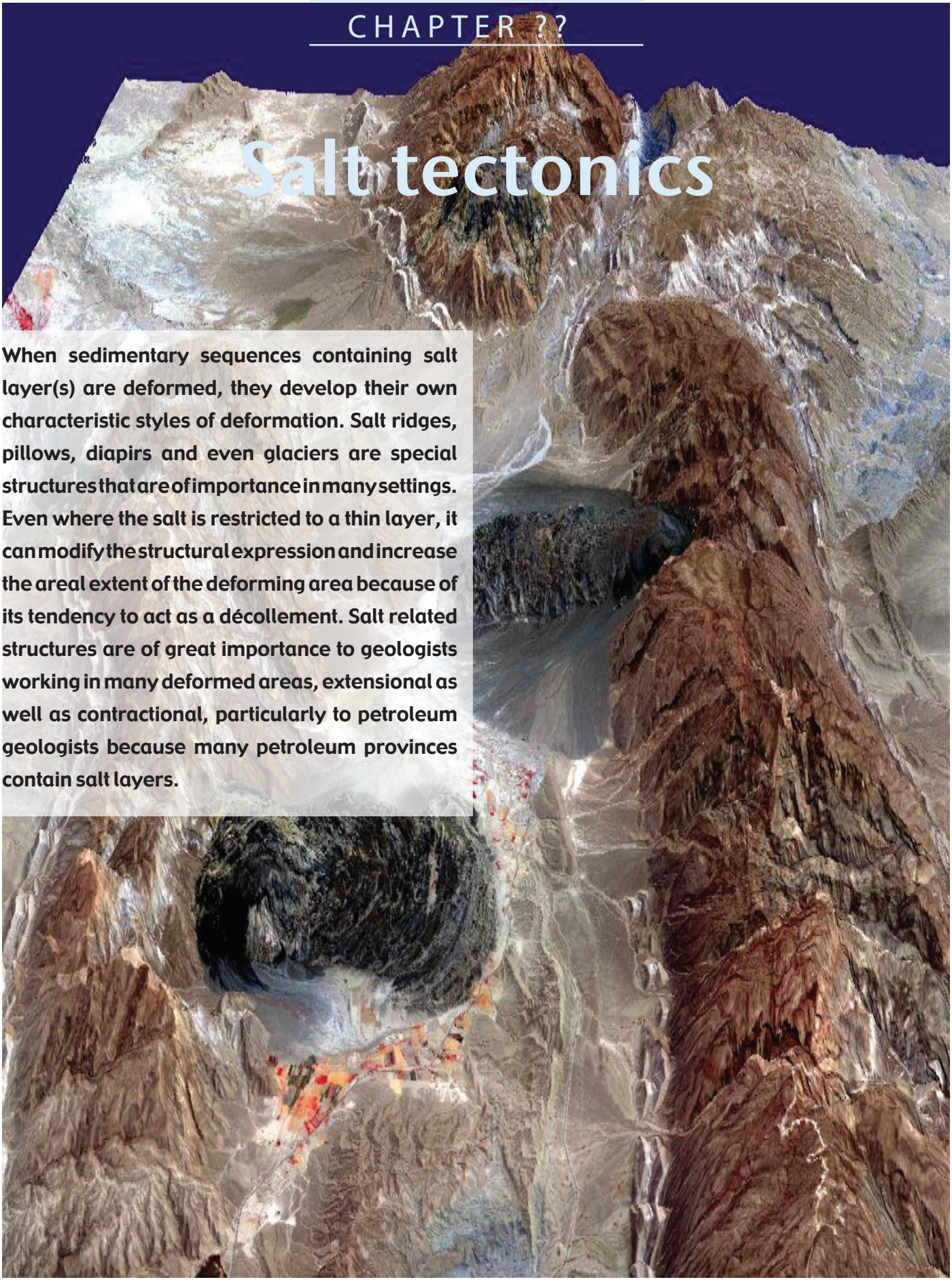

When sedimentary sequences containing salt layer(s) are deformed, they develop their own characteristic styles of deformation. Salt ridges, pillows, diapirs and even glaciers are special structures that are of importance in many settings. Even where the salt is restricted to a thin layer, it can modify the structural expression and increase the areal extent of the deforming area because of its tendency to act as a décollement. Salt related structures are of great importance to geologists working in many deformed areas, extensional as well as contractional, particularly to petroleum geologists because many petroleum provinces contain salt layers.

1.1 Introduction

Salt layers form integral parts of the stratigraphic column in many sedimentary basins (Fig. X.1), including cratonic basins, rift basins, passive margin basins and foreland basins, and plays a significant role when salt-bearing sedimentary basins are exposed to deformation, be it in an extensional, contractional or strike-slip setting. We use the term *salt tectonics* when salt is involved in deformation to the extent that it influences the type, geometry, localization and/or extent of deformation structures that form. This term covers any salt-related deformation and deformation structures, including salt detachment-related deformation, while the term *halokinesis*, formed by the greek words for salt or halite (halos) and movement (kinesis), is merely the study of the mechanisms and structures caused by vertical salt movement in the upper crust.

The influence of salt during deformation depends on its thickness, extent and position in the stratigraphic column, the degree of basement reactivation and the physical properties of the overlying strata. The deformation can be local and unrelated to plate-tectonic strain, completely driven by density contrasts between the salt and its overburden. In other cases, and perhaps more commonly, salt plays a more passive or reactive role in a region under influence of a regional tectonic stress field. In this chapter we will look at some of the most common structures associated with salt movement, after a quick look at what makes salt so special.

1.2 Salt properties and rheology

Salt has physical and rheological properties that make it fundamentally different from most other common rocks. First of all, pure halite[1] has the relatively low density of 2.160 g/cm^3. This makes salt less dense than most carbonate rocks, but denser than recently deposited siliciclastic sediments. However, as sediments compact physically and chemically during burial, their density increases with increasing burial depth. Salt, which is more or less nonporous in the first place, is almost incompressible and hence does not become much denser with increasing overburden. Thus, a density inversion occurs once the compacting overburden becomes denser than the salt. At that point a gravitationally unstable situation is established which, under certain conditions, can result in flow of salt towards the surface.

SALT PROPERTIES

-Common constituent of sedimentary basins
-Mechanically very weak
-Low density
-High heat conductivity
-Almost incompressible
-Impermeable
-Viscous, behaves like a fluid
-Causes wide areas of deformation
-Enhances horizontal detachments
-Creates structural fluid traps

The buoyancy of a salt layer is controlled by the density of its overburden. Compaction of the overburden during burial increases its density, and at depths of 1-2 km siliciclastic sediments tend to have densities in excess of 2.2 g/cm^3. This depth depends on the type of sediment, and for siliciclastic sediments clay compacts faster than sand. Simple calculations can be performed by summing the density of the rock minerals (ρ_s) and that of the pore fluid (ρ_f):

$$\rho = \Phi\rho_f + (1-\Phi)\rho_s$$

In this formula the porosity (Φ) reflects the compaction. For a silisiclastic

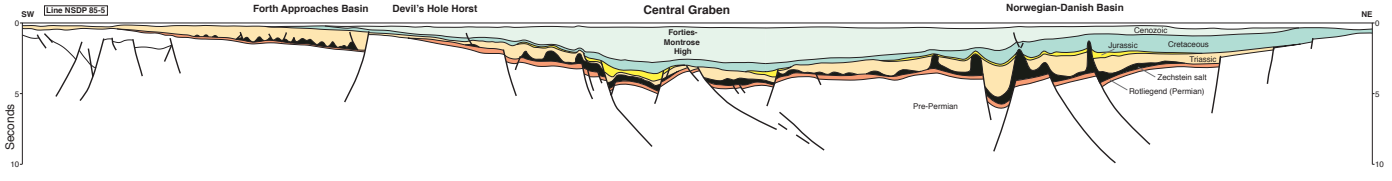

Figure X.1 Crossection (interpreted seismic line) through the southern North Sea, showing the Permian salt in black. Location shown in Fig. ?. From Zanella, Coward & McGrandle 2003). The location of the central part of this profile is shown in Fig. 12.NS MAP

1 In general, salt layers tend to be impure, and include other minerals such as anhydrite, gypsum and clay minerals.

of 30% porosity, a density of 2.7 g/cm^3, and with salt pore water (1.04 g/cm^3), the rock density is approximately the same as somewhat impure salt (2.2 g/cm^3). Hence, a porosity lower than 30% is required for the overburden to become denser than the salt. This occurs at lower depths if the sediment is finegrained, perhaps as little as a few hundred meters, while some sandstones have a porosity of 30% at 2 km depth. Thus, the depth at which salt can start to rise depends on the local properties of the sedimentary sequence overlying any given salt layers.

For salt to reach the surface by buoyancy alone, it is required that the average density of the *entire* siliciclastic overburden exceeds that of salt. This requires at least 1600 m, and more commonly more than 3000 m of overburden.

Salt layers become buoyant and gravitationally unstable when buried to the depth where the overburden is denser than the salt, and can then potentially start to flow.

Rheologically, salt deforms plastically during loading even at surface conditions. Only if strain rates become high, such as those associated with earthquakes and mining (or when hit by a hammer), salt will fracture. Under most other geologic conditions, salt will flow as a viscoelastic medium. This is why salt mines are being used as (nuclear) waste repositories.

The elastic component of salt deformation can be neglected for most purposes because of the low relaxation rates involved, and the flow can be considered viscous. In more detail, two deformation mechanisms dominate salt deformation; wet diffusion and dislocation creep. Wet diffusion (p. ...) is the dominating deformation mechanism when there is some water present in the salt, which is usually the case in a buried stratigraphic sequence. Since wet diffusion involves transport along grain boundaries and surface area increases with decreasing grain size, wet diffusion is generally faster and thus more important in fine-grained than coarse-grained salt. Low strain rate and differential stresses also promote wet diffusion. Dry salt, with no fluids to transport matter, is different. In that case dislocation creep is the principal deformation mechanism. Either of these deformation mechanisms is easily activated in salt, meaning that salt has very low yield strength and thus flows very easily. Together with the fact that salt is almost incompressible under most geologic conditions, this means that salt can be treated as a fluid in geologic modeling.

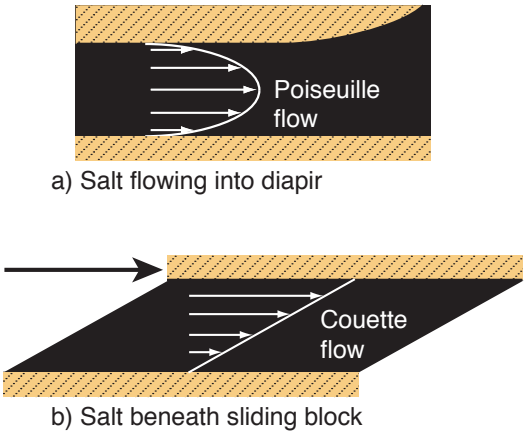

Figure X.3 The two principal types of flow occuring in deforming salt layers Arrows indicate velocity and the velocity profile is parabolic in a) and linear in b).

1.3 Salt diapirism, salt geometry and the flow of salt

Salt structures

Salt volumes in the crust has for along time been

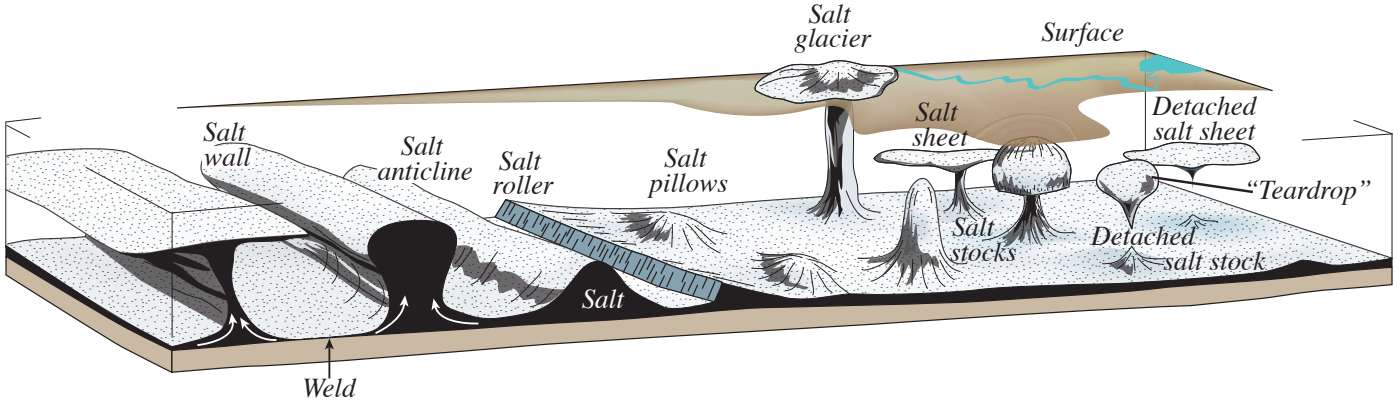

Figure X.2 Shapes of salt structures and their names. Maturity increases from the central part of the figure to the left and right.

known to take on a variety of geometric shapes, from elongated structures such as salt anticlines and salt pillows to more localized structures such as salt stocks (Fig. X.2). Many of these structures are referred to as diapirs. The term *diapir* derives from the greek words for through (dia) and pierce (peran) and is used in geology about a body, usually of salt, magma or water saturated mud or sand, that gravitationally moves upward and intrude the overburden. Hence, some structures such as *salt pillows* and *salt anticlines* that just bend and uplift the overlying layers are not diapirs sensu stricto, because they do not intrude or pierce the overburden. However, most of these structures represent various stages that could (have) lead to the formation of a true diapir. The process through which a diapir develops is known as *diapirism*.

A salt diapir is a mass of salt that has flowed upward into the overburden.

The flow of salt from a layer into a salt structure is usually referred to as *salt withdrawal* or, although *salt expulsion* would be a physically more correct term. In simple terms, there are two principal types of flow. One (*Poiseuille flow*) occurs when salt flows into a salt structure during the growth of a salt anticline or diapir (Fig. X.3a). In this case flow is restricted by the viscous shear forces acting along the boundaries of the salt, an effect known as *boundary drag*. This effect causes the salt to flow faster in the central part of the salt layer than along the top and bottom. Hence, thin salt layers flow slower than thick ones, implying that flow in a thick (tens of meters or more) salt layer may become significantly slowed down when the salt is reduced to a thin (e.g. a few tens of meters thick) layer. If the salt becomes completely exhausted the boundary layers become attached to each other, and the contact is referred to as a *salt weld* (Fig. X.2). A salt weld may pin salt anticlines and domes, and thus terminate the growth of salt structures.

The other type of flow is known as *Couette flow* (Fig. X.3b), and occurs in a simple shear-type deformation within the salt layer as the overburden is translated relative to the substrate. This type of flow is typical for salt layers acting as décollement, however the two types of flows can be superposed on each other. Ideally, in Couette flow there is no boundary effect of the type occurring in Poiseuille flow.

Salt diapir geometries

Salt diapirs can take on a variety of forms. In plan view they may be elongated, typically along

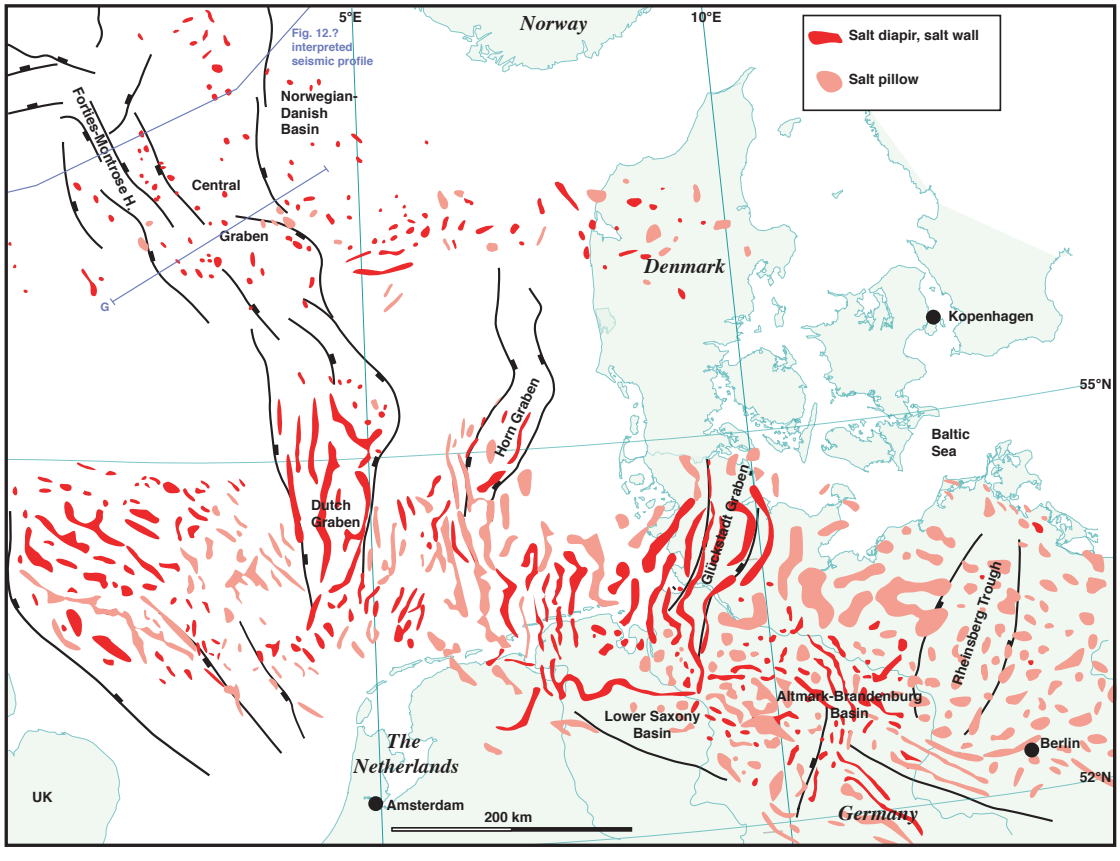

Figure X.4 Map of salt structures and the main faults of the southern North Sea basin and northern Europe. Note close connection

the direction of regional faulting or graben axis, or they may be circular (Fig. X.4 and X.5). Some portray a triangular geometry in crossections, with the salt thinning upward. This is common where salt structures are connected with faults in the overburden (see reactive salt structures below). If they rather stand up with a more or less cylindrical shape they are known as *salt stocks* (Fig. X.6). However, many diapirs have a stem and a wider upper part, known as the *bulb*. In extreme cases the stem may be missing, so that the salt bulb is completely detached from its source layer. Such isolated salt bulbs are sometimes called *teardrop diapirs*. Diapirs can also flatten out and join at one and sometimes several stratigraphic levels, forming various types of *salt stock canopies*.

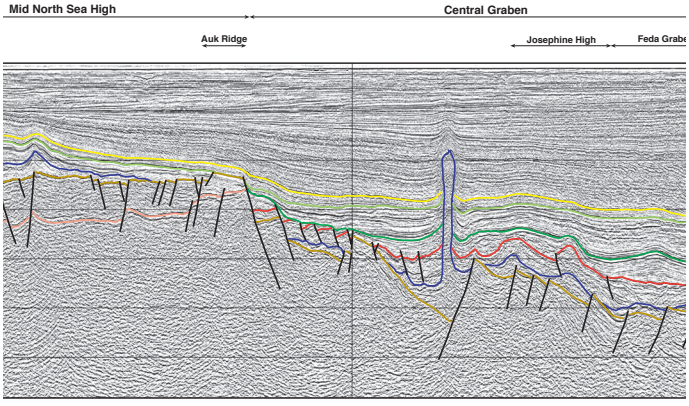

Figure X.6 Profile G in Fig. MAP. From

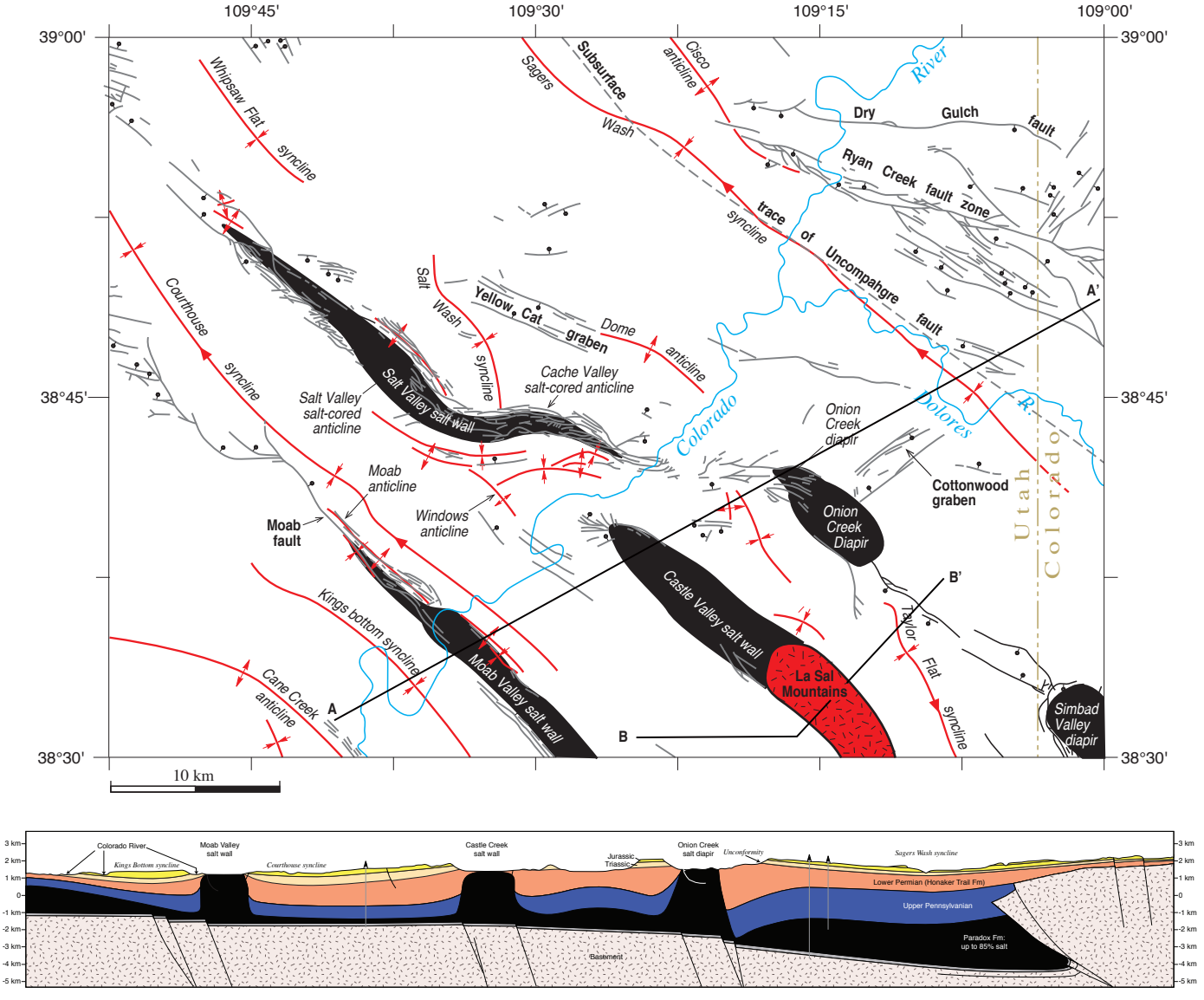

Figure X.5 Salt structures in the Moab area of SE Utah in map view and crossection. Elongated salt walls dominate, but more circular diapirs also occur. The salt walls seem to follow the trend of long-lived faults in the basement, but younger collapse-related faults occur in the overburden. Did these salt structures initiate and grow during contraction or extension? Simple questions are sometimes hard to answer.

SALT OR IMPACT STRUCTURE?

It can be difficult to decide whether a circular structure is salt diapir-related structure or an impact structure. Both mechanisms produce circular structures with faults, disturbed stratigraphy etc.

Upheaval Dome in Canyonlands National Park, Utah, is one such example. It is located in the marginal parts of the Paradox Basin, which contains salt of Carboniferous age. Salt movement in this area has caused a series of salt anticlines, notably in the Moab and Arches National Park area, but circular structures of the Upheaval Dome type are absent.

Silverpit "Crater" is a similar structure in the North Sea, identified from seismic interpretation as a depression containing circular faults (ring faults). It has also been claimed to be an impact as well as a salt structure, and the issue is far from settled. So how do we separate between impact and salt diapir structures?

The best structure to look for is perhaps evidence of shocked quartz, planar deformation lamellae that are diagnostic of the high pressure deformation related to a meteor impact event. The lamellae are bands of dislocations arranged in crystallographic directions, and can be seen under the Transmission Electron Microscop. Such lamellae have been reported from the Upheaval Dome structure (Buchner and Kenkmann 2008), supporting the view that this is primarily an impact structure rather than a salt structure.

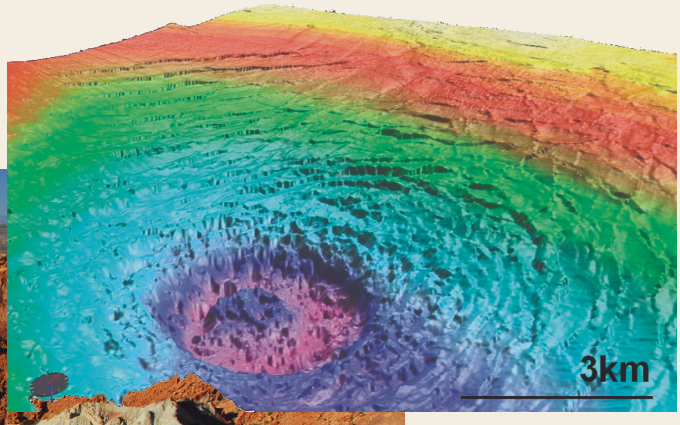

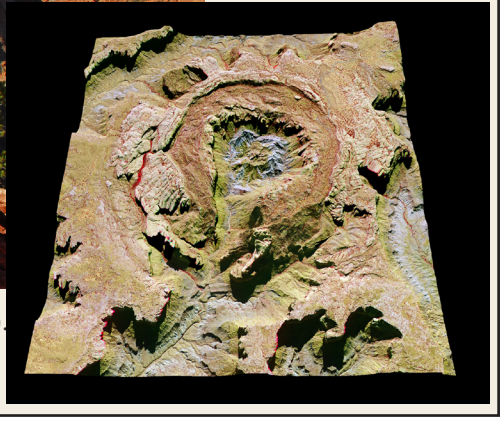

Upper right: Seismic interpretation of the Silverpit structure (Stewart & Allen, 2005). Above: Central part of Upheaval Dome, Utah. Right: Terrain model of Upheaval Dome.

Modeling salt diapirs

Early workers noted the role of the density contrast between salt and the overburden and the ability for salt to flow even at geologically low temperatures. They modeled not only the salt, but also the overlying denser sediments as fluids. By means of the sentrifuge and other experimental setups, diapirs very similar to salt diapirs observed in the upper crust were produced. In fluid experiments, the dense fluid ("sediments") will sink into the underlying less dense fluid ("salt"). A gradual development of diapirs can be produced in this way, from open anticlines or pillows to isolated volumes of salt that intrude the overburden[2].

There is now general consensus that modeling the overburden as a fluid is a gross oversimplification. Fluids have no shear strength, whereas actual rocks and sediments do. Hence, the ability of salt to ascend and the geometry of the resulting salt structure depend largely on the strength of the overburden and how it deforms, as will be explored later in this chapter. In fact, also salt has shear strength, but it is small compared to other rocks and sediments. For this reason, physical models where silicone gel represents the salt and sand is used as overburden have successfully been used over the past few decades.

2 If the overburden behaves like a perfect fluid, it does not break but simply thin during the rise of the salt. In this special case the salt structure is not a diapir sensu stricto.

Controls on salt flow

Even though salt overlain by denser layers represents a gravitationally instable situation, the salt will not move unless there is a gravitational or mechanical anomaly of some kind. *Differential loading* is a common factor that can cause salt to move. If an area for some reason is more heavily loaded than its circumference, the salt starts to flow away from the area of maximum loading. This difference can, for example, be caused by a lateral variation in overburden thickness and/or slope (Fig. X7a) or by variations in lithology and rock density (sedimentary facies variations, local occurrence of lava etc.). Also, a difference in elevation can trigger salt flow, as indicated in Fig. X.7b.

While salt can flow solely in response to vertical loading, salt structures are commonly associated with faults and folds, indicating that tectonic strain played a role during salt movement. If a salt body is shortened, the weak salt is likely to flow upward and shorten in the horizontal direction, like toothpaste being squeezed from a tube. In the case of regional extension, horizontal stretching or unloading causes the salt to expand laterally and thin vertically. In this simple model the boundaries on each side of our salt body control the flow of salt, and this boundary effect can be referred to as *displacement loading*.

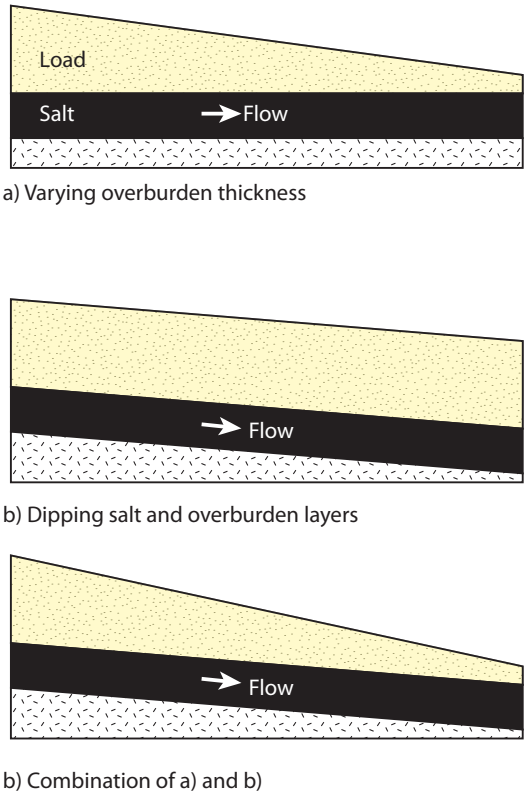

Figure X.7 Situations where salt can flow because of differences in overburden thickness or pressure (a) and elevation (b). The models have restricted (pinned) ends so that the overburden cannot slide on the salt.

Thermal loading refers to the fact that hot salt expands and becomes more buoyant. This can accelerate salt flow towards the surface. It has also been suggested that thermal loading can result in convection (hot salt rising and cool salt sinking within the salt structure). This may not be an important process in most salt structures, but could explain some peculiarly coiled salt structures (vortex structures) found in Iran FIGURE HERE?.

For a salt structure to initiate it has to overcome the strength of its roof. As discussed above, sedimentary layers become denser with burial and lithification, and thereby create the density inversion required for gravity-driven salt movement. At the same time the strength of the overburden increases

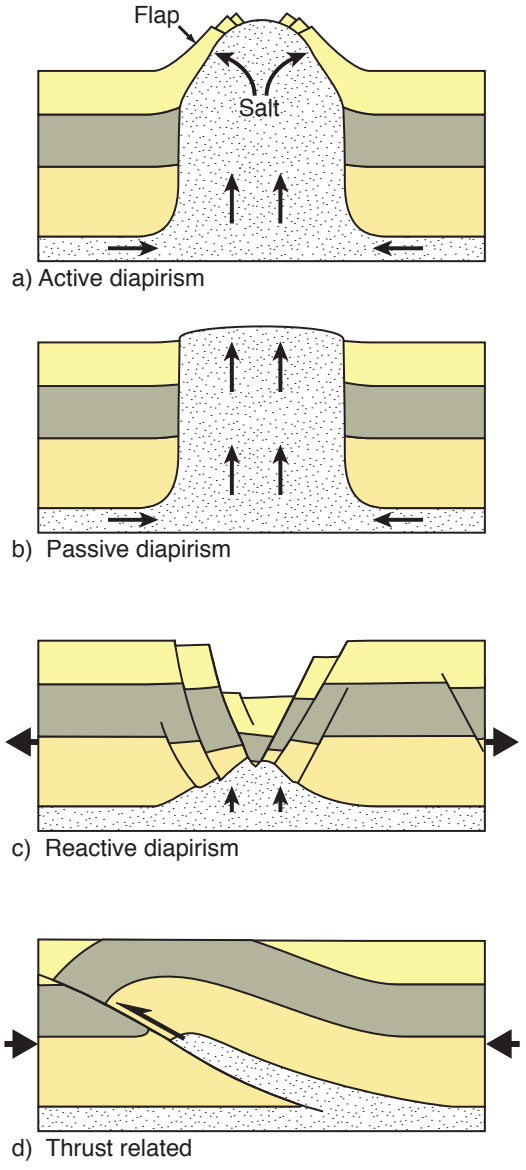

Figure X.8 Main classes of diapirs and diapirism. a) Actively, driven by density contrast and forceful ascent of salt (bouyancy), b) passively as sediments are deposited around the salt structure, c) Reactive, or in response to extension, and d) salt movement in hanging wall of thrust fault during contraction.

during lithification, making it harder for salt to move upward. Is it at all possible for a salt layer to break through lithified roof rocks? Physical considerations tell us that it is very unlikely to happen without assistance from tectonic faulting or fracturing, except for rare cases where the roof contains enough halite or gypsum to behave ductilely.

Salt diapirism usually requires weakening of the roof through fracturing and faulting.

Subsidiary structures associated with salt structures

Salt flow may affect the wall rock, simply because of the friction between the flowing salt and its surroundings. Hence, synclines or so-called flaps, which is layers that forcefully have been bent upward during diapirism (Fig. X.8a), may develop along the steep walls of salt structures. These are true drag folds in the sense that they grow during salt movement. However, since salt is almost incompressible while other sediments compact, differential compaction can cause apparent drag along upward-thinning salt structures. Whether there is a forceful effect of the salt on the walls in a diapir depends on the process of diapirism – as will be discussed in the next section.

Above a salt structure is a gentle dome structure in most cases (Fig. X.9), which again could be related to compaction as well as salt growth. Faults above the top of a salt diapir are common, and in most cases these are normal faults that form as the layers are bent and stretched during salt movement. However, in rare cases reverse faults can occur above the margins of salt diapirs due to forceful jacking of the roof by the salt. In either case, faults above salt structures tend to reflect the map-view geometry of the salt structure, so that circular diapirs develop circular patterns of faults, while elliptical diapirs and salt walls develop faults with more linear traces. Concentric faults are commonly seen above circular salt diapirs (Fig. X.9), and can in many cases be related to the collapse of salt structures. In addition, radial faults have been described from salt domes, created by the expansion of the underlying salt. Small-scale fractures also form above salt structures, and concentric, radial and other patterns have been reported.

Within the salt itself there will be significant strain gradients, since the velocity decays to zero towards the adjacent rocks. The flow is probably simple along a salt layer, but within salt structures the pattern can be more complex. This is clear from the folded pattern of bedding observed in salt domes (salt mines), and relates to the non-linear flow of salt as it enters the structures and passes ramps or other irregularities. Folding occur as bedding rotates into the constrictional field of the instantaneous strain ellipse, as illustrated on page ??.

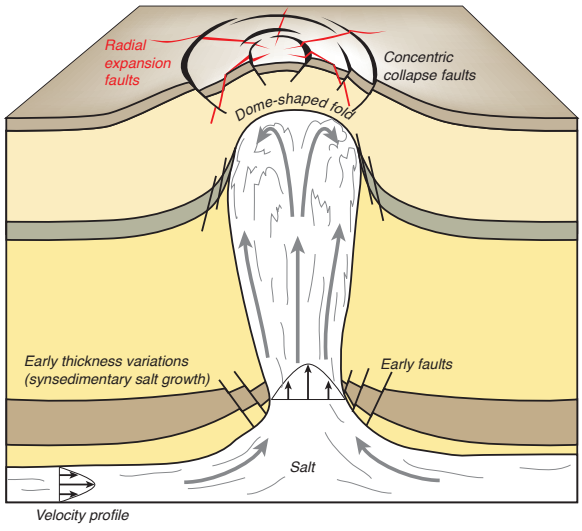

Figure X.9 Some common subsidiary structures associated with salt domes.

1.4 Rising diapirs: processes

Once a diapir starts rising it will develop into a diapir with a shape that depends on the sedimentation or erosion rate, tectonic regime, strength of the overburden, any gravitational loading, temperature of the salt, salt layer thickness and extent (salt availability), and more. In the traditional models of diapirism, diapirs force their way upward through the overburden, driven by differential, thermal or displacement loading. During such *active diapirism,* flaps of the roof is forced aside, causing significant upward rotation of layers along the upper parts of the salt walls (Fig. X.8a). As mentioned above, gravity inversion alone is generally not sufficient to initiate active diapirism, but once a diapir is established and the overburden becomes thin it can evolve as an active diapir, driven by buoyancy forces.

Passive diapirism is a term used about exposed diapirs that rise continually at a rate that more or less keeps pace with sedimentation (Fig. X.8a). Surrounding sediments subside as they compact and as the source salt layer thins while salt moves into the adjacent diapir structure. If the salt rise rate is greater than the sedimentation rate, the diapir widens upward. In the opposite case, where the rise rate is less than sedimentation rate, the diapir thins upward.

Passive diapirism comes to an end once the source layer is depleted, and from then on the diapir becomes buried.

In some cases the overburden is significantly affected by faulting, and salt fills inn spaces between fault blocks (Fig. X.8c). In this case the salt rises as a reaction to tectonic strain, usually extension, and the process is known as *reactive diapirism*. Experiments have shown that reactive diapirism ceases once extension comes to a halt, demonstrating its dependence on active extensional strain. Contractional deformation can also drive diapirism, as salt can be emplaced into its overburden in the hanging wall of a thrust fault (Fig. X.8d).

The close interaction between faulting and salt diapirism calls for a closer look at salt tectonics in different tectonic regimes.

1.5 Salt diapirism in the extensional regime

Many salt accumulations occur in continental extensional basins and passive continental margins. Since such settings tend to experience prolonged or repeated periods of extension, many salt layers are affected by regional extensional tectonics. Specifically, most salt diapir provinces are found to have initiated during regional extension. However, later contraction can modify the salt diapirs, as discussed below.

As illustrated by physical experiments, extensional faulting and fracturing weakens the overburden so that reactive diapirism can start. Graben formation in

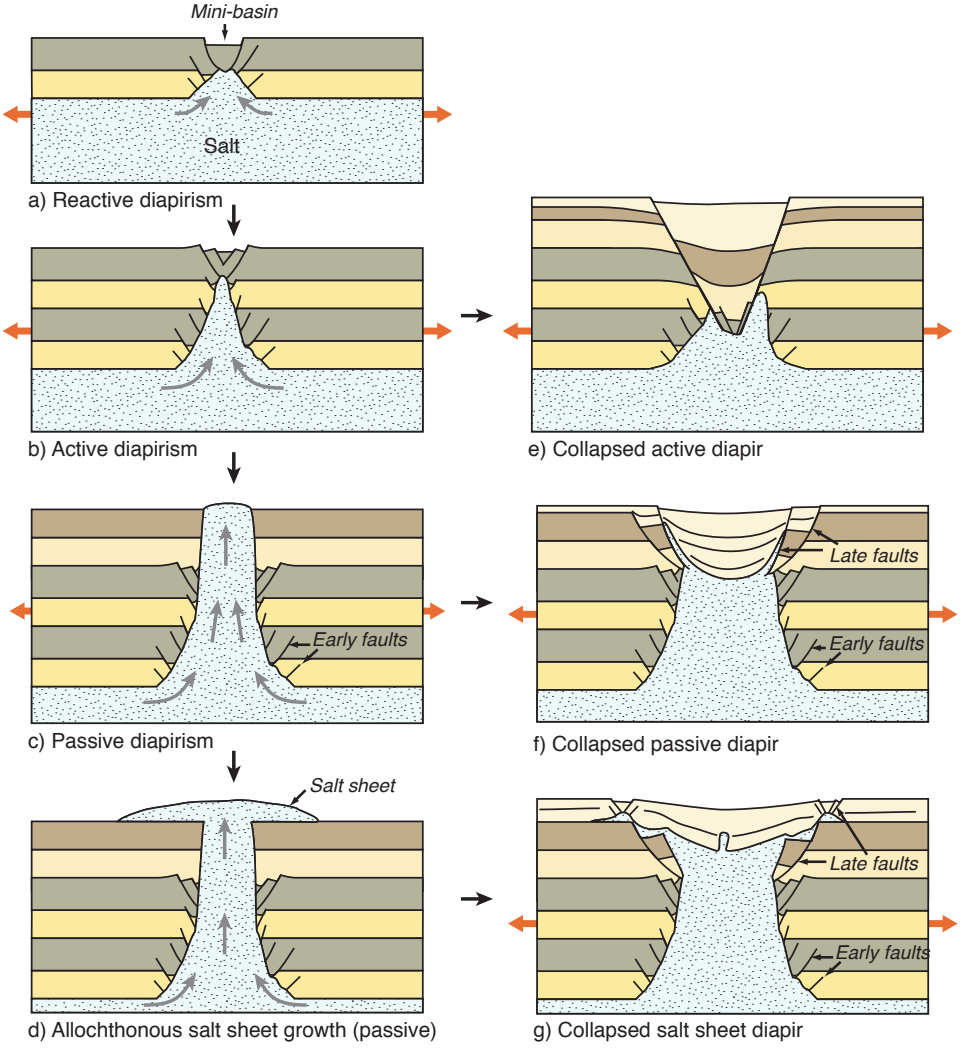

Figure X.10 Illustration of a complete and idealized evolution of a surfacing salt diapir through stages of reactive (a), active (b), and passive (c-d) diapirism. At any time the salt structure can collapse, giving rise to structures shown at the right-hand side (e-g).

the overburden typically result in a triangular shaped diapir that rises as extension proceeds and provides space for the salt (Fig. X.10a). The graben structure above the salt is topped by a local mini-basin at this stage, although salt emplacement reduces the depth of this basin. The graben as shown in Fig. X.10a is symmetric, but can also be asymmetric with a single dominant master fault. This type of structure is known as a *salt roller* (Fig. X.2). The continued evolution of a salt roller involves thickening of the salt in the footwall side of the fault. We will here discuss possible future stages of a more or less symmetric salt structure.

When the overburden above the salt diapir becomes thin enough and sufficiently weakened by extensional faulting, the salt can start to actively (buoyantly) force itself upward if the overburden is, on average, denser than the salt (Fig. X.10b). There is now a significant difference in density between the salt structure and its surroundings, and the extra weight of the compacting wall sediments pressurizes the salt and causes it to flow into the salt structure. This loading can be enough to drive salt diapirism, meaning that extension is not necessarily present at this stage. During this passive stage the roof layers are domed and stretched, resulting in steeply dipping layers or flaps along the upper margins of the salt diapir.

If the source layer is thick enough, the salt can reach the surface and act as a passive diapir (Fig. X.10c). Hence, salt can flow by reactive, active and passive diapirism during the rise of a diapir in an extensional setting. The salt may even end up flowing laterally at the surface (typically the sea bottom) as an autochthonous *salt sheet* (Fig. X.10d). Note how early faults are present in the deepest parts of the salt walls even for diapirs evolving into the most mature stages (Fig. X.10 c and d), showing that the diapir initiated during a phase of regional extension.

Salt structures may go through all the stages shown in Fig. X.10 a-d, but the evolution may also stop at any time during the process, or reverse in the sense of salt diapir collapse. The right hand column if Fig. X.10 shows the result of collapse of salt diapirs after various stages of growth. The actual evolution in any given example depends on the balance between extension rate, sedimentation rate, the viscosity (temperature, pureness) of the salt and salt availability (thickness of salt layer). During extension, the width of the salt diapir increases, so the flow of salt into the structure must more than balance the extension rate for the structure to grow.

If the structure widens too fast during extension, collapse will occur. Clearly, if salt source layer is exhausted and a salt weld is formed, collapse will occur during continued extension regardless of the extension rate. A history of growth and collapse, or rise and fall of a salt diapir is very common, and reproduced nicely in laboratory experiments where extension rate and sedimentation rate are controlled.

1.6 Diapirism in the contractional regime

When a sedimentary sequence overlying a salt layer is shortened during regional contraction, the sequence above the salt may buckle. The buckling creates lower-pressure antiformal crests into which the salt flows and in this way accommodates the folding of its overburden. Long salt anticlines form in this way, and may cause significant variations in thickness if the process is synsedimentary, with thinning or pinching out of layers towards the antiformal crests.

The formation of salt anticlines during

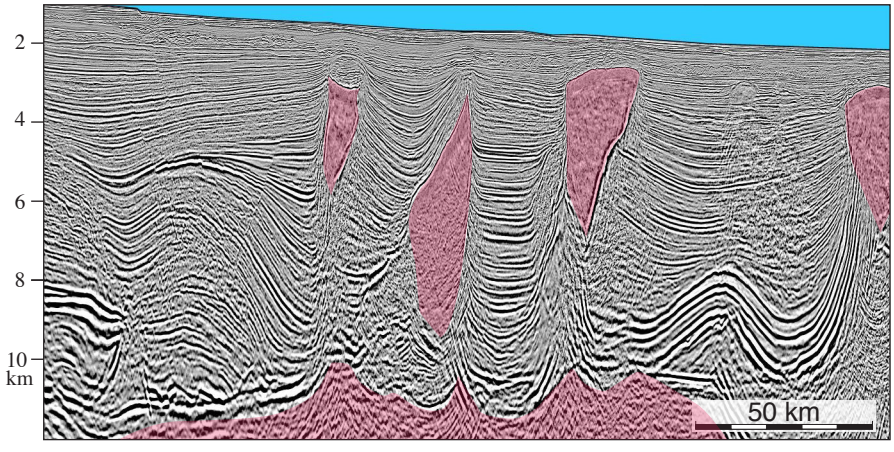

Figure X.11 Depth migrated seismic section from the submarine Mississippi Canyon, Gulf of Mexico, showing teardrop diapirs (detached salt stocks). The source salt layer is located at ~11 km depth. Folds indicate the role of contraction in the shaping of these salt structures. Image provided courtesy of TSG-NOPEC.

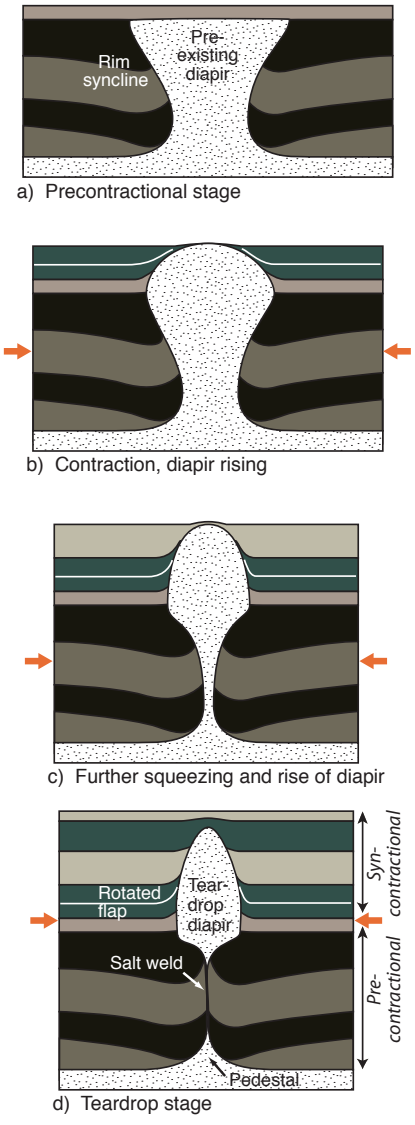

Figure X.12 Schematic illustration of the conversion of a hourglass-shaped diapir formed during extension to a teardrop diapir during subsequent contraction.

contractional folding of the overburden does not result in diapirism per se, since the overburden is still intact. Piercement can occur by means of thrust formation, as shown in Fig. X.8d, but the geometry of the resulting salt structure is very asymmetric and not very similar to classical diapir structures of the kinds shown in Fig. X.2. Most extensive diapir structures found in areas of regional contraction are amplified and otherwise reworked structures that originally formed during regional extension. Already existing salt diapirs represent weak elements in the stratigraphy, and are prone to accumulate much of the shortening. When this occurs, the salt structures become narrower and salt is squeezed upward and also laterally if the salt reaches the surface.

Teardrop diapirs

A spectrum of interesting structures can emerge from contractional amplification of salt structures. One class is *teardrop diapirs* (Fig. X.11), where an originally upward-widening diapir is squeezed to the point that a salt weld forms in the middle of the structure. The upper and isolated part is the teardrop, and the lower root structure is called a pedestal. Salt flows upward during this process, in many cases fueled by the component of buoyancy involved, but also because there is a free surface at the top. In fact, buoyancy is not required for this process to occur, since the tectonic squeezing or pressurizing of the salt is sufficient. Examples of teardrop structures are commonly seen on seismic data from areas where shortening of salt structures has occurred (Fig. X.12). In cases where the salt weld of a teardrop structure is inclined the weld may become activated as a reverse fault during continued shortening. The final geometry of a teardrop diapir and related structures depends on the preexisting geometry and rate of sedimentation. It also matters if the contraction is by pure shear alone, as in Fig. X.12 or if a component of shear along the

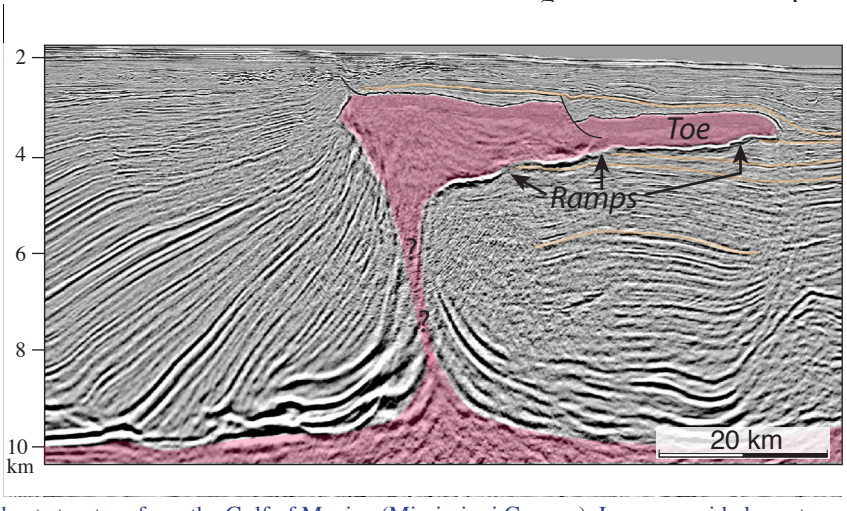

Figure X.13 Classical salt sheet structure from the Gulf of Mexico (Mississippi Canyon). Image provided courtesy of TSG-NOPEC.

salt layer is involved.

Salt sheets

In some cases salt can reach the surface and extrude like a very slow flowing erupting lava coming up from a volcanic feeder. Salt that flows out as sheets on the surface is called *allochthonous*, because it stratigraphically overlies younger rock or sediment layers, similar to a (allochthonous) thrust nappe. Salt sheets can form in contractional as well as extensional settings. An example of the latter is shown in Fig. X.11d, and occurs where vertical salt movement in a surfacing diapir (feeder) is larger than the sedimentation rate. If no sediments are deposited, the salt sheet follows the top of the upper bed, and will be confined to this stratigraphic level upon burial. However, if sedimentation accompanies salt extrusion, the salt will climb or ramp up-section away from the feeder at a rate that depends on the sedimentation rate versus the salt extrusion rate. The formation of salt sheet by extrusion resulting from passive diapirism is called *extrusive advance*.

Salt sheets commonly exhibit strongly asymmetric geometries, of which a characteristic example is portrayed in Fig. X.13. This type of structure is believed to form from partly buried sheets with a free (exposed) toe on one side. The toe of such an asymmetric structure advances laterally in what is referred to as *open-toed advance*, making the asymmetry of the structure more pronounced with time. After some time a thrust may develop underneath the advancing toe in some cases, driven either by gravity spreading alone or by regional contraction.

The effect of regional contraction is to form more inclined structures, and the end member in this spectrum of salt sheet structures is thrust structures where salt has been thrust up a ramp to a higher level

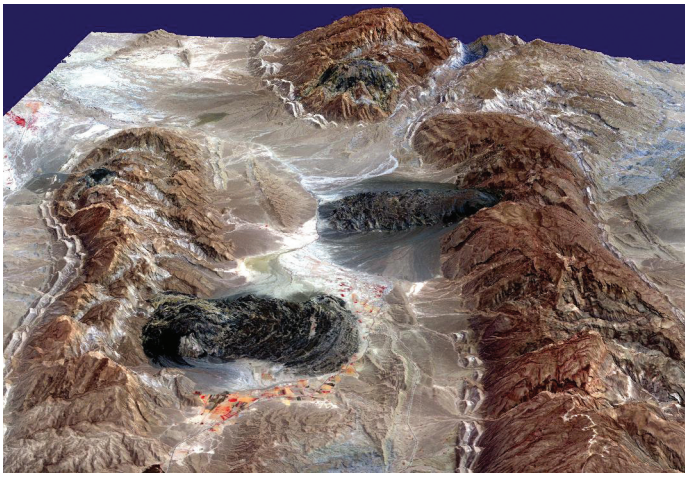

Figure X.14 Two salt glaciers in southern Iran. Credit: ASA/GSFC/METI/ERSDAC/JAROS, and U.S./Japan ASTER Science Team

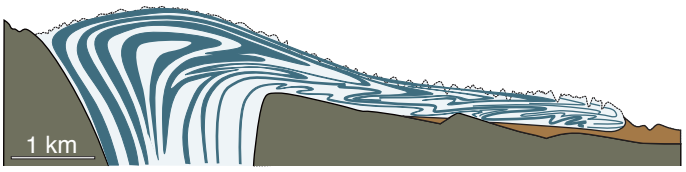

Figure X.15 Schematic crossection through one of many salt glaciers in Iran. Based on Talbot (1998).

(Fig. X.8d). These type of salt sheets can become large, and are characteristic of fold-and-thrust belts involving salt layers. In rare cases salt diapirs may also spread laterally between a stratigraphically higher salt layer and its roof. This can occur during delamination of the layers between the two salt layers, or during contraction where the uppermost layer buckles. In general, however, salt sheets form at the surface of the crust, and salt sheets within sedimentary sequences, such as the one shown in Fig. X.13, has been buried under later sediments.

Salt sheets can form from several salt diapirs at the same time, and if they are close enough the salt can coalesce to form a continuous unit, or salt canopy, that can cover large areas. Once formed, the canopy can act as any other salt layer, with the creation of secondary diapirs piercing higher stratigraphic units.

Salt glaciers

Where salt flows out of a diapir on the surface it flows gravitationally. In dry regions, such as Iran, the flow occurs during periods of rainfall, when the salt is wet. Otherwise, the upper part of the salt sheets deforms brittlely by jointing. This shows the effect of fluids on deformation mechanism; wet conditions favor plastic deformation.

Salt can flow down surface slopes much like glaciers, and (parts of) salt sheets that flow in a preferred direction on the surface are referred to as *salt glaciers* (Fig. X.14). The Zargos Mountains in Iran is known for its salt glaciers, but salt glaciers can also occur under sea level if the extrusion of salt is faster than the rate of dissolution of salt by the seawater. This is the case in the Gulf of Mexico, where several submarine salt glaciers have been mapped.

During the downhill flow of salt, the salt deform by folding due to the non-constant velocity field (velocity increasing from the base upward). Recumbent folds on a variety of scales can be seen, the largest of which can be mapped out (Fig. X.15). These folds are similar (class 2) folds, because they involve no mechanical layering and simply form because the passive layering enters the contractional field during shearing (flow).

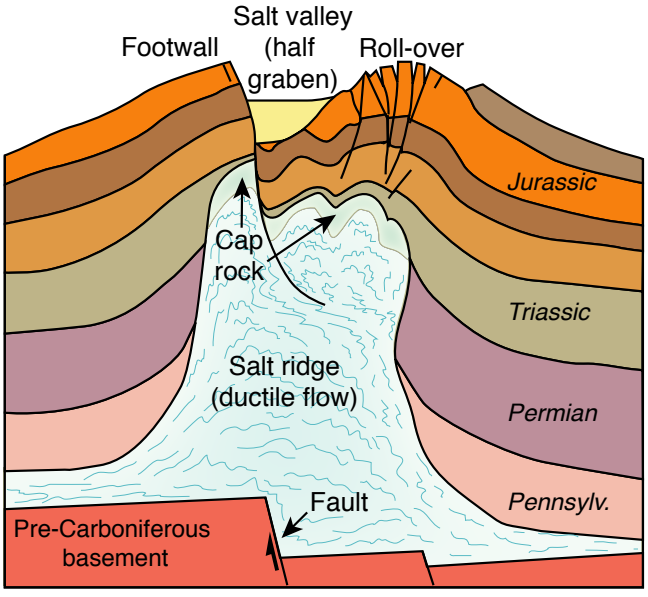

Figure X.16 Generalized crossection through the salt walls of the Paradox Basin in SE Utah. The collapse structure at the top of the salt is in part generated by reactivation of a regional system of Tertiary joints during Salt dissolution, although most of the faulting are related with cataclastic deformation bands that must have formed earlier and at greater depths.

1.7 Salt collapse by carstification

Salt structures whose top are at or close to the surface are exposed to dissolution by meteoric water. The process is carstification, and bears similarities to carst formation in limestones and marbles. In both cases carstification can lead to gravity collapse of overlying rocks and sediments, but the solubility of salt is higher (~360 g/l) and thus the potential of gravity collapse greater. The result can be fault systems above the salt structure that could form long after salt movement came to a halt. Such structures can be difficult to distinguish between crestal grabens and circular fault systems that form during extensional down-building of a salt structure during regional extension, and there can be an effect of both at the same time. The salt ridges in the Paradox Basin of SE Utah is one of several places where salt dissolution have been interpreted to have caused relatively recent collapse of salt walls, probably by reactivation of already established faults at the crest (Fig. X.16). The presence of a cap rock at the top of the salt, i.e. a residual rock consisting mostly of gypsum and clay, shows that salt dissolution has occurred.

1.8 Salt décollements

One of the most important roles of salt is to act as a mechanically weak décollement, be it in extensional settings such as passive continental margins, or contractional settings such as orogenic wedges (fold-and-thrust belts). The presence of salt can make a great difference regarding finite strain and strain distribution in the deforming area. In general, its very weak nature enables much wider areas to be deformed, provided that the salt layer is extensive. It also allows for, and usually causes, decoupling of the substrate and the overburden.

While salt structures such as diapirs only form when a thick salt layer is present, décollements can form in salt layers just a few meters, decimeters or even centimeters thick. Such salt layers are common in both rift settings and, particularly, continental margin settings, and it is very common that they develop into décollements where extensional fault systems detach on the salt layer(s). This causes a decoupling of the fault systems above and beneath the salt layer, which may exhibit significant differences in style and geometry.

The most extreme expressions of salt décollement tectonics occur on some passive continental margins, such as offshore Angola. In these areas, ocean-dipping salt layers allow for gravity-driven sliding of the overburden. The dip is low, commonly only a few degrees, but this is sufficient in many cases due to the low strength of salt. The overall strain pattern is the same as for any gravity sliding process: extension in the rear and contraction in the front (Fig. X.17). In the upper part, extreme extension can separate blocks above the salt. So-called *rafts* form where extensional faults completely separate the fault blocks above the salt décollement (Fig. X.17). Rafting in the sense that fault blocks ride as separated blocks on a salt layer is particularly common in the western passive margin

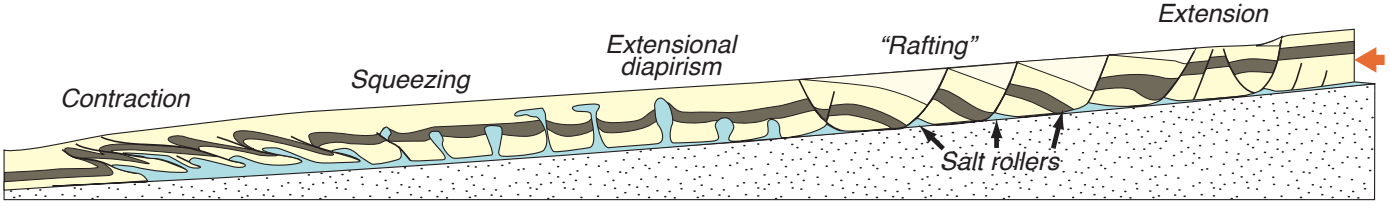

Figure X.17 Schematic illustration of structures commonly found on passive continental margins with salt detachment

of Africa.

Salt décollement in contractional settings serves as any other décollement, separating a deforming wedge with multiple reverse faults, some normal faults and décollement folds from an undeformed basement (Fig. Previous chapter). The main difference lies in the low friction of salt décollements, causing the above-lying wedge of deformed rocks tot become long and thin in crossection (se p. ??) and hence to extend farther into the foreland than normally would have been the case. Thus, salt décollements make orogenic belts wider.

Folding create irregularities that can lead to salt diapirism, particularly through the development of salt ridges or salt anticlines. In fact, buckling is the common explanation why salt anticlines form in some areas instead of salt diapirs.

Balancing
Perfect, because salt accommodates most space problems that normally occur along the base of a deformed section.

Related structures: mud diapirs and shallow intrusions

---***---

Salt is important because of

Further reading:

Brun, J. P. & Fort, X. 2004. Compressional salt tectonics (Angolan margin). Tectonophysics 382, 129-150.

Gutiérrez, F. 2004. Origin of the salt valleys in the Canyonlands section of the Colorado Plateau Evaporite-dissolution collapse versus tectonic subsidence. Geomorphology 57, 423-435.

Hudec, M. R. & Jackson, J. A. 2007. Terra infirma: understanding salt tectonics. Earth-Science Reviews 82, 1-28.

Stewart, S. A. 2006. Implications of passive salt diapir kinematics for reservoir segmentation by radial and concentric faults. Marine and Petroleum Geology 23, 843-853.

Vendeville, B. C. & Jackson, M. P. A. 1992. The fall of diapirs during thin-skinned extension. Marine and Petr. Geol. 9, 354-371.

Vendeville, B. C. & Jackson, M. P. A. 1992. The rise of diapirs during thin-skinned extension. Marine and Petr. Geol. 9, 331-353.

References:

Buchner, E. & Kenkmann, T. 2008. Upheaval Dome, Utah, USA: Impact origin confirmed. Geology 36, 227-230.

Gutiérrez, F. 2004. Origin of the salt valleys in the Canyonlands section of the Colorado Plateau Evaporite-dissolution collapse versus tectonic subsidence. Geomorphology 57, 423-435.

Stewart, S. A. & Allen, P. J. 2005. 3D seismic refl ection mapping of the Silverpit multi-ringed crater, North Sea. Geological Society of America Bulletin 117, 354-368.

Zanella, E., Coward, M. P. & McGrandle, A. 2003. Crustal structure. In: The Millennium Atlas, petroleum geology of the central and northern North Sea (edited by Evans, D., Graham, C., Armour, A. & Bathurst, P.). The Geological Society of London, 35-43.

Dictionary

Active folding: Folding of layers by layer-parallel shortening controlled by contrasts in viscosity between layers (buckling).

Accommodation zone: Zone between two overlapping fault segments where offset is transferred from one fault segment to the other. Used specifically about the zone connecting two oppositely dipping half-grabens (Rosendahl et al. 1986).

Axial surface: The theoretical surface connecting the hinge lines of consecutive surfaces in a fold structure.

Axial plane: A planar axial surface, not necessarily parallel to the bisecting surface.

Axial plane cleavage: Cleavage that is subparallel to the axial surface of a fold. The cleavage must have formed during the process of folding.

Axial trace: The theoretical line that connects hinge points across a fold.

Axially symmetric extension: Extension in one principal direction (X axis of the strain ellipsoid) and equal shortening in the other two (Y and Z). Implies perfect constructional strain. Equal to *uniform extension*.

Axially symmetric shortening: Shortening in one principal direction (Z) and equal extension in the other two (Y and X). Implies perfect flattening strain. Equal to *uniform shortening*.

Allochthonous: Tectonic unit that has been transported too far for direct correlation with the substrate. Derived from Greek: ”allo” means “different” and ”chthon” means “ground”. Typically used for nappes that have moved tens of kilometer or more.

Angular shear: Change in angle for a pair of lines that were orthogonal before deformation. More specifically, the angular shear along a reference line is the change in angle of a line that was perpendicular to the reference line before deformation.

Antithetic fault: From the Greek word ”antithethemi”, to oppose. An antithetic fault is a fault dipping in the opposite direction of an adjacent master fault or dominating fault set.

Aperture: The distance between the two walls of a fracture.

Area change: Change in area due to deformation. Implies volume change unless compensated for in the third dimension.

Asperity: Irregularity along a fracture surface.

Autochthonous: Lithologic unit in or along an orogenic belt that has not been tectonically transported. The Greek word ”auto” means “the same” in this connection.

Balancing: The construction or interpretation of a geologic profile or 3D model that can be reconstructed by means of geologically realistic processes to a geologically sound undeformed state.

Bending: Folding mechanism that occurs where forces are applied at a high angle to the layering.

Bisecting surface: Surface that divides a fold into two parts. When the bisecting surface is vertical, the limbs should have the same dip.

Blastomylonite: A mylonite that has recrystallized posttectonically: Grains show no preferred orientation (equant grains) and little or no internal strain.

Blind fault: Fault that terminates without reaching another fault or the surface. Traditionally used in thrust fault terminology (blind thrust).

Boudinage: The process leading to the formation of boudins.

Boudins: Structures forming during systematic segmentation of preexisting layers. Classical boudins form by extension of layers that are more competent than the matrix. Also see *foliation boudinage*.

Branch line: A line of intersection between two intersecting faults. Used about any type of fault (normal, reverse or strike-slip)

Branch point: Point in a section or map where two fault traces join.

Breached relay ramp: Relay ramp that has been cut by a fault, transforming it from a *soft-linked* into a *hard-linked overlap* structure.

Breccia: Cohesive or non-cohesive fault rocks consisting of randomly oriented fragments resulting from brittle fracturing. Breccia fragments must constitute >30% of the rock.

Brittle deformation: Deformation by fracturing (discontinuous deformation).

Brittle deformation mode: Deformation by means of brittle deformation mechanisms (fracturing, frictional sliding, cataclastic flow).

Buckle folds: Folds that form by buckling. They show a certain regularity with regard to wavelength and amplitude as a function of layer thickness and the viscosity contrast between layer(s) and the matrix.

Buckling: A folding mechanism that occurs when layers that are more competent (higher viscosity) than the matrix are compressed parallel to the layering. As stress increases the layer becomes unstable and buckles through the amplification of minute irregularities along the layer interfaces.

Cataclasis: Brittle crushing of grains (grain size reduction), accompanied with frictional sliding and rotation. Derived from a Greek word for crushing.

Cataclastic flow: Flow of rock during deformation by means of cataclasis, but at a scale that makes the deformation continuous and distributed over a zone.

Cataclastic deformation bands: Deformation bands where cataclasis is an important deformation mechanism.

Cataclasite: Cohesive and fine-grained fault rock. Cataclasites are subdivided into those that have 10-50% matrix (protocataclasite), 50-90% matrix (cataclasite) and>90% matrix (ultracataclasite).

Chevron fold: Fold with angular hinge and where the axial surface is more or less perpendicular to σ_1.

Chocolate tablet boudinage: Boudinage in two directions (in the X-Y plane), forming more or less square or rectangular boudins in three dimensions.

Clay smear: Smearing or, less commonly, injection of clay along the fault core.

Clay Smear Potential: CSP, relationship between the thickness of a faulted clay layer and the distance from the clay layer along the fault in a sequence of sandstone with one or more clay layers. CSP is used in fault sealing analysis.

Clay injection: Injection of clay along a fault, normally because a tension fracture opens due to local overpressure.

Cleavage: A tectonic foliation formed at low-grade metamorphic conditions and related to folding. A cleaved rock breaks more easily along the cleavage.

Cleavage refraction: A change in cleavage orientation across an interface between layers of contrasting competence.

Coaxial deformation: Lines along the principal strain axes have the same orientation before and after the deformation.

Coble creep: See *grain boundary diffusion*.

CPS: Se *fault seal potential*.

Coaxial deformation: Lines along the principal strain axes have the same orientations before and after the deformation.

Coaxial deformation history: Lines along ISA do not rotate during the deformation; W_k=0. The principal strain axes (X, Y and Z) remain constant throughout the deformation history.

Cohesion: The solidness of a medium. A cohesive rock does not fall apart very easily, while a non-cohesive medium easily disintegrates. Cementation increases cohesion in sedimentary rocks and fault gouges.

Compaction bands: Deformation bands involving compaction without shear.

Compaction cleavage: Cleavage formed by lithostatic compaction of sediments into sedimentary rocks. Best developed in mudrocks.

Competency: A relative expression that compares the mechanical strength or resistance against flow of a layer or object to that of its adjacent layers or matrix. Competent objects are more resistant against flow than their matrix.

Compression: Expression used extensively about compressional stresses. Some use it about strain too, but contraction or shortening is a better word than compression in this case.

Conjugate faults: Two intersecting faults that formed under the same stress field. Such faults show opposite sense of shear and about 30° to σ_1.

Constant-horizontal-stress reference state: Reference state of stress assuming that the lithosphere has no shear strength at a certain depth and that it behaves like a fluid below this compensation depth.

Constitutive laws: Laws or equations describing the relationship between stress and strain.

Continuous cleavage: Cleavage where the distance between individual cleavage domains are indistinguishable in hand sample, i.e. less than 1 mm.

Contraction: Reduction in length of a line, layer, area or object. Synonymous with shortening. Usually a one-dimensional effect, but can also be considered in two or three dimensions, e.g. axially symmetric extension/flattening.

Crenulation cleavage: Cleavage formed by microfolding at low-metamorphic conditions of phyllosilicate-rich and well-foliated rocks.

Crenulation lineation: Lineation formed by crenulation of phyllosilicate-rich layers. Closely related to intersection lineations.

Creep: Generally used about slow geological processes. More specifically used about the (slow) way that permanent plastic deformation accumulates at long-term constant stress by various micro-scale or atomic-scale deformation mechanisms (diffusion creep, dislocation creep etc.).

Creep mechanisms: Deformation mechanisms at work in a crystal or crystal aggregate that respond to sustaining stress by gradual accumulation of plastic strain. These are separated into diffusion creep (grain boundary diffusion, volume diffusion, pressure solution) and dislocation creep (dislocation climb, dislocation glide and recrystallization).

Damage zone: Zone of brittle deformation structures (fractures, deformation bands and/or stylolites) around a fault. The zone has a density of such structures that is higher than the surrounding rocks.

Décollement: Large-scale detachment, i.e. fault or shear zone that is located along a weak layer in the crust or in a stratigraphic sequence (e.g. salt or shale). The term is used in both extensional and contractional settings.

Deformation: The change of the shape, position and/or orientation as a result of external forces. The deformation is found by comparing the undeformed and the deformed states.

Deformation bands (I): Millimeter-thick zones of strain localization formed by grain reorganization and/or grain crushing. Shear bands with some compaction across the band form the most common type.

Deformation bands (II): Microscopic zones in a mineral grain with similar optical orientation (extinction), forming between dislocation walls.

Deformation gradient tensor: See *deformation matrix*

Deformation matrix: Transformation matrix that relates the undeformed and the deformed states of a deformation. A fixed deformation matrix describes a linear transformation and therefore homogeneous deformation. It represents a complete description of the deformation (but not the deformation history).

Deformation mechanisms: Mechanisms at the microscale that are active during plastic deformation, including cataclasis, dry and wet diffusion and recrystallization.

Detachment: Low-angle or horizontal fault or shear zone separating an upper plate (hanging wall) from a lower plate (footwall). Detachments are typically reactivated weak layers or structures.

Detachment folds: Folds formed above a detachment, where lower layers are undisturbed by the folding. The detachment is typically a weak layer (e.g. salt or shale) while the folded layers are more competent (e.g. limestone).

Deviatoric stress: The difference between the total stress and the mean stress. Often related (equated by some) to tectonic stress.

Dilation: Volume increase (positive) or decrease (negative). Also used about area change.

Dip isogons: Theoretical lines connecting points of equal dip on the upper and lower boundaries of a folded layer oriented in an upright position (vertical bisecting surface).

Dip separation: Apparent fault displacement as observed in a vertical section in the dip direction of the fault. Dip separation equals true displacement for dip-slip faults.

Displacement: The difference, represented by a vector, between the location of a point before and after deformation. For faults displacement is the relative motion of two originally adjacent points on each side of the fault.

Displacement-length ratio: The ratio between the maximum displacement of a fault and its length. Usually measured on a cross section or a map, which introduces a sectional uncertainty.

Displacement vector: Vector connecting the positions of a material point (e.g. a sand grain) before and after deformation.

Displacement field: The field of vectors describing the distortion of points in a deformed medium, i.e. vectors connecting the pre- and post-deformational positions of particles.. The displacement field gives important information about the deformation, e.g., plane strain, convergent or divergent, and contains information about strain.

Domino faults: Set of parallel normal faults separated rotated fault blocks (domino blocks) where bedding is dipping antithetic to the faults.

Differential stress: The difference between the largest and smallest principal stresses, i.e. the diameter of the Mohr circle.

Diffusion: The moving of vacancies (holes) in an atomic lattice. Volume diffusion occurs within the lattice, while grain boundary diffusion (Coble creep) occurs along the grain boundaries.

Dilation (US), dilatation (UK): Volume change, usually implying volume loss (negative dilation being volume gain). Isotropic dilation or volume change involves the same amount of shortening (or extension) in all directions. A common example of anisotropic dilation is uniaxial strain (compaction).

Dilation band: Deformation band where displacement is dilational (volume increase) without shear. Dilation bands show an increase in porosity and are relatively uncommon as compared to other types of deformation bands.

Dip-slip fault: Fault with the slip vector oriented along the dip direction of the fault surface, i.e. a perfectly reverse or normal fault.

Dip separation: Apparent fault displacement in a vertical section in the dip direction of the fault. Dip separation equals true displacement for dip-slip faults.

Dipmeter log: Well log showing dip and azimuth of planar features based on interpretations of resitivity measurements along the well bore. Measurements are done by running a dipmeter tool through the wellbore, and the planar features represent bedding, deformation bands or fractures.

Disaggregation band: A deformation band formed by granular flow (rotation and frictional sliding of grains). Commonly form in sand and poorly consolidated sandstones.

Disjunctive cleavage: Domainal cleavage that is independent of previous foliation(s). Typical for very-low grade metamorphic medasediments. May be divided into stylolitic, anastomosing, rough and smooth, according to the morphology of the domains. Disjunctive cleavage contrasts to crenulation cleavages, where a preexisting foliation is reworked by microfolding and solution.

Dislocation: An atomic-scale defect within a crystal lattice. Dislocations can move by means of glide and climb mechanisms and dislocation formation and motion causes plastic deformation. Edge and screw dislocations are the principal types of dislocations in naturally deformed rocks.

Dislocaion creep: Motion of dislocations in a crystal where mechanisms called climb and cross slip are used to by-pass obstacles in the lattice.

Dislocation walls: Concentration of dislocations forming walls within a crystal. Dislocation walls mark the boundary between deformation bands and subgrains.

Domainal cleavage: Cleavage composed of domains of different minerals, usually micaceous M-domains and quartzofeldspatic QF-domains. When individual domains are visible in hand sample, the cleavage is a spaced cleavage.

Domino fault model: Model where parallel normal faults define fault blocks that rotate like domino bricks during deformation. Also called book-shelf mechanism. Blocks are by definition rigid, but the *soft domino model* allows for internal block deformation.

Drag: Zone of folding on one or both sides of a fault. The folding must be related to the fault formation and/or growth.

Ductile: Continuous deformation at the scale of observation, resulting from any deformation mechanism (brittle or plastic). Some geologists restrict the term to crystal-plastic deformation.

Duplex: Tectonic unit consisting of a series of horses that are arranged in a piggy-back fashion between a sole and a roof thrust. Also used about similar structures in extensional and strike-slip settings (extensional and strike-slip duplexes).

Dynamic analysis: The analysis explores the relationship between stress and strain.

Dynamic recrystallization: Synkinematic recrystallization, i.e. continual crystallization during deformation. Revealed in shear zones by slightly non-equant grains that define a new fabric at an angle to the foliation.

Extension: A measure of how much longer a line or object has become due to deformation.

Extension fracture: Fracture formed by extension perpendicular to the fracture walls. The amount of extension can be minute, as for joints, or can be larger, as for veins.

Elastic deformation: Deformation (strain) that disappears when the applied stress is removed.

Effective stress: The total stress minus the pore pressure in a porous rock or sediment.

Elongation: $e=(l-l_0)/l_0$, where l_0 and l are the lengths of the line before and after the deformation, respectively.

Fabric: The configuration of planar and/or linear objects in a penetratively deformed rock. An L-fabric is composed of linear features, while an S-fabric consists of planar elements.

Failure envelope: The curve enveloping a series of Mohr's circles representing different differential and mean stress values (different positions along the x-axis of the Mohr diagram). Each circle touches the envelope. The failure envelope describes the stress conditions at failure for different stress conditions for a given medium (rock).

Fault: Surface or narrow tabular zone with displacement parallel to the surface (zone). Generally used about brittle structures (structures dominated by brittle deformation mechanisms).

Fault-bend fold: Fold forming above a ramp along a thrust fault as the hanging wall accommodates to the ramp geometry.

Fault core: Central high-strain zone of a fault where most of the displacement is taken up. Enveloped by the fault damage zone. The fault core can consist of non-cohesive rock flour or strongly sheared phyllosilicate-rich rock called fault gauge, or cohesive cataclasite, and can contain lenses of wall rock. The core thickness can vary from less than 1 mm for small (meter-scale) faults to around ten meters for large (km-displacement) faults.

Fault cut: Stratigraphic section missing in a well due to omission by faulting. The fault cut is estimated based on stratigraphic information from near-by wells or outcrops.

Fault cut-off line: The line of intersection between a fault surface and another (usually stratigraphic) surface cut by the fault. There are two such lines, known as hanging-wall and footwall cut-off lines.

Fault juxtaposition diagram: Diagram illustrating the lithological contact relations along a particular fault, e.g. sand-sand, sand-shale etc. Closely related to *triangle diagrams*, which are general juxtaposition diagrams for a synthetic fault (gradually changing displacement).

Fault plane solution: Stereographic projection containing information about the first motion caused by an earthquake based on seismic observations from a number of seismographs. It consists of two orthogonal planes separating compressional from tensional motion. One of these planes represents the fault orientation. The beach-ball style plots also give us the sense of slip (normal, reverse etc.) and approximate locations of the principal stress axes.

Fault-propagation fold: Fold forming ahead of a propagating fault. Traditionally used about thrust faults, but can be used about any type of fault (normal, strike-slip or reverse).

Fault strain: Strain calculated for an area or volume affected by numerous faults. As a concept, two and three-dimensional strain applies only to ductile (continuous) deformation, but since ductility is scale dependent, it can, as an approximation, be applied to fractured rocks with distributed fractures.

Fault trace: Intersection between a fault and any given surface, such as the surface of the Earth, a stratigraphic interface or a cross section.

Fault zone: A series of subparallel faults, forming a zone. The thickness of the zone must be small relative to its length.

Flexural shear: Fold mechanism where layers are sheared by simple shear. The shear is zero at the hinge point, increasing away from the hinge toward the inflection point. Sense of shear is away from the hinge zone, i.e. opposite on the two limbs.

Flexural slip: Slip along bedding interfaces during folding. As for flexural shear, slip increases away from the hinge line, being opposite on the two limbs. Typical in folded layers of high contrasts in strength.

Floor thrust: Low-angle fault that defines the upper limitation of a duplex structure. Synonymous to sole thrust.

Flow: A term used about rocks in the perspective of geologic time: Given enough time and appropriate physical conditions (temperature, pressure, fluid availability), rocks flow by means of plastic or brittle deformation mechanisms. A distinction can be made between cataclastic flow and plastic flow.

Flow apophyses: Apophyses separating domains of different particle motion during flow (deformation).

Flow laws: Mathematical models describing the relation between deformation rate, stress and deformation mechanism fore a given rock.

Flow pattern: The pattern outlined by the particle paths during flow (distributed deformation).

Flow parameters: Parameters describing the deformation at any instant or interval of the deformation history. For steady-state deformation, they are representative for the entire deformation history. Important flow parameters are the velocity field, flow apophyses, ISA and vorticity.

Fold axis: The straight hinge line of a cylindrical fold.

Fold hinge: See *hinge*.

Fold nappe: Nappe that is internally folded throughout and appears to have originated by shearing of an inverted fold limb.

Fold limb: The two parts of the fold that are separated by the hinge zone, i.e. by the area of maximum curvature.

Foliation: Usually a tectonic planar structure formed in the plastic regime. Foliations are characterized by flattening across the structure. Also used about primary structures such as bedding or magmatic layering, in which case the term primary (in contrast to secondary or tectonic) foliation should be used.

Foliation boudinage: The formation of boudins in strongly foliated metamorphic rocks, where the boudins are separated by en-echelon arranged shear fractures, small shear zones or extension fractures.

Foliation fish: Volume in a strongly foliated rock that is back-rotated relative to the rest of the rock, displaying a fish-like geometry.

Footwall uplift: Uplift of the footwall of a normal fault, which typically is in the order of 10% of the fault throw.

Foreland: The peripheral or frontal part of a thrust region or orogenic belt, dominated by thin-skinned tectonics and very low to non-metamorphic conditions.

Fracture: A sharp planar discontinuity. An ideal fracture is narrow (significantly thinner than 1 mm), involves a displacement discontinuity as well as being a mechanical discontinuity, and it is weak so that the rock preferentially breaks along the fracture. It also conducts fluids. A distinction is drawn between extension fractures and shear fractures.

Fracture cleavage: A dense array of fractures that mimic a cleavage. While ordinary cleavage involves shortening across the cleavage, fracture cleavage involves shear along or extension across the structure. The term is a bit confusing and should be used with care.

Fracture toughness: A material's resistance against continued growth of an existing fracture. High fracture toughness implies high resistance against fracture propagation and therefore low propagation rates.

Frictional sliding: Sliding on a fracture that has a certain friction without activation of plastic deformation mechanisms.

Floor thrust: Thrust fault defining the base of a duplex structure or the basal thrust of a nappe or nappe complex, i.e. a sole thrust.

Flower structure: The upward-splitting and widening of strike-slip faults as seen in cross sections, especially on seismic sections.

Footwall: The surface underneath a non-vertical fault.

General shear: Used synonymous to subsimple shear by several geologists.

Gouge: Pulverized rock located in the core to faults and formed by frictional sliding during fault motions. Gouge is incohesive and typically silty or clay-rich.

Graben: German for grave. A depression bounded by two more or less strike-parallel but oppositely dipping normal faults or vertical faults.

Grain boundary diffusion: Diffusion of crystal vacancies along grain boundaries – a plastic deformation mechanism. Also called Coble-creep.

Grain boundary sliding: Plastic deformation mechanism where grains slide along side as a result of diffusion (not to be confused with frictional grain boundary sliding, which is a brittle mechanism).

Granular flow: Particles flowing by frictional sliding and rolling (translation and rigid rotation). Typical for deformation of loose sand or soil. Synonymous with particulate flow.

Growth fault: A shallow normal fault that has moved during deposition of sediments on the hanging-wall side. The hanging wall strata thicken toward the fault and amay also be more corse-grained close to the fault. The fault displacement increases downwards as fault dip decreases.

Hackles, hackle marks: Plumose curvilinear patterns defined by gentle relief on extension fractures, radiating from the nucleation point of the fracture or fanning away from a curvilinear axis. Identical to *plumose structures*.

Half graben: Structural depression controlled by one master normal fault and typically also antithetic (oppositely-dipping) minor normal faults in the rotated hanging-wall layers. An *asymmetric graben* is a graben structure intermediate between a perfect half graben and a symmetric graben.

Hard link: Expression used in fault overlap zones where the overlapping faults are connected by at least one fault that is mappable at the scale of observation.

Hanging wal (US), hangingwall (UK): The rock volume above a dipping fault.

Heave: The horizontal component of the dip-separation of a fault. Equal to the horizontal component of the actual displacement vector for dip-slip faults.

Heterogeneous deformation: Deformation varies within the area or volume in question. or inhomogeneous deformation. Also called *inhomogeneous deformation*.

Heterogeneous strain: The state of strain (strain ellipse or ellipsoid) varies within the area or volume in question. Also called *inhomogeneous strain*.

High-angle fault: Fault dipping more than 30°.

Hinge: The area of maximum curvature of a folded surface, i.e. the zone that connects the fold limbs.

Hinge point: Point of maximum curvature on a folded surface

Hinge line: The line of maximum curvature, i.e. the line defined by consecutive hinge points on a folded surface. Linear and known as the fold axis for cylindrical folds.

Hinge zone: Zone of maximum curvature on a fold.

Hinterland: The central or internal zone of an orogen, as opposed to the foreland. The hinterland is characterized by basement involvement and locally high metamorphic grade.

Homogeneous deformation: Deformation is everywhere the same within the area or volume in question.

Homogeneous strain: The state of strain is the same within the area or volume in question, meaning that the strain in the entire area or volume can be represented by a single strain ellipse or ellipsoid.

Horse: The smallest tectonic unit in thrust terminology: a tectonic sheet bounded by thrust faults on each side and occurring in trains in duplex structures. S-shaped geometry common. Now also used in normal fault terminology (horses in extensional duplexes).

Horst: Elongate area that is stratigraphically elevated relative to rocks on each side. A horst is bounded by normal faults that are vertical or dipping away from the horst.

Hydrostatic stress: State of stress where the stress is the same in all directions (spherical stress ellipsoid). Occurs in fluids only, incluing magma.

Imbrication zone: A series of reverse faults dipping in the same direction and soling out on a floor thrust, but not necessarily bounded by a roof thrust. Also used about similar constellations of normal faults.

Incremental strain ellipse: Strain ellipse for a small part of the total deformation history. The sum of all of the incremental strain ellipse will be the finite or total strain ellipse.

Inhomogeneous deformation/strain: See *heterogeneous deformation/strain*

Instantaneous strain axes: Directions of maximum ongoing stretching (ISA_1), minimum stretching (maximum shortening; ISA_3) and an intermediate axis perpendicular to the other two (ISA_2). These axes are defined at any instant during the deformation.

Interlimb angle: The angle between the two limbs of a fold.

Intersection lineation: Lineation formed by the intersection between two planar structures, such as bedding and a cleavage.

Inversion: 1) Turning stratigraphy upside-down by means of recumbend folding (inverted limb). 2) Reactivating a normal fault as a reverse fault. 3) Turning a basin into a high and vice versa (related to the previous definition).

ISA: se *instantaneous stretching axes*

Isochoric: Constant volume or area.

Juxtaposition: Description of the geological strata that are in contact across a fault. Commonly expressed in a juxtaposition or triangle diagram.

Kinematics: From Greek ”kinema”, meaning to move. The description of how rock masses or objects in rocks move as a result of deformation.

Kinematic vorticity number: W_k, dimensionless number representing the ratio between the rate of rotation of the strain ellipsoid and the rate at which strain accumulates. $W_k=0$ for pure shear and 1 for simple shear.

Kinematic indicator: Any structure indicating the kinematics (typically sense of shear) during a deformation event. Examples include shear bands in mylonites, rotated porphyroclasts, drag folds and riedel shears associated with faults.

Kink folds: Small (typical cm-scale) angular folds with straight hinges, thought to form with axial planes at an acute angle to σ_1.

Lineament: Straight or gently curved line feature on the surface of the Earth or another planet, identified and mapped by means of remote sensing imagery. A lineament should be likely to represent a geologic structure or lithologic contact.

Lineation: Linear structure formed by means of tectonic strain, e.g. rotated amphibole needles in an amphibolite, stretched aggregates of quartz and feldspar in a granitic gneiss, or striations on a fault surfac. The linear objects are pervasive (metamorphic rocks) or limited to a fracture (brittle regime).

Listric: From Greek "listros", meaning spoon shaped. Geometric term that describes the downward flattening geometry of some faults. Faults that steepen by depth are sometimes called antilistric.

Lithostatic reference state: Reference state of stress in the crust where the crust is considered a medium without shear strength (i.e., a fluid) and where stress in any direction is the product of density, depth and *g*.

Lithostatic pressure: The product of the density and height of the overlying rock layers, multiplied by *g*.

Low-angle fault: Fault dipping less than 30°.

Metamorphic core complex: Exposed portion (window) of the metamorphic rocks of the lower plate (footwall) of a low-angle normal fault (detachment). According to the original use of this term, the upper plate should be exposed to brittle deformation while the lower one contains mylonitic rocks formed in the plastic regime.

Mean stress: The arithmetic mean (average) of the principal stresses.

Mica fish: Mica grains with pointed and oppositely bent tails, typically delimited by shear bands. Characteristic of micaceous mylonites.

Mineral lineation: Lineation deformed by parallel-arranged minerals on a surface or throughout a given volume of rocks.

Mineral fiber lineation: Lineation formed by growth of fibrous or elongated minerals, such as quartz, serpentine and actinolite.

Missing section, see *fault cut.*

Mode I fracture: Extension fracture (opening mode).

Mode II fracture: Shear fracture, where the movement is into and out of the plane of observation. Also known as the sliding mode.

Mode III fracture: Shear fracture with movement parallel to the edge, i.e. the plane of observation is parallel to the slip vector. Also called the tearing mode.

Mylonite: Well-foliated tectonic rock formed by intense plastic deformation of rock, usually at middle crustal levels and deeper. Normally characterized by grain size reduction, although grain size increase can occur when fine-grained rocks become mylonitized. Subordinate brittle deformation can occur. Subdivided into protomylonite, mylonite and ultramylonite depending on the degree of recrystallization.

Mylonitic foliation: The foliation formed during mylonitization: usually a strong and compositional foliation defined by parallel minerals and mineral aggregates, lenses and parallel layers reflecting primary structures such as dikes and bedding.

Mylonitization: The process that transforms a rock to a mylonite. This occurs predominantly by means of plastic deformation mechanisms, but also brittle micro-fracturing can be important.

Nabarro-Herring creep: See *volume diffusion.*

Non-coaxial deformation: Lines along the principal strain axes do no have the same orientation before and after the deformation.

Non-coaxial deformation history: Lines along ISA as well as the principal strain axes rotate during the deformation history: $W_k \neq 0$.

Non-steady state deformation: The particle paths and flow parameters such as ISA and W_k varies during the deformation history.

Normal drag: Rotation of layers in the walls of a fault so that the curvature is consistent with sense of offset on the fault.

Normal fault: Fault where the hanging wall has moved down relative to the footwall. Normal faults are extensional with respect to a horizontal layer or the surface of the Earth.

Normal stress: Stress or stress component acting perpendicular to the surface of reference.

Oblate: Disk-shaped geometry, used to describe the strain ellipsoid. For perfect oblate objects the maximum and intermediate axes (X and Y) are of the same length: X=Y>>Z.

Oblique-slip fault: Fault where the displacement vector is dipping at a lower angle than the dip of the fault, i.e. a mixture of strike-slip and either normal- or reverse movement.

Orogenic wedge: The wedge-shaped (as seen in cross section) area of allochthons in an orogenic zone or mountain range: thickest in the hinterland and thinning toward the foreland.

Overlap zone: Zone between overlapping fault segments. Can be hard linked, where the overlapping folds are physically connected, or soft linked where the strain in the overlap zone is ductile (continuous deformation). A relay ramp is a common expression of the latter.

Overlapping faults: Two faults with approximately the same strike orientation but laterally offset with respect to each other so that the fault tips are misaligned. The tips have grown past each other by a length that is much smaller than the fault length, and the two faults must be close enough that their elastic strain fields overlap.

Overpressure: Term used to describe the case where the pore pressure in a stratigraphic unit exceeds the hydrostatic pressure. This can occur in a highly porous and permeable unit (e.g. sandstone) that is captured between two impermeable layers (e.g. shale) so that the pore fluid cannot escape. Further lithostatic loading (burial) will then generate an overpressure, which reduces the *effective stress* and counteracts physical compaction.

Parautochthonous: Almost autochthonous rocks in an orogen, only short transportation. The rocks can easily be correlated with the autochthonous.

Particulate flow: Same as granular flow

Passiv folding: Folding where the layering has no mechanical influence (no competency contrast): the layers merely act as markers.

Pencil cleavage: Two differently oriented cleavages in shales causing the shale to break into pencil-like fragments. Typically a combination of compaction and tectonic strain.

Phyllitic cleavage: Continuous cleavage formed under lower-middle greenschist facies conditions in phyllitic rocks.

Pinch-and-swell structures: Necking of (usually) competent layers without the formation of true boudins.

Plastic deformation: Ductile deformation resulting from plastic deformation mechanisms. Plastic deformation produces a non-recoverable change in shape (permanent strain) without failure by rupture. Also see *plastic behavior*.

Perfect plastic deformation: Time-independent plastic deformation where strain rate has no influence on the stress-strain curve. Perfect plastic deformation does not show any work (strain) hardening or softening.

Perfect plastic material: Incompressible material that accumulate permanent strain at a constant stress level and where this level of stress (the yield stress) cannot be increased even if we tried to: the yield stress is independent of strain rate.

Permanent strain: Strain that remains after the removal of the stress field that caused the strain.

Phyllosilicate deformation bands: Deformation bands where phyllosilicates have reoriented to form a local fabric along the band. Common in phyllosilicate-bearing sands and sandstones. Also called phyllosilicate framework structures.

Plane strain: Strain where the intermediate strain axis (Y) remains unaffected by the deformation (Y=1). There is therefore no particle motion perpendicular to the X-Z plane. Plane strain produce strain ellipsoids that plot along the diagonal (k=1) of the Flinn diagram.

Plastic behavior: Deformation only occurs at a given yield stress. The deformation is permanent, and both strain hardening and softening may occur. From a soil or rock mechanic's point of view, plastic behavior doesn't have to involve plastic deformation mechanisms. Hence, materials such as clay can show plastic behavior.

Plastic deformation: General meaning in this book: Deformation that accumulates strain by means of dislocation movements and diffusion. In a strict sense, diffusion should be kept separate from plastic deformation mechanisms. In terms of rheology (regardless of deformation mechanisms), plastic deformation is simply the accumulation of permanent deformation without fracturing in response to stress. Soil mechanics people therefore regard clay as a (quasi-)plastic material.

Plastic deformation mechanisms: Mechanisms operative during plastic deformation. These are dislocation glide and creep, diffusive mass transfer, and (non-frictional) grain boundary sliding (superplasticity).

Plasticity: Deformation mechanisms where atomic bonds are broken while material coherency or cohesion is maintained. Note however that soil mechanicists relate plasticity merely to rheology (the accumulation of permanent strain).

Plumose structures: Subtle pattern (relief) on joints that resembles the structure of a feather, indicating the growth direction of joints. The pattern points toward the nucleation point of the joint. Commonly found on joints in fine-grained rocks. Also called *hackle marks*.

Pore pressure: The pressure in the fluid (water, oil or gas) filling the pore space in a porous rock.

Porphyroclast: Mineral grain, typically feldspar, in a strongly sheared rock that is larger than the surrounding grains (matrix). Porphyroclasts tend to be relicts of large crystals that are more resistant against grain-size reducing processes. Common in mylonites where they can have asymmetric tails that reflect sense of shear.

Pressure solution: Wet diffusion along grain boundaries. The only type of diffusion that can occur at sum-metamorphic temperatures. Commonly called dissolution or solution when found in sedimentary rocks, because temperature and chemical factors seem to be more important than pressure during compaction of sediments.

Pressure-solution cleavage: Tectonic cleavage defined by subparallel solution seams. Common in limestones.

Principal planes of stress: The planes in a stress field that do not contain shear stresses. These planes are perpendicular to the principal stress axes.

Principal stresses: Principal stress is the normal stress on a plane with no shear stress. There are two such stress vectors in two dimensions, and three in 3D, and they are mutually orthogonal. These are known as the principal stresses or principal stress vectors. They define the orientation and shape of the stress ellipse or ellipsoid.

Principal strain axes: The two (three) orthogonal axes of the strain ellipse (ellipsoid) that represent the directions and amounts of maximum extension (X) and shortening (Y). The strain ellipsoid has a third, intermediate axis (Z) that is orthogonal to the other two.

Principal stress axes: The three orthogonal axes (two in two dimensions) defining the directions of the principal stresses and therefore the stress ellipsoid.

Prolate: Elongate three-dimensional shape reminiscent of a cigar. A perfectly prolate object has a major principal strain that is much longer than the other two axes, which are of equal length: X>>Y=Z.

Process zone: The zone ahead of a fracture where the rock is "processed" or softened through the formation of numerous microcracks. The process zone moves along with the tip during tip propagation.

Pseudotachylyte (US), *pseudotachylite* (UK): Glass or devitrified glass formed as a result of frictional melting during faulting.

Pull-apart basin: Basin formed in an extensional overlap or releasing bend of a strike-slip fault or fault zone.

Pure shear: Plane strain coaxial deformation where particles move symmetrically around the principal axes of the strain ellipse in the X-Y plane. Flow apophyses are prthogonal and $W_k=0$.

Ramp: The steep and relatively short segment of a thrust fault as it climbs to a higher level in the stratigraphy. Now also used about steep segments connecting two low-angle normal fault segments. Also see *relay ramp*.

Ramp-flat-ramp geometry: A fault with a subhorizontal central segment bounded by steeper segments at each end.

Recrystallization: Process occurring during deformation, metamorphism and diagenesis of minerals by means of grain boundary migration and/or the formation of new grain boundaries. The "purpose" of recrystallization is to reduce the energy of a mineral represented by dislocations, point defects, subgrains and grain boundaries. Recrystallization that occurs during deformation is known as dynamic, whereas temperature-controlled recrystallization is static. Minerals can also recrystallize into new minerals with different compositions, typically related to metamorphic reactions during temperature and pressure changes.

Relay: The overlap zone between overlapping fault segments.

Relay ramp: Folded area in a relay formed by flexing of layers between the fault tips. Usually used about subhorizontal layers that are given a ramp-like geometry in the overlap zone. The folding is due to strain transfer between the two faults.

Releasing bend: A bend along a strike-slip fault that has generated local extension.

Repeated section: Stratigraphic section that is repeated in a well because of faulting, i.e. the opposite of missing section. Whether one observes repeated or missing section depends on the orientations of the fault and the well. A vertical well gives repeated section across reverse or thrust faults.

Restoration: Expression used about the reconstruction of a geologic section, map or 3D model to its pre-deformational situation.

Reverse drag: Rotation of layers in the hanging wall of a fault so that the curvature is inconsistent with sense of offset on the fault. Roll-over structures, which are related to fault geometry, are the most common example of reverse drag.

Reverse fault: Fault where the hanging wall has moved up relative to the footwall, implying shortening of horizontal layers.

Rheology: The study of flow (rheo in Greek) of any rock and other material that deform as a continuum under the influence of stress. Elasticity, viscosity and combinations of these are different rheological behaviors.

Rheological stratigraphy: The rheological stratification of the lithosphere or part of the lithosphere, where a subdivision can be made into layers of contrasting rheological properties.

Restraining bends: Bends on strike-slip faults that generate local contraction (transpression).

Ribs or *Rib marks*: Elliptical (conchoidal) structures occurring on extension fractures, centered on the nucleation point of the fracture. They are ridges or furrows where the fracture has a slightly anomalous orientation and are perpendicular to *hackle marks*.

Riedel shears: Sets of subsidiary slip surfaces arranged en echelon, each Riedel or R shear being oblique to the zone. Also found along larger slip surfaces, where they are oriented oblique to the main slip surface. An antithetic set (R' or R prime) also occurs, although less commonly than R shears.

Rolling hinge model: Dynamic model where the upper part of an initially steep normal fault flattens as offset accumulates. The hinge of the curved fault moves or "rolls" toward the hanging wall due to isostatic adjustments during faulting. The result can be a *metamorphic core complex*.

Roll-over: The fold structure defined by the steepening of otherwise horizontal hangingwall layers toward a normal fault. Normally related to a downward-flattening (listric) fault.

Roof thrust: Low-angle fault that defines the upper limitation of a duplex structure.

Scaling: Changing natural physical quantities to those appropriate for a given laboratory setup. In addition to the scaling of lengths, such as the thickness of the crust etc., it may be necessary to scale quantities such as strain rate, temperature, viscosity, stress, cohesion and grain size.

Scale model: A model that has been properly scaled down (or up) from some natural example.

Schistosity: Tectonic foliation defined by coarse-grained platy minerals in rocks deformed under upper greenschist and amphibolite facies conditions.

Sealing fault: Fault in porous and permeable rocks such as sandstones that is non-permeable and therefore prevents fluid to pass across the fault. Shale or clay smearing as well as a membrane of non-permeable fault gouge can cause faults to be sealing even if there is sand-sand contact along the fault surface.

SFF: See *Shale Smear Factor*.

SGR: *See Shale Gouge Ratio*.

Shale Gouge Ratio (SGR): Ratio used in fault sealing analysis, relating the amount of shale that has passed a point at a fault surface and the local fault throw.

Shale Smear Factor (SSF): Ratio between fault throw and the thickness of the shale source layer. SSF is used in the evaluation of the sealing properties of faults.

Shear bands: Small-scale (mm or cm-scale) shear zones in well-foliated mylonitic rocks. Single sets of shear bands make an oblique angle to the foliation that indicates the sense of shear in sheared rocks.

Shear fracture: Fracture with detectable wall-parallel displacement. Different from *fault* in that it only consists of a single fracture, while faults are composed of a number of linked fractures.

Shear sense indicators: See *kinematic indicators*.

Shear strain (γ): The tangent value of the change in angle ψ experienced by two originally perpendicular lines.

Shear strain rate: The rate at which shear strain accumulates.

Shear stress: Stress acting parallel to a plane of reference.

Shear zone: Tabular strain zone dominated by ductile (continuous) deformation, typically dominated by simple shear.
Shortening: See *contraction*.
Similar fold: Fold where the inner and outer arc have exactly the same shape, implying that the distance between the arcs parallel to the axial trace is everywhere the same. Similar folds are Class 2 folds according to Ramsay's dip isogon-based classification.
Simple shear: Non-coaxial plane strain deformation where particles move along straight lines and W_k=1.
Slaty cleavage: Tectonic cleavage in slate that forms by reorientation and pressure solution (diffusion) of minerals.
Slickolites: The peaks or "teeth" on tectonic stylolites.
Slip: 1) Shear motion localized to a surface (slip surface). 2) Movement of a dislocation front within a crystallographic plane.
Slip plane: 1) Planar slip surface. 2) Crystal lattice plane along which dislocations move.
Slip surface: Well-defined surface or narrow (< 1 mm) zone along which slip has occurred. In principal, the amount of slip can be from a few centimeters to several kilometers, but large displacements tend to produce a zone (not suface) of brittle shearing known as fault core. A slip plane and a fault are the equivalent terms to some geologists.
Sole thrust: Low-angle thrust fault that marks the base of a tectonic unit.
Soft domino model: See *domino model*.
Soft link: Expression used about fault overlap zones where there is no fault connecting the two overlapping fault segments. Instead, a *relay ramp* may be present.
Spaced cleavage: Cleavage where the width of the cleavage domains is at least 1 mm, i.e. distinguishable in a rock sample.
Splay faults: Smaller faults horse-tailing from a fault near its tip point.
Static recrystallization: Recrystallization of a rock or mineral grain (shortly) after deformation. Characterized by equigranular texture unstrained grains (no pronounced undulatory extinction under the microscope etc.).
Steady state deformation: Deformation where particle paths and flow parameters such as ISA and W_k are constant throughout the deformation history.
Steady-state flow: Deformation of a material at constant strain rate. Also se *steady state deformation*.
Strain: Change in length (1D) or shape (2D or 3D) due to deformation. Primarily defined for continuous (ductile) deformation, but is also used in areas of faulting: see *fault strain*.
Strain ellipse: The ellipse resulting from the deformation of a unit sphere passively present in the deforming medium. The strain ellipse has two principal axes that define the directions of maximum, minimum and intermediate strains (principal strain axes).
Strain markers: Objects reflecting the state of strain in a deformed medium, i.e. lines or objects of known undeformed length, shape and/or orientation.
Strain rate: The rate or speed at which strain accumulates. Two different types of strain rate are in common use: elongation rate and shear strain rate.
Strain hardening: The effect that the stress level must be increased in order to maintain a fixed strain rate. Best constrained in the laboratory during rock mechanics experiments. In a shear zone or deformation band setting, strain hardening means that it is easier to deform the wall rock than to continue the deformation in the zone or band. Strain hardening is also referred to as deformation hardening or work hardening.
Strain softening: The effect that the stress level must be decreased in order to maintain a fixed strain rate, i.e. opposite to *strain hardening*.
Strain partitioning: The physical decomposition of strain into different components at anything from micro- to mesoscale. For example: Transpression can be partitioned into zones of pure and simple shear, e.g. along obliquely convergent plate boundaries. At the cm-scale, simple shear can be partitioned into oblique shear bands and domains experiencing back-rotation.
Stretching (s): s=1+e, where e is elongation (extension). Equal to the betafactor reported in regional estimates of the stretching of a basin.
Stretching lineation: Lineation formed by tectonic stretching of objects, such as mineral aggregates and conglomerate clasts.
Stress: Stress on a surface is the force over the area on which it is applied. Typically decomposed into a normal and a shear component. The complete state of stress in a point is given by the stress tensor and illustrated by the *stress ellipsoid*.

Structural geology: The knowledge of the structure of the crust and the underlying processes at various scales.

Stress ellipsoid: Ellipsoid that describes the state of stress at a point. A point represents the intersection of an infinite number of planes, and the normal stress to any given plane at that point is the distance from the point to the ellipse, measured perpendicular to the plane in question. The axes of the ellipse are the principal stresses (maximum, minimum and intermediate normal stresses, designated σ_1, σ_2 and σ_3), oriented perpendicular to the principal planes of stress. A stress ellipsoid only exists when all three principal stresses are compressive or tensile.

Striations, striae: Linear scratches and grooves on a slip surface, formed by frictional movement of the hanging wall against the footwall of a fault.

Strike-slip fault: Fault where the displacement is horizontal. Strike-slip fault are dextral (right-lateral) or sinistral (left-lateral).

Subgrains: Part of a mineral grain that has a uniform optical, and therefore also crystallographic, orientation that differs from that of the rest of the grain. At the crystal lattice scale, subgrains are accumulations of dislocations in the form of dislocation walls.

Sub-simple shear: Planar deformation intermediate between simple and pure shear, i.e. $0<Wk<1$ and the flow apophyses make an acute angle.

Synthetic fault: Term used about a small fault dipping in the same direction as an adjacent main fault.

Tangential longitudinal strain: Fold mechanism where lines that were orthogonal to the folded layer before folding remain so also after the folding is over. The mechanism implies outer-arc extension and inner-arc contraction.

Tectonics: From the Greek word "tektos" – to build. The knowledge of how the crust of the Earth is being built through plate interactions and the results of related movements and processes. Also used about similar processes not directly related to plate tectonics, e.g. glaciotectonics.

Tectonite: Strongly strained rock, usually a mylonite. A distinction is made between L-tectonites (strong lineation), S-tectonites (strong foliation) and LS-tectonites (pronounced foliation and lineation).

Tension: Pull that can (but doesn't have to) result in extension.

Tension fractures, tension cracks: Expression used about extension fractures with small openings perpendicular to the walls, i.e. Mode I or opening mode fractures. Many geologists find it useful to reserve the term tension for stress, in which case the term tension fractures should be restricted to extension fractures formed under tension.

Tensor: An n^{th} order tensor is an object that has m^n components, m being the dimension. 0^{nd} order tensors are scalars, 1^{st} order tensors are vectors, while 2^{nd} and higher order tensors are matrices. Tensors have properties that are independent of coordinate systems. For instance, the deformation matrix (2^{nd} or 3^{rd} order tensor in section or space) will describe the strain ellipsoid and dilation regardless of the related coordinate system.

Thick-skinned deformation: Orogenic deformation involving the basement and not only the overlying sedimentary cover.

Thin-skinned deformation: Orogenic deformation not involving the basement, only the overlying sedimentary cover. Basement nappes may still occur in the orogenic wedge, but these basement rocks must stem from an area far away of the area in question.

Throw: The vertical component of the dip separation of faults.

Thrust fault: Low-angle reverse fault with considerable displacement (10 km or more). More informally used about any low-angle reverse fault, regardless of the amount of displacement.

Transcurrent faults: Strike-slip faults with unconstrained tip (c.f. transform faults).

Transected fold: Fold whose axial planar cleavage is oblique with respect to the axial surface of the fold.

Transfer fault: Fault that transfers offset from one fault to another.

Transform fault: Strike-slip fault that defines a plate boundary. Transform faults transfer movement between mid-ocean ridge segments or island-arc bounding faults.

Translation: Rigid movement without any rotation or strain. The displacement field consists of parallel and equally long displacement vectors.

Transmissibility: The ability of a fault to transmit fluids in a hydrocarbon or water reservoir.

Transposed layering: Layering formed by tectonic flattening of originally crosscutting elements (dikes, beds, cross beds, magmatic banding, tectonic foliation etc.) into a

composite foliation. The process involves high strain and the foliation reflect the flattening (X-Y) plane of the strain ellipsoid. Transposed layering is commonly seen in gneisses formed in the lower crust.

Transpression: Strike-slip zone with additional simultaneous shortening across the zone. Usually a three-dimensional deformation where the strain ellipses plot off the k=1 diagonal of the Flinn diagram.

Transtension: Strike-slip zone with additional simultaneous extension across the zone

Triangle diagram: Diagram showing the juxtaposition of beds for a continuously ingreasing offset. The input for the construction of a triangle diagram is the local stratigraphy. Factors such as SGR values can be calculated and incorporated into triangle diagrams.

Trishear: Model for the deformation ahead of a propagating fault tip, where shear is fanning out into an upward-widening zone of heterogeneous ductile isochoric deformation expressed by (fault propagation) folding of horizontal layers.

Uniaxial contraction/shortening: Contraction in one direction and no strain in the plane perpendicular to this direction. Compaction of sediments is a common example. Uniaxial shortening is an example of anisotropic *dilation*.

Uniaxial extension: Extension in one direction and no strain in the plane perpendicular to this direction. Uniaxial extension implies volume increase.

Uniaxial-strain reference state: Model of the state of stress in the crust, where stress arises as a consequence of vertical compaction only (i.e. uniaxial compaction). Stresses arise because rocks cannot expand or contract in the horizontal plane and the stress level increases downward with the weight of the overburden.

Uniaxial contraction: Contraction in one direction and no strain in the plane perpendicular to this direction. Uniaxial extension implies volume increase and is the type of strain generated during compaction of sediments.

Velocity field: A vector field describing the velocities of particles at any given moment during the deformation history.

Vergence: Term related to the geometry of asymmetric folds. The vergence direction is the direction of apparent shear if the fold is considered to be a result of simple shear.

Viscosity: A measure of the resistance of a fluid to deform under shear stress or, less formally, of a medium's resistance to flow. "Thick" fluids therefore have a higher viscosity than "thin" or runny fluids. Over geologic time, rocks in the middle and lower crust can be considered as fluids with very high viscosity.

Viscous material: Material showing a linear relationship between shear stress and shear strain. Viscous materials also show a linear relationship between shear stress and shear strain rate.

Volume change: See *dilation*.

Volume diffusion: Diffusion creep where vacancies migrate through the crystal lattice. Also known as Nabarro-Herring Creep.

Wall rock: The rock on each side of a shear zone or a fault.

Work hardening/softening: More or less the same as strain or deformation hardening/softening, but strictly relates to the work (energy) involved rather than the level of stress.

Vorticity: The local angular rate of rotation in a fluid or, in other words, a measure of how fast a fluid rotates or circulates. Applied to rocks deforming (or flowing) in the plastic regime. Mathematically vorticity is the curl of the velocity, and therefore a vector whose axis is along the axis of rotation. It can be visualized by considering a tiny portion of the fluid or flowing rock freezing into an undeformable sphere. The vorticity vector is the axis of rotation through that sphere and the angular velocity (an expression of rotation rate) is half the vorticity. If the sphere does not rotate there is no vorticity.

Wing crack: Tension fracture forming at the tips of shear fractures during fracture growth or reactivation.

Yield point: The point on a stress-strain curve that marks the transition from elastic to permanent deformation.

Yield stress: The critical stress that it takes for a rock to flow (yield).